

# THE ADAPTIVE NATURE OF PALLADIUM REACTIVITY IN SYNTHESIS

Thesis by

Daniel David Caspi

In Partial Fulfillment of the Requirements for the Degree of

Doctor of Philosophy

California Institute of Technology

Pasadena, California

2008

(Defended February 15, 2008)

© 2008

Daniel David Caspi

All Rights Reserved



*To my family*

## ACKNOWLEDGEMENTS

I would like to express my deepest gratitude to my advisor, mentor, and friend, Professor Brian Stoltz. His enthusiasm and constant support have made graduate school one of the most rewarding experiences of my life. I admire him for his dedication to his group, his strive for perfection, his insight into science, and his genuine concern for the well-being of his students. Working under his supervision has been an incredible privilege, and I have greatly appreciated his seemingly infinite curiosity about chemistry. I always remember feeling far more excited about the state of my project on the way out of his office than I did going in. I sincerely thank Brian for fostering my personal development and maturation as a scientist, and his amazing ability to balance a highly challenging work environment with good humor and compassion. I have also greatly appreciated the support of his wife Erna, and thanks to Harry, I will forever have a fellow Stoltz lab member with whom to celebrate my birthday with every year.

I would also like to extend a wholehearted thanks to the members of my thesis committee: Professors Bob Grubbs, Bill Goddard, and Peter Dervan. Professor Grubbs, the chair of my committee, has been extremely supportive, and he also was an instrumental component of my job search. I am grateful for all of the advice and input he has given me, and I am awed by his humility. I felt honored to be a part of the Caltech community's celebration when he received the Nobel prize. Professor Goddard taught me in one of my first classes at Caltech, and I have been learning from him ever since. His ability to juggle such a multitude of projects is impressive, and he has always brought insightful questions and good humor to the table. I am also indebted to Professor Dervan,

who generously stepped in to be the final member of my committee. Even though he is my most recent committee member, his willingness to provide guidance and support has been outstanding. I would also like to thank Professors MacMillan and Peters for their tenure on my committee, and for helping to shape me as a scientist during the earlier portion of graduate school. Although not official members, I would also like to warmly acknowledge Professors John Bercaw, Dennis Dougherty, and Dave Tirrell, with whom I have had a number of enjoyable discussions. I greatly admire their skillful leadership and willingness to listen, and I aspire to model my future management style after theirs.

I would also like to express my gratitude to my high school chemistry teacher, Mr. Jack Coakley, who was the first person to attract my interest to this field. His enthusiasm made learning chemistry incredibly fun, which is really hard to do since *everyone* had a “terrible high school chemistry teacher.” He made chemistry tangible and exciting for me, which ultimately led me to pursue it as my college major.

While at UCSD, I was introduced to organic chemistry by Professors Nat Finney and Yitzhak Tor. I am incredibly grateful to them for getting me excited about the field, as well as for discussions we had years later about graduate schools and research. I would also like to extend a warm thanks to Professors Charles Perrin and Robert Continetti, whose chemistry courses were especially memorable and who exposed me to more advanced topics. I am especially indebted to Dr. Jorge Gomez of the Medicinal Chemistry department at Metabasis Therapeutics, Inc., who took me in as a student intern during my last two years of college. He gave me the finest training I could have ever imagined, and he made continual efforts to expose me to every aspect of being a modern synthetic chemist. His patience, natural teaching ability, and intelligence made for an

unforgettable experience, and my time with him at Metabasis clinched my decision to become an organic chemist. I cannot thank him enough for his support over the years. I would also like to sincerely acknowledge Drs. Serge Boyer and Max Dang, from whom I learned a great deal during that time as well.

I have also had the great pleasure and privilege of working alongside so many talented chemists over my time in the Stoltz lab. Eric Ferreira and Jeff Bagdanoff, as well as my classmates Dave Ebner and Ryan McFadden, were my teammates on the palladium(II) oxidative kinetic resolution project. Their enthusiasm and collective wisdom made for a fantastic way to start graduate school.

Shortly thereafter, I sought to apply some of our lab's palladium(II) methodology to total synthesis, and I was lucky to end up collaborating with Neil Garg on the dragmacidin F project. Neil was an outstanding role model and coworker, and joining forces with him was one of the most enjoyable experiences I have had at Caltech. I cannot thank him enough for his insightful scientific contributions and his overwhelming input of time and energy into my personal growth as an organic chemist. I have always admired his stellar ability to teach, and I have no doubt that his current students (he is now *Professor* Garg) feel the same way. Outside of the lab, I am also indebted to both Neil and his wife Lindsey for their great friendship and support.

I would like to thank Dr. Haiming Zhang for all of his hard work getting the telomestatin project off the ground, as well as his friendly emails to see how things were progressing. Tim Dong is acknowledged for making some key improvements along the early part of the synthesis, and I had a lot of fun training him over the summer; I am sure he will be very successful in graduate school. I am also indebted to J. T. Mohr, who has

graciously taken on this project, and has already made some important contributions. I have full confidence entrusting the project to him, and I am excited to see what the future directions bring. In addition to being an exceptional chemist, J. T. is one of the few people I know who is an absolute encyclopedia of information. To my surprise, he was even able to recite the third ingredient of Coke from memory! Outside of the doors of Crellin, Church, and Gates, I have also become close friends with J. T. and his wife Sarah, and I really value their friendship.

I would also like to extend an enormous thank you to all of the Stoltz Group members, both past and present. There are far too many people to list all of them individually, but I am indebted to all of them at one time or another for their advice and expertise. In particular, in addition to the names already mentioned, I would like to thank Dr. Richmond Sarpong, Eric Ashley, Raissa Trend, Uttam Tambar, and Dr. Yeeman Ramtohl for their generously dispensed help and guidance during my early days here. Richmond was an exemplary role model, and I learned a great deal just being around him. He set the bar very high, and I have always admired his dedication. I would also like to express my deep gratitude for his support during my job search. Raissa's abilities to think critically are unparalleled, and I feel grateful to have learned so much from her. I also appreciated sharing many delicious tacos and perhaps even more spirited discussions. I feel incredibly privileged to have become close friends with Uttam, who is a first-rate scientist and an even better human being. There's no way I would have made it through graduate school without his sense of humor, advice, and friendship. Yeeman always took time to help me with chemistry, and he is one of the most easy-going people I have ever met. He had a great attitude about life, and he definitely brought a calming

influence to the lab. I would like to extend a warm thanks to Eric Ashley, who was extremely knowledgeable and helpful, and always took time out of his day to be of assistance with a mechanism or a troublesome reaction. Finally, Mike Krout, who joined during my second year, has also been incredibly generous with his expertise. In addition to being a terrific scientist and a wealth of knowledge, both he and his fiancée Kristy have become close friends of mine.

I would also like to extend my gratitude to Tim Funk, Dr. Chris Douglas, and Dr. Tom Driver, who were regular attendees at our weekly Stoltz group meetings and were generous in sharing their wisdom. I benefited tremendously from interacting with them. I also want to acknowledge the generosity of the other research groups at Caltech, in particular, the Hsieh-Wilson, Dougherty, Dervan, Grubbs, Peters, MacMillan, and Bercaw groups. I have borrowed reagents, expertise, and equipment, from time to time and I have always felt like everyone went out of their way to be helpful. David Chenoweth from the Dervan lab has been very accommodating; he spent a great deal of time training me to use their analytical and preparatory instrumentation. I am also extremely grateful to the American Chemical Society, TRDRP, and Eli Lilly for funding portions of my graduate school research.

I would like to extend my sincere gratitude to my long-term baymates Jenny Roizen, Dr. Dave White, Dr. Zoli Novák, and Dr. Andy Harned. Your good humor and scientific input made for a friendly and fun work environment, and made my daily life very pleasant. I also want to show my appreciation to J. T. Mohr, Mike Krout, Jenny Roizen, John Enquist, Kevin Allan, Sandy Ma, Hosea Nelson, and Dr. Andy McClory for

proofreading portions of this document. This thesis has been much improved by their meticulous corrections and contributions.

There are so many talented staff at Caltech, and I have been repeatedly astonished by how much care and personal attention they have given me. I am grateful to Drs. Scott Ross and Chris Brandow for their hard work in the NMR laboratory, and for their help with advanced experiments. I am tremendously indebted to Tom Dunn for his MacGyver-like ability to repair just about anything. He has always been so easy to count on, especially with regards to the NMR facility. Dr. Mona Shahgholi and Naseem Torian are acknowledged for their assistance obtaining numerous mass spectra. I would like to extend my gratitude to Drs. Larry Henling and Mike Day for solving a crystal structure on the telomestatin project, Rick Gerhart for being a master of glass and an expert on Hawaii, and Joe Drew, Moises Renteria, and Terry James, for many lively conversations and general assistance. Lynne Martinez is incredibly sweet, and somehow manages to do a great job handling our ever-growing group. And, the latest departmental addition, Dr. Scott Virgil, has already become one my favorite people with whom to discuss chemistry problems. His expert suggestions his contributions on the telomestatin project have had, and I'm sure will continue to have, a large impact. I am extremely grateful to Chris Smith, who played a key role in my job search and was a tremendous resource. Anne Penney has always been good to me, and Dian Buchness is one of the primary reasons I am at Caltech today. If it weren't for her persistent emails, I probably would never have visited. Laura Howe seems to be doing a terrific job in her place, and has been incredibly helpful while I have been finishing up.

In the tradition of Uttam Tambar, I'd also like to acknowledge the staff at Amigos, and the staff at the newer and trendier Magnolia Lounge. Their refreshing beverages have helped to commemorate many a good time, and have helped to rejuvenate dampened spirits as well. I would be completely lost without my friends Lori Lee and Mel Pribisko, who have always been there for me. I appreciate all of the deep conversations and savory foods that we have shared. I will really miss having you around. Sarah Threlfall, you are a lifesaver. You have always been there for me, over and above what I ever expected, and have helped me in more ways than I can count. I owe you big time.

To my extended family in Los Angeles—Betty and Grant Hyun; Vicki, Glenn, Ari, and Jaime Ziegel; and Henry, Wendy, Matt, and Josh David—your support has been truly invaluable. I have always felt surrounded by your love and kindness. I would also like to thank Marlana Chang, who has been a shining beam of light in my life and an invaluable source of support for me. Her love helped to renew my strength on more than one occasion, and I am indebted to her for that. I hope to be as much of an ally to her on our new adventure together in Chicago. Last, but certainly not least, I would also like to thank my mom, my dad, and my sister, Sara. Your love and support over the years has enabled me to cross the finish line.



## ABSTRACT

Both Pd(0) and Pd(II) have had, and continue to have, far-reaching impacts on organic synthesis. The versatile nature of palladium, in conjunction with the mechanistic understanding and predictive models that have been elucidated, has permitted a wealth of exploration into the seemingly endless potential of this metal. The utility of palladium is described in the context of the syntheses of the pharmaceutical agents Prozac<sup>®</sup> and Singulair<sup>®</sup>, as well as the natural products drarmacidin F and telomestatin.

First, the palladium-catalyzed aerobic oxidative kinetic resolution for the enantioselective preparation of a variety of pharmaceutical substances, including Prozac<sup>®</sup> and Singulair<sup>®</sup>, is described. In this regard, the versatility of this resolution is further demonstrated by the diversity of the substrates chosen for this study, and for the first time this work extends the utility of the resolution to include amino alcohol derivatives and highly functionalized benzylic alcohols.

Secondly, an enantiodivergent strategy for the total chemical synthesis of both (+)- and (–)-drarmacidin F from a single enantiomer of quinic acid has been developed and successfully implemented. Although unique, the synthetic routes to these antipodes share a number of key features, including novel Pd(0) reductive isomerization reactions, Pd(II)-mediated oxidative carbocyclization reactions, halogen-selective Suzuki couplings, and high-yielding late-stage Neber rearrangements.

Finally, progress toward the total synthesis of the potent telomerase inhibitor telomestatin is described. Palladium-mediated cross-coupling reactions are employed to assemble oligooxazole intermediates from oxazole building blocks. Additionally, this strategy utilizes a minimum number of protecting groups, and proposes a unique aryl–aryl macrocyclization as the last step of the synthesis. In addition to the biological relevance of the desired target, a successful total synthesis of telomestatin would also enable rapid access to the preparation of telomestatin analogs. This would allow for the investigation of key interactions between telomestatin and the G-quadruplex.

## TABLE OF CONTENTS

Dedication .....	iii
Acknowledgements.....	iv
Abstract .....	xi
Table of Contents .....	xii
List of Figures .....	xvii
List of Schemes .....	xxviii
List of Tables.....	xxxix
List of Abbreviations .....	xxxiii

### CHAPTER ONE: Palladium in Organic Synthesis ..... 1

1.1 Background.....	1
1.1.1 Introduction .....	1
1.2 Palladium(0) and Palladium(II).....	2
1.2.1 Oxidation States of Palladium .....	2
1.2.2 General Reactivity.....	3
1.2.3 Palladium(0) Reactivity .....	4
1.2.4 Palladium(II) Reactivity.....	6
1.3 Conclusion .....	9
1.4 Notes and References .....	10

### CHAPTER TWO: The Resolution of Important Pharmaceutical Building Blocks by Palladium-Catalyzed Aerobic Oxidation of Secondary Alcohols.....14

2.1 Background.....	14
---------------------	----

2.1.1 Introduction .....	14
2.1.2 Mechanism of the Pd-Catalyzed Oxidative Kinetic Resolution .....	17
2.2 The Oxidative Kinetic Resolution of Pharmaceutical Building Blocks .....	18
2.2.1 Pharmaceutical Targets .....	18
2.2.2 Resolution of Pharmaceutical Intermediates .....	20
2.3 Conclusion .....	22
2.4 Experimental Section.....	24
2.4.1 Materials and Methods.....	24
2.4.2 Methods of Determination for Enantiomeric Excess and % Conversion....	25
2.4.3 Optical Rotations of New Compounds.....	26
2.4.4 Representative Procedures for Oxidative Kinetic Resolution.....	27
2.4.5 Representative Procedure for Ketone Recycling.....	29
2.4.6 Preparative Procedures .....	30
2.5 Notes and References .....	40
APPENDIX ONE: Spectra Relevant to Chapter Two .....	45
CHAPTER THREE: The Total Syntheses of (+)- and (-)-Dragmacidin F .....	62
3.1 Background.....	62
3.1.1 Introduction .....	62
3.1.2 Biosynthesis.....	63
3.1.3 Previous Synthetic Studies.....	64
3.1.4 Isolation and Bioactivity of Dragmacidin F .....	65
3.1.5 Retrosynthetic Analysis of Dragmacidin F .....	66

3.2 The Total Synthesis of (+)-Dragmacidin F.....	67
3.2.1 Synthesis of Cyclization Substrates.....	67
3.2.2 Intramolecular Heck Cyclization .....	70
3.2.3 Intramolecular Oxidative Cyclization.....	71
3.2.4 Assembling the Carbon Skeleton of Dragmacidin F.....	79
3.2.5 End-Game: Total Synthesis of (+)-Dragmacidin F .....	80
3.4 The Total Synthesis of (–)-Dragmacidin F.....	85
3.4.1 An Enantiodivergent Strategy for the Preparation of (–)-Dragmacidin F...85	
3.4.2 The Development of a Reductive Isomerization Reaction .....	87
3.4.3 The Scope and Mechanism of the Reductive Isomerization Reaction .....	90
3.4.4 Constructing the [3.3.1] Bicycle En Route to (–)-Dragmacidin F .....	96
3.4.5 End-Game: Total Synthesis of (–)-Dragmacidin F .....	98
3.5 Conclusion .....	100
3.6 Experimental Section.....	102
3.6.1 Materials and Methods.....	102
3.6.2 Preparative Procedures.....	104
3.7 Notes and References .....	178
APPENDIX TWO: Synthetic Summary for (+)- and (–)-Dragmacidin F .....	194
APPENDIX THREE: Spectra Relevant to Chapter Three .....	198
CHAPTER FOUR: Progress Toward The Total Synthesis of Telomestatin .....	335

4.1 Background.....	335
4.1.1 Telomeres and Telomerase .....	335
4.1.2 Isolation and Biological Activity .....	337
4.1.3 Biosynthesis.....	338
4.1.4 Previous Synthetic Studies.....	339
4.1.5 Retrosynthetic Analysis of Telomestatin.....	343
4.2 Progress Toward The Total Synthesis of Telomestatin.....	345
4.2.1 Synthesis of Left-hand Trisoxazole Iodo Acid.....	345
4.2.2 Synthesis of Right-hand Tetrakisoxazole Amino Alcohol .....	347
4.2.3 Late-Stage and Proposed Endgame .....	349
4.3 Conclusion .....	350
4.4 Experimental Section.....	352
4.4.1 Materials and Methods.....	352
4.4.2 Preparative Procedures .....	354
4.5 Notes and References .....	372
APPENDIX FOUR: Spectra Relevant to Chapter Four .....	385
APPENDIX FIVE: X-Ray Crystallography Reports Relevant to Chapter Four .....	418
APPENDIX SIX: Notebook Cross-Reference.....	434
Comprehensive Bibliography .....	440
Index.....	472

About the Author .....	481
------------------------	-----

## LIST OF FIGURES

### CHAPTER ONE

Figure 1.2.1	Types of Pd(0)- and Pd(II)-mediated transformations .....	3
Figure 1.2.2	Generalized Pd(0) and Pd(II) reactivity cycle .....	4

### CHAPTER TWO

Figure 2.2.1	Pharmaceutical substances .....	19
--------------	---------------------------------	----

### APPENDIX ONE

Figure A1.1	<sup>1</sup> H NMR (300 MHz, CDCl <sub>3</sub> ) of compound <b>67</b> .....	46
Figure A1.2	Infrared spectrum (thin film/NaCl) of compound <b>67</b> .....	47
Figure A1.3	<sup>13</sup> C NMR (75 MHz, CDCl <sub>3</sub> ) of compound <b>67</b> .....	47
Figure A1.4	<sup>1</sup> H NMR (300 MHz, CDCl <sub>3</sub> ) of compound <b>68</b> .....	48
Figure A1.5	Infrared spectrum (thin film/NaCl) of compound <b>68</b> .....	49
Figure A1.6	<sup>13</sup> C NMR (75 MHz, CDCl <sub>3</sub> ) of compound <b>68</b> .....	49
Figure A1.7	<sup>1</sup> H NMR (300 MHz, CDCl <sub>3</sub> ) of compound <b>69</b> .....	50
Figure A1.8	Infrared spectrum (thin film/NaCl) of compound <b>69</b> .....	51
Figure A1.9	<sup>13</sup> C NMR (75 MHz, CDCl <sub>3</sub> ) of compound <b>69</b> .....	51
Figure A1.10	<sup>1</sup> H NMR (300 MHz, CDCl <sub>3</sub> ) of compound <b>70</b> .....	52
Figure A1.11	Infrared spectrum (thin film/NaCl) of compound <b>70</b> .....	53
Figure A1.12	<sup>13</sup> C NMR (75 MHz, CDCl <sub>3</sub> ) of compound <b>70</b> .....	53
Figure A1.13	<sup>1</sup> H NMR (300 MHz, CDCl <sub>3</sub> ) of compound <b>73</b> .....	54
Figure A1.14	Infrared spectrum (thin film/NaCl) of compound <b>73</b> .....	55
Figure A1.15	<sup>13</sup> C NMR (75 MHz, CDCl <sub>3</sub> ) of compound <b>73</b> .....	55
Figure A1.16	<sup>1</sup> H NMR (300 MHz, C <sub>6</sub> D <sub>6</sub> ) of compound <b>75</b> .....	56
Figure A1.17	Infrared spectrum (thin film/NaCl) of compound <b>75</b> .....	57
Figure A1.18	<sup>13</sup> C NMR (75 MHz, C <sub>6</sub> D <sub>6</sub> ) of compound <b>75</b> .....	57
Figure A1.19	<sup>1</sup> H NMR (300 MHz, C <sub>6</sub> D <sub>6</sub> ) of compound <b>77</b> .....	58

Figure A1.20	Infrared spectrum (thin film/NaCl) of compound <b>77</b> .....	59
Figure A1.21	$^{13}\text{C}$ NMR (75 MHz, $\text{C}_6\text{D}_6$ ) of compound <b>77</b> .....	59
Figure A1.22	$^1\text{H}$ NMR (300 MHz, $\text{C}_6\text{D}_6$ ) of compound <b>78</b> .....	60
Figure A1.23	Infrared spectrum (thin film/NaCl) of compound <b>78</b> .....	61
Figure A1.24	$^{13}\text{C}$ NMR (75 MHz, $\text{C}_6\text{D}_6$ ) of compound <b>78</b> .....	61

### CHAPTER THREE

Figure 3.1.1	The pyrazinone-containing drarmacidins.....	63
Figure 3.3.1	Absolute stereochemistry of drarmacidins D–F ( <b>82–84</b> ).....	85
Figure 3.4.1	Rational design of reductive isomerization substrate <b>131</b> .....	89
Figure 3.4.2	Model for reductive isomerization reactivity.....	96

### APPENDIX THREE

Figure A3.1	$^1\text{H}$ NMR (300 MHz, $\text{CDCl}_3$ ) of compound <b>165</b> .....	199
Figure A3.2	Infrared spectrum (thin film/NaCl) of compound <b>165</b> .....	200
Figure A3.3	$^{13}\text{C}$ NMR (75 MHz, $\text{CDCl}_3$ ) of compound <b>165</b> .....	200
Figure A3.4	$^1\text{H}$ NMR (300 MHz, $\text{CD}_3\text{OD}$ ) of compound <b>166</b> .....	201
Figure A3.5	Infrared spectrum (KBr pellet) of compound <b>166</b> .....	202
Figure A3.6	$^{13}\text{C}$ NMR (75 MHz, $\text{CD}_3\text{OD}$ ) of compound <b>166</b> .....	202
Figure A3.7	$^1\text{H}$ NMR (300 MHz, $\text{CDCl}_3$ ) of compound <b>95</b> .....	203
Figure A3.8	Infrared spectrum (thin film/NaCl) of compound <b>95</b> .....	204
Figure A3.9	$^{13}\text{C}$ NMR (75 MHz, $\text{CDCl}_3$ ) of compound <b>95</b> .....	204
Figure A3.10	$^1\text{H}$ NMR (300 MHz, $\text{CDCl}_3$ ) of compound <b>97</b> .....	205
Figure A3.11	Infrared spectrum (thin film/NaCl) of compound <b>97</b> .....	206
Figure A3.12	$^{13}\text{C}$ NMR (75 MHz, $\text{CDCl}_3$ ) of compound <b>97</b> .....	206
Figure A3.13	$^1\text{H}$ NMR (300 MHz, $\text{CDCl}_3$ ) of compound <b>98</b> .....	207
Figure A3.14	Infrared spectrum (thin film/NaCl) of compound <b>98</b> .....	208
Figure A3.15	$^{13}\text{C}$ NMR (75 MHz, $\text{CDCl}_3$ ) of compound <b>98</b> .....	208
Figure A3.16	$^1\text{H}$ NMR (300 MHz, $\text{CDCl}_3$ ) of compound <b>96</b> .....	209
Figure A3.17	Infrared spectrum (thin film/NaCl) of compound <b>96</b> .....	210



Figure A3.18	$^{13}\text{C}$ NMR (75 MHz, $\text{CDCl}_3$ ) of compound <b>96</b> .....	210
Figure A3.19	$^1\text{H}$ NMR (300 MHz, $\text{CDCl}_3$ ) of compound <b>101</b> .....	211
Figure A3.20	Infrared spectrum (thin film/ $\text{NaCl}$ ) of compound <b>101</b> .....	212
Figure A3.21	$^{13}\text{C}$ NMR (75 MHz, $\text{CDCl}_3$ ) of compound <b>101</b> .....	212
Figure A3.22	$^1\text{H}$ NMR (300 MHz, $\text{CDCl}_3$ ) of compound <b>170</b> .....	213
Figure A3.23	Infrared spectrum (thin film/ $\text{NaCl}$ ) of compound <b>170</b> .....	214
Figure A3.24	$^{13}\text{C}$ NMR (75 MHz, $\text{CDCl}_3$ ) of compound <b>170</b> .....	214
Figure A3.25	$^1\text{H}$ NMR (300 MHz, $\text{CDCl}_3$ ) of compound <b>91</b> .....	215
Figure A3.26	Infrared spectrum (thin film/ $\text{NaCl}$ ) of compound <b>91</b> .....	216
Figure A3.27	$^{13}\text{C}$ NMR (75 MHz, $\text{CDCl}_3$ ) of compound <b>91</b> .....	216
Figure A3.28	$^1\text{H}$ NMR (300 MHz, $\text{CDCl}_3$ ) of compound <b>172</b> .....	217
Figure A3.29	Infrared spectrum (thin film/ $\text{NaCl}$ ) of compound <b>172</b> .....	218
Figure A3.30	$^{13}\text{C}$ NMR (75 MHz, $\text{CDCl}_3$ ) of compound <b>172</b> .....	218
Figure A3.31	$^1\text{H}$ NMR (300 MHz, $\text{CDCl}_3$ ) of compound <b>92</b> .....	219
Figure A3.32	Infrared spectrum (thin film/ $\text{NaCl}$ ) of compound <b>92</b> .....	220
Figure A3.33	$^{13}\text{C}$ NMR (75 MHz, $\text{CDCl}_3$ ) of compound <b>92</b> .....	220
Figure A3.34	$^1\text{H}$ NMR (300 MHz, $\text{CDCl}_3$ ) of compound <b>90</b> .....	221
Figure A3.35	$^1\text{H}$ NMR (300 MHz, $\text{C}_6\text{D}_6$ ) of compound <b>90</b> .....	222
Figure A3.36	Infrared spectrum (thin film/ $\text{NaCl}$ ) of compound <b>90</b> .....	223
Figure A3.37	$^{13}\text{C}$ NMR (75 MHz, $\text{C}_6\text{D}_6$ ) of compound <b>90</b> .....	223
Figure A3.38	$^1\text{H}$ NMR (300 MHz, $\text{C}_6\text{D}_6$ ) of compound <b>102</b> .....	224
Figure A3.39	$^1\text{H}$ NMR (300 MHz, $\text{CDCl}_3$ ) of compound <b>102</b> .....	225
Figure A3.40	Infrared spectrum (thin film/ $\text{NaCl}$ ) of compound <b>102</b> .....	226
Figure A3.41	$^{13}\text{C}$ NMR (75 MHz, $\text{CDCl}_3$ ) of compound <b>102</b> .....	226
Figure A3.42	$^1\text{H}$ NMR (300 MHz, $\text{C}_6\text{D}_6$ ) of compound <b>107</b> .....	227
Figure A3.43	Infrared spectrum (thin film/ $\text{NaCl}$ ) of compound <b>107</b> .....	228
Figure A3.44	$^{13}\text{C}$ NMR (75 MHz, $\text{C}_6\text{D}_6$ ) of compound <b>107</b> .....	228
Figure A3.45	$^1\text{H}$ NMR (300 MHz, $\text{C}_6\text{D}_6$ ) of compound <b>108</b> .....	229
Figure A3.46	Infrared spectrum (thin film/ $\text{NaCl}$ ) of compound <b>108</b> .....	230
Figure A3.47	$^{13}\text{C}$ NMR (75 MHz, $\text{C}_6\text{D}_6$ ) of compound <b>108</b> .....	230
Figure A3.48	$^1\text{H}$ NMR (300 MHz, $\text{C}_6\text{D}_6$ ) of compound <b>109</b> .....	231

Figure A3.49	Infrared spectrum (thin film/NaCl) of compound <b>109</b> .....	232
Figure A3.50	$^{13}\text{C}$ NMR (75 MHz, $\text{C}_6\text{D}_6$ ) of compound <b>109</b> .....	232
Figure A3.51	$^1\text{H}$ NMR (300 MHz, $\text{C}_6\text{D}_6$ ) of compound <b>110</b> .....	233
Figure A3.52	Infrared spectrum (thin film/NaCl) of compound <b>110</b> .....	234
Figure A3.53	$^{13}\text{C}$ NMR (75 MHz, $\text{C}_6\text{D}_6$ ) of compound <b>110</b> .....	234
Figure A3.54	$^1\text{H}$ NMR (300 MHz, $\text{C}_6\text{D}_6$ ) of compound <b>111</b> .....	235
Figure A3.55	Infrared spectrum (thin film/NaCl) of compound <b>111</b> .....	236
Figure A3.56	$^{13}\text{C}$ NMR (75 MHz, $\text{C}_6\text{D}_6$ ) of compound <b>111</b> .....	236
Figure A3.57	$^1\text{H}$ NMR (300 MHz, $\text{C}_6\text{D}_6$ ) of compound <b>173</b> .....	237
Figure A3.58	Infrared spectrum (thin film/NaCl) of compound <b>173</b> .....	238
Figure A3.59	$^{13}\text{C}$ NMR (75 MHz, $\text{C}_6\text{D}_6$ ) of compound <b>173</b> .....	238
Figure A3.60	$^1\text{H}$ NMR (300 MHz, $\text{C}_6\text{D}_6$ ) of compound <b>112</b> .....	239
Figure A3.61	Infrared spectrum (thin film/NaCl) of compound <b>112</b> .....	240
Figure A3.62	$^{13}\text{C}$ NMR (75 MHz, $\text{C}_6\text{D}_6$ ) of compound <b>112</b> .....	240
Figure A3.63	$^1\text{H}$ NMR (300 MHz, $\text{C}_6\text{D}_6$ ) of compound <b>113</b> .....	241
Figure A3.64	Infrared spectrum (thin film/NaCl) of compound <b>113</b> .....	242
Figure A3.65	$^{13}\text{C}$ NMR (75 MHz, $\text{C}_6\text{D}_6$ ) of compound <b>113</b> .....	242
Figure A3.66	$^1\text{H}$ NMR (300 MHz, $\text{C}_6\text{D}_6$ ) of compound <b>114</b> .....	243
Figure A3.67	Infrared spectrum (thin film/NaCl) of compound <b>114</b> .....	244
Figure A3.68	$^{13}\text{C}$ NMR (75 MHz, $\text{C}_6\text{D}_6$ ) of compound <b>114</b> .....	244
Figure A3.69	$^1\text{H}$ NMR (300 MHz, $\text{C}_6\text{D}_6$ ) of compound <b>176</b> .....	245
Figure A3.70	Infrared spectrum (thin film/NaCl) of compound <b>176</b> .....	246
Figure A3.71	$^{13}\text{C}$ NMR (75 MHz, $\text{CDCl}_3$ ) of compound <b>176</b> .....	246
Figure A3.72	$^1\text{H}$ NMR (300 MHz, $\text{C}_6\text{D}_6$ ) of compound <b>115</b> .....	247
Figure A3.73	Infrared spectrum (thin film/NaCl) of compound <b>115</b> .....	248
Figure A3.74	$^{13}\text{C}$ NMR (75 MHz, $\text{C}_6\text{D}_6$ ) of compound <b>115</b> .....	248
Figure A3.75	$^1\text{H}$ NMR (300 MHz, $\text{C}_6\text{D}_6$ ) of compound <b>177</b> .....	249
Figure A3.76	Infrared spectrum (thin film/NaCl) of compound <b>177</b> .....	250
Figure A3.77	$^{13}\text{C}$ NMR (75 MHz, $\text{C}_6\text{D}_6$ ) of compound <b>177</b> .....	250
Figure A3.78	$^1\text{H}$ NMR (300 MHz, $\text{C}_6\text{D}_6$ ) of compound <b>89</b> .....	251
Figure A3.79	Infrared spectrum (thin film/NaCl) of compound <b>89</b> .....	252

Figure A3.80	$^{13}\text{C}$ NMR (75 MHz, $\text{C}_6\text{D}_6$ ) of compound <b>89</b> .....	252
Figure A3.81	$^1\text{H}$ NMR (300 MHz, $\text{CDCl}_3$ ) of compound <b>118</b> .....	253
Figure A3.82	Infrared spectrum (thin film/ $\text{NaCl}$ ) of compound <b>118</b> .....	254
Figure A3.83	$^{13}\text{C}$ NMR (75 MHz, $\text{CDCl}_3$ ) of compound <b>118</b> .....	254
Figure A3.84	$^1\text{H}$ NMR (300 MHz, $\text{CDCl}_3$ ) of compound <b>119</b> .....	255
Figure A3.85	Infrared spectrum (thin film/ $\text{NaCl}$ ) of compound <b>119</b> .....	256
Figure A3.86	$^{13}\text{C}$ NMR (75 MHz, $\text{CDCl}_3$ ) of compound <b>119</b> .....	256
Figure A3.87	$^1\text{H}$ NMR (300 MHz, $\text{CDCl}_3$ ) of compound <b>120</b> .....	257
Figure A3.88	Infrared spectrum (thin film/ $\text{NaCl}$ ) of compound <b>120</b> .....	258
Figure A3.89	$^{13}\text{C}$ NMR (75 MHz, $\text{CDCl}_3$ ) of compound <b>120</b> .....	258
Figure A3.90	$^1\text{H}$ NMR (600 MHz, $\text{CD}_3\text{OD}$ ) of compound <b>124</b> .....	259
Figure A3.91	$^1\text{H}$ NMR (300 MHz, $\text{CD}_3\text{OD}$ ) of compound <b>121</b> .....	260
Figure A3.92	Infrared spectrum (thin film/ $\text{NaCl}$ ) of compound <b>121</b> .....	261
Figure A3.93	$^{13}\text{C}$ NMR (75 MHz, $\text{CD}_3\text{OD}$ ) of compound <b>121</b> .....	261
Figure A3.94	$^1\text{H}$ NMR (300 MHz, $\text{CD}_3\text{OD}$ ) of compound <b>125</b> .....	262
Figure A3.95	Infrared spectrum (thin film/ $\text{NaCl}$ ) of compound <b>125</b> .....	263
Figure A3.96	$^{13}\text{C}$ NMR (75 MHz, $\text{CD}_3\text{OD}$ ) of compound <b>125</b> .....	263
Figure A3.97	$^1\text{H}$ NMR (600 MHz, $\text{CD}_3\text{OD}$ ) of (+)-dragmacidin F ( <b>84</b> ) .....	264
Figure A3.98	Infrared spectrum (thin film/ $\text{NaCl}$ ) of (+)-dragmacidin F ( <b>84</b> ) .....	265
Figure A3.99	$^{13}\text{C}$ NMR (125 MHz, $\text{CD}_3\text{OD}$ ) of (+)-dragmacidin F ( <b>84</b> ) .....	265
Figure A3.100	$^1\text{H}$ NMR (300 MHz, $\text{CDCl}_3$ ) of compound <b>129</b> .....	266
Figure A3.101	Infrared spectrum (thin film/ $\text{NaCl}$ ) of compound <b>129</b> .....	267
Figure A3.102	$^{13}\text{C}$ NMR (75 MHz, $\text{CDCl}_3$ ) of compound <b>129</b> .....	267
Figure A3.103	$^1\text{H}$ NMR (300 MHz, $\text{C}_6\text{D}_6$ ) of compound <b>180</b> .....	268
Figure A3.104	Infrared spectrum (thin film/ $\text{NaCl}$ ) of compound <b>180</b> .....	269
Figure A3.105	$^{13}\text{C}$ NMR (75 MHz, $\text{C}_6\text{D}_6$ ) of compound <b>180</b> .....	269
Figure A3.106	$^1\text{H}$ NMR (300 MHz, $\text{C}_6\text{D}_6$ ) of compound <b>132</b> .....	270
Figure A3.107	Infrared spectrum (thin film/ $\text{NaCl}$ ) of compound <b>132</b> .....	271
Figure A3.108	$^{13}\text{C}$ NMR (75 MHz, $\text{C}_6\text{D}_6$ ) of compound <b>132</b> .....	271
Figure A3.109	$^1\text{H}$ NMR (300 MHz, $\text{C}_6\text{D}_6$ ) of compound <b>133</b> .....	272
Figure A3.110	Infrared spectrum (thin film/ $\text{NaCl}$ ) of compound <b>133</b> .....	273

Figure A3.111	$^{13}\text{C}$ NMR (75 MHz, $\text{C}_6\text{D}_6$ ) of compound <b>133</b> .....	273
Figure A3.112	$^1\text{H}$ NMR (300 MHz, $\text{C}_6\text{D}_6$ ) of compound <b>131</b> .....	274
Figure A3.113	Infrared spectrum (thin film/ $\text{NaCl}$ ) of compound <b>131</b> .....	275
Figure A3.114	$^{13}\text{C}$ NMR (75 MHz, $\text{C}_6\text{D}_6$ ) of compound <b>131</b> .....	275
Figure A3.115	$^1\text{H}$ NMR (300 MHz, $\text{C}_6\text{D}_6$ ) of compound <b>127</b> .....	276
Figure A3.116	Infrared spectrum (thin film/ $\text{NaCl}$ ) of compound <b>127</b> .....	277
Figure A3.117	$^{13}\text{C}$ NMR (75 MHz, $\text{C}_6\text{D}_6$ ) of compound <b>127</b> .....	277
Figure A3.118	$^1\text{H}$ NMR (300 MHz, $\text{C}_6\text{D}_6$ ) of compound <b>135</b> .....	278
Figure A3.119	Infrared spectrum (thin film/ $\text{NaCl}$ ) of compound <b>135</b> .....	279
Figure A3.120	$^{13}\text{C}$ NMR (75 MHz, $\text{C}_6\text{D}_6$ ) of compound <b>135</b> .....	279
Figure A3.121	$^1\text{H}$ NMR (300 MHz, $\text{C}_6\text{D}_6$ ) of compound <b>138</b> .....	280
Figure A3.122	Infrared spectrum (thin film/ $\text{NaCl}$ ) of compound <b>138</b> .....	281
Figure A3.123	$^{13}\text{C}$ NMR (75 MHz, $\text{C}_6\text{D}_6$ ) of compound <b>138</b> .....	281
Figure A3.124	$^1\text{H}$ NMR (300 MHz, $\text{CDCl}_3$ ) of compound <b>137</b> .....	282
Figure A3.125	Infrared spectrum (thin film/ $\text{NaCl}$ ) of compound <b>137</b> .....	283
Figure A3.126	$^{13}\text{C}$ NMR (75 MHz, $\text{CDCl}_3$ ) of compound <b>137</b> .....	283
Figure A3.127	$^1\text{H}$ NMR (300 MHz, $\text{CD}_3\text{OD}$ ) of compound <b>181</b> .....	284
Figure A3.128	$^1\text{H}$ NMR (300 MHz, $\text{CDCl}_3$ ) of compound <b>140</b> .....	285
Figure A3.129	Infrared spectrum (thin film/ $\text{NaCl}$ ) of compound <b>140</b> .....	286
Figure A3.130	$^{13}\text{C}$ NMR (75 MHz, $\text{CDCl}_3$ ) of compound <b>140</b> .....	286
Figure A3.131	$^1\text{H}$ NMR (300 MHz, $\text{CDCl}_3$ ) of compound <b>141</b> .....	287
Figure A3.132	Infrared spectrum (thin film/ $\text{NaCl}$ ) of compound <b>141</b> .....	288
Figure A3.133	$^{13}\text{C}$ NMR (125 MHz, $\text{CDCl}_3$ ) of compound <b>141</b> .....	288
Figure A3.134	$^1\text{H}$ NMR (300 MHz, $\text{CDCl}_3$ ) of compound <b>142</b> .....	289
Figure A3.135	Infrared spectrum (thin film/ $\text{NaCl}$ ) of compound <b>142</b> .....	290
Figure A3.136	$^{13}\text{C}$ NMR (75 MHz, $\text{CDCl}_3$ ) of compound <b>142</b> .....	290
Figure A3.137	$^1\text{H}$ NMR (300 MHz, $\text{CDCl}_3$ ) of compound <b>143</b> .....	291
Figure A3.138	Infrared spectrum (thin film/ $\text{NaCl}$ ) of compound <b>143</b> .....	292
Figure A3.139	$^{13}\text{C}$ NMR (75 MHz, $\text{CDCl}_3$ ) of compound <b>143</b> .....	292
Figure A3.140	$^1\text{H}$ NMR (300 MHz, $\text{CDCl}_3$ ) of compound <b>144</b> .....	293
Figure A3.141	Infrared spectrum (thin film/ $\text{NaCl}$ ) of compound <b>144</b> .....	294

Figure A3.142	$^{13}\text{C}$ NMR (75 MHz, $\text{CDCl}_3$ ) of compound <b>144</b> .....	294
Figure A3.143	$^1\text{H}$ NMR (300 MHz, $\text{CDCl}_3$ ) of compound <b>145</b> .....	295
Figure A3.144	Infrared spectrum (thin film/ $\text{NaCl}$ ) of compound <b>145</b> .....	296
Figure A3.145	$^{13}\text{C}$ NMR (75 MHz, $\text{CDCl}_3$ ) of compound <b>145</b> .....	296
Figure A3.146	$^1\text{H}$ NMR (300 MHz, $\text{C}_6\text{D}_6$ ) of compound <b>146</b> .....	297
Figure A3.147	Infrared spectrum (thin film/ $\text{NaCl}$ ) of compound <b>146</b> .....	298
Figure A3.148	$^{13}\text{C}$ NMR (75 MHz, $\text{C}_6\text{D}_6$ ) of compound <b>146</b> .....	298
Figure A3.149	$^1\text{H}$ NMR (300 MHz, $\text{C}_6\text{D}_6$ ) of compound <b>147</b> .....	299
Figure A3.150	Infrared spectrum (thin film/ $\text{NaCl}$ ) of compound <b>147</b> .....	300
Figure A3.151	$^{13}\text{C}$ NMR (75 MHz, $\text{C}_6\text{D}_6$ ) of compound <b>147</b> .....	300
Figure A3.152	$^1\text{H}$ NMR (300 MHz, $\text{C}_6\text{D}_6$ ) of compound <b>148</b> .....	301
Figure A3.153	Infrared spectrum (thin film/ $\text{NaCl}$ ) of compound <b>148</b> .....	302
Figure A3.154	$^{13}\text{C}$ NMR (75 MHz, $\text{C}_6\text{D}_6$ ) of compound <b>148</b> .....	302
Figure A3.155	$^1\text{H}$ NMR (300 MHz, $\text{C}_6\text{D}_6$ ) of compound <b>149</b> .....	303
Figure A3.156	Infrared spectrum (thin film/ $\text{NaCl}$ ) of compound <b>149</b> .....	304
Figure A3.157	$^{13}\text{C}$ NMR (75 MHz, $\text{C}_6\text{D}_6$ ) of compound <b>149</b> .....	304
Figure A3.158	$^1\text{H}$ NMR (300 MHz, $\text{C}_6\text{D}_6$ ) of compound <b>150</b> .....	305
Figure A3.159	Infrared spectrum (thin film/ $\text{NaCl}$ ) of compound <b>150</b> .....	306
Figure A3.160	$^{13}\text{C}$ NMR (75 MHz, $\text{C}_6\text{D}_6$ ) of compound <b>150</b> .....	306
Figure A3.161	$^1\text{H}$ NMR (300 MHz, $\text{C}_6\text{D}_6$ ) of compound <b>151</b> .....	307
Figure A3.162	Infrared spectrum (thin film/ $\text{NaCl}$ ) of compound <b>151</b> .....	308
Figure A3.163	$^{13}\text{C}$ NMR (75 MHz, $\text{C}_6\text{D}_6$ ) of compound <b>151</b> .....	308
Figure A3.164	$^1\text{H}$ NMR (300 MHz, $\text{CDCl}_3$ ) of compound <b>152</b> .....	309
Figure A3.165	Infrared spectrum (thin film/ $\text{NaCl}$ ) of compound <b>152</b> .....	310
Figure A3.166	$^{13}\text{C}$ NMR (75 MHz, $\text{CDCl}_3$ ) of compound <b>152</b> .....	310
Figure A3.167	$^1\text{H}$ NMR (300 MHz, $\text{CDCl}_3$ ) of compound <b>153</b> .....	311
Figure A3.168	$^1\text{H}$ NMR (300 MHz, $\text{C}_6\text{D}_6$ ) of compound <b>153</b> .....	312
Figure A3.169	Infrared spectrum (thin film/ $\text{NaCl}$ ) of compound <b>153</b> .....	313
Figure A3.170	$^{13}\text{C}$ NMR (75 MHz, $\text{C}_6\text{D}_6$ ) of compound <b>153</b> .....	313
Figure A3.171	$^1\text{H}$ NMR (300 MHz, $\text{C}_6\text{D}_6$ ) of compound <b>128</b> .....	314
Figure A3.172	Infrared spectrum (thin film/ $\text{NaCl}$ ) of compound <b>128</b> .....	315

Figure A3.173	$^{13}\text{C}$ NMR (75 MHz, $\text{C}_6\text{D}_6$ ) of compound <b>128</b> .....	315
Figure A3.174	$^1\text{H}$ NMR (300 MHz, $\text{C}_6\text{D}_6$ ) of compound <b>156</b> .....	316
Figure A3.175	Infrared spectrum (thin film/ $\text{NaCl}$ ) of compound <b>156</b> .....	317
Figure A3.176	$^{13}\text{C}$ NMR (75 MHz, $\text{C}_6\text{D}_6$ ) of compound <b>156</b> .....	317
Figure A3.177	$^1\text{H}$ NMR (300 MHz, $\text{C}_6\text{D}_6$ ) of compound <b>157</b> .....	318
Figure A3.178	Infrared spectrum (thin film/ $\text{NaCl}$ ) of compound <b>157</b> .....	319
Figure A3.179	$^{13}\text{C}$ NMR (75 MHz, $\text{C}_6\text{D}_6$ ) of compound <b>157</b> .....	319
Figure A3.180	$^1\text{H}$ NMR (300 MHz, $\text{C}_6\text{D}_6$ ) of compound <b>158</b> .....	320
Figure A3.181	Infrared spectrum (thin film/ $\text{NaCl}$ ) of compound <b>158</b> .....	321
Figure A3.182	$^{13}\text{C}$ NMR (75 MHz, $\text{C}_6\text{D}_6$ ) of compound <b>158</b> .....	321
Figure A3.183	$^1\text{H}$ NMR (300 MHz, $\text{C}_6\text{D}_6$ ) of compound <b>159</b> .....	322
Figure A3.184	Infrared spectrum (thin film/ $\text{NaCl}$ ) of compound <b>159</b> .....	323
Figure A3.185	$^{13}\text{C}$ NMR (75 MHz, $\text{C}_6\text{D}_6$ ) of compound <b>159</b> .....	323
Figure A3.186	$^1\text{H}$ NMR (300 MHz, $\text{C}_6\text{D}_6$ ) of compound <b>160</b> .....	324
Figure A3.187	Infrared spectrum (thin film/ $\text{NaCl}$ ) of compound <b>160</b> .....	325
Figure A3.188	$^{13}\text{C}$ NMR (125 MHz, $\text{C}_6\text{D}_6$ ) of compound <b>160</b> .....	325
Figure A3.189	$^1\text{H}$ NMR (300 MHz, $\text{C}_6\text{D}_6$ ) of compound <b>161</b> .....	326
Figure A3.190	Infrared spectrum (thin film/ $\text{NaCl}$ ) of compound <b>161</b> .....	327
Figure A3.191	$^{13}\text{C}$ NMR (125 MHz, $\text{C}_6\text{D}_6$ ) of compound <b>161</b> .....	327
Figure A3.192	$^1\text{H}$ NMR (300 MHz, $\text{C}_6\text{D}_6$ ) of compound <b>187</b> .....	328
Figure A3.193	Infrared spectrum (thin film/ $\text{NaCl}$ ) of compound <b>187</b> .....	329
Figure A3.194	$^{13}\text{C}$ NMR (75 MHz, $\text{C}_6\text{D}_6$ ) of compound <b>187</b> .....	329
Figure A3.195	$^1\text{H}$ NMR (300 MHz, $\text{C}_6\text{D}_6$ ) of compound <b>162</b> .....	330
Figure A3.196	Infrared spectrum (thin film/ $\text{NaCl}$ ) of compound <b>162</b> .....	331
Figure A3.197	$^{13}\text{C}$ NMR (125 MHz, $\text{C}_6\text{D}_6$ ) of compound <b>162</b> .....	331
Figure A3.198	$^1\text{H}$ NMR (300 MHz, $\text{C}_6\text{D}_6$ ) of compound <b>163</b> .....	332
Figure A3.199	Infrared spectrum (thin film/ $\text{NaCl}$ ) of compound <b>163</b> .....	333
Figure A3.200	$^{13}\text{C}$ NMR (125 MHz, $\text{C}_6\text{D}_6$ ) of compound <b>163</b> .....	333
Figure A3.201	$^1\text{H}$ NMR (600 MHz, $\text{CD}_3\text{OD}$ ) of (–)-dragmacidin F ( <b>84</b> ) .....	334

## CHAPTER FOUR

Figure 4.1.1	The two-stage M1/M2 model of senescence .....	336
Figure 4.1.2	Telomestatin, G-quartet, and G-quadruplex structures .....	337

## APPENDIX FOUR

Figure A4.1	$^1\text{H}$ NMR (300 MHz, $\text{CDCl}_3$ ) of compound <b>219</b> .....	386
Figure A4.2	Infrared spectrum (thin film/ $\text{NaCl}$ ) of compound <b>219</b> .....	387
Figure A4.3	$^{13}\text{C}$ NMR (75 MHz, $\text{CDCl}_3$ ) of compound <b>219</b> .....	387
Figure A4.4	$^1\text{H}$ NMR (300 MHz, $\text{DMSO}-d_6$ ) of compound <b>220</b> .....	388
Figure A4.5	Infrared spectrum (KBr pellet) of compound <b>220</b> .....	389
Figure A4.6	$^{13}\text{C}$ NMR (75 MHz, $\text{DMSO}-d_6$ ) of compound <b>220</b> .....	389
Figure A4.7	$^1\text{H}$ NMR (300 MHz, $\text{CDCl}_3$ ) of compound <b>214</b> .....	390
Figure A4.8	Infrared spectrum (thin film/ $\text{NaCl}$ ) of compound <b>214</b> .....	391
Figure A4.9	$^{13}\text{C}$ NMR (75 MHz, $\text{CDCl}_3$ ) of compound <b>214</b> .....	391
Figure A4.10	$^1\text{H}$ NMR (300 MHz, $\text{DMSO}-d_6$ ) of compound <b>247</b> .....	392
Figure A4.11	Infrared spectrum (KBr pellet) of compound <b>247</b> .....	393
Figure A4.12	$^{13}\text{C}$ NMR (75 MHz, $\text{DMSO}-d_6$ ) of compound <b>247</b> .....	393
Figure A4.13	$^1\text{H}$ NMR (300 MHz, $\text{DMSO}-d_6$ ) of compound <b>224</b> .....	394
Figure A4.14	Infrared spectrum (thin film/ $\text{NaCl}$ ) of compound <b>224</b> .....	395
Figure A4.15	$^{13}\text{C}$ NMR (125 MHz, $\text{DMSO}-d_6$ ) of compound <b>224</b> .....	395
Figure A4.16	$^1\text{H}$ NMR (300 MHz, $\text{DMSO}-d_6$ ) of compound <b>225</b> .....	396
Figure A4.17	Infrared spectrum (thin film/ $\text{NaCl}$ ) of compound <b>225</b> .....	397
Figure A4.18	$^{13}\text{C}$ NMR (75 MHz, $\text{DMSO}-d_6$ ) of compound <b>225</b> .....	397
Figure A4.19	$^1\text{H}$ NMR (300 MHz, $\text{CDCl}_3$ ) of compound <b>226</b> .....	398
Figure A4.20	Infrared spectrum (thin film/ $\text{NaCl}$ ) of compound <b>226</b> .....	399
Figure A4.21	$^{13}\text{C}$ NMR (75 MHz, $\text{CDCl}_3$ ) of compound <b>226</b> .....	399
Figure A4.22	$^1\text{H}$ NMR (300 MHz, $\text{CDCl}_3$ ) of compound <b>227</b> .....	400
Figure A4.23	Infrared spectrum (thin film/ $\text{NaCl}$ ) of compound <b>227</b> .....	401
Figure A4.24	$^{13}\text{C}$ NMR (75 MHz, $\text{CDCl}_3$ ) of compound <b>227</b> .....	401
Figure A4.25	$^1\text{H}$ NMR (300 MHz, $\text{DMSO}-d_6$ ) of compound <b>228</b> .....	402

Figure A4.26	Infrared spectrum (KBr pellet) of compound <b>228</b> .....	403
Figure A4.27	$^{13}\text{C}$ NMR (75 MHz, $\text{DMSO}-d_6$ ) of compound <b>228</b> .....	403
Figure A4.28	$^1\text{H}$ NMR (300 MHz, $\text{DMSO}-d_6$ ) of compound <b>230</b> .....	404
Figure A4.29	Infrared spectrum (thin film/ $\text{NaCl}$ ) of compound <b>230</b> .....	405
Figure A4.30	$^{13}\text{C}$ NMR (75 MHz, $\text{DMSO}-d_6$ ) of compound <b>230</b> .....	405
Figure A4.31	$^1\text{H}$ NMR (300 MHz, $\text{CDCl}_3$ ) of compound <b>232</b> .....	406
Figure A4.32	Infrared spectrum (thin film/ $\text{NaCl}$ ) of compound <b>232</b> .....	407
Figure A4.33	$^{13}\text{C}$ NMR (75 MHz, $\text{CDCl}_3$ ) of compound <b>232</b> .....	407
Figure A4.34	$^1\text{H}$ NMR (300 MHz, $\text{CDCl}_3$ ) of compound <b>233</b> .....	408
Figure A4.35	Infrared spectrum (thin film/ $\text{NaCl}$ ) of compound <b>233</b> .....	409
Figure A4.36	$^{13}\text{C}$ NMR (75 MHz, $\text{CDCl}_3$ ) of compound <b>233</b> .....	409
Figure A4.37	$^1\text{H}$ NMR (500 MHz, $\text{C}_6\text{D}_6$ , 70 °C) of compound <b>235</b> .....	410
Figure A4.38	Infrared spectrum (thin film/ $\text{NaCl}$ ) of compound <b>235</b> .....	411
Figure A4.39	$^{13}\text{C}$ NMR (125 MHz, $\text{CDCl}_3$ ) of compound <b>235</b> .....	411
Figure A4.40	$^1\text{H}$ NMR (500 MHz, $\text{CDCl}_3$ , 50 °C) of compound <b>236</b> .....	412
Figure A4.41	Infrared spectrum (thin film/ $\text{NaCl}$ ) of compound <b>236</b> .....	413
Figure A4.42	$^{13}\text{C}$ NMR (125 MHz, $\text{CDCl}_3$ ) of compound <b>236</b> .....	413
Figure A4.43	$^1\text{H}$ NMR (500 MHz, $\text{CDCl}_3$ , 50 °C) of compound <b>238</b> .....	414
Figure A4.44	Infrared spectrum (thin film/ $\text{NaCl}$ ) of compound <b>238</b> .....	415
Figure A4.45	$^{13}\text{C}$ NMR (75 MHz, $\text{CDCl}_3$ ) of compound <b>238</b> .....	415
Figure A4.46	$^1\text{H}$ NMR (500 MHz, $\text{CDCl}_3$ ) of compound <b>215</b> .....	416
Figure A4.47	Infrared spectrum (thin film/ $\text{NaCl}$ ) of compound <b>215</b> .....	417
Figure A4.48	$^{13}\text{C}$ NMR (75 MHz, $\text{CDCl}_3$ ) of compound <b>215</b> .....	417

## APPENDIX FIVE

Figure A5.1.1	Iodobisoxazole triflate <b>226</b> with 50% probability ellipsoids .....	419
Figure A5.1.2	Molecule A .....	422
Figure A5.1.3	Molecule B .....	422
Figure A5.1.4	Overlap of molecule A and B emphasizing the torsion angle around the C(6)-O(3) bond .....	423



Figure A5.1.5	Overlap of molecule A and B emphasizing the torsion angle around the O(3)-S bond .....	424
Figure A5.1.6	Packing in the unit cell with the I(1)-N(1B) interaction emphasized.....	425
Figure A5.1.7	Stereo view of the packing in the unit cell with the I(1)-N(1B) interaction emphasized .....	425

## LIST OF SCHEMES

### CHAPTER ONE

Scheme 1.1.1	Examples of well-known Pd-mediated transformations .....	2
Scheme 1.2.1	Representative Pd(0) catalytic cycle .....	5
Scheme 1.2.2	Pd(0) catalysis in Fukuyama's synthesis of (–)-strychnine.....	6
Scheme 1.2.3	Representative Pd(II) catalytic cycle .....	8
Scheme 1.2.4	Pd(II) catalysis in Tietze's synthesis of vitamin E .....	9

### CHAPTER TWO

Scheme 2.1.1	Oxidative kinetic resolution of racemic secondary alcohols.....	15
Scheme 2.1.2	Pd-catalyzed aerobic heterocyclizations and carbocyclizations.....	15
Scheme 2.1.3	Mechanism of the Pd-catalyzed oxidative kinetic resolution.....	18
Scheme 2.2.1	Recycling and functionalization in the Prozac <sup>®</sup> series .....	21
Scheme 2.2.2	Recycling and functionalization in the Singulair <sup>®</sup> series .....	22

### CHAPTER THREE

Scheme 3.1.1	Dragmacidin D ( <b>82</b> ) as the proposed biosynthetic precursor to dragmacidins E and F ( <b>83</b> and <b>84</b> ).....	64
Scheme 3.1.2	Synthetic summary for dragmacidin D ( <b>82</b> ) .....	65
Scheme 3.1.3	Retrosynthetic analysis of dragmacidin F ( <b>84</b> ).....	67
Scheme 3.2.1	Functionalization of quinic acid and $\pi$ -allyl reduction studies .....	69
Scheme 3.2.2	Reductive isomerization of lactone <b>95</b> .....	70
Scheme 3.2.3	Synthesis of cyclization substrates <b>91</b> and <b>92</b> .....	70
Scheme 3.2.4	Intramolecular Heck reaction of <b>91</b> .....	71
Scheme 3.2.5	Related precedent for the Pd(II) oxidative carbocyclization strategy to form <b>90</b> .....	72
Scheme 3.2.6	Comparison between DMSO and ethyl nicotinate conditions in the indole cyclization.....	75

Scheme 3.2.7	Catalysis in the Pd(II) oxidative cyclization of acetate <b>107</b> .....	76
Scheme 3.2.8	Comparison between oxidative and classical Heck cyclizations in the preparation of <b>90</b> .....	79
Scheme 3.2.9	Synthesis of the carbon scaffold of dragmacidin F ( <b>84</b> ).....	80
Scheme 3.2.10	Synthesis of ketone <b>119</b> .....	81
Scheme 3.2.11	Neber rearrangement to prepare amino ketone <b>121</b> .....	82
Scheme 3.2.12	Detailed mechanism of Neber rearrangement .....	83
Scheme 3.2.13	Completion of the total synthesis of (+)-dragmacidin F ( <b>84</b> ).....	84
Scheme 3.4.1	An enantiodivergent strategy from quinic acid ( <b>93</b> ) to access (+)- and (–)-dragmacidin F ( <b>84</b> ) .....	86
Scheme 3.4.2	Critical results from reductive isomerization studies .....	88
Scheme 3.4.3	Synthesis and reductive isomerization of carbonate <b>131</b> .....	90
Scheme 3.4.4	Mechanism of reductive isomerization: Deuterium-labeling studies.....	91
Scheme 3.4.5	Mechanism of reductive isomerization: Tandem hydrogenation/elimination studies.....	91
Scheme 3.4.6	Mechanism of reductive isomerization: $\pi$ -allyl studies.....	92
Scheme 3.4.7	Mechanism of reductive isomerization: Single electron transfer studies.....	93
Scheme 3.4.8	Pd(II) oxidative cyclization of <b>127</b> .....	97
Scheme 3.4.9	Completion of the total synthesis of (–)-dragmacidin F ( <b>84</b> ).....	100

## APPENDIX TWO

Scheme A2.1	The synthesis of boronic ester <b>89</b> .....	195
Scheme A2.2	The synthesis of (+)-dragmacidin F ( <b>84</b> ) .....	196
Scheme A2.3	The synthesis of (–)-dragmacidin F ( <b>84</b> ).....	197

## CHAPTER FOUR

Scheme 4.1.1	Proposed biosynthesis of telomestatin ( <b>189</b> ) .....	339
Scheme 4.1.2	Peptide-bond formation-cyclization-oxidation sequence .....	340
Scheme 4.1.3	Taiho Pharmaceutical total synthesis of telomestatin ( <b>189</b> ).....	341
Scheme 4.1.4	Doi and Takahashi total synthesis of telomestatin ( <b>189</b> ).....	342
Scheme 4.1.5	Retrosynthetic analysis of telomestatin ( <b>189</b> ).....	344
Scheme 4.2.1	Synthesis of left-hand trisoxazole iodo acid <b>211</b> .....	345
Scheme 4.2.2	Synthesis and X-ray characterization of <b>222</b> .....	346
Scheme 4.2.3	Synthesis of methylbisoxazole ester <b>233</b> .....	347
Scheme 4.2.4	Synthesis of methyloxazole triflate <b>240</b> .....	348
Scheme 4.2.5	Synthesis of right-hand tetrakisoxazole amino alcohol <b>212</b> .....	349
Scheme 4.2.6	Late stage and proposed endgame.....	350

## LIST OF TABLES

### CHAPTER TWO

Table 2.1.1	Original Pd-catalyzed oxidative kinetic resolution.....	16
Table 2.1.2	Rate-accelerated Pd-catalyzed oxidative kinetic resolution .....	17
Table 2.2.1	Chloroform-based Pd-catalyzed oxidation kinetic resolution.....	21
Table 2.4.1	Methods for determination of enantiomeric excess.....	25
Table 2.4.2	Methods for determination of % conversion .....	25
Table 2.4.3	Optical rotations of oxidative kinetic resolution substrates .....	26

### CHAPTER THREE

Table 3.2.1	Optimization of Pd(II) oxidative carbocyclization .....	73
Table 3.2.2	Pd(II) oxidative carbocyclization substrate scope .....	77
Table 3.4.1	Reductive isomerization of allylic lactones and carbonates.....	94
Table 3.4.2	Pd(II) oxidative carbocyclization substrate scope in the (-)- <i>nat</i> -dragmacidin F series .....	98

### APPENDIX FIVE

Table A5.1.1	Crystal data and structure refinement for <b>226</b> (CCDC 282586) ....	420
Table A5.1.2	Atomic coordinates ( $\times 10^4$ ) and equivalent isotropic displacement parameters ( $\text{\AA}^2 \times 10^3$ ) for <b>226</b> (CCDC 282586). ....	426
Table A5.1.3	Bond lengths [ $\text{\AA}$ ] and angles [ $^\circ$ ] for <b>226</b> (CCDC 282586).....	427
Table A5.1.4	Anisotropic displacement parameters ( $\text{\AA}^2 \times 10^4$ ) for <b>226</b> (CCDC 282586) .....	430
Table A5.1.5	Hydrogen coordinates ( $\times 10^4$ ) and isotropic displacement parameters ( $\text{\AA}^2 \times 10^3$ ) for <b>226</b> (CCDC 282586) .....	431
Table A5.1.6	Torsion angles [ $^\circ$ ] for <b>226</b> (CCDC 282586) .....	432
Table A5.1.7	CH $\cdots$ N hydrogen bonds for <b>226</b> (CCDC 282586) [ $\text{\AA}$ and $^\circ$ ] .....	433

## APPENDIX SIX

Table A6.1	Compounds appearing in Chapter 2.....	435
Table A6.2	Compounds appearing in Chapter 3.....	436
Table A6.3	Compounds appearing in Chapter 4.....	439

## LIST OF ABBREVIATIONS

Å	Ångstrom
$[\alpha]_D$	specific rotation at wavelength of sodium D line
Ac	acetyl, acetate
app.	apparent
aq.	aqueous
Ar	aryl
atm	atmosphere
Bn	benzyl
Boc	<i>tert</i> -butoxycarbonyl
BOXAX	2,2'-Bis(oxazolyl)-1,1'-binaphthyl
bp	boiling point
BQ	benzoquinone
br	broad
Bu	butyl
<i>n</i> -Bu	butyl
<i>t</i> -Bu	<i>tert</i> -Butyl
<i>c</i>	concentration for specific rotation measurements
°C	degrees Celsius
calc'd	calculated
cat.	catalytic
Cbz	carbobenzyloxy
CCDC	Cambridge Crystallographic Data Centre
CDI	1,1'-carbonyldiimidazole
CI	chemical ionization

comp.	complex
Cy	cyclohexyl
d	doublet
DBU	1,8-diazabicyclo[5.4.0]undec-7-ene
DCE	dichloroethane
dba	dibenzylideneacetone
dec.	decomposition
dppb	1,4-bis(diphenylphosphino)butane
dppf	1,1'-bis(diphenylphosphino)ferrocene
DMA	<i>N,N</i> -dimethylacetamide
DMAP	4-dimethylaminopyridine
DMF	<i>N,N</i> -dimethylformamide
DMSO	dimethyl sulfoxide
DNA	(deoxy)ribonucleic acid
dr	diastereomeric ratio
EC <sub>50</sub>	median effective concentration (50%)
EDC	<i>N</i> -(3-dimethylaminopropyl)- <i>N'</i> -ethylcarbodiimide
ee	enantiomeric excess
EI	electron impact
equiv	equivalent
ESI	electrospray ionization
Et	ethyl
FAB	fast atom bombardment
g	gram(s)
GC	gas chromatography
gCOSY	gradient-selected correlation spectroscopy
h	hour(s)



HIV	human immunodeficiency virus
HMDS	1,1,1,3,3,3-hexamethyldisilazane
HOBt	1-hydroxybenzotriazole
HPLC	high performance liquid chromatography
HRMS	high resolution mass spectroscopy
HSV	herpes simplex virus
$h\nu$	light
Hz	hertz
IC <sub>50</sub>	median inhibition concentration (50%)
IR	infrared (spectroscopy)
$J$	coupling constant
$\lambda$	wavelength
L	liter
m	multiplet or milli
$m$	meta
$m/z$	mass to charge ratio
$\mu$	micro
M	metal or molar
Me	methyl
MHz	megahertz
min	minute(s)
mol	mole(s)
mp	melting point
Ms	methanesulfonyl (mesyl)
MS	molecular sieves
n	nano
N	normal

nb	norbornadiene
NBS	<i>N</i> -bromosuccinimide
NMO	<i>N</i> -methylmorpholine <i>N</i> -oxide
NMR	nuclear magnetic resonance
NOE	nuclear Overhauser effect
NOESY	nuclear Overhauser enhancement spectroscopy
Nu	nucleophile
[O]	oxidation
<i>o</i>	ortho
<i>p</i>	para
PDC	pyridinium dichromate
Pin	pinacolato
Ph	phenyl
pH	hydrogen ion concentration in aqueous solution
PhH	benzene
ppm	parts per million
PPTs	pyridinium <i>p</i> -toluenesulfonate
Pr	propyl
<i>i</i> -Pr	isopropyl
Py	pyridine
q	quartet
ref	reference
R <sub>f</sub>	retention factor
rt	room temperature
s	singlet or strong or selectivity factor
sat.	saturated
SEM	(trimethylsilyl)ethoxymethyl

SET	single electron transfer
sp	species or (–)-sparteine
t	triplet
TBAF	tetrabutylammonium fluoride
TBHP	<i>tert</i> -butyl hydroperoxide
TBS	<i>tert</i> -butyldimethylsilyl
TCNE	tetracyanoethylene
Tf	trifluoromethanesulfonyl (trifyl)
TFA	trifluoroacetic acid
TFE	2,2,2-trifluoroethanol
THF	tetrahydrofuran
TIPS	triisopropylsilyl
TLC	thin-layer chromatography
TMS	trimethylsilyl
TON	turnover number
Tr	trityl
Ts	<i>p</i> -toluenesulfonyl (tosyl)
UV	ultraviolet
w	weak
w/v	weight to volume
v/v	volume to volume
X	anionic ligand or halide

## CHAPTER ONE

### Palladium in Organic Synthesis

#### 1.1 Background

##### 1.1.1 Introduction

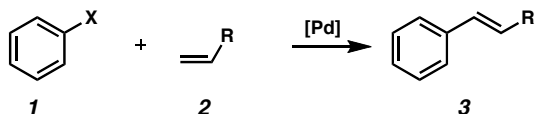
Palladium (Pd), named after the asteroid Pallas, is arguably the most versatile and ubiquitous metal in modern organic synthesis.<sup>1,2</sup> Palladium-mediated processes have become essential tools, spanning countless applications in the syntheses of natural products, polymers, agrochemicals, and pharmaceuticals. In part, this far-reaching scope is due to palladium's ability to participate in catalytic transformations, as well as its high functional group tolerance. Nearly every area of organic synthesis has been impacted by this versatile transition metal, which has fundamentally changed the way retrosynthetic analysis is approached.

Palladium can be used to conduct myriad transformations with organic molecules. In fact, there are a number of well-known name reactions that feature this metal, including the Heck, Suzuki, Stille, and Buchwald-Hartwig cross-couplings; the Wacker process;<sup>3</sup> and the Tsuji-Trost allylation (Scheme 1.1.1).<sup>1,2</sup> In addition, Pd also enables hydrogenation; hydrogenolysis; carbonylation; the formation of C–C, C–O, C–N, and C–S bonds; cycloisomerization; and even pericyclic reactions.<sup>1,2</sup> Palladium-based methods often proceed under mild conditions affording high yields, with excellent levels of stereo-, regio-, and chemoselectivity. Domino catalysis, where multiple Pd-catalyzed

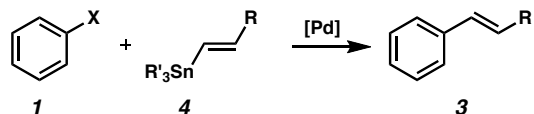
transformations are carried out in a single operation, is also a powerful extension of this chemistry.<sup>1u</sup>

### Scheme 1.1.1

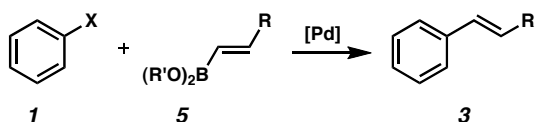
Heck



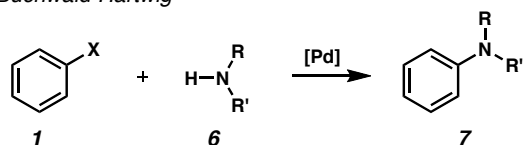
Stille



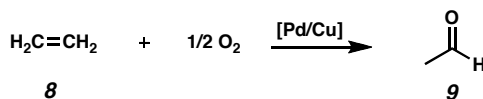
Suzuki



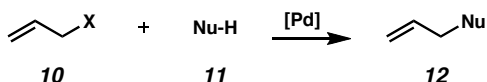
Buchwald-Hartwig



Wacker



Tsuji-Trost



## 1.2 Palladium(0) and Palladium(II)

### 1.2.1 Oxidation States of Palladium

Although palladium can exist in a number of different oxidation states, useful organic methods are dominated by the use of Pd(0) and Pd(II),<sup>1,2</sup> although the utility of Pd(IV)<sup>4</sup> has been steadily emerging in its own right. The remaining oxidation states have not, as of yet, found practical applications, and their observation remains rare.<sup>5</sup> The increased stability of the even-numbered oxidation states (e.g., 0, +2, +4) can be rationalized by the low tendency of palladium to undergo one-electron or radical processes; conversely, it readily participates in two-electron oxidation or reduction.<sup>2a</sup>

Palladium's ability to undergo facile and reversible two-electron operations has contributed to its widespread use as a catalyst, since each oxidation state can yield different chemistry (see Figure 1.2.1 for examples of reaction classes). Reactions such as cross-couplings and olefin hydrogenation are common to the Pd(0) platform, while transformations such as alcohol oxidation and cycloisomerization can be achieved using Pd(II).

*Figure 1.2.1*

***Types of Transformations***

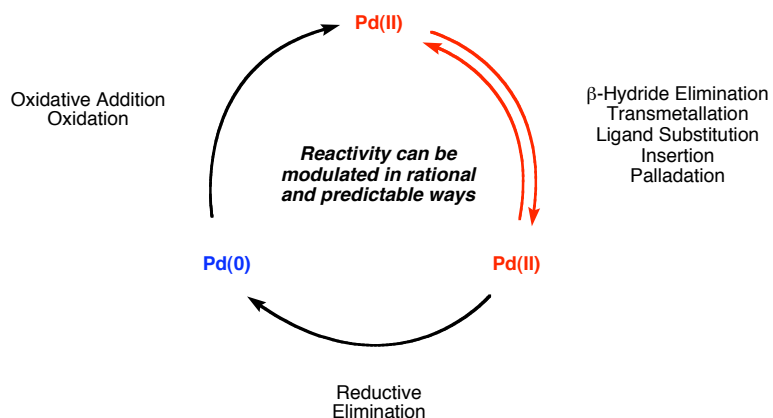
Pd <sup>0</sup>	Pd <sup>II</sup>
Cross-couplings	Wacker Process
Allylic Alkylation	Cycloisomerization
Hydrogenation	Alcohol Oxidation
Hydrogenolysis	Allylic Oxidation
Carbonylation	Allylic Rearrangements

### 1.2.2 General Reactivity

The bulk of the organopalladium literature is centered on the use of Pd(0) and Pd(II). Although many reports do not clearly delineate the active catalyst (e.g., Pd(II) precatalysts can be used to generate Pd(0) in situ), in general, palladium-catalyzed reactions proceed through the simplified cycle presented in Figure 1.2.2. Pd(0) can undergo either oxidation or oxidative addition, which affords a Pd(II) complex. Pd(II) complexes can generate new Pd(II) complexes via processes such as  $\beta$ -hydride elimination, transmetallation, ligand substitution, insertion, or palladation. Finally, reductive elimination converts the Pd(II) complex back to Pd(0). This mechanistic understanding, combined with the ability of ligands and reaction parameters to modulate

the reactivity of palladium, has allowed for a substantial amount of rational design in this field.

Figure 1.2.2



### 1.2.3 Palladium(0) Reactivity

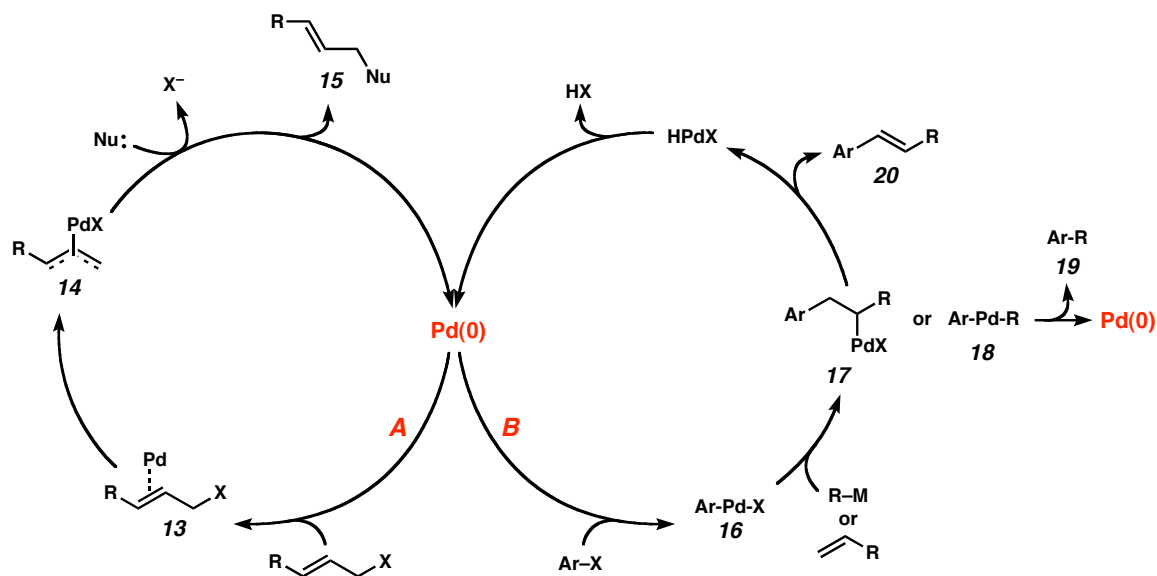
Palladium(0) catalysis has been the focal point of palladium research over the past several decades. A popular method of preparing Pd(0) complexes is via an in situ reduction of a Pd(II) species by reagents such as alkenes, alcohols, amines, phosphines, or metal hydrides. Considered to be nucleophilic, Pd(0) complexes contain a  $d^{10}$  palladium, and they are easily oxidized to the Pd(II) state; thus most of the catalytic processes using Pd(0) generally begin with oxidative addition. In general, increasing the electron density on palladium promotes oxidative addition.

One frequent mode of reactivity characteristic of Pd(0) involves the complexation of an olefin with an allylic leaving group, and subsequent oxidative addition (e.g., Pd(0)  $\rightarrow$  **13**  $\rightarrow$  **14**) to generate a Pd(II)  $\pi$ -allyl complex (**14**, Path A, Scheme 1.2.1). Subsequent

nucleophilic attack, which occurs predominately at the less-hindered carbon of the palladium  $\pi$ -allyl complex, affords the product (**15**) and regenerates the Pd(0) catalyst.

Another common reaction pathway for Pd(0) is regularly observed in cross-coupling chemistry. Specifically, oxidative addition to a molecular bond (e.g., Ar-X) forms an electrophilic Pd(II) complex (e.g., **16**, Path B). At this juncture, any number of Pd(II) reactions can take place, such as olefin insertion (**16**  $\rightarrow$  **17**) or transmetalation (**16**  $\rightarrow$  **18**). Pd(0) is eventually regenerated by a reductive elimination sequence;  $\beta$ -hydride elimination of **17** produces **20** and HPdX, which becomes Pd(0) and HX upon reductive elimination. Similarly, reductive elimination of **18** affords the product (**19**) and Pd(0) directly.

*Scheme 1.2.1*

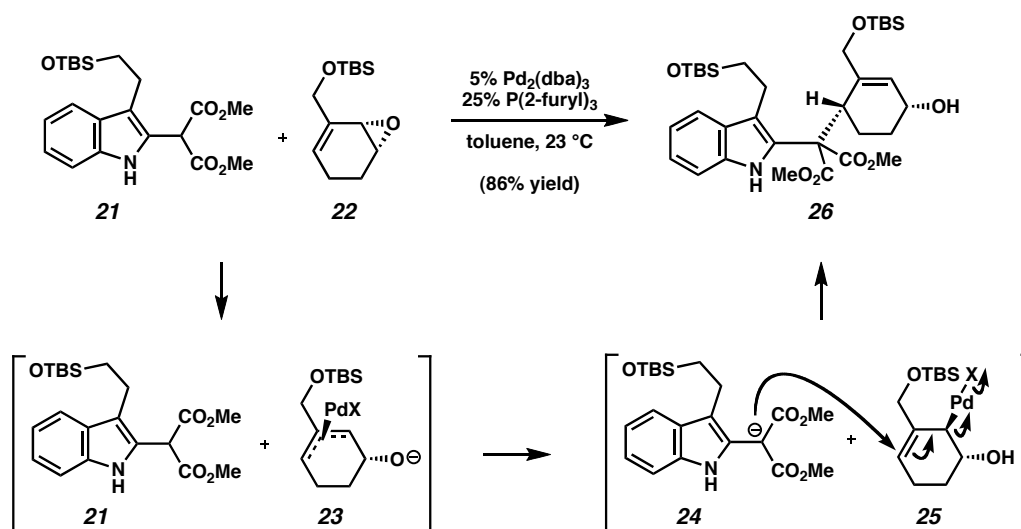


Fukuyama recently carried out a relevant example of Pd(0) catalysis in the early steps of his total synthesis of (–)-strychnine.<sup>6</sup> Indole malonate **21** and vinyl epoxide **22**



were treated with Pd(0) at room temperature (Scheme 1.2.2). Initial oxidative addition to the vinyl epoxide produced Pd(II)  $\pi$ -allyl complex **23**, and the resulting alkoxide was quenched by malonate **21** to form **24**. The malonate anion (**24**) then attacked the electrophilic palladium(II) complex (**25**) in a stereo- and regioselective manner to yield the product (**26**). This product is an intermediate in the synthesis of (–)-strychnine, and was subsequently carried forward to complete the total synthesis.

*Scheme 1.2.2*



#### 1.2.4 Palladium(II) Reactivity

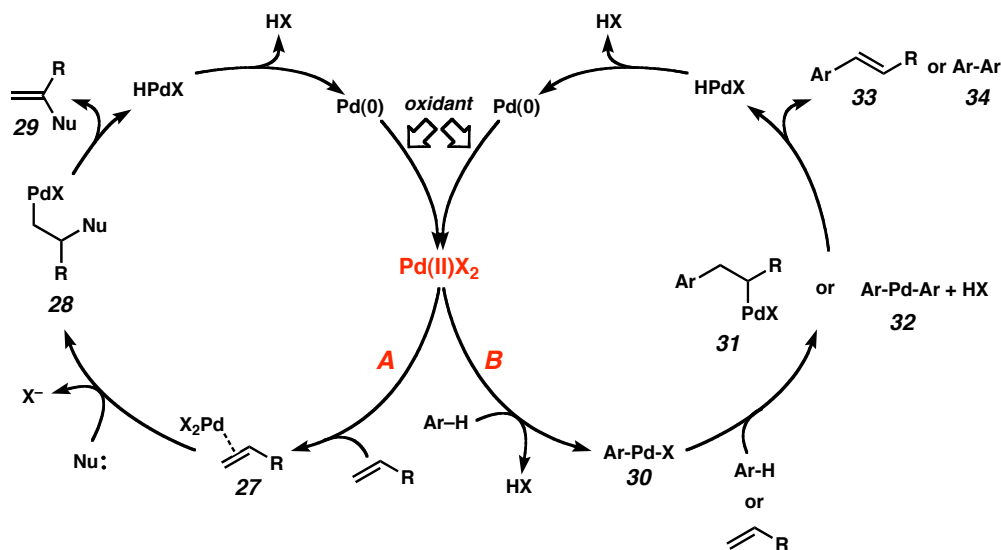
Palladium(II) catalysis, in contrast to palladium(0), has received significantly less attention from the synthetic community in the past, although there has been a revitalized interest within the last several years.<sup>1i-k</sup> Pd(II) complexes are typically electrophilic and air stable, and thus usually interact with electron-rich functionalities such as olefins, alkynes, and arenes. The lack of Pd(II) research may initially seem surprising, considering that Pd(II) also promotes useful modes of reactivity (see Figure 1.2.1).

However, one of the main complications that has been problematic in the development of Pd(II) methodology is the difficulty of reoxidizing  $\text{Pd}(0) \rightarrow \text{Pd}(\text{II})$ . Completion of the catalytic cycle to regenerate Pd(II) requires the presence of a stoichiometric oxidant, such as  $\text{CuCl}_2$ ,  $\text{Cu}(\text{OAc})_2$ , benzoquinone, *tert*-butyl hydroperoxide (TBHP),  $\text{MnO}_2$ ,  $\text{HNO}_3$ , and most recently  $\text{O}_2$ . Not unexpectedly, the addition of these oxidants to a reaction has often interfered with the catalyst/ligand system (or the substrates themselves), and has led to complications in maintaining chemo- or stereoselective processes.

A typical reaction with electrophilic Pd(II) commences with the complexation of an olefin by Pd(II) (**27**, Path A, Scheme 1.2.3). An intermolecular or intramolecular nucleophilic attack on the resulting olefin complex can then occur, generally at the more substituted position of the olefin (**28**, Path A—Wacker-type mechanism). Although any number of Pd(II) processes can occur at this stage (see Figure 1.2.2), the final product typically results from  $\beta$ -hydride elimination (e.g., **28**  $\rightarrow$  **29**). The resultant palladium hydride,  $\text{HPdX}$ , then undergoes a reductive elimination–oxidation sequence to regenerate the active Pd(II) catalyst.<sup>7</sup>

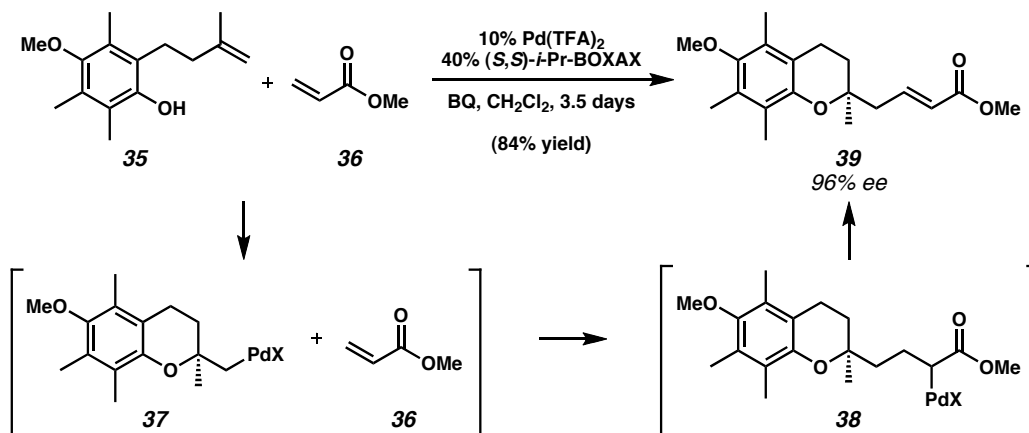
Alternatively, a pathway involving direct attack of the  $\text{Pd}(\text{II})\text{X}_2$  complex by a nucleophile (e.g., an arene) is also possible (**30**, Path B—Friedel-Crafts-type mechanism).<sup>8</sup> In a similar fashion, this complex (**30**) can then participate in traditional Pd(II) pathways such as a successive Friedel-Crafts type attack to form **31**, or olefin insertion to form **32**. Although different processes may be observed,  $\beta$ -hydride elimination and reductive elimination sequences are likely to be the final steps in the cycle prior to reoxidation of palladium.

Scheme 1.2.3



A recent report disclosed by Tietze pertaining to the synthesis of vitamin E highlights the synthetic utility of  $\text{Pd(II)}$ .<sup>9</sup> Tietze's synthetic route relied upon a critical cyclization event, in which phenol **35** and methyl acrylate (**36**) were exposed to a chiral  $\text{Pd(II)}$  salt where (*S,S*)-*i*-Pr-BOXAX served as the ligand (Scheme 1.2.4). Enantiofacial coordination of the palladium to the olefin of phenol **35**, followed by oxypalladation, results in the formation of the key tertiary stereogenic center, which then leaves palladium(II) intermediate **37** without an accessible  $\beta$ -hydride. Without a competing  $\beta$ -hydride elimination pathway, intermediate **37** is able to react further, and underwent a Heck coupling with methyl acrylate (**36**) to afford  $\text{Pd(II)}$  complex **38**. Restoration of the enoate through  $\beta$ -hydride elimination then generated the product (**39**), as well as a  $\text{Pd(II)}$  hydride,  $\text{X-Pd-H}$ . Reductive elimination to liberate  $\text{HX}$  then afforded a  $\text{Pd(0)}$  species, which could be reoxidized to  $\text{Pd(II)}$  using benzoquinone. The chroman product (**39**) obtained by Tietze was later elaborated to furnish vitamin E.

Scheme 1.2.4



### 1.3 Conclusion

In summary, both Pd(0) and Pd(II) have had, and continue to have, far-reaching impacts on organic synthesis. The versatile nature of palladium, in conjunction with the mechanistic understanding and predictive models that have been elucidated, has permitted a wealth of exploration into the seemingly endless potential of this metal. Additionally, deficiencies in the Pd(II) and Pd(IV) literature are likely to be remedied as greater control over the oxidation of palladium(0) is achieved.

## 1.4 Notes and References

- (1) (a) Beccalli, E. M.; Broggini, G.; Martinelli, M.; Sottocornola, S. *Chem. Rev.* **2007**, 107, 5318–5365. (b) Muzart, J. *J. Mol. Catal. A: Chem.* **2007**, 276, 62–72. (c) Zeni, G.; Larock, R. C. *Chem. Rev.* **2006**, 106, 4644–4680. (d) Buchwald, S. L.; Mauger, C.; Mignani, G.; Scholz, U. *Adv. Synth. Catal.* **2006**, 348, 23–39. (e) Cacchi, S.; Fabrizi, G. *Chem. Rev.* **2005**, 105, 2873–2920. (f) Zeni, G.; Larock, R. C. *Chem. Rev.* **2004**, 104, 2285–2309. (g) Muzart, J. *Tetrahedron* **2005**, 61, 5955–6008. (h) Muzart, J. *Tetrahedron* **2005**, 61, 9423–9463. (i) Stahl, S. S. *Angew. Chem., Int. Ed.* **2004**, 43, 3400–3420. (j) Sigman, M. S.; Schultz, M. J. *Org. Biomol. Chem.* **2004**, 2, 2551–2554. (k) Stoltz, B. M. *Chem. Lett.* **2004**, 33, 362–367. (l) Tietze, L. F.; Ila, H.; Bell, H. P. *Chem. Rev.* **2004**, 104, 3453–3516. (m) Nishimura, T.; Uemura, S. *Synlett* **2004**, 201–216. (n) Dounay, A. B.; Overman, L. E. *Chem. Rev.* **2003**, 103, 2945–2963. (o) Agrofoglio, L. A.; Gillaizeau, I.; Saito, Y. *Chem. Rev.* **2003**, 103, 1875–1916. (p) Negishi, E.-I.; Anastasia, L. *Chem. Rev.* **2003**, 103, 1979–2017. (q) Kiss, G. *Chem. Rev.* **2001**, 101, 3435–3456. (r) Beletskaya, I. P.; Cheprakov, A. V. *Chem. Rev.* **2000**, 100, 3009–3066. (s) Zimmer, R.; Dinesh, C. U.; Nandanan, E.; Khan, F. A. *Chem. Rev.* **2000**, 100, 3067–3125. (t) Amatore, C.; Jutand, A. *Acc. Chem. Res.* **2000**, 33, 314–321. (u) Poli, G.; Giambastiani, G.; Heumann, A. *Tetrahedron* **2000**, 56, 5959–5989. (v) Miyaura, N.; Suzuki, A. *Chem. Rev.* **1995**, 95, 2457–2483. (w) Tsuji, J. *Synthesis* **1990**, 739–749.

- (2) (a) *Handbook of Organopalladium Chemistry for Organic Synthesis*; Negishi, E., Ed.; Wiley-Interscience: New York, 2002. (b) Tsuji, J. *Palladium Reagents and Catalysts: Innovations in Organic Synthesis*; Wiley and Sons: New York, 1995. (c) Tsuji, J. *Palladium Reagents and Catalysts: New Perspectives for the 21st Century*; Wiley and Sons: New York, 2003. (d) *Palladium in Organic Synthesis*; Tsuji, J., Ed.; Springer: Berlin, 2005. (e) Heck, R. F. *Palladium Reagents in Organic Synthesis*; Academic Press: New York, 1985. (f) Li, J. J.; Gribble, G. W. *Palladium in Heterocyclic Chemistry*; Pergamon: New York, 2000. (g) Heumann, A.; Jens, K.-J.; Reglier, M. *Progress in Inorganic Chemistry*; Karlin, K. D., Ed.; Wiley and Sons: New York, 1994; Vol. 42, pp. 483–576.
- (3) For a recent review, see: Punniyamurthy, T.; Velusamy, S.; Iqbal, J. *Chem. Rev.* **2005**, *105*, 2329–2365 and references therein.
- (4) For recent examples of Pd(IV) transformations, see the following references and references therein: (a) Desai, L. V.; Sanford, M. S. *Angew. Chem., Int. Ed.* **2007**, *46*, 5737–5740. (b) Yu, J. Q.; Giri, R.; Chen, X. *Org. Biomol. Chem.* **2006**, *4*, 4041–4047. (c) Daugulis, O.; Zaitsev, V. G.; Shabasov, D.; Pham, O.-N.; Lazareva, A. *Synlett* **2006**, 3382–3388. (d) Bressy, C.; Alberico, D.; Lautens, M. *J. Am. Chem. Soc.* **2005**, *127*, 13148–13149.
- (5) For recent examples of Pd(I), see: (a) Escobar-Nuricumbo, J. J.; Campos-Alvarado, C.; Ríos-Moreno, G.; Morales-Morales, D.; Walsh, P. J.; Parra-Hake, M. *Inorg.*

- Chem.* **2007**, *46*, 6182–6189. (b) Stromnova, T. A.; Shishilov, O. N.; Dayneko, M. V.; Monakhov, K. Y.; Churakov, A. V.; Kuz'mina, L. G.; Howard, J. A. K. *J. Organomet. Chem.* **2006**, *691*, 3730–3736. For a review of Pd(I), see: (c) Temkin, O. N.; Bruk, L. G. *Russ. Chem. Rev.* **1983**, *52*, 117–137. For a example of Pd(III), see: (d) Cotton, F. A.; Koshevoy, I. O.; Lahuerta, P.; Murillo, C. A.; Sanaú, M.; Ubeda, M. A.; Zhao, Q. *J. Am. Chem. Soc.* **2006**, *128*, 13674–13675 and references therein. For a recent example of Pd(V), see: (e) Shimada, S.; Li, Y.-H.; Choe, Y.-K.; Tanaka, M.; Bao, M.; Uchimar, T. *Proc. Nat. Acad. Sci.* **2007**, *104*, 7758–7763. For a example of Pd(VI), see: (f) Crabtree, R. H. *Science* **2002**, *295*, 288–289. (g) Chen, W.; Shimada, S.; Tanaka, M. *Science* **2002**, *295*, 308–310.
- (6) Kaburagi, Y.; Tokuyama, T.; Fukuyama, T. *J. Am. Chem. Soc.* **2004**, *126*, 10246–10247.
- (7) The pathway for reoxidation of Pd may not necessarily proceed through Pd(0); rather, it may involve the direct insertion of O<sub>2</sub> into a Pd hydride. For recent discussions concerning the mechanistic details of Pd oxidation by molecular oxygen, see: (a) Gligorich, K. M.; Sigman, M. S. *Angew. Chem., Int. Ed.* **2006**, *45*, 6612–6615. (b) Popp, B. V.; Stahl, S. S. *J. Am. Chem. Soc.* **2007**, *129*, 4410–4422. (c) Chowdhury, S.; Rivalta, I.; Russo, N.; Sicilia, E. *Chem. Phys. Lett.* **2007**, *443*, 183–189. (d) Keith, J. M.; Goddard, W. A., III; Oxgaard, J. *J. Am. Chem. Soc.* **2007**, *129*, 10361–10369.

- (8) Pd(II) complexes such as **30** can also be generated via transmetallation (e.g.,  $\text{Pd(II)X}_2 + \text{Ar-M} \rightarrow \text{Ar-Pd-X} + \text{MX}$ ). For a recent example, see: Lindh, J.; Enquist, P.-A.; Pilotti, Å.; Nilsson, P.; Larhed, M. *J. Org. Chem.* **2007**, *72*, 7957–7962 and references therein.
- (9) (a) Tietze, L. F.; Sommer, K. M.; Zinngrebe, J.; Stecker, F. *Angew. Chem., Int. Ed.* **2005**, *44*, 257–259. For a recent synthetic application of a Pd(II) heterocyclization from our group, see: (b) Liu, Q.; Ferreira, E. M.; Stoltz, B. M. *J. Org. Chem.* **2007**, *72*, 7352–7358.



## CHAPTER TWO

### The Resolution of Important Pharmaceutical Building Blocks by Palladium-Catalyzed Aerobic Oxidation of Secondary Alcohols

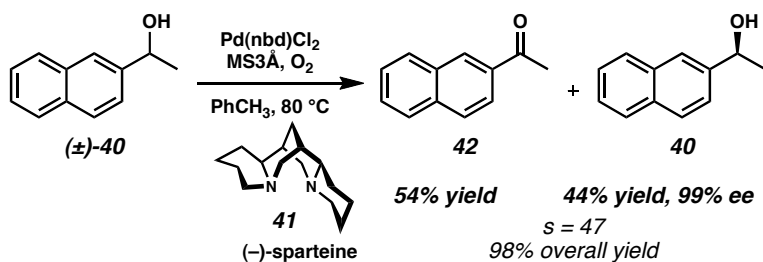
#### 2.1 Background

##### 2.1.1 Introduction

As part of a general program initiated in the area of asymmetric dehydrogenation chemistry, our laboratory recently reported the oxidative kinetic resolution of secondary alcohols. Our method employs a simple palladium dichloride catalyst precursor  $[\text{Pd}(\text{nbd})\text{Cl}_2]$  in conjunction with (–)-sparteine (**41**), which serves as both ligand and base, and molecular oxygen as the stoichiometric oxidant (Scheme 2.1.1).<sup>1,2,3</sup> In this resolution, one enantiomer of a secondary alcohol (e.g., (±)-**40**) is preferentially oxidized to the ketone (e.g., **42**), leaving behind the other, slower-reacting enantiomer of the alcohol (e.g., **40**). The relative reaction rates of each enantiomer, referred to as *selectivity* ( $k_{\text{rel}}$  or  $s$ ), can be computed from the enantiomeric excess of the alcohol at a given conversion.<sup>4</sup>

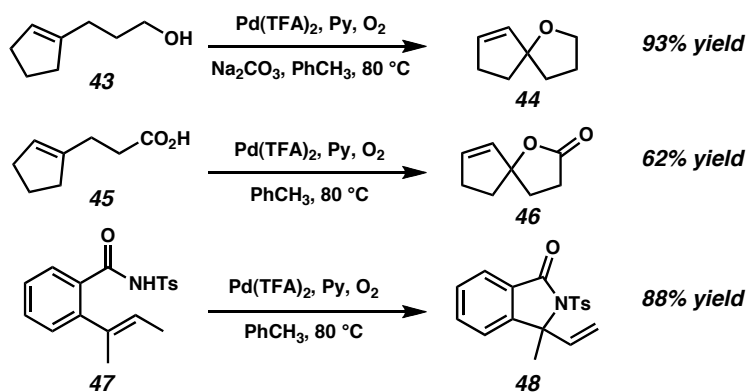
This palladium/sparteine system proved useful for the resolution of simple benzylic and allylic alcohols, as well as the desymmetrization of meso-diols, with selectivities ranging from 6.6–47.1 (Scheme 2.1.1).<sup>4</sup> Additionally, the use of dehydrogenative Pd(II) catalysis has been extended to oxidative cyclizations including both heterocyclizations and carbocyclizations (Scheme 2.1.2).<sup>5</sup>

Scheme 2.1.1

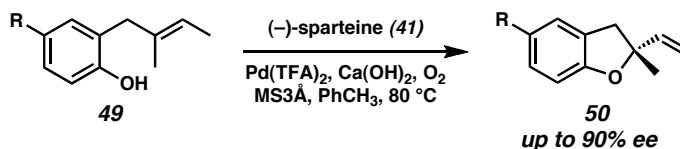


Scheme 2.1.2

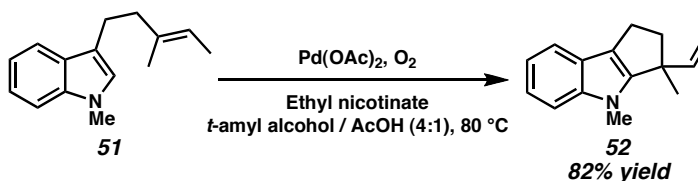
## Aerobic Heteroatom/Olefin Cyclizations



## Enantioselective Aerobic Heteroatom/Olefin Cyclizations



## Aerobic Carbocyclizations via C–H Bond Functionalization



Since the initial report,<sup>1a</sup> a number of conceptual improvements to the original oxidative kinetic resolution system have been made that allow a range of secondary alcohols (e.g., **40**) to be resolved with a variety of differing experimental procedures depending on the substrate.<sup>1b,1c</sup> A second method was developed employing  $\text{Cs}_2\text{CO}_3$  and *t*-

BuOH as additives, which provided generally higher selectivities and shorter reaction times under lower reaction temperatures (Table 2.1.1).<sup>1b</sup> Additionally, a third iteration of our reaction replaced toluene with chloroform, which enabled us to run these transformations at room temperature using ambient air as the stoichiometric oxidant (Table 2.1.2).<sup>1c</sup>

Table 2.1.1

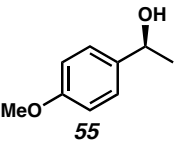
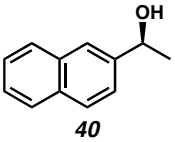
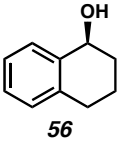
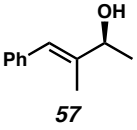
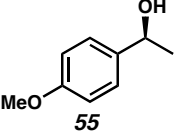
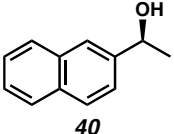
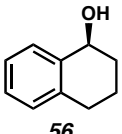
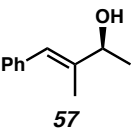
$  \begin{array}{c}  \text{Pd(nbd)Cl}_2 \text{ (5 mol \%)} \\  \text{(-)-sparteine (41, 12 mol \%)} \\  \text{MS3A, Cs}_2\text{CO}_3 \\  \text{O}_2 \text{ or air, CHCl}_3, 23^\circ\text{C}  \end{array}  \xrightarrow{\hspace{1cm}}  \begin{array}{c}  \text{R}^1\text{C(=O)R}^2 \\  \text{54}  \end{array}  +  \begin{array}{c}  \text{R}^1\text{CH(OH)R}^2 \\  \text{53}  \end{array}  $						
entry	unreacted alcohol, major enantiomer	O <sub>2</sub> source	time	conversion (%)	ee ROH (%)	s
1	 55	O <sub>2</sub>	48 h	62.6	99.9	27.1
		air	24 h	62.3	99.8	25.4
2	 40	O <sub>2</sub>	48 h	59.3	99.6	31.1
		air	24 h	55.5	98.0	37.3
3	 56	O <sub>2</sub>	24 h	57.5	98.0	27.6
		air	16 h	60.2	99.6	28.0
4	 57	O <sub>2</sub>	48 h	62.6	98.7	17.9
		air	44 h	64.7	98.9	15.7

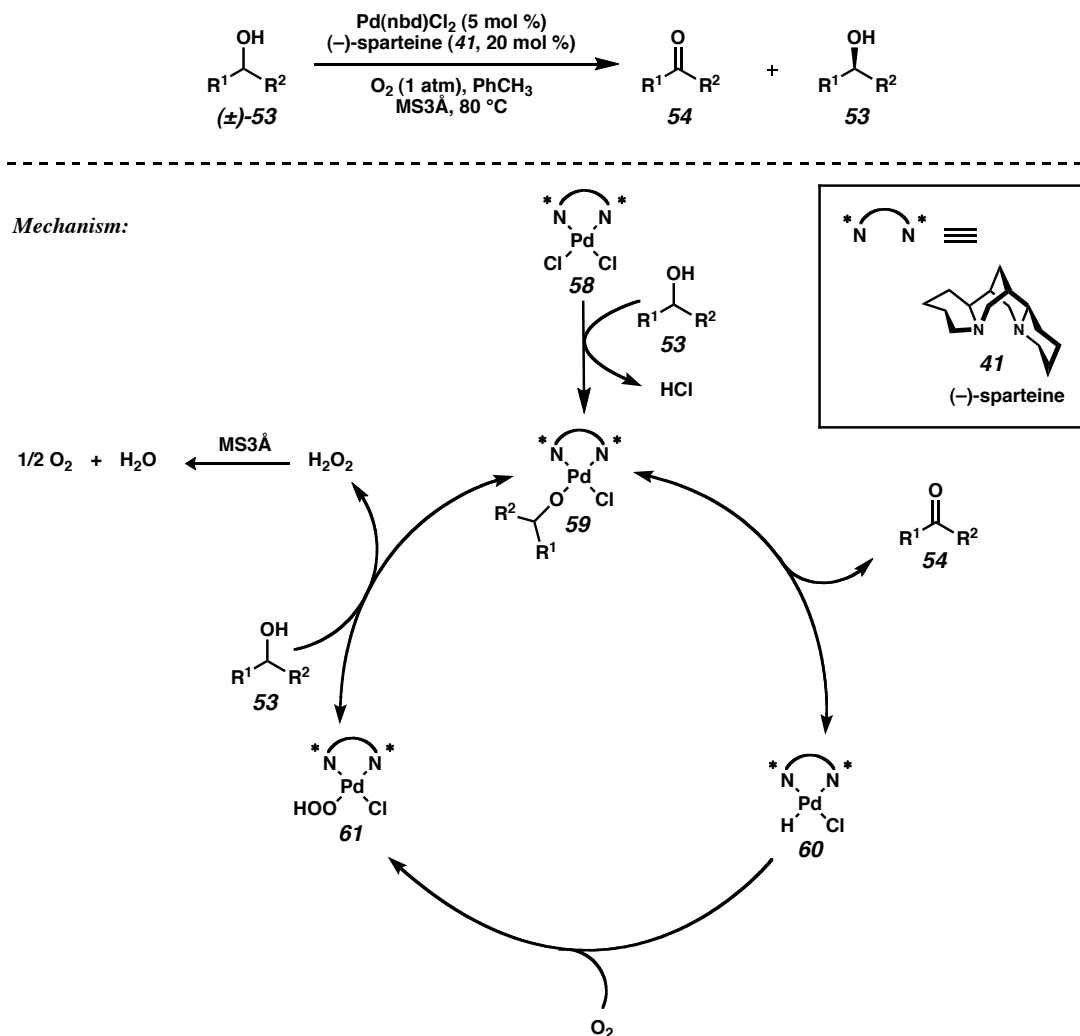
Table 2.1.2

$  \begin{array}{c}  \text{Pd(nbd)Cl}_2 \text{ (5 mol \%)} \\  \text{(-)-sparteine (41, 12 mol \%)} \\  \text{MS3Å, Cs}_2\text{CO}_3 \\  \text{O}_2 \text{ or air, CHCl}_3, 23^\circ\text{C}  \end{array}  \xrightarrow{\hspace{1cm}}  \begin{array}{c}  \text{R}^1\text{C(=O)R}^2 \\  \text{54}  \end{array}  +  \begin{array}{c}  \text{R}^1\text{CH(OH)R}^2 \\  \text{53}  \end{array}  $						
entry	unreacted alcohol, major enantiomer	atm	time	conversion (%)	ee ROH (%)	s
1	 55	O <sub>2</sub>	48 h	62.6	99.9	27.1
		air	24 h	62.3	99.8	25.4
2	 40	O <sub>2</sub>	48 h	59.3	99.6	31.1
		air	24 h	55.5	98.0	37.3
3	 56	O <sub>2</sub>	24 h	57.5	98.0	27.6
		air	16 h	60.2	99.6	28.0
4	 57	O <sub>2</sub>	48 h	62.6	98.7	17.9
		air	44 h	64.7	98.9	15.7

### 2.1.2 Mechanism of the Pd-Catalyzed Oxidative Kinetic Resolution

The general mechanism envisioned for this reaction is outlined in Scheme 2.1.3.<sup>6</sup> Starting with a palladium(II)-ligand complex (**58**), ligand substitution with a chiral substrate molecule (**53**) affords Pd(II) alkoxide **59**. This complex (**59**) can undergo  $\beta$ -hydride elimination to afford palladium hydride **60**, and generate oxidized substrate molecule **54**. Oxidation of the palladium with molecular oxygen then gives rise to **61**,<sup>7</sup> which can undergo ligand substitution with another substrate molecule (**53**) and continue the catalytic cycle. Finally, the hydrogen peroxide that is produced in the final step is proposed to be disproportionated into oxygen and water via the action of MS3Å.<sup>3</sup>

Scheme 2.1.3



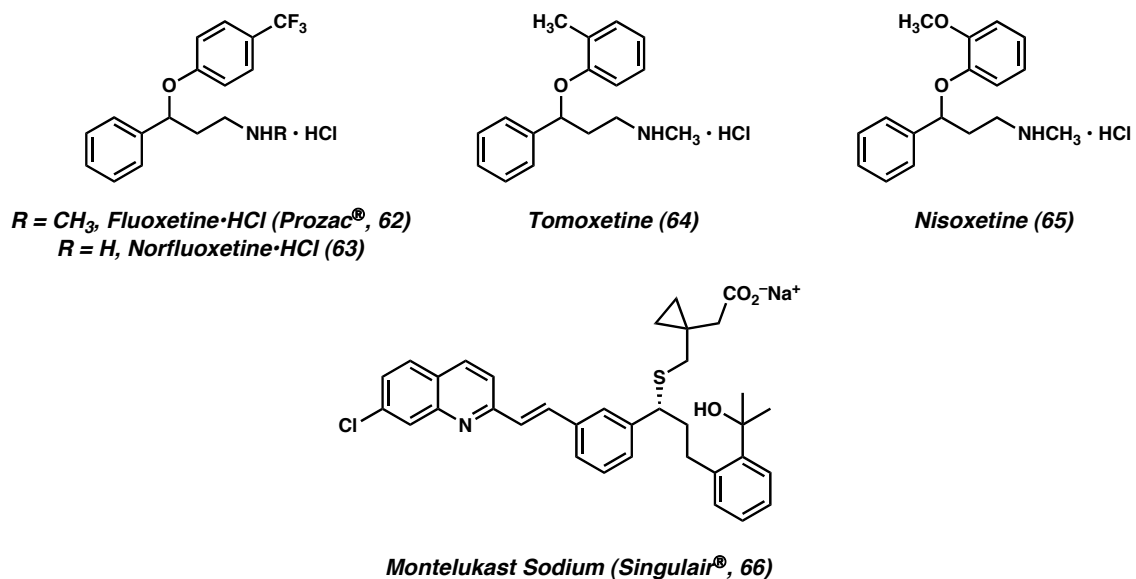
## 2.2 The Oxidative Kinetic Resolution of Pharmaceutical Building Blocks

### 2.2.1 Pharmaceutical Targets

Although this oxidative kinetic resolution system had been optimized and studied in detail, it had primarily only been tested with simple, commercially-available benzylic alcohols. To demonstrate the potential synthetic utility of our palladium-catalyzed enantioselective alcohol oxidation, we investigated the oxidative kinetic resolution of a diverse set of small molecules representing key building blocks of bioactive,

pharmaceutically relevant materials (Figure 2.2.1).<sup>8</sup> These pharmaceutical substances included A) the antidepressants fluoxetine hydrochloride (Prozac<sup>®</sup>, **62**), norfluoxetine (**63**), tomoxetine (**64**), and nisoxetine (**65**),<sup>9</sup> and B) the orally active leukotriene receptor antagonist montelukast sodium (Singulair<sup>®</sup>, **66**).<sup>10,11</sup> These compounds were specifically chosen due to the inclusion of a key benzylic or allylic alcohol in the known synthetic routes (i.e., **67–70**, Table 2.2.1). We believed that these pharmaceutical agents would represent an ideal testing ground for our new asymmetric methodology.

Figure 2.2.1



### 2.2.2 Resolution of Pharmaceutical Intermediates

To this end, we prepared a number of key intermediates by literature procedures and subjected them to kinetic resolution using a variety of our palladium-catalyzed aerobic conditions.<sup>12</sup> To our delight, all of the intermediates were resolved to high enantiomeric excess and with good-to-excellent selectivity (*s*) between the *R* and *S* enantiomers (*s* = 9.0–17.9).<sup>4</sup> As shown in Table 2.2.1, the amino alcohol derivatives **67** and **68**, relevant to the antidepressants **62–65**, could be resolved under our original conditions, employing Pd(nbd)Cl<sub>2</sub>, (–)-sparteine (**41**), and O<sub>2</sub>.<sup>1a</sup> While acetamide **68** was reasonably selective (*s* = 9), the more synthetically versatile Boc derivative **67** could be resolved with a selectivity factor of nearly 18.

Notably, carbamate **67** could be easily converted to *N*-methyl derivative **71** by reduction with LiAlH<sub>4</sub> (78% yield) or to primary amine **72** by treatment with TFA (68% yield), and ketone **73** could be recycled to (±)-**67** by quantitative reduction with NaBH<sub>4</sub> (Scheme 2.2.1). Amino alcohol intermediates **71** and **72** could then be converted to pharmaceutically-relevant compounds **62–65** using known procedures.<sup>9</sup>

Table 2.2.1

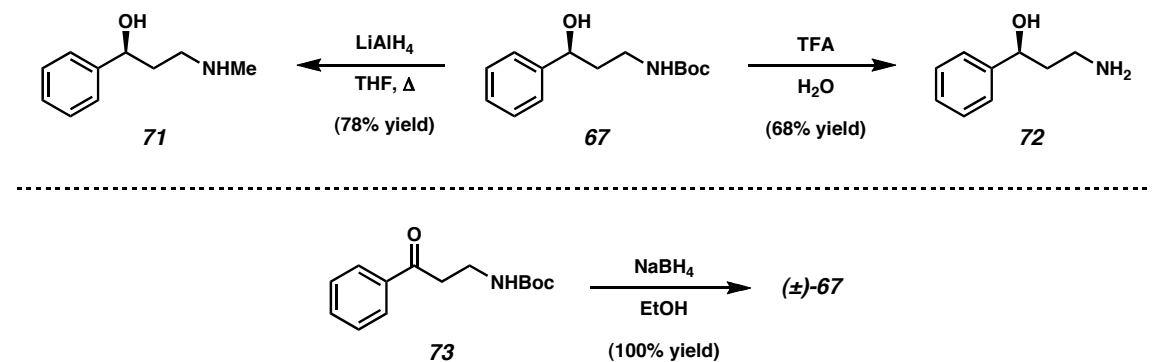
$$\text{R}^1\text{CH}(\text{OH})\text{R}^2 \xrightarrow{\text{Pd(nbd)Cl}_2, (-)\text{-sparteine (41)}} \text{R}^1\text{C(=O)R}^2 + \text{R}^1\text{CH}(\text{OH})\text{R}^2$$

$(\pm)\text{-53} \quad \quad \quad 54 \quad \quad \quad 53$

entry	unreacted alcohol, major enantiomer	method <sup>a</sup>	time	conversion (%)	ee ROH (%) <sup>e</sup>	<i>s</i>
1	 <b>67</b>	A	24 h	57.5 <sup>c</sup>	93.1	17.9
2	 <b>68</b>	A	14.5 h	70.0 <sup>c</sup>	97.0	9.0
3	 <b>69</b>	B <sup>b</sup>	4.5 h	62.5 <sup>d</sup>	92.9	11.2
4	 <b>70</b>	B <sup>b</sup>	4.5 h	70.6 <sup>c</sup>	99.9	15.3

<sup>a</sup> Method A: 5 mol % Pd(nbd)Cl<sub>2</sub>, 20 mol % (–)-sparteine (**41**), MS3Å, O<sub>2</sub> (1 atm), 0.1 M in PhCH<sub>3</sub>, 80 °C. Method B: 5 mol % Pd(nbd)Cl<sub>2</sub>, 20 mol % (–)-sparteine (**41**), 0.5 equiv Cs<sub>2</sub>CO<sub>3</sub>, 1.5 equiv *t*-BuOH, MS3Å, O<sub>2</sub> (1 atm), 0.25 M in PhCH<sub>3</sub>, 60 °C. <sup>b</sup> Performed at 80 °C. <sup>c</sup> Conversion determined by isolated yield. <sup>d</sup> Conversion determined by <sup>1</sup>H NMR. <sup>e</sup> Enantiomeric excess (ee) determined by chiral HPLC. Total mass recovery in all cases was greater than 85%.

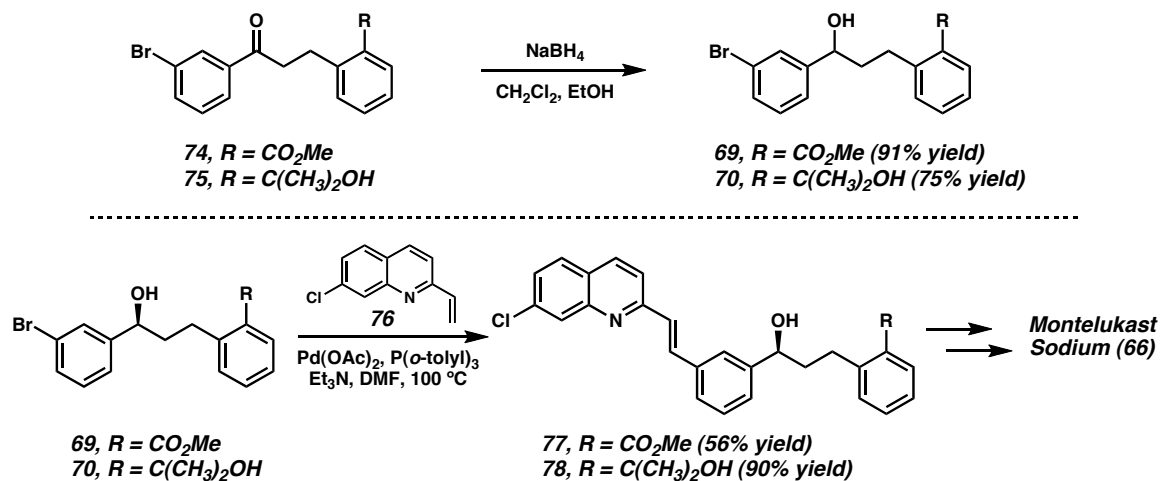
Scheme 2.2.1





The molecules relevant to the Singlair<sup>®</sup> system also resolved quite efficiently under our conditions (Table 2.2.1, entries 3 and 4). In order to minimize the experimental time involved for the resolution of compounds **69** and **70**, we chose to employ our recently described base-accelerated conditions.<sup>1b</sup> Smooth and rapid kinetic resolution was observed for both substrates (4.5 h) leading to production of the relevant enantiomer en route to Singlair<sup>®</sup>. Importantly, these resolutions provide a notable example of the functional group compatibility of the rate-accelerated system, as both aryl bromides and benzoate esters are tolerated in the oxidation. Again, the corresponding ketones **74** and **75** could be easily recycled via borohydride reduction. Furthermore, intermolecular Heck reaction of both **69** and **70** provided access to elaborated benzylic alcohols **77** and **78**, intermediates used in the production of montelukast sodium (Scheme 2.2.2).

Scheme 2.2.2



## 2.3 Conclusion

In conclusion, we have employed the palladium-catalyzed aerobic oxidative kinetic resolution of secondary alcohols for the enantioselective preparation of a variety

of pharmaceutical substances including Prozac<sup>®</sup> (**62**) and Singulair<sup>®</sup> (**66**). These examples demonstrate the power and utility of the methods to overcome many subtleties of substrate functionality. In this regard, the versatility of this resolution is further demonstrated by the diversity of the substrates chosen for this study, and for the first time this work extends the utility of the resolution to include amino alcohol derivatives and highly functionalized benzylic alcohols. Efforts to develop new catalyst systems and expand the utility and generality of asymmetric aerobic dehydrogenations continue.

## 2.4 Experimental Section

### 2.4.1 Materials and Methods

Unless stated otherwise, reactions were conducted in flame-dried glassware under an atmosphere of nitrogen using anhydrous solvents (either freshly distilled or passed through activated alumina columns). All commercially obtained reagents were used as received. Reaction temperatures were controlled using an IKAmag temperature modulator. Thin-layer chromatography (TLC) was conducted with E. Merck silica gel 60 F254 pre-coated plates, (0.25 mm) and visualized using a combination of UV, anisaldehyde, and potassium permanganate staining. ICN silica gel (particle size 0.032–0.063 mm) was used for flash column chromatography. Analytical chiral HPLC was performed on a Chiralcel<sup>®</sup> OJ or Chiralpak<sup>®</sup> AD column (each is 4.6 mm x 250 mm) obtained from Daicel Chemical Industries, Ltd. Analytical achiral GC was performed using an Agilent DB-WAX (30.0 m x 0.25 mm) column. <sup>1</sup>H NMR spectra were recorded on a Varian Mercury 300 (at 300 MHz) and are reported relative to Me<sub>4</sub>Si ( $\delta$  0.0). Data for <sup>1</sup>H NMR spectra are reported as follows: chemical shift ( $\delta$  ppm), multiplicity, coupling constant (Hz), and integration. <sup>13</sup>C NMR spectra were recorded on a Varian Mercury 300 (at 75 MHz) and are reported relative to Me<sub>4</sub>Si ( $\delta$  0.0). Data for <sup>13</sup>C NMR spectra are reported in terms of chemical shift. IR spectra were recorded on a Perkin Elmer Paragon 1000 spectrometer and are reported in frequency of absorption (cm<sup>-1</sup>). Optical rotations were measured with a Jasco P-1010 polarimeter. High-resolution mass spectra were obtained from the California Institute of Technology Mass Spectral Facility. Chemicals were purchased from the Sigma-Aldrich Chemical Company, Milwaukee, WI.

## 2.4.2 Methods of Determination for Enantiomeric Excess and % Conversion

Table 2.4.1. Methods for determination of enantiomeric excess

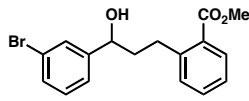
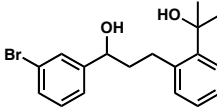
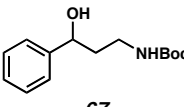
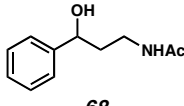
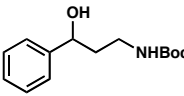
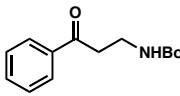
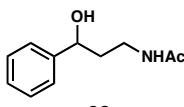
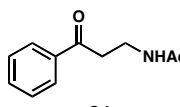
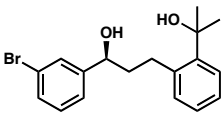
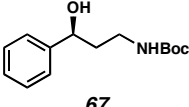
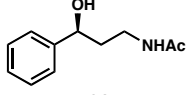
Entry	Substrate	HPLC Assay	Conditions	Retention Time (min)	
				(R)-isomer	(S)-isomer
1	 <b>69</b>	Chiralpak <sup>®</sup> AD	5% EtOH/hexanes 1.0 mL/min 254 nm	15.8	17.1
2	 <b>70</b>	Chiralcel <sup>®</sup> OJ	5% EtOH/hexanes 1.0 mL/min 210 nm	17.8	15.0
3.	 <b>67</b>	Chiralcel <sup>®</sup> OJ	8% 2-propanol/hexanes 1.0 mL/min 210 nm	10.5	20.1
4	 <b>68</b>	Chiralpak <sup>®</sup> AD	6% 2-propanol/hexanes 1.0 mL/min 210 nm	27.9	23.8

Table 2.4.2. Methods for determination of % conversion

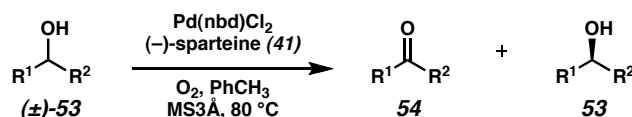
Entry	Substrate	Ketone	GC Conditions	Retention Time (min)	
				Alcohol	Ketone
1	 <b>67</b>	 <b>73</b>	70 °C, 15 min; 7 °C/min to 240 °C; hold 20 min  1.0 mL/min carrier gas flow	48.1	42.2
2	 <b>68</b>	 <b>81</b>	70 °C, 15 min; 7 °C/min to 240 °C; hold 20 min  1.0 mL/min carrier gas flow	53.5	45.1

### 2.4.3 Optical Rotations of New Compounds

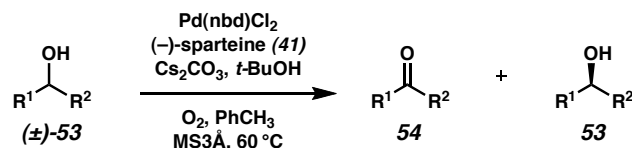
Table 2.4.3. Optical rotations (refer to Table 2.2.1 for relevant % enantiomeric excess)

Entry	Substrate	Rotation
1	 <b>70</b>	$[\alpha]_{\text{D}}^{26} -31.7^{\circ}$ ( <i>c</i> 1.0, benzene) <sup>13</sup>
2	 <b>67</b>	$[\alpha]_{\text{D}}^{25} -15.4^{\circ}$ ( <i>c</i> 1.0, CHCl <sub>3</sub> ) <sup>13</sup>
3	 <b>68</b>	$[\alpha]_{\text{D}}^{25} -23.6^{\circ}$ ( <i>c</i> 1.3, CHCl <sub>3</sub> ) <sup>14</sup>

#### 2.4.4 Representative Procedures for Oxidative Kinetic Resolution

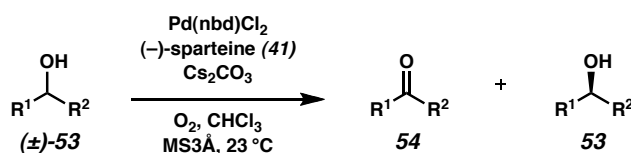


**Kinetic Resolution Conditions A: “Original Conditions.”**<sup>1a</sup> To an oven-dried reaction tube with stir bar was added oven-dried powdered 3Å molecular sieves (250 mg). After cooling, Pd(nbd)Cl<sub>2</sub> (6.7 mg, 0.025 mmol) followed by toluene (2.5 mL) and then (–)-sparteine (**41**, 23.4 mg, 23 µL, 0.10 mmol) were added. The reaction tube was then vacuum evacuated and purged with O<sub>2</sub> (3x), and the tube was heated to 80 °C with vigorous stirring under O<sub>2</sub> atmosphere (1 atm) for 20 min. A solution of alcohol **53** (0.50 mmol) in toluene (2.5 mL) was added, and the reaction was allowed to proceed under O<sub>2</sub> atmosphere (1 atm) at 80 °C. Aliquots were filtered through a small plug of silica gel (Et<sub>2</sub>O eluent), evaporated, and analyzed. Purification of ketone **54** and enantioenriched alcohol **53** was accomplished by direct chromatography of the crude reaction mixture.



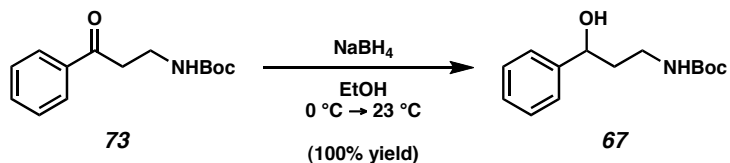
**Kinetic Resolution Conditions B: “Rate-Accelerated Conditions.”**<sup>1b</sup> To an oven-dried reaction tube with stir bar was added oven-dried powdered 3Å molecular sieves (500 mg). After cooling, Pd(nbd)Cl<sub>2</sub> (13.5 mg, 0.05 mmol), followed by toluene (2 mL) and then (–)-sparteine (**41**, 46.9 mg, 46 µL, 0.20 mmol) were added. The reaction tube was then vacuum evacuated and purged with O<sub>2</sub> (3x), and the tube was heated (60 °C) with vigorous stirring under O<sub>2</sub> atmosphere (1 atm) for 20 min. Finely powdered

anhydrous  $\text{Cs}_2\text{CO}_3$  (162.9 mg, 0.50 mmol) was added, followed by a solution of alcohol **53** (1.0 mmol), *t*-butanol (111.2 mg, 143  $\mu\text{L}$ , 1.5 mmol) and toluene (2 mL). The reaction was allowed to proceed under  $\text{O}_2$  atmosphere (1 atm) at 60  $^\circ\text{C}$ . Aliquots were filtered through a small plug of silica gel ( $\text{Et}_2\text{O}$  eluent), evaporated, and analyzed. Purification of ketone **54** and enantioenriched alcohol **53** was accomplished by direct chromatography of the crude reaction mixture.



**Kinetic Resolution Conditions C: “Chloroform Conditions.”**<sup>1c</sup> To an oven-dried reaction tube with stir bar was added oven-dried powdered 3Å molecular sieves (500 mg). After cooling,  $\text{Pd(nbd)Cl}_2$  (13.5 mg, 0.05 mmol), followed by chloroform (2 mL, stabilized with amylenes) and then (–)-sparteine (**41**, 28.1 mg, 27.6  $\mu\text{L}$ , 0.12 mmol) were added. The reaction tube was then vacuum evacuated and purged with  $\text{O}_2$  (3x), and the reaction was stirred vigorously at 23  $^\circ\text{C}$  under  $\text{O}_2$  atmosphere (1 atm) for 15 min. Finely powdered anhydrous  $\text{Cs}_2\text{CO}_3$  (130.3 mg, 0.40 mmol) was added, followed by a solution of alcohol **53** (1.0 mmol) in chloroform (2 mL). The reaction was allowed to proceed under  $\text{O}_2$  atmosphere (1 atm) at 23  $^\circ\text{C}$ . Aliquots were filtered through a small plug of silica gel ( $\text{Et}_2\text{O}$  eluent), evaporated, and analyzed. Purification of ketone **54** and enantioenriched alcohol **53** was accomplished by direct chromatography of the crude reaction mixture.

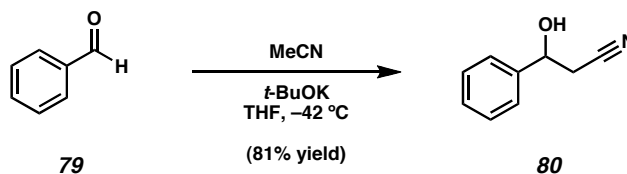
### 2.4.5 Representative Procedure for Ketone Recycling



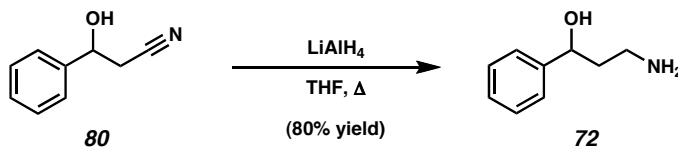
**Carbamate 67.** To keto-carbamate **73** (113.3 mg, 0.45 mmol) in EtOH (2.0 mL) was added  $\text{NaBH}_4$  (40.0 mg, 1.0 mmol) at  $0\text{ }^\circ\text{C}$ . After stirring for 3 h and allowing the reaction to warm to  $23\text{ }^\circ\text{C}$ , saturated aq.  $\text{NH}_4\text{Cl}$  was added dropwise at  $0\text{ }^\circ\text{C}$ . The mixture was diluted with EtOAc (1 mL) and  $\text{H}_2\text{O}$  (1 mL) and the phases were partitioned. The aqueous phase was extracted with EtOAc (3 x 1 mL). The organic extracts were combined and passed over a small plug of silica gel (EtOAc eluent). The solvent was removed in vacuo to afford carbamate **67** (113.8 mg, 100% yield).



### 2.4.6 Preparative Procedures

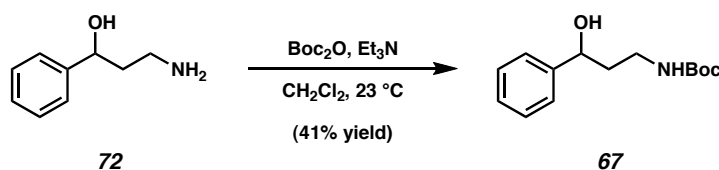


**Nitrile 80.**<sup>9c</sup> A flask charged with THF (100 mL) and acetonitrile (3.2 mL, 57.1 mmol) was cooled to  $-42\text{ }^{\circ}\text{C}$  and treated dropwise with a solution of *t*-BuOK (7.1 g, 63.3 mmol) in THF (25 mL). After stirring for 45 min, freshly distilled benzaldehyde (**79**, 5.7 mL, 56.4 mmol) was added dropwise. The reaction was allowed to warm to  $-15\text{ }^{\circ}\text{C}$  over a 4 h period, and then was quenched by slow addition of saturated aq.  $\text{NH}_4\text{Cl}$  (35 mL). The layers were partitioned, and the aqueous phase was extracted with  $\text{Et}_2\text{O}$  (2 x 100 mL). The combined organics were washed with  $\text{H}_2\text{O}$  (2 x 20 mL) and saturated aq.  $\text{NaCl}$  (20 mL), dried over  $\text{MgSO}_4$ , and concentrated under reduced pressure. The residue was flash chromatographed (1:1  $\text{Et}_2\text{O}$ :hexanes eluent) to give nitrile **80** (6.69 g, 81% yield) as a colorless oil.  $R_f$  0.16 (1:1  $\text{Et}_2\text{O}$ :hexanes); characterization data for this compound have been previously reported.<sup>9a</sup>



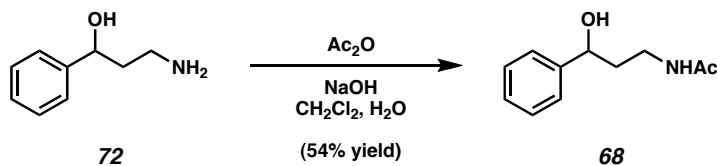
**Amino alcohol 72.** A flask was charged with a suspension of  $\text{LiAlH}_4$  (2.92 g, 77.0 mmol) in THF (100 mL). After cooling to  $0\text{ }^{\circ}\text{C}$ , the suspension was treated with nitrile **80** (4.54 g, 30.9 mmol) dropwise, and the resulting brown mixture was heated to reflux for 5 h. The reaction was cooled to  $0\text{ }^{\circ}\text{C}$ , and quenched by slow addition of  $\text{H}_2\text{O}$  (3

mL), followed by 15% w/v aq. NaOH (3 mL), and finally by H<sub>2</sub>O (9 mL). The crude green sludge was vacuum filtered and washed well with Et<sub>2</sub>O. The filtrate was concentrated under reduced pressure to a green oil, and partitioned between EtOAc (100 mL) and 15% w/v aq. NaOH (30 mL). The aqueous phase was extracted with EtOAc (2 x 100 mL), and the combined organic layers were dried over Na<sub>2</sub>SO<sub>4</sub>. The solvent was evaporated in vacuo to afford amino alcohol **72** (3.74 g, 80% yield) as a dark orange oil, which was used without further purification. *R<sub>f</sub>* 0.0 (1:1 EtOAc:hexanes); characterization data for this compound have been previously reported.<sup>9a</sup>

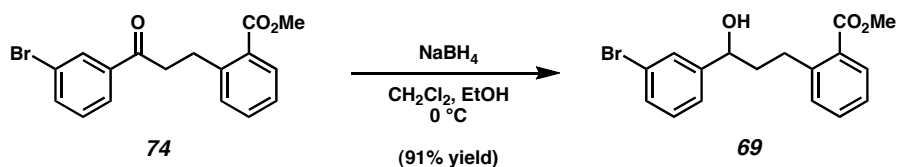


**Carbamate 67.** To amino alcohol **72** (2.14 g, 14.1 mmol) in CH<sub>2</sub>Cl<sub>2</sub> (25 mL) was added Et<sub>3</sub>N (2.8 mL, 20.1 mmol) over 1–2 min at 23 °C, followed by Boc<sub>2</sub>O (3.09 g, 14.2 mmol). The reaction was stirred for 2 h, then quenched by addition of saturated aq. NH<sub>4</sub>Cl (15 mL). The phases were partitioned, and the aqueous phase was extracted with CH<sub>2</sub>Cl<sub>2</sub> (2 x 30 mL). The organic extracts were combined, washed with saturated aq. NaHCO<sub>3</sub> (15 mL), H<sub>2</sub>O (15 mL), and saturated aq. NaCl (15 mL), and dried over MgSO<sub>4</sub>. The crude product was concentrated in vacuo, and passed over a short plug of silica gel (20:1 CH<sub>2</sub>Cl<sub>2</sub>:MeOH eluent). A solid was precipitated from the residue by treatment with hexanes:Et<sub>2</sub>O (10:1, 10 mL), and the solvent was evaporated in vacuo. This material was then recrystallized from hexanes:Et<sub>2</sub>O (10:1, 10 mL), filtered, and rinsed with ice-cold pentane (3 x 5 mL) to afford carbamate **67** (1.44 g, 41% yield) as a white solid. *R<sub>f</sub>* 0.60 (7:1 CH<sub>2</sub>Cl<sub>2</sub>:MeOH); <sup>1</sup>H NMR (300 MHz, CDCl<sub>3</sub>) δ 7.37–7.23 (m, 5H), 4.84 (br s, 1H),

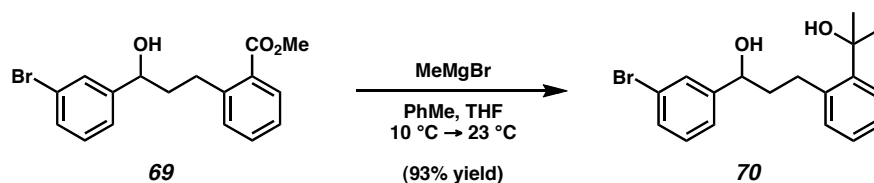
4.77–4.69 (m, 1H), 3.55–3.36 (m, 1H), 3.22–3.09 (m, 1H), 2.94 (br s, 1H), 1.88–1.80 (m, 2H), 1.44 (s, 3H);  $^{13}\text{C}$  NMR (75 MHz,  $\text{CDCl}_3$ )  $\delta$  157.1, 144.5, 128.6, 127.6, 125.8, 79.8, 71.9, 39.8, 37.8, 28.6; IR (film) 3360 (br), 1688, 1515, 1281, 1252, 1170  $\text{cm}^{-1}$ ; HRMS-FAB  $m/z$ :  $[\text{M} + \text{H}]^+$  calc'd for  $\text{C}_{14}\text{H}_{22}\text{NO}_3$ , 252.1600; found, 252.1600.



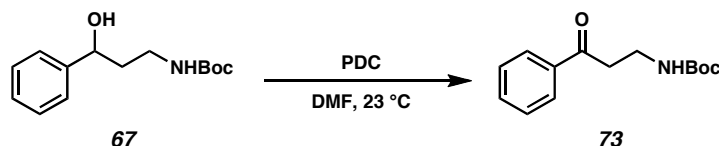
**Acetamide 68.** To amino alcohol **72** (1.61 g, 10.6 mmol) in  $\text{CH}_2\text{Cl}_2$  (17 mL) and aq. 1.4 N NaOH (17 mL, 23.8 mmol) was added acetic anhydride (1.3 mL, 13.8 mmol) at 23 °C. After the biphasic reaction was stirred for 5 h, the layers were partitioned, and the aqueous phase was extracted with  $\text{CH}_2\text{Cl}_2$  (3 x 30 mL). The combined organics were washed with  $\text{H}_2\text{O}$  (15 mL) and saturated aq. NaCl (15 mL), then dried over  $\text{MgSO}_4$ . The solvent was evaporated under reduced pressure, and the crude material was passed over a short plug of silica gel (20:1  $\text{CH}_2\text{Cl}_2$ :MeOH eluent). After concentrating to a yellow oil, hexanes: $\text{Et}_2\text{O}$  (10:1, 10 mL) was added, which precipitated a yellow solid. The solvent was evaporated in vacuo, and the yellow solid was triturated with pentane: $\text{Et}_2\text{O}$  (12:1), and collected by vacuum filtration to afford acetamide **68** (1.10 g, 54% yield) as a pale yellow solid.  $R_f$  0.50 (9:1  $\text{CH}_2\text{Cl}_2$ :MeOH);  $^1\text{H}$  NMR (300 MHz,  $\text{CDCl}_3$ )  $\delta$  7.37–7.24 (m, 5H), 5.96 (br s, 1H), 4.72 (dd,  $J = 7.4, 5.8$  Hz, 1H), 3.73–3.59 (m, 1H), 3.28–3.14 (m, 1H), 3.19 (br s, 1H), 1.97 (s, 3H), 1.90–1.81 (m, 2H);  $^{13}\text{C}$  NMR (75 MHz,  $\text{CDCl}_3$ )  $\delta$  171.5, 144.4, 128.6, 127.5, 125.8, 72.0, 39.0, 37.0, 23.3; IR (film): 3295 (br), 1651, 1556  $\text{cm}^{-1}$ ; HRMS-FAB ( $m/z$ ):  $[\text{M} + \text{H}]^+$  calc'd for  $\text{C}_{11}\text{H}_{16}\text{NO}_2$ , 194.1181; found, 194.1190.



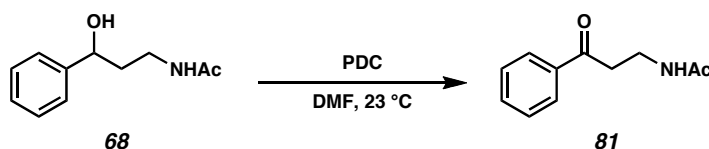
**Bromo Methyl Ester 69.** To 2-[3-(3-bromophenyl)-3-oxopropyl]benzoic acid methyl ester<sup>15</sup> (**74**, 1.763 g, 5.08 mmol), previously described by Larsen, et al.,<sup>10a</sup> in EtOH (12 mL) and CH<sub>2</sub>Cl<sub>2</sub> (12 mL), was added NaBH<sub>4</sub> (208.8 mg, 5.52 mmol) portionwise over a 5-min period at 0 °C. The reaction was stirred for 3.5 h at 0 °C, then quenched by slow addition of 0.1 N HCl (45 mL). After stirring 30 min, the mixture was poured over CH<sub>2</sub>Cl<sub>2</sub> (75 mL) and the phases were partitioned. The aqueous phase was extracted with CH<sub>2</sub>Cl<sub>2</sub> (75 mL), and the organic extracts were combined, washed with H<sub>2</sub>O (15 mL) and brine (15 mL), and dried over MgSO<sub>4</sub>. The solvent was evaporated in vacuo, and the crude product was chromatographed (7:1 hexanes:EtOAc eluent) to provide the product as a viscous oil. The residual solvent was removed by lyophilization from benzene to afford bromo methyl ester **69** (1.61 g, 91% yield) as a white-to-off-white solid. *R*<sub>f</sub> 0.44 (4:1 hexanes:EtOAc); <sup>1</sup>H NMR (300 MHz, CDCl<sub>3</sub>) δ 7.88 (app. dd, *J* = 8.1, 1.5 Hz, 1H), 7.50 (app. t, *J* = 1.7 Hz, 1H), 7.46–7.33 (m, 2H), 7.28–7.14 (m, 4H), 4.64 (app. t, *J* = 6.2 Hz, 1H), 3.87 (s, 3H), 3.16–2.97 (m, 3H), 2.06–1.97 (m, 2H); <sup>13</sup>C NMR (75 MHz, CDCl<sub>3</sub>) δ 168.4, 147.2, 143.7, 132.4, 131.2, 130.9, 130.3, 130.0, 129.2, 129.0, 126.2, 124.5, 122.6, 72.6, 52.5, 41.6, 30.4; IR (film) 3460 (br), 1722, 1263, 1083 cm<sup>-1</sup>; HRMS-EI *m/z*: [M - H]<sup>+</sup> calc'd for C<sub>17</sub>H<sub>16</sub>BrO<sub>3</sub>, 347.0283; found, 347.0274.



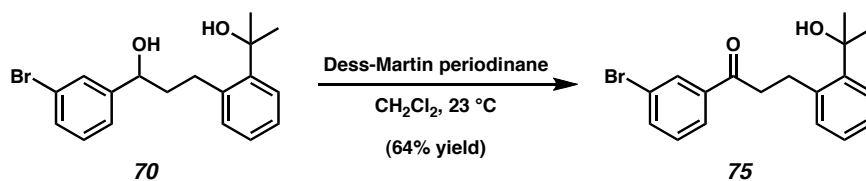
**Bromo Diol 70.** To bromo methyl ester **69** (1.502 g, 4.30 mmol) in THF (9 mL) and toluene (9 mL) was added MeMgBr (2.78 M in Et<sub>2</sub>O, 8.5 mL, 23.4 mmol) in a rapid dropwise fashion at 10 °C. The solution was stirred at 23 °C for 3.5 h after the addition was complete, then quenched by slow addition of saturated aq. NH<sub>4</sub>Cl. The resulting mixture was poured over Et<sub>2</sub>O (50 mL) and brine (25 mL). The organic phase was dried over MgSO<sub>4</sub>, and chromatographed (7:1 hexanes:EtOAc → 3:1 hexanes:EtOAc). The fractions containing the methyl ketone (slightly higher R<sub>f</sub> than the desired product) were concentrated in vacuo and resubjected to the initial reaction conditions. After purification in the same manner described above, all of the product containing fractions were combined and evaporated in vacuo. The viscous oil was lyophilized from benzene to provide bromo diol **70** (1.39 g, 93% combined yield) as a white-to-off-white solid. R<sub>f</sub> 0.33 (3:2 hexanes:EtOAc); <sup>1</sup>H NMR (300 MHz, CDCl<sub>3</sub>) δ 7.49 (app. s, 1H), 7.37–7.31 (m, 2H), 7.26–7.09 (m, 5H), 4.61 (dd, *J* = 8.6, 4.1 Hz, 1H), 3.26–3.14 (m, 1H), 3.12–3.01 (m, 1H), 2.21 (br s, 1H), 2.15–1.95 (m, 3H), 1.67 (s, 3H), 1.64 (s, 3H); <sup>13</sup>C NMR (75 MHz, CDCl<sub>3</sub>) δ 147.2, 144.9, 140.0, 131.4, 130.3, 130.0, 129.1, 127.4, 125.8, 125.6, 124.5, 122.6, 74.5, 72.5, 42.2, 32.4, 32.3, 29.7; IR (film) 3356 (br), 1069 cm<sup>-1</sup>; HRMS-EI *m/z*: [M - H]<sup>+</sup> calc'd for C<sub>18</sub>H<sub>20</sub>BrO<sub>2</sub>, 349.0628; found, 349.0631.



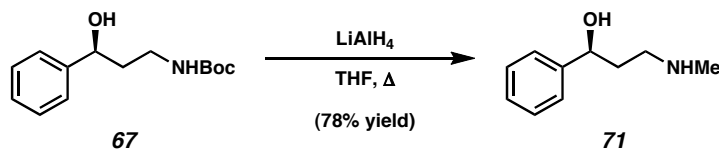
**Keto-Carbamate 73.** To carbamate **67** (27.5 mg, 0.11 mmol) in DMF (2 mL) was added pyridinium dichromate (237 mg, 0.63 mmol) at 23 °C. After 10 h, the reaction mixture was diluted in Et<sub>2</sub>O (5 mL) and brine (5 mL), and the phases were partitioned. The aqueous phase was extracted with Et<sub>2</sub>O (2 x 5 mL), and the organic extracts were combined, dried over MgSO<sub>4</sub>, and concentrated in vacuo. The residue was chromatographed (20:1 → 10:1 hexanes:EtOAc eluent) to afford keto-carbamate **73** as a solid, which was used as an authentic standard to confirm the oxidative kinetic resolution product of carbamate **67**. *R<sub>f</sub>* 0.50 (1:1 EtOAc:hexanes); <sup>1</sup>H NMR (300 MHz, CDCl<sub>3</sub>) δ 7.97–7.90 (m, 2H), 7.61–7.51 (m, 1H), 7.49–7.39 (m, 2H), 5.13 (br s, 1H), 3.53 (q, *J* = 5.9 Hz, 2H), 3.19 (t, *J* = 5.5 Hz, 2H), 1.41 (s, 9H); <sup>13</sup>C NMR (75 MHz, CDCl<sub>3</sub>) δ 199.4, 156.1, 136.7, 133.6, 128.8, 128.1, 79.3, 38.8, 35.6, 28.5; IR (film) 1682, 1506, 1172 cm<sup>-1</sup>; HRMS-FAB *m/z*: [M + H]<sup>+</sup> calc'd for C<sub>14</sub>H<sub>20</sub>NO<sub>3</sub>, 250.1443; found, 250.1441.



**Keto-Acetamide 81.** Compound **81** was prepared in an analogous manner to keto-carbamate **73**. The characterization data for this compound have been previously reported by Knochel.<sup>16</sup>

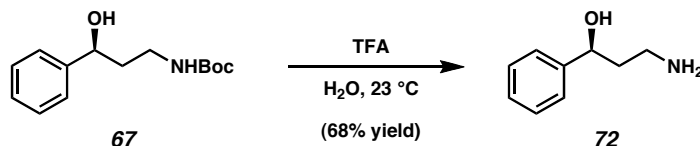


**Bromo Hydroxy Propanone 75.** To bromo diol **70** (51.6 mg, 0.15 mmol) in  $\text{CH}_2\text{Cl}_2$  (2.5 mL) was added Dess-Martin periodinane (70.7 mg, 0.17 mmol). The mixture was stirred for 3 h at  $23^\circ\text{C}$ , and then chromatographed directly (1:1  $\text{Et}_2\text{O}$ :pentane eluent) to provide bromo hydroxy propanone **75** (33.0 mg, 64% yield) as a solid. This product was used as an authentic standard to confirm the oxidative kinetic resolution product of bromo diol **70**.  $R_f$  0.60 (3:2 hexanes: $\text{EtOAc}$ );  $^1\text{H}$  NMR (300 MHz,  $\text{C}_6\text{D}_6$ )  $\delta$  8.06 (app. t,  $J = 1.7$  Hz, 1H), 7.86–7.81 (m, 1H), 7.57 (app. ddd, 1H,  $J = 7.7, 1.6, 1.1$  Hz, 1H), 7.25–7.20 (m, 1H), 7.11–6.98 (m, 3H), 6.65 (app. td,  $J = 10.8, 3.9$  Hz), 3.43 (app. t,  $J = 7.7$  Hz, 2H), 2.98–2.91 (m, 2H), 1.44–1.41 (m, 6H);  $^{13}\text{C}$  NMR (75 MHz,  $\text{C}_6\text{D}_6$ )  $\delta$  198.1, 146.4, 140.5, 139.5, 136.0, 132.2, 131.8, 130.6, 127.7, 127.1, 126.4, 126.4, 123.4, 73.8, 42.4, 32.6 (2C), 29.2; IR (film) 3452 (br), 1684, 1198  $\text{cm}^{-1}$ ; HRMS-FAB  $m/z$ :  $[\text{M} + \text{H}]^+$  for  $\text{C}_{18}\text{H}_{20}\text{O}_2\text{Br}$  calc'd, 347.0647; found, 347.0632.

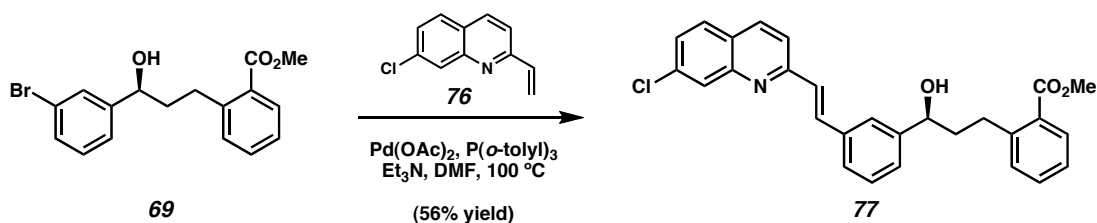


**(S)-Methyl Amine 71.** To a suspension of  $\text{LiAlH}_4$  (56.8 mg, 1.5 mmol) in THF (1.5 mL) was added enantioenriched carbamate **67** (47.5 mg, 0.19 mmol). The reaction was heated to reflux for 5.5 h, and then quenched at  $0^\circ\text{C}$  by slow addition of  $\text{H}_2\text{O}$  (50  $\mu\text{L}$ ), followed by 15% w/v aq. NaOH (50  $\mu\text{L}$ ), and finally by  $\text{H}_2\text{O}$  (150  $\mu\text{L}$ ). The mixture was filtered, and the filter cake was rinsed well with  $\text{Et}_2\text{O}$ . The filtrate was evaporated

under reduced pressure, diluted in  $\text{CH}_2\text{Cl}_2$  (1 mL), washed with saturated aq. NaCl (0.5 mL), and dried over  $\text{Na}_2\text{SO}_4$ . The solvent was evaporated under reduced pressure, which provided methyl amine **71** (24.5 mg, 78% yield) as an oil.  $[\alpha]_D^{26} -33.7^\circ$  ( $c$  0.81,  $\text{CHCl}_3$ ). lit<sup>17</sup>:  $[\alpha]_D^{23} -37.4^\circ$  ( $c$  1%,  $\text{CHCl}_3$ ).



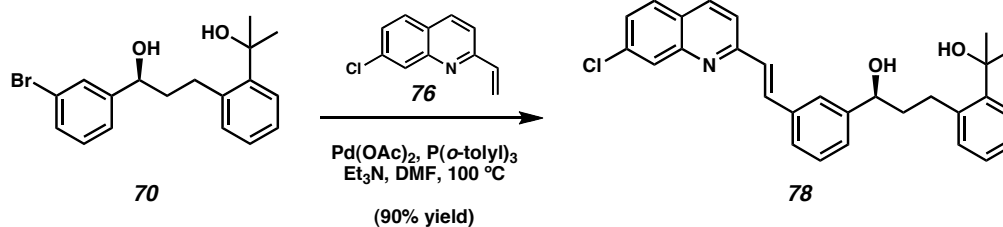
**(S)-Amino Alcohol 72.** To enantioenriched carbamate **67** (25.2 mg, 0.1 mmol) was added a mixture of trifluoroacetic acid (1.0 mL) and  $\text{H}_2\text{O}$  (0.2 mL). The solution was stirred at  $23^\circ\text{C}$  for 48 h, and then the volatiles were removed in vacuo. The aqueous residue was made basic using 5 N aq. NaOH (1 mL), and extracted with  $\text{CH}_2\text{Cl}_2$  (3 x 1 mL). The combined organic extracts were dried over  $\text{Na}_2\text{SO}_4$  and concentrated in vacuo to afford title compound **72** (10.2 mg, 68% yield) as a solid. Characterization data for this compound have been previously reported.<sup>9a</sup>  $[\alpha]_D^{25} -40.5^\circ$  ( $c$  0.5, MeOH). lit:<sup>9a</sup>  $[\alpha]_D^{25} -43.65^\circ$  ( $c$  1, MeOH).



**(S)-Chloroquinoline Methyl Ester 77.**<sup>10b,18</sup> To enantioenriched bromo methyl ester **69** (83.8 mg, 0.24 mmol) was added  $\text{Pd}(\text{OAc})_2$  (3.0 mg, 0.013 mmol),  $\text{P}(\text{o-tolyl})_3$  (12.7 mg, 0.042 mmol), 2-ethenyl-7-chloroquinoline<sup>10a</sup> (**76**, 47.0 mg, 0.25 mmol), and



DMF (0.7 mL). The dark mixture was degassed three times using the freeze-pump-thaw technique, and then Et<sub>3</sub>N (93  $\mu$ L, 0.67 mmol) was added. The reaction was heated to 100 °C for 3 h, then cooled to 23 °C. The crude mixture was diluted with EtOAc (2 mL) and H<sub>2</sub>O (2 mL). The phases were partitioned, and the aqueous phase was extracted with EtOAc (3 x 2 mL). The combined organic extracts were dried by passage over a short plug of silica gel (EtOAc eluent), and the solvent was evaporated in vacuo. The residue was purified by flash chromatography (5:1 hexanes:EtOAc eluent). Desired chloroquinoline methyl ester **77** (62.0 mg, 56% yield) was obtained as a solid after evaporation of solvent under reduced pressure, and lyophilization from benzene. *R*<sub>f</sub> 0.21 (3:2 hexanes:EtOAc); <sup>1</sup>H NMR (300 MHz, C<sub>6</sub>D<sub>6</sub>) 8.35 (app. d, *J* = 1.6 Hz, 1H), 7.92–7.85 (m, 2H), 7.68 (s, 1H), 7.43–7.36 (m, 3H), 7.29–6.89 (m, 8H), 4.67 (t, *J* = 5.8 Hz, 1H), 3.43 (s, 3H), 3.30–3.10 (m, 2H), 2.65 (br s, 1H), 2.11 (m, 2H); <sup>13</sup>C NMR (75 MHz, C<sub>6</sub>D<sub>6</sub>, 27/28 °C) 168.5, 157.5, 149.7, 146.9, 145.1, 137.2, 136.1, 136.0, 132.7, 131.9, 131.5, 130.2, 129.3, 129.3, 129.1, 128.9, 127.3, 127.1, 126.7, 126.5, 126.2, 125.7, 120.6, 73.6, 52.0, 42.5, 31.2; IR (film) 3407 (br), 1719, 1607, 1497, 1258 cm<sup>-1</sup>; HRMS-FAB *m/z*: [M + H]<sup>+</sup> calc'd for C<sub>28</sub>H<sub>25</sub>NO<sub>3</sub>Cl, 458.1523; found, 458.1517. lit (*R*)-**77**:<sup>10b</sup> [ $\alpha$ ]<sub>D</sub><sup>22</sup> +28.3° (99.5% ee, *c* 1, CHCl<sub>3</sub>). The absolute configuration of **77** was determined by optical rotation and chiral HPLC,<sup>19</sup> and no degradation of enantiopurity was observed in the conversion of starting material (**69**) to product (**77**).



**(S)-Chloroquinoline Diol 78.**<sup>18,19</sup> To enantioenriched bromo diol **70** (41.6 mg, 0.12 mmol) was added  $\text{Pd}(\text{OAc})_2$  (1.9 mg, 0.008 mmol),  $\text{P}(o\text{-tolyl})_3$  (10.8 mg, 0.035 mmol), 2-ethenyl-7-chloroquinoline<sup>10a</sup> (**76**, 23.9 mg, 0.12 mmol), and DMF (0.35 mL). The dark mixture was degassed three times using the freeze-pump-thaw technique, and then  $\text{Et}_3\text{N}$  (40  $\mu\text{L}$ , 0.29 mmol) was added. The reaction was heated to  $100\text{ }^\circ\text{C}$  for 3 h, then cooled to  $23\text{ }^\circ\text{C}$ . The crude mixture was chromatographed directly (9:1 hexanes:EtOAc  $\rightarrow$  3:1 hexanes:EtOAc eluent). Desired chloroquinoline diol **78** (49.2 mg, 90% yield) was obtained as a solid after evaporation of solvent under reduced pressure and lyophilization from benzene.  $R_f$  0.11 (3:2 hexanes:EtOAc);  $^1\text{H}$  NMR (300 MHz,  $\text{C}_6\text{D}_6$ ) 8.32 (app. d,  $J = 1.6\text{ Hz}$ , 1H), 7.82 (app. d,  $J = 16.5\text{ Hz}$ , 1H), 7.69 (app. s, 1H), 7.42–7.31 (m, 4H), 7.29–7.00 (m, 8H), 4.68 (dd,  $J = 8.2, 4.4\text{ Hz}$ , 1H), 3.97 (br s, 1H), 3.45–3.32 (m, 1H), 3.21–3.10 (m, 1H), 2.96 (br s, 1H), 2.23–2.09 (m, 2H), 1.50 (s, 1H), 1.48 (s, 1H);  $^{13}\text{C}$  NMR (75 MHz,  $\text{C}_6\text{D}_6$ , 28/29  $^\circ\text{C}$ ) 157.5, 149.5, 146.8, 146.1, 141.1, 137.1, 136.2, 136.0, 135.9, 132.2, 129.3, 129.3, 129.0, 129.0, 128.9, 127.8, 127.3, 126.8, 126.3, 126.2, 125.8, 120.4, 74.3, 73.4, 43.0, 32.6, 32.4, 30.4; IR (film) 3361 (br), 1607, 1498  $\text{cm}^{-1}$ ; HRMS-FAB  $m/z$ :  $[\text{M} + \text{H}]^+$  calc'd for  $\text{C}_{29}\text{H}_{29}\text{NO}_2\text{Cl}$ , 458.1887; found, 458.1886. The absolute configuration of **78** was determined by chiral HPLC,<sup>19</sup> and no degradation of enantiopurity was observed in the conversion of starting material (**70**) to product (**78**).

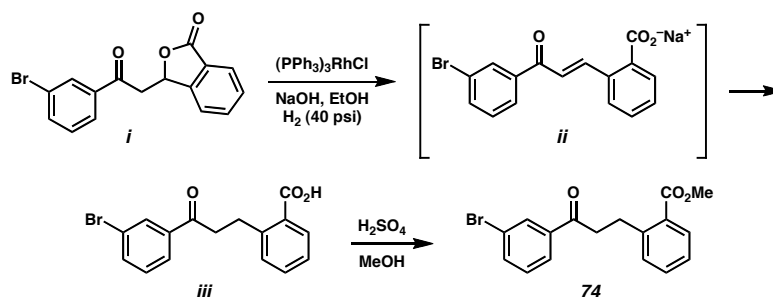
## 2.5 Notes and References

- (1) (a) Ferreira, E. M.; Stoltz, B. M. *J. Am. Chem. Soc.* **2001**, *123*, 7725–7726. (b) Bagdanoff, J. T.; Ferreira, E. M.; Stoltz, B. M. *Org. Lett.* **2003**, *5*, 835–837. (c) Bagdanoff, J. T.; Stoltz, B. M. *Angew. Chem., Int. Ed.* **2004**, *43*, 353–357.
- (2) Simultaneous to our publication, a related system was reported; see: Jensen, D. R.; Pugsley, J. S.; Sigman, M. S. *J. Am. Chem. Soc.* **2001**, *123*, 7475–7476.
- (3) The kinetic resolutions in references 1 and 2 were based on a non-asymmetric alcohol oxidation employing Pd(OAc)<sub>2</sub>, pyridine, and O<sub>2</sub>, see: Nishimura, T.; Ohe, K.; Uemura, S. *J. Org. Chem.* **1999**, *64*, 6750–6755.
- (4) The selectivity factor (*s*) was determined using the equation:  $s = k_{\text{rel}}[\text{fast/slow}] = \ln[(1 - C)(1 - ee)]/\ln[(1 - C)(1 + ee)]$ , where C = conversion. For an excellent discussion of kinetic resolutions, see: Kagan, H. B.; Fiaud, J. C. In *Topics in Stereochemistry*; Eliel, E. L., Ed.; Wiley & Sons: New York, 1988; Vol. 18, pp 249–330.
- (5) (a) Trend, R. M.; Ramtohul, Y. K.; Ferreira, E. M.; Stoltz, B. M. *Angew. Chem., Int. Ed.* **2003**, *42*, 2892–2895. (b) Ferreira, E. M.; Stoltz, B. M. *J. Am. Chem. Soc.* **2003**, *125*, 9578–9579.

- (6) A model for the observed stereochemistry was recently proposed: (a) Trend, R. M.; Stoltz, B. M. *J. Am. Chem. Soc.* **2004**, *126*, 4482–4483. (b) Nielsen, R. J.; Keith, J. M.; Stoltz, B. M.; Goddard, W. A., III *J. Am. Chem. Soc.* **2004**, *126*, 7967–7974.
- (7) For recent discussions concerning the mechanistic details of Pd oxidation by molecular oxygen, see: (a) Gligorich, K. M.; Sigman, M. S. *Angew. Chem., Int. Ed.* **2006**, *45*, 6612–6615. (b) Popp, B. V.; Stahl, S. S. *J. Am. Chem. Soc.* **2007**, *129*, 4410–4422. (c) Chowdhury, S.; Rivalta, I.; Russo, N.; Sicilia, E. *Chem. Phys. Lett.* **2007**, *443*, 183–189. (d) Keith, J. M.; Goddard, W. A., III; Oxgaard, J. *J. Am. Chem. Soc.* **2007**, *129*, 10361–10369.
- (8) Portions of this chapter are reproduced in part, with permission, from: Caspi, D. D.; Ebner, D. C.; Bagdanoff, J. T.; Stoltz, B. M. *Adv. Synth. Catal.* **2004**, *346*, 185–189 (Copyright 2004 Wiley-VCH Verlag GmbH & Co.KGaA).
- (9) (a) Mitchell, D.; Koenig, T. M. *Synth. Commun.* **1995**, *25*, 1231–1238. (b) Kumar, A.; Ner, D. H.; Dike, S. Y. *Tetrahedron Lett.* **1991**, *32*, 1901–1904. (c) Koenig, T. M.; Mitchell, D. *Tetrahedron Lett.* **1994**, *35*, 1339–1342. (d) Ali, I. S.; Sudalai, A. *Tetrahedron Lett.* **2002**, *43*, 5435–5436. (e) Kumar, A.; Ner, D. H.; Dike, S. Y. *Ind. J. Chem.* **1992**, *31B*, 803–809 and references therein.

- (10) (a) Larsen, R. D.; Corley, E. G.; King, A. O.; Carroll, J. D.; Davis, P.; Verhoeven, T. R.; Reider, P. J.; Labelle, M.; Gauthier, J. Y.; Xiang, Y. B.; Zamboni, R. J. *J. Org. Chem.* **1996**, *61*, 3398–3405. (b) King, A. O.; Corley, E. G.; Anderson, R. K.; Larsen, R. D.; Verhoeven, T. R.; Reider, P. J.; Xiang, Y. B.; Belley, M.; Leblanc, Y.; Labelle, M.; Prasit, P.; Zamboni, R. J. *J. Org. Chem.* **1993**, *58*, 3731–3735. (c) Bhupathy, M.; McNamara, J. M.; Sidler, D. R.; Volante, R. P.; Bergan, J. J. (Merck & Co., Inc.). WO 95/18107, 1995. (d) Bhupathy, M.; McNamara, J. M.; Sidler, D. R.; Volante, R. P.; Bergan, J. (Merck & Co., Inc.), U.S. Patent 5,614,632, 1997, and references therein.
- (11) (a) Kuethe, J. T.; Wong, A.; Wu, J.; Davies, I. W.; Dormer, P. G.; Welch, C. J.; Hillier, M. C.; Hughes, D. L.; Reider, P. J. *J. Org. Chem.* **2002**, *67*, 5993–6000. (b) Desai, R. C.; Cicala, P.; Meurer, L. C.; Finke, P. E. *Tetrahedron Lett.* **2002**, *43*, 4569–4570 and references therein.
- (12) Substrates were tested under all of the available oxidative kinetic resolution protocols (see reference 1), and the best results are reported.
- (13) The absolute configurations of **67** and **70** were assigned by conversion to known compounds (**67** → **72** and **70** → **78**).
- (14) The absolute configuration of **68** was assigned by analogy to known compounds.

- (15) In our hands, the reported benzofuranone reduction with Wilkinson's catalyst<sup>10a</sup> (**i** → **ii** → **iii**) did not proceed as described unless the starting material was further purified. This could be accomplished by filtering benzofuranone **i** in boiling EtOAc to remove insoluble impurities. Additionally, the product obtained after the benzofuranone reduction did not match the reported values for benzoic acid **iii**; however, brief exposure to acidic MeOH (conditions for the subsequent esterification reaction, **iii** → **74**) quantitatively converted it to the reported compound (**iii**).



- (16) Duddu, R.; Eckhardt, M.; Furlong, M.; Knoess, H. P.; Berger, S.; Knochel, P. *Tetrahedron* **1994**, *50*, 2415–2432.
- (17) Robertson, D. W.; Krushinski, J. H.; Fuller, R. W.; Leander, J. D. *J. Med. Chem.* **1988**, *31*, 1412–1417.
- (18) The NMR characterization data have been previously reported in  $CDCl_3$ . In our hands, these compounds slowly decomposed in  $CDCl_3$ , so we have reported these data in  $C_6D_6$ .

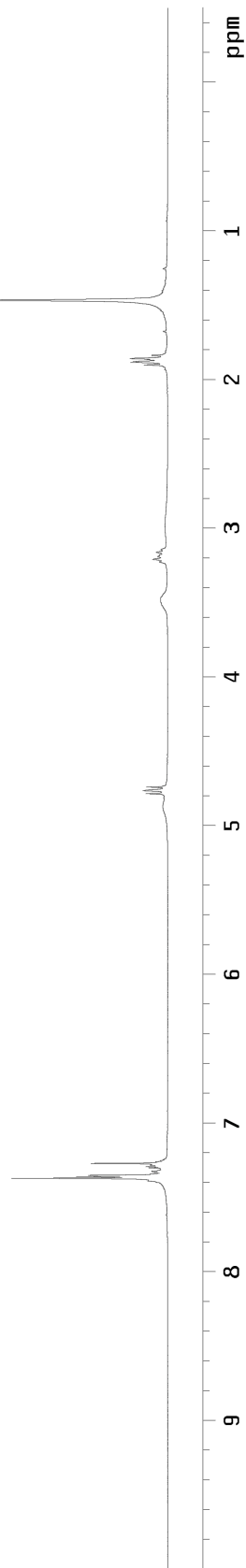
- (19) O'Brien, T.; Crocker, L.; Thompson, R.; Thompson, K.; Toma, P. H.; Conlon, D. A.; Feibush, B.; Moeder, C.; Bicker, G.; Grinberg, N. *Anal. Chem.* **1997**, 69, 1999–2007.

## **APPENDIX ONE**

### **Spectra Relevant to Chapter Two:**

**The Resolution of Important Pharmaceutical Building Blocks by Palladium-  
Catalyzed Aerobic Oxidation of Secondary Alcohols**





*Figure A1.1*  $^1\text{H}$  NMR (300 MHz,  $\text{CDCl}_3$ ) of compound **67**

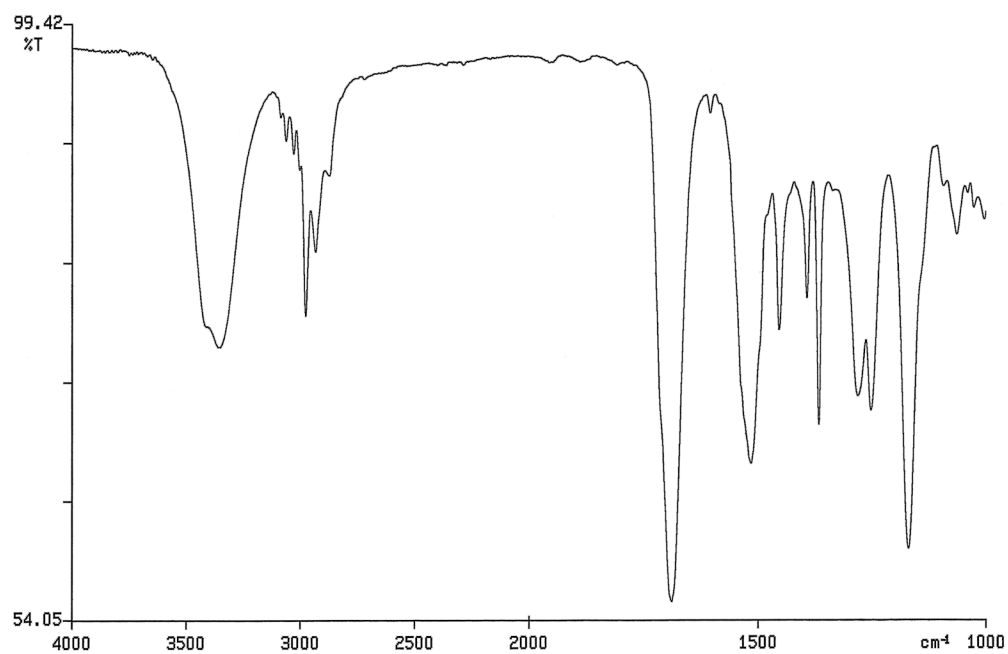


Figure A1.2 Infrared spectrum (thin film/NaCl) of compound **67**

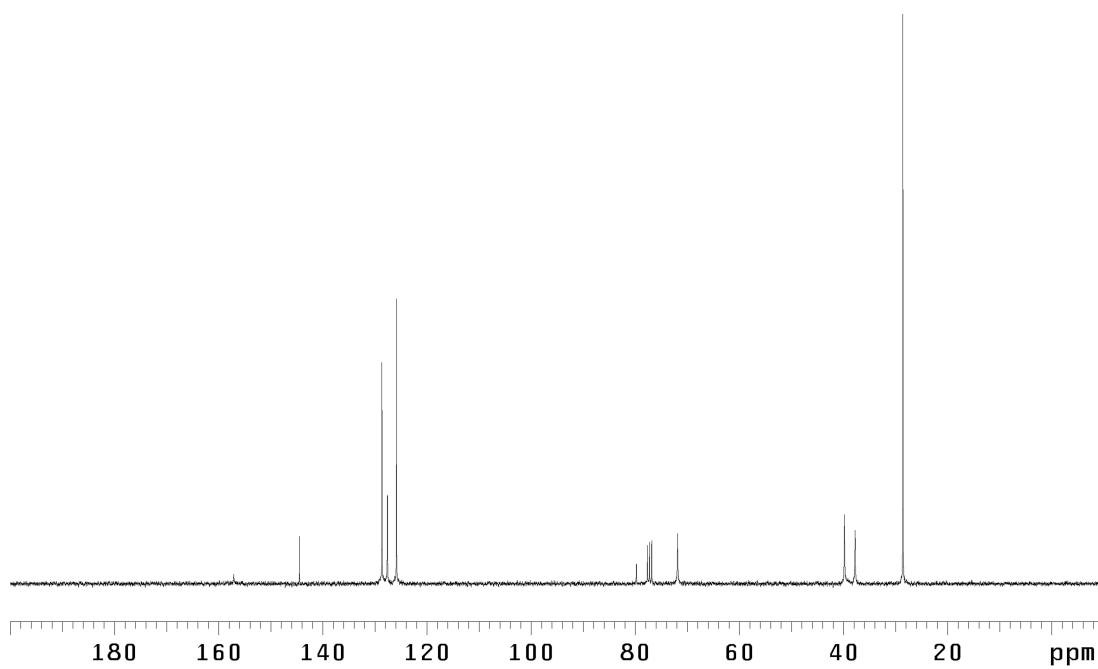


Figure A1.3 <sup>13</sup>C NMR (75 MHz, CDCl<sub>3</sub>) of compound **67**

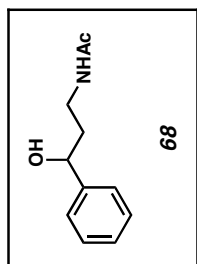
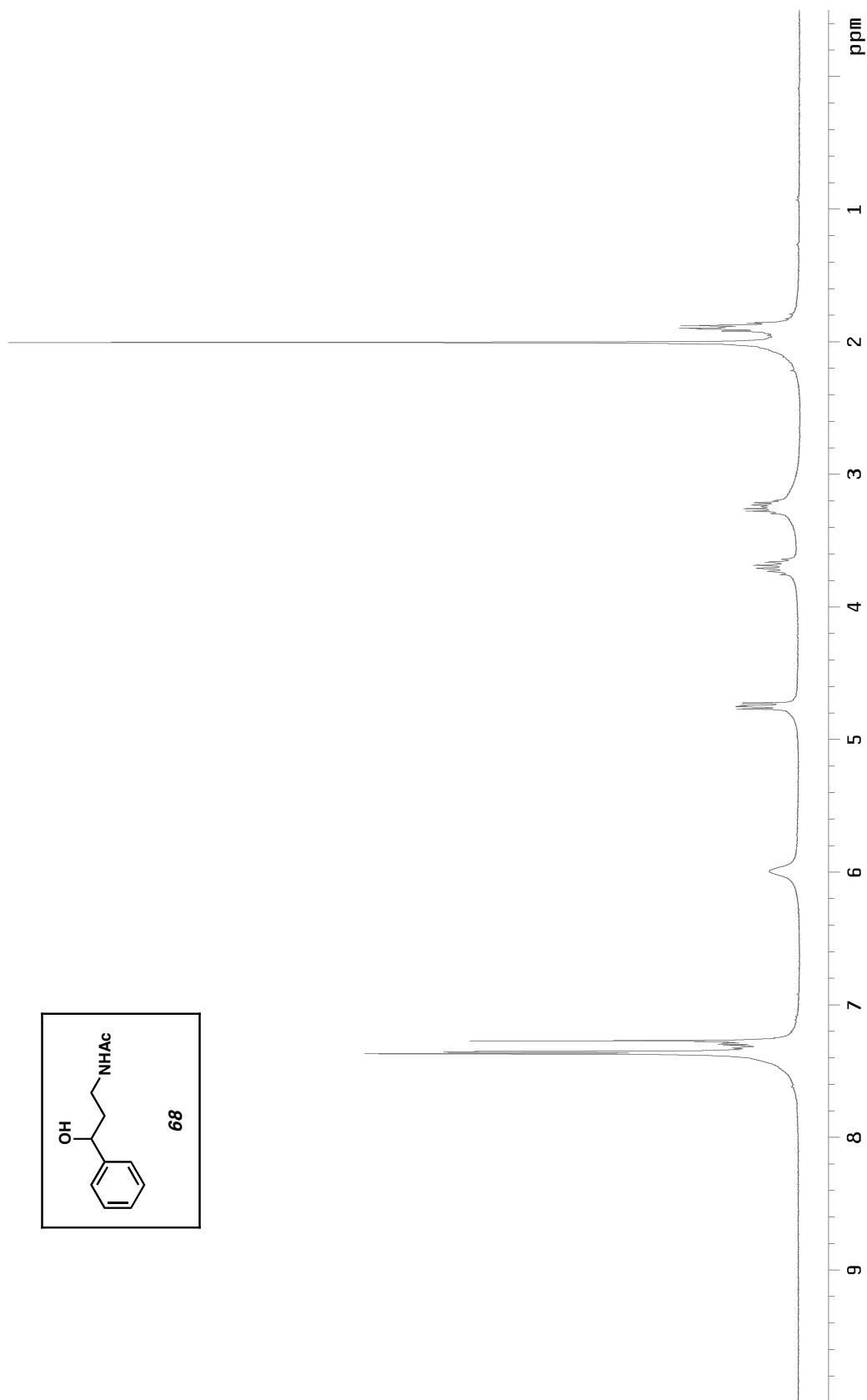


Figure A1.4  $^1\text{H}$  NMR (300 MHz,  $\text{CDCl}_3$ ) of compound **68**

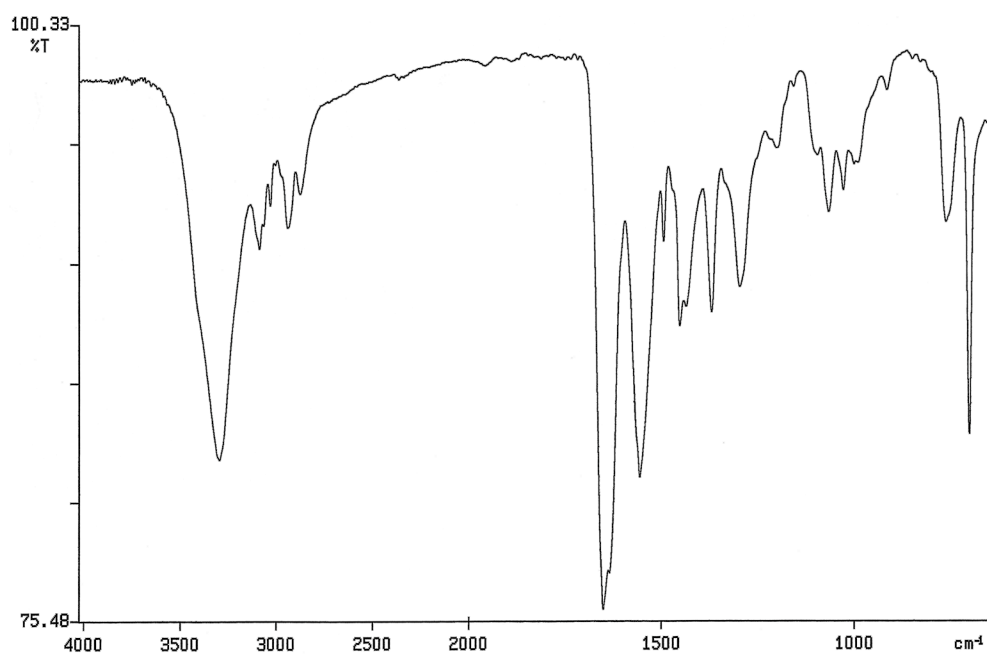


Figure A1.5 Infrared spectrum (thin film/NaCl) of compound **68**

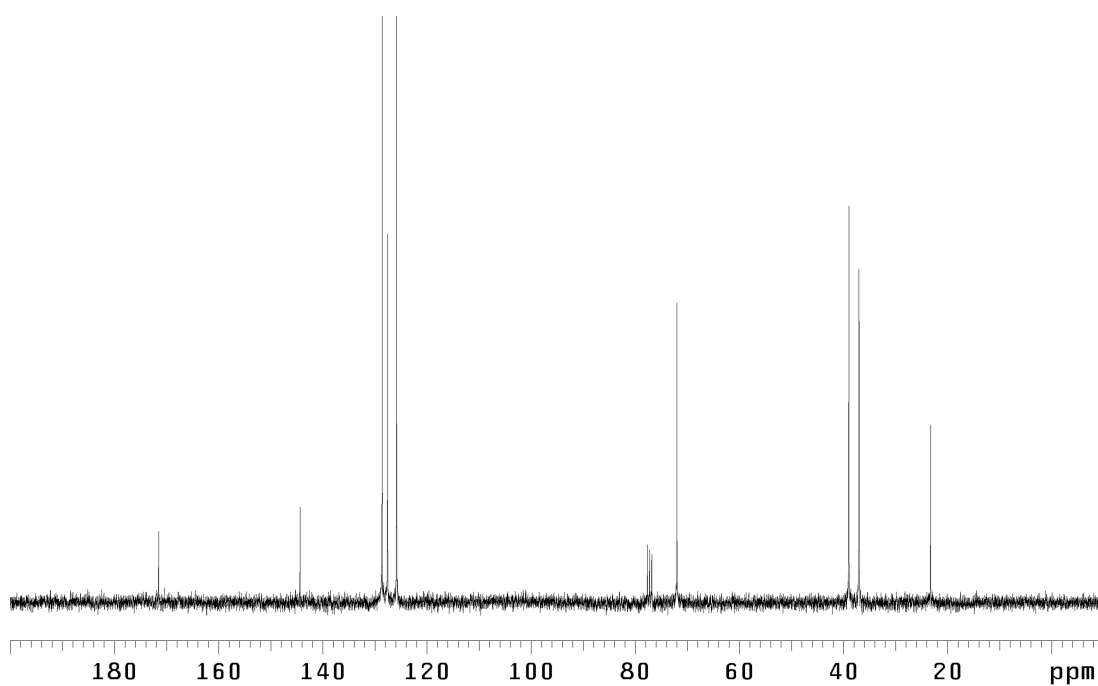
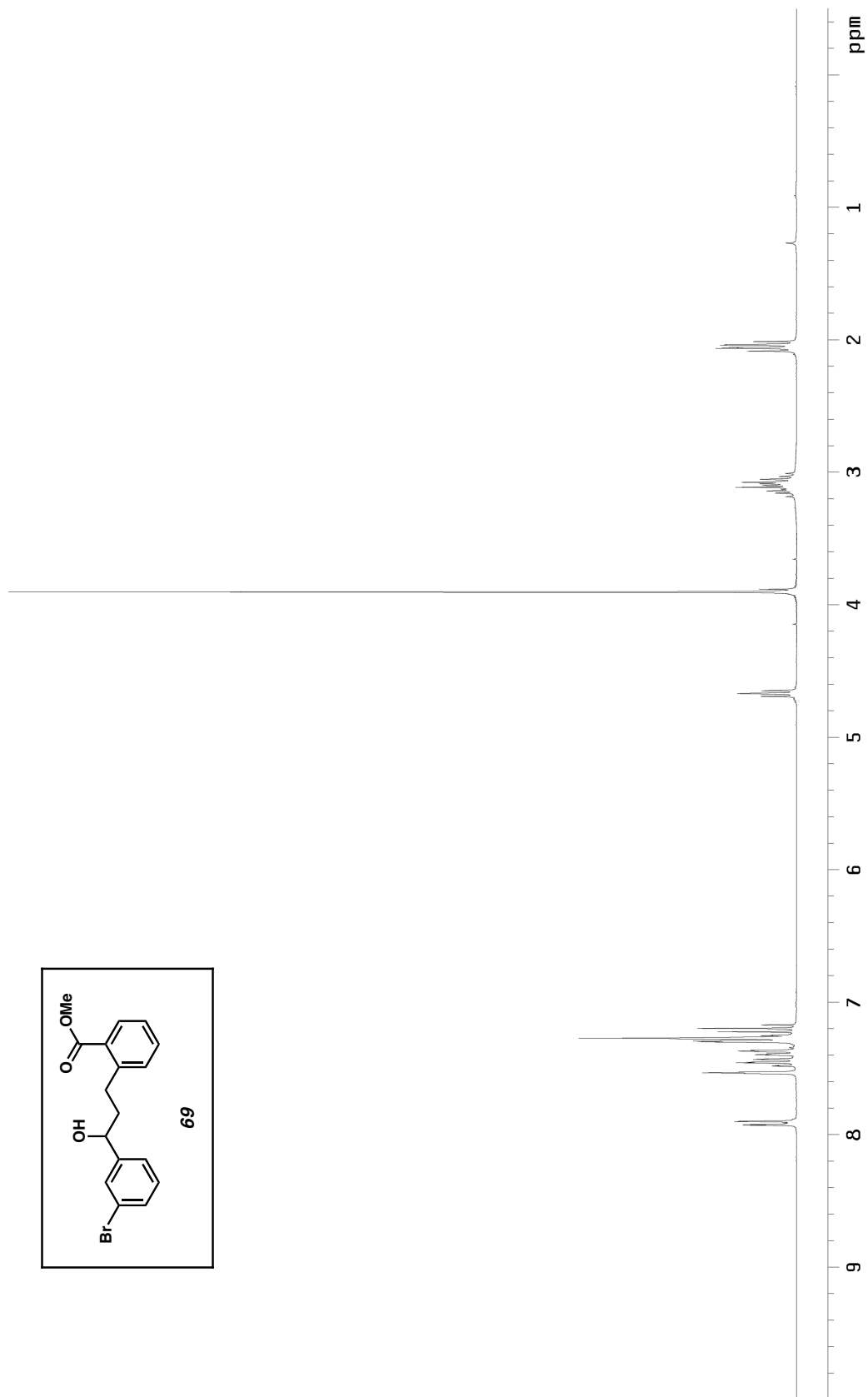
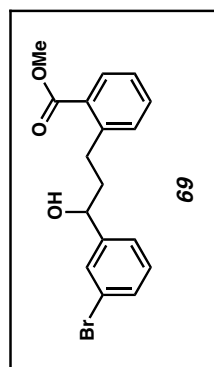


Figure A1.6 <sup>13</sup>C NMR (75 MHz, CDCl<sub>3</sub>) of compound **68**



*Figure A1.7*  $^1\text{H}$  NMR (300 MHz,  $\text{CDCl}_3$ ) of compound **69**

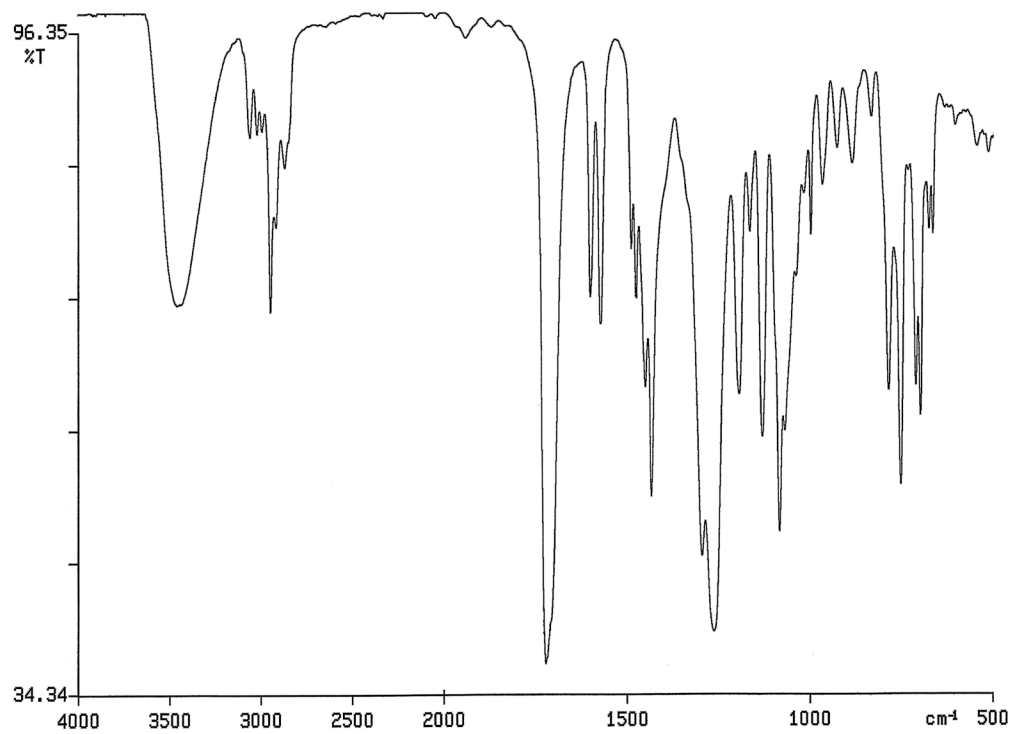


Figure A1.8 Infrared spectrum (thin film/NaCl) of compound **69**

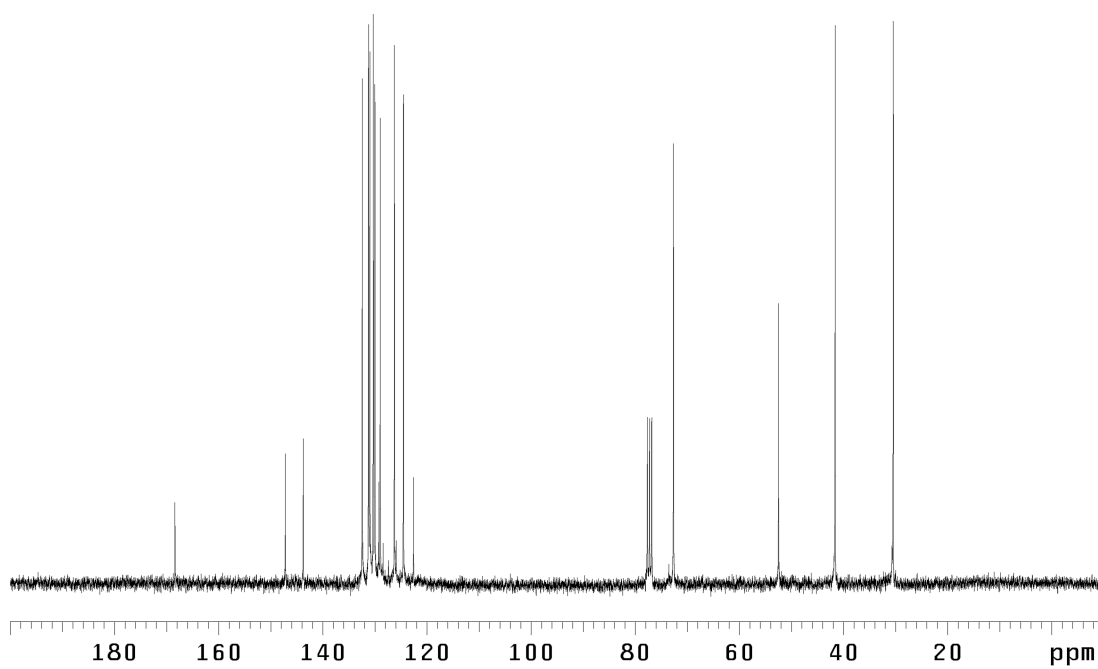


Figure A1.9  $^{13}\text{C}$  NMR (75 MHz,  $\text{CDCl}_3$ ) of compound **69**

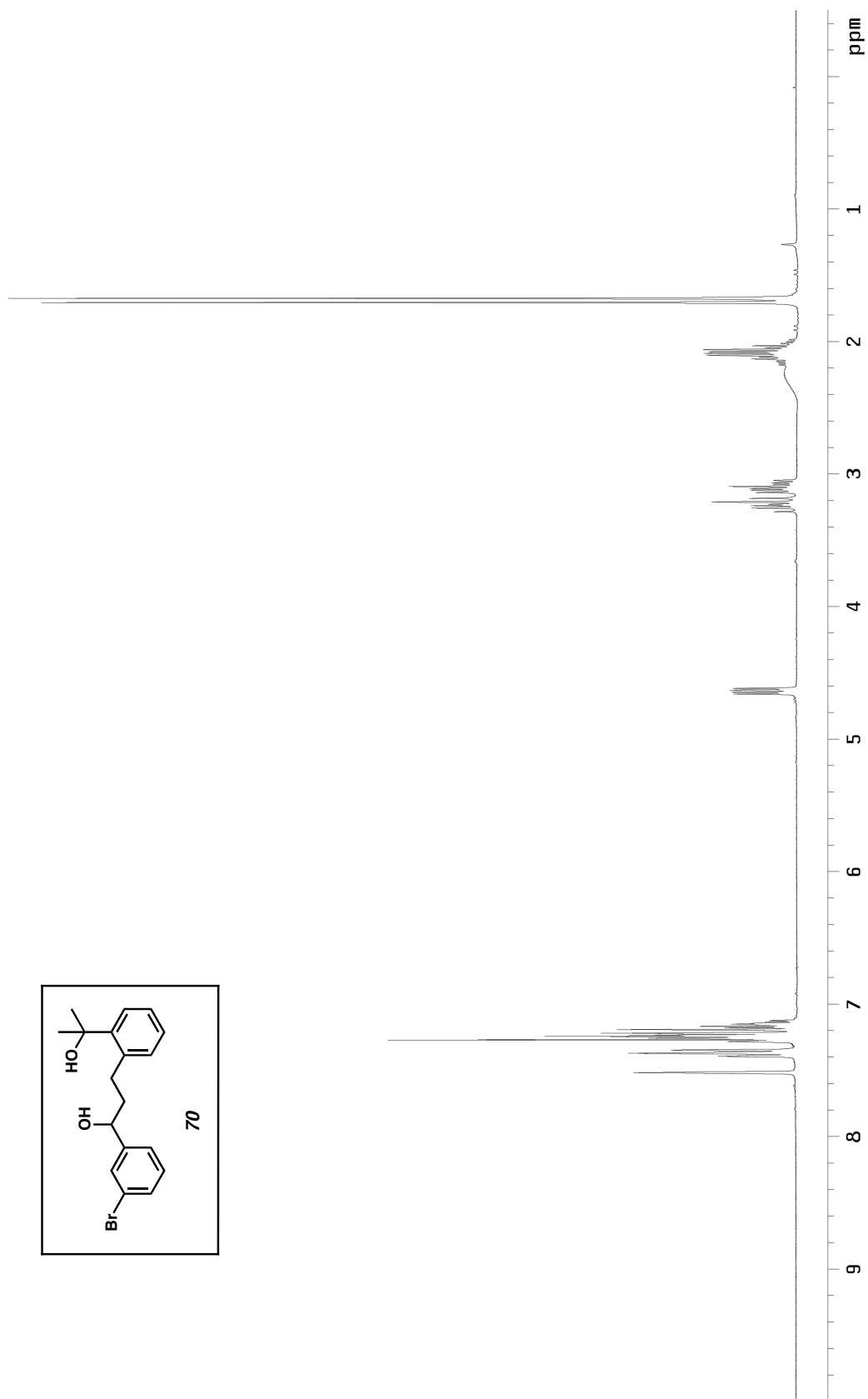
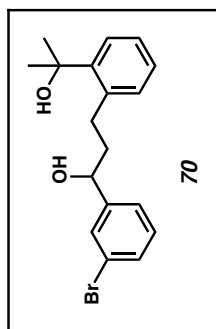


Figure A1.10 <sup>1</sup>H NMR (300 MHz, CDCl<sub>3</sub>) of compound **70**

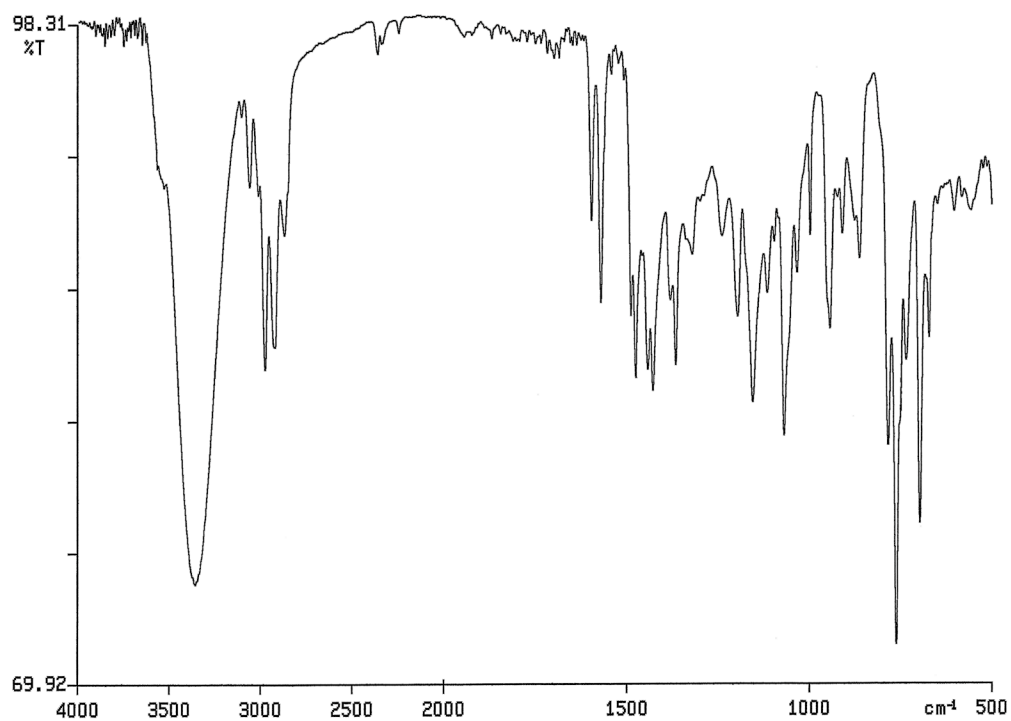


Figure A1.11 Infrared spectrum (thin film/NaCl) of compound **70**

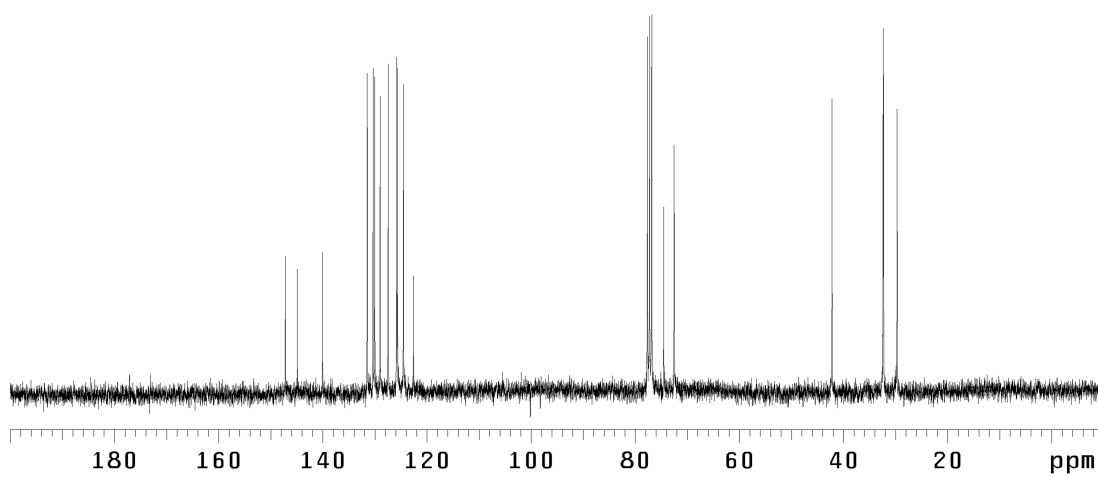
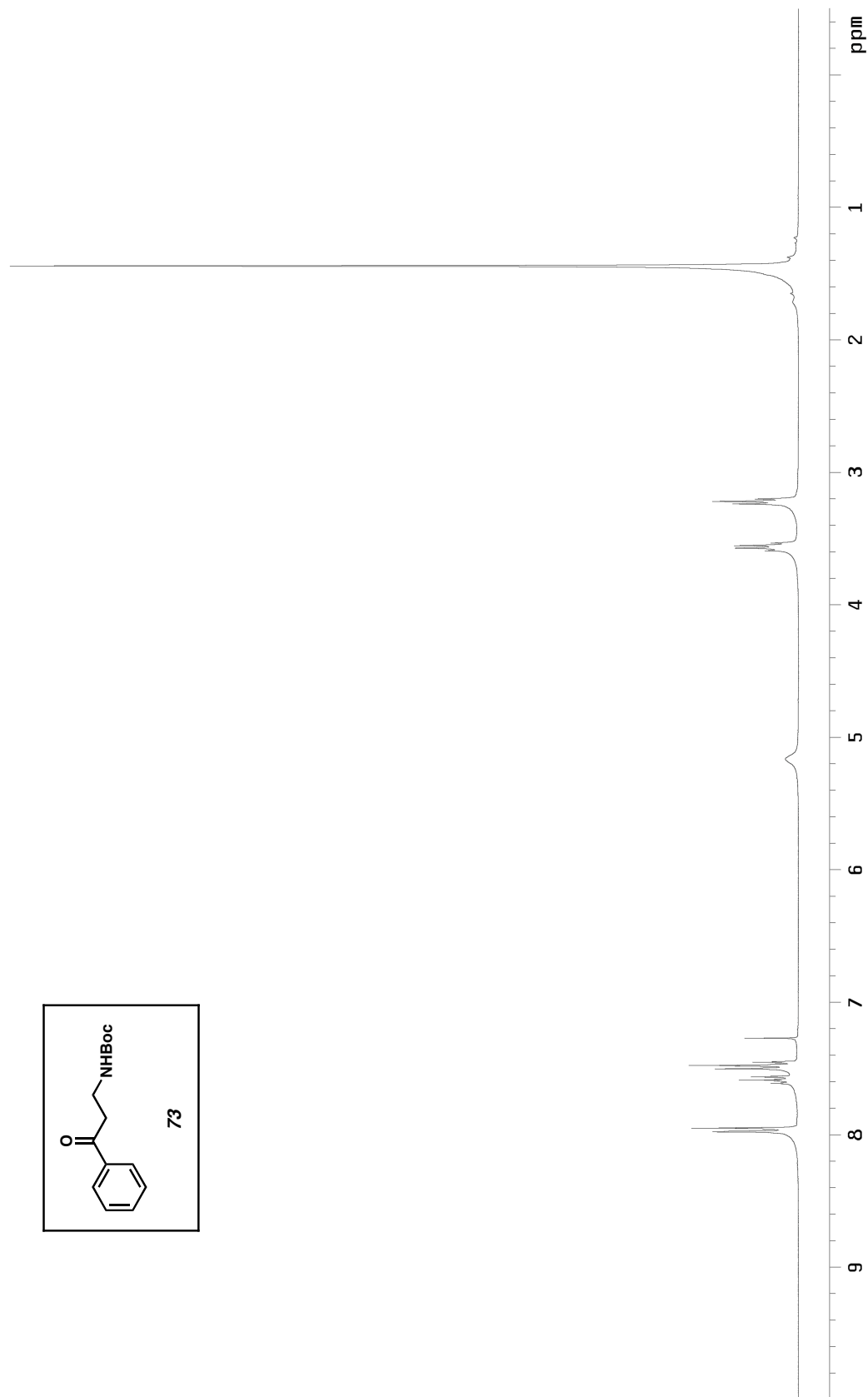
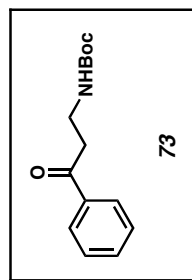


Figure A1.12 <sup>13</sup>C NMR (75 MHz, CDCl<sub>3</sub>) of compound **70**





*Figure A1.13*  $^1\text{H}$  NMR (300 MHz,  $\text{CDCl}_3$ ) of compound **73**

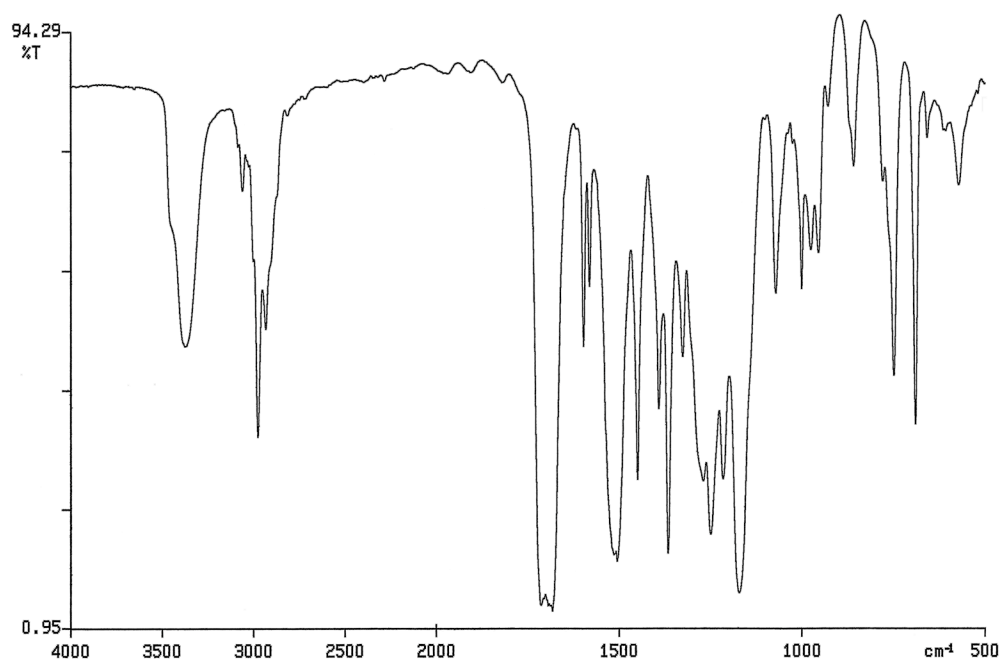


Figure A1.14 Infrared spectrum (thin film/NaCl) of compound **73**

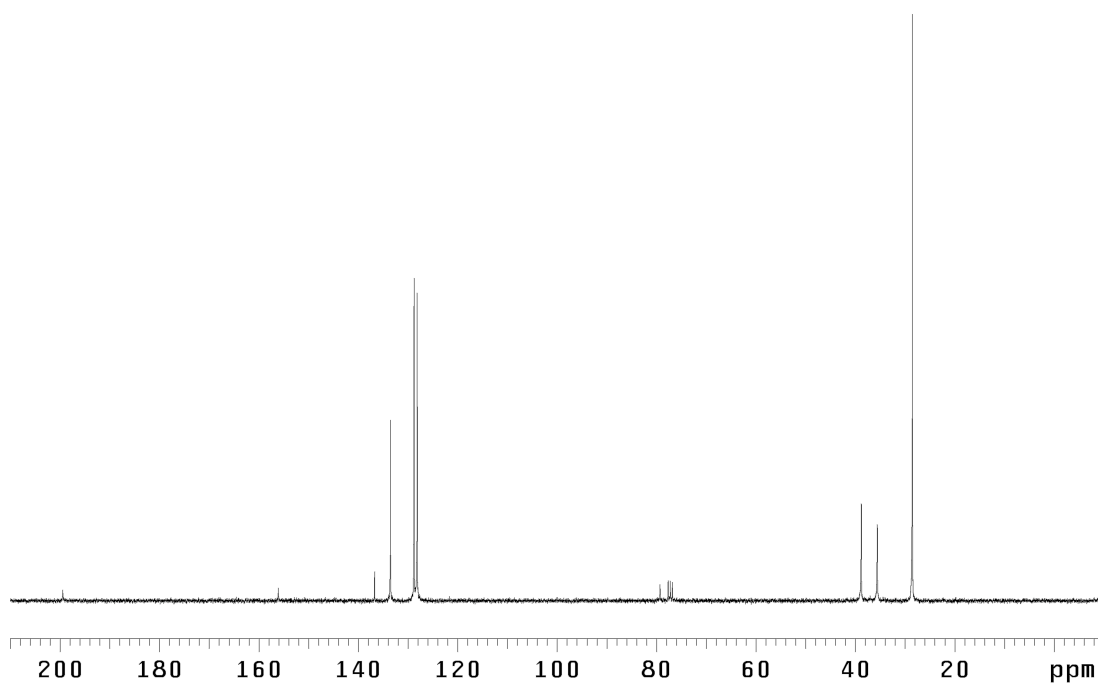


Figure A1.15 <sup>13</sup>C NMR (75 MHz, CDCl<sub>3</sub>) of compound **73**

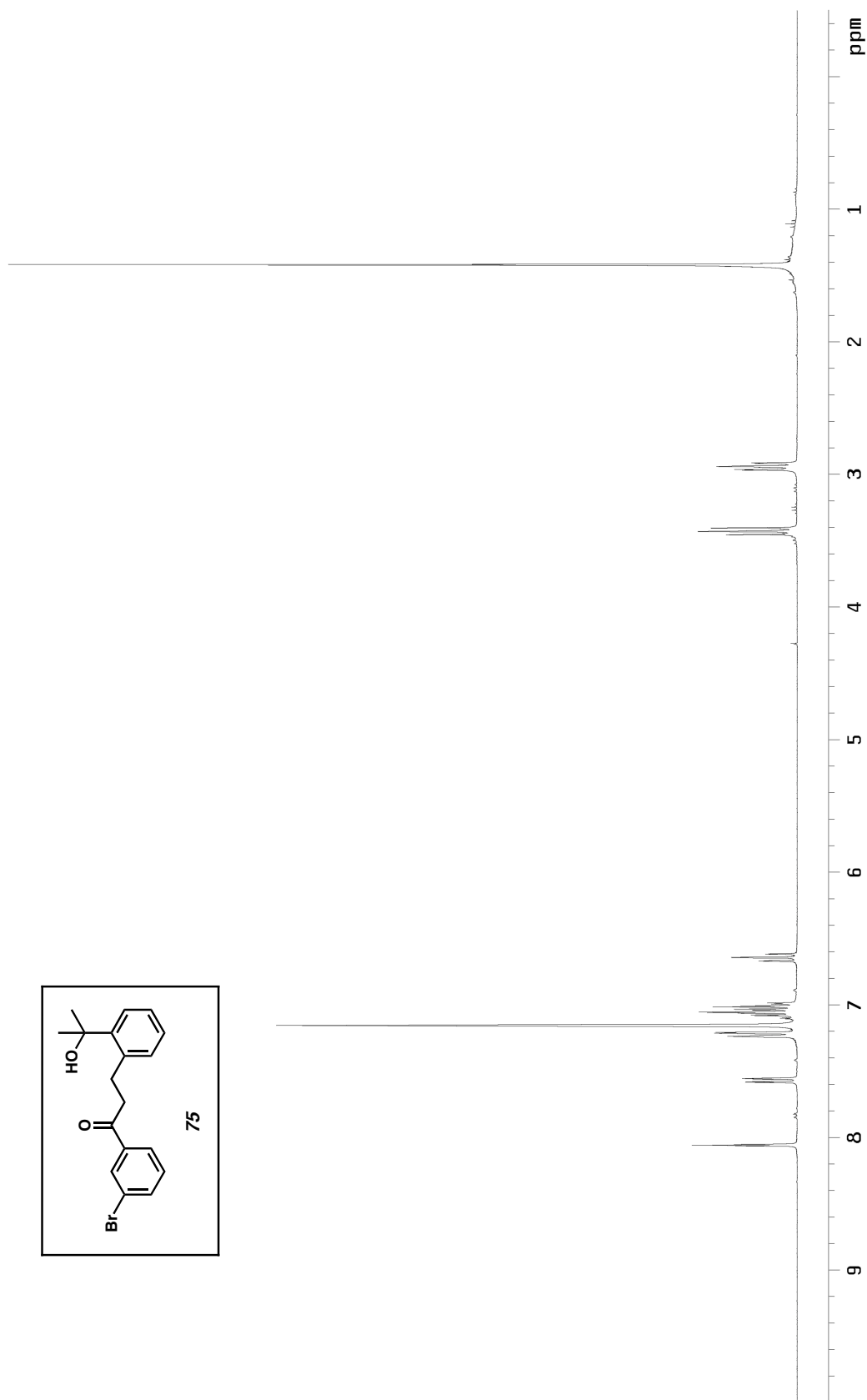


Figure A1.16  $^1\text{H}$  NMR (300 MHz,  $\text{C}_6\text{D}_6$ ) of compound **75**

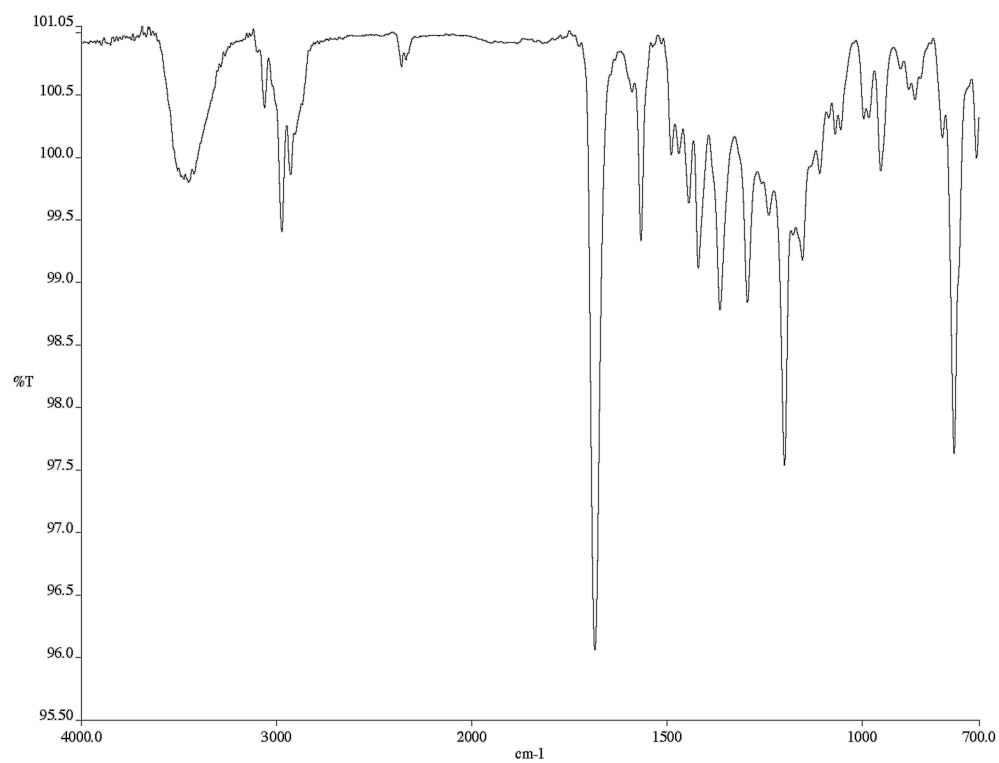


Figure A1.17 Infrared spectrum (thin film/NaCl) of compound **75**

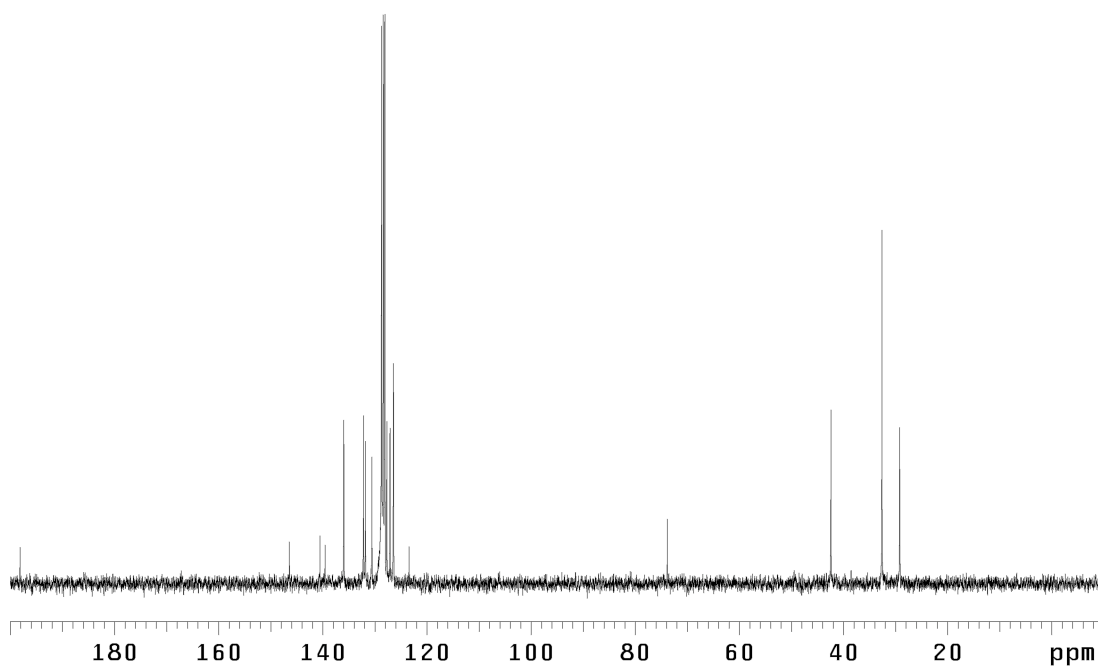


Figure A1.18 <sup>13</sup>C NMR (75 MHz, C<sub>6</sub>D<sub>6</sub>) of compound **75**

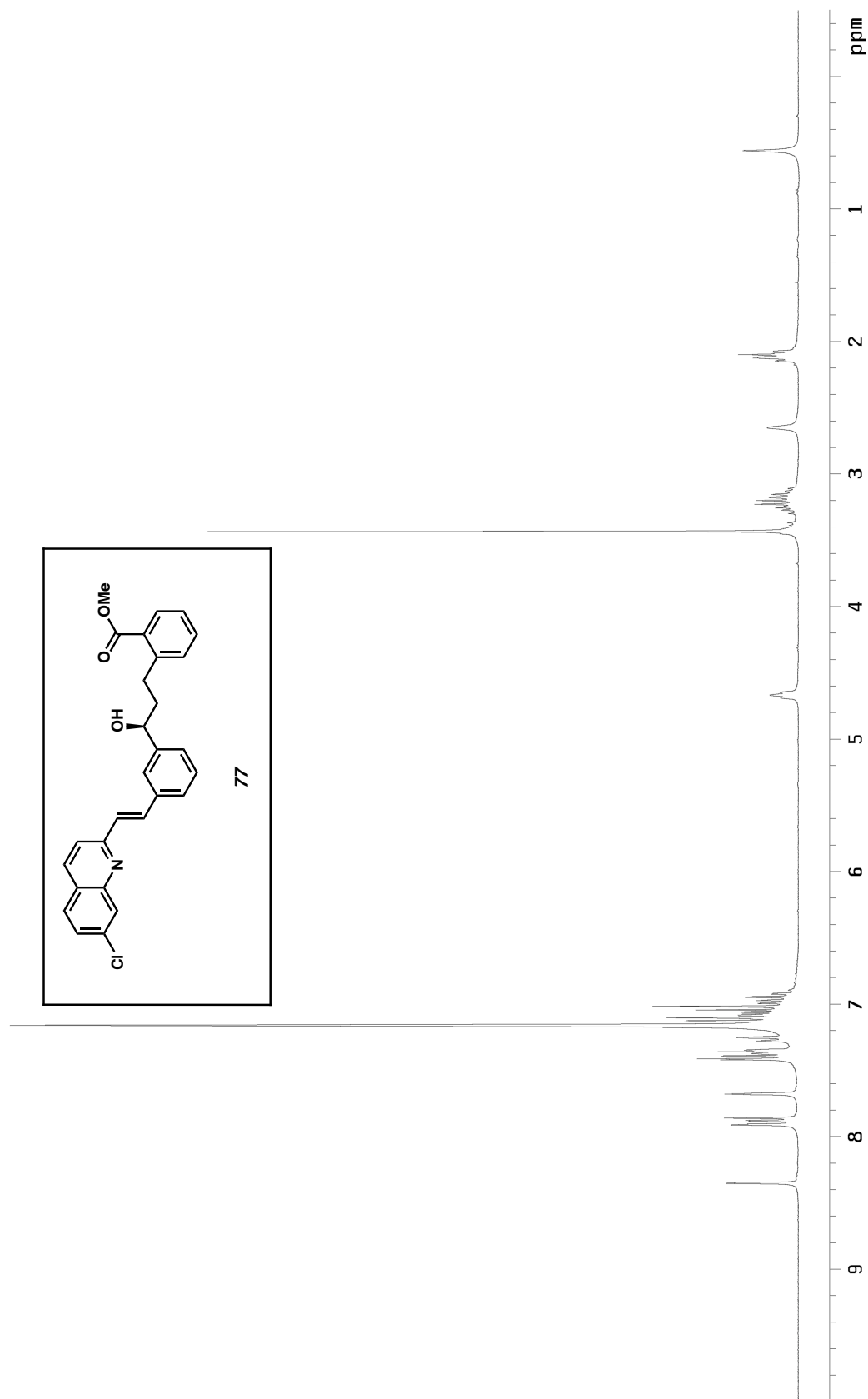


Figure A1.19  $^1\text{H}$  NMR (300 MHz,  $\text{C}_6\text{D}_6$ ) of compound **77**

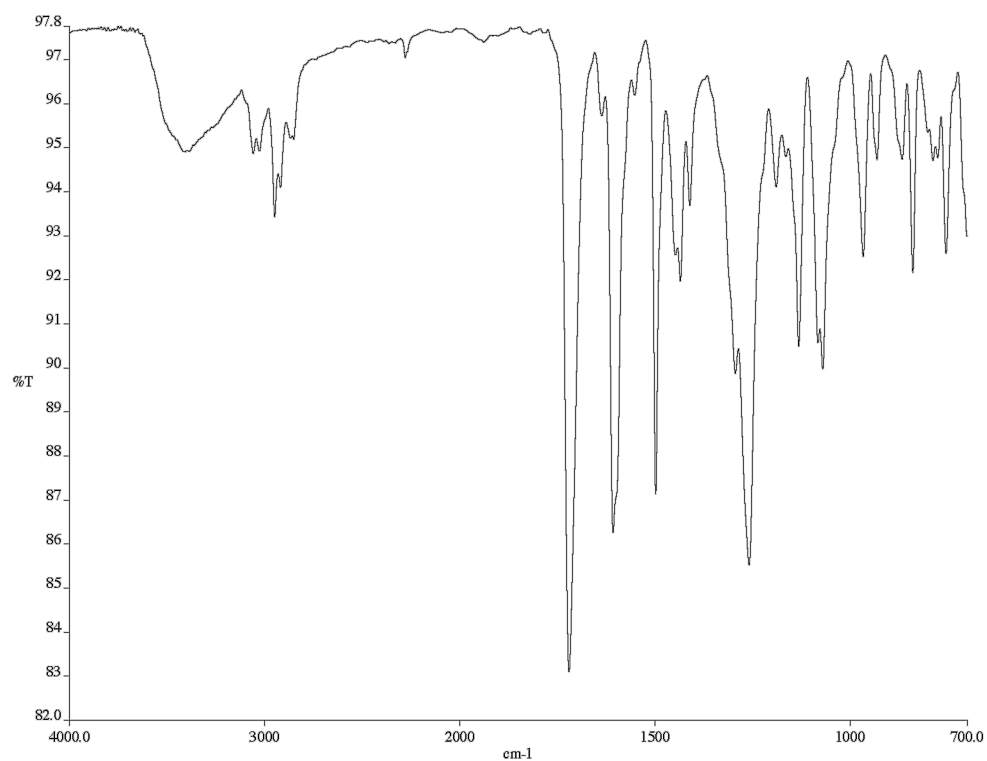


Figure A1.20 Infrared spectrum (thin film/NaCl) of compound **77**

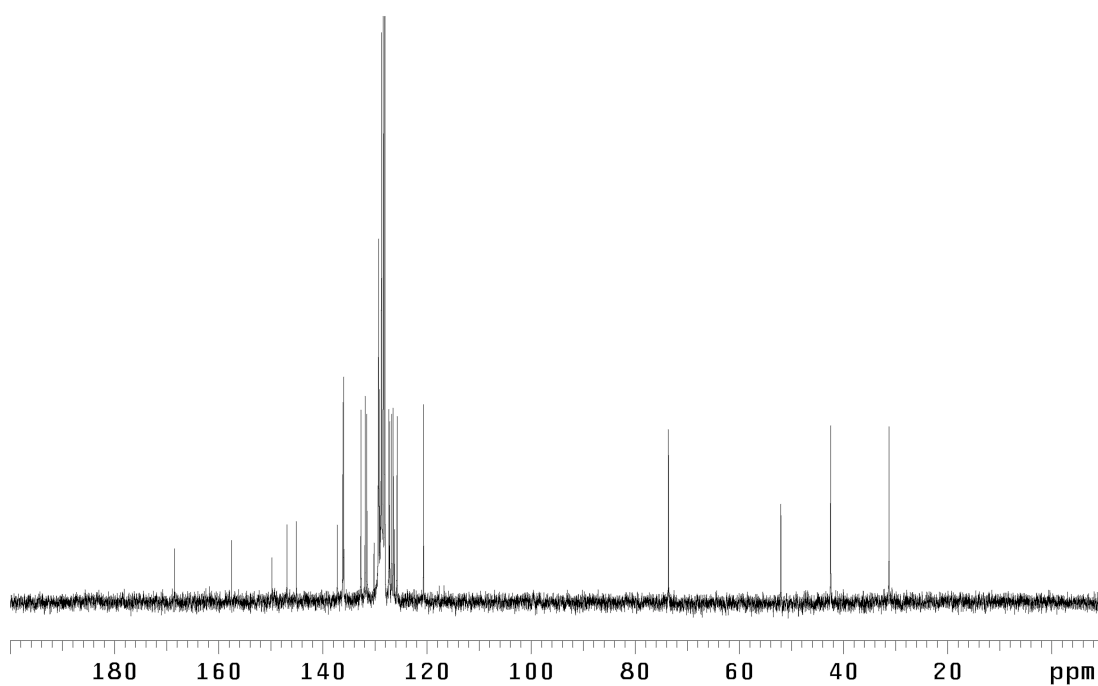


Figure A1.21 <sup>13</sup>C NMR (75 MHz, C<sub>6</sub>D<sub>6</sub>) of compound **77**

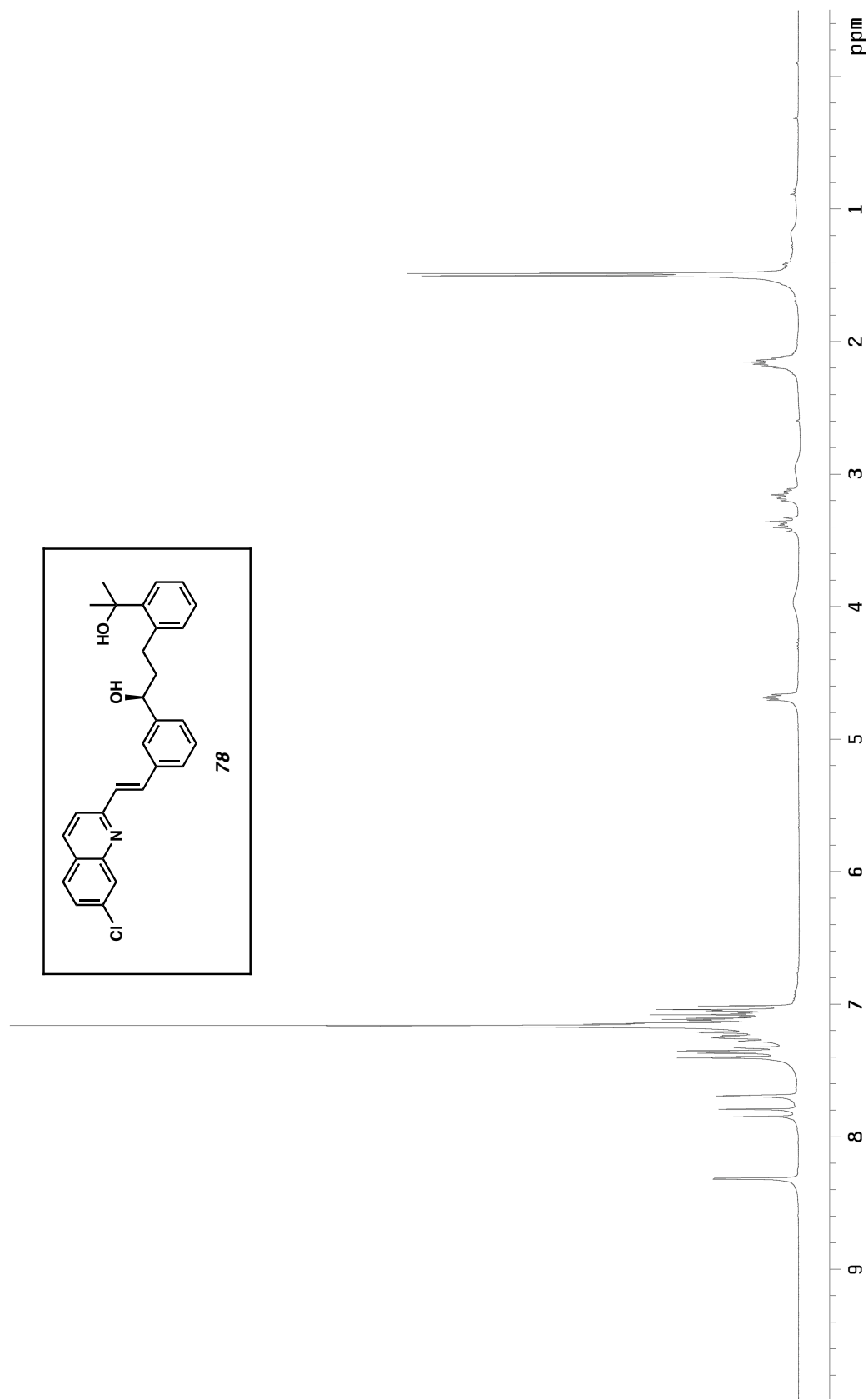


Figure A1.22  $^1\text{H}$  NMR (300 MHz,  $\text{CDCl}_3$ ) of compound **78**

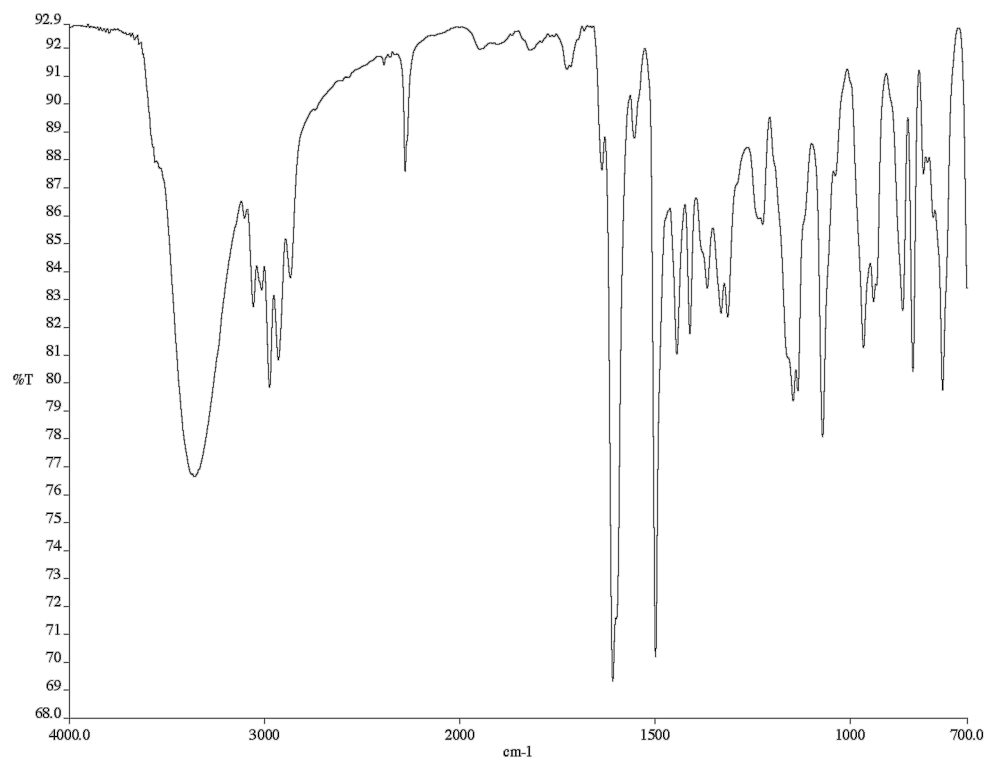


Figure A1.23 Infrared spectrum (thin film/NaCl) of compound **78**

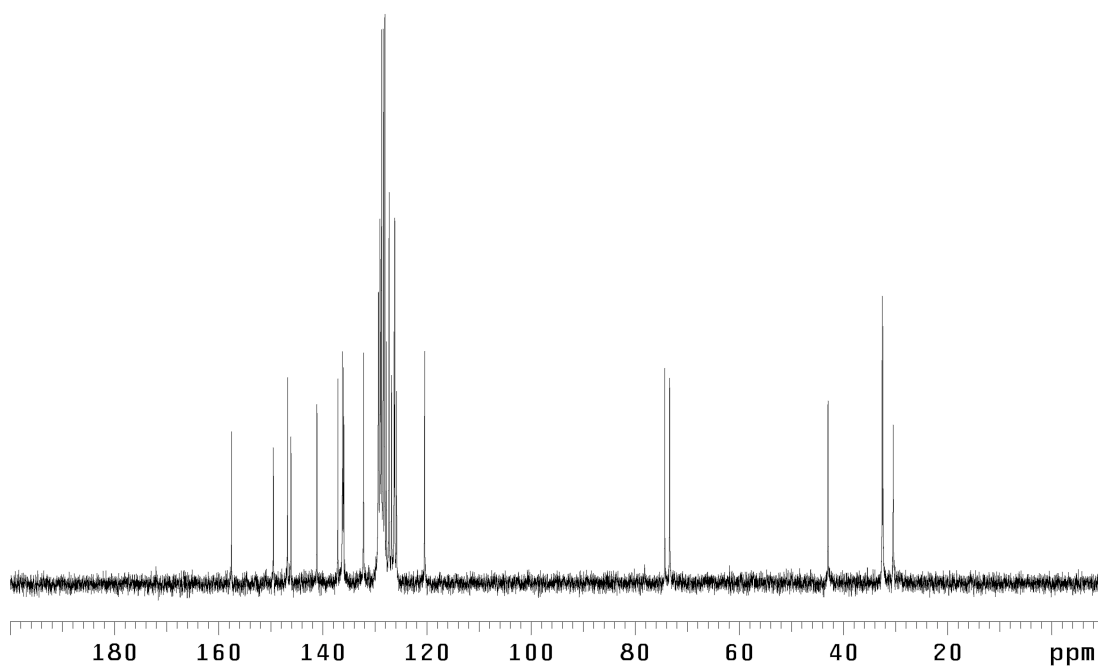


Figure A1.24 <sup>13</sup>C NMR (75 MHz, C<sub>6</sub>D<sub>6</sub>) of compound **78**



## CHAPTER THREE

### The Total Syntheses of (+)- and (-)-Dragmacidin F<sup>†</sup>

#### 3.1 Background

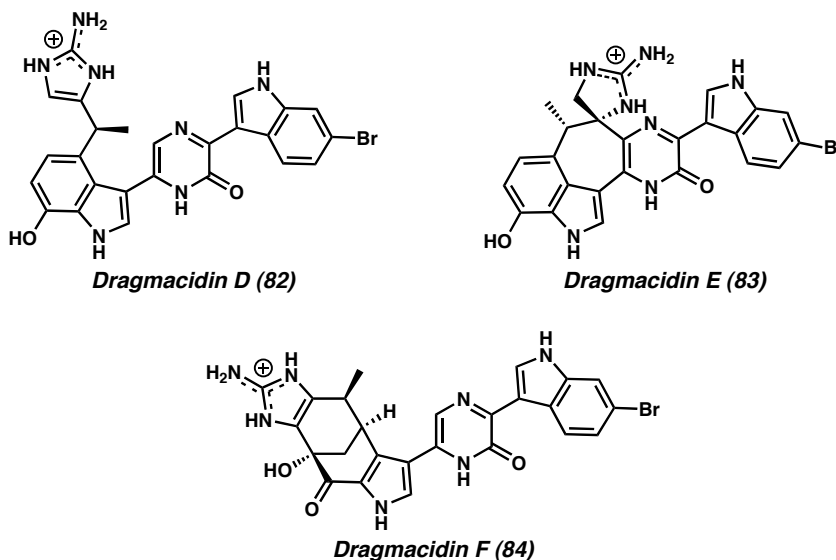
##### 3.1.1 Introduction

Over the past several decades, the search for natural products in marine environments has led to the discovery of a number of biologically active bis(indole) alkaloids.<sup>1</sup> These compounds, as well as their unnatural analogs, have shown promise as leads for the development of novel therapeutics, particularly in the area of cancer.<sup>2</sup> Of the many bis(indole) alkaloids found in nature, the dragmacidins have received considerable attention from the scientific community over the past decade due to their broad range of biological activity and complex structures.<sup>3,4,5</sup> This structurally elaborate class of bromoindole marine alkaloids was isolated from a variety of deep-water sponges including *Dragmacidon*, *Halicortex*, *Spongosorites*, and *Hexadella*, and the tunicate *Didemnum candidum*. As part of a research program geared toward the synthesis of complex heterocyclic natural products, our laboratory initiated an effort in the fall of 2000 to synthesize those dragmacidins that possess a pyrazinone core, namely, dragmacidins D, E, and F (Figure 3.1.1, **82–84**).<sup>4</sup>

---

<sup>†</sup> This work was performed in collaboration with Neil K. Garg, a graduate student in the Stoltz group (Ph.D. 2005).

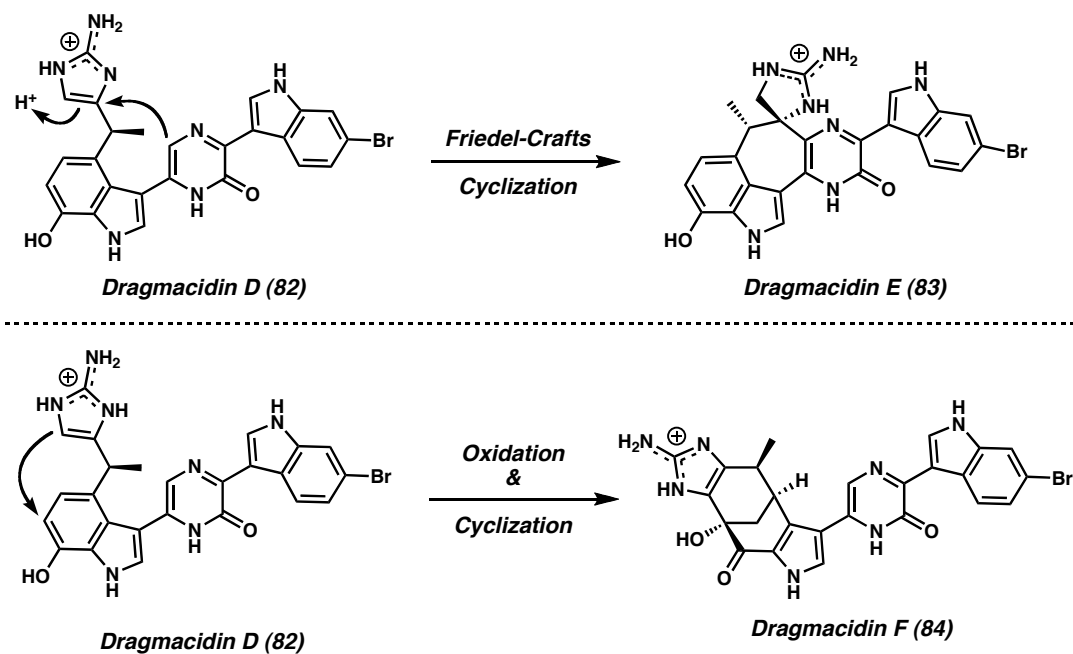
Figure 3.1.1



### 3.1.2 Biosynthesis

Dragmacidin D (**82**),<sup>4a,b</sup> was selected as a primary target predominantly because it was believed to be the biosynthetic precursor to dragmacidins E (**83**) and F (**84**).<sup>4c</sup> (Scheme 3.1.1). Dragmacidins D (**82**) and E (**83**) are related via a Friedel-Crafts cyclization between the pyrazinone and aminoimidazole groups of dragmacidin D, which occurs in order to construct the seven-membered ring of dragmacidin E (i.e., **82** → **83**). Although **84** does not contain a bis(indole) framework, it is presumed to be derived biosynthetically from dragmacidin D (**82**) via an oxidative de-aromatization/cyclization process (i.e., **82** → **84**). Related oxidation pathways for tryptophan derivatives have been observed in nature.<sup>6</sup> Furthermore, dragmacidin D (**82**) seemed to be the least structurally complex of the pyrazinone-containing dragmacidin family members, and therefore a suitable entry point into this class.

Scheme 3.1.1

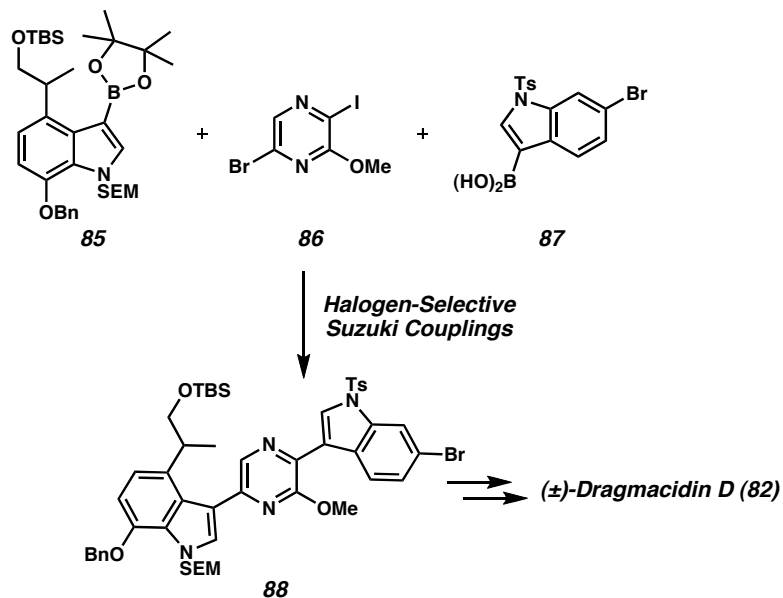


### 3.1.3 Previous Synthetic Studies

In 2002, our laboratory reported the total synthesis of ( $\pm$ )-dragmacidin D (**82**), the first of any of these three unique dragmacidin alkaloids to be prepared.<sup>7</sup> The highly convergent approach to **82** relied on a series of halogen-selective Suzuki cross-couplings of **85**, **86**, and **87** to build the bis(indole)pyrazine skeleton (**88**) of the natural product (Scheme 3.1.2). In addition, the appropriate selection and cleavage sequence of protecting groups proved to be of critical importance, as only highly specific arrangements permitted successful late-stage manipulations. We hypothesized that this general synthetic strategy could also be applied to the other pyrazinone-containing members of the dragmacidin family. Having developed a strategy to construct the bis(indole)pyrazinone core of dragmacidin D (**82**), we set out to extend the scope of our halogen-selective Suzuki coupling methodology to the synthesis of related natural

products. We reasoned that our approach could be amenable to the preparation of the antiviral agent dragmacidin F (**84**),<sup>4c</sup> which is perhaps the most daunting target of the dragmacidin natural products.<sup>8,9</sup>

*Scheme 3.1.2*



### 3.1.4 Isolation and Bioactivity of Dragmacidin F

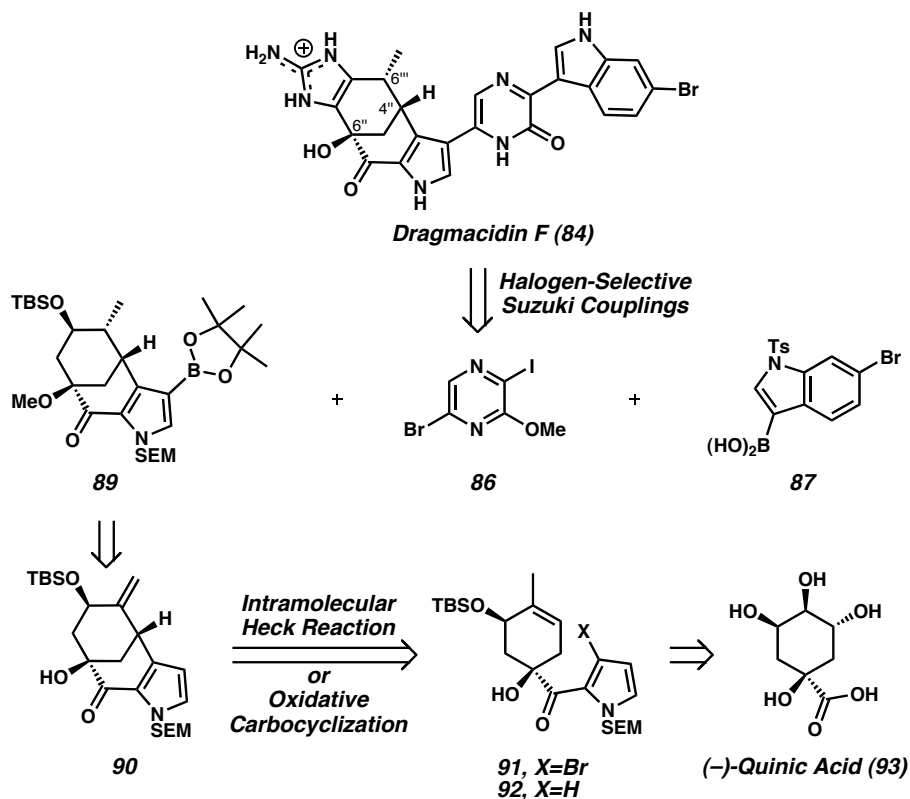
Dragmacidin F (**84**) was isolated in 2000 from the ethanol extracts of the Mediterranean sponge *Halicortex* sp. This marine natural product exhibits in vitro antiviral activity against herpes simplex virus (HSV-I;  $EC_{50} = 95.8 \mu\text{M}$ ) and human immunodeficiency virus (HIV-I;  $EC_{50} = 0.91 \mu\text{M}$ ),<sup>4c</sup> and thus is an attractive target from a biological perspective. In addition, dragmacidin F (**84**) possesses a variety of structural features that make it an attractive target for total synthesis. These synthetic challenges include the differentially substituted pyrazinone, the bridged [3.3.1] bicyclic ring system, which is fused to both the trisubstituted pyrrole and aminoimidazole heterocycles, and the

installation and maintenance of the 6-bromoindole fragment. Given the limited supply of dragmacidin F (**84**) available from natural sources, a successful synthetic approach to **84** could also facilitate the production of sufficient quantities of material needed for advanced biological studies.

### 3.1.5 Retrosynthetic Analysis of Dragmacidin F

Our retrosynthetic analysis for dragmacidin F (**84**) is shown in Scheme 3.1.3. On the basis of our experience with dragmacidin D (**82**), we reasoned that the aminoimidazole moiety would best be incorporated at a late stage in the synthesis.<sup>7</sup> The carbon skeleton of the natural product would then arise via a series of halogen-selective Suzuki cross-coupling reactions (**89** + **86** + **87**). Pyrazine **86** and indoloboronic acid **87** were both readily accessible,<sup>7</sup> while pyrroloboronic ester **89** perhaps could be derived from pyrrole-fused bicycle **90**, our key retrosynthetic intermediate. We then targeted bicycle **90** from two related directions: a Pd(0)-mediated intramolecular Heck reaction<sup>10</sup> of bromopyrrole **91**, and a Pd(II)-promoted oxidative carbocyclization<sup>11</sup> involving *des*-bromopyrrole **92**. The successful implementation of the latter method was particularly attractive since it is closely aligned with our interest in Pd(II)-catalyzed dehydrogenation reactions.<sup>12</sup> Both of the cyclization substrates (**91** and **92**) could be prepared from commercially available (–)-quinic acid (**93**).<sup>13</sup> At the time of this synthetic effort, the absolute stereochemistry of natural dragmacidin F (**84**) was not known; thus, the absolute stereochemistry of our target (**84**) was chosen arbitrarily.

## Scheme 3.1.3



## 3.2 The Total Synthesis of (+)-Dragmacidin F

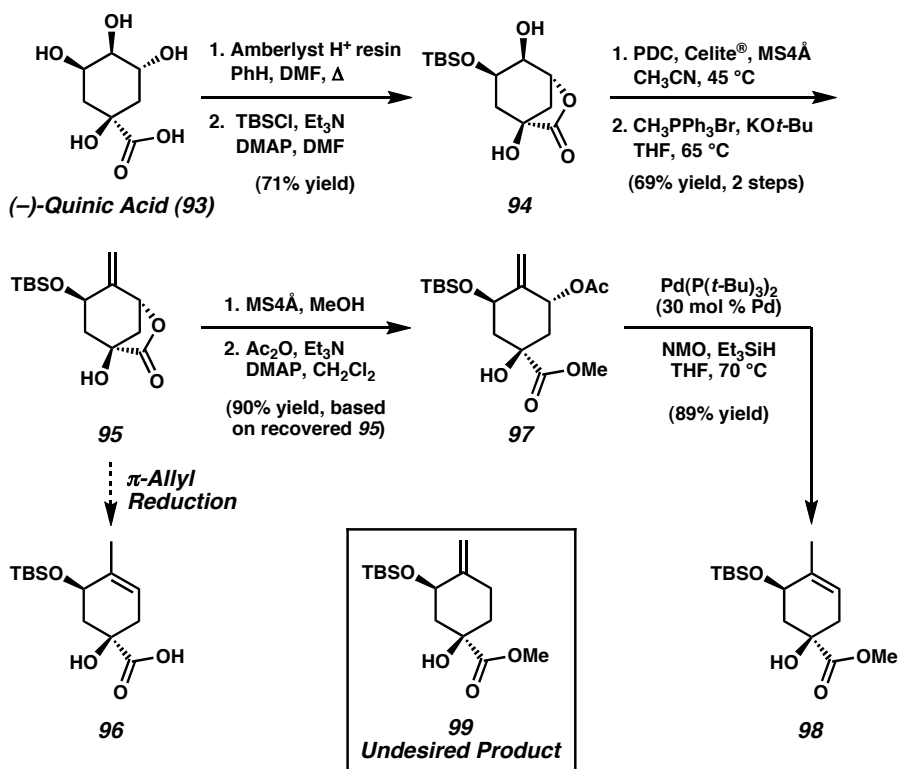
## 3.2.1 Synthesis of Cyclization Substrates

Our synthesis of dragmacidin F (**84**) began with a known two-step protocol involving lactonization and silylation of (–)-quinic acid (**93**) to afford bicyclic lactone **94** (Scheme 3.2.1).<sup>14</sup> Subsequent oxidation and Wittig olefination of **94** produced exomethylene lactone **95** in good yield. Initially, we envisioned the direct conversion of lactone **95** to unsaturated carboxylic acid **96** by executing a homogeneous Pd(0)-catalyzed  $\pi$ -allyl hydride addition reaction.<sup>15</sup> Despite considerable experimentation, however, exposure of lactone **95** to a variety of Pd and hydride sources under standard conditions<sup>15</sup> led to the formation of complex product mixtures. As a result, a more

stepwise approach was tried. Methanolysis of lactone **95** followed by acetylation of the resulting 2° alcohol<sup>16</sup> gave rise to allylic acetate **97**, another potential substrate for  $\pi$ -allyl reduction chemistry. Although **97** did react under most literature protocols, undesired exocyclic olefin **99** was typically the major product observed, and **98** could not be isolated by conventional purification techniques. This was not an altogether unexpected outcome; in fact, overcoming the practical problem of regioselectivity (e.g., **98** vs. **99**) in nucleophilic addition to  $\pi$ -allylpalladium complexes has been the subject of intense study.<sup>17</sup>

After substantial optimization, we were able to access **98** as the major product by employing stoichiometric  $\text{Pd}(\text{P}(t\text{-Bu})_3)_2$ <sup>18</sup> in the presence of triethylsilane as a reductant. Further refinements designed to facilitate catalysis led to a reduced Pd loading (30 mol %) when *N*-methylmorpholine-*N*-oxide (NMO) was used as an additive.<sup>19</sup> Under these conditions, cyclohexene **98** was obtained in 89% yield as a single olefin regioisomer. Unfortunately, this transformation often gave inconsistent results and was particularly sensitive to oxygen, water, and the quality of  $\text{Et}_3\text{SiH}$ . These difficulties coupled with the high catalyst loading resulted in substantial material throughput problems. We therefore sought yet another method to prepare cyclohexene **98**, or a closely related derivative thereof (i.e., **96**), in a more facile and preparative manner.

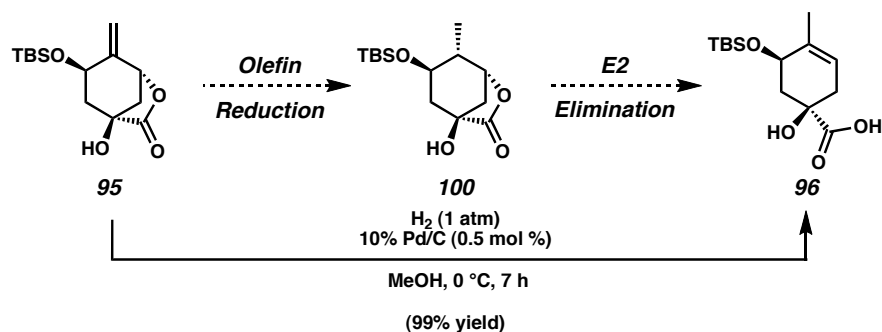
Scheme 3.2.1



In our revised plan, we conceived a two-step route to obtain carboxylic acid **96** via diastereoselective reduction of olefin **95** followed by base-promoted elimination of the carboxylate functionality of **100** (Scheme 3.2.2). The first part of this sequence was attempted by exposing olefin **95** to standard catalytic hydrogenation conditions (Pd/C, 1 atm H<sub>2</sub>). Surprisingly, these conditions led to the production of a compound that was more polar than we expected for simple olefin hydrogenation (i.e., **100**). To our delight, the product was identified as unsaturated carboxylic acid **96**. Under our optimized reaction conditions (0.5 mol % Pd/C, 1 atm H<sub>2</sub>, MeOH, 0 °C), essentially quantitative reductive isomerization to **96** was observed.<sup>20,21</sup>

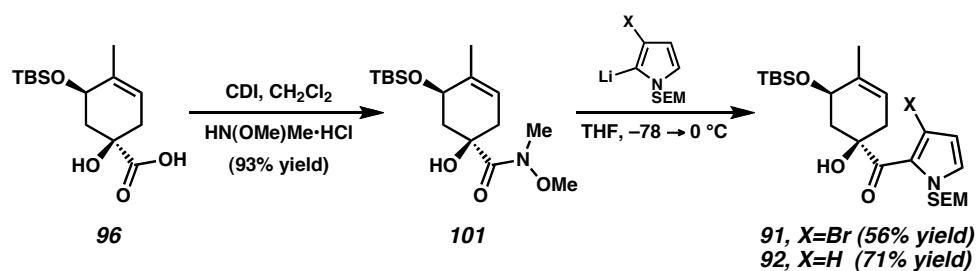


Scheme 3.2.2



With facile access to cyclohexene carboxylic acid **96**, preparation of the key cyclization precursors proceeded without difficulty. Activation of acid **96** with CDI followed by the addition of  $\text{HN}(\text{OMe})\text{Me}\cdot\text{HCl}$  afforded Weinreb amide **101** (Scheme 3.2.3). The Weinreb amide functionality was then displaced with the appropriate lithiopyrrole<sup>22</sup> reagent to produce Heck cyclization substrate **91**<sup>23</sup> and oxidative cyclization substrate **92**.

Scheme 3.2.3

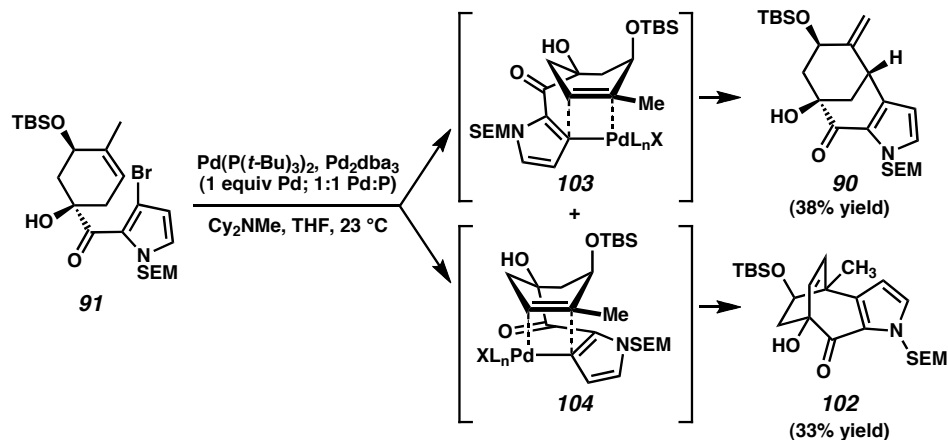


### 3.2.2 Intramolecular Heck Cyclization

With the pyrrole-fused cyclohexene substrates in hand, Neil Garg carried out extensive studies in order to achieve the intramolecular Heck cyclization of bromopyrrole

**91**. Attempts to utilize standard procedures were unsuccessful,<sup>10</sup> likely due to the thermal instability of the bromopyrrole moiety. However, implementation of the room-temperature conditions developed by Fu<sup>24</sup> provided the desired [3.3.1] bicyclic product (**90**), albeit in low yield (Scheme 3.2.4). Unfortunately, the formation of **90** was hampered by competitive production of [3.2.2] bicycle **102**. Although efforts to optimize temperature, solvent, base, and concentration were not met with success, it was found that increased quantities of Pd improved the ratio of the desired [3.3.1] bicycle (**90**) to the undesired [3.2.2] bicycle (**102**). In addition, the ratio of **90** to **102** decreased over time,<sup>25</sup> suggesting that the active catalytic species varied during the course of the reaction or that selectivity changed as the concentration of  $R_3NH^+Br^-$  increased.

Scheme 3.2.4

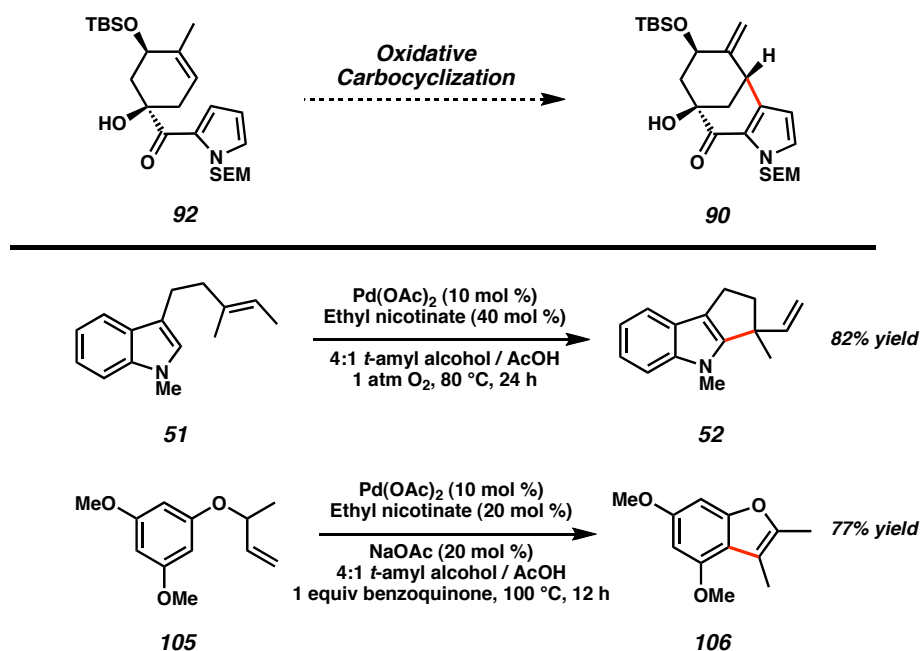


### 3.2.3 Intramolecular Oxidative Cyclization

Although the Heck reaction was useful for preparing reasonable quantities of bicycle **90**, an alternative and potentially more selective route to **90** was desired. In conjunction with ongoing research in our group,<sup>12</sup> we turned to the Pd(II)-mediated C–C

bond forming approach. In this scenario, C(3)-unsubstituted pyrrole **92** would undergo intramolecular carbocyclization to afford **90** (Scheme 3.2.5). Previously in our laboratories, indoles (e.g., **51**) and electron-rich aryl ethers (e.g., **105**) had been shown to be competent cyclization substrates. However, pyrrole heterocycles had never been tested in this regard, especially not to form bridged bicycles.

Scheme 3.2.5



As a starting point, stoichiometric Pd(II) was employed for the oxidative cyclization reaction to eliminate the need for a co-oxidant, which could complicate preliminary studies. Catalytic methods could, in theory, be devised once these stoichiometric conditions were optimized. Protocols reported by our group were initially tried, however, these conditions did not afford any of desired bicycle **90** (Table 3.2.1, entry 1). Indeed, initial experimentation revealed that neither pyridine, ethyl nicotinate,

nor triphenylphosphine were effective ligands for promoting cyclization in the presence of  $\text{Pd}(\text{OAc})_2$ .<sup>12c,d</sup>

Although these initial conditions failed, a control experiment omitting the ligand did produce a trace amount of desired bicycle **90** (entry 2). Interestingly, a number of byproducts were also discovered in the reaction pot of entry 2, which appeared to be caused by *t*-amyl alcohol incorporation into the starting material and product.<sup>26</sup> Thus, substituting *t*-butyl alcohol for *t*-amyl alcohol as solvent (entry 3) and conducting the reaction under an atmosphere of dioxygen led to the consumption of all starting material and production of desired bicycle **90** as the major product by crude  $^1\text{H}$  NMR in 15% isolated yield.<sup>27</sup>

Table 3.2.1

**92**  $\xrightarrow[\text{Oxidative Heck Reaction}]{\text{Pd(II)-Mediated}}$  **90** + **102**

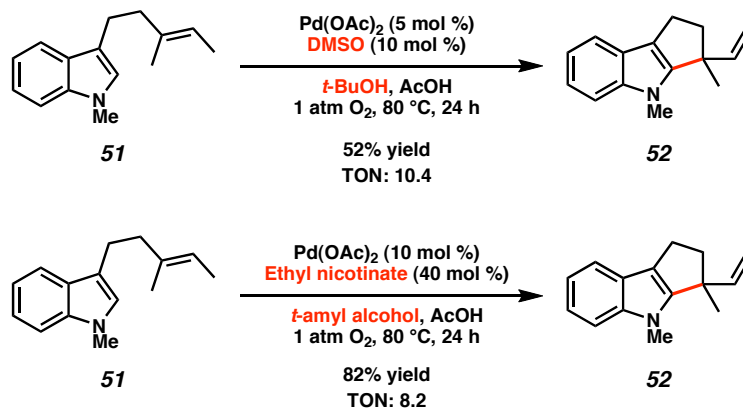
entry	conditions	result	
1	$\text{Pd}(\text{OAc})_2$ (stoichiometric or cat w/ $\text{O}_2$ ) ethyl nicotinate, pyridine or $\text{PPh}_3$ <i>t</i> -amyl OH, AcOH, 80 °C	no reaction, starting material recovered	
2	$\text{Pd}(\text{OAc})_2$ (1 equiv) <i>t</i> -amyl OH, AcOH, 80 °C	<b>90</b> trace	<b>102</b> not observed
3	$\text{Pd}(\text{OAc})_2$ (1 equiv) <i>t</i> -BuOH, AcOH, 80 °C, $\text{O}_2$	<b>90</b> 15% yield	<b>102</b> not observed
4	$\text{Pd}(\text{OAc})_2$ (stoichiometric or cat w/ $\text{O}_2$ ) ethyl nicotinate, pyridine or $\text{PPh}_3$ <i>t</i> -BuOH, AcOH, 80 °C	no reaction, starting material recovered	
5	$\text{Pd}(\text{OAc})_2$ (1 equiv), DMSO <i>t</i> -BuOH, AcOH, 80 °C, 2 h	<b>90</b> 56% yield	<b>102</b> not observed
6	$\text{Pd}(\text{OAc})_2$ (1 equiv), DMSO dioxane, AcOH, 80 °C, 7.5 h	<b>90</b> 41% yield	<b>102</b> not observed
7	$\text{Pd}(\text{OAc})_2$ (1 equiv), DMSO <i>t</i> -BuOH, AcOH, 60 °C, 10 h	<b>90</b> 74% yield	<b>102</b> not observed

Upon learning that the use of *t*-amyl alcohol was deleterious to this cyclization, both pyridine and phosphine-based ligands were reinvestigated with *t*-butanol (entry 4). Unfortunately, however, the desired transformation was rendered inactive under these conditions. On the basis of these results, we hypothesized that an ideal ligand would be sufficient to stabilize the palladium complex without being overly coordinating as to halt the reactivity in the cyclization.<sup>28</sup> Thus, a focused investigation of possible ligands was undertaken. A marked improvement was realized when DMSO was employed;<sup>29</sup> the desired cyclization product could be obtained in 56% yield (entry 5). Dioxane was also competent as a *t*-butanol substitute, though a diminished yield of product was obtained (entry 6). Subsequent optimization of temperature, solvent, and reaction time led to an ideal set of conditions whereby the desired [3.3.1] bicycle (**90**) was isolated as the sole product in 74% yield (entry 7). This transformation is particularly noteworthy since it results in functionalization of the electronically deactivated and sterically congested C(3) position of acyl pyrrole **92**.<sup>30,31</sup> Importantly, the undesired [3.2.2] bicycle (**102**) seen as a byproduct in the classical Heck reaction has never been observed as a product of the oxidative Heck cyclization of substrate **92**.

Despite considerable experimentation, we were unable to render the conversion of acyl pyrrole **92** to bicycle **90** catalytic in Pd in the presence of a stoichiometric oxidant (e.g., O<sub>2</sub> or benzoquinone). This difficulty has been attributed to the extreme sensitivity of both the starting material and desired product to oxidative decomposition.<sup>32,33</sup> This hypothesis is corroborated by related catalytic pyrrole cyclizations that were described after the report of this work,<sup>34</sup> as well as an unoptimized study that we conducted in the conversion of **51** → **52** (Scheme 3.2.6). Applying our DMSO-based conditions in the

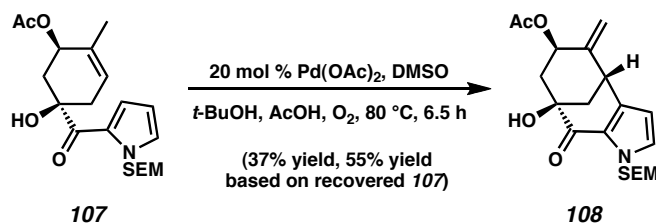
same cyclization yields a similar turnover number (10.4) to the one initially reported (8.2).<sup>12c</sup> These collective results suggest that palladium is capable of reoxidation under these conditions, and thus in principle, is also able to function in a catalytic manner.

*Scheme 3.2.6*




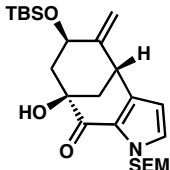

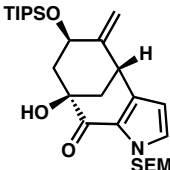
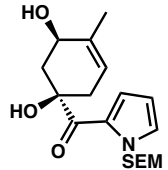

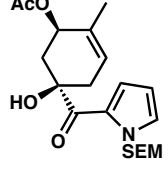
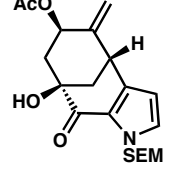
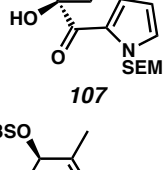
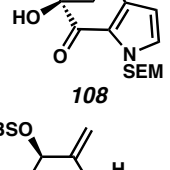

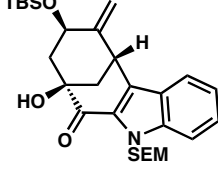
Notably, we have observed some catalysis in the cyclization of a closely related substrate, acetate **107** (Scheme 3.2.7). In this case, oxidative Heck cyclization using 20 mol %  $\text{Pd}(\text{OAc})_2$ , under 1 atm of  $\text{O}_2$ , afforded [3.3.1] bicycle **108** in 37% yield (55% based on recovered **107**). As isolated yields and catalyst turnover for this process were low, and bicycle **108** was not directly useful for our total synthesis goals, we elected to utilize the stoichiometric Pd-mediated oxidative Heck reaction (**92**  $\rightarrow$  **90**) as a means to advance material en route to dragmacidin F.

Scheme 3.2.7



We also explored the Pd(II)-mediated carbocyclization of a number of substrates related to TBS ether **92** (Table 3.2.2, entry 1). For instance, the TIPS ether analog (entry 2) underwent cyclization, albeit in lower yield with respect to the parent TBS compound. However, if the 2° alcohol was left unprotected altogether (entry 3)<sup>35</sup> or the substrate possessed a 3° methyl ether (entry 4)<sup>36</sup>, formation of the desired bicyclic products was not observed. Interestingly, the acetate derivative readily participated in the cyclization reaction (entry 5). As previously described, exposure of the acetate substrate to catalytic conditions (20 mol % Pd, 1 atm O<sub>2</sub>) also led to the formation of the desired product, although in modest yield with a TON of 1.9 (entry 6). It was also possible to annulate C(3) of related indole substrates under our standard conditions (entry 7).

Table 3.2.2<sup>a</sup>

entry	substrate	product	temp (°C)	time	yield <sup>b</sup>
1	 <b>92</b>	 <b>90</b>	60	10 h	74%
2	 <b>109</b>	 <b>110</b>	60	13.5 h	51% (63%)
3	 <b>111</b>	—	80	complex mixture	
4	 <b>112</b>	—	80	no reaction	
5	 <b>107</b>	 <b>108</b>	80	1.8 h	53% (66%)
6	 <b>107</b>	 <b>108</b>	80 <sup>c</sup>	6.5 h	37% (55%)
7	 <b>113</b>	 <b>114</b>	80	2.5 h	49%

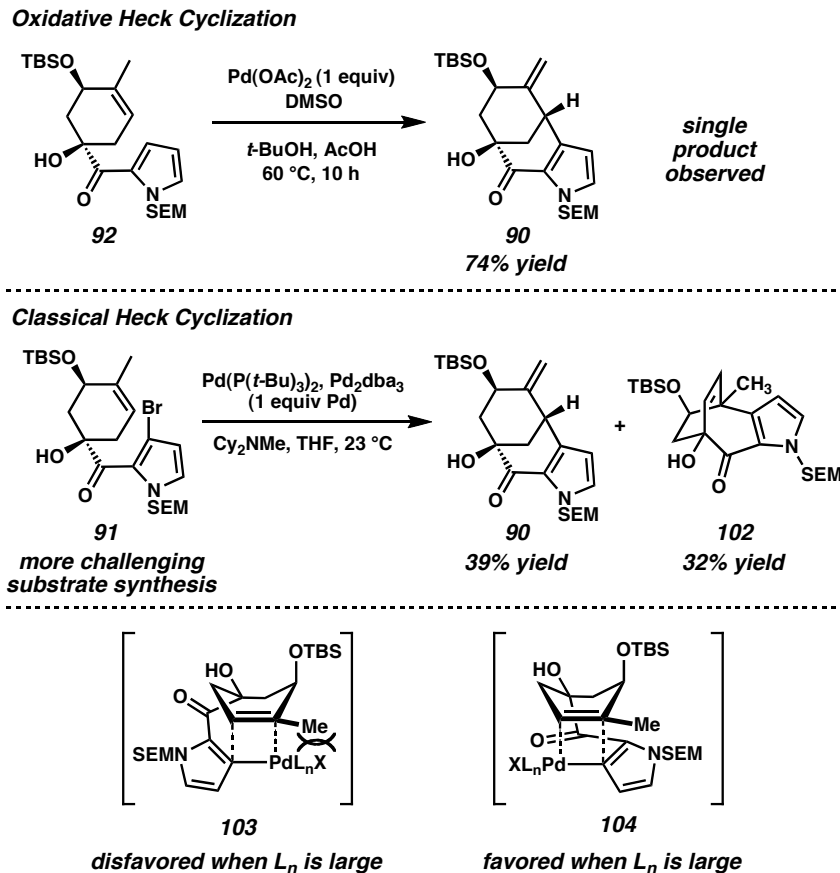
<sup>a</sup> Standard Conditions: 1 equiv Pd(OAc)<sub>2</sub>, 2 equiv DMSO, *t*-BuOH:AcOH (4:1, 0.01 M). <sup>b</sup> Isolated Yield. Number in parentheses represents the yield based on recovered starting material. <sup>c</sup> 20 mol % Pd(OAc)<sub>2</sub>, 40 mol % DMSO, *t*-BuOH:AcOH (4:1, 0.01 M), O<sub>2</sub> (1 atm)

In the context of our total synthesis objective, the oxidative Heck reaction strategy is advantageous compared to the classical Heck route for preparing [3.3.1] bicycle **90** on



the basis of several factors (Scheme 3.2.8): a) the oxidative Heck approach does not require the synthesis of a halogenated starting material (i.e., **91**), which can sometimes be significantly challenging;<sup>23,37</sup> b) using identical palladium loadings, the oxidative Heck cyclization provides bicycle **90** in nearly twice the chemical yield as the classical Heck reaction; c) the oxidative Heck reaction furnishes bicycle **90** as a single product, whereas the classical Heck reaction requires a more tedious chromatographic separation of the undesired [3.2.2] bicycle (**102**). Although more detailed mechanistic studies are pending, we partially attribute the differences in product distribution between the two strategies to the effects of ligands. More specifically, the use of bulky  $P(t\text{-Bu})_3$  ligands in the classical Heck cyclization could favor olefin insertion transition state **104** over **103**, as it would place the large  $\text{PdL}_n\text{X}$  away from the more substituted position of the olefin undergoing insertion.

Scheme 3.2.8

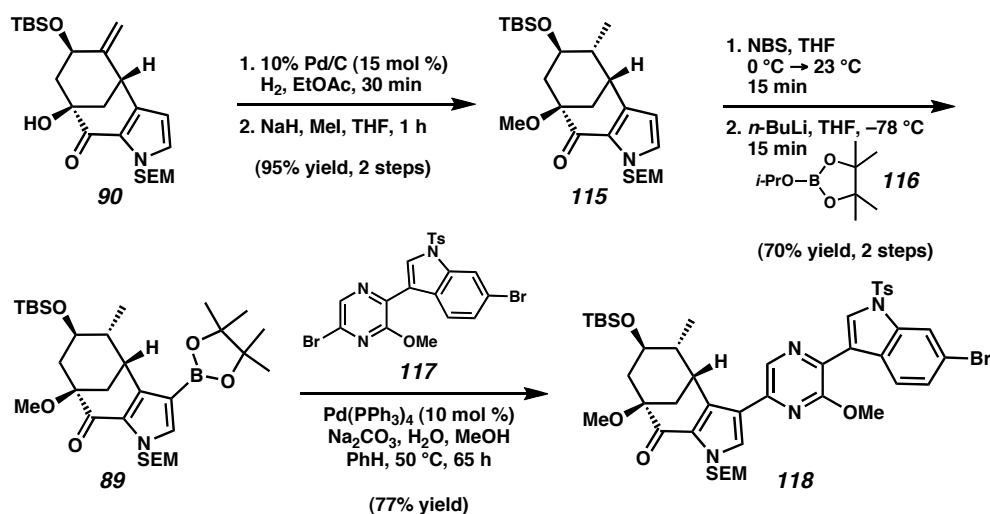


### 3.2.4 Assembling the Carbon Skeleton of Dragmacidin F

With the [3.3.1] bicyclic framework in hand (i.e., **90**), we focused our attention on constructing the full carbon skeleton of dragmacidin F (**118**, Scheme 3.2.9). The final stereocenter present in the natural product was installed via catalytic hydrogenation of olefin **90**, and was followed by methylation of the 3° alcohol to produce bis(ether) **115**. The methyl protecting group was selected initially for its robustness<sup>16</sup> and would presumably allow for the exploration of late-stage chemistry in the form of a model system.<sup>38</sup> Methyl ether **115** was then elaborated via regioselective bromination of the pyrrole and metalation to boronic ester **89**. In the critical halogen-selective Suzuki

fragment coupling, pyrroloboronic ester **89** was reacted with dibromide **117** (prepared from **86** + **87**)<sup>7</sup> under Pd(0) catalysis. By analogy to our dragmacidin D studies,<sup>7</sup> we were pleased to find that at 50 °C, the desired C–C bond forming reaction took place to afford the fully coupled product (**118**) in 77% yield. Importantly, the indolylbromide moiety was maintained under these reaction conditions.

Scheme 3.2.9

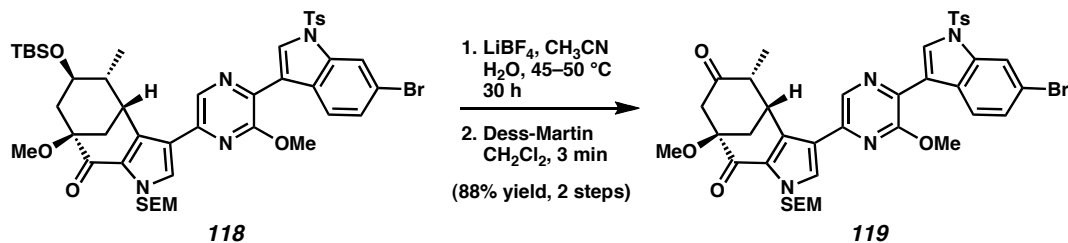


### 3.2.5 End-Game: Total Synthesis of (+)-Dragmacidin F

With the carbon framework completed, few tasks remained in order to finish the total synthesis of dragmacidin F (**84**), namely, removal of all protecting groups and installation of the aminoimidazole unit. Of particular note is the similarity of these synthetic challenges to those encountered in our total synthesis of dragmacidin D (**82**).<sup>7</sup> Not surprisingly, we decided to utilize the methods that were already familiar to us in order to elaborate **118** to the desired natural product (**84**). To this end, we anticipated that the presence of an amino group  $\alpha$  to the ketone would allow for eventual introduction of

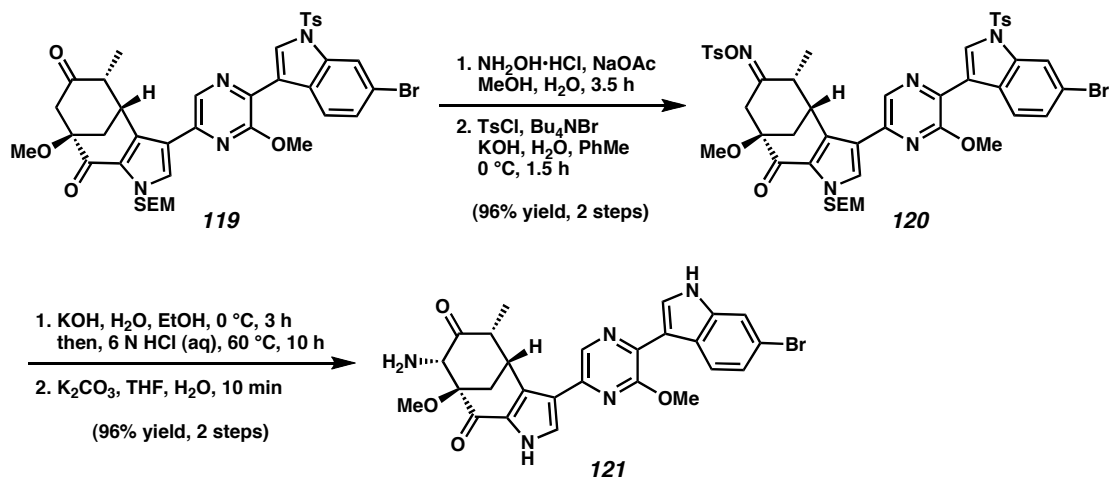
the aminoimidazole moiety. Therefore, selective cleavage of silyl ether **118**, followed by oxidation with Dess-Martin periodinane, produced ketone **119** (Scheme 3.2.10).

*Scheme 3.2.10*



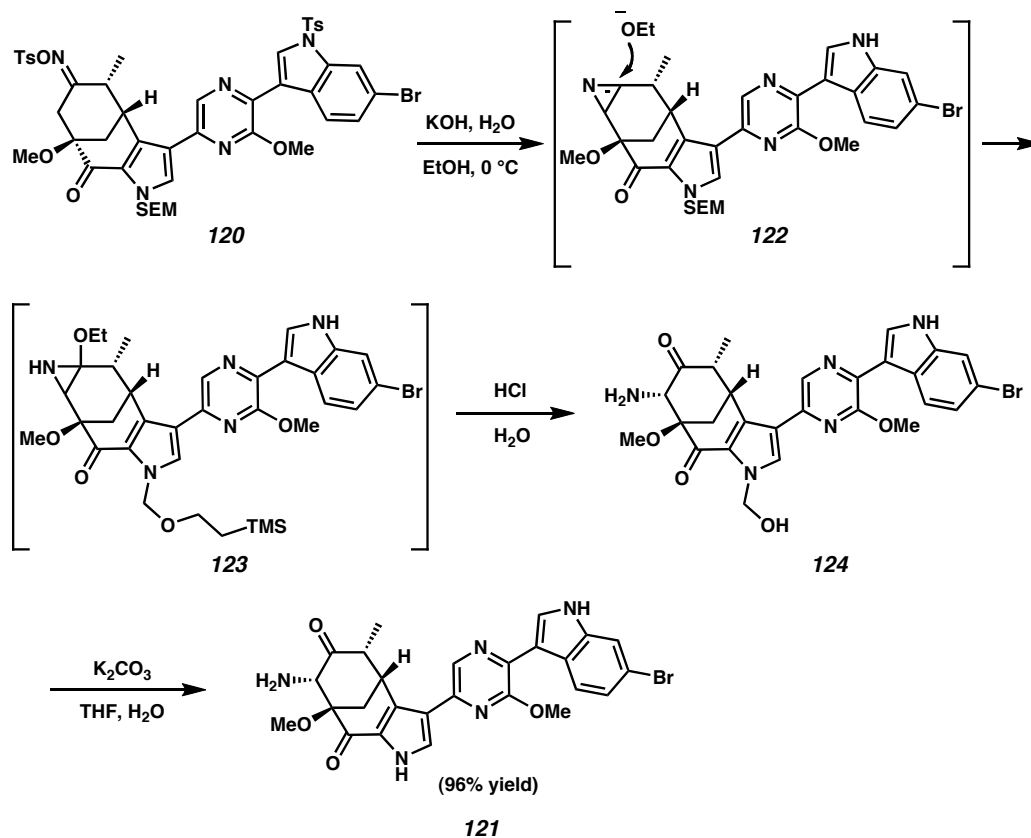
Although attempts to introduce the necessary  $\alpha$ -amino group failed under numerous literature protocols,<sup>8b</sup> Neil Garg skillfully managed the installation of this substituent using a Neber rearrangement.<sup>39,40</sup> In this scenario, an activated oxime derivative would undergo alkoxide-promoted rearrangement to furnish an  $\alpha$ -amino ketone. Thus, ketone **119** was converted to tosyloxime **120** via standard conditions (Scheme 3.2.11). Gratifyingly, exposure of substrate **120** to aqueous KOH in ethanol led to Neber rearrangement. After optimization, we found that simply exposing tosyloxime **120** to i) KOH, ii) HCl, and iii)  $\text{K}_2\text{CO}_3$  produced  $\alpha$ -amino ketone **121** as a single regio- and stereochemical isomer in excellent yield.<sup>41,42,43</sup> Furthermore, under these reaction conditions, both the tosyl and SEM protective groups were quantitatively removed from their corresponding heterocycles. To the best of our knowledge, this is the first example of a successful Neber rearrangement in the context of natural product synthesis.<sup>44</sup>

Scheme 3.2.11



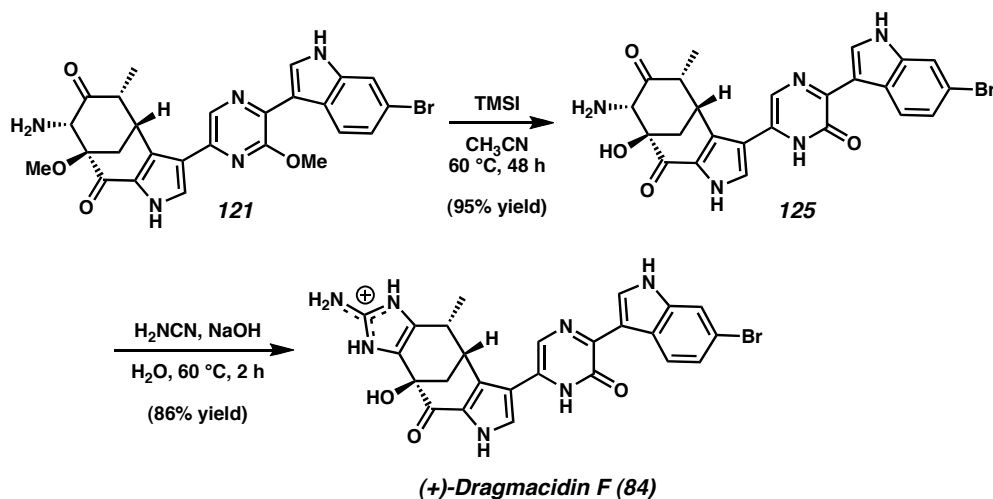
A more detailed look at the possible mechanism of the Neber rearrangement/deprotection sequence is shown in Scheme 3.2.12. Exposure of tosyloxime **120** to KOH in ethanol likely leads to the formation of detosylated azirine **122**, which is attacked by ethoxide to afford ethoxyaziridine **123**.<sup>40a,45</sup> Following acid-mediated hydrolysis, the amino ketone moiety is installed with concomitant partial cleavage of the SEM protective group (**123** → **124**).<sup>41b,46</sup> Finally, treatment of hemiaminal **124** with  $\text{K}_2\text{CO}_3$  removes the remaining portion of the SEM group, thus giving rise to the deprotected amino ketone (**121**).

Scheme 3.2.12



In order to unveil the masked pyrazinone functionality, Neber rearrangement product **121** was treated with TMSI at  $60\text{ }^\circ\text{C}$  (Scheme 3.2.13).<sup>16</sup> Fortuitously, both the pyrazinone and the  $3^\circ$  alcohol functionalities were revealed simultaneously (**121**  $\rightarrow$  **125**). In the final step of the synthesis, the penultimate amino ketone (**125**) was subjected to cyanamide and aqueous  $\text{NaOH}$  to produce enantiopure dragmacidin F (**84**).<sup>7,47</sup> Our efficient and enantiospecific route allows access to **84** in 7.8% overall yield in just 21 steps from (–)-quinic acid (**93**).

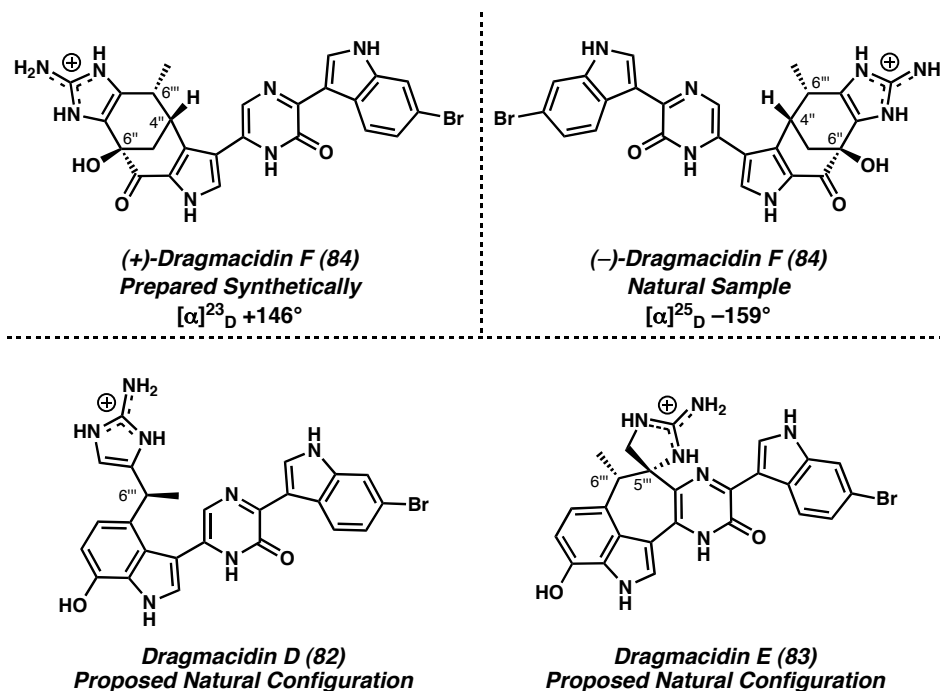
Scheme 3.2.13



### 3.3 The Absolute Stereochemistry of the Pyrazinone-Containing Dragmacidins.

Synthetic dragmacidin F (**84**) was spectroscopically identical (<sup>1</sup>H NMR, <sup>13</sup>C NMR, IR, UV, HPLC) to a sample obtained from natural sources,<sup>3f</sup> with the exception of the sign of rotation (natural:  $[\alpha]_D^{25} -159^\circ$  (*c* 0.4, MeOH); synthetic:  $[\alpha]_D^{23} +146^\circ$  (*c* 0.45, MeOH)). Thus, our synthesis from (–)-quinic acid (**93**) established, for the first time, the absolute configuration of natural dragmacidin F (**84**) to be (4''*S*, 6''*S*, 6'''*S*) as shown in Figure 3.3.1.<sup>48</sup> On the basis of the hypothesis that dragmacidins D, E, and F are biosynthetically related, it is likely that the absolute stereochemical configurations of natural dragmacidins D (**82**) and E (**83**) are (6'''*S*) and (5'''*R*, 6'''*S*), respectively. Having developed a route to the unnatural antipode of dragmacidin F ((+)-**84**), we set out to extend our approach to the total synthesis of (–)-**84**.

Figure 3.3.1



### 3.4 The Total Synthesis of (-)-Dragmacidin F

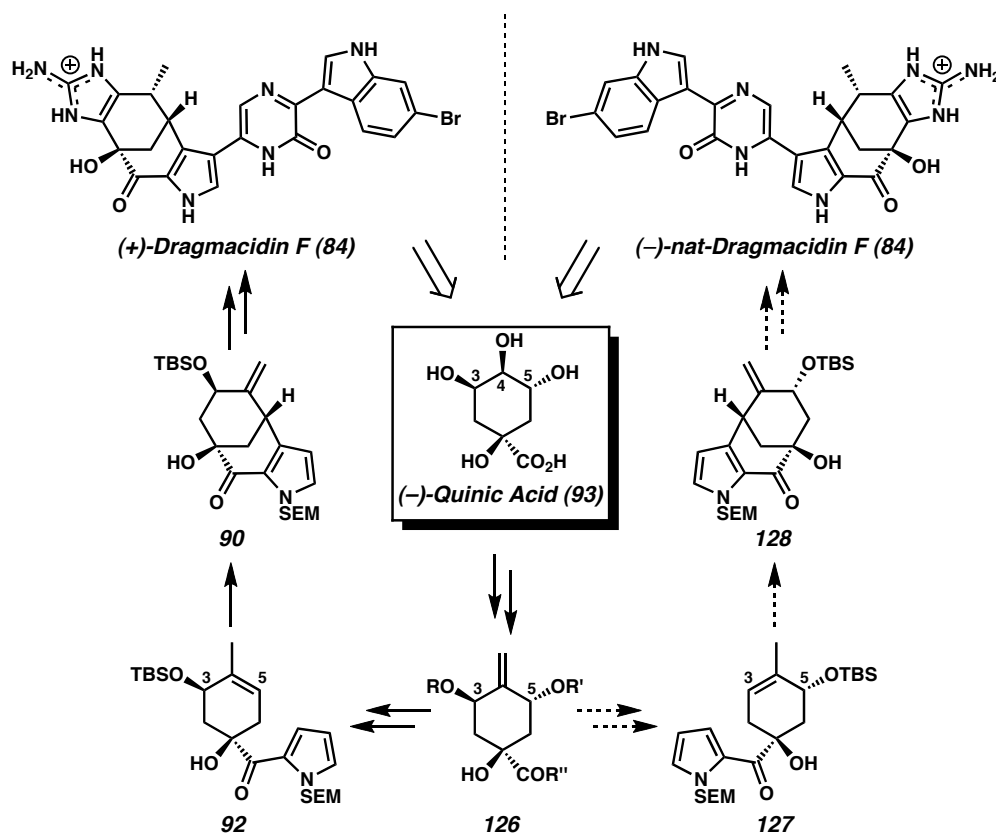
#### 3.4.1 An Enantiodivergent Strategy for the Preparation of (-)-Dragmacidin F

As described above, naturally occurring and readily available (-)-quinic acid (**84**)<sup>13</sup> had served as the starting material for our synthetic approach to (+)-**84**. Unfortunately, the (+)-enantiomer of **93** is not easily accessible,<sup>49</sup> and we were confronted with the possibility that our synthesis would not be amenable to the preparation of our new target molecule, (-)-dragmacidin F ((-)-**84**). We reasoned, however, that it might be possible to exploit (-)-quinic acid (**93**) in an enantiodivergent manner that would allow access to both (+)- and (-)-**84** (Scheme 3.4.1).<sup>50</sup> For such an approach to succeed, (-)-quinic acid (**93**) would be elaborated via selective manipulation of the C(3), C(4), and C(5) hydroxyl groups to a pseudo-*C*<sub>2</sub>-symmetric<sup>51</sup> derivative (**126**) en route to pyrrolocyclohexene **127**, the diastereomer of which (i.e., **92**) was employed in our



synthesis of (+)-**84**. Analogous to our approach to (+)-**84** (i.e., **92**  $\rightarrow$  **90**), we anticipated that **127** could undergo oxidative carbocyclization to afford annulated pyrrole **128**. Bicyclic **128** would then be elaborated to (–)-dragmacidin F ((–)-**84**). Of the key transformations outlined in Scheme 3.4.1, we were familiar with the Pd-mediated oxidative carbocyclizations and the late-stage manipulations of related compounds; however, the successful preparation of (–)-dragmacidin F ((–)-**84**) would rely heavily on the identification of a suitable quinic acid derivative (**126**), the facile synthesis of that compound, and the rapid conversion of **126** to the requisite cyclization substrate (**92**).

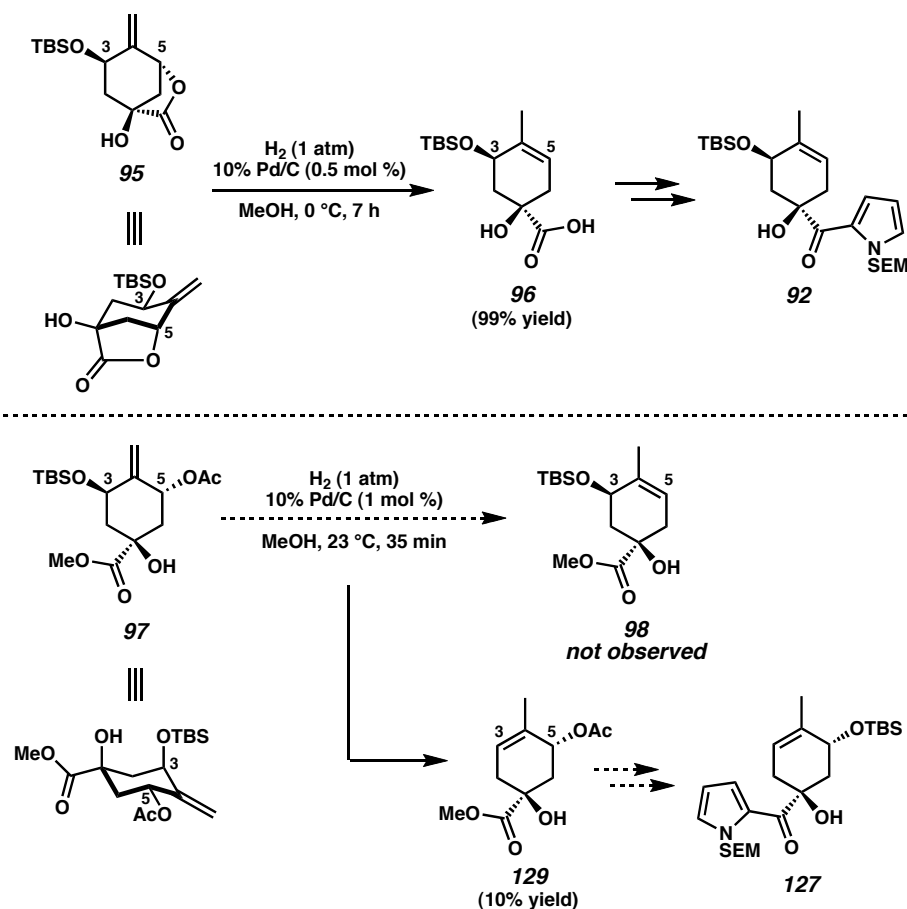
Scheme 3.4.1



### 3.4.2 The Development of a Reductive Isomerization Reaction

Fortunately, potential solutions to these problems had become apparent during our studies of a novel reductive isomerization reaction discovered in our synthesis of (+)-dragmacidin F ((+)-**84**). Two critical results are shown in Scheme 3.4.2. In the first experiment, treatment of lactone **95** with Pd/C and H<sub>2</sub> in methanol at 0 °C furnished carboxylic acid **96** in essentially quantitative yield via reductive loss of the C(5) carboxylate with concomitant olefin migration (i.e., net S<sub>N</sub>2' reduction). In the second experiment, a closely related derivative (**97**) was exposed to similar reaction conditions.<sup>52</sup> Surprisingly, the reductive isomerization reaction proceeded with loss of the C(3) silyl ether rather than the C(5) acetate, thus producing small quantities of allylic acetate **129** instead of the anticipated product (**98**).<sup>53</sup> The observation that (*t*-Bu)Me<sub>2</sub>SiO<sup>-</sup> was preferentially ejected from compound **97** despite the clear superiority of AcO<sup>-</sup> as a leaving group led us to consider that the C(3) silyl ether moiety was positioned in an axial orientation, thereby facilitating its elimination.<sup>54</sup> This preferred conformation of **97** represents a cyclohexane ring-flip with respect to lactone **95**, and thus gives rise to the reductive isomerization product (**129**) possessing a Δ<sub>3,4</sub> olefin. Importantly, the possibility existed that the unexpected product obtained from this reaction (i.e., **129**) could be converted to cyclization substrate **127** (diastereomeric to **92**).

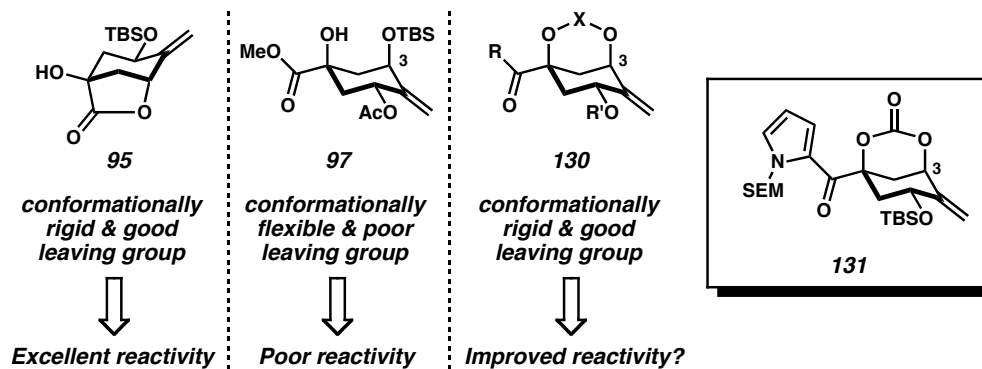
Scheme 3.4.2



Our efforts to optimize the reductive isomerization of **97** to **129** were hampered by competitive hydrogenation of the olefin moiety of **97**, a complication not observed in the high-yielding conversion of **95** to **96**. Although both processes presumably involve the elimination of an axially disposed leaving group,<sup>54</sup> we reasoned that the successful conversion of **95** to **96** was due to the carboxylate being conformationally restricted to an axial orientation, while substrate **97** possessed a poorer leaving group ( $t\text{-BuMe}_2\text{SiO}^-$ ) and was free to adopt alternate conformations (Figure 3.4.1). We hypothesized that derivatives of **97** containing an axially-locked leaving group at C(3) (e.g., **130**) would be more suitable substrates for the reductive isomerization reaction. Thus, carbonate **131**

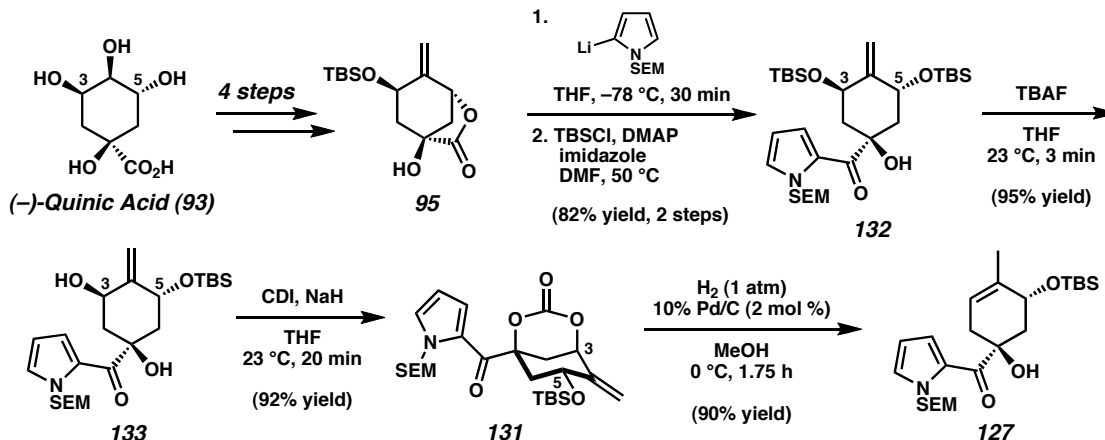
was identified as the key (–)-quinic acid derived intermediate en route to the desired cyclization substrate (**127**), and became the focus of our efforts.

Figure 3.4.1



Our synthesis of carbonate **131** began with bicyclic lactone **95**, a derivative of (–)-quinic acid (**93**) that was used in our total synthesis of (+)-**84** (Scheme 3.4.3). Addition of 2-lithio-SEM-pyrrole<sup>22</sup> followed by TBS protection afforded bis(silylether) **132** in good yield. This pseudo- $C_2$ -symmetric compound then underwent rapid diastereoselective mono-desilylation upon treatment with TBAF in THF to produce the *syn* 1,3-diol **133**.<sup>55</sup> Importantly, this desymmetrization proceeded with complete selectivity and allowed us to efficiently differentiate the C(3) and C(5) positions of the cyclohexyl moiety. Diol **133** was smoothly converted to bicyclic carbonate **131** in the presence of CDI, effectively restricting the C(3) substituent to an axial disposition. Gratifyingly, exposure of carbonate **131** to our reductive isomerization conditions (2 mol % Pd/C, H<sub>2</sub>, MeOH, 0 °C) led to the selective formation of the desired cyclization substrate (**127**) in 90% yield.<sup>56</sup>

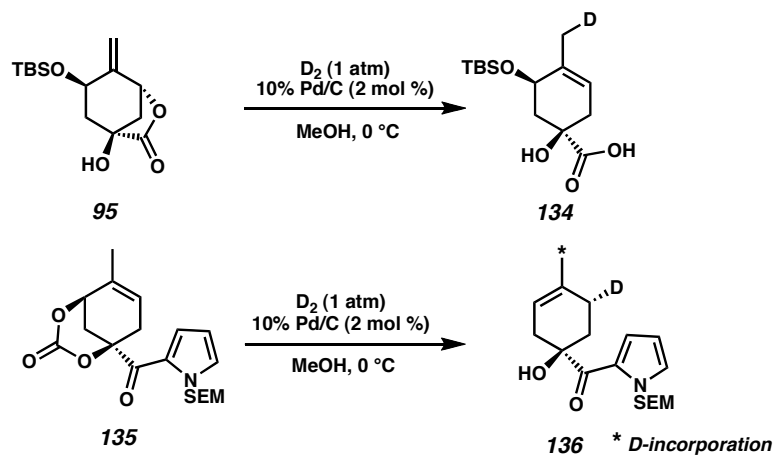
Scheme 3.4.3



### 3.4.3 The Scope and Mechanism of the Reductive Isomerization Reaction

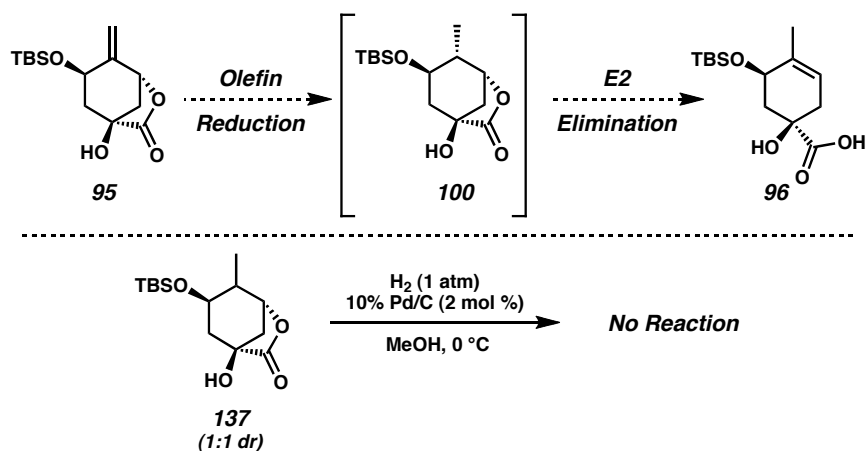
On the basis of these results, we set out to examine the unusual reactivity of the heterogeneous palladium system.<sup>57</sup> Intrigued by our initial results (**95**  $\rightarrow$  **96** and **131**  $\rightarrow$  **127**), we began a more detailed study of this reductive isomerization by examining the origin of the hydrogen atom in the newly formed C-H bond. Experiments employing D<sub>2</sub> indicate that the deuterium delivered at the allylic positions of **134** and **136** originates from D<sub>2</sub>, whereas no C-D incorporation was observed by using CD<sub>3</sub>OD (Scheme 3.4.4).<sup>58</sup> Furthermore, deuterium incorporation occurs with complete stereoselectivity (**135**  $\rightarrow$  **136**), with additional incorporation at the exocyclic methyl group.<sup>59</sup>

Scheme 3.4.4



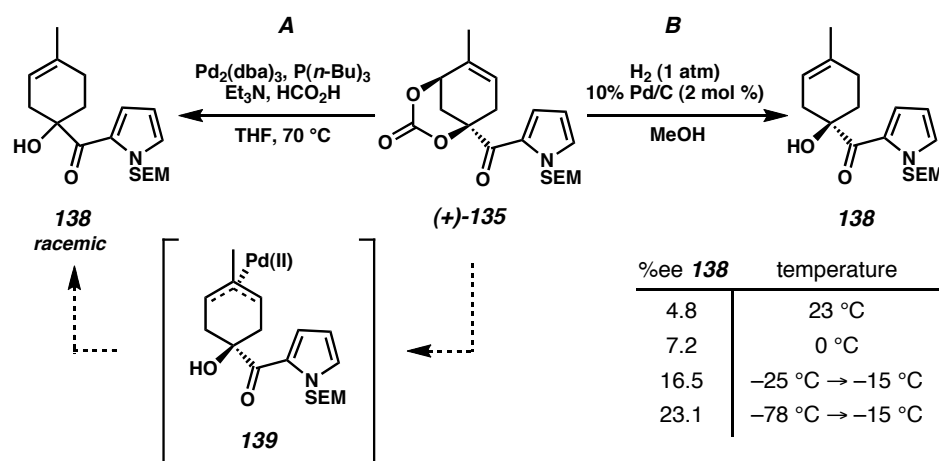
In terms of mechanism, we considered the simple possibility that our transformation could be proceeding in a tandem fashion via hydrogenation of the olefin followed by E2 elimination (e.g., **95**  $\rightarrow$  **100**  $\rightarrow$  **96**, Scheme 3.4.5). However, submission of an independently prepared sample of saturated lactone **137** (1:1 dr) to the identical reaction conditions (10% Pd/C,  $H_2$ , MeOH, 0 °C) led to no reaction, allowing us to dismiss its potential as a viable intermediate.<sup>60</sup>

Scheme 3.4.5



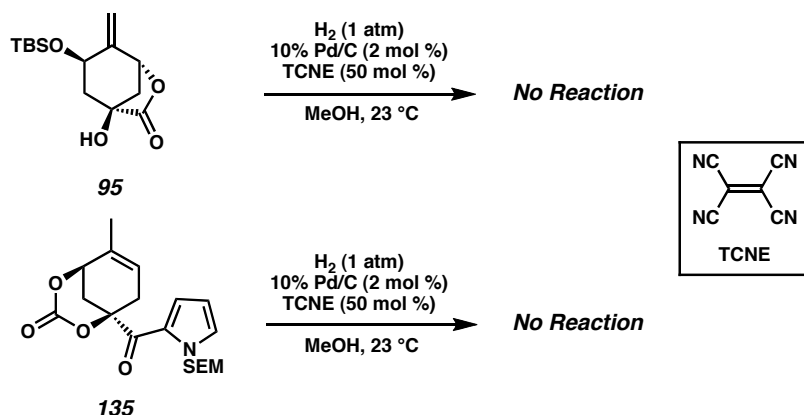
A  $\pi$ -allyl mechanism could be probed by using carbonate-bearing trisubstituted olefin **135**. Under  $\pi$ -allyl hydrogenolysis conditions, racemic **138** was obtained (Scheme 3.4.6A).<sup>41b</sup> Interestingly, analysis by chiral HPLC revealed that, under our reductive isomerization conditions at 0 °C, cyclohexene **138** was produced in 7.2% ee (Scheme 3.4.6B). In fact, by lowering the reaction temperature, up to 23.1% ee could be achieved.<sup>41b</sup> Although complete optical purity was not maintained in the product, this result suggests a reaction pathway that does not solely involve a meso- $\pi$ -allylpalladium complex (e.g., **139**).<sup>61</sup>

Scheme 3.4.6



Recently, both Sajiki and Hara have invoked a single-electron transfer (SET) mechanism for other transformations involving the use of 10% Pd/C and MeOH.<sup>62</sup> In accordance with this hypothesis, exposing either lactone **95** or carbonate **135** to our standard conditions in the presence of tetracyanoethylene (TCNE) as a SET inhibitor completely halts all reactivity, even at 23 °C (Scheme 3.4.7).<sup>63</sup>

Scheme 3.4.7



We prepared a number of substrates to assess the generality of this reaction (Table 3.4.1).<sup>64</sup> As a starting point, a simple variant of lactone **95** bearing an acetate on the secondary allylic alcohol was synthesized (i.e., **140**). We were pleased to see that **140** could be converted to carboxylic acid **141** in good yield (entry 1). The use of allylic acetate **97** as a substrate (entry 2), on the other hand, led to an unexpected result. We anticipated that methyl ester **98** would be the observed product because acetate is a superior leaving group to silanolate (see Scheme 3.4.2, *vide supra*). However, the compound obtained (i.e., **129**) resulted from a net loss of the OTBS group.<sup>65</sup> Notably, none of the byproducts formed under homogeneous  $\pi$ -allyl protocols were observed under these heterogeneous conditions (**98**, **99**, **iv**<sup>20</sup>, see Scheme 3.2.1, *vide supra*). In order to probe this result further, a version of **97** with exchanged protecting groups on the secondary alcohols was prepared (**142**, entry 3). In this case, elimination of acetate occurred.<sup>65</sup>



Table 3.4.1<sup>a</sup>

entry	substrate	product	time	yield <sup>b</sup>
1			15 min	71%
2 <sup>c</sup>			1 h 35 min	3% <sup>d</sup> 10% <sup>e,f</sup>
3 <sup>c,g</sup>			1.5 h	27%
4			129 R = Ac 1 h	81%
5			143 R = TBS 8 min	94%
6			147 R = Ac 20 min	94%
7			149 R = H 15 min	80%
8			4 h	90%
9			1 h	68%
10 <sup>g</sup>			1.3 h	91%

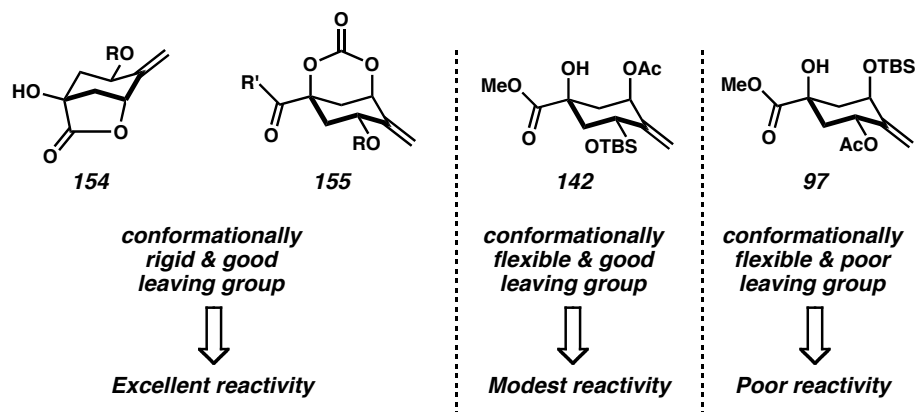
<sup>a</sup> Standard conditions: H<sub>2</sub> (balloon, 1 atm), 10% Pd/C (2 mol % Pd), MeOH, 0 °C. <sup>b</sup> Isolated yield. <sup>c</sup> Yield based on <sup>1</sup>H NMR integration. <sup>d</sup> 10% Pd/C (0.5 mol % Pd). <sup>e</sup> 10% Pd/C (1 mol % Pd). <sup>f</sup> Reaction performed at 23 °C. <sup>g</sup> Product formed in 7.2% ee.

Due to the success of the rigid bicyclic lactone framework in this reaction, we reasoned that the reactivity of **97** and **142** might be improved by restricting them as bicyclic carbonates (**144** and **145**). These carbonate-containing substrates were well tolerated and led to competent production of the corresponding methyl esters (entries 4 and 5). Additionally, carbonates with adjacent heterocyclic moieties such as pyrrole (**146** and **148**) and indole (**150**) could be converted into their reductively isomerized counterparts in excellent yields (entries 6–8 and 10). The use of an acetate protecting group on the secondary allylic alcohol (entries 1, 4, and 6), or an unprotected alcohol altogether (entry 7), did not significantly influence the overall reaction efficiency. Interestingly, replacement of the carbonate moiety with a dioxasilyl linkage led solely to diastereoselective hydrogenation of the olefin (entry 9).<sup>66</sup> Somewhat surprisingly, reductive isomerization using a trisubstituted olefin was also quite facile (entry 10, cf. Scheme 3.4.6).<sup>67</sup>

A model to rationalize some of these anomalous differences in reactivity is presented in Figure 3.4.2, which is an extended version of the model conceived in our initial hypothesis (see Figure 3.4.1, vide supra). An examination of the three-dimensional structures of the starting materials in Table 3.4.1 reveals that the leaving group is positioned preferentially in an axial orientation with respect to the six-membered ring.<sup>68</sup> Furthermore, structurally rigid bicyclic lactones and carbonates with locked axial leaving groups (e.g., **154** and **155**) exhibited enhanced yields relative to their more flexible monocyclic counterparts (**142** and **97**). The difference in yield between substrates **142** and **97** can be attributed to leaving group ability (i.e.  $\text{AcO}^- > \text{Me}_2(t\text{-Bu})\text{SiO}^-$ ). This leaving group effect was also observed when the carbonate functionality was replaced

with a dioxasilyl moiety (entry 9), in which case only direct olefin hydrogenation occurred.

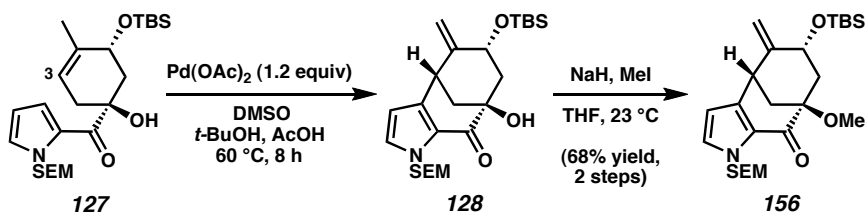
Figure 3.4.2



### 3.4.4 Constructing the [3.3.1] Bicycle En Route to (–)-Dragmacidin F

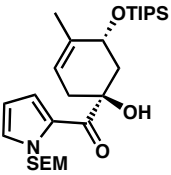
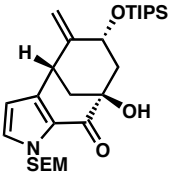
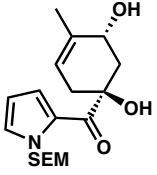
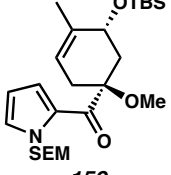
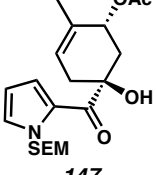
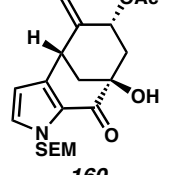
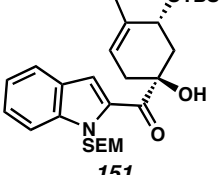
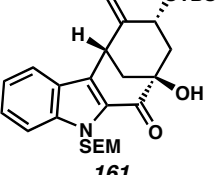
After assembling target substrate **127**, we turned our attention to the key Pd(II)-mediated cyclization reaction (Scheme 3.4.8). Substrate **127** was treated with 1.2 equiv of Pd(OAc)<sub>2</sub> under conditions similar to those described earlier, at which point, the desired pyrrole-fused bicycle (**128**) formed as a single regio- and stereoisomer. Notably, bond formation between the pyrrole functionality and C(3) of **127** occurred even in the presence of the bulky C(5) silyl ether group positioned syn to the acyl pyrrole subunit. Following protection of the 3° alcohol, [3.3.1] bicycle **156** was obtained in 68% yield for the two-step process.

Scheme 3.4.8



We also explored the Pd(II)-mediated carbocyclization of a number of substrates related to the diastereomeric counterpart (**127**) of TBS ether **92** (cf. Table 3.2.2, *vide supra*). The TIPS ether analog underwent smooth cyclization (Table 3.4.2, entry 1), while the use of the hydroxy derivative<sup>35</sup> (entry 2) or the 3° methyl ether derivative<sup>36</sup> (entry 3) did not lead to any product formation. Additionally, the substrates bearing acetate (entry 4) and indole (entry 5) moieties participated in the cyclization reaction. In general, the results of this study (Table 3.4.2) mirrored the results of their diastereomeric counterparts in Table 3.2.2, albeit in lower yields. This decrease in reactivity could be attributed, at least in part, to the steric repulsion between the newly forming bond at C(3) and the protected alcohol at C(5).

Table 3.4.2<sup>a</sup>

entry	substrate	product	temp (°C)	time	yield <sup>b</sup>
1	 157	 158	80	2.3 h	51% (70%)
2	 149	—	80	complex mixture <sup>c</sup>	
3	 159	—	80	no reaction	
4	 147	 160	60 <sup>d</sup>	11 h	10% <sup>e</sup>
5	 151	 161	80	2.3 h	34%

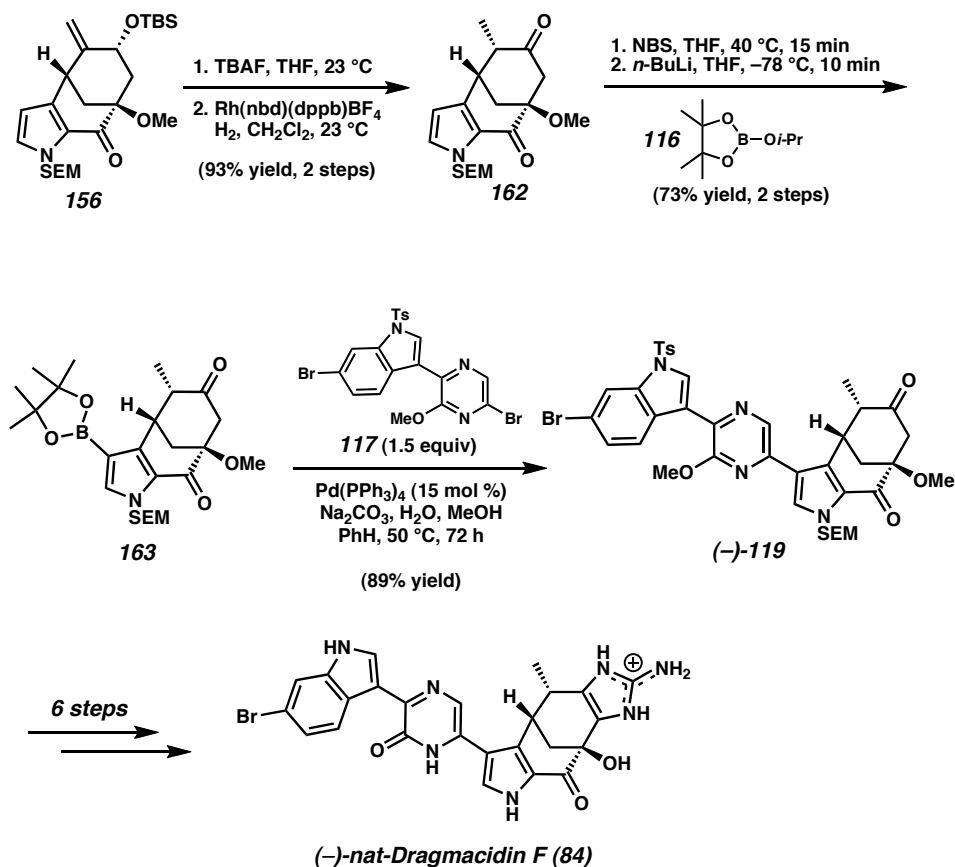
<sup>a</sup> Standard Conditions: 1 equiv Pd(OAc)<sub>2</sub>, 2 equiv DMSO, *t*-BuOH:AcOH (4:1, 0.01 M). <sup>b</sup> Isolated Yield. Number in parentheses represents the yield based on recovered starting material. <sup>c</sup> Trace product may have formed in this reaction, but could not be isolated. <sup>d</sup> At 80 °C, trace product formation and substantial decomposition were observed.

### 3.4.5 End-Game: Total Synthesis of (–)-Dragmacidin F

Despite the similarity of **156** to its diastereomeric counterpart (**115**, Scheme 3.2.9) employed in the synthesis of (+)-dragmacidin F (**84**), attempts to carry out similar elaborations using previously developed protocols were unsuccessful. Thus, a slightly

modified end-game route was conceived and carried out by Neil Garg. Cleavage of the TBS ether of **156** using TBAF in THF, followed by a tandem olefin isomerization/tautomerization process using Brown's cationic rhodium catalyst<sup>69</sup> Rh(nbd)(dppb)BF<sub>4</sub> and H<sub>2</sub>, formed ketone **162** as a single diastereomer in 93% yield over two steps (Scheme 3.4.9).<sup>70</sup> Position-selective bromination and low-temperature metalation of the pyrrole in the presence of two ketones gave rise to boronic ester **163**. Subsequent halogen-selective cross-coupling of **163** with dibromide **117** afforded the desired Suzuki adduct (–)-**119** (89% yield), the enantiomer of which had been employed in the synthesis of (+)-dragmacidin F. Finally, Suzuki adduct (–)-**119** was converted to (–)-dragmacidin F ((–)-**84**) via our previously described six-step protocol (vide supra). Synthetic and natural (–)-**84**<sup>3f</sup> were spectroscopically identical, including the sign of optical rotation (natural (–)-**84**:  $[\alpha]_D^{25} -159^\circ$  (*c* 0.4, MeOH); synthetic (–)-**84**:  $[\alpha]_D^{23} -148^\circ$  (*c* 0.2, MeOH)).<sup>41b</sup>

Scheme 3.4.9



### 3.5 Conclusion

In summary, we have developed an enantiodivergent strategy to access both antipodes of drarmacidin F (**84**) from a single enantiomer of readily available (–)-quinic acid (**93**). Our highly efficient syntheses provide (+)-**84** in 7.8% overall yield and (–)-**84** in 9.3% overall yield beginning from **93**. The routes that we have developed to (+)- and (–)-**84** are concise and feature a number of key transformations, namely: a) highly efficient functionalizations of (–)-**93** to differentiate C(3) and C(5), b) novel reductive isomerization reactions, c) sterically demanding Pd(II)-mediated oxidative carbocyclizations, d) halogen-selective Suzuki cross-coupling reactions, and e) high-

yielding late-stage Neber rearrangements. Advanced biological testing of both synthetic antipodes of dragmacidin F is currently underway.



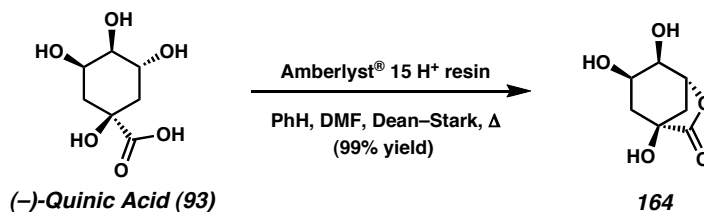
### 3.6 Experimental Section

#### 3.6.1 Materials and Methods

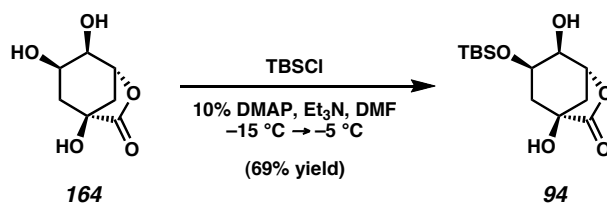
Unless stated otherwise, reactions were conducted in flame-dried glassware under an atmosphere of nitrogen using anhydrous solvents (either freshly distilled or passed through activated alumina columns). 10% Pd/C was purchased from Aldrich Chemical Company, Inc. (20,569-9). All commercially obtained reagents were used as received. Reaction temperatures were controlled using an IKAmag temperature modulator. Thin-layer chromatography (TLC) was conducted with E. Merck silica gel 60 F254 pre-coated plates (0.25 mm) and visualized using a combination of UV, anisaldehyde, ceric ammonium molybdate, and potassium permanganate staining. ICN silica gel (particle size 0.032–0.063 mm) was used for flash column chromatography. Disposable Sep-Pak C<sub>18</sub> Vac Cartridges were purchased from Waters and used for all reversed-phase filtrations. HPLC analysis was performed on a Beckman Gold system using a Rainin C<sub>18</sub>, Microsorb MV, 5  $\mu$ m, 300 x 4.6 mm reversed-phased column in 0.1% (w/v) TFA with acetonitrile/H<sub>2</sub>O as eluent and a flow rate of 1.0 mL/min, gradient elution of 1.25% acetonitrile/min. Preparatory reversed-phase HPLC was performed on a Beckman HPLC with a Waters DeltaPak 25 x 100 mm, 100  $\mu$ m C<sub>18</sub> column equipped with a guard, 0.1% (w/v) TFA with acetonitrile/H<sub>2</sub>O as eluent, and gradient elution of 0.50% acetonitrile/min. For all reversed-phase purifications, H<sub>2</sub>O (18M $\Omega$ ) was obtained from a Millipore MiliQ water purification system and TFA from Halocarbon, Inc. <sup>1</sup>H NMR spectra were recorded on a Varian Mercury 300 (at 300 MHz), a Varian Inova 500 (at 500 MHz), or a Varian Inova 600 (at 600 MHz) and are reported relative to Me<sub>4</sub>Si ( $\delta$  0.0). Data for <sup>1</sup>H NMR spectra are reported as follows: chemical shift ( $\delta$  ppm), multiplicity,

coupling constant (Hz), and integration.  $^{13}\text{C}$  NMR spectra were recorded on a Varian Mercury 300 (at 75 MHz), or a Varian Inova 500 (at 125 MHz) and are reported relative to  $\text{Me}_4\text{Si}$  ( $\delta$  0.0). Data for  $^{13}\text{C}$  NMR spectra are reported in terms of chemical shift. IR spectra were recorded on a Perkin Elmer Paragon 1000 spectrometer or a Perkin Elmer Spectrum BXII spectrometer and are reported in frequency of absorption ( $\text{cm}^{-1}$ ). Optical rotations were measured with a Jasco P-1010 polarimeter. High-resolution mass spectra were obtained from the California Institute of Technology Mass Spectral Facility. Analytical chiral HPLC was performed on a Chiralpak<sup>®</sup> AD column (4.6 mm x 250 mm) obtained from Daicel Chemical Industries, Ltd.

### 3.6.2 Preparative Procedures

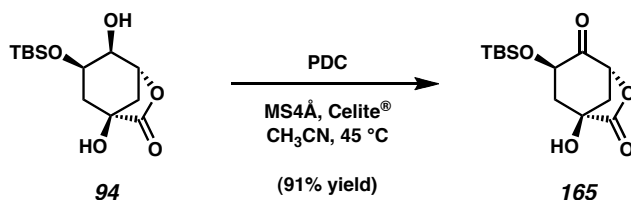


**Lactone 164.** A mixture of D-(-)-quinic acid (**93**) (50.0 g, 260.2 mmol), Amberlyst<sup>®</sup> 15 ion-exchange resin (7 g, 35 mmol), benzene (500 mL), and DMF (125 mL) was refluxed under a Dean-Stark trap for 16 h. The reaction mixture was cooled to 23 °C and filtered over a pad of Celite<sup>®</sup>. The filtrate was then evaporated under reduced pressure to afford a thick oil, which was diluted with CH<sub>2</sub>Cl<sub>2</sub> (150 mL). Hexanes (250 mL) was added and the resulting mixture was allowed to sit at 23 °C for 2 h. The product was collected by vacuum filtration and was further dried in vacuo to afford lactone **164** (44.9 g, 99% yield) as a white powder. *R<sub>f</sub>* 0.40 (3:1 EtOAc:acetone); characterization data for this compound have been previously reported.<sup>14a</sup>



**TBS Lactone 94.** To a mixture of lactone **164** (90.0 g, 517 mmol), DMAP (6.31 g, 51.7 mmol), triethylamine (90 mL, 646 mmol), and DMF (345 mL) at -15 °C was added TBSCl (84.9 g, 563 mmol) in 3 equal portions over 30 min. The temperature was maintained between -20 °C and -15 °C during the addition. The reaction mixture was allowed to warm to -5 °C over 3 h, quenched by the addition of 5% aq. citric acid (120 mL), and then warmed to 23 °C. The solvent was removed in vacuo, and the crude

product was diluted with 5% aq. citric acid (350 mL) and extracted with Et<sub>2</sub>O (1 x 500 mL, 2 x 400 mL). The combined organic layers were washed with H<sub>2</sub>O (2 x 400 mL) and brine (400 mL), dried over MgSO<sub>4</sub>, and evaporated under reduced pressure. The product was triturated with hexanes (750 mL) and collected by vacuum filtration. It was further dried under vacuum to afford TBS lactone **94** (102.8 g, 69% yield) as a dry white solid. *R<sub>f</sub>* 0.48 (1:1 hexanes:EtOAc); *R<sub>f</sub>* 0.28 (2:1 Et<sub>2</sub>O:hexanes); characterization data for this compound have been previously reported.<sup>14b</sup>

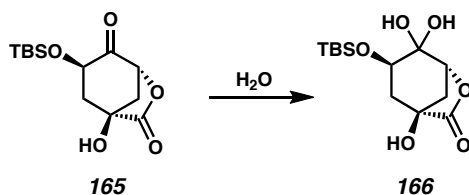


**Keto Lactone 165.** A mixture of TBS lactone **94** (3.72 g, 12.90 mmol), powdered 4Å activated molecular sieves (2.79 g), Celite® (2.79 g), pyridinium dichromate (12.13 g, 32.2 mmol), and acetonitrile (185 mL) was heated to 45 °C for 24 h. The reaction was allowed to cool to 23 °C, and then was filtered over a plug of silica gel topped with Celite® (EtOAc eluent). The solvent was removed under reduced pressure to afford a brown oil, which was further purified by passage over a plug of silica gel (1:1 hexanes:EtOAc eluent). Evaporating the solvent in vacuo afforded keto lactone **165** (3.35 g, 91% yield) as a pale yellow oil.

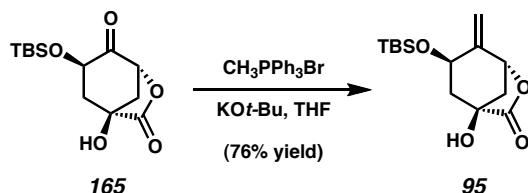
*Alternate Procedure.* Powdered 4Å activated molecular sieves (184.6 g) were agitated and flame-dried under vacuum for approximately 30 min until a fine, powder-like consistency was obtained. Upon cooling to 23 °C, CH<sub>2</sub>Cl<sub>2</sub> (540 mL) was introduced, and the slurry was cooled to 0 °C. Freshly prepared pyridinium dichromate<sup>71</sup> (148.7 g,

395.3 mmol) was added, and the resulting heterogeneous orange mixture was treated with TBS lactone **94** (70.04 g, 242.8 mmol) portionwise over 4 min. After the addition was complete, the reaction was stirred for 5 min and then freshly distilled AcOH (49.0 mL, 856.0 mmol) was added dropwise over a 20-min period. The reaction temperature was maintained at 0 °C for 15 min after the addition was complete, and the mixture was then stirred at 23 °C. After 10 h, the reaction was judged complete by <sup>1</sup>H NMR. The dark mixture was evenly divided into 3 portions, each of which was filtered over a pad of silica gel (10 cm diameter x 7.5 cm height, EtOAc eluent). The filtrates were combined and evaporated in vacuo to afford a dark liquid, and this residue was further coevaporated with toluene (3 x 150 mL). The crude product was diluted in a mixture of hexanes:EtOAc (10:1; 250 mL) and filtered over a pad of powdered Na<sub>2</sub>SO<sub>4</sub> to remove insoluble impurities. The filtrate was evaporated, and dried in vacuo, to afford keto lactone **165** (55.27 g, 80% yield) as a brown, waxy solid. This material was used immediately in the next step without further purification. *Unstable to TLC conditions*; <sup>1</sup>H NMR (300 MHz, CDCl<sub>3</sub>): δ 4.71 (d, *J* = 6.6 Hz, 1H), 4.52 (dd, *J* = 10.3, 8.9 Hz, 1H), 2.95 (s, 1H), 2.88–2.79 (m, 1H), 2.57–2.47 (m, 1H), 2.39 (d, *J* = 12.4 Hz, 1H), 2.13 (dd, *J* = 12.4 Hz, 10.5 Hz, 1H), 0.88 (s, 9H), 0.11 (s, 3H), 0.02 (s, 3H); <sup>13</sup>C NMR (75 MHz, CDCl<sub>3</sub>): δ 202.6, 177.4, 79.0, 72.0, 70.6, 43.2, 42.6, 25.8 (3C), 18.5, –4.6, –5.3; IR (film): 3444 (br), 2931, 2858, 1799, 1753, 1254, 1144, 1111 cm<sup>–1</sup>; HRMS-FAB (*m/z*): [M + H]<sup>+</sup> calc'd for C<sub>13</sub>H<sub>23</sub>O<sub>5</sub>Si, 287.1315; found, 287.1316; [α]<sub>D</sub><sup>19</sup> –96.47° (*c* 1.0, C<sub>6</sub>H<sub>6</sub>).

*NOTE: Exposure of keto lactone 165 to water (e.g., aqueous workup, or prolonged exposure to silica gel) led to the formation of hydrate 166, as a white powder.*



**Hydrate 166.** *Unstable to TLC conditions*; mp 104–6 °C;  $^1\text{H}$  NMR (300 MHz,  $\text{CD}_3\text{OD}$ ):  $\delta$  4.46 (d,  $J = 5.8$  Hz, 1H), 3.75 (dd,  $J = 10.7, 7.0$  Hz, 1H), 2.48–2.31 (comp. m, 2H), 2.10–2.00 (m, 1H), 1.76 (app. t,  $J = 11.4$  Hz, 1H), 0.93 (s, 9H), 0.14 (s, 3H), 0.12 (s, 3H);  $^{13}\text{C}$  NMR (75 MHz,  $\text{CD}_3\text{OD}$ ):  $\delta$  179.4, 93.2, 81.8, 73.0, 72.3, 41.5, 40.9, 26.5 (3C), 19.1, –4.3, –4.7; IR (KBr): 3440 (br), 3374 (br), 2929, 2858, 1782, 1256, 1108, 1070  $\text{cm}^{-1}$ ; HRMS-Cl ( $m/z$ ):  $[\text{M} + \text{H}]^+$  calc'd for  $\text{C}_{13}\text{H}_{24}\text{O}_6\text{Si}$ , 304.1342; found, 304.1336;  $[\alpha]_D^{19}$  –54.29° ( $c$  1.0, MeOH).

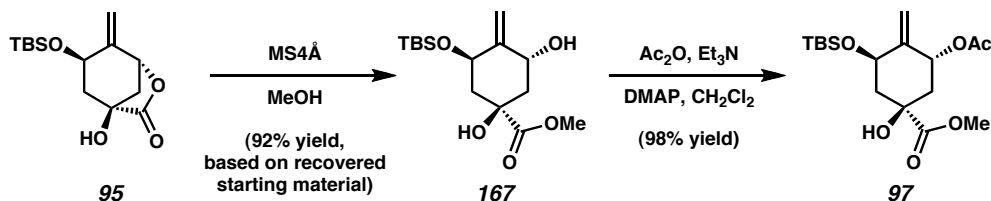


**Methylene Lactone 95.** To  $\text{CH}_3\text{PPh}_3\text{Br}$  (105 mg, 0.293 mmol) in THF (2.8 mL) at 0 °C was added potassium *t*-butoxide (31.3 mg, 0.279 mmol). The mixture was warmed to 23 °C and stirred for an additional 10 min. Keto lactone **165** (40 mg, 0.140 mmol) in THF (1 mL) was added and stirring was continued at 23 °C for 15 min. The reaction mixture was then refluxed for 2 h and cooled to 23 °C. The solvent was removed under reduced pressure, and the residue was partitioned between  $\text{Et}_2\text{O}$  (3 mL) and brine (1.5 mL). The layers were separated, and the aqueous layer was further extracted with  $\text{Et}_2\text{O}$  (3 x 1 mL). The combined organic layers were washed with brine (1.5 mL), dried by passage over a plug of silica gel ( $\text{Et}_2\text{O}$  eluent, then 2:1 hexanes: $\text{EtOAc}$  eluent), and

evaporated under reduced pressure. The crude product was purified by flash chromatography (2:1 hexanes:EtOAc eluent) to afford methylene lactone **95** (30 mg, 76% yield) as a white solid.

*Alternate Procedure.* To  $\text{CH}_3\text{PPh}_3\text{Br}$  (82.9 g, 232.1 mmol) in THF (1.10 L) at 23 °C was added potassium *t*-butoxide (23.8 g, 212.1 mmol) in one portion. The mixture was stirred for 2 h, then cooled to 0 °C. Keto lactone **165** (54.5 g, 190.3 mmol) in THF (240 mL) was added dropwise over a 30 min period. The reaction was allowed to warm slowly to 23 °C over 9 h, then quenched by the addition of ice-cold 15% aq.  $\text{NH}_4\text{Cl}$  (500 mL). The solvent was evaporated under reduced pressure, and the residue was partitioned between  $\text{Et}_2\text{O}$  (500 mL) and  $\text{H}_2\text{O}$  (100 mL). The aqueous phase was extracted with  $\text{Et}_2\text{O}$  (3 x 250 mL), and the combined organics were washed with  $\text{H}_2\text{O}$  (100 mL) and brine (100 mL) and dried over  $\text{MgSO}_4$ . Evaporation of the solvent afforded a crude yellow oil, which was filtered over a plug of silica gel (4:1 pentane: $\text{Et}_2\text{O}$   $\rightarrow$  3:2 pentane: $\text{Et}_2\text{O}$  eluent). After evaporating the solvent in vacuo, the residue was triturated with ice-cold pentane (40 mL). The white solid was filtered and washed with ice-cold pentane (2 x 2 mL). A second crop was collected from the filtrate after concentrating its volume to 15 mL. Drying the collected material in vacuo afforded methylene lactone **95** (22.1 g, 41% yield) as a white solid.  $R_f$  0.59 (1:1 hexanes:EtOAc); mp 87–88 °C;  $^1\text{H}$  NMR (300 MHz,  $\text{CDCl}_3$ ):  $\delta$  5.25–5.23 (m, 1H), 5.13–5.10 (m, 1H), 5.07 (d,  $J$  = 6.0 Hz, 1H), 4.38–4.29 (m, 1H), 2.85 (s, 1H), 2.67–2.59 (m, 1H), 2.31–2.21 (m, 1H), 2.09 (d,  $J$  = 11.5 Hz, 1H), 1.86 (app. t,  $J$  = 11.3 Hz, 1H), 0.89 (s, 9H), 0.06 (s, 6H);  $^{13}\text{C}$  NMR (75 MHz,  $\text{CDCl}_3$ ):  $\delta$  178.1, 144.8, 111.0, 79.4, 73.1, 67.1, 44.7, 44.7, 26.0 (3C), 18.5, –4.5, –4.7; IR (film): 3426 (br),

2956, 2931, 2858, 1791, 1254, 1120, 1071  $\text{cm}^{-1}$ ; HRMS-FAB ( $m/z$ ):  $[\text{M} + \text{H}]^+$  calc'd for  $\text{C}_{14}\text{H}_{25}\text{O}_4\text{Si}$ , 285.1522; found, 285.1519;  $[\alpha]_D^{19} -101.71^\circ$  ( $c$  1.0,  $\text{CHCl}_3$ ).



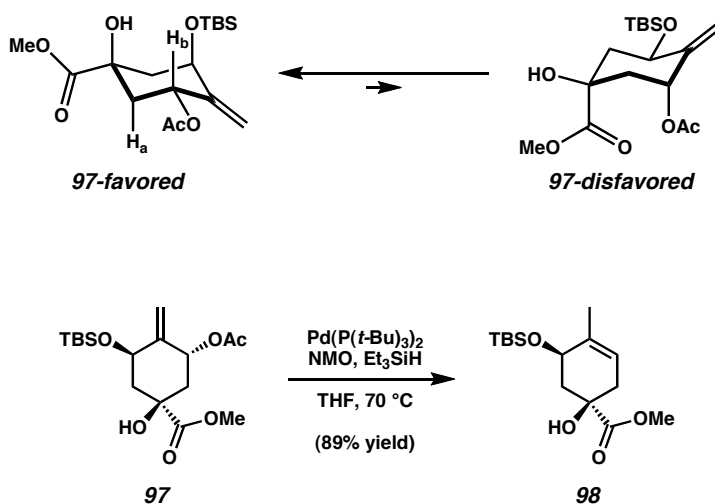
**Methyl Ester 97.** To lactone **95** (420 mg, 1.477 mmol) and activated oven-dried  $4\text{\AA}$  molecular sieves (100 mg) was added  $\text{MeOH}$  (15 mL). The reaction mixture was stirred at  $23^\circ\text{C}$  for 5.5 h, then filtered over a short plug of Celite<sup>®</sup> ( $\text{EtOAc}$  eluent). After evaporation of the reaction mixture under reduced pressure, the residue was purified by flash column chromatography (2:1 hexanes: $\text{EtOAc}$  eluent) to afford starting material lactone **95** (82 mg, 20% yield) and siloxy diol **167** (345 mg, 74% yield, 92% yield based on recovered starting material), which was used directly in the subsequent reaction.

To siloxy diol **167** (80.0 mg, 0.253 mmol) in  $\text{CH}_2\text{Cl}_2$  (1.5 mL) was added  $\text{Et}_3\text{N}$  (71  $\mu\text{L}$ , 0.506 mmol),  $\text{DMAP}$  (3 mg, 0.0253 mmol), followed by  $\text{Ac}_2\text{O}$  (31  $\mu\text{L}$ , 0.329 mmol). The reaction mixture was stirred at  $23^\circ\text{C}$  for 10 min, quenched with saturated aq.  $\text{NaHCO}_3$  (5 mL), and extracted with  $\text{CH}_2\text{Cl}_2$  (3 x 15 mL). The combined organic layers were filtered over a plug of silica gel ( $\text{CH}_2\text{Cl}_2$  eluent, then  $\text{EtOAc}$  eluent) and evaporated under reduced pressure. The crude product was purified by flash chromatography (3:1 hexanes: $\text{EtOAc}$  eluent) to afford methyl ester **97** (89.0 mg, 98% yield) as a colorless oil.  $R_f$  0.50 (1:1 hexanes: $\text{EtOAc}$ );  $^1\text{H}$  NMR (300 MHz,  $\text{CDCl}_3$ ):  $\delta$  5.90–5.81 (m, 1H), 4.96 (br s, 1H), 4.94 (br s, 1H), 4.91–4.89 (m, 1H), 4.67 (app. t,  $J = 3.2$  Hz, 1H), 3.74 (s, 3H), 2.38 (ddd,  $J = 12.7, 5.2, 2.2$  Hz, 1H), 2.19–2.03 (comp. m, 2H), 2.09 (s, 3H), 1.93 (app. t,



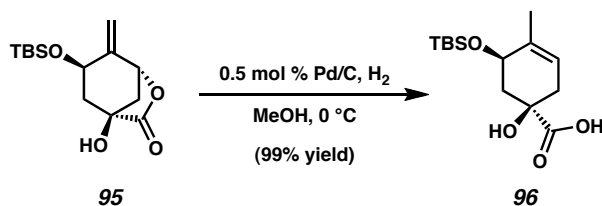
$J = 12.1$  Hz, 1H), 0.87 (s, 9H), 0.09 (s, 3H), 0.08 (s, 3H);  $^{13}\text{C}$  NMR (75 MHz,  $\text{CDCl}_3$ ):  $\delta$  173.7, 169.6, 146.3, 108.5, 76.5, 75.1, 68.0, 52.9, 42.7, 41.2, 25.8 (3C), 21.1, 18.1,  $-4.6$ ,  $-5.2$ ; IR (film) 3464 (br), 2954, 2932, 2858, 2888, 1739 (br), 1369, 1233 (br), 1124, 1098, 1072, 1036  $\text{cm}^{-1}$ ; HRMS-FAB ( $m/z$ ):  $[\text{M} + \text{H}]^+$  calc'd for  $\text{C}_{17}\text{H}_{31}\text{O}_6\text{Si}$ , 359.1890; found, 359.1900;  $[\alpha]_{\text{D}}^{26} -26.61^\circ$  (c 1.0,  $\text{C}_6\text{H}_6$ ).

The stable chair conformer of methyl ester **97** was determined using homodecoupling NMR experiments. The coupling constant between  $\text{H}_a$  and  $\text{H}_b$  was measured as  $J_{ab} = 10.7$  Hz.



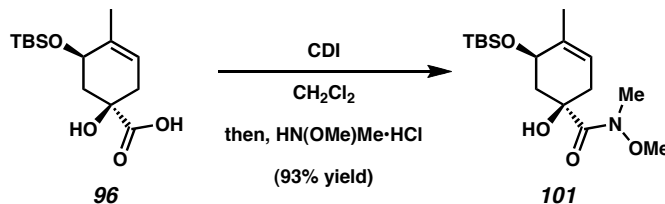
**Siloxycyclohexene 98.** Methyl ester **97** (94 mg, 0.262 mmol),  $\text{Pd}(\text{P}(t\text{-Bu})_3)_2$  (40.2 mg, 0.0786 mmol), anhydrous *N*-methylmorpholine *N*-oxide (307 mg, 2.52 mmol), THF (5.2 mL), and freshly distilled  $\text{Et}_3\text{SiH}$  (1.67 mL, 10.5 mmol) were combined under a glovebox atmosphere. The reaction mixture was immediately removed from the glovebox and placed in a  $70^\circ\text{C}$  oil bath. After 3.5 h, the reaction mixture was cooled to  $0^\circ\text{C}$ , and the volatiles were removed under reduced pressure. Saturated aq.  $\text{NH}_4\text{Cl}$  (15 mL) was added, and the mixture was extracted with  $\text{Et}_2\text{O}$  (3 x 25 mL). The combined organic

layers were washed with brine (15 mL), dried over  $\text{MgSO}_4$ , and evaporated under reduced pressure. The crude product was purified by flash chromatography (5:1 hexanes:EtOAc eluent) to afford siloxycyclohexene **98** (70 mg, 89% yield) as a pale yellow oil.  $R_f$  0.55 (2:1 hexanes:EtOAc);  $^1\text{H}$  NMR (300 MHz,  $\text{CDCl}_3$ ):  $\delta$  5.49–5.42 (m, 1H), 4.62 (s, 1H), 4.18–4.12 (m, 1H), 3.76 (s, 3H), 2.45–2.38 (comp. m, 2H), 2.16–2.10 (comp. m, 2H), 1.79–1.74 (m, 3H), 0.88 (s, 9H), 0.13 (s, 3H), 0.12 (s, 3H);  $^{13}\text{C}$  NMR (75 MHz,  $\text{CDCl}_3$ ):  $\delta$  175.3, 133.7, 120.9, 73.0, 68.7, 52.6, 38.4, 36.9, 25.9 (3C), 21.4, 18.0, –4.3, –4.7; IR (film) 3478 (br), 2955, 2858, 1740, 1451, 1253, 1217, 1111, 1065, 1037  $\text{cm}^{-1}$ ; HRMS-FAB ( $m/z$ ):  $[\text{M} + \text{H}]^+$  calc'd for  $\text{C}_{15}\text{H}_{19}\text{O}_4\text{Si}$ , 301.1835; found, 301.1835;  $[\alpha]_D^{24} +77.62^\circ$  (c 0.47,  $\text{CHCl}_3$ ).

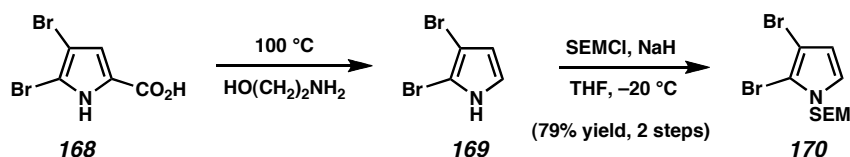


**Acid 96.** A mixture of methylene lactone **95** (4.0 g, 14.1 mmol) and 10% Pd/C (80 mg, 0.075 mmol) in methanol (120 mL) was cooled to 0 °C. The reaction vessel was evacuated and back-filled with  $\text{H}_2$  (3x). After 7 h at 0 °C, the mixture was filtered over a pad of Celite<sup>®</sup> (MeOH eluent), and the solvent was evaporated under reduced pressure to afford a colorless oil. Residual solvent was removed by holding the crude product under vacuum for 10 h, providing acid **96** (4.0 g, 99% yield), which was used immediately without further purification.  $R_f$  0.28 (1:1 hexanes:EtOAc; 1% acetic acid);  $^1\text{H}$  NMR (300 MHz,  $\text{CDCl}_3$ ):  $\delta$  5.88 (s, 1H), 5.53–5.48 (m, 1H), 4.16–4.11 (m, 1H), 2.71–2.60 (m, 1H), 2.36–2.22 (m, 1H), 2.18 (dd,  $J = 14.3, 3.9$  Hz, 1H), 2.08–2.01 (m, 1H), 1.79–1.76 (m,

3H), 0.89 (s, 9H), 0.15–0.13 (comp. m, 6H);  $^{13}\text{C}$  NMR (75 MHz,  $\text{CDCl}_3$ ):  $\delta$  176.4, 133.2, 121.1, 73.6, 68.6, 37.9, 35.9, 25.8 (3C), 21.4, 18.0,  $-4.5$ ,  $-4.7$ ; IR (film): 3356 (br), 2956, 2931, 2858, 1768 (br), 1718 (br), 1255, 1063  $\text{cm}^{-1}$ ; HRMS-FAB ( $m/z$ ):  $[\text{M} + \text{H}]^+$  calc'd for  $\text{C}_{14}\text{H}_{27}\text{O}_4\text{Si}$ , 287.1679; found, 287.1675;  $[\alpha]_D^{19} +37.58^\circ$  ( $c$  1.0,  $\text{C}_6\text{H}_6$ ).



**Weinreb Amide 101.** To acid **96** (4.0 g, 14.1 mmol) in  $\text{CH}_2\text{Cl}_2$  (70 mL) at 23 °C was added 1,1'-carbonyldiimidazole (3.65 g, 22.5 mmol) in equal portions over 15 min. After the final addition, stirring was continued for 10 min, then *N,O*-dimethylhydroxylamine  $\cdot$  HCl (3.43 g, 35.16 mmol) was added in one portion. The reaction was allowed to stir at 23 °C for 3 h.  $\text{Et}_2\text{O}$  was added (50 mL), and the reaction mixture was filtered. The filtrate was evaporated, diluted with  $\text{Et}_2\text{O}$  (125 mL), washed with 5% aq. citric acid (2 x 50 mL) and brine (50 mL), and dried over  $\text{MgSO}_4$ . The crude product was purified by flash chromatography (3:1 hexanes: $\text{EtOAc}$  eluent) to afford Weinreb amide **101** (4.29 g, 93% yield) as a colorless oil.  $R_f$  0.42 (2:1 hexanes: $\text{EtOAc}$ );  $^1\text{H}$  NMR (300 MHz,  $\text{CDCl}_3$ ):  $\delta$  5.43 (m, 1H), 4.72 (s, 1H), 4.17–4.11 (m, 1H), 3.71 (s, 3H), 3.22 (s, 3H), 2.59–2.24 (comp. m, 3H), 2.03 (dd,  $J = 14.6, 4.1$  Hz, 1H), 1.75–1.71 (m, 3H), 0.86 (s, 9H), 0.11 (s, 3H), 0.09 (s, 3H);  $^{13}\text{C}$  NMR (75 MHz,  $\text{CDCl}_3$ , 15/16 C):  $\delta$  133.5, 121.5, 74.3, 69.4, 61.2, 38.1, 35.9, 26.0, 25.9 (3C), 21.3, 18.1,  $-4.3$ ,  $-4.7$ ; IR (film): 3463 (br), 2956, 2932, 2858, 1655, 1362, 1254  $\text{cm}^{-1}$ ; HRMS-EI ( $m/z$ ):  $[\text{M} + \text{H}]^+$  calc'd for  $\text{C}_{16}\text{H}_{32}\text{NO}_4\text{Si}$ , 330.2101; found, 330.2085;  $[\alpha]_D^{19} +41.13^\circ$  ( $c$  1.0,  $\text{CHCl}_3$ ).

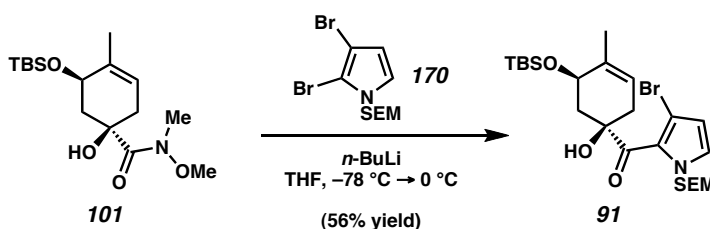


**Dibromopyrrole 170.** A solution of 4,5-dibromopyrrole carboxylic acid (**168**)<sup>72</sup> (6.05 g, 22.5 mmol) in ethanolamine (36 mL) was heated to 100 °C for 2 h, cooled to 23 °C, and poured into a mixture of Et<sub>2</sub>O (200 mL) and 0.5 N aq. HCl (300 mL). The layers were separated, and the aqueous layer was extracted with Et<sub>2</sub>O (2 x 250 mL). The combined organic layers were washed with brine (200 mL), dried over MgSO<sub>4</sub>, and concentrated to 100 mL. The solution was diluted with hexanes (100 mL), filtered over a plug of silica gel (2:1 hexanes:Et<sub>2</sub>O eluent), and concentrated to 150 mL. THF (100 mL) was added, and the solution was concentrated to 100 mL. This solvent exchange procedure was repeated 2 additional times (2 x 100 mL THF) to afford 2,3-dibromopyrrole (**169**) as a solution in THF, which was used immediately in the subsequent reaction.

*CAUTION: Concentrating the above described solutions to dryness or near-dryness leads to rapid decomposition of 2,3-dibromopyrrole (**169**).<sup>37</sup>*

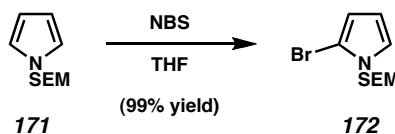
To 2,3-dibromopyrrole (**169**) in THF at –20 °C was added NaH (60% dispersion in mineral oil, 1.51 g, 37.8 mmol) in 3 equal portions over 3 min. After 10 min at –20 °C, SEMCl (4.8 mL, 27.1 mmol) was added dropwise over 1 min. The reaction mixture was allowed to warm to –8 °C over 40 min and was then quenched with saturated aq. NH<sub>4</sub>Cl (30 mL). After warming to 23 °C, the reaction mixture was diluted with Et<sub>2</sub>O (75 mL) and H<sub>2</sub>O (20 mL), and the layers were separated. The aqueous layer was further extracted

with Et<sub>2</sub>O (2 x 50 mL). The combined organic layers were washed with brine (50 mL), dried over MgSO<sub>4</sub>, and evaporated under reduced pressure. The crude product was purified by flash chromatography (6:1 hexanes:CH<sub>2</sub>Cl<sub>2</sub>, then 4:1 hexanes:CH<sub>2</sub>Cl<sub>2</sub> eluent) to afford dibromopyrrole **170** (6.25 g, 79% yield) as a yellow oil. *R<sub>f</sub>* 0.17 (6:1 hexanes:CH<sub>2</sub>Cl<sub>2</sub>); <sup>1</sup>H NMR (300 MHz, CDCl<sub>3</sub>): δ 6.82 (d, *J* = 3.6 Hz, 1H), 6.25 (d, *J* = 3.3 Hz, 1H), 5.21 (s, 2H), 3.48 (t, *J* = 8.1 Hz, 2H), 0.88 (t, *J* = 8.1 Hz, 2H), −0.03 (s, 9H); <sup>13</sup>C NMR (75 MHz, CDCl<sub>3</sub>): δ 123.1, 112.3, 103.7, 99.8, 77.8, 66.2, 17.9, −1.2 (3C); IR (film): 2953, 2896, 1514, 1470, 1279, 1250, 1109, 1084 cm<sup>−1</sup>; HRMS-EI (*m/z*): [*M* + H]<sup>+</sup> calc'd for C<sub>10</sub>H<sub>17</sub>NOSiBr<sub>2</sub>, 352.9446; found, 352.9435.



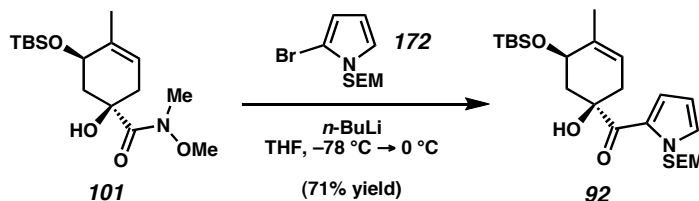
**Bromo Acyl Pyrrole 91.** To dibromopyrrole **170** (6.02 g, 17.06 mmol) in THF (114 mL) at −78 °C was added *n*-BuLi (2.5 M in hexanes, 6.7 mL, 16.8 mmol) dropwise over 1 min. After 10 min at −78 °C, Weinreb amide **101** (1.58 g, 4.80 mmol) in THF (15 mL) was added dropwise over 30 seconds. The reaction vessel was immediately warmed to 0 °C, stirred for 90 min, and cooled to −78 °C. The reaction was quenched with saturated aq. NH<sub>4</sub>Cl (15 mL), then warmed to 23 °C. The volatiles were removed in vacuo, and the residue was partitioned between Et<sub>2</sub>O (75 mL) and H<sub>2</sub>O (30 mL). The layers were separated, and the aqueous layer was further extracted with Et<sub>2</sub>O (2 x 50 mL). The combined organic layers were washed with brine (50 mL), dried over MgSO<sub>4</sub>, and evaporated under reduced pressure. The crude product was purified by flash

chromatography (11:9 CH<sub>2</sub>Cl<sub>2</sub>:hexanes eluent) to afford bromo acyl pyrrole **91** (1.47 g, 56% yield) as a colorless oil. *R<sub>f</sub>* 0.29 (11:9 hexanes:CH<sub>2</sub>Cl<sub>2</sub>); <sup>1</sup>H NMR (300 MHz, CDCl<sub>3</sub>): δ 6.77 (d, *J* = 2.9 Hz, 1H), 6.20 (d, *J* = 2.7 Hz, 1H), 5.53–5.47 (m, 1H), 5.35 (d, *J* = 10.4 Hz, 1H), 5.29 (d, *J* = 10.4 Hz, 1H), 4.72 (s, 1H), 4.18–4.14 (m, 1H), 3.31 (t, *J* = 8.2 Hz, 2H), 2.65–2.53 (m, 1H), 2.53–2.41 (m, 1H), 2.32 (dt, *J* = 14.3, 1.7 Hz, 1H), 2.15 (dd, *J* = 14.2 Hz, 4 Hz, 1H), 1.79–1.76 (m, 3H), 0.87 (s, 9H), 0.81 (t, *J* = 8.2 Hz, 2H), 0.12 (s, 6H), –0.06 (s, 9H); <sup>13</sup>C NMR (75 MHz, CDCl<sub>3</sub>): δ 201.9, 133.2, 129.6, 125.0, 121.6, 112.5, 101.8, 78.9, 78.6, 68.9, 66.2, 38.6, 37.4, 26.0 (3C), 21.5, 18.1, 17.8, –1.2 (3C), –4.1, –4.7; IR (film): 3477 (br), 2953, 1664 (br), 1400, 1253, 1101 cm<sup>–1</sup>; HRMS-EI (*m/z*): [M + H]<sup>+</sup> calc'd for C<sub>24</sub>H<sub>43</sub>NO<sub>4</sub>Si<sub>2</sub>Br, 544.1914; found, 544.1903; [α]<sub>D</sub><sup>19</sup> +1.64° (*c* 1.0, CHCl<sub>3</sub>).



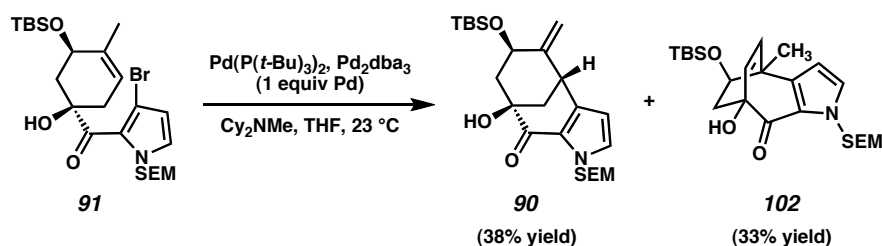
**Bromopyrrole 172.** To SEM pyrrole **171**<sup>22</sup> (1.25 g, 6.33 mmol) in THF (125 mL) at 23 °C was added freshly recrystallized NBS (1.127 g, 6.33 mmol) in one portion. After stirring for 5 min, additional NBS was added (15 mg, 0.084 mmol), and the reaction was immediately judged complete by TLC. The reaction mixture was poured into saturated aq. NaHCO<sub>3</sub> (100 mL) and extracted with Et<sub>2</sub>O (1 x 100 mL, 2 x 50 mL). The combined organic layers were washed with brine (75 mL), dried over MgSO<sub>4</sub>, and evaporated under reduced pressure. The crude product was purified by passage over a plug of silica gel (CH<sub>2</sub>Cl<sub>2</sub> eluent) to afford bromopyrrole **172** (1.73 g, 99% yield) as a pale yellow oil. *R<sub>f</sub>* 0.53 (1:1 CH<sub>2</sub>Cl<sub>2</sub>:hexanes); <sup>1</sup>H NMR (300 MHz, CDCl<sub>3</sub>): δ 6.83 (app. t, *J* = 2.5 Hz, 1H),

6.18–6.16 (comp. m, 2H), 5.22 (s, 2H), 3.53–3.46 (m, 2H), 0.92–0.85 (m, 2H), –0.03 (s, 9H);  $^{13}\text{C}$  NMR (75 MHz,  $\text{CDCl}_3$ ):  $\delta$  122.9, 111.9, 110.1, 102.0, 76.7, 66.0, 17.9, –1.2 (3C); IR (film): 2953, 2895, 1264, 1249, 1108, 1085  $\text{cm}^{-1}$ ; HRMS-EI ( $m/z$ ):  $[\text{M} + \text{H}]^+$  calc'd for  $\text{C}_{10}\text{H}_{18}\text{NOSiBr}$ , 275.0341; found, 275.0331.



**Acyl Pyrrole 92.** To bromopyrrole **172** (1.73 g, 6.26 mmol) in THF (42 mL) at  $-78\text{ }^{\circ}\text{C}$  was added  $n\text{-BuLi}$  (2.25 M in hexanes, 2.7 mL, 6.16 mmol) dropwise over 1 min. After 10 min at  $-78\text{ }^{\circ}\text{C}$ , Weinreb amide **101** (655 mg, 1.99 mmol) in THF (5 mL) was added dropwise over 1 min. The reaction vessel was immediately warmed to  $0\text{ }^{\circ}\text{C}$ , stirred for 25 min, and cooled to  $-78\text{ }^{\circ}\text{C}$ . The reaction mixture was quenched with saturated aq.  $\text{NH}_4\text{Cl}$  (10 mL), then warmed to  $23\text{ }^{\circ}\text{C}$ . The volatiles were removed under reduced pressure. The residue was partitioned between  $\text{Et}_2\text{O}$  (75 mL) and  $\text{H}_2\text{O}$  (50 mL), and the layers were separated. The aqueous layer was further extracted with  $\text{Et}_2\text{O}$  (2 x 40 mL). The combined organic layers were washed with brine (50 mL), dried over  $\text{MgSO}_4$ , and evaporated under reduced pressure. The crude product was purified by flash chromatography (23:1 hexanes: $\text{EtOAc}$ , then 15:1 hexanes: $\text{EtOAc}$  eluent) to afford acyl pyrrole **92** (656 mg, 71% yield) as a colorless oil.  $R_f$  0.30 (9:1 hexanes: $\text{EtOAc}$ );  $^1\text{H}$  NMR (300 MHz,  $\text{CDCl}_3$ ):  $\delta$  7.66 (dd,  $J = 4.0, 1.7\text{ Hz}$ , 1H), 7.06 (dd,  $J = 2.5, 1.7\text{ Hz}$ , 1H), 6.19 (dd,  $J = 4.0, 2.5\text{ Hz}$ , 1H), 5.71 (d,  $J = 10.4\text{ Hz}$ , 1H), 5.67 (d,  $J = 10.0\text{ Hz}$ , 1H), 5.52–5.47 (m, 1H), 4.90 (s, 1H), 4.19 (app. t,  $J = 3.1\text{ Hz}$ , 1H), 3.51 (t,  $J = 8.3\text{ Hz}$ , 2H), 2.52–2.46

(comp. m, 2H), 2.19–2.16 (comp. m, 2H), 1.80–1.78 (m, 3H), 0.92–0.88 (comp. m, 11H), 0.13 (s, 6H), –0.06 (s, 9H);  $^{13}\text{C}$  NMR (75 MHz,  $\text{CDCl}_3$ , 22/24 °C):  $\delta$  193.7, 133.5, 129.9, 128.0, 123.8, 121.7, 109.0, 78.2, 69.4, 66.3, 38.6, 38.3, 26.0 (3C), 21.5, 18.1, –1.2 (3C), –4.2, –4.7; IR (film): 3476, 2954, 2931, 2859, 1639, 1412, 1310, 1251, 1085  $\text{cm}^{-1}$ ; HRMS-EI ( $m/z$ ):  $[\text{M} + \text{H}]^+$  calc'd for  $\text{C}_{24}\text{H}_{44}\text{NO}_4\text{Si}_2$ , 466.2809; found, 466.2822;  $[\alpha]_D^{19}$  +34.25° ( $c$  1.0,  $\text{C}_6\text{H}_6$ ).



**[3.3.1] Bicycle 90.** Bromo acyl pyrrole **91** (52.0 mg, 0.0955 mmol),  $\text{Pd}_2\text{dba}_3$  (21.9 mg, 0.0239 mmol),  $\text{Pd}(\text{P}(t\text{-Bu})_3)_2$  (24.4 mg, 0.0477 mmol), THF (1.2 mL), and  $\text{Cy}_2\text{NMe}$  (24.3  $\mu\text{L}$ , 0.115 mmol) were combined under a glovebox atmosphere and stirred at 23 °C for 10 h. The reaction vessel was removed from the glovebox, diluted with 3:1 hexanes:EtOAc (2 mL), and filtered over a plug of silica gel topped with Celite® (3:1 hexanes:EtOAc eluent). The solvent was removed under reduced pressure, and the residue was purified by flash chromatography ( $\text{CH}_2\text{Cl}_2$ , then 3:1 hexanes:EtOAc eluent). The crude product was further purified by flash chromatography (6:1 hexanes:EtOAc eluent) to afford [3.3.1] bicycle **90** (16.7 mg, 38% yield) and [3.2.2] bicycle **102** (14.4 mg, 33% yield), both as pale yellow oils.

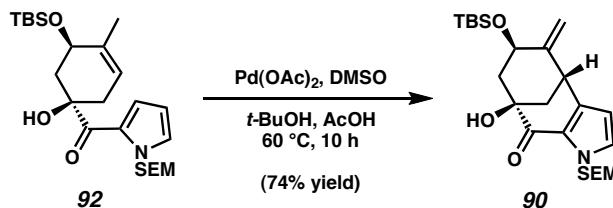
**[3.3.1] Bicycle 90:**  $R_f$  0.20 (4:1 hexanes:EtOAc);  $^1\text{H}$  NMR (300 MHz,  $\text{CDCl}_3$ ):  $\delta$  7.07 (d,  $J = 2.7$  Hz, 1H), 6.05 (d,  $J = 2.7$  Hz, 1H), 5.71 (d,  $J = 9.9$  Hz, 1H), 5.58 (d,  $J = 9.9$  Hz,



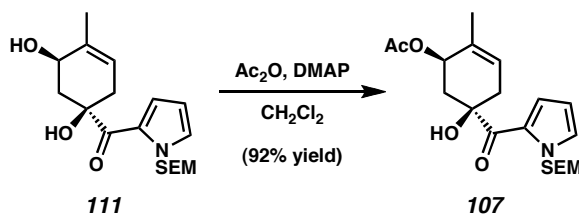
1H), 5.09–5.05 (m, 2H), 4.00 (s, 1H), 3.99–3.90 (m, 1H), 3.84 (app. t,  $J = 3.0$  Hz, 1H), 3.55–3.47 (m, 2H), 2.39 (app. dt,  $J = 7.4, 3.8$  Hz, 1H), 2.13–2.03 (comp. m, 2H), 1.73 (app. t,  $J = 11.8$  Hz, 1H), 0.98–0.76 (comp. m, 11H), –0.04 (s, 9H), –0.11 (s, 6H);  $^1\text{H}$  NMR (300 MHz,  $\text{C}_6\text{D}_6$ ):  $\delta$  6.53 (d,  $J = 2.5$  Hz, 1H), 5.77 (d,  $J = 2.8$  Hz, 1H), 5.55 (d,  $J = 10.2$  Hz, 1H), 5.32 (app. t,  $J = 1.9$  Hz, 1H), 5.26 (d,  $J = 10.2$  Hz, 1H), 5.01–4.97 (m, 1H), 4.29 (s, 1H), 4.27–4.19 (m, 1H), 3.59–3.47 (comp. m, 3H), 2.45–2.31 (comp. m, 2H), 2.16 (dd,  $J = 12.1, 3.0$  Hz, 1H), 2.07 (app. t,  $J = 11.8$  Hz, 1H), 0.92–0.89 (comp. m, 11H), 0.01 (s, 9H), –0.06 (s, 3H), –0.07 (s, 3H);  $^{13}\text{C}$  NMR (75 MHz,  $\text{C}_6\text{D}_6$ ):  $\delta$  191.5, 149.4, 141.8, 132.0, 125.5, 108.5, 107.4, 76.8, 75.8, 68.4, 66.3, 48.9, 45.5, 40.7, 26.3 (3C), 18.8, 18.2, –0.8 (3C), –4.4, –4.7; IR (film): 3480, 2953, 2858, 1651, 1420, 1318, 1251, 1100, 1077  $\text{cm}^{-1}$ ; HRMS-FAB ( $m/z$ ):  $[\text{M}]^+$  calc'd for  $\text{C}_{24}\text{H}_{41}\text{NO}_4\text{Si}_2$ , 463.2574; found, 463.2577;  $[\alpha]_{\text{D}}^{23}$  –275.07° ( $c$  1.0,  $\text{CHCl}_3$ ).

**[3.2.2] Bicycle 102:**  $R_f$  0.42 (5:1 hexanes:EtOAc);  $^1\text{H}$  NMR (300 MHz,  $\text{C}_6\text{D}_6$ ):  $\delta$  6.55 (d,  $J = 2.7$  Hz, 1H), 6.23 (d,  $J = 8.8$  Hz, 1H), 5.96 (d,  $J = 3.3$  Hz, 1H), 5.94 (d,  $J = 9.2$  Hz, 1H), 5.59 (d,  $J = 10.4$  Hz, 1H), 5.40 (d,  $J = 9.9$  Hz, 1H), 5.32 (s, 1H), 3.82–3.75 (m, 1H), 3.46 (t,  $J = 7.7$  Hz, 2H), 2.46 (dd,  $J = 13.7, 7.7$  Hz, 1H), 2.25 (dd,  $J = 13.7, 1.6$  Hz, 1H), 1.52 (s, 3H), 0.92 (s, 9H), 0.82 (t,  $J = 8.0$  Hz, 2H), –0.03 (s, 3H), –0.08 (s, 3H), –0.09 (s, 9H);  $^1\text{H}$  NMR (300 MHz,  $\text{CDCl}_3$ ):  $\delta$  6.98 (d,  $J = 2.7$  Hz, 1H), 6.15 (d,  $J = 2.7$  Hz, 1H), 6.02 (d,  $J = 9.3$  Hz, 1H), 5.98 (d,  $J = 8.8$  Hz, 1H), 5.69 (d,  $J = 9.9$  Hz, 1H), 5.62 (d,  $J = 9.9$  Hz, 1H), 4.93 (s, 1H), 3.81 (d,  $J = 7.7$  Hz, 1H), 3.50 (t,  $J = 8.0$  Hz, 2H), 2.36 (dd,  $J = 14.3, 7.7$  Hz, 1H), 1.94 (dd,  $J = 14.3, 1.6$  Hz, 1H), 1.55 (s, 3H), 0.91–0.83 (comp. m, 11H), 0.02 (s, 3H), 0.01 (s, 3H), –0.07 (s, 9H);  $^{13}\text{C}$  NMR (75 MHz,  $\text{CDCl}_3$ ):  $\delta$  188.7,

144.1, 139.4, 134.5, 129.1, 121.8, 107.7, 78.2, 77.8, 73.3, 66.4, 45.7, 45.0, 26.0 (3C), 22.2, 18.2, 18.0, -1.25 (3C), -4.1, -4.6; IR (film): 3432, 2955, 2858, 1645, 1250, 1081  $\text{cm}^{-1}$ ; HRMS-EI ( $m/z$ ):  $[\text{M} + \text{H}]^+$  calc'd for  $\text{C}_{24}\text{H}_{42}\text{NO}_4\text{Si}_2$ , 464.2652; found, 464.2665;  $[\alpha]_D^{19} +19.22^\circ$  ( $c$  1.0,  $\text{C}_6\text{H}_6$ ).

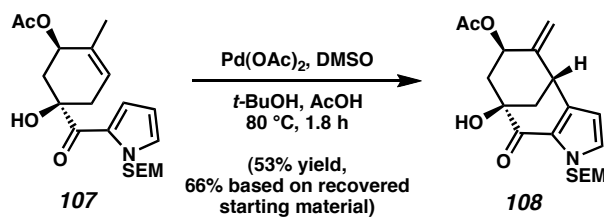


*Alternate Procedure.* To acyl pyrrole **92** (106.0 mg, 0.227 mmol) was added  $\text{Pd}(\text{OAc})_2$  (51.1 mg, 0.227 mmol), DMSO (32.3  $\mu\text{L}$ , 0.455 mmol),  $t$ -BuOH (18.2 mL), and AcOH (4.5 mL). The mixture was heated to 60  $^\circ\text{C}$  for 10 h, cooled to 23  $^\circ\text{C}$ , and filtered over a plug of silica gel (3:1 hexanes:EtOAc eluent). The solvent was evaporated, and the residue was again filtered over a plug of silica gel (3:1 hexanes:EtOAc eluent). After removal of solvent in vacuo, the product was purified by flash chromatography on silica gel (6:1 hexanes:EtOAc eluent) to afford [3.3.1] bicycle **90** (78.4 mg, 74% yield) as a pale yellow oil.



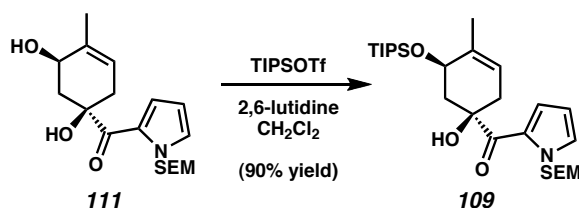
**Allylic Acetate 107.** To allylic alcohol **111**<sup>73</sup> (131.0 mg, 0.37 mmol) in  $\text{CH}_2\text{Cl}_2$  (7.5 mL) at 23  $^\circ\text{C}$  was added DMAP (68.1 mg, 0.56 mmol) followed by  $\text{Ac}_2\text{O}$  (53  $\mu\text{L}$ , 0.56 mmol). After stirring for 50 min, the reaction was quenched by the addition of

saturated aq.  $\text{NaHCO}_3$  (10 mL).  $\text{Et}_2\text{O}$  (30 mL) was added, the phases were partitioned, and the aqueous phase was extracted with  $\text{Et}_2\text{O}$  (3 x 30 mL). The combined organics were washed successively with  $\text{H}_2\text{O}$  (10 mL) and brine (10 mL), dried over  $\text{MgSO}_4$ , and evaporated in vacuo. Flash chromatography of the crude product (7:3 hexanes: $\text{Et}_2\text{O}$  eluent) provided allylic acetate **107** (134.4 mg, 92%) as a colorless oil.  $R_f$  0.21 (4:1 hexanes: $\text{EtOAc}$ );  $^1\text{H}$  NMR (300 MHz,  $\text{C}_6\text{D}_6$ ):  $\delta$  7.71 (dd,  $J = 3.9, 1.7$  Hz, 1H), 6.76 (dd,  $J = 2.6, 1.8$  Hz, 1H), 6.10 (dd,  $J = 4.0, 2.6$  Hz, 1H), 5.63 (d,  $J = 10.2$  Hz, 1H), 5.57 (d,  $J = 9.9$  Hz, 1H), 5.50–5.45 (m, 1H), 5.32–5.26 (m, 1H), 3.45 (t,  $J = 7.8$  Hz, 2H), 3.39 (s, 1H), 2.69–2.58 (m, 1H), 2.51–2.35 (comp. m, 2H), 2.28 (app. dt,  $J = 8.6, 5.0$  Hz, 1H), 1.60–1.57 (comp. m, 6H), 0.84 (t,  $J = 7.8$  Hz, 2H),  $-0.07$  (s, 9H);  $^{13}\text{C}$  NMR (75 MHz,  $\text{C}_6\text{D}_6$ ):  $\delta$  193.4, 169.9, 131.2, 130.6, 128.3, 124.6, 124.0, 109.2, 78.5, 77.6, 69.7, 66.4, 38.4, 38.3, 20.9, 20.8, 18.3,  $-1.0$  (3C); IR (film) 3458 (br), 2924, 1734, 1641, 1314, 1372, 1247, 1085  $\text{cm}^{-1}$ ; HRMS-FAB ( $m/z$ ):  $[\text{M} + \text{H}]^+$  calc'd for  $\text{C}_{20}\text{H}_{32}\text{NO}_5\text{Si}$ , 394.2050; found, 394.2030;  $[\alpha]_D^{27} +22.38^\circ$  (c 1.0,  $\text{C}_6\text{H}_6$ ).



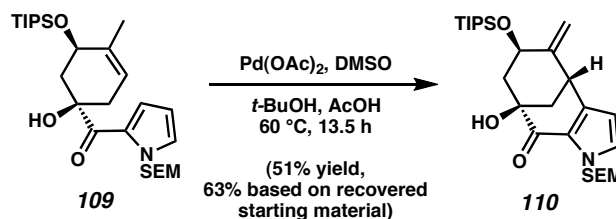
**Allylic Acetate 108.** For representative procedures, see oxidative cyclization of **92**  $\rightarrow$  **90** or **113**  $\rightarrow$  **114**. Purified by preparative thin-layer chromatography (4:1  $\text{CH}_2\text{Cl}_2$ : $\text{Et}_2\text{O}$  eluent). *Note:* Table 3.2.2, Entry 5 was performed in a round-bottom flask fitted with reflux condenser and an  $\text{O}_2$  balloon.  $R_f$  0.56 (4:1  $\text{CH}_2\text{Cl}_2$ : $\text{Et}_2\text{O}$ );  $^1\text{H}$  NMR (300 MHz,  $\text{C}_6\text{D}_6$ ):  $\delta$  6.52 (d,  $J = 2.7$  Hz, 1H), 5.76 (d,  $J = 2.7$  Hz, 1H), 5.51–5.41 (m, 1H), 5.46

(d,  $J = 10.4$  Hz, 1H), 5.27 (d,  $J = 10.4$  Hz, 1H), 4.93 (app. t,  $J = 1.7$  Hz, 1H), 4.91–4.88 (m, 1H), 4.35 (s, 1H), 3.56 (t,  $J = 7.7$  Hz, 2H), 3.47 (app. t,  $J = 3.1$  Hz, 1H), 2.49–2.36 (comp. m, 2H), 2.17–2.09 (m, 1H), 1.94 (app. t,  $J = 12.0$  Hz, 1H), 1.55 (s, 3H), 0.96–0.86 (m, 2H), –0.01 (s, 9H);  $^{13}\text{C}$  NMR (75 MHz,  $\text{C}_6\text{D}_6$ ):  $\delta$  190.6, 169.2, 145.5, 141.0, 132.4, 125.4, 108.6, 106.8, 76.8, 75.4, 69.0, 66.5, 45.3, 44.5, 40.9, 20.6, 18.2, –0.9 (3C); IR (film) 3469 (br), 2952, 1743, 1651, 1237, 1093, 1037  $\text{cm}^{-1}$ ; HRMS-FAB ( $m/z$ ):  $[\text{M}+\text{H}]^+$  calc'd for  $\text{C}_{20}\text{H}_{30}\text{NO}_5\text{Si}$ , 392.1893; found, 392.1886;  $[\alpha]_{\text{D}}^{27} -389.72^\circ$  ( $c$  0.6,  $\text{C}_6\text{H}_6$ ).

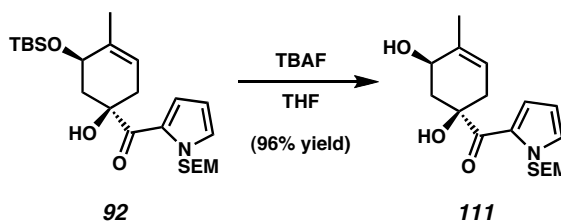


**TIPS Ether 109.** To allylic alcohol **111**<sup>73</sup> (50.7 mg, 0.14 mmol) in  $\text{CH}_2\text{Cl}_2$  (5 mL) at 23 °C was added 2,6-lutidine (34  $\mu\text{L}$ , 0.29 mmol), followed by TIPSOTf (44  $\mu\text{L}$ , 0.16 mmol). After stirring 5 min, saturated aq.  $\text{NH}_4\text{Cl}$  (5 mL) was added to quench the reaction. The phases were partitioned, and the aqueous phase was extracted with  $\text{CH}_2\text{Cl}_2$  (3 x 20 mL). The combined organic extracts were washed with brine (5 mL), and dried over  $\text{MgSO}_4$ . Following evaporation of the solvent in vacuo, the crude product was purified by flash chromatography (9:1 hexanes:EtOAc eluent) to provide TIPS ether **109** (65.8 mg, 90%) as a colorless oil.  $R_f$  0.58 (4:1 hexanes:EtOAc);  $^1\text{H}$  NMR (300 MHz,  $\text{C}_6\text{D}_6$ ):  $\delta$  8.12 (dd,  $J = 3.9, 1.6$  Hz, 1H), 6.77 (dd,  $J = 2.5, 1.6$  Hz, 1H), 6.15 (dd,  $J = 3.9, 2.5$  Hz, 1H), 5.69 (d,  $J = 10.1$  Hz, 1H), 5.65 (d,  $J = 9.6$  Hz, 1H), 5.34–5.29 (m, 1H), 5.00 (s, 1H), 4.24–4.19 (m, 1H), 3.49 (t,  $J = 7.8$  Hz, 2H), 2.69–2.63 (comp. m, 2H), 2.50–2.42 (m, 1H), 2.40–2.32 (m, 1H), 1.78–1.74 (m, 3H), 1.09–0.97 (comp. m, 21H), 0.85 (t,  $J =$

7.8 Hz, 2H),  $-0.06$  (s, 9H);  $^{13}\text{C}$  NMR (75 MHz,  $\text{C}_6\text{D}_6$ ):  $\delta$  194.1, 133.8, 130.3, 129.0, 124.7, 122.8, 109.2, 78.9, 78.5, 70.5, 66.3, 39.6, 39.4, 22.0, 18.7 (3C), 18.7 (3C), 18.4, 13.3 (3C),  $-0.9$  (3C); IR (film) 3472 (br), 2947, 2868, 1639, 1413, 1310, 1249, 1084  $\text{cm}^{-1}$ ; HRMS-FAB ( $m/z$ ):  $[\text{M} + \text{H}]^+$  calc'd for  $\text{C}_{27}\text{H}_{50}\text{NO}_4\text{Si}_2$ , 508.3278; found, 508.3273;  $[\alpha]_D^{27} +29.49^\circ$  (c 1.0,  $\text{C}_6\text{H}_6$ ).

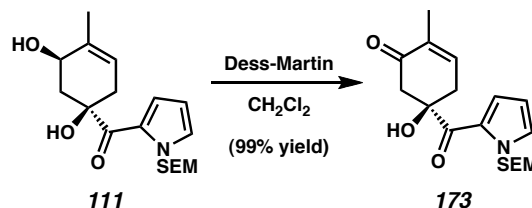


**TIPS Ether 110.** For representative procedures, see oxidative cyclization of **92**  $\rightarrow$  **90** or **113**  $\rightarrow$  **114**. Purified by preparative thin-layer chromatography (4:1 hexanes:EtOAc eluent).  $R_f$  0.29 (4:1 hexanes:EtOAc);  $^1\text{H}$  NMR (300 MHz,  $\text{C}_6\text{D}_6$ ):  $\delta$  6.54 (d,  $J = 2.7$  Hz, 1H), 5.78 (d,  $J = 2.7$  Hz, 1H), 5.52 (d,  $J = 10.1$  Hz, 1H), 5.41 (app. t,  $J = 2.1$  Hz, 1H), 5.32 (d,  $J = 10.1$  Hz, 1H), 5.02 (app. t,  $J = 2.3$  Hz, 1H), 4.38–4.29 (m, 1H), 4.25 (s, 1H), 3.59–3.45 (comp. m, 3H), 2.50–2.38 (comp. m, 2H), 2.21–2.04 (comp. m, 2H), 1.09–0.78 (comp. m, 23H),  $-0.01$  (s, 9H);  $^{13}\text{C}$  NMR (75 MHz,  $\text{C}_6\text{D}_6$ ):  $\delta$  191.5, 149.6, 141.7, 131.8, 125.6, 108.5, 107.5, 76.9, 75.9, 68.6, 66.5, 49.2, 40.7, 18.6 (3C) 18.6 (3C), 18.2, 13.1 (3C),  $-0.9$  (3C); IR (film) 3478 (br), 2946, 2867, 1650, 1100, 1080  $\text{cm}^{-1}$ ; HRMS-EI ( $m/z$ ):  $[\text{M}]^+$  calc'd for  $\text{C}_{27}\text{H}_{47}\text{NO}_4\text{Si}_2$ , 505.3044; found, 505.3041;  $[\alpha]_D^{27} -207.44^\circ$  (c 0.6,  $\text{C}_6\text{H}_6$ ).

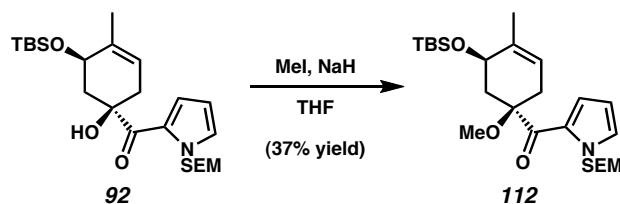


**Allylic Alcohol 111.** To allylic silyl ether **92** (100.0 mg, 0.21 mmol) in THF (5 mL) at 23 °C was added TBAF (1.0 M in THF, 250  $\mu$ L, 0.25 mmol). After stirring 5 min, the reaction mixture was quenched by the addition of saturated aq.  $\text{NH}_4\text{Cl}$  (5 mL). The reaction was poured into  $\text{Et}_2\text{O}$  (5 mL) and  $\text{H}_2\text{O}$  (5 mL), and the phases were partitioned. The aqueous phase was extracted with  $\text{Et}_2\text{O}$  (4 x 3 mL), and the combined organic extracts were dried by passage over a plug of  $\text{SiO}_2$  gel ( $\text{Et}_2\text{O}$  eluent). The solvent was evaporated in vacuo, and the residue was passed over another plug of  $\text{SiO}_2$  gel ( $\text{Et}_2\text{O}$  eluent) to afford allylic alcohol **111** (72.8 mg, 96% yield) as a colorless oil.  $R_f$  0.38 (2:1 hexanes: $\text{EtOAc}$ );  $^1\text{H}$  NMR (300 MHz,  $\text{C}_6\text{D}_6$ ):  $\delta$  7.01 (dd,  $J = 4.1, 1.7$  Hz, 1H), 6.70 (dd,  $J = 2.5, 1.7$  Hz, 1H), 5.99 (dd,  $J = 4.1, 2.8$  Hz, 1H), 5.52 (d,  $J = 10.0$  Hz, 1H), 5.49 (d,  $J = 10.2$  Hz, 1H), 5.31–5.25 (m, 1H), 4.95 (s, 1H), 3.93–3.84 (m, 1H), 3.60 (app. d,  $J = 9.6$  Hz, 1H), 3.41 (t,  $J = 7.8$  Hz, 2H), 2.77–2.65 (m, 1H), 2.27–2.16 (comp. m, 3H), 1.93–1.89 (m, 3H), 0.82 (t,  $J = 7.7$  Hz, 2H),  $-0.08$  (s, 9H);  $^{13}\text{C}$  NMR (75 MHz,  $\text{C}_6\text{D}_6$ ):  $\delta$  194.0, 136.2, 131.0, 126.9, 123.5, 120.0, 109.5, 78.8, 77.8, 68.1, 66.6, 41.0, 38.7, 21.7, 18.3,  $-1.0$  (3C); IR (film) 3388 (br), 2953, 1632, 1412, 1309, 1249, 1086  $\text{cm}^{-1}$ ; HRMS-FAB ( $m/z$ ):  $[\text{M} + \text{H}]^+$  calc'd for  $\text{C}_{18}\text{H}_{30}\text{NO}_4\text{Si}$ , 352.1944; found, 352.1941;  $[\alpha]_D^{27} +31.11^\circ$  (c 1.0,  $\text{C}_6\text{H}_6$ ).

For entry 2 (Table 3.2.2) and entry 8 (Table 3.4.2), small quantities of enone **173** were observed. An authentic sample was prepared as follows:



**Enone 173.** To allylic alcohol **111** (11.4 mg, 0.032 mmol) in  $\text{CH}_2\text{Cl}_2$  (1 mL) was added Dess-Martin periodinane (31.4 mg, 0.074 mmol). After stirring for 20 min, a solution of saturated  $\text{Na}_2\text{S}_2\text{O}_3$ : saturated  $\text{NaHCO}_3$  (1:1, 1 mL) was added to quench the reaction. The phases were partitioned, and the aqueous phase was extracted with  $\text{Et}_2\text{O}$  (1 x 4 mL). The combined organics were dried by passage over a plug of  $\text{SiO}_2$ , and the solvent was evaporated in vacuo. The residue was purified by preparative thin layer chromatography (1:1 hexanes:EtOAc eluent) to furnish enone **173** (11.4 mg, 99% yield) as a pale yellow oil.  $R_f$  0.40 (2:1 hexanes:EtOAc);  $^1\text{H}$  NMR (300 MHz,  $\text{C}_6\text{D}_6$ ):  $\delta$  7.03 (dd,  $J = 4.1, 1.4$  Hz, 1H), 6.68 (dd,  $J = 2.5, 1.6$  Hz, 1H), 5.97 (dd,  $J = 4.1, 2.7$  Hz, 1H), 5.92–5.87 (m, 1H), 5.48 (d,  $J = 9.6$  Hz, 1H), 5.43 (d,  $J = 9.6$  Hz, 1H), 3.40 (t,  $J = 7.8$  Hz, 2H), 3.25 (s, 1H), 2.98 (d,  $J = 16.0$  Hz, 1H), 2.83–2.73 (m, 1H), 2.66 (dd,  $J = 16.3, 1.6$  Hz, 1H), 2.25–2.14 (m, 1H), 1.84–1.81 (m, 3H), 0.82 (t,  $J = 7.8$  Hz, 2H),  $-0.08$  (s, 9H);  $^{13}\text{C}$  NMR (75 MHz,  $\text{C}_6\text{D}_6$ ):  $\delta$  195.2, 191.4, 138.9, 135.8, 131.1, 126.7, 123.5, 109.5, 80.3, 78.7, 66.6, 49.5, 38.4, 18.3, 16.4,  $-1.0$  (3C); IR (film) 3424 (br), 2953, 1677, 1639, 1412, 1249, 1085  $\text{cm}^{-1}$ ; HRMS-FAB ( $m/z$ ):  $[\text{M} + \text{H}]^+$  calc'd for  $\text{C}_{18}\text{H}_{28}\text{NO}_4\text{Si}$ , 350.1788; found, 350.1784;  $[\alpha]_{\text{D}}^{27} -21.94^\circ$  (c 1.0,  $\text{C}_6\text{H}_6$ ).

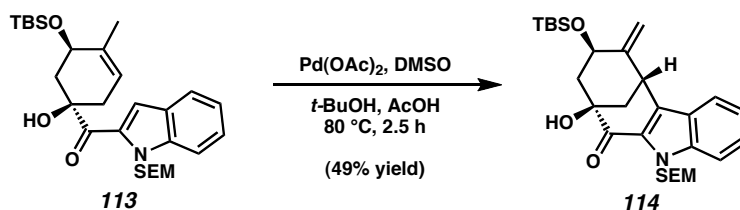


**Methyl Ether 112.** To allylic silyl ether **92** (55.0 mg, 0.12 mmol) in THF (2 mL) at 23 °C was added NaH (60% dispersion in mineral oil, 95.5 mg, 2.39 mmol). After stirring for 5 min, MeI (200  $\mu$ L, 3.21 mmol) was added. After stirring for 30 min, saturated aq.  $\text{NH}_4\text{Cl}$  (2 mL) was added dropwise over 1 min to quench the reaction. EtOAc (1 mL) was added, and the phases were partitioned. The aqueous phase was extracted with EtOAc (2 x 1 mL), and the combined organic extracts were washed with brine (1 mL) and dried over  $\text{MgSO}_4$ . After evaporation of the solvent in vacuo, the residue was purified by flash chromatography (9:1 hexanes:EtOAc eluent) to afford methyl ether **112** (21.1 mg, 37% yield).  $R_f$  0.53 (4:1 hexanes:EtOAc);  $^1\text{H}$  NMR (300 MHz,  $\text{C}_6\text{D}_6$ ):  $\delta$  7.76 (dd,  $J$  = 3.9, 1.6 Hz, 1H), 6.69 (dd,  $J$  = 2.5, 1.5 Hz, 1H), 6.08 (dd,  $J$  = 3.9, 2.5 Hz, 1H), 5.64 (d,  $J$  = 9.6 Hz, 1H), 5.45 (d,  $J$  = 10.1 Hz, 1H), 5.35–5.30 (m, 1H), 4.52–4.43 (m, 1H), 3.45 (t,  $J$  = 7.8 Hz, 2H), 3.10 (s, 3H), 2.99–2.85 (comp. m, 2H), 2.36–2.25 (m, 1H), 2.22 (dd,  $J$  = 12.4, 9.2 Hz, 1H), 1.82–1.79 (m, 3H), 0.98 (s, 9H), 0.88–0.82 (m, 2H), 0.09 (s, 3H), 0.07 (s, 3H),  $-0.05$  (s, 9H);  $^{13}\text{C}$  NMR (75 MHz,  $\text{C}_6\text{D}_6$ , 24/25 C):  $\delta$  193.2, 136.5, 130.0, 122.2, 120.7, 109.2, 84.6, 78.2, 70.1, 66.4, 51.7, 42.4, 35.0, 26.4 (3C), 20.3, 18.6, 18.4,  $-1.0$  (3C),  $-3.7$ ,  $-4.4$ ; IR (film) 2954, 1645, 1412, 1250, 1079  $\text{cm}^{-1}$ ; HRMS-FAB ( $m/z$ ):  $[\text{M} + \text{H}]^+$  calc'd for  $\text{C}_{25}\text{H}_{46}\text{NO}_4\text{Si}_2$ , 480.2965; found, 480.2958;  $[\alpha]_D^{27} +43.57^\circ$  ( $c$  1.0,  $\text{C}_6\text{H}_6$ ).

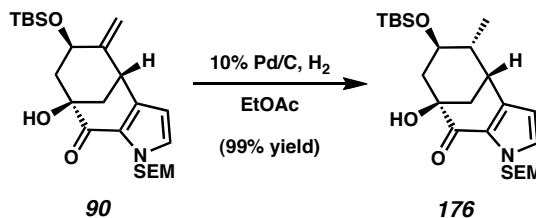




mL) was added, the phases were partitioned, and the aqueous phase was extracted with Et<sub>2</sub>O (2 x 75 mL). The combined organic extracts were washed successively with H<sub>2</sub>O (15 mL) and brine (15 mL), and dried over MgSO<sub>4</sub>. Following evaporation of the solvent in vacuo, the crude product was purified by flash chromatography (19:1 hexanes:EtOAc eluent) to furnish indole **113** (92.2 mg, 36% yield) as a colorless oil. *R<sub>f</sub>* 0.48 (4:1 hexanes:EtOAc); <sup>1</sup>H NMR (300 MHz, C<sub>6</sub>D<sub>6</sub>): δ 8.41 (s, 1H), 7.64–7.60 (m, 1H), 7.50–7.46 (m, 1H), 7.28–7.21 (m, 1H), 7.10–7.04 (m, 1H), 6.03–5.95 (m, 2H), 5.35–5.30 (m, 1H), 5.23 (s, 1H), 3.96–3.92 (m, 1H), 3.58 (t, *J* = 7.8 Hz, 2H), 2.77–2.57 (comp. m, 2H), 2.42–2.35 (m, 1H), 2.35–2.28 (m, 1H), 1.70–1.67 (m, 3H), 0.93–0.81 (m, 2H), 0.89 (s, 9H), 0.00 (s, 3H), –0.02 (s, 3H), –0.10 (s, 9H); <sup>13</sup>C NMR (75 MHz, C<sub>6</sub>D<sub>6</sub>): δ 196.9, 141.0, 133.7, 132.8, 127.5, 126.8, 124.1, 122.3, 121.9, 117.8, 112.2, 79.3, 74.1, 69.9, 66.0, 39.3, 39.3, 26.2 (3C), 21.6, 18.4, 18.3, –0.9 (3C), –4.3, –4.6; IR (film) 3466 (br), 2954, 1655, 1250, 1072 cm<sup>–1</sup>; HRMS-EI (*m/z*): [*M*]<sup>+</sup> calc'd for C<sub>28</sub>H<sub>45</sub>NO<sub>4</sub>Si<sub>2</sub>, 515.2887; found, 515.2893; [α]<sub>D</sub><sup>27</sup> –12.17° (*c* 1.0, C<sub>6</sub>H<sub>6</sub>).



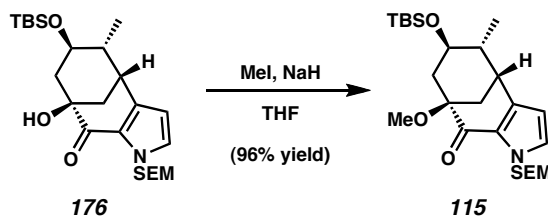
**Indole 114.** To indole **113** (23.5 mg, 0.05 mmol) was added Pd(OAc)<sub>2</sub> (10.2 mg, 0.05 mmol), DMSO (6.5 μL, 0.09 mmol), *t*-BuOH (3.6 mL), and AcOH (0.9 mL). The mixture was heated at 80 °C for 2.5 h, cooled to 23 °C, and filtered over a plug of silica gel (EtOAc eluent). The solvent was evaporated, and the crude product was purified by flash chromatography on silica gel (19:1 hexanes:EtOAc eluent) to afford pure [3.3.1]



**Reduced [3.3.1] Bicycle 176.** [3.3.1] Bicycle **90** (360 mg, 0.78 mmol), 10% Pd/C (130 mg, 0.12 mmol), and EtOAc (8 mL) were combined, and the reaction vessel was evacuated and back-filled with H<sub>2</sub> (1 atm). The reaction mixture was stirred under H<sub>2</sub> for 30 min, then filtered over a plug of silica gel topped with Celite® (EtOAc eluent) to afford reduced [3.3.1] bicycle **176** as a colorless oil (358 mg, 99% yield). R<sub>f</sub> 0.28 (5:1 hexanes:EtOAc); <sup>1</sup>H NMR (300 MHz, C<sub>6</sub>D<sub>6</sub>): δ 6.55 (d, *J* = 2.5 Hz, 1H), 5.74 (d, *J* = 2.5 Hz, 1H), 5.56 (d, *J* = 10.2 Hz, 1H), 5.30 (d, *J* = 10.2 Hz, 1H), 4.27 (s, 1H), 3.59–3.45 (m, 2H), 3.19 (ddd, *J* = 12.9, 7.7, 3.3 Hz, 1H), 2.58 (dd, *J* = 6.5, 3.2 Hz, 1H), 2.37–2.20

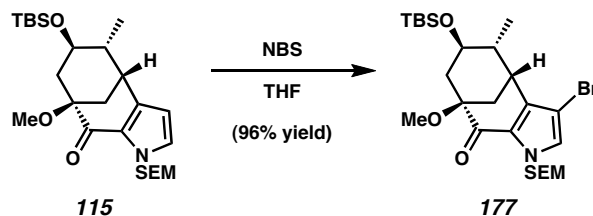
(comp. m, 2H), 2.06–1.90 (comp. m, 2H), 1.63–1.50 (m, 1H), 1.00 (d,  $J = 6.6$  Hz, 3H), 0.94–0.89 (comp. m, 11H),  $-0.02$  (s, 9H),  $-0.06$  (s, 3H),  $-0.09$  (s, 3H);  $^{13}\text{C}$  NMR (75 MHz,  $\text{C}_6\text{D}_6$ ):  $\delta$  190.8, 140.4, 131.3, 125.2, 110.1, 76.6, 75.6, 71.8, 66.1, 46.8, 44.3, 40.0, 37.3, 25.9 (3C), 18.1, 17.9, 16.5,  $-1.2$  (3C),  $-4.0$ ,  $-4.6$ ; IR (film): 3473 (br), 2953, 2931, 2857, 1651, 1420, 1249, 1079  $\text{cm}^{-1}$ ; HRMS-EI ( $m/z$ ):  $[\text{M} + \text{H}]^+$  calc'd for  $\text{C}_{24}\text{H}_{44}\text{NO}_4\text{Si}_2$ , 466.2809; found, 466.2804;  $[\alpha]_D^{19} -166.30^\circ$  ( $c$  1.0,  $\text{C}_6\text{H}_6$ ).

*NOTE: In some instances, trace phosphine contaminants from the Heck reaction (i.e., **91**  $\rightarrow$  **90**) prevented the reduction from occurring. Simply working up the reaction and re-exposing it to the identical reaction conditions (as described above) allowed the reduction to proceed.*



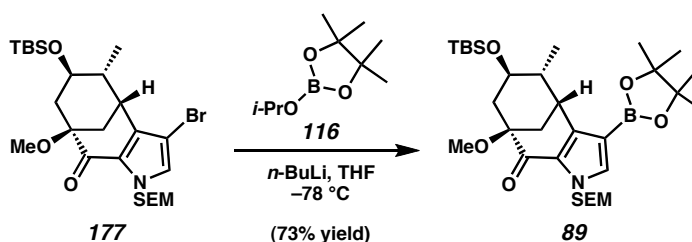
**Methyl Ether 115.** To reduced [3.3.1] bicycle **176** (358 mg, 0.77 mmol) in THF (7.7 mL) at 23 °C was added NaH (60% dispersion in mineral oil, 123 mg, 3.08 mmol). After stirring for 2 min at 23 °C, MeI was added (335  $\mu\text{L}$ , 5.38 mmol). The resulting mixture was stirred for 1 h, cooled to 0 °C, and quenched with saturated aq.  $\text{NH}_4\text{Cl}$  (4 mL), then warmed to 23 °C.  $\text{Et}_2\text{O}$  (10 mL) and  $\text{H}_2\text{O}$  (5 mL) were added, and the layers were separated. The aqueous layer was further extracted with  $\text{Et}_2\text{O}$  (2 x 15 mL). The combined organic layers were washed with brine (20 mL), dried over  $\text{MgSO}_4$ , and evaporated under reduced pressure. The crude product was purified by flash

chromatography (4:1 hexanes:EtOAc eluent) to afford methyl ether **115** (354 mg, 96% yield) as a colorless oil.  $R_f$  0.34 (5:1 hexanes:EtOAc);  $^1\text{H}$  NMR (300 MHz,  $\text{C}_6\text{D}_6$ ):  $\delta$  6.58 (d,  $J = 2.8$  Hz, 1H), 5.78 (d,  $J = 2.5$  Hz, 1H), 5.57 (d,  $J = 10.2$  Hz, 1H), 5.54 (d,  $J = 10.2$  Hz, 1H), 3.65–3.50 (m, 2H), 3.37 (s, 3H), 3.22 (ddd,  $J = 12.9, 7.9, 3.1$  Hz, 1H), 2.68 (dd,  $J = 6.5, 3.2$  Hz, 1H), 2.59–2.49 (comp. m, 2H), 1.86 (dd,  $J = 12.4$  Hz, 11.3 Hz, 1H), 1.72–1.56 (m, 2H), 1.04 (d,  $J = 6.9$  Hz, 3H), 0.93–0.85 (comp. m, 11H), –0.02 (s, 9H), –0.07 (s, 3H), –0.10 (s, 3H);  $^{13}\text{C}$  NMR (75 MHz,  $\text{C}_6\text{D}_6$ , 24/25 °C):  $\delta$  189.4, 138.3, 130.4, 109.7, 81.9, 76.9, 72.4, 66.2, 51.8, 45.9, 41.3, 41.2, 37.6, 26.4 (3C), 18.5, 18.3, 17.0, –0.9 (3C), –3.6, –4.4; IR (film): 2954, 1657, 1421, 1250, 1085  $\text{cm}^{-1}$ ; HRMS-EI ( $m/z$ ):  $[\text{M} + \text{H}]^+$  calc'd for  $\text{C}_{25}\text{H}_{46}\text{NO}_4\text{Si}_2$ , 480.2965; found, 480.2970;  $[\alpha]_D^{19}$  –172.9° (c 1.0,  $\text{C}_6\text{H}_6$ ).



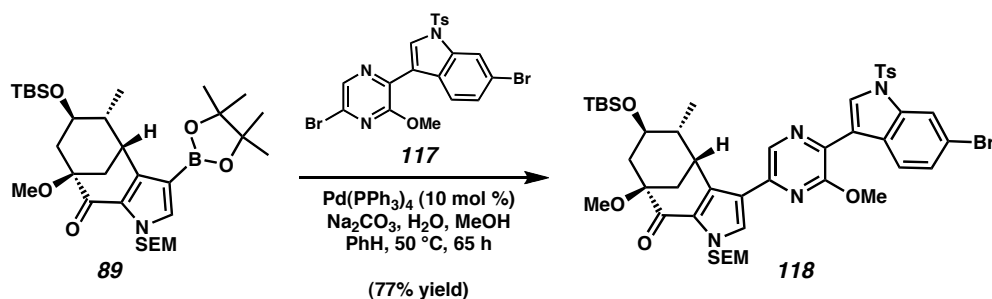
**Bromide 177.** To methyl ether **115** (305 mg, 0.64 mmol) in THF (6 mL) at 0 °C was added freshly recrystallized NBS (147 mg, 0.83 mmol). After stirring for 10 min at 0 °C, the reaction mixture was warmed to 23 °C, and additional NBS (30 mg, 0.17 mmol) was added. After 5 min, the reaction was quenched with saturated aq.  $\text{Na}_2\text{S}_2\text{O}_3$ , diluted with  $\text{H}_2\text{O}$  (15 mL), and extracted with  $\text{Et}_2\text{O}$  (3 x 15 mL). The combined organic layers were washed with brine (15 mL), dried over  $\text{MgSO}_4$ , and evaporated under reduced pressure. The crude product was purified by flash chromatography (5:1 hexanes:EtOAc eluent) to afford bromide **177** (340 mg, 96% yield) as a colorless oil.  $R_f$  0.55 (3:1 hexanes:EtOAc);  $^1\text{H}$  NMR (300 MHz,  $\text{C}_6\text{D}_6$ ):  $\delta$  6.57 (s, 1H), 5.46 (d,  $J = 10.2$  Hz, 1H),

5.34 (d,  $J = 10.2$  Hz, 1H), 3.57–3.41 (m, 2H), 3.32–3.20 (m, 4H), 2.88 (dd,  $J = 6.5, 3.2$  Hz, 1H), 2.46 (ddd,  $J = 12.2, 5.1, 2.5$  Hz, 1H), 2.28 (app. dt,  $J = 7.4, 4.0$  Hz, 1H), 1.78 (app. t,  $J = 11.8$  Hz, 1H), 1.69–1.57 (m, 1H), 1.52 (dd,  $J = 11.8, 3.0$  Hz, 1H), 1.19 (d,  $J = 6.9$  Hz, 3H), 0.91–0.80 (comp. m, 11H),  $-0.05$  (s, 9H),  $-0.09$  (s, 3H),  $-0.12$  (s, 3H);  $^{13}\text{C}$  NMR (75 MHz,  $\text{C}_6\text{D}_6$ ):  $\delta$  189.6, 147.2, 137.2, 130.1, 98.4, 81.8, 77.0, 72.1, 66.6, 51.8, 45.8, 42.4, 41.0, 35.9, 26.3 (3C), 18.5, 18.3, 17.8,  $-0.9$  (3C),  $-3.7$ ,  $-4.3$ ; IR (film): 2954, 2930, 1664, 1249, 1089  $\text{cm}^{-1}$ ; HRMS-EI ( $m/z$ ):  $[\text{M} + \text{H}]^+ - \text{H}_2$  calc'd for  $\text{C}_{25}\text{H}_{43}\text{NO}_4\text{Si}_2\text{Br}$ , 556.1914; found, 556.1928;  $[\alpha]_{\text{D}}^{19} -98.22^\circ$  ( $c$  1.0,  $\text{C}_6\text{H}_6$ ).



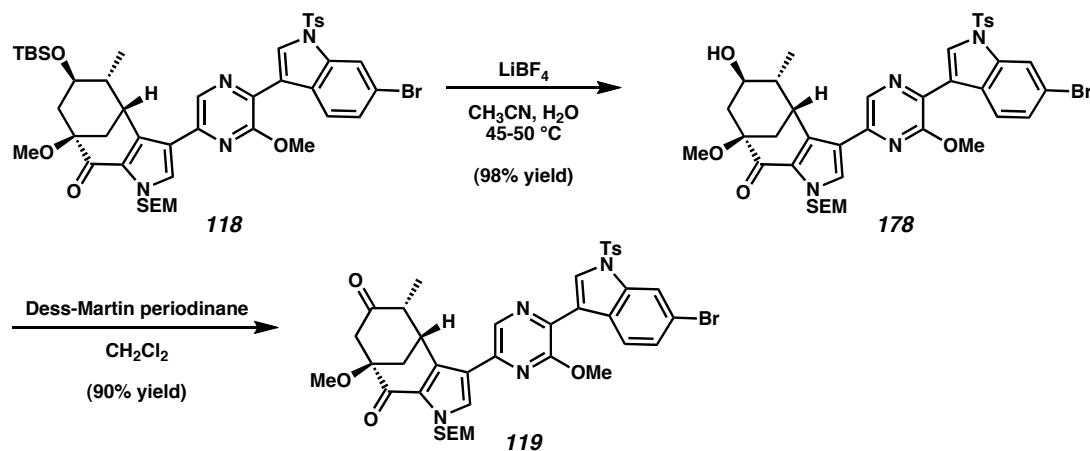
**Boronic Ester 89.** To bromide **177** (116 mg, 0.21 mmol) and 2-isopropoxy-4,4,5,5-tetramethyl-1,3,2-dioxaborolane (**116**) (847  $\mu\text{L}$ , 4.15 mmol) in THF (10.4 mL) at  $-78^\circ\text{C}$  was added  $n\text{-BuLi}$  (2.3 M in hexanes, 1.35 mL, 3.11 mmol) dropwise over 2 min. After stirring for 15 min at  $-78^\circ\text{C}$ , the reaction mixture was quenched with saturated aq.  $\text{NH}_4\text{Cl}$ , warmed to  $23^\circ\text{C}$ , and diluted with  $\text{H}_2\text{O}$  (10 mL). The mixture was extracted with  $\text{Et}_2\text{O}$  (3 x 15 mL). The combined organic layers were washed with brine (15 mL), dried over  $\text{MgSO}_4$ , and evaporated under reduced pressure. The crude product was purified by flash chromatography (4:1 hexanes:EtOAc with 0.5%  $\text{Et}_3\text{N}$  eluent) to afford boronic ester **89** (92 mg, 73% yield) as a white powder, which was used immediately in the next step.  $R_f$  0.50 (3:1 hexanes:EtOAc); mp  $143\text{--}145^\circ\text{C}$ ;  $^1\text{H}$  NMR (300 MHz,  $\text{C}_6\text{D}_6$ ):  $\delta$  7.42 (s, 1H), 5.55 (d,  $J = 10.1$  Hz, 1H), 5.51 (d,  $J = 9.8$  Hz, 1H), 3.74–3.68 (m, 1H), 3.60–3.50 (m,

2H), 3.43–3.36 (m, 1H), 3.33 (s, 3H), 2.65–2.53 (comp. m, 2H), 1.91 (app. t,  $J = 11.8$  Hz, 1H), 1.89–1.80 (m, 1H), 1.68 (dd,  $J = 11.8, 2.8$  Hz, 1H), 1.34 (d,  $J = 6.6$  Hz, 3H), 1.15 (s, 6H), 1.14 (s, 6H), 0.94–0.81 (comp. m, 11H), –0.04 (s, 3H), –0.05 (s, 9H), –0.07 (s, 3H);  $^{13}\text{C}$  NMR (75 MHz,  $\text{C}_6\text{D}_6$ , 30/31 °C):  $\delta$  190.1, 145.1, 139.3, 130.2, 83.5 (2C), 82.0, 77.2, 72.6, 66.5, 51.7, 46.1, 42.0, 41.6, 36.8, 26.4 (3C), 25.4 (2C), 25.2 (2C), 18.5, 18.3, 16.9, –0.9 (3C), –3.6, –4.3; IR (film): 2953, 2931, 2858, 1658, 1543, 1249, 1141, 1085  $\text{cm}^{-1}$ ; HRMS-FAB ( $m/z$ ):  $[\text{M} + \text{H}]^+$  calc'd for  $\text{C}_{31}\text{H}_{57}\text{BNO}_6\text{Si}_2$ , 606.3818; found, 606.3805;  $[\alpha]_{\text{D}}^{19} -98.84^\circ$  ( $c$  1.0,  $\text{C}_6\text{H}_6$ ).



**Suzuki Adduct 118.** Bromopyrazine **117** (46.5 mg, 0.087 mmol), boronic ester **89** (35 mg, 0.058 mmol), benzene (1.15 mL), methanol (231  $\mu\text{L}$ ), 2 M aq.  $\text{Na}_2\text{CO}_3$  (96  $\mu\text{L}$ ), and tetrakis(triphenylphosphine)palladium(0) (6.7 mg, 0.0058 mmol) were combined and deoxygenated by sparging with argon for 5 min. The reaction vessel was evacuated, purged with  $\text{N}_2$ , sealed, heated to 50 °C for 65 h, cooled to 23 °C, then quenched by the addition of  $\text{Na}_2\text{SO}_4$  (200 mg). Following filtration over a pad of silica gel (2:1 hexanes:EtOAc eluent) and evaporation to dryness under reduced pressure, the remaining residue was purified by flash chromatography (3:1 hexanes:EtOAc eluent) to afford Suzuki adduct **118** (41.5 mg, 77% yield) as a yellow oil.  $R_f$  0.43 (2:1 hexanes:EtOAc);  $^1\text{H}$  NMR (300 MHz,  $\text{CDCl}_3$ ):  $\delta$  8.61 (d,  $J = 8.5$  Hz, 1H), 8.45 (s, 1H),

8.44 (s, 1H), 8.16 (d,  $J = 1.5$  Hz, 1H), 7.80 (d,  $J = 8.5$  Hz, 2H), 7.59 (s, 1H), 7.40 (dd,  $J = 8.5, 1.8$  Hz, 1H), 7.23 (d,  $J = 7.9$  Hz, 2H), 5.85 (d,  $J = 10.0$  Hz, 1H), 5.78 (d,  $J = 10.0$  Hz, 1H), 4.27–4.21 (m, 1H), 4.19 (s, 3H), 3.72–3.59 (m, 2H), 3.34 (s, 3H), 3.13–3.02 (m, 1H), 2.87–2.77 (m, 1H), 2.32 (s, 3H), 2.22–2.12 (m, 1H), 1.98–1.89 (m, 1H), 1.82–1.72 (m, 1H), 1.67 (app. t,  $J = 11.7$  Hz, 1H), 1.04–0.83 (m, 2H), 0.78 (s, 9H), 0.72 (d,  $J = 6.7$  Hz, 3H), –0.02 (s, 9H), –0.09 (s, 3H), –0.16 (s, 3H);  $^{13}\text{C}$  NMR (75 MHz,  $\text{CDCl}_3$ , 44/45 °C):  $\delta$  190.0, 156.2, 145.7, 143.6, 136.9, 135.7, 135.5, 135.0, 132.7, 130.3 (2C), 130.2, 129.3, 128.8, 128.5, 127.3, 127.1 (2C), 125.3, 120.5, 119.0, 116.9, 116.4, 81.3, 77.2, 71.4, 66.7, 54.3, 51.6, 44.8, 41.8, 40.2, 34.8, 25.9 (3C), 21.8, 18.1, 16.1, –1.1 (3C), –4.0, –4.7; IR (film): 2952, 1660, 1555, 1372, 1372, 1190, 1140, 1089  $\text{cm}^{-1}$ ; HRMS-FAB ( $m/z$ ):  $[\text{M}]^+$  calc'd for  $\text{C}_{45}\text{H}_{59}\text{N}_4\text{O}_7\text{Si}_2\text{SBr}$ , 934.2826; found, 934.2829;  $[\alpha]_{\text{D}}^{21} +51.73^\circ$  ( $c$  1.0,  $\text{CHCl}_3$ ).

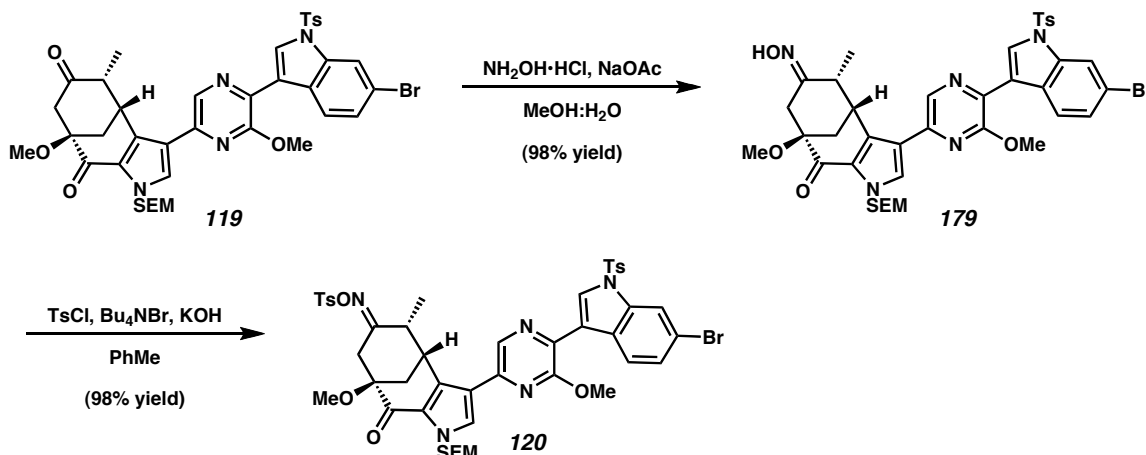


**Ketone 119.** Suzuki adduct **118** (113 mg, 0.121 mmol),  $\text{LiBF}_4$  (113 mg, 1.21 mmol), acetonitrile (6 mL), and water (600  $\mu\text{L}$ ) were heated to  $45\text{--}50^\circ\text{C}$ . After 9 h, additional  $\text{LiBF}_4$  (30 mg, 0.32 mmol) was introduced, and heating was continued. After 6 h, additional  $\text{LiBF}_4$  (35 mg, 0.32 mmol) was introduced, and heating was continued for 16 h. The reaction mixture was cooled to  $23^\circ\text{C}$ , quenched with 10% aq. citric acid (10



mL), and extracted with EtOAc (3 x 20 mL). The combined organic layers were dried over  $\text{MgSO}_4$  and evaporated under reduced pressure. The crude product was purified by flash chromatography (3:1 EtOAc:hexanes eluent) to yield alcohol **178** (96.9 mg, 98% yield) as a yellow oil, which was used in the subsequent step without further purification.  $R_f$  0.44 (3:1 EtOAc:hexanes).

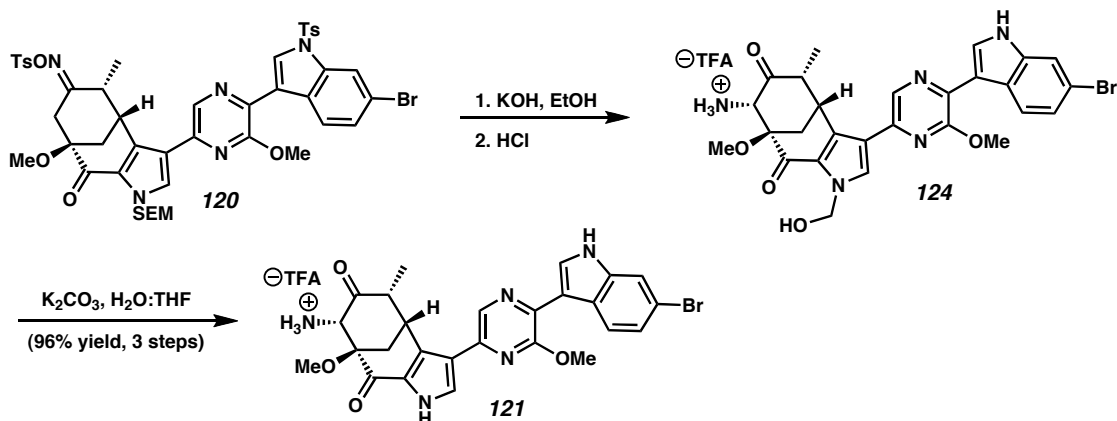
To alcohol **178** (96 mg, 0.117 mmol) in  $\text{CH}_2\text{Cl}_2$  (2.0 mL) at 23 °C was added Dess-Martin periodinane (74.3 mg, 0.175 mmol). The mixture was stirred for 3 min, quenched with a solution of saturated aq.  $\text{NaHCO}_3$  and saturated aq.  $\text{Na}_2\text{S}_2\text{O}_3$  (1:1, 5 mL), stirred for 5 min, and extracted with EtOAc (3 x 15 mL). The combined organic layers were washed with brine (15 mL), dried over  $\text{MgSO}_4$ , and evaporated under reduced pressure. The crude product was purified by flash chromatography (1:1 hexanes:EtOAc eluent) to yield ketone **119** (86 mg, 90% yield) as a yellow foam.  $R_f$  0.48 (1:1 hexanes:EtOAc);  $^1\text{H}$  NMR (300 MHz,  $\text{CDCl}_3$ ):  $\delta$  8.61 (d,  $J$  = 8.5 Hz, 1H), 8.45 (s, 1H), 8.42 (s, 1H), 8.18 (d,  $J$  = 1.7 Hz, 1H), 7.81 (d,  $J$  = 8.5 Hz, 2H), 7.56 (s, 1H), 7.42 (dd,  $J$  = 8.7, 1.8 Hz, 1H), 7.25 (d,  $J$  = 7.7 Hz, 2H), 5.77 (d,  $J$  = 10.5 Hz, 1H), 5.72 (d,  $J$  = 10.2 Hz, 1H), 4.62–4.56 (m, 1H), 4.20 (s, 3H), 3.57 (app. dt,  $J$  = 8.2, 1.8 Hz, 2H), 3.43 (s, 3H), 3.14–3.06 (m, 1H), 2.91–2.81 (m, 1H), 2.74 (s, 2H), 2.40 (dd,  $J$  = 12.5, 2.9 Hz, 1H), 2.34 (s, 3H), 0.96–0.88 (m, 2H), 0.78 (d,  $J$  = 6.6 Hz, 3H), –0.02 (s, 9H);  $^{13}\text{C}$  NMR (75 MHz,  $\text{CDCl}_3$ , 37/39 °C):  $\delta$  207.2, 188.0, 156.1, 145.7, 143.2, 136.3, 135.7, 134.9, 132.6, 130.7, 130.3 (2C), 128.8, 128.4, 127.3, 127.1 (2C), 125.4, 120.5, 119.0, 116.8, 116.3, 82.4, 77.1, 66.9, 54.3, 52.2, 52.0, 49.2, 40.2, 35.2, 21.8, 18.1, 12.2, –1.2 (3C); IR (film): 2950, 1716, 1664, 1557, 1373, 1190, 1178, 1090  $\text{cm}^{-1}$ ; HRMS-FAB ( $m/z$ ):  $[\text{M}]^+$  calc'd for  $\text{C}_{39}\text{H}_{43}\text{N}_4\text{O}_7\text{SiSBr}$ , 818.1805; found, 818.1836;  $[\alpha]_D^{21} +71.61^\circ$  (c 1.0,  $\text{CHCl}_3$ ).



**Tosyl Oxime 120.** To ketone **119** (50.0 mg, 0.061 mmol),  $\text{NH}_2\text{OH}\cdot\text{HCl}$  (85 mg, 1.22 mmol), and  $\text{NaOAc}\cdot 3\text{H}_2\text{O}$  (125 mg, 0.915 mmol) was added methanol (2.5 mL), followed by  $\text{H}_2\text{O}$  (350  $\mu\text{L}$ ), then additional methanol (5 mL). The homogeneous solution was stirred at 23 °C for 8 h, and the solvent was removed under reduced pressure.  $\text{H}_2\text{O}$  (15 mL) was added, and the resulting mixture was extracted with EtOAc (3 x 15 mL). The combined organic layers were washed with brine (15 mL), dried over  $\text{MgSO}_4$ , and evaporated under reduced pressure. The crude product was further purified by filtration over a plug of silica gel (EtOAc eluent) to yield oxime **179** (50.1 mg, 98% yield) as a yellow foam, which was used without purification in the subsequent reaction.  $R_f$  0.46 (1:1 hexanes:EtOAc).

To a solution of oxime **179** (20.0 mg, 0.0240 mmol),  $\text{TsCl}$  (14.0 mg, 0.0734 mmol), and  $\text{Bu}_4\text{NBr}$  (1.0 mg, 0.0031 mmol) in toluene (2.0 mL) at 0 °C was added 50% aq.  $\text{KOH}$  (310  $\mu\text{L}$ ). The reaction mixture was stirred at 0 °C for 2 h, quenched with ice-cold  $\text{H}_2\text{O}$  (1.5 mL) and extracted with ice-cold EtOAc (5 x 1 mL). The combined organic layers were washed with brine (1 mL), dried by passage over a plug of silica gel (EtOAc eluent), and evaporated under reduced pressure. The crude product was purified by flash

chromatography (1:1 hexanes:EtOAc eluent) to yield tosyl oxime **120** (23.3 mg, 98% yield) as a yellow foam.  $R_f$  0.48 (1:1 hexanes:EtOAc);  $^1\text{H}$  NMR (300 MHz,  $\text{CDCl}_3$ ):  $\delta$  8.63 (d,  $J = 8.5$  Hz, 1H), 8.46 (s, 1H), 8.41 (s, 1H), 8.19 (d,  $J = 1.4$  Hz, 1H), 7.81 (d,  $J = 8.3$  Hz, 2H), 7.65 (d,  $J = 8.0$  Hz, 2H), 7.51 (s, 1H), 7.44 (dd,  $J = 8.7, 1.5$  Hz, 1H), 7.28–7.19 (comp. m, 4H), 5.87 (d,  $J = 10.2$  Hz, 1H), 5.42 (d,  $J = 10.2$  Hz, 1H), 4.45–4.43 (m, 1H), 4.20 (s, 3H), 3.67–3.53 (comp. m, 3H), 3.38 (s, 3H), 2.98–2.89 (m, 1H), 2.87–2.77 (m, 1H), 2.42 (s, 3H), 2.35 (s, 3H), 2.12 (d,  $J = 14.0$  Hz, 2H), 1.05–0.85 (m, 2H), 0.78 (d,  $J = 6.6$  Hz, 3H),  $-0.02$  (s, 9H);  $^{13}\text{C}$  NMR (75 MHz,  $\text{CDCl}_3$ ):  $\delta$  187.2, 165.8, 156.3, 145.8, 144.8, 143.5, 135.8, 135.7, 135.3, 135.0, 132.9, 132.6, 130.4 (2C), 129.9, 129.4 (2C), 129.1 (2C), 128.9, 128.4, 128.0, 127.5, 127.2 (2C), 125.3, 120.3, 119.2, 116.8, 116.5, 80.8, 77.4, 67.2, 54.4, 52.2, 42.5, 40.3, 36.5, 36.2, 21.9, 21.9, 18.1, 13.7,  $-1.1$  (3C); IR (film): 2946, 1665, 1555, 1373, 1191, 1178, 1140  $\text{cm}^{-1}$ ; HRMS-FAB ( $m/z$ ):  $[\text{M}]^+$  calc'd for  $\text{C}_{46}\text{H}_{50}\text{N}_5\text{O}_9\text{SiS}_2\text{Br}$ , 987.2002; found, 987.2038;  $[\alpha]_D^{20} +139.01^\circ$  ( $c$  1.0,  $\text{CHCl}_3$ ).

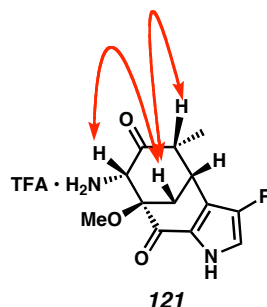


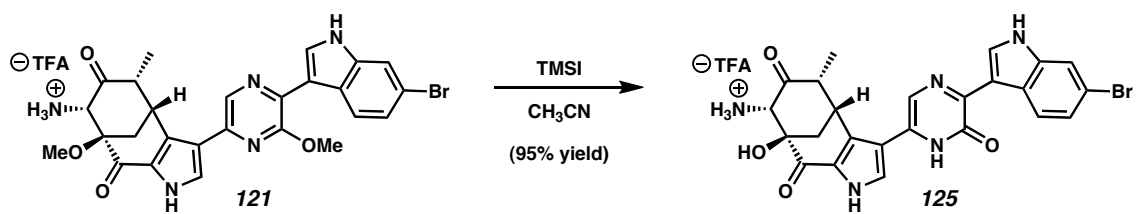
**Aminoketone 121.** To a stirred solution of tosyl oxime **120** (23.3 mg, 0.0236 mmol) in EtOH (3.5 mL) at 0 °C was added 50% aq. KOH (450  $\mu$ L) dropwise over 1 min. The reaction mixture was stirred at 0 °C for 3 h, then 6 N aq. HCl (5 mL) was added. The reaction mixture was heated to 60 °C for 10 h, cooled to 23 °C, and purified by reversed-phase filtration through a Sep-Pak column: loaded with water containing 0.1% (w/v) TFA, washed with 15% acetonitrile:water containing 0.1% (w/v) TFA to remove salts, then 70% acetonitrile:water containing 0.1% (w/v) TFA to collect the crude product. The solvents were removed under reduced pressure to afford hemiaminal **124**, which was used immediately in the subsequent reaction. Although hemiaminal **124** is typically used in crude form, it has been observed by  $^1\text{H}$  NMR.  $^1\text{H}$  NMR (600 MHz,  $\text{CD}_3\text{OD}$ ):  $\delta$  8.61 (d,  $J$  = 8.2 Hz, 1H), 8.52 (s, 1H), 8.24 (s, 1H), 7.94 (s, 1H), 7.60 (s, 1H), 7.25 (d,  $J$  = 9.2 Hz, 1H), 5.72 (d,  $J$  = 10.1 Hz, 1H), 5.65 (d,  $J$  = 10.1 Hz, 1H), 4.85–4.82 (m, 1H), 4.49 (s, 1H), 4.21 (s, 3H), 3.47 (s, 3H), 3.36–3.30 (m, 1H), 3.26 (dd,  $J$  = 12.8, 2.7 Hz, 1H), 2.61 (dd,  $J$  = 12.8, 2.7 Hz, 1H), 0.85 (d,  $J$  = 7.3 Hz, 3H).

To hemiaminal **124** and  $\text{K}_2\text{CO}_3$  (60 mg, 0.434 mmol) in THF (2 mL) at 23 °C was added  $\text{H}_2\text{O}$  (200  $\mu$ L). The reaction mixture was stirred for 10 min, then purified by reversed-phase filtration through a Sep-Pak column: loaded with water containing 0.1%

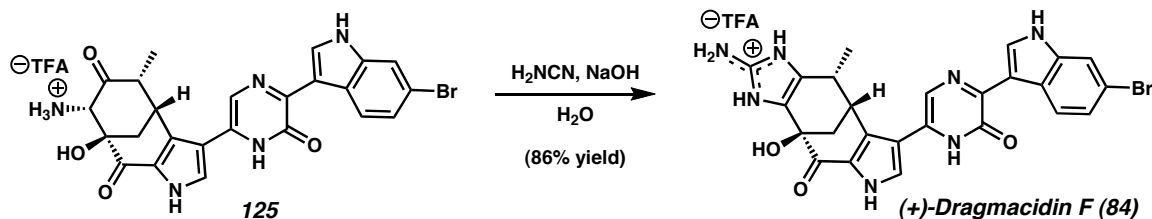
(w/v) TFA, washed with 10% acetonitrile:water containing 0.1% (w/v) TFA to remove salts, then 70% acetonitrile:water containing 0.1% (w/v) TFA to collect the crude product. After removal of solvents under reduced pressure, the crude material was further purified by reversed-phased HPLC. Concentration under reduced pressure provided aminoketone **121** (15.0 mg, 96% yield) as an orange/red oil.  $^1\text{H}$  NMR (300 MHz,  $\text{CD}_3\text{OD}$ ):  $\delta$  8.60 (d,  $J = 8.5$  Hz, 1H), 8.53 (s, 1H), 8.23 (s, 1H), 7.81 (s, 1H), 7.61 (d,  $J = 1.4$  Hz, 1H), 7.25 (dd,  $J = 8.7, 1.8$  Hz, 1H), 4.82–4.78 (m, 1H), 4.46 (s, 1H), 4.21 (s, 3H), 3.47 (s, 3H), 3.41–3.30 (m, 1H), 3.26 (dd,  $J = 12.9, 3.9$  Hz, 1H), 2.61 (dd,  $J = 12.9, 3.0$  Hz, 1H), 0.88 (d,  $J = 6.6$  Hz, 3H);  $^{13}\text{C}$  NMR (75 MHz,  $\text{CD}_3\text{OD}$ , 25/26 C):  $\delta$  203.5, 183.3, 156.8, 142.4, 139.9, 139.1, 136.3, 133.4, 130.7, 129.9, 129.6, 126.9, 125.5, 124.5, 123.1, 116.9, 115.4, 112.6, 84.3, 66.0, 54.5, 52.9, 40.4, 36.6, 12.2; IR (film): 3156 (br), 2935, 1674, 1531, 1447, 1409, 1203, 1135  $\text{cm}^{-1}$ ; HRMS-FAB ( $m/z$ ):  $[\text{M} + \text{H}]^+$  calc'd for  $\text{C}_{26}\text{H}_{25}\text{N}_5\text{O}_4\text{Br}$ , 550.1090; found, 550.1071;  $[\alpha]_D^{20} +99.19^\circ$  (c 0.87, MeOH).

The relative stereochemistry of deprotected aminoketone **121** was determined by NOE experiments. Medium-strength NOE interactions were observed as indicated below.<sup>75</sup> Analogous NOE interactions were observed for hemiaminal **124** and deprotected aminoketone **125**.

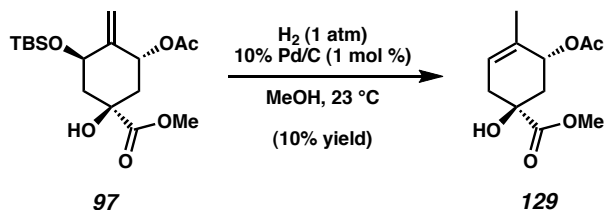




**Deprotected Aminoketone 125.** To a stirred solution of aminoketone **121** (7.5 mg, 0.0113 mmol) in MeCN (1 mL) at 0 °C was added TMSI (500  $\mu$ L, 3.51 mmol) dropwise over 30 sec. The reaction mixture was heated to 60 °C for 48 h, cooled to 0 °C, then transferred dropwise into a chilled solution (0 °C) of saturated aqueous sodium metabisulfite (5 mL). The mixture was diluted with 6 N HCl (15 mL), stirred at 0 °C for 20 min, then purified by reversed-phase filtration through a Sep-Pak column: loaded with water containing 0.1% (w/v) TFA, washed with 1 N HCl, 10% acetonitrile:water containing 0.1% (w/v) TFA to remove salts, then 60% acetonitrile:water containing 0.1% (w/v) TFA to collect the crude product. After removal of solvents under reduced pressure, the crude material was further purified by reversed-phase HPLC. Concentration under reduced pressure provided deprotected aminoketone **125** (6.8 mg, 95% yield) as an orange/red oil.  $^1\text{H}$  NMR (300 MHz,  $\text{CD}_3\text{OD}$ ):  $\delta$  8.69 (s, 1H), 8.59 (d,  $J$  = 8.5 Hz, 1H), 7.69 (s, 1H), 7.61 (d,  $J$  = 1.7 Hz, 1H), 7.57 (s, 1H), 7.27 (dd,  $J$  = 8.5, 1.7 Hz, 1H), 4.40 (s, 1H), 4.06–3.98 (m, 1H), 3.31–3.21 (m, 1H), 2.87 (dd,  $J$  = 13.2, 3.3 Hz, 1H), 2.79 (dd,  $J$  = 13.1, 2.9 Hz, 1H), 0.85 (d,  $J$  = 6.6 Hz, 3H);  $^{13}\text{C}$  NMR (75 MHz,  $\text{CD}_3\text{OD}$ , 23/24 C):  $\delta$  203.4, 186.0, 157.4, 139.1, 136.3, 132.5, 132.4, 130.2, 130.1, 128.2, 126.7, 126.7, 125.6, 124.9, 117.1, 115.4, 113.6, 79.3, 67.1, 49.6, 45.5, 36.7, 12.3; IR (film): 3164 (br), 2927, 1674, 1451, 1207, 1143  $\text{cm}^{-1}$ ; HRMS-FAB ( $m/z$ ):  $[\text{M} + \text{H}]^+$  calc'd for  $\text{C}_{24}\text{H}_{21}\text{N}_5\text{O}_4\text{Br}$ , 522.0777; found, 522.0783;  $[\alpha]_D^{22} +86.88^\circ$  ( $c$  0.33, MeOH).

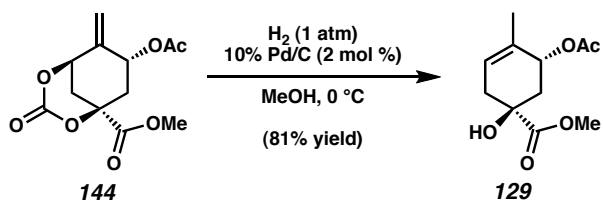


**(+)-Dragmacidin F (84).** To deprotected aminoketone **125** (3.6 mg, 0.0056 mmol) and cyanamide (120 mg, 2.86 mmol) in H<sub>2</sub>O (2 mL, degassed by sparging with argon) at 23 °C was added 10% aq. NaOH (80 μL). The reaction mixture was heated to 60 °C for 2 h, cooled to 23 °C, then purified by reversed-phase filtration through a Sep-Pak column: loaded with water containing 0.1% (w/v) TFA, washed with 10% acetonitrile:water containing 0.1% (w/v) TFA to remove salts, then 60% acetonitrile:water containing 0.1% (w/v) TFA to collect the crude product. After removal of solvents under reduced pressure, the product was further purified by reversed-phase HPLC. Concentration under reduced pressure afforded (+)-dragmacidin F (**84**, 3.2 mg, 86% yield) as an orange/red oil. <sup>1</sup>H NMR (600 MHz, CD<sub>3</sub>OD): δ 8.69 (s, 1H), 8.59 (d, *J* = 8.7 Hz, 1H), 7.68 (s, 1H), 7.60 (s, 1H), 7.47 (s, 1H), 7.26 (d, *J* = 8.7 Hz, 1H), 4.12 (br s, 1H), 3.40–3.34 (m, 1H), 2.73 (dd, *J* = 12.0, 2.9 Hz, 1H), 2.45 (d, *J* = 11.6 Hz, 1H), 0.92 (d, *J* = 7.0 Hz, 3H); <sup>13</sup>C NMR (125 MHz, CD<sub>3</sub>OD, 22/25 °C): δ 188.5, 157.5, 149.6, 139.1, 132.6, 132.4, 128.5, 128.4, 126.7, 126.2, 125.6, 124.9, 124.8, 123.3, 117.1, 115.4, 113.7, 72.8, 45.3, 36.9, 33.3, 15.9; IR (film): 3175 (br), 2925, 1679, 1637, 1205, 1141 cm<sup>-1</sup>; UV (MeOH) λ<sub>max</sub> 283, 389 nm; HRMS-FAB (*m/z*): [M + H]<sup>+</sup> calc'd for C<sub>25</sub>H<sub>21</sub>N<sub>7</sub>O<sub>3</sub>Br, 546.0889; found, 546.0883; [α]<sub>D</sub><sup>23</sup> +146.21° (*c* 0.45, MeOH).



**Acetoxycyclohexene 129.** A mixture of methyl ester **97** (50.0 mg, 0.140 mmol) and 10% Pd/C (1.5 mg, 0.0014 mmol) in MeOH (1.3 mL) was stirred under an  $\text{H}_2$  atmosphere at 23 °C. After 35 min, the reaction mixture was filtered over a Celite<sup>®</sup> plug (MeOH eluent), and the solvent was evaporated in vacuo.  $^1\text{H}$  NMR integration showed that acetoxycyclohexene **129** was formed in approximately 10% yield.

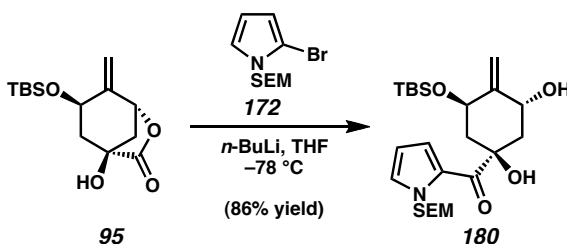
*Alternate Procedure.* A mixture of methyl ester **97** (21.4 mg, 0.06 mmol) and 10% Pd/C (0.3 mg, 0.0003 mmol) in MeOH (1.5 mL) was cooled to 0 °C. The reaction vessel was then evacuated and back-filled with  $\text{H}_2$  (4x). After 1 h, the reaction mixture was filtered over a Celite<sup>®</sup> plug (MeOH eluent), and the solvent was evaporated in vacuo.  $^1\text{H}$  NMR integration showed that acetoxycyclohexene **129** was formed in approximately 3% yield. An analytical sample of **129** was prepared via an alternate route as follows:



A mixture of acetoxycarbonate **144**<sup>76</sup> (18.5 mg, 0.07 mmol) and 10% Pd/C (1.4 mg, 0.001 mmol) in MeOH (1.3 mL) was cooled to 0 °C. The reaction vessel was then evacuated and back-filled with  $\text{H}_2$  (3x). After 1 h at 0 °C, the reaction mixture was filtered over a Celite<sup>®</sup> plug (MeOH eluent), and the solvent was evaporated in vacuo. The residue was purified by flash chromatography (1:1 EtOAc:hexanes eluent) to afford

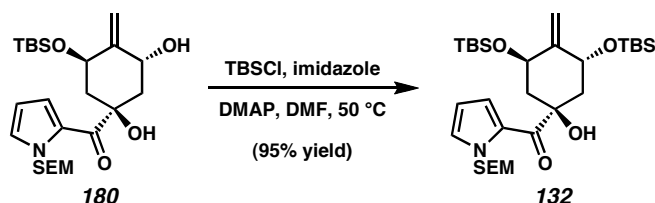


acetoxycyclohexene **129** (12.6 mg, 81% yield) as a colorless oil.  $R_f$  0.46 (2:1 EtOAc:hexanes);  $^1\text{H}$  NMR (300 MHz,  $\text{CDCl}_3$ ):  $\delta$  5.57–5.48 (comp. m, 2H), 3.77 (s, 3H), 3.06 (br s, 1H), 2.69–2.58 (m, 1H), 2.29–2.20 (m, 1H), 2.16–1.91 (comp. m, 2H), 2.05 (s, 3H), 1.69–1.66 (m, 3H);  $^{13}\text{C}$  NMR (75 MHz,  $\text{CDCl}_3$ ):  $\delta$  176.1, 170.9, 132.7, 122.0, 73.8, 70.7, 53.2, 37.1, 35.3, 21.3, 19.2; IR (film) 3477 (br), 2953, 1736, 1239  $\text{cm}^{-1}$ ; HRMS-FAB ( $m/z$ ):  $[\text{M} + \text{H}]^+$  calc'd for  $\text{C}_{11}\text{H}_{17}\text{O}_5$ , 229.1076; found 229.1066;  $[\alpha]_D^{25}$   $-3.31^\circ$  ( $c$  0.6,  $\text{CHCl}_3$ ).



**Anti-diol 180.** To 2-bromo SEM pyrrole (**172**, 4.66 g, 16.87 mmol) in THF (112 mL) at  $-78^\circ\text{C}$  was added  $n\text{-BuLi}$  (2.5 M in hexanes, 6.04 mL, 15.09 mmol) dropwise over 1 min. After 7 min at  $-78^\circ\text{C}$ , lactone **95** (1.26 g, 4.44 mmol) in THF (10 mL) was added dropwise over 1 min. The reaction vessel was immediately warmed to  $-42^\circ\text{C}$ , stirred for 30 min, and cooled to  $-78^\circ\text{C}$ . The reaction mixture was quenched with saturated aq.  $\text{NH}_4\text{Cl}$  (50 mL), then warmed to  $23^\circ\text{C}$ . The volatiles were removed under reduced pressure. The residue was partitioned between  $\text{Et}_2\text{O}$  (125 mL) and  $\text{H}_2\text{O}$  (100 mL), and the layers were separated. The aqueous layer was further extracted with  $\text{Et}_2\text{O}$  (2 x 125 mL). The combined organic layers were washed with brine (75 mL), dried over  $\text{MgSO}_4$ , and evaporated under reduced pressure. The crude product was purified by flash chromatography (4:1 hexanes:EtOAc eluent) to afford *anti*-diol **180** (1.84 g, 86% yield) as a pale yellow foam.  $R_f$  0.48 (2:1 hexanes:EtOAc);  $^1\text{H}$  NMR (300 MHz,  $\text{C}_6\text{D}_6$ ):  $\delta$  8.11

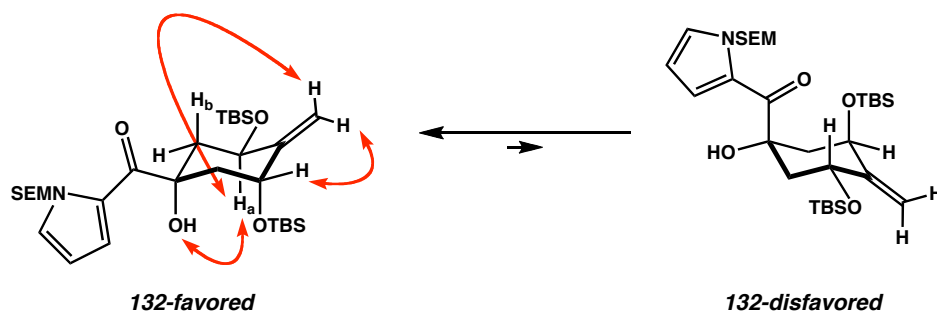
(dd,  $J = 4.1, 1.7$  Hz, 1H), 6.78 (app. t,  $J = 2.1$  Hz, 1H), 6.15 (dd,  $J = 4.0, 2.6$  Hz, 1H), 5.71 (d,  $J = 9.9$  Hz, 1H), 5.58 (d,  $J = 10.2$  Hz, 1H), 5.26 (s, 1H), 5.17 (app. t,  $J = 1.8$  Hz, 1H), 4.92–4.82 (m, 1H), 4.76–4.73 (m, 1H), 4.45 (app. t,  $J = 3.0$  Hz, 1H), 3.47 (t,  $J = 7.7$  Hz, 2H), 2.66 (ddd,  $J = 12.4, 5.2, 2.5$  Hz, 1H), 2.39 (dd,  $J = 14.4, 2.9$  Hz, 1H), 2.20 (app. dt,  $J = 8.7, 4.8$  Hz, 1H), 1.92 (app. t,  $J = 12.0$  Hz, 1H), 0.88–0.80 (comp. m, 12H), –0.04 (s, 3H), –0.06 (s, 3H), –0.06 (s, 9H);  $^{13}\text{C}$  NMR (75 MHz,  $\text{C}_6\text{D}_6$ ):  $\delta$  192.8, 151.6, 130.5, 128.6, 124.8, 109.3, 108.3, 83.0, 78.5, 76.7, 66.4, 66.2, 48.5, 42.1, 26.1 (3C), 18.4, 18.4, –0.9 (3C), –4.4, –5.1; IR (film): 3456 (br), 2953, 1637, 1406, 1250, 1091  $\text{cm}^{-1}$ ; HRMS-FAB ( $m/z$ ):  $[\text{M} + \text{H}]^+$  calc'd for  $\text{C}_{24}\text{H}_{44}\text{NO}_5\text{Si}_2$ , 482.2758; found, 482.2751;  $[\alpha]_{\text{D}}^{28} -21.18^\circ$  (c 1.0,  $\text{C}_6\text{H}_6$ ).

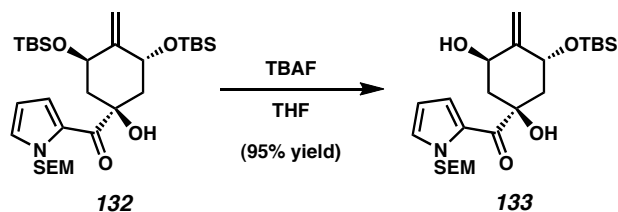


**Bis(silylether) 132.** To a solution of *anti*-diol **180** (253.1 mg, 0.53 mmol), imidazole (147.1 mg, 2.16 mmol), and DMAP (23.5 mg, 0.19 mmol) in DMF (5.0 mL), was added TBSCl (152.5 mg, 1.01 mmol). The solution was warmed to 50 °C for 70 min, cooled to 0 °C, then quenched by the addition of 10% (w/v) aq. citric acid (10 mL).  $\text{Et}_2\text{O}$  (40 mL) was added, and the layers were partitioned. The aqueous phase was further extracted with  $\text{Et}_2\text{O}$  (2 x 30 mL). The combined organic extracts were washed with brine (15 mL), dried over  $\text{MgSO}_4$ , and evaporated under reduced pressure. The crude product was purified by flash chromatography (9:1 hexanes:EtOAc eluent) to provide bis(silylether) **132** (296.0 mg, 95% yield) as a colorless oil that solidified under reduced

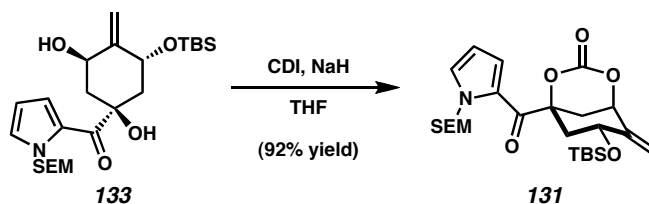
pressure.  $R_f$  0.61 (4:1 hexanes:EtOAc);  $^1\text{H}$  NMR (300 MHz,  $\text{C}_6\text{D}_6$ ):  $\delta$  8.17 (dd,  $J = 4.0$ , 1.8 Hz, 1H), 6.76 (dd,  $J = 2.5$ , 1.7 Hz, 1H), 6.14 (dd,  $J = 4.0$ , 2.6 Hz, 1H), 5.68 (d,  $J = 9.9$  Hz, 1H), 5.62 (d,  $J = 10.2$  Hz, 1H), 5.37 (s, 1H), 5.32 (app. t,  $J = 2.1$  Hz, 1H), 5.22–5.14 (m, 1H), 4.77 (app. t,  $J = 1.9$  Hz, 1H), 4.50 (app. t,  $J = 3.0$  Hz, 1H), 3.47 (t,  $J = 7.8$  Hz, 2H), 2.82 (ddd,  $J = 12.7$ , 5.1, 2.6 Hz, 1H), 2.45 (dd,  $J = 14.6$ , 2.8 Hz, 1H), 2.27–2.18 (comp. m, 2H), 0.99 (s, 9H), 0.88 (s, 9H), 0.82 (t,  $J = 7.8$  Hz, 2H), 0.17 (s, 3H), 0.14 (s, 3H), 0.00 (s, 3H),  $-0.04$  (s, 3H),  $-0.07$  (s, 9H);  $^{13}\text{C}$  NMR (75 MHz,  $\text{C}_6\text{D}_6$ , 29/30 C):  $\delta$  192.6, 151.6, 130.4, 124.5, 109.3, 108.6, 83.2, 78.5, 76.8, 67.4, 66.3, 49.3, 42.1, 26.4 (3C), 26.1 (3C), 18.9, 18.4, 18.3,  $-0.9$  (3C),  $-4.3$ ,  $-4.4$ ,  $-4.5$ ,  $-5.1$ ; IR (film): 3464 (br), 1953, 2929, 1640, 1405, 1309, 1251, 1094  $\text{cm}^{-1}$ ; HRMS-FAB ( $m/z$ ):  $[\text{M} + \text{H}]^+$  calc'd for  $\text{C}_{30}\text{H}_{58}\text{NO}_5\text{Si}_3$ , 596.3623; found, 596.3594;  $[\alpha]_D^{27} -7.16^\circ$  ( $c$  1.0,  $\text{C}_6\text{H}_6$ ).

The stable chair conformer of bis(silylether) **132** was determined using a combination of NOESY-1D, gCOSY, and homodecoupling NMR experiments. Medium-strength NOE interactions were observed as indicated below.<sup>75</sup> The coupling constant between  $\text{H}_a$  and  $\text{H}_b$  was measured as  $J_{ab} = 11.0$  Hz.

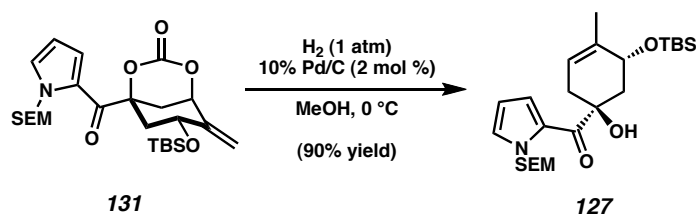




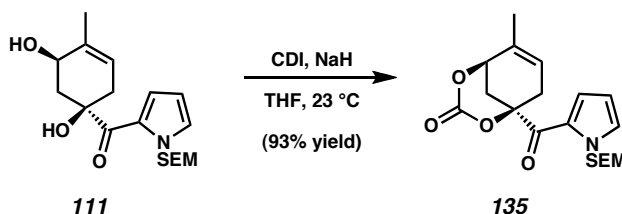
**Syn-diol 133.** To bis(silylether) **132** (113.9 mg, 0.19 mmol) in THF (10.0 mL) was added TBAF (1.0 M in THF, 195  $\mu$ L, 0.20 mmol) in a dropwise fashion over 1 min. The reaction mixture was stirred for 2 min, quenched with saturated aq. NH<sub>4</sub>Cl (15 mL), then poured into EtOAc (40 mL). The layers were partitioned, and the aqueous layer was further extracted with EtOAc (2 x 40 mL). The combined organic extracts were successively washed with H<sub>2</sub>O (15 mL) and brine (15 mL), dried over MgSO<sub>4</sub>, and evaporated under reduced pressure. The residue was purified by flash chromatography (7:1 hexanes:EtOAc eluent) to furnish *syn*-diol **133** (87.5 mg, 95% yield) as a pale yellow oil.  $R_f$  0.29 (4:1 hexanes:EtOAc); <sup>1</sup>H NMR (300 MHz, C<sub>6</sub>D<sub>6</sub>):  $\delta$  7.09 (dd,  $J$  = 4.1, 1.4 Hz, 1H), 6.63 (dd,  $J$  = 2.3, 1.5 Hz, 1H), 5.89 (dd,  $J$  = 4.1, 2.5 Hz, 1H), 5.51–5.39 (comp. m, 4H), 5.27–5.19 (m, 1H), 5.01 (app. t,  $J$  = 2.1 Hz, 1H), 4.52–4.46 (m, 1H), 3.86 (d,  $J$  = 8.0 Hz, 1H), 3.37 (t,  $J$  = 7.7 Hz, 2H), 2.45–2.23 (comp. m, 3H), 2.04 (app. dt,  $J$  = 8.4, 4.9 Hz, 1H), 0.99 (s, 9H), 0.79 (t,  $J$  = 7.8 Hz, 2H), 0.14 (s, 3H), 0.11 (s, 3H), –0.09 (s, 9H); <sup>13</sup>C NMR (75 MHz, C<sub>6</sub>D<sub>6</sub>):  $\delta$  191.6, 152.9, 131.4, 126.4, 124.0, 109.8, 108.5, 81.2, 78.8, 74.7, 67.4, 66.6, 49.0, 43.3, 26.4 (3C), 18.9, 18.3, –1.0 (3C), –4.5, –4.5; IR (film): 3363 (br), 2954, 1631, 1410, 1314, 1250, 1101 (br) cm<sup>–1</sup>; HRMS-FAB ( $m/z$ ): [M + H]<sup>+</sup> calc'd for C<sub>24</sub>H<sub>44</sub>NO<sub>5</sub>Si<sub>2</sub>, 482.2758; found, 482.2780; [ $\alpha$ ]<sub>D</sub><sup>27</sup> –27.06° ( $c$  1.0, C<sub>6</sub>H<sub>6</sub>).



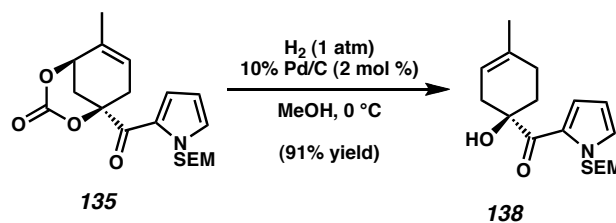
**Carbonate 131.** To *syn*-diol **133** (68.2 mg, 0.14 mmol) and 1,1'-carbonyldiimidazole (37.0 mg, 0.23 mmol) in THF (2.6 mL) was added NaH (60% dispersion in mineral oil, 21.9 mg, 0.55 mmol) in one portion. The reaction was stirred for 20 min at 23 °C, then quenched by addition of saturated aq. NH<sub>4</sub>Cl (20 mL). The reaction mixture was poured into EtOAc (30 mL), the layers were partitioned, and the aqueous layer was further extracted with EtOAc (2 x 30 mL). The combined organic extracts were successively washed with H<sub>2</sub>O (10 mL) and brine (10 mL), dried over MgSO<sub>4</sub>, and evaporated under reduced pressure. Purification of the residue by flash chromatography (6:1 hexanes:EtOAc eluent) afforded carbonate **131** (65.8 mg, 92% yield) as a colorless oil. *R<sub>f</sub>* 0.29 (4:1 hexanes:EtOAc); <sup>1</sup>H NMR (300 MHz, C<sub>6</sub>D<sub>6</sub>): δ 7.91 (dd, *J* = 4.1, 1.7 Hz, 1H), 6.68 (dd, *J* = 2.8, 1.7 Hz, 1H), 6.02 (dd, *J* = 4.3, 2.6 Hz, 1H), 5.51 (d, *J* = 9.9 Hz, 1H), 5.43 (d, *J* = 9.9 Hz, 1H), 5.24 (app. t, *J* = 1.9 Hz, 1H), 4.84–4.75 (m, 1H), 4.69 (app. t, *J* = 1.8 Hz, 1H), 4.46 (dd, *J* = 3.9, 1.9 Hz, 1H), 3.39 (t, *J* = 7.7 Hz, 2H), 2.78 (ddd, *J* = 13.5, 6.1, 2.5 Hz, 1H), 2.12–1.98 (comp. m, 2H), 1.92–1.85 (m, 1H), 0.86 (s, 9H), 0.81 (t, *J* = 7.8 Hz, 2H), –0.07 to –0.08 (comp. m, 12H), –0.10 (s, 3H); <sup>13</sup>C NMR (75 MHz, C<sub>6</sub>D<sub>6</sub>): δ 185.9, 147.2, 146.4, 132.1, 126.7, 125.0, 112.2, 110.3, 87.9, 80.3, 78.8, 66.8, 66.5, 46.1, 33.7, 26.2 (3C), 18.6, 18.3, –1.0 (3C), –4.7, –5.0; IR (film): 2954, 1764, 1641, 1413, 1354, 1251, 1173, 1089 cm<sup>–1</sup>; HRMS-FAB (*m/z*): [M + H]<sup>+</sup> calc'd for C<sub>25</sub>H<sub>42</sub>NO<sub>6</sub>Si<sub>2</sub>, 508.2551; found, 508.2560; [α]<sub>D</sub><sup>27</sup> –54.78° (*c* 1.0, C<sub>6</sub>H<sub>6</sub>).



**Pyrrolocyclohexene 127.** A mixture of carbonate **131** (40.0 mg, 0.08 mmol) and 10% Pd/C (1.7 mg, 0.002 mmol) in MeOH (1.0 mL) was cooled to 0 °C. The reaction vessel was then evacuated and back-filled with H<sub>2</sub> (3x). After 1.75 h at 0 °C, the reaction mixture was filtered over a Celite<sup>®</sup> plug (MeOH eluent), and the solvent was evaporated in vacuo. The residue was purified by flash chromatography (9:1 hexanes:EtOAc eluent) to afford pyrrolocyclohexene **127** (33.1 mg, 90% yield) as a colorless oil. *R<sub>f</sub>* 0.53 (4:1 hexanes:EtOAc); <sup>1</sup>H NMR (300 MHz, C<sub>6</sub>D<sub>6</sub>): δ 6.94 (dd, *J* = 4.1, 1.4 Hz, 1H), 6.64 (dd, *J* = 2.6, 1.5 Hz, 1H), 5.89 (dd, *J* = 4.0, 2.6 Hz, 1H), 5.54 (d, *J* = 10.2 Hz, 1H), 5.45 (d, *J* = 10.2 Hz, 1H), 5.39–5.33 (m, 1H), 4.87–4.78 (m, 1H), 4.78 (s, 1H), 3.40 (t, *J* = 7.8 Hz, 2H), 2.97–2.85 (m, 1H), 2.48 (dd, *J* = 12.5, 9.8 Hz, 1H), 2.34–2.26 (m, 1H), 2.21–2.08 (m, 1H), 1.95–1.90 (m, 3H), 0.96 (s, 9H), 0.81 (t, *J* = 7.8 Hz, 2H), 0.06 (s, 3H), 0.03 (s, 3H), –0.08 (s, 9H); <sup>13</sup>C NMR (75 MHz, C<sub>6</sub>D<sub>6</sub>): δ 193.8, 138.5, 131.0, 126.4, 123.1, 120.1, 109.7, 78.8, 78.2, 69.6, 66.5, 44.7, 38.9, 26.4 (3C), 20.6, 18.6, 18.3, –1.0 (3C), –3.8, –4.5; IR (film): 3431 (br), 2954, 1634, 1414, 1250, 1089 (br) cm<sup>–1</sup>; HRMS-FAB (*m/z*): [*M* + H]<sup>+</sup> calc'd for C<sub>24</sub>H<sub>44</sub>NO<sub>4</sub>Si<sub>2</sub>, 466.2809; found, 466.2804; [*α*]<sub>D</sub><sup>28</sup> +26.19° (*c* 1.0, C<sub>6</sub>H<sub>6</sub>).



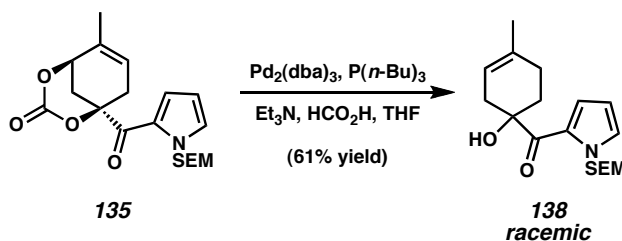
**Pyrrolocarbonate 135.** To diol **111** (114.5 mg, 0.33 mmol) in THF (6 mL) at 23 °C was added 1,1'-carbonyldiimidazole (86.9 mg, 0.54 mmol) followed by NaH (60% dispersion in mineral oil, 55.2 mg, 1.38 mmol). After stirring for 40 min at 23 °C, saturated aq.  $\text{NH}_4\text{Cl}$  (10 mL) was added to quench the reaction and EtOAc (50 mL) was added. The phases were partitioned, and the aqueous layer was further extracted with EtOAc (2 x 75 mL). The combined organic layers were successively washed with  $\text{H}_2\text{O}$  (15 mL) and brine (15 mL), dried over  $\text{MgSO}_4$ , and evaporated under reduced pressure. The residue was purified by flash chromatography (4:1 hexanes:EtOAc eluent) to provide pyrrolocarbonate **135** (114.3 mg, 93% yield) as a pale yellow oil.  $R_f$  0.53 (1:1 hexanes:EtOAc);  $^1\text{H}$  NMR (300 MHz,  $\text{C}_6\text{D}_6$ ):  $\delta$  7.85 (dd,  $J = 4.1, 1.4$  Hz, 1H), 6.70 (dd,  $J = 2.7, 1.8$  Hz, 1H), 6.04 (dd,  $J = 4.1, 2.7$  Hz, 1H), 5.52 (d,  $J = 9.9$  Hz, 1H), 5.48 (d,  $J = 10.0$  Hz, 1H), 4.91–4.86 (m, 1H), 3.78 (app. t,  $J = 3.0$  Hz, 1H), 3.41 (t,  $J = 7.8$  Hz, 2H), 2.42–2.37 (comp. m, 2H), 1.97 (ddd,  $J = 14.1, 3.3, 1.0$  Hz, 1H), 1.83 (dd,  $J = 14.2, 2.3$  Hz, 1H), 1.40 (app. q,  $J = 2.0$  Hz, 3H), 0.83 (t,  $J = 7.8$  Hz, 2H),  $-0.07$  (s, 9H);  $^{13}\text{C}$  NMR (75 MHz,  $\text{C}_6\text{D}_6$ ):  $\delta$  187.6, 147.5, 132.6, 131.9, 127.1, 125.1, 122.6, 110.2, 85.9, 78.7, 73.8, 66.5, 37.9, 30.4, 21.0, 18.3,  $-1.0$  (3C); IR (film) 2952, 1751, 1643, 1413, 1178,  $1093\text{ cm}^{-1}$ ; HRMS-EI ( $m/z$ ):  $[\text{M}]^+$  calc'd for  $\text{C}_{19}\text{H}_{27}\text{NO}_5\text{Si}$ , 377.1658; found, 377.1655;  $[\alpha]_D^{24} +2.72^\circ$  (c 1.0,  $\text{C}_6\text{H}_6$ ).



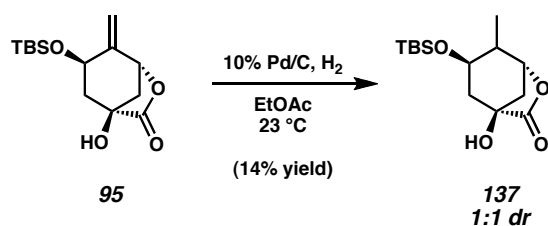
**Trisubstituted Olefin 138.** A mixture of pyrrolocarbonate **135** (41.6 mg, 0.11 mmol) and 10% Pd/C (2.3 mg, 0.002 mmol) in MeOH (2.0 mL) was cooled to 0 °C. The reaction vessel was then evacuated and back-filled with H<sub>2</sub> (3x). After 1.3 h at 0 °C, the reaction mixture was filtered over a Celite® plug (MeOH eluent) and the solvent was evaporated in vacuo. The residue was purified by preparative thin-layer chromatography (13:4:3 hexanes:EtOAc:CH<sub>2</sub>Cl<sub>2</sub> eluent) to afford pyrrolocyclohexene **138** (33.5 mg, 91% yield) as a colorless oil. *R<sub>f</sub>* 0.64 (13:7 hexanes:EtOAc); <sup>1</sup>H NMR (300 MHz, C<sub>6</sub>D<sub>6</sub>): δ 7.16 (dd, *J* = 4.0, 1.5 Hz, 1H), 6.72 (dd, *J* = 2.7, 1.6 Hz, 1H), 6.02 (dd, *J* = 4.0, 2.7 Hz, 1H), 5.56 (s, 2H), 5.35–5.28 (m, 1H), 3.98 (s, 1H), 3.43 (t, *J* = 7.8 Hz, 2H), 2.98–2.85 (m, 1H), 2.51–2.33 (m, 1H), 2.24–2.10 (comp. m, 2H), 1.88–1.73 (comp. m, 2H), 1.67–1.63 (m, 3H), 0.82 (t, *J* = 7.8 Hz, 2H), –0.08 (s, 9H); <sup>13</sup>C NMR (75 MHz, C<sub>6</sub>D<sub>6</sub>): δ 195.5, 134.0, 130.6, 127.3, 123.1, 118.5, 109.3, 78.7, 76.8, 66.5, 38.4, 34.2, 27.2, 24.1, 18.3, –1.0 (3C); IR (film) 3441 (br), 2957, 1727, 1632, 1413, 1084 cm<sup>–1</sup>; HRMS-FAB (*m/z*): [M + H]<sup>+</sup> calc'd for C<sub>18</sub>H<sub>30</sub>NO<sub>3</sub>Si, 336.1995; found, 336.1993; [α]<sub>D</sub><sup>24</sup> –0.02° (*c* 1.0, C<sub>6</sub>H<sub>6</sub>); 7.2% ee as measured by chiral HPLC (2% EtOH:hexanes eluent). Retention times: 13.9 min, 15.6 min.



A racemic sample was prepared as follows:

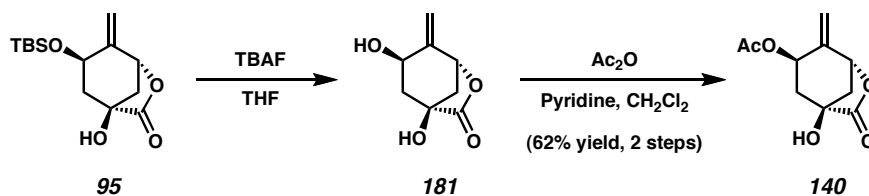


To carbonate **135** (9.9 mg, 0.03 mmol) and  $\text{Pd}_2(\text{dba})_3$  (2.7 mg, 0.003 mmol) was added THF (800  $\mu\text{L}$ ) followed by  $\text{P}(n\text{-Bu})_3$  (2.8  $\mu\text{L}$ , 0.011 mmol),  $\text{Et}_3\text{N}$  (5.2  $\mu\text{L}$ , 0.04 mmol) and formic acid (1.6  $\mu\text{L}$ , 0.04 mmol).<sup>77</sup> The solution was stirred at 23 °C for 3 h, and was then heated to 70 °C for 70 min. The reaction was cooled to 23 °C and purified directly by preparative thin-layer chromatography (4:1 hexanes:EtOAc eluent). The crude product was then re-purified by preparative thin-layer chromatography (13:4:3 hexanes:EtOAc: $\text{CH}_2\text{Cl}_2$  eluent) to provide an a racemic, analytical sample of **138** (5.4 mg, 61% yield).



**Reduced Lactone 137.** A mixture of methylene lactone **95** (63.1 mg, 0.22 mmol) and 10% Pd/C (39.8 mg, 0.04 mmol) in EtOAc (2 mL) was evacuated and back-filled with  $\text{H}_2$  (3x). After 7 min at 23 °C, the mixture was filtered over a pad of Celite<sup>®</sup> (EtOAc eluent) and the solvent was evaporated in vacuo. The crude product was purified by flash chromatography (2:1 hexanes:EtOAc eluent) to provide reduced lactone **137** (8.7 mg, 14% yield) as a white amorphous solid and a 1:1 mixture of diastereomers.  $R_f$  0.59 (1:1

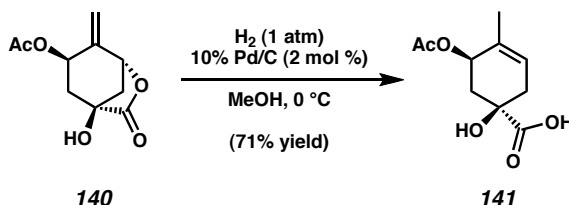
hexanes:EtOAc);  $^1\text{H}$  NMR (300 MHz,  $\text{CDCl}_3$ , 1:1 mixture of diastereomers):  $\delta$  4.68–4.63 (m, 1H), 4.51 (d,  $J$  = 6.4 Hz, 1H), 4.04–3.94 (m, 1H), 3.45 (ddd,  $J$  = 12.9, 6.2, 4.1 Hz, 1H), 2.63 (app. d,  $J$  = 10.1 Hz, 1H), 2.49 (ddd,  $J$  = 11.2, 6.4, 3.2 Hz, 1H), 2.44–2.33 (m, 1H), 2.29–2.22 (comp. m, 2H), 2.14 (ddd,  $J$  = 12.1, 6.6, 2.9 Hz, 1H), 2.08 (app. d,  $J$  = 11.2 Hz, 1H), 2.00–1.82 (comp. m, 3H), 1.65–1.54 (comp. m, 2H), 1.12 (d,  $J$  = 6.9 Hz, 3H), 0.92 (d,  $J$  = 7.4 Hz, 3H), 0.86 (s, 9H), 0.85 (s, 9H), 0.03–0.02 (comp. m, 6H), 0.02–0.01 (comp. m, 6H);  $^{13}\text{C}$  NMR (75 MHz,  $\text{CDCl}_3$ , 1:1 mixture of diastereomers):  $\delta$  178.5, 178.2, 80.4, 80.0, 73.5, 72.8, 71.4, 67.0, 44.8, 43.6, 41.9, 41.4, 37.4, 35.9, 25.9 (6C), 18.2, 18.1, 16.1, 10.7, –4.0, –4.6, –4.6, –4.8; IR (film) 3424 (br), 2930, 1787, 1099  $\text{cm}^{-1}$ ; HRMS-EI ( $m/z$ ):  $[\text{M}]^+$  calc'd for  $\text{C}_{14}\text{H}_{26}\text{O}_4\text{Si}$ , 286.1600; found, 286.1612;  $[\alpha]_D^{25}$  –64.48° ( $c$  1.0,  $\text{C}_6\text{H}_6$ ).



**Acetoxylactone 140.** To lactone **95** (510.1 mg, 1.80 mmol) in THF (25 mL) and freshly distilled AcOH (300  $\mu\text{L}$ , 5.24 mmol) was added TBAF (1.0 M in THF, 4.0 mL, 4.0 mmol) in a dropwise fashion over 3 min. The reaction was stirred for 16 h, and then the solvent was evaporated in vacuo to afford hydroxylactone **181**, which was used immediately in the subsequent reaction. Although hydroxylactone **181** is typically used in crude form, it has been observed by  $^1\text{H}$  NMR.  $R_f$  0.25 (3:1 EtOAc:hexanes).  $^1\text{H}$  NMR (300 MHz,  $\text{CD}_3\text{OD}$ ):  $\delta$  5.27 (dd,  $J$  = 2.4, 1.1 Hz, 1H), 5.20–5.17 (m, 1H), 5.11 (d,  $J$  = 6.1

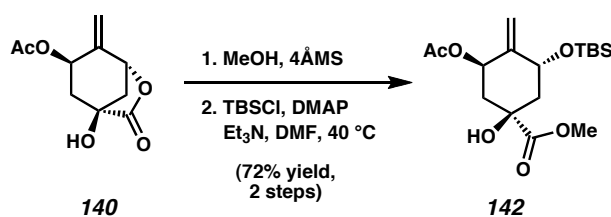
Hz, 1H), 4.26 (app ddt,  $J = 10.7, 7.5, 2.4$  Hz, 1H), 2.63 (ddd,  $J = 11.3, 6.1, 3.1$  Hz, 1H), 2.34 (ddd,  $J = 11.4, 7.4, 3.3$  Hz, 1H), 1.98 (d,  $J = 11.4$  Hz, 1H), 1.72 (t,  $J = 11.3$ , 1H).

Hydroxylactone **181** was dissolved in  $\text{CH}_2\text{Cl}_2$  (17 mL) and pyridine (1.02 mL, 12.6 mmol) was added. A solution of  $\text{Ac}_2\text{O}$  (355  $\mu\text{L}$ , 3.76 mmol) in  $\text{CH}_2\text{Cl}_2$  (355  $\mu\text{L}$ ) was added via syringe pump at a rate of 170  $\mu\text{L}/\text{h}$ . After the addition was complete, the reaction was quenched by the addition of 10% (w/v) aq. citric acid (35 mL). The layers were separated and the aqueous layer was extracted with  $\text{CH}_2\text{Cl}_2$  (2 x 50 mL). The combined organic extracts were dried over  $\text{MgSO}_4$ , and the solvent was evaporated under reduced pressure. The crude product was purified by flash chromatography (3:2 hexanes:EtOAc eluent) to provide acetoxylactone **140** (235 mg, 62% yield, 2 steps) as a white crystalline solid.  $R_f$  0.52 (3:1 EtOAc:hexanes); mp 87–89 °C;  $^1\text{H}$  NMR (300 MHz,  $\text{CDCl}_3$ ):  $\delta$  5.54–5.44 (m, 1H), 5.16 (d,  $J = 2.4$  Hz, 1H), 5.09–5.04 (comp. m, 2H), 3.26 (br s, 1H), 2.70 (ddd,  $J = 11.4, 6.1, 2.9$  Hz, 1H), 2.52–2.42 (m, 1H), 2.14–2.08 (m, 1H), 2.12 (s, 3H), 1.87 (dd,  $J = 12.0, 10.4$  Hz, 1H);  $^{13}\text{C}$  NMR (75 MHz,  $\text{CDCl}_3$ ):  $\delta$  177.7, 169.9, 140.4, 111.6, 79.2, 72.9, 67.4, 44.2, 40.3, 21.0; IR (film) 3441 (br), 1790, 1743, 1240, 1128, 1042  $\text{cm}^{-1}$ ; HRMS-EI ( $m/z$ ):  $[\text{M} + \text{H}]^+$  calc'd for  $\text{C}_{10}\text{H}_{13}\text{O}_5$ , 213.0763; found, 213.0769;  $[\alpha]_{\text{D}}^{25} -229.70^\circ$  ( $c$  1.0,  $\text{C}_6\text{H}_6$ ).



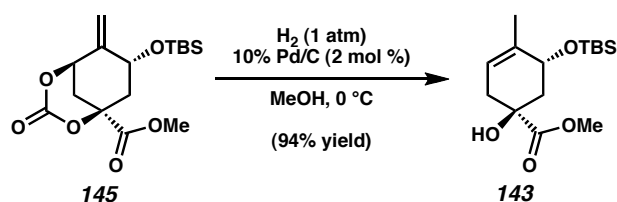
**Acid 141.** For representative procedures, see reductive isomerization of **131**  $\rightarrow$  **127** or **135**  $\rightarrow$  **138**. Purified by preparative thin-layer chromatography (19:1:1

EtOAc:MeOH:AcOH eluent).  $R_f$  0.53 (19:1:1 EtOAc:MeOH:AcOH);  $^1\text{H}$  NMR (300 MHz,  $\text{CDCl}_3$ ):  $\delta$  7.31 (br s, 1H), 5.66–5.60 (m, 1H), 5.39–5.32 (m, 1H), 2.68–2.54 (m, 1H), 2.39–2.23 (comp. m, 2H), 2.14–2.00 (m, 1H), 2.06 (s, 3H), 1.74–1.69 (m, 3H);  $^{13}\text{C}$  NMR (125 MHz,  $\text{CDCl}_3$ ):  $\delta$  178.9, 170.7, 130.8, 123.7, 72.5, 68.9, 36.6, 35.7, 21.4, 20.6; IR (film) 3440 (br), 2938, 1728, 1242  $\text{cm}^{-1}$ ; HRMS-FAB ( $m/z$ ):  $[\text{M} + \text{Na}]^+$  calc'd for  $\text{C}_{10}\text{H}_{14}\text{O}_5\text{Na}$ , 237.0739; found, 237.0744;  $[\alpha]_D^{25} +83.74^\circ$  ( $c$  1.0,  $\text{CHCl}_3$ ).

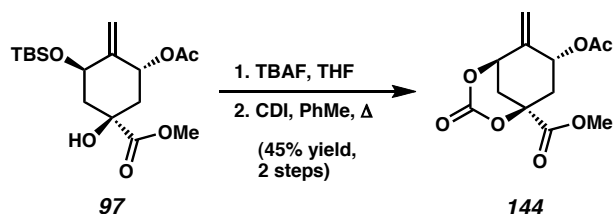


**Methyl Ester 142.** To acetoxylactone **140** (310 mg, 1.46 mmol) and oven-dried powdered 4ÅMS (220 mg) was added MeOH (20 mL). The suspension was stirred for 1 h, and then filtered over Celite<sup>®</sup> (EtOAc eluent). The filtrate was evaporated in vacuo, and was subsequently passed over a plug of  $\text{SiO}_2$  gel (EtOAc eluent). Following evaporation of the solvent under reduced pressure, this material was used in the next step without further purification.  $R_f$  0.33 (3:1 EtOAc:hexanes). To this crude material in DMF (7.3 mL) was added  $\text{Et}_3\text{N}$  (1.63 mL, 11.7 mmol) and DMAP (17.8 mg, 0.15 mmol). TBSCl (880 mg, 5.84 mmol) was added, and the solution was warmed to 40  $^\circ\text{C}$ . After stirring for 1 h, the solution was allowed to cool to 23  $^\circ\text{C}$  and quenched by the addition of 10% (w/v) aq. citric acid (10 mL). The reaction mixture was poured over  $\text{H}_2\text{O}$  (10 mL) and  $\text{Et}_2\text{O}$  (40 mL), and the phases were partitioned. The aqueous phase was extracted with  $\text{Et}_2\text{O}$  (2 x 30 mL), and the combined organic extracts were washed with brine (15 mL) and dried over  $\text{MgSO}_4$ . Following evaporation of the solvent in vacuo, the crude

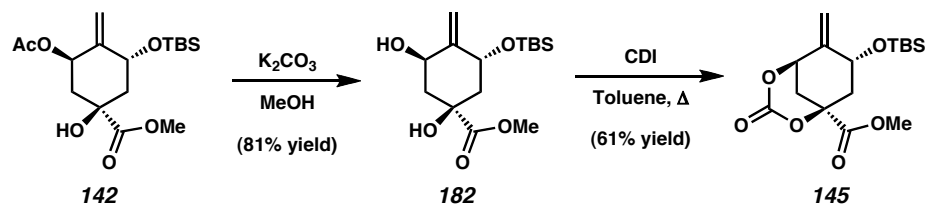
product was purified by flash chromatography (2:1 hexanes:EtOAc eluent) to afford methyl ester **142** (376 mg, 72% yield, 2 steps) as a white solid.  $R_f$  0.53 (1:1 hexanes:EtOAc);  $^1\text{H}$  NMR (300 MHz,  $\text{CDCl}_3$ ):  $\delta$  5.62 (app. t,  $J = 3.7$  Hz, 1H), 5.24 (app. t,  $J = 1.9$  Hz, 1H), 5.10 (app. t,  $J = 1.7$  Hz, 1H), 4.73–4.63 (m, 1H), 3.74 (s, 3H), 3.16 (br s, 1H), 2.14 (dd,  $J = 14.9, 4.3$  Hz, 1H), 2.09–2.00 (comp. m, 2H), 2.03 (s, 3H), 1.90 (dd,  $J = 12.5, 10.6$  Hz, 1H), 0.88 (s, 9H), 0.05 (s, 6H);  $^{13}\text{C}$  NMR (75 MHz,  $\text{CDCl}_3$ ):  $\delta$  175.5, 170.2, 146.6, 111.7, 75.3, 74.0, 66.8, 53.2, 45.7, 38.8, 26.0 (3C), 21.5, 18.4, –4.8, –4.9; IR (film) 3481 (br), 2955, 2930, 2858, 1734 (br), 1372, 1251, 1237, 1124, 1108, 1069, 1016  $\text{cm}^{-1}$ ; HRMS-FAB ( $m/z$ ):  $[\text{M} + \text{H}]^+$  calc'd for  $\text{C}_{17}\text{H}_{31}\text{O}_6\text{Si}$ , 359.1890; found, 359.1894;  $[\alpha]_D^{26} -7.32^\circ$  ( $c$  1.0,  $\text{CHCl}_3$ ).



**Methyl Ester 143.** For representative procedures, see reductive isomerization of **131**  $\rightarrow$  **127** or **135**  $\rightarrow$  **138**. Purified by flash chromatography (7:3 hexanes:EtOAc eluent).  $R_f$  0.62 (1:1 hexanes:EtOAc);  $^1\text{H}$  NMR (300 MHz,  $\text{CDCl}_3$ ):  $\delta$  5.38–5.31 (m, 1H), 4.44–4.34 (m, 1H), 3.78 (s, 3H), 3.10 (br s, 1H), 2.65–2.53 (m, 1H), 2.08–1.89 (comp. m, 3H), 1.74–1.70 (m, 3H), 0.88 (s, 9H), 0.08 (s, 3H), 0.06 (s, 3H);  $^{13}\text{C}$  NMR (75 MHz,  $\text{CDCl}_3$ ):  $\delta$  176.9, 137.2, 119.0, 74.5, 68.2, 53.2, 40.8, 35.8, 26.1 (3C), 20.1, 18.3, –4.1, –4.6; IR (film) 3492 (br), 2954, 2857, 1730, 1249, 1095  $\text{cm}^{-1}$ ; HRMS-FAB ( $m/z$ ):  $[\text{M} + \text{H}]^+$  calc'd for  $\text{C}_{15}\text{H}_{29}\text{O}_4\text{Si}$ , 301.1835; found, 301.1841;  $[\alpha]_D^{24} +29.49^\circ$  ( $c$  1.0,  $\text{C}_6\text{H}_6$ ).

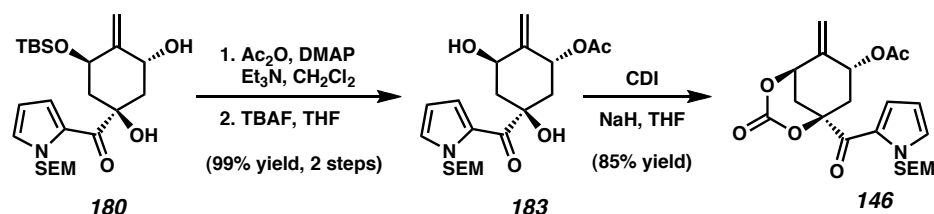


**Acetoxycarbonate 144.** To a solution of methyl ester **97** (44.8 mg, 0.12 mmol) in THF (2 mL) was added TBAF (1.0 M in THF, 140  $\mu$ L, 0.14 mmol). After 3 min of stirring, the reaction was quenched by the addition of saturated aq.  $\text{NH}_4\text{Cl}$  (2 mL). EtOAc (4 mL) was added, and the phases were partitioned. The aqueous phase was further extracted with EtOAc (2 x 2 mL). The combined organic layers were successively washed with  $\text{H}_2\text{O}$  (1 mL) and brine (1 mL), and dried over  $\text{MgSO}_4$ . The solvent was evaporated in vacuo, and the residue was dissolved in toluene (4 mL). 1,1'-carbonyldiimidazole (82.1 mg, 0.51 mmol) was added, and the mixture was heated at reflux for 2 h. After cooling to 23  $^\circ\text{C}$ , the crude reaction mixture was directly purified by flash column chromatography (3:2 hexanes:EtOAc eluent) to afford pure acetoxycarbonate **144** (16.9 mg, 45% yield, 2 steps).  $R_f$  0.15 (1:1 hexanes:EtOAc);  $^1\text{H}$  NMR (300 MHz,  $\text{CDCl}_3$ ):  $\delta$  5.70–5.62 (m, 1H), 5.25 (app. d,  $J$  = 2.5 Hz, 1H), 5.19 (app. d,  $J$  = 2.5 Hz, 1H), 5.16 (dd,  $J$  = 4.1, 1.9 Hz, 1H), 3.81 (s, 3H), 2.84 (ddd,  $J$  = 13.4, 6.4, 2.7 Hz, 1H), 2.55–2.48 (m, 1H), 2.32–2.26 (m, 1H), 2.12 (s, 3H), 1.96 (dd,  $J$  = 13.3, 11.1 Hz, 1H);  $^{13}\text{C}$  NMR (75 MHz,  $\text{CDCl}_3$ ):  $\delta$  169.3, 168.3, 146.6, 140.2, 113.7, 81.6, 79.5, 66.4, 53.7, 39.3, 32.7, 20.9; IR (film) 1763 (br), 1230, 1180, 1120  $\text{cm}^{-1}$ ; HRMS-FAB ( $m/z$ ):  $[\text{M} + \text{H}]^+$  calc'd for  $\text{C}_{12}\text{H}_{15}\text{O}_7$ , 271.0818; found, 271.0810;  $[\alpha]_D^{25}$   $-154.53^\circ$  ( $c$  1.0,  $\text{C}_6\text{H}_6$ ).



**TBS Carbonate 145.** To methyl ester **142** (201 mg, 0.56 mmol) in MeOH (5 mL) was added powdered  $\text{K}_2\text{CO}_3$  (150 mg, 1.09 mmol). After stirring 10 min, the MeOH was evaporated in vacuo and the residue was diluted in  $\text{Et}_2\text{O}$  (50 mL) and saturated aq.  $\text{NH}_4\text{Cl}$  (25 mL). The layers were partitioned, and the aqueous phase was extracted with  $\text{Et}_2\text{O}$  (25 mL). The combined organics were successively washed with  $\text{H}_2\text{O}$  (15 mL) and brine (15 mL), and dried over  $\text{MgSO}_4$ . The solvent was evaporated in vacuo, and *syn*-diol **182** (143.9 mg, 81% yield) was carried on to the next step without further purification.  $R_f$  0.38 (1:1 hexanes:EtOAc).

To *syn*-diol **182** (48.9 mg, 0.15 mmol) in toluene (3 mL) was added 1,1'-carbonyldiimidazole (80 mg, 0.50 mmol), and the reaction mixture was heated to reflux for 2.5 h. After cooling to 23 °C, the residue was chromatographed directly (7:3 hexanes:EtOAc eluent) to afford TBS carbonate **145** (32.2 mg, 61% yield).  $R_f$  0.47 (1:1 hexanes:EtOAc);  $^1\text{H}$  NMR (300 MHz,  $\text{CDCl}_3$ ):  $\delta$  5.34 (dd,  $J = 2.2, 1.1$  Hz, 1H), 5.21–5.19 (m, 1H), 5.15 (dd,  $J = 4.0, 1.8$  Hz, 1H), 4.55–4.47 (m, 1H), 3.82 (s, 3H), 2.62 (ddd,  $J = 13.6, 6.2, 2.6$  Hz, 1H), 2.45 (ddd,  $J = 14.2, 4.1, 2.7$  Hz, 1H), 2.26 (dd,  $J = 14.2, 1.8$  Hz, 1H), 1.92 (dd,  $J = 13.5, 10.7$  Hz, 1H), 0.90 (s, 9H), 0.08 (s, 3H), 0.07 (s, 3H);  $^{13}\text{C}$  NMR (75 MHz,  $\text{CDCl}_3$ ):  $\delta$  168.6, 147.2, 144.9, 113.4, 82.1, 79.9, 65.7, 53.6, 43.5, 33.0, 25.9 (3C), 18.3, –4.7, –4.9; IR (film) 2957, 2930, 2857, 1748 (br), 1254, 1178, 1103, 1054  $\text{cm}^{-1}$ ; HRMS-FAB ( $m/z$ ):  $[\text{M} + \text{H}]^+$  calc'd for  $\text{C}_{16}\text{H}_{27}\text{O}_6\text{Si}$ , 343.1577; found, 343.1592;  $[\alpha]_D^{26}$  –81.11° (c 1.0,  $\text{C}_6\text{H}_6$ ).

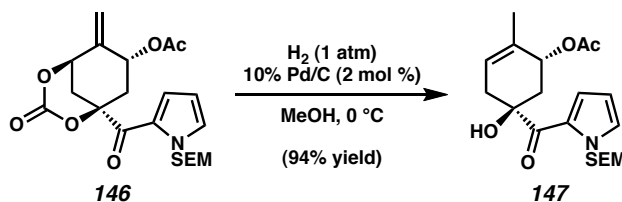


**Acetoxycarbonate 146.** To *anti*-diol **180** (1.77 g, 3.68 mmol) in  $\text{CH}_2\text{Cl}_2$  (25 mL) at 23 °C was added  $\text{Et}_3\text{N}$  (1.28 mL, 9.19 mmol) and DMAP (45 mg, 0.368 mmol), followed by  $\text{Ac}_2\text{O}$  (451  $\mu\text{L}$ , 4.78 mmol). The reaction mixture was stirred for 5 min, and then additional  $\text{Ac}_2\text{O}$  (125  $\mu\text{L}$ , 1.32 mmol) was added. Stirring was continued for 5 min, and then another portion of  $\text{Ac}_2\text{O}$  (100  $\mu\text{L}$ , 1.06 mmol) was added. After 5 min, the reaction mixture was quenched with saturated aq.  $\text{NaHCO}_3$  (15 mL). The volatile solvents were removed under reduced pressure. The residue was diluted with  $\text{H}_2\text{O}$  (30 mL) and extracted with  $\text{EtOAc}$  (3 x 70 mL). The combined organic layers were dried over  $\text{MgSO}_4$ , and evaporated under reduced pressure. Subsequent filtration over a short plug of silica gel afforded the crude product, which was used immediately in the following reaction.  $R_f$  0.63 (2:1 hexanes: $\text{EtOAc}$ ).

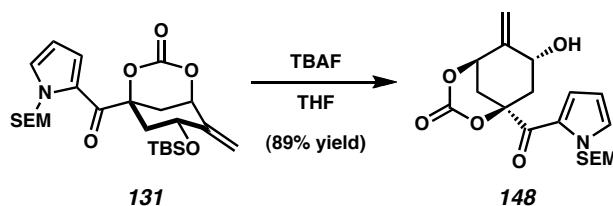
To the crude product in THF (25 mL) was added TBAF (1.0 M in THF, 3.85 mL, 3.85 mmol). After 2 min of stirring, the reaction was quenched by the addition of saturated aq.  $\text{NH}_4\text{Cl}$  (30 mL) and the volatile solvents were removed under reduced pressure. The residue was diluted with  $\text{H}_2\text{O}$  (50 mL) and extracted with  $\text{EtOAc}$  (3 x 60 mL). The combined organic layers were washed with brine (30 mL), dried over  $\text{MgSO}_4$ , and evaporated under reduced pressure. The crude product was purified by flash chromatography (3:2 hexanes: $\text{EtOAc}$  eluent) to afford acetoxycyclohexene **183** (1.49 g, 99% yield, 2 steps) as a colorless oil.  $R_f$  0.23 (2:1 hexanes: $\text{EtOAc}$ ).



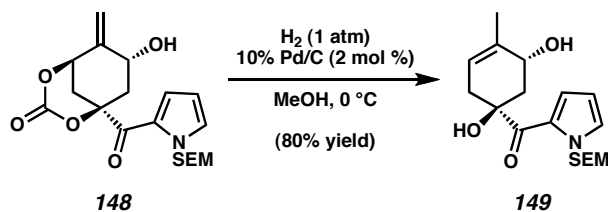
To acetoxycyclohexene **183** (222 mg, 0.542 mmol) and 1,1'-carbonyldiimidazole (132 mg, 0.813 mmol) in THF (10.8 mL) at 23 °C was added NaH (60% dispersion in mineral oil, 54 mg, 1.35 mmol). After 2 min of stirring, the reaction was quenched by the addition of saturated aq. NH<sub>4</sub>Cl (10 mL) and the volatile solvents were removed under reduced pressure. The residue was diluted with H<sub>2</sub>O (50 mL) and extracted with EtOAc (3 x 50 mL). The combined organic layers were washed with brine (30 mL), dried over MgSO<sub>4</sub>, and evaporated under reduced pressure. The crude product was purified by flash chromatography (2:1 hexanes:EtOAc eluent) to afford acetoxycarbonate **146** (200.1 mg, 85% yield) as a colorless oil. *R<sub>f</sub>* 0.25 (2:1 hexanes:EtOAc); <sup>1</sup>H NMR (300 MHz, C<sub>6</sub>D<sub>6</sub>): δ 7.75 (dd, *J* = 4.3, 1.5 Hz, 1H), 6.74 (dd, *J* = 2.5, 1.7 Hz, 1H), 6.03 (dd, *J* = 4.3, 2.6 Hz, 1H), 5.89–5.79 (m, 1H), 5.47 (s, 2H), 4.90 (d, *J* = 2.2 Hz, 1H), 4.73 (d, *J* = 1.9 Hz, 1H), 4.54 (dd, *J* = 3.9, 1.9 Hz, 1H), 3.40 (t, *J* = 7.8 Hz, 2H), 2.82 (ddd, *J* = 13.4, 6.3, 2.3 Hz, 1H), 2.03 (dd, *J* = 14.6, 1.9 Hz, 1H), 1.95 (ddd, *J* = 14.6, 3.8, 2.4 Hz, 1H), 1.81 (dd, *J* = 13.2, 11.3 Hz, 1H), 1.63 (s, 3H), 0.81 (t, *J* = 7.8 Hz, 2H), –0.08 (s, 9H); <sup>13</sup>C NMR (75 MHz, C<sub>6</sub>D<sub>6</sub>): δ 185.4, 168.9, 146.8, 141.6, 132.3, 126.4, 125.4, 112.6, 110.4, 87.4, 80.0, 78.7, 67.3, 66.5, 41.7, 33.3, 20.5, 18.3, –1.0 (3C); IR (film) 2953, 1764, 1643, 1413, 1356, 1234, 1177, 1129, 1106, 1086, 1048 cm<sup>–1</sup>; HRMS-FAB (*m/z*): [M + H]<sup>+</sup> calc'd for C<sub>21</sub>H<sub>30</sub>NO<sub>7</sub>Si, 436.1792; found, 436.1807; [α]<sub>D</sub><sup>27</sup> –112.57° (*c* 1.0, C<sub>6</sub>H<sub>6</sub>).



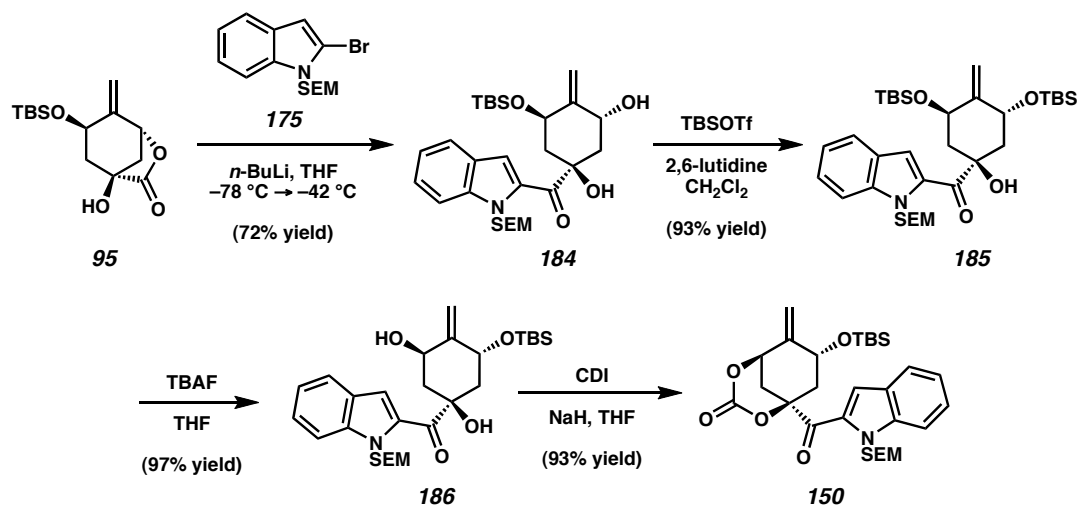
**Allylic Acetate 147.** A mixture of acetoxycarbonate **146** (734 mg, 1.69 mmol) and 10% Pd/C (36 mg, 0.03 mmol) in MeOH (17 mL) was cooled to 0 °C. The reaction vessel was then evacuated and back-filled with H<sub>2</sub> (3x). After 20 min at 0 °C, the reaction mixture was filtered over a Celite® plug (MeOH eluent) and the solvent was evaporated in vacuo. The residue was purified by flash chromatography (3:1 hexanes:EtOAc eluent) to afford allylic acetate **147** (625 mg, 94% yield). *R<sub>f</sub>* 0.56 (2:1 hexanes:EtOAc); <sup>1</sup>H NMR (300 MHz, C<sub>6</sub>D<sub>6</sub>): δ 7.05 (dd, *J* = 4.1, 1.7 Hz, 1H), 6.69 (dd, *J* = 2.2, 1.4 Hz, 1H), 6.07–5.98 (m, 1H), 5.95 (dd, *J* = 3.9, 2.8 Hz, 1H), 5.53 (d, *J* = 9.9 Hz, 1H), 5.47 (d, *J* = 9.9 Hz, 1H), 5.36–5.30 (m, 1H), 4.09 (br s, 1H), 3.42 (t, *J* = 7.8 Hz, 2H), 2.80 (ddd, *J* = 18.0, 5.2, 2.6 Hz, 1H), 2.43 (ddd, *J* = 12.6, 6.1, 1.7 Hz, 1H), 2.34 (dd, *J* = 12.4, 9.6 Hz, 1H), 2.17–2.06 (m, 1H), 1.72–1.69 (m, 3H), 1.68 (s, 3H), 0.82 (t, *J* = 7.8 Hz, 2H), –0.08 (s, 9H); <sup>13</sup>C NMR (75 MHz, C<sub>6</sub>D<sub>6</sub>): δ 193.3, 170.4, 133.8, 130.9, 126.9, 123.1, 122.7, 109.5, 78.7, 78.3, 71.9, 66.6, 39.6, 38.2, 21.0, 19.4, 18.3, –1.0 (3C); IR (film) 3438 (br), 2951, 1735, 1717, 1636, 1413, 1370, 1241, 1082, 1024 cm<sup>–1</sup>; HRMS-FAB (*m/z*): [M + H]<sup>+</sup> calc'd for C<sub>20</sub>H<sub>32</sub>NO<sub>5</sub>Si, 394.2050; found, 394.2031; [α]<sub>D</sub><sup>27</sup> –9.91° (*c* 1.0, C<sub>6</sub>H<sub>6</sub>).



**Hydroxycarbonate 148.** To carbonate **131** (41.8 mg, 0.08 mmol) in THF (1 mL) was added TBAF (1.0 M in THF, 85  $\mu$ L, 0.085 mmol) at 23 °C. After stirring 3 min, the reaction was quenched by the addition of saturated aq.  $\text{NH}_4\text{Cl}$  (1 mL). EtOAc (1 mL) was added, the phases were partitioned, and the aqueous phase was extracted with EtOAc (3 x 1 mL). The combined organics were washed successively with  $\text{H}_2\text{O}$  (1 mL) and brine (1 mL), and dried over  $\text{MgSO}_4$ . The solvent was evaporated in vacuo, and the crude product was purified by flash chromatography (1:1 hexanes:EtOAc eluent) to provide hydroxycarbonate **148** (28.7 mg, 89% yield) as a colorless oil.  $R_f$  0.29 (1:1 hexanes:EtOAc);  $^1\text{H}$  NMR (300 MHz,  $\text{C}_6\text{D}_6$ ):  $\delta$  7.77 (dd,  $J = 4.1, 1.4$  Hz, 1H), 6.72 (app. t,  $J = 2.1$  Hz, 1H), 6.08 (dd,  $J = 4.1, 2.3$  Hz, 1H), 5.48 (d,  $J = 10.1$  Hz, 1H), 5.42 (d,  $J = 10.1$  Hz, 1H), 5.29 (app. t,  $J = 1.6$  Hz, 1H), 4.78–4.75 (m, 1H), 4.52–4.42 (comp. m, 2H), 3.40 (t,  $J = 8.0$  Hz, 2H), 2.67 (ddd,  $J = 13.4, 6.1, 2.6$  Hz, 1H), 2.47 (app. d,  $J = 5.5$  Hz, 1H), 2.00 (dd,  $J = 14.4, 1.6$  Hz, 1H), 1.91–1.81 (comp. m, 2H), 0.83 (t,  $J = 7.8$  Hz, 2H), –0.07 (s, 9H);  $^{13}\text{C}$  NMR (75 MHz,  $\text{C}_6\text{D}_6$ ):  $\delta$  185.8, 147.9, 145.9, 132.0, 126.6, 125.1, 112.2, 110.2, 88.1, 80.6, 78.7, 66.6, 65.4, 45.2, 33.4, 18.2, –1.0 (3C); IR (film) 3455 (br), 2953, 2895, 1756, 1644, 1414, 1360, 1250, 1179, 1082 (br)  $\text{cm}^{-1}$ ; HRMS-FAB ( $m/z$ ):  $[\text{M} + \text{H}]^+$  calc'd for  $\text{C}_{19}\text{H}_{28}\text{NO}_6\text{Si}$ , 394.1686; found, 394.1690;  $[\alpha]_D^{26}$  –77.69° ( $c$  1.0,  $\text{C}_6\text{H}_6$ ).



**Allylic alcohol 149.** A mixture of hydroxycarbonate **148** (34.2 mg, 0.09 mmol) and 10% Pd/C (1.5 mg, 0.001 mmol) in MeOH (1.4 mL) was cooled to 0 °C. The reaction vessel was then evacuated and back-filled with H<sub>2</sub> (3x). After 15 min at 0 °C, the reaction mixture was filtered over a Celite<sup>®</sup> plug (MeOH eluent) and the solvent was evaporated in vacuo. The residue was purified by flash chromatography (3:1 hexanes:EtOAc eluent) to afford allylic alcohol **149** (24.3 mg, 80% yield) as a colorless oil. *R<sub>f</sub>* 0.33 (1:1 hexanes:EtOAc); <sup>1</sup>H NMR (300 MHz, C<sub>6</sub>D<sub>6</sub>): δ 7.19 (dd, *J* = 4.0, 1.6 Hz, 1H), 6.69 (dd, *J* = 2.4, 1.6 Hz, 1H), 5.98 (dd, *J* = 4.1, 2.5 Hz, 1H), 5.50 (d, *J* = 10.1 Hz, 1H), 5.46 (d, *J* = 9.8 Hz, 1H), 5.27–5.21 (m, 1H), 4.45–4.34 (m, 1H), 3.99 (s, 1H), 3.41 (t, *J* = 7.8 Hz, 2H), 2.91–2.79 (m, 1H), 2.26 (dd, *J* = 12.9, 8.1 Hz, 1H), 2.20–2.03 (comp. m, 3H), 1.87–1.83 (m, 3H), 0.82 (t, *J* = 7.8 Hz, 2H), –0.08 (s, 9H); <sup>13</sup>C NMR (75 MHz, C<sub>6</sub>D<sub>6</sub>): δ 194.3, 137.9, 130.9, 126.9, 123.5, 119.9, 109.5, 78.7, 78.4, 68.4, 66.6, 43.9, 38.8, 19.9, 18.3, –1.0 (3C); IR (film) 3407 (br), 2953, 2920, 1629, 1412, 1309, 1250, 1081 cm<sup>–1</sup>; HRMS-FAB (*m/z*): [M + H]<sup>+</sup> calc'd for C<sub>18</sub>H<sub>30</sub>NO<sub>4</sub>Si, 352.1944; found, 352.1931; [α]<sub>D</sub><sup>25</sup> +21.44° (*c* 1.0, C<sub>6</sub>H<sub>6</sub>).



**Indolocarbonate 150.** To 2-bromo SEM indole (**175**, 345.0 mg, 1.06 mmol) in THF (7 mL) cooled to  $-78\text{ }^{\circ}\text{C}$  was added *n*-BuLi (2.5 M in hexanes, 380  $\mu\text{L}$ , 0.95 mmol) dropwise over 1 min. The reaction was stirred for 7 min, and then a solution of lactone **95** (80.8 mg, 0.28 mmol) in THF (1 mL) was added dropwise over 2 min. The solution was warmed to  $-42\text{ }^{\circ}\text{C}$ , and stirred for 1 h. The reaction was quenched at  $-78\text{ }^{\circ}\text{C}$  by the addition of saturated aq.  $\text{NH}_4\text{Cl}$  (3 mL), and was allowed to thaw slowly to  $23\text{ }^{\circ}\text{C}$ .  $\text{Et}_2\text{O}$  (50 mL) and  $\text{H}_2\text{O}$  (10 mL) were added, the phases were partitioned, and the aqueous phase was extracted with  $\text{Et}_2\text{O}$  (2 x 50 mL). The combined organic extracts were washed with brine (15 mL) and dried over  $\text{MgSO}_4$ . Following evaporation of the solvent in vacuo, the crude product was purified by flash chromatography (9:1 hexanes:EtOAc eluent) to afford *anti*-diol **184** (108.9 mg, 72% yield) as a pale yellow foam.  $R_f$  0.40 (4:1 hexanes:EtOAc).

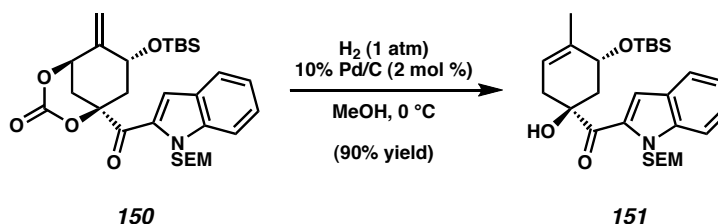
To *anti*-diol **184** (762.8 mg, 1.43 mmol) in  $\text{CH}_2\text{Cl}_2$  (20 mL) at  $23\text{ }^{\circ}\text{C}$  was added 2,6-lutidine (360  $\mu\text{L}$ , 3.09 mmol). The solution was treated with TBSOTf (480  $\mu\text{L}$ , 2.09 mmol), and was stirred for 10 min. The reaction was quenched by the addition of saturated aq.  $\text{NH}_4\text{Cl}$  (50 mL). The phases were partitioned, and the aqueous phase was

extracted with  $\text{CH}_2\text{Cl}_2$  (4 x 50 mL). The combined organic extracts were washed with brine (15 mL) and dried over  $\text{MgSO}_4$ . Following evaporation of the solvent in vacuo, the crude product was purified by flash chromatography (9:1 hexanes:EtOAc eluent) to afford bis(silylether) **185** (859.6 mg, 93% yield) as a white solid.  $R_f$  0.48 (4:1 hexanes:EtOAc).

To bis(silylether) **185** (859.6 mg, 1.33 mmol) in THF (34 mL) at 23 °C was added TBAF (1.0 M in THF, 1.40 mL, 1.40 mmol) in a dropwise fashion over 1 min. After stirring 5 min, the reaction was quenched by the addition of saturated aq.  $\text{NH}_4\text{Cl}$  (50 mL).  $\text{Et}_2\text{O}$  (50 mL) was added, the phases were partitioned, and the aqueous phase was extracted with  $\text{Et}_2\text{O}$  (75 mL x 2). The combined organics were washed with brine (25 mL), dried over  $\text{MgSO}_4$ , and evaporated under reduced pressure. The residue was purified by flash chromatography (9:1 hexanes:EtOAc  $\rightarrow$  4:1 hexanes:EtOAc eluent) to afford *syn*-diol **186** (687.1 mg, 97% yield) as a pale yellow foam.  $R_f$  0.28 (4:1 hexanes:EtOAc).

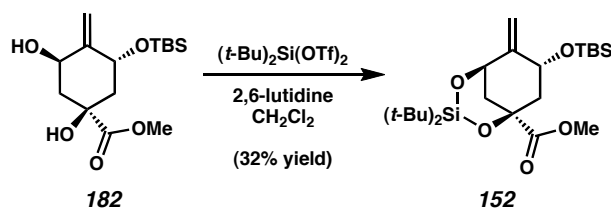
To *syn*-diol **186** (687.1 mg, 1.29 mmol) in THF (30 mL) at 23 °C was added NaH (60% dispersion in mineral oil, 167.0 mg, 4.18 mmol). When  $\text{H}_2$  evolution ceased (3 min), 1,1'-carbonyldiimidazole (331.3 mg, 2.04 mmol) was added in one portion. The reaction was quenched after 30 min of stirring with saturated aq.  $\text{NH}_4\text{Cl}$  (50 mL).  $\text{Et}_2\text{O}$  (50 mL) was added, the phases were partitioned, and the aqueous phase was extracted with  $\text{Et}_2\text{O}$  (75 mL x 2). The combined organics were washed with brine (25 mL), dried over  $\text{MgSO}_4$ , and evaporated under reduced pressure. The residue was purified by flash chromatography (9:1 hexanes:EtOAc eluent) to furnish indolocarbonate **150** (668.9 mg, 93% yield) as a white foam.  $R_f$  0.37 (4:1 hexanes:EtOAc);  $^1\text{H}$  NMR (300 MHz,  $\text{C}_6\text{D}_6$ ):  $\delta$

8.24 (d,  $J = 0.8$  Hz, 1H), 7.45 (app. dt,  $J = 4.5, 2.8$  Hz, 1H), 7.38–7.34 (m, 1H), 7.24–7.18 (m, 1H), 7.03–6.97 (m, 1H), 5.86 (d,  $J = 10.6$  Hz, 1H), 5.77 (d,  $J = 10.4$  Hz, 1H), 5.26 (dd,  $J = 2.0, 1.5$  Hz, 1H), 4.88–4.79 (m, 1H), 4.74 (app. t,  $J = 1.7$  Hz, 1H), 4.54 (dd,  $J = 3.9, 2.0$  Hz, 1H), 3.51–3.44 (m, 2H), 2.86 (ddd,  $J = 13.5, 6.0, 2.3$  Hz, 1H), 2.11–1.92 (comp. m, 3H), 0.87 (s, 9H), 0.80 (t,  $J = 7.7$  Hz, 2H), –0.05 (s, 3H), –0.07 (s, 3H), –0.12 (s, 9H);  $^{13}\text{C}$  NMR (75 MHz,  $\text{C}_6\text{D}_6$ ):  $\delta$  188.9, 147.0, 146.2, 141.5, 130.7, 127.9, 127.3, 124.7, 122.4, 118.2, 112.5, 111.9, 88.3, 80.2, 74.1, 66.7, 66.2, 46.1, 33.6, 26.2 (3C), 18.6, 18.3, –1.0 (3C), –4.7, –4.9; IR (film) 2954, 1765, 1656, 1355, 1170, 1086  $\text{cm}^{-1}$ ; HRMS-EI ( $m/z$ ):  $[\text{M}]^+$  calc'd for  $\text{C}_{29}\text{H}_{43}\text{NO}_6\text{Si}_2$ , 557.2629; found, 557.2632;  $[\alpha]_{\text{D}}^{23}$  –34.29 (c 1.0,  $\text{C}_6\text{H}_6$ ).



**Acyl Indole 151.** A mixture of indolocarbonate **150** (230.2 mg, 0.41 mmol) and 10% Pd/C (8.8 mg, 0.008 mmol) in MeOH (10 mL) was cooled to 0 °C. The reaction vessel was then evacuated and back-filled with  $\text{H}_2$  (3x). After 4 h at 0 °C, the reaction mixture was filtered over a Celite<sup>®</sup> plug (MeOH eluent) and the solvent was evaporated in vacuo. The residue was purified by flash chromatography (9:1 hexanes:EtOAc eluent) to afford acyl indole **151** (192.2 mg, 90% yield) as a pale yellow oil.  $R_f$  0.48 (4:1 hexanes:EtOAc);  $^1\text{H}$  NMR (300 MHz,  $\text{C}_6\text{D}_6$ ):  $\delta$  7.43–7.42 (m, 1H), 7.42–7.39 (m, 1H), 7.39–7.37 (m, 1H), 7.24–7.17 (m, 1H), 7.07–7.01 (m, 1H), 5.90 (d,  $J = 10.6$  Hz, 1H), 5.82 (d,  $J = 10.6$  Hz, 1H), 5.41–5.35 (m, 1H), 4.87–4.77 (m, 1H), 4.29 (s, 1H), 3.51 (t,  $J$

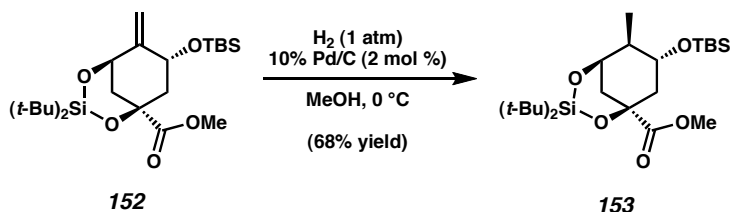
= 7.8 Hz, 2H), 3.03–2.92 (m, 1H), 2.66–2.57 (m, 1H), 2.43–2.35 (m, 1H), 2.23–2.11 (m, 1H), 1.95–1.92 (m, 3H), 0.96 (s, 9H), 0.82 (t,  $J = 7.8$  Hz, 2H), 0.08 (s, 3H), 0.06 (s, 3H), –0.12 (s, 9H);  $^{13}\text{C}$  NMR (75 MHz,  $\text{C}_6\text{D}_6$ ):  $\delta$  197.1, 141.0, 138.7, 130.7, 127.4, 127.0, 124.0, 122.3, 119.9, 116.1, 112.2, 79.3, 74.2, 69.5, 66.2, 44.4, 38.8, 26.4 (3C), 20.6, 18.6, 18.3, –1.0 (3C), –3.8, –4.5; IR (film) 3449 (br), 2954, 1643, 1249, 1092  $\text{cm}^{-1}$ ; HRMS-EI ( $m/z$ ):  $[\text{M}]^+$  calc'd for  $\text{C}_{28}\text{H}_{45}\text{NO}_4\text{Si}_2$ , 515.2887; found, 515.2875;  $[\alpha]_D^{27}$  –27.67° ( $c$  1.0,  $\text{C}_6\text{H}_6$ ).



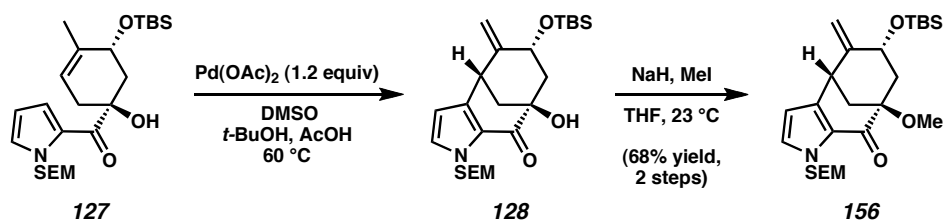
**Dioxasilylcyclohexane 152.** To *syn*-diol **182** (19.3 mg, 0.06 mmol) in  $\text{CH}_2\text{Cl}_2$  (1.2 mL) was added 2,6-lutidine (30  $\mu\text{L}$ , 0.26 mmol) followed by rapid dropwise addition of  $(t\text{-Bu})_2\text{Si(OTf)}_2$  (30  $\mu\text{L}$ , 0.08 mmol) over 1 min. The reaction was stirred for 16 h at 23 °C, and then quenched by the addition of saturated aq.  $\text{NH}_4\text{Cl}$  (1 mL). The phases were partitioned, and the aqueous phase was extracted with  $\text{CH}_2\text{Cl}_2$  (3 x 1 mL). The combined organic extracts were dried over  $\text{MgSO}_4$  and evaporated in vacuo. Purification by preparative thin-layer chromatography (11:2 hexanes:EtOAc eluent) afforded dioxasilylcyclohexane **152** (9.0 mg, 32% yield) as a colorless oil.  $R_f$  0.50 (4:1 hexanes:EtOAc);  $^1\text{H}$  NMR (300 MHz,  $\text{CDCl}_3$ ):  $\delta$  5.17 (app. t,  $J = 1.9$  Hz, 1H), 5.14–5.06 (comp. m, 2H), 4.78 (dd,  $J = 3.8, 2.1$  Hz, 1H), 3.73 (s, 3H), 2.71 (app. dt,  $J = 9.1, 4.9$  Hz, 1H), 2.42 (ddd,  $J = 13.1, 7.2, 2.9$  Hz, 1H), 2.00–1.80 (comp. m, 2H), 1.08 (s, 9H), 1.07 (s, 9H), 0.89 (s, 9H), 0.06 (s, 6H);  $^{13}\text{C}$  NMR (75 MHz,  $\text{CDCl}_3$ ):  $\delta$  173.6, 150.2, 110.6,



76.8, 74.9, 66.6, 52.6, 45.4, 39.1, 29.2 (3C), 28.7 (3C), 26.0 (3C), 21.7, 21.6, 18.3, -4.3, -4.5; IR (film) 2937, 2860, 1758, 1739, 1473, 1243, 1112  $\text{cm}^{-1}$ ; HRMS-EI ( $m/z$ ):  $[\text{M}]^+$  calc'd for  $\text{C}_{23}\text{H}_{44}\text{O}_5\text{Si}_2$ , 456.2727; found, 456.2740;  $[\alpha]_{\text{D}}^{21} -47.35^\circ$  ( $c$  1.0,  $\text{C}_6\text{H}_6$ ).



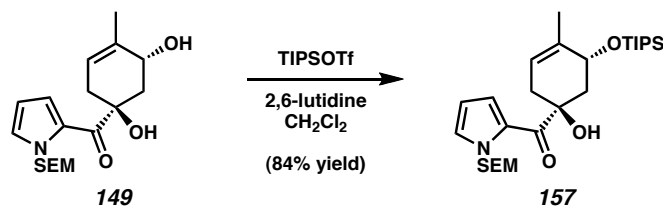
**Reduced Dioxasilycyclohexane 153.** For representative procedures, see reductive isomerization of **131**  $\rightarrow$  **127** or **135**  $\rightarrow$  **138**. Purified by preparative thin-layer chromatography (4:1 hexanes:EtOAc eluent).  $R_f$  0.82 (1:1 hexanes:EtOAc);  $^1\text{H}$  NMR (300 MHz,  $\text{CDCl}_3$ ):  $\delta$  4.30–4.19 (comp. m, 2H), 3.73 (s, 3H), 2.64 (ddd,  $J = 14.5, 4.0, 3.1$  Hz, 1H), 2.29 (ddd,  $J = 13.4, 5.9, 2.9$  Hz, 1H), 1.88–1.72 (comp. m, 2H), 1.53–1.43 (m, 1H), 1.15 (d,  $J = 6.6$  Hz, 3H), 1.09 (s, 9H), 1.06 (s, 9H), 0.86 (s, 9H), 0.02 (s, 3H), 0.02 (s, 3H);  $^1\text{H}$  NMR (300 MHz,  $\text{C}_6\text{D}_6$ ):  $\delta$  4.47 (app. dt,  $J = 9.9, 5.6$  Hz, 1H), 3.97–3.92 (m, 1H), 3.32 (s, 3H), 2.71–2.58 (comp. m, 2H), 1.99 (dd,  $J = 13.3, 10.3$  Hz, 1H), 1.63 (dd,  $J = 14.4, 1.7$  Hz, 1H), 1.44–1.31 (m, 1H), 1.28 (d,  $J = 6.4$  Hz, 3H), 1.20 (s, 9H), 1.19 (s, 9H), 1.00 (s, 9H), 0.14 (s, 3H), 0.10 (s, 3H);  $^{13}\text{C}$  NMR (75 MHz,  $\text{C}_6\text{D}_6$ ):  $\delta$  173.7, 77.6, 74.1, 70.1, 52.1, 45.9, 44.8, 38.6, 29.8 (3C), 29.4 (3C), 26.4 (3C), 22.2, 22.1, 18.5, 15.9, -3.2, -3.8; IR (film) 2954, 2936, 2895, 2860, 1757, 1739, 1258, 1146, 1100, 1081  $\text{cm}^{-1}$ ; HRMS-EI ( $m/z$ ):  $[\text{M}]^+$  calc'd for  $\text{C}_{23}\text{H}_{46}\text{O}_5\text{Si}_2$ , 458.2884; found, 458.2886;  $[\alpha]_{\text{D}}^{25} -52.92^\circ$  ( $c$  1.0,  $\text{CHCl}_3$ ).



**[3.3.1] Bicycle 128.** To pyrrolocyclohexene **127** (40.0 mg, 0.0859 mmol) was added Pd(OAc)<sub>2</sub> (23.0 mg, 0.103 mmol), DMSO (14.6  $\mu$ L, 0.206 mmol), *t*-BuOH (6.9 mL), and AcOH (1.7 mL). The mixture was heated to 60 °C for 8 h, cooled to 23 °C, and filtered over a plug of silica gel (2:1 hexanes:EtOAc eluent). The solvent was evaporated, and the product was purified by flash chromatography on silica gel (8:1 hexanes:EtOAc eluent) to afford [3.3.1] bicycle **128** contaminated with a trace amount of pyrrolocyclohexene **127**. Although this material was carried on to the subsequent step without further purification, an analytical sample of **128** was obtained by flash chromatography on silica gel (12:1 hexanes:EtOAc eluent) as a colorless oil. *R*<sub>f</sub> 0.64 (3:1 hexanes:EtOAc); <sup>1</sup>H NMR (300 MHz, C<sub>6</sub>D<sub>6</sub>):  $\delta$  6.64 (d, *J* = 2.5 Hz, 1H), 6.25 (d, *J* = 10.2 Hz, 1H), 5.84 (d, *J* = 2.8 Hz, 1H), 5.07 (d, *J* = 9.9 Hz, 1H), 4.79 (br s, 1H), 4.66 (br s, 1H), 4.24–4.19 (m, 1H), 4.19 (s, 1H), 3.68–3.51 (m, 2H), 3.43–3.38 (m, 1H), 2.61 (app. dt, *J* = 7.3, 3.9 Hz, 1H), 2.21–2.10 (m, 2H), 2.06–1.98 (m, 1H), 0.99–0.77 (m, 2H), 0.72 (s, 9H), –0.04 (s, 9H), –0.11 (s, 3H), –0.24 (s, 3H); <sup>13</sup>C NMR (75 MHz, C<sub>6</sub>D<sub>6</sub>):  $\delta$  192.0, 148.6, 142.7, 130.5, 126.3, 113.2, 108.3, 77.0, 73.4, 73.0, 66.6, 48.5, 45.5, 40.2, 26.1 (3C), 18.4, 18.3, –1.0 (3C), –4.4, –5.1; IR (film): 3468 (br), 2951, 1648, 1422, 1250, 1094, 1062 cm<sup>–1</sup>; HRMS-FAB (*m/z*): [M + H]<sup>+</sup> calc'd for C<sub>24</sub>H<sub>42</sub>NO<sub>4</sub>Si<sub>2</sub>, 464.2652; found, 464.2661; [ $\alpha$ ]<sub>D</sub><sup>27</sup> +319.22° (*c* 1.0, C<sub>6</sub>H<sub>6</sub>).

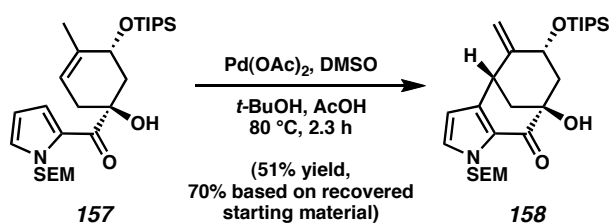
**Methyl Ether 156.** The crude mixture of **127** and **128** obtained from the previous step was dissolved in THF (1.5 mL) at 23 °C, and NaH (60% dispersion in mineral oil, 17

mg, 0.429 mmol) was added. After stirring for 1 min at 23 °C, MeI was added (53  $\mu$ L, 0.859 mmol). The resulting mixture was stirred for 1.5 h, quenched with saturated aq.  $\text{NH}_4\text{Cl}$  (1.5 mL), and extracted with  $\text{Et}_2\text{O}$  (4 x 1 mL). The combined organic layers were washed with brine (1 mL), dried by passage over a plug of silica gel (EtOAc eluent), and evaporated under reduced pressure. The crude product was purified by flash chromatography (10:1 hexanes:EtOAc eluent) to afford methyl ether **156** (28.2 mg, 68% yield, 2 steps) as a colorless oil.  $R_f$  0.43 (5:1 hexanes:EtOAc);  $^1\text{H}$  NMR (300 MHz,  $\text{C}_6\text{D}_6$ ):  $\delta$  6.62 (d,  $J$  = 2.6 Hz, 1H), 6.43 (d,  $J$  = 10.3 Hz, 1H), 5.86 (d,  $J$  = 2.6 Hz, 1H), 5.06 (d,  $J$  = 10.0 Hz, 1H), 4.84 (d,  $J$  = 1.5 Hz, 1H), 4.69 (d,  $J$  = 1.5 Hz, 1H), 4.29–4.22 (m, 1H), 3.42–3.52 (m, 2H), 3.45 (app. t,  $J$  = 2.8 Hz, 1H), 3.39 (s, 3H), 2.79 (app. dt,  $J$  = 7.4, 3.8 Hz, 1H), 2.49 (app. dt,  $J$  = 8.1, 4.4 Hz, 1H), 1.96 (dd,  $J$  = 13.8, 4.7 Hz, 1H), 1.70 (dd,  $J$  = 11.7, 3.2 Hz, 1H), 0.96–0.82 (m, 2H), 0.73 (s, 9H), –0.06 (s, 9H), –0.11 (s, 3H), –0.23 (s, 3H);  $^{13}\text{C}$  NMR (75 MHz,  $\text{C}_6\text{D}_6$ ):  $\delta$  189.2, 149.2, 140.9, 129.6, 128.9, 112.9, 107.6, 79.0, 77.3, 72.7, 66.6, 51.5, 46.3, 41.7, 39.9, 26.1 (3C), 18.4, 18.4, –1.0 (3C), –4.4, –5.1; IR (film): 2951, 1661, 1426, 1250, 1113, 1066; HRMS-FAB ( $m/z$ ):  $[\text{M} + \text{H}]^+$  calc'd for  $\text{C}_{25}\text{H}_{44}\text{NO}_4\text{Si}_2$ , 478.2809; found, 478.2815;  $[\alpha]_D^{27} +312.37^\circ$  (c 1.0,  $\text{C}_6\text{H}_6$ ).

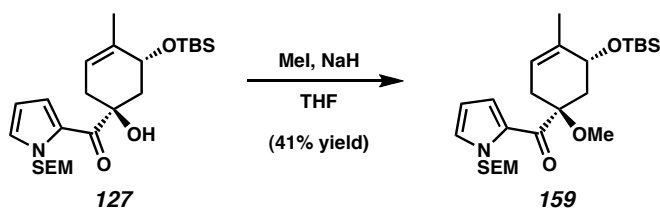


**TIPS Ether 157.** To allylic alcohol **149** (48.5 mg, 0.14 mmol) in  $\text{CH}_2\text{Cl}_2$  (5 mL) at 23 °C was added 2,6-lutidine (32  $\mu$ L, 0.27 mmol), followed by TIPSOTf (42  $\mu$ L, 0.16 mmol). After stirring 5 min, saturated aq.  $\text{NH}_4\text{Cl}$  (5 mL) was added to quench the

reaction. The phases were partitioned, and the aqueous phase was extracted with  $\text{CH}_2\text{Cl}_2$  (3 x 20 mL). The combined organic extracts were washed with brine (5 mL), and dried over  $\text{MgSO}_4$ . Following evaporation of the solvent in vacuo, the crude product was purified by flash chromatography (19:1 hexanes:EtOAc  $\rightarrow$  9:1 hexanes:EtOAc eluent) to provide TIPS ether **157** (58.5 mg, 84%) as a colorless oil.  $R_f$  0.48 (4:1 hexanes:EtOAc);  $^1\text{H}$  NMR (300 MHz,  $\text{C}_6\text{D}_6$ ):  $\delta$  6.98 (dd,  $J = 4.1, 1.4$  Hz, 1H), 6.64 (dd,  $J = 2.5, 1.6$  Hz, 1H), 5.91 (dd,  $J = 4.1, 2.7$  Hz, 1H), 5.50 (d,  $J = 10.0$  Hz, 1H), 5.46 (d,  $J = 10.0$  Hz, 1H), 5.39–5.33 (m, 1H), 5.07–4.98 (m, 1H), 4.79 (s, 1H), 3.39 (t,  $J = 7.8$  Hz, 2H), 2.97–2.85 (m, 1H), 2.55–2.46 (m, 1H), 2.44–2.36 (m, 1H), 2.20–2.08 (m, 1H), 2.05–2.00 (m, 3H), 1.16–1.02 (comp. m, 21H), 0.80 (t,  $J = 7.8$  Hz, 2H),  $-0.08$  (s, 9H);  $^{13}\text{C}$  NMR (75 MHz,  $\text{C}_6\text{D}_6$ ):  $\delta$  193.9, 139.1, 131.0, 126.3, 123.0, 119.9, 109.7, 78.8, 78.2, 70.1, 66.6, 44.9, 38.9, 20.8, 18.9 (3C), 18.8 (3C), 18.3, 13.5 (3C),  $-1.0$  (3C); IR (film) 3431 (br), 2946, 2866, 1631, 1413, 1382, 1250, 1094  $\text{cm}^{-1}$ ; HRMS-FAB ( $m/z$ ):  $[\text{M} + \text{H}]^+$  calc'd for  $\text{C}_{27}\text{H}_{50}\text{NO}_4\text{Si}_2$ , 508.3278; found, 508.3264;  $[\alpha]_{\text{D}}^{27} +14.46^\circ$  ( $c$  1.0,  $\text{C}_6\text{H}_6$ ).

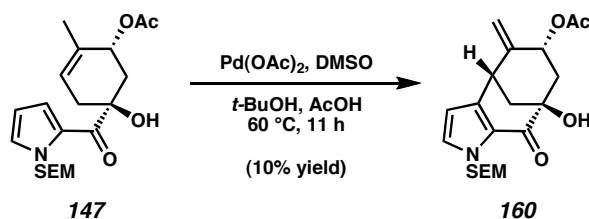


**TIPS Ether 158.** For representative procedures, see oxidative cyclization of **92**  $\rightarrow$  **90** or **113**  $\rightarrow$  **114**. Purified by preparative thin-layer chromatography (9:1  $\text{CH}_2\text{Cl}_2$ : $\text{Et}_2\text{O}$  eluent).  $R_f$  0.48 (4:1 hexanes:EtOAc);  $R_f$  0.65 (4:1  $\text{Et}_2\text{O}$ : $\text{CH}_2\text{Cl}_2$ );  $^1\text{H}$  NMR (300 MHz,  $\text{C}_6\text{D}_6$ ):  $\delta$  6.62 (d,  $J = 2.7$  Hz, 1H), 6.26 (d,  $J = 10.1$  Hz, 1H), 5.86 (d,  $J = 2.7$  Hz, 1H), 5.06 (d,  $J = 10.1$  Hz, 1H), 4.84 (app. d,  $J = 1.6$  Hz, 1H), 4.73 (app. d,  $J = 1.6$  Hz, 1H),

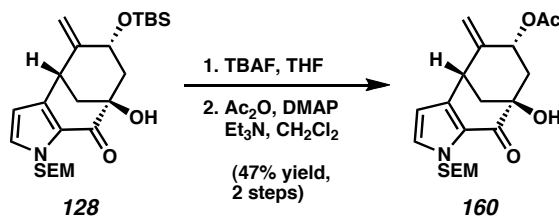


**Methyl Ether 159.** To allylic silyl ether **127** (10 mg, 0.02 mmol) in THF (1 mL) at 23 °C was added NaH (60% dispersion in mineral oil, 17 mg, 0.43 mmol). After stirring for 5 min, MeI (37 µL, 0.59 mmol) was added, and the reaction was stirred for 30 min. Saturated aq. NH<sub>4</sub>Cl (2 mL) was added slowly to quench the reaction mixture, and Et<sub>2</sub>O (1 mL) was added. The phases were partitioned, and the aqueous phase was extracted with Et<sub>2</sub>O (2 x 1 mL). The combined organic extracts were dried over MgSO<sub>4</sub>, evaporated in vacuo, and purified by flash chromatography (19:1 hexanes:EtOAc eluent) to afford methyl ether **159** (4.2 mg, 41% yield). R<sub>f</sub> 0.51 (4:1 hexanes:EtOAc); <sup>1</sup>H NMR (300 MHz, C<sub>6</sub>D<sub>6</sub>): δ 7.78 (dd, *J* = 4.1, 1.7 Hz, 1H), 6.73 (dd, *J* = 2.5, 1.7 Hz, 1H), 6.10 (dd, *J* = 4.0, 2.6 Hz, 1H), 5.64 (d, *J* = 9.9 Hz, 1H), 5.59 (d, *J* = 9.9 Hz, 1H), 5.29–5.23 (m, 1H), 4.62–4.53 (m, 1H), 3.47 (t, *J* = 2.8 Hz, 2H), 3.14 (s, 3H), 2.77 (ddd, *J* = 13.7, 5.4, 2.4 Hz, 1H), 2.70–2.58 (m, 1H), 2.53–2.41 (m, 1H), 2.32 (dd, *J* = 13.8, 9.9 Hz, 1H),

1.84–1.80 (m, 3H), 0.97 (s, 9H), 0.84 (t,  $J = 7.8$  Hz, 2H), 0.09 (s, 6H),  $-0.08$  (s, 9H);  $^{13}\text{C}$  NMR (75 MHz,  $\text{C}_6\text{D}_6$ ):  $\delta$  193.7, 137.6, 130.4, 129.2, 122.4, 119.8, 109.5, 85.8, 78.3, 69.6, 66.4, 52.6, 38.8, 34.9, 26.4 (3C), 20.3, 18.6, 18.3,  $-1.0$  (3C),  $-3.8$ ,  $-4.4$ ; IR (film) 2953, 2930, 2857, 1644, 1412, 1250, 1078  $\text{cm}^{-1}$ ; HRMS-EI ( $m/z$ ):  $[\text{M}]^+$  calc'd for  $\text{C}_{25}\text{H}_{45}\text{NO}_4\text{Si}_2$ , 479.2887; found, 479.2887;  $[\alpha]_D^{27} +7.38^\circ$  ( $c$  0.6,  $\text{C}_6\text{H}_6$ ).



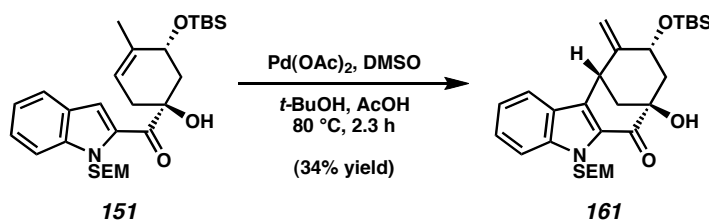
**[3.3.1] Bicycle 160.** For representative procedures, see oxidative cyclization of **92**  $\rightarrow$  **90** or **113**  $\rightarrow$  **114**. A 10% yield of **160** was obtained based on  $^1\text{H}$  NMR integration relative to benzothiazole as an internal standard. An analytical sample of **160** was prepared as follows:



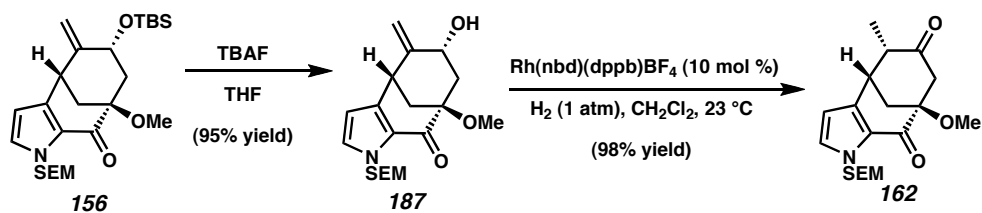
To silyl ether **128** (10.4 mg, 0.02 mmol) in THF (1 mL) was added TBAF (1.0 M in THF, 75  $\mu\text{L}$ , 0.075 mmol) dropwise over 1 min at 23  $^\circ\text{C}$ . After 23 h, the reaction was quenched by the addition of saturated aq.  $\text{NH}_4\text{Cl}$  (1 mL). The aqueous layer was extracted with  $\text{EtOAc}$  (4 x 1 mL), and the combined organics were dried over  $\text{MgSO}_4$  and evaporated in vacuo. Purification of the crude product by preparative thin-layer

chromatography (1:1 hexanes:EtOAc eluent) afforded the crude diol, which was used in the subsequent reaction.  $R_f$  0.09 (7:3 hexanes:EtOAc).

To a vial containing the crude diol in  $\text{CH}_2\text{Cl}_2$  (1.1 mL) was added DMAP (2.2 mg, 0.02 mmol) and  $\text{Et}_3\text{N}$  (31  $\mu\text{L}$ , 0.22 mmol), followed by  $\text{Ac}_2\text{O}$  (31  $\mu\text{L}$ , 0.33 mmol). The vial was sealed and heated at 50 °C for 40 min. The reaction was allowed to cool to 23 °C, and saturated aq.  $\text{NaHCO}_3$  (1 mL) was added. The aqueous layer was extracted with EtOAc (4 x 1 mL), and the combined organics were dried over  $\text{MgSO}_4$  and evaporated in vacuo. Purification of the residue by preparative thin-layer chromatography (7:3 hexanes:EtOAc) afforded [3.3.1] bicycle **160** (4.1 mg, 47% yield, 2 steps) as a colorless oil.  $R_f$  0.22 (7:3 hexanes:EtOAc);  $^1\text{H}$  NMR (300 MHz,  $\text{C}_6\text{D}_6$ ):  $\delta$  6.53 (d,  $J$  = 2.3 Hz, 1H), 5.73 (d,  $J$  = 2.3 Hz, 1H), 5.53 (d,  $J$  = 10.1 Hz, 1H), 5.49–5.45 (m, 1H), 5.39 (d,  $J$  = 10.1 Hz, 1H), 5.12 (d,  $J$  = 1.4 Hz, 1H), 4.92 (d,  $J$  = 1.8 Hz, 1H), 4.20 (s, 1H), 3.67–3.52 (m, 2H), 3.33–3.29 (m, 1H), 2.50 (app. dt,  $J$  = 7.7, 4.0 Hz, 1H), 2.12 (ddd,  $J$  = 14.7, 2.7, 1.8 Hz, 1H), 2.04 (dd,  $J$  = 12.1, 3.0 Hz, 1H), 1.96 (dd,  $J$  = 14.7, 5.5 Hz, 1H), 1.35 (s, 3H), 0.91–0.85 (m, 2H), –0.04 (s, 9H);  $^{13}\text{C}$  NMR (125 MHz,  $\text{C}_6\text{D}_6$ ):  $\delta$  191.4, 169.0, 143.6, 142.3, 131.2, 126.1, 117.5, 108.2, 76.8, 73.1, 72.9, 66.7, 44.5, 44.0, 40.0, 20.8, 18.3, –1.0 (3C); IR (film) 3471 (br), 2951, 1738, 1650, 1231, 1094  $\text{cm}^{-1}$ ; HRMS-EI ( $m/z$ ):  $[\text{M}]^+$  calc'd for  $\text{C}_{20}\text{H}_{29}\text{NO}_5\text{Si}$ , 391.1815; found, 391.1800;  $[\alpha]_D^{24}$  +396.32° ( $c$  0.5,  $\text{C}_6\text{H}_6$ ).



**[3.3.1] Bicycle 161.** For representative procedures, see oxidative cyclization of **92**  $\rightarrow$  **90** or **113**  $\rightarrow$  **114**. Purified by preparative thin-layer chromatography (4:1 hexanes:EtOAc eluent).  $R_f$  0.55 (4:1 hexanes:EtOAc);  $^1\text{H}$  NMR (300 MHz,  $\text{C}_6\text{D}_6$ ):  $\delta$  7.51–7.48 (m, 1H), 7.48–7.46 (m, 1H), 7.27–7.21 (m, 1H), 7.08–7.02 (m, 1H), 6.63 (d,  $J$  = 10.7 Hz, 1H), 5.59 (d,  $J$  = 10.7 Hz, 1H), 4.89 (app. d,  $J$  = 1.4 Hz, 1H), 4.68 (app. d,  $J$  = 1.7 Hz, 1H), 4.20–4.15 (m, 1H), 4.13 (s, 1H), 3.79–3.58 (comp. m, 3H), 2.69 (app. dt,  $J$  = 7.6, 4.0 Hz, 1H), 2.23 (dd,  $J$  = 11.8, 3.0 Hz, 1H), 2.20–2.12 (m, 1H), 2.09–2.01 (m, 1H), 1.03–0.79 (m, 2H), 0.51 (s, 9H),  $-0.07$  (s, 9H),  $-0.25$  (s, 3H),  $-0.69$  (s, 3H);  $^{13}\text{C}$  NMR (125 MHz,  $\text{C}_6\text{D}_6$ , 27/28  $^\circ\text{C}$ ):  $\delta$  195.3, 147.4, 141.4, 134.7, 129.8, 127.8, 121.8, 121.6, 113.8, 112.4, 74.1, 73.7, 72.9, 66.2, 48.6, 45.2, 38.1, 25.7 (3C), 18.2, 18.1,  $-1.0$  (3C),  $-5.0$ ,  $-5.3$ ; IR (film) 3475 (br), 2951, 1656, 1250, 1061  $\text{cm}^{-1}$ ; HRMS-EI ( $m/z$ ):  $[\text{M}]^+$  calc'd for  $\text{C}_{28}\text{H}_{43}\text{NO}_4\text{Si}_2$ , 513.2731; found, 513.2730;  $[\alpha]_D^{24} +216.18^\circ$  ( $c$  0.25,  $\text{C}_6\text{H}_6$ ).



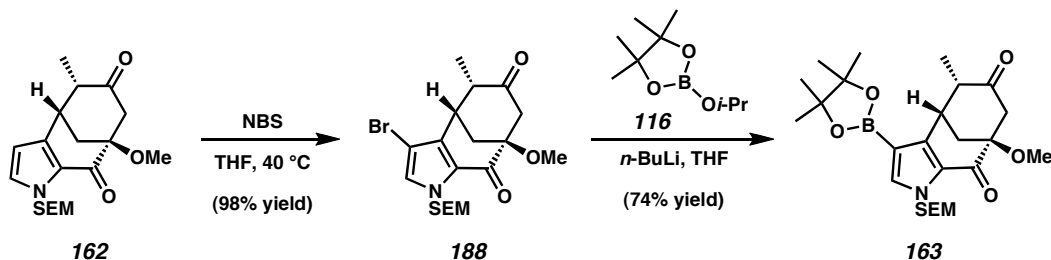
**Ketone 162.** To methyl ether **156** (120 mg, 0.25 mmol) in THF (12.5 mL) was added TBAF (1.0 M in THF, 750  $\mu\text{L}$ , 0.75 mmol). The reaction mixture was stirred for 4 h, quenched with saturated aq.  $\text{NH}_4\text{Cl}$  (10 mL), diluted with  $\text{H}_2\text{O}$  (5 mL), and extracted with EtOAc (3 x 25 mL). The combined organic extracts were washed with brine (15



mL), dried over  $\text{MgSO}_4$ , and evaporated under reduced pressure. The residue was purified by flash chromatography (1:1 hexanes:EtOAc eluent) to furnish allylic alcohol **187** (86 mg, 95% yield) as a pale yellow oil.  $R_f$  0.12 (2:1 hexanes:EtOAc);  $^1\text{H}$  NMR (300 MHz,  $\text{C}_6\text{D}_6$ ):  $\delta$  6.60 (d,  $J = 2.8$  Hz, 1H), 5.81 (d,  $J = 2.8$  Hz, 1H), 5.64 (d,  $J = 10.2$  Hz, 1H), 5.58 (d,  $J = 10.2$  Hz, 1H), 4.80 (d,  $J = 1.7$  Hz, 1H), 4.64 (d,  $J = 1.7$  Hz, 1H), 4.15–4.09 (m, 1H), 3.68–3.59 (m, 2H), 3.42 (t,  $J = 3.2$  Hz, 1H), 3.36 (s, 3H), 2.72 (app. dt,  $J = 7.4, 3.9$  Hz, 1H), 2.58 (app. dt,  $J = 8.1, 4.9$  Hz, 1H), 1.89 (dd,  $J = 14.2, 5.1$  Hz, 1H), 1.65 (dd,  $J = 11.6, 3.0$  Hz, 1H), 0.97–0.88 (m, 2H), 0.59 (d,  $J = 3.9$  Hz, 1H), –0.03 (s, 9H);  $^{13}\text{C}$  NMR (75 MHz,  $\text{C}_6\text{D}_6$ , 18/19 C):  $\delta$  189.4, 149.4, 140.6, 130.4, 113.8, 107.4, 78.9, 76.7, 72.0, 66.2, 51.6, 44.3, 41.1, 39.5, 18.4, –0.9 (3C); IR (film): 3460 (br), 2951, 1659, 1424, 1248, 1111, 1023  $\text{cm}^{-1}$ ; HRMS-FAB ( $m/z$ ):  $[\text{M} + \text{H}]^+$  calc'd for  $\text{C}_{19}\text{H}_{30}\text{NO}_4\text{Si}$ , 364.1944; found, 364.1942;  $[\alpha]_D^{24} +330.71^\circ$  ( $c$  1.0,  $\text{C}_6\text{H}_6$ ).

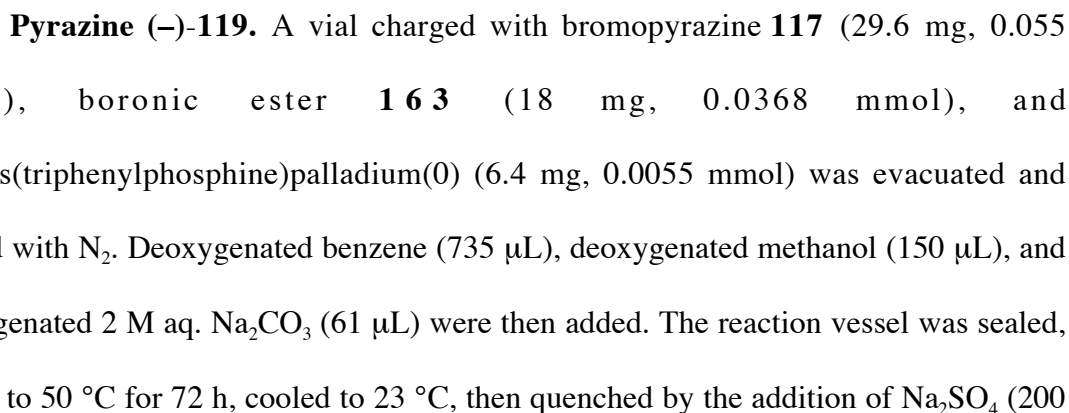
Allylic alcohol **187** (44.0 mg, 0.121 mmol) and freshly prepared  $\text{Rh}(\text{nbd})(\text{dppb})\text{BF}_4$  (8.6 mg, 0.0121 mmol)<sup>69</sup> were combined under a glovebox atmosphere. The reaction vessel was carefully sealed and removed from the glovebox.  $\text{CH}_2\text{Cl}_2$  (12.0 mL) was added, and a balloon of  $\text{H}_2$  (1 atm) was applied without purging. After 3 h of stirring, the reaction mixture was filtered over a plug of silica gel ( $\text{CH}_2\text{Cl}_2$ , then 2:1 hexanes:EtOAc eluent) to afford ketone **162** (43.0 mg, 98% yield) as a colorless oil.  $R_f$  0.30 (2:1 hexanes:EtOAc);  $^1\text{H}$  NMR (300 MHz,  $\text{C}_6\text{D}_6$ ):  $\delta$  6.53 (d,  $J = 2.5$  Hz, 1H), 5.66 (d,  $J = 2.5$  Hz, 1H), 5.50 (d,  $J = 10.5$  Hz, 1H), 5.36 (d,  $J = 10.2$  Hz, 1H), 3.57–3.38 (m, 2H), 3.34 (s, 3H), 2.98 (dd,  $J = 14.3, 2.5$  Hz, 1H), 2.70–2.64 (m, 1H), 2.57–2.47 (m, 1H), 2.43 (d,  $J = 14.3$  Hz, 1H), 2.11–1.99 (m, 1H), 1.69 (dd,  $J = 12.2, 2.6$  Hz, 1H), 0.95 (d,  $J = 6.6$  Hz, 3H), 0.84 (t,  $J = 8.0$  Hz, 2H), –0.03 (s, 9H);  $^{13}\text{C}$  NMR (125 MHz,  $\text{C}_6\text{D}_6$ ):  $\delta$

205.7, 187.9, 137.5, 131.1, 126.6, 109.7, 82.9, 76.8, 66.4, 52.7, 52.3, 48.1, 41.0, 37.7, 18.3, 13.0,  $-1.0$  (3C); IR (film): 2952, 2931, 1716, 1660, 1421, 1123, 1097, 1076  $\text{cm}^{-1}$ ; HRMS-FAB ( $m/z$ ):  $[M + H]^+ - H_2$  calc'd for  $C_{19}H_{28}NO_4Si$ , 362.1788; found, 362.1778;  $[\alpha]_D^{27} +163.23^\circ$  ( $c$  1.0,  $C_6H_6$ ).

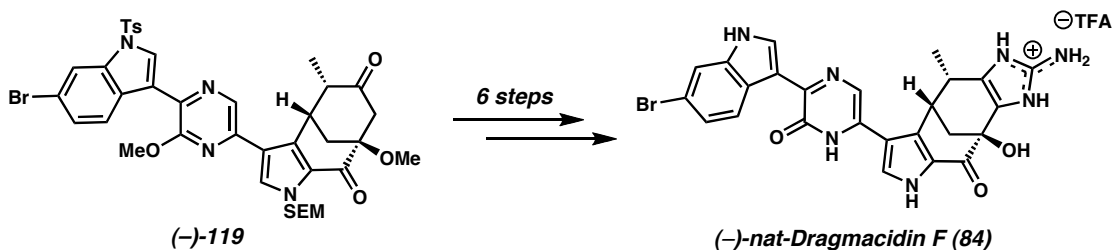


**Boronic Ester 163.** A flask wrapped in aluminum foil at 23  $^\circ\text{C}$  was charged with ketone **162** (25 mg, 0.0689 mmol), THF (5 mL), and freshly recrystallized NBS (37.5 mg, 0.211 mmol). The reaction vessel was placed in a 40  $^\circ\text{C}$  oil bath, stirred for 15 min, then cooled to 0  $^\circ\text{C}$ . The reaction was quenched with saturated aq.  $\text{Na}_2\text{S}_2\text{O}_3$  (10 mL), diluted with  $\text{H}_2\text{O}$  (5 mL), and extracted with  $\text{Et}_2\text{O}$  (3 x 20 mL). The combined organic layers were washed with brine (15 mL), dried over  $\text{MgSO}_4$ , and evaporated under reduced pressure to afford the crude product. Further purification by flash column chromatography (3:1 hexanes:EtOAc eluent) afforded bromide **188** (29.9 mg, 98% yield) as a colorless oil.  $R_f$  0.45 (2:1 hexanes:EtOAc).

To bromide **188** (27 mg, 0.061 mmol) and 2-isopropoxy-4,4,5,5-tetramethyl-1,3,2-dioxaborolane (**116**, 510  $\mu\text{L}$ , 2.5 mmol) in THF (7 mL) at  $-78^\circ\text{C}$  was added  $n\text{-BuLi}$  (2.5 M in hexanes, 730  $\mu\text{L}$ , 0.183 mmol) dropwise over 3 min. After stirring for an additional 10 min at  $-78^\circ\text{C}$ , the reaction mixture was quenched with saturated aq.  $\text{NH}_4\text{Cl}$  (7 mL), warmed to 23  $^\circ\text{C}$ , diluted with  $\text{H}_2\text{O}$  (10 mL), and extracted with EtOAc (3 x 20



mg). Following filtration over a pad of silica gel (3:1 EtOAc:hexanes eluent) and evaporation to dryness under reduced pressure, the residue was purified by flash column chromatography (2:1  $\rightarrow$  1:1 hexanes:EtOAc eluent) to afford pyrazine (–)-**119** (26.8 mg, 89% yield) as a yellow foam.  $R_f$ ,  $^1\text{H}$  NMR,  $^{13}\text{C}$  NMR, HRMS, and IR characterization data for (+)-**119** are reported earlier in this section.  $[\alpha]_D^{27} -72.92^\circ$  ( $c$  1.0,  $\text{CHCl}_3$ ).



(–)-**Dragmacidin F (84)**. Pyrazine (–)-**119** was converted to (–)-dragmacidin F (**84**) by methods described earlier in this section.  $^1\text{H}$  NMR,  $^{13}\text{C}$  NMR, HRMS, and IR characterization data for (+)-**84** are also reported above.  $[\alpha]_D^{29} -148.33^\circ$  ( $c$  0.20, MeOH). For comparison, natural (–)-dragmacidin F (**84**):  $[\alpha]_D^{25} -159^\circ$  ( $c$  0.40, MeOH).<sup>4c</sup>

### 3.7 Notes and References

- (1) (a) Blunt, J. W.; Copp, B. R.; Munro, M. H. G.; Northcote, P. T.; Prinsep, M. R. *Nat. Prod. Rep.* **2004**, *21*, 1–49. (b) Aygün, A.; Pindur, U. *Curr. Med. Chem.* **2003**, *10*, 1113–1127. (c) Faulkner, D. J. *Nat. Prod. Rep.* **2002**, *19*, 1–48. (d) Pindur, U.; Lemster, T. *Curr. Med. Chem.* **2001**, *8*, 1681–1698.
- (2) (a) Yang, C.-G.; Huang, H.; Jiang, B. *Curr. Org. Chem.* **2004**, *8*, 1691–1720. (b) Jin, Z. *Nat. Prod. Rep.* **2003**, *20*, 584–605. (c) Hibino, S.; Choshi, T. *Nat. Prod. Rep.* **2002**, *19*, 148–180. (d) Sasaki, S.; Ehara, T.; Sakata, I.; Fujino, Y.; Harada, N.; Kimura, J.; Nakamura, H.; Maeda, M. *Bioorg. Med. Chem. Lett.* **2001**, *11*, 583–585.
- (3) For the isolation of the piperazine-containing dragmacidins, see: (a) Kohmoto, S.; Kashman, Y.; McConnell, O. J.; Rinehart, K. L., Jr.; Wright, A.; Koehn, F. *J. Org. Chem.* **1988**, *53*, 3116–3118. (b) Morris, S. A.; Andersen, R. J. *Tetrahedron* **1990**, *46*, 715–720. (c) Fahy, E.; Potts, B. C. M.; Faulkner, D. J.; Smith, K. *J. Nat. Prod.* **1991**, *54*, 564–569.
- (4) For the isolation of the pyrazinone-containing dragmacidins, see: (a) Wright, A. E.; Pomponi, S. A.; Cross, S. S.; McCarthy, P. *J. Org. Chem.* **1992**, *57*, 4772–4775. (b) Capon, R. J.; Rooney, F.; Murray, L. M.; Collins, E.; Sim, A. T. R.; Rostas, J. A. P.; Butler, M. S.; Carroll, A. R. *J. Nat. Prod.* **1998**, *61*, 660–662. (c) Cutignano, A.; Bifulco, G.; Bruno, I.; Casapullo, A.; Gomez-Paloma, L.; Riccio, R. *Tetrahedron*

- 2000**, 56, 3743–3748. (d) Wright, A. E.; Pomponi, S. A.; Jacobs, R. S. PCT Int. Appl. WO 9942092, August 26, 1999.
- (5) For synthetic work aimed toward the piperazine-containing drarmacidins, see: (a) Jiang, B.; Smallheer, J. M.; Amaral-Ly, C.; Wuonola, M. A. *J. Org. Chem.* **1994**, 59, 6823–6827. (b) Whitlock, C. R.; Cava, M. P. *Tetrahedron Lett.* **1994**, 35, 371–374. (c) Kawasaki, T.; Enoki, H.; Matsumura, K.; Ohyama, M.; Inagawa, M.; Sakamoto, M. *Org. Lett.* **2000**, 2, 3027–3029. (d) Miyake, F. Y.; Yakushijin, K.; Horne, D. A. *Org. Lett.* **2000**, 2, 3185–3187. (e) Yang, C.-G.; Wang, J.; Tang, X.-X.; Jiang, B. *Tetrahedron: Asymmetry* **2002**, 13, 383–394. (f) Kawasaki, T.; Ohno, K.; Enoki, H.; Umemoto, Y.; Sakamoto, M. *Tetrahedron Lett.* **2002**, 43, 4245–4248. For studies targeting drarmacidins D, E, or F, see: (g) Jiang, B.; Gu, X.-H. *Bioorg. Med. Chem.* **2000**, 8, 363–371. (h) Jiang, B.; Gu, X.-H. *Heterocycles* **2000**, 53, 1559–1568. (i) Yang, C.-G.; Wang, J.; Jiang, B. *Tetrahedron Lett.* **2002**, 43, 1063–1066. (j) Miyake, F. Y.; Yakushijin, K.; Horne, D. A. *Org. Lett.* **2002**, 4, 941–943. (k) Yang, C.-G.; Liu, G.; Jiang, B. *J. Org. Chem.* **2002**, 67, 9392–9396. (l) Feldman, K. S.; Ngermmeesri, P. *Org. Lett.* **2005**, 7, 5449–5452. (m) Huntley, R. J.; Funk, R. L. *Org. Lett.* **2006**, 8, 4775–4778.
- (6) McIntire, W. S.; Wemmer, D. E.; Chistoserdov, A.; Lidstrom, M. E. *Science* **1991**, 252, 817–824.
- (7) Garg, N. K.; Sarpong, R.; Stoltz, B. M. *J. Am. Chem. Soc.* **2002**, 124, 13179–13184.

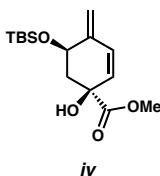
- (8) Portions of this chapter are reproduced in part, with permission, from: (a) Garg, N. K.; Caspi, D. D.; Stoltz, B. M. *J. Am. Chem. Soc.* **2004**, *126*, 9552–9553 (Copyright 2004 American Chemical Society). (b) Garg, N. K.; Caspi, D. D.; Stoltz, B. M. *J. Am. Chem. Soc.* **2005**, *127*, 5970–5978 (Copyright 2005 American Chemical Society). (c) Caspi, D. D.; Garg, N. K.; Stoltz, B. M. *Org. Lett.* **2005**, *7*, 2513–2516 (Copyright 2005 American Chemical Society). (d) Garg, N. K.; Caspi, D. D.; Stoltz, B. M. *Synlett* **2006**, 3081–3087 (Copyright 2006 Georg Thieme Verlag Stuttgart: New York).
- (9) (a) Garg, N. K.; Stoltz, B. M. *Chem. Commun.* **2006**, 3769–3779. (b) Garg, N. K. "The total synthesis of dragmacidins D and F." Ph.D. Thesis, California Institute of Technology, 2005. <http://resolver.caltech.edu/CaltechETD:etd-03222005-133937>
- (10) For recent reviews of the Heck reaction, see: (a) Dounay, A. B.; Overman, L. E. *Chem. Rev.* **2003**, *103*, 2945–2963. (b) Beletskaya, I. P.; Cheprakov, A. V. *Chem. Rev.* **2000**, *100*, 3009–3066. (c) Amatore, C.; Jutand, A. *J. Organomet. Chem.* **1999**, *576*, 254–278.
- (11) For related examples of Pd-mediated carbocyclizations in natural product synthesis, see: (a) Baran, P. S.; Corey, E. J. *J. Am. Chem. Soc.* **2002**, *124*, 7904–7905. (b) Williams, R. M.; Cao, J.; Tsujishima, H.; Cox, R. J. *J. Am. Chem. Soc.* **2003**, *125*, 12172–12178.

- (12) (a) Stoltz, B. M. *Chem. Lett.* **2004**, 33, 362–367. (b) Trend, R. M.; Ramtohl, Y. K.; Ferreira, E. M.; Stoltz, B. M. *Angew. Chem., Int. Ed.* **2003**, 42, 2892–2895. (c) Ferreira, E. M.; Stoltz, B. M. *J. Am. Chem. Soc.* **2003**, 125, 9578–9579. (d) Zhang, H.; Ferreira, E. M.; Stoltz, B. M. *Angew. Chem., Int. Ed.* **2004**, 43, 6144–6148. (e) Ferreira, E. M.; Zhang, H.; Stoltz, B. M. *Tetrahedron* **2008**, (in press).
- (13) For reviews and examples regarding the use of (–)-quinic acid in natural product synthesis, see: (a) Barco, A.; Benetti, S.; De Risi, C.; Marchetti, P.; Pollini, G. P.; Zanirato, V. *Tetrahedron: Asymmetry* **1997**, 8, 3515–3545. (b) Huang, P.-Q. *Youji Huaxue* **1999**, 19, 364–373. (c) Hanessian, S.; Pan, J.; Carnell, A.; Bouchard, H.; Lesage, L. *J. Org. Chem.* **1997**, 62, 465–473. (d) Hanessian, S. In *Total Synthesis of Natural Products: The "Chiron" Approach*, Baldwin, E. J., Ed.; Pergamon Press: Oxford, 1983; pp. 206–208.
- (14) (a) Philippe, M.; Sepulchre, A. M.; Gero, S. D.; Loibner, H.; Streicher, W.; Stutz, P. *J. Antibiot.* **1982**, 35, 1507–1512. (b) Manthey, M. K.; González-Bello, C.; Abell, C. *J. Chem. Soc., Perkin Trans. 1* **1997**, 625–628.
- (15) For a review, see: Tsuji, J.; Mandai, T. *Synthesis* **1996**, 1–24.
- (16) Greene, T. W.; Wuts, P. G. M. *Protective Groups in Organic Synthesis*, 4<sup>th</sup> Ed.; Wiley-Interscience: New York, 2006.



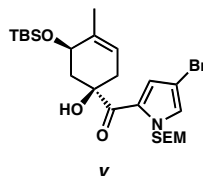
- (17) For reviews, see: (a) *Handbook of Organopalladium Chemistry for Organic Synthesis*; Negishi, E., Ed.; Wiley-Interscience: New York, 2002. (b) Trost, B. M.; Van Vranken, D. L. *Chem. Rev.* **1996**, 96, 395–422. (c) Trost, B. M. *Chem. Pharm. Bull.* **2002**, 50, 1–14. (d) Poli, G.; Giambastiani, G.; Heumann, A. *Tetrahedron* **2000**, 56, 5959–5989. (e) Hayashi, T. *J. Organomet. Chem.* **1999**, 576, 195–202. (f) Helmchen, G. *J. Organomet. Chem.* **1999**, 576, 203–214. (g) Nomura, N.; Tsurugi, K. Yoshida, N.; Okada, M. *Curr. Org. Syn.* **2005**, 2, 21–38. (h) Tsuji, J. *J. Synth. Org. Chem. Japan* **1999**, 57, 1036–1050. (i) Trost, B. M. *J. Org. Chem.* **2004**, 69, 5813–5837. (j) Trost, B. M.; Crawley, M. L. *Chem. Rev.* **2003**, 103, 2921–2943. (k) *Comprehensive Organic Synthesis*; Godleski, S. A., Trost, B. M., Fleming, I., Eds.; Pergamon Press: New York, 1991.
- (18) Despite its widespread use in modern cross-coupling chemistry, to the best of our knowledge, this is the first report of  $\text{Pd}(\text{P}(t\text{-Bu})_3)_2$  being used for a  $\pi$ -allyl palladium substitution reaction. For recent examples of  $\text{Pd}(\text{P}(t\text{-Bu})_3)_2$  in cross coupling reactions, see: Hills, I. D.; Fu, G. C. *J. Am. Chem. Soc.* **2004**, 126, 13178–13179 and references therein.
- (19) For the use of NMO as an additive in Stille couplings, see: Han, X.; Stoltz, B. M.; Corey, E. J. *J. Am. Chem. Soc.* **1999**, 121, 7600–7605.
- (20) Treatment of **97** under a variety of standard homogeneous  $\pi$ -allyl reduction conditions<sup>15</sup> led to the formation of **98**, **99**, and **iv**, all of which presumably arise

from loss of  $^-OAc$ . In stark contrast, exposure of **97** to heterogeneous reductive isomerization conditions did not produce any of these compounds (see Scheme 3.4.2).



- (21) 10% Pd/C was purchased from Aldrich (205699). This has been demonstrated to be a safe and nearly neutral hydrogenation catalyst, see: (a) Sajiki, H.; Ikawa, T.; Hirota, K. *Tetrahedron Lett.* **2003**, *44*, 7407–7410. (b) Ikawa, T.; Sajiki, H.; Hirota, K. *Tetrahedron* **2004**, *60*, 6189–6195.
- (22) For the discovery and use of SEM pyrrole, see: (a) Edwards, M. P.; Ley, S. V.; Lister, S. G.; Palmer, B. D. *J. Chem. Soc., Chem. Commun.* **1983**, 630–633. (b) Muchowski, J. M.; Solas, D. R. *J. Org. Chem.* **1984**, *49*, 203–205. (c) Edwards, M. P.; Ley, S. V.; Lister, S. G.; Palmer, B. D.; Williams, D. J. *J. Org. Chem.* **1984**, *49*, 3503–3516. (d) Edwards, M. P.; Doherty, A. M.; Ley, S. V.; Organ, H. M. *Tetrahedron* **1986**, *42*, 3723–3729.

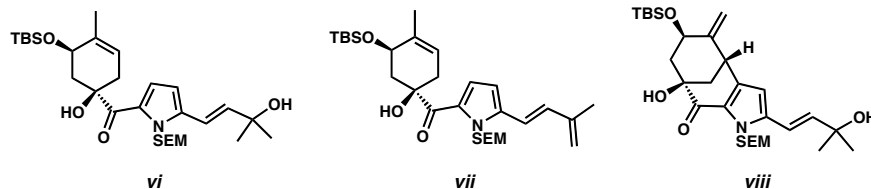
- (23) During the conversion of **101** to **91**, 2,4-disubstituted pyrrole **v** was formed as a byproduct.



- (24) Littke, A. F.; Fu, G. C. *J. Am. Chem. Soc.* **2001**, *123*, 6989–7000.

- (25) By conducting reactions in THF-*d*<sub>8</sub>, it was possible to monitor Heck reactions by <sup>1</sup>H NMR.

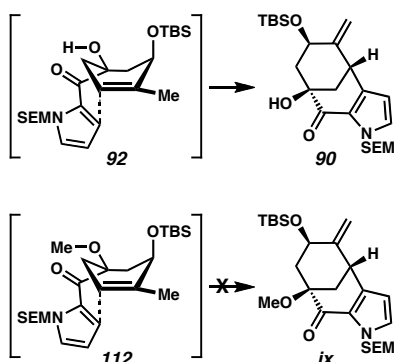
- (26) The use of *t*-amyl alcohol in the cyclization of **92** → **90** led to the formation of byproducts such as **vi**, **vii**, and **viii**. Additionally, simply re-exposing **90** to the *t*-amyl alcohol-based reaction conditions, led to the formation of **viii**.



- (27) This reaction was performed using stoichiometric Pd(OAc)<sub>2</sub>. The atmosphere of dioxygen seemed to enhance the overall conversion, but this reaction also proceeded under an inert atmosphere. In either case, the formation of Pd black was observed.

- (28) Although pyridine and ethyl nicotinate failed to perform in this cyclization, employing more electron-deficient pyridines (such as 3,4,5-trihalogenated pyridines) led to production of desired bicycle **90**.
- (29) DMSO has commonly been employed in oxidative Pd(II) chemistry. See: (a) Larock, R. C.; Hightower, T. R. *J. Org. Chem.* **1993**, 58, 5298–5300. (b) Van Benthem, R. A. T. M.; Hiemstra, H.; Michels, J. J.; Speckamp, W. N. *J. Chem. Soc., Chem. Commun.* **1994**, 357–359. (c) Rönn, M.; Bäckvall, J.-E.; Andersson, P. G. *Tetrahedron Lett.* **1995**, 36, 7749–7752. (d) Chen, M. S.; White, M. C. *J. Am. Chem. Soc.* **2004**, 126, 1346–1347. (e) Stahl, S. S. *Angew. Chem., Int. Ed.* **2004**, 43, 3400–3420. See also references therein.
- (30) Gilow, H. M.; Hong, Y. H.; Millirons, P. L.; Snyder, R. C.; Casteel, W. J., Jr. *J. Heterocycl. Chem.* **1986**, 23, 1475–1480.
- (31) Reactions conducted in the presence of acetic acid-*d* led to deuterium incorporation in the pyrrole ring of both the starting material (**92**) and the product (**90**), mostly at C(4).
- (32) The instability of pyrroles to oxidants is well known. See: (a) Ciamician, G.; Silber, P. *Chem. Ber.* **1912**, 45, 1842–1845. (b) Bernheim, F.; Morgan, J. E. *Nature* **1939**, 144, 290. (c) Chierici, L.; Gardini, G. P. *Tetrahedron* **1966**, 22, 53–56.

- (33) The instability of the starting material and product to oxidation was confirmed by a series of control experiments wherein aliquots of reactions were carefully monitored by  $^1\text{H}$  NMR analysis using benzothiazole as an internal standard. In the presence of oxidants, substantial non-specific decomposition readily occurred.
- (34) Recently, related oxidative cyclizations of pyrrole substrates have been reported. See: (a) Beccalli, E. M.; Brogini, G.; Martinelli, M.; Paladino, G. *Tetrahedron* **2005**, *61*, 1077–1082. (b) Beck, E. M.; Grimster, N. P.; Hatley, R.; Gaunt, M. J. *J. Am. Chem. Soc.* **2006**, *128*, 2528–2529.
- (35) Direct oxidation of starting material to the corresponding enone was observed.
- (36) The lack of reactivity of the 3° methyl ether substrate (**112**) vs. **92** may be due to the transition state. In order to form bicycle **90**, a nearly coplanar arrangement between the tertiary alcohol and the carbonyl of **92** is required, which may also be facilitated via an intramolecular hydrogen bond. In the case of the tertiary methyl ether (**112**), the additional steric bulk of the methyl group may disfavor this orientation.



- (37) The Heck route required the use of 2,3-dibromopyrrole, an extremely unstable compound. For a discussion regarding the instability of bromopyrroles, see: Audebert, P.; Bidan, G. *Synthetic Metals* **1986**, *15*, 9–22.
- (38) In preliminary investigations, late-stage chemistry in the presence of a reactive 3° alcohol was unsuccessful.
- (39) Neber, P. W.; Friedolsheim, A. V. *Justus Liebigs Ann. Chem.* **1926**, *449*, 109–134.
- (40) (a) For a review, see: O'Brien, C. *Chem. Rev.* **1964**, *64*, 81–89. (b) For a recent study involving the Neber rearrangement, see: Ooi, T.; Takahashi, M.; Doda, K.; Maruoka, K. *J. Am. Chem. Soc.* **2002**, *124*, 7640–7641.
- (41) (a) Purified by reversed-phase chromatography using trifluoroacetic acid in the eluent. (b) See 3.6 *Experimental Section* for details.
- (42) Derivatives of **120** bearing a free 3° alcohol or a TMS-protected 3° alcohol produced complex mixtures of products when subjected to Neber rearrangement conditions.
- (43) Acid-promoted dimerization of the amino ketone functionalities was not observed.

- (44) (a) Woodward reported a Neber rearrangement during synthetic studies involving lysergic acid. Unfortunately, the Neber rearrangement product could not be further utilized in the synthesis. See: Kornfeld, E. C.; Fornefeld, E. J.; Kline, G. B.; Mann, M. J.; Morrison, D. E.; Jones, R. G.; Woodward, R. B. *J. Am. Chem. Soc.* **1956**, 78, 3087–3114. (b) For the use of the Neber rearrangement in drug discovery, see: Chung, J. Y. L.; Ho, G.-J.; Chartrain, M.; Roberge, C.; Zhao, D.; Leazer, J.; Farr, R.; Robbins, M.; Emerson, K.; Mathre, D. J.; McNamara, J. M.; Hughes, D. L.; Grabowski, E. J. J.; Reider, P. J. *Tetrahedron Lett.* **1999**, 40, 6739–6743.
- (45) The intermediacy of azirines in Neber rearrangements is well accepted. These azirines presumably arise from transient nitrenes. See: (a) House, H. O.; Berkowitz, W. F. *J. Org. Chem.* **1963**, 28, 307–311. (b) House, H. O.; Berkowitz, W. F. *J. Org. Chem.* **1963**, 28, 2271–2276.
- (46) Hemiaminal **124** has been isolated and characterized by  $^1\text{H}$  NMR.
- (47) Boehm, J. C.; Gleason, J. G.; Pendrak, I.; Sarau, H. M.; Schmidt, D. B.; Foley, J. J.; Kingsbury, W. D. *J. Med. Chem.* **1993**, 36, 3333–3340.
- (48) Dragmacidin numbering convention, see reference 4c.
- (49) (a) (+)-Quinic acid ((+)-**93**) is commercially available in limited quantities from Interbioscreen Ltd. (50 mg/\$305 USD). (b) (+)-Quinic acid ((+)-**93**) potentially

could be prepared via multistep synthesis by applying methods used for the preparation of (–)-quinic acid (**93**). See: Rapado, L. P.; Bulugahapitiya, V.; Renaud, P. *Helv. Chim. Acta* **2000**, 83, 1625–1632 and references therein. (c) Enantiopure (–)-quinic acid (**93**) can also be racemized. See: Grewe, R.; Lorenzen, W.; Vining, L. *Chem. Ber.* **1954**, 87, 793–802.

- (50) Surprisingly, despite its widespread use in natural product synthesis and its near symmetry, (–)-quinic acid (**93**) has rarely been used in an enantiodivergent manner. For examples, see: (a) Ulibarri, G.; Nadler, W.; Skrydstrup, T.; Audrain, H.; Chiaroni, A.; Riche, C.; Grierson, D. S. *J. Org. Chem.* **1995**, 60, 2753–2761. (b) Ulibarri, G.; Audrain, H.; Nadler, W.; Lhermitte, H.; Grierson, D. S. *Pure Appl. Chem.* **1996**, 68, 601–604. (c) Barros, M. T.; Maycock, C. D.; Ventura, M. R. *J. Chem. Soc., Perkin Trans. 1* **2001**, 166–173.
- (51) If  $R = R'$ , **126** is considered to be pseudo- $C_2$ -symmetric. Pseudo- $C_2$ -symmetric molecules are those that would be  $C_2$ -symmetric if they did not contain a central chirotopic, nonstereogenic center. For discussions, see: (a) Schreiber, S. L. *Chem. Scr.* **1987**, 27, 563–566. (b) Poss, C. S.; Schreiber, S. L. *Acc. Chem. Res.* **1994**, 27, 9–17. (c) Magnuson, S. R. *Tetrahedron* **1995**, 51, 2167–2213. (d) Eliel, E. L.; Wilen, S. H.; Mander, L. N. *Stereochemistry of Organic Compounds*; Wiley-Interscience: New York, 1994.



- (52) Olefin **97** was also exposed to the reaction conditions used for the reductive isomerization of **95** to **96**. Only trace quantities of **129** were produced under those conditions.<sup>41b,53b</sup>
- (53) (a) Yield determined based on <sup>1</sup>H NMR integration. (b) The material isolated was predominantly a mixture of diastereomeric olefin hydrogenation products.
- (54) The favored conformation of **97** depicted in Scheme 3.4.2 is consistent with <sup>1</sup>H NMR studies.<sup>41b</sup>
- (55) <sup>1</sup>H NMR experiments show that the C(3) silyl ether of **132** is axially disposed.<sup>41b</sup> For similar examples of axial-selective TBS cleavage promoted by TBAF, see: (a) Craig, B. N.; Janssen, M. U.; Wickersham, B. M.; Rabb, D. M.; Chang, P. S.; O’Leary, D. J. *J. Org. Chem.* **1996**, *61*, 9610–9613. (b) Meier, R.-M.; Tamm, C. *Helv. Chim. Acta*, **1991**, *74*, 807–818.
- (56) For a classic example involving the use of conformational analysis to solve stereochemical problems in total synthesis, see: Woodward, R. B.; Bader, F. E.; Bickel, H.; Frey, A. J.; Kierstead, R. W. *Tetrahedron* **1958**, *2*, 1–57.
- (57) Isolated examples of similar reactivity using Pd/C, H<sub>2</sub> and a protic solvent have been reported in the literature, see: (a) Paulson, D. R.; Gilliam, L. S.; Terry, V. O.; Farr, S. M.; Parker, E. J.; Tang, F. Y. N.; Ullman, R.; Ribar, G. *J. Org. Chem.* **1978**,

43, 1783–1787. (b) Dauben, W. G.; Hance, P. D. *J. Am. Chem. Soc.* **1955**, 77, 2451–2453. (c) Dauben, W. G.; Hayes, W. K.; Schwarz, J. S. P.; McFarland, J. W. *J. Am. Chem. Soc.* **1960**, 82, 2232–2238.

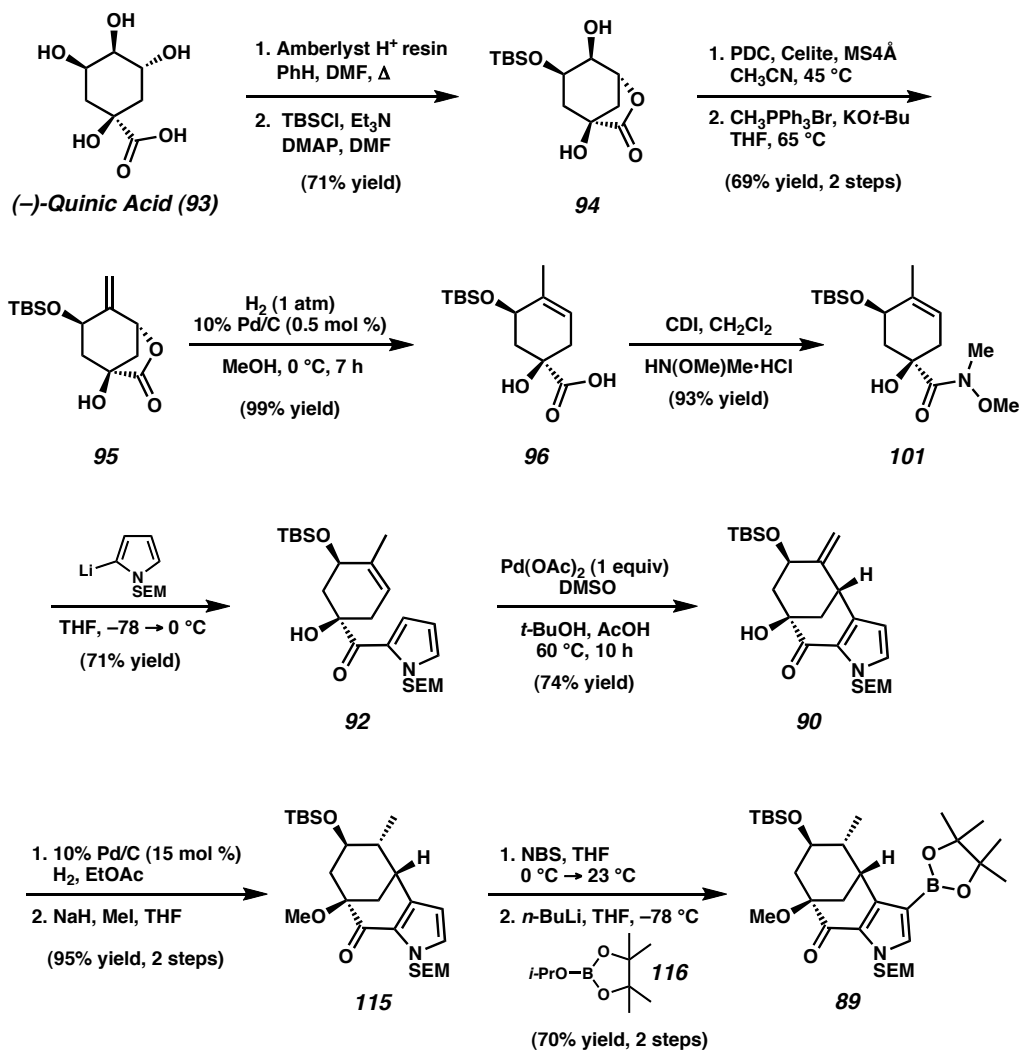
- (58) Complete deuterium incorporation was observed at the internal allylic positions by  $^1\text{H}$  and  $^2\text{H}$  NMR (See Scheme 3.4.4). Although nearly complete deuterium incorporation was observed at the exocyclic methyl group, this may only be occurring after initial reductive isomerization. See reference 59.
- (59) Control experiments demonstrate that the deuterium incorporation at the exocyclic methyl group can happen after the reductive isomerization has occurred. The stereochemistry of the deuterium in **136** was elucidated by  $^1\text{H}$  NMR homonuclear decoupling and NOESY-1D experiments.
- (60) Conducting this experiment in the presence of **95** did not lead to consumption of **137**.
- (61) Few examples of heterogeneous Pd/C-mediated allylic substitution have been reported, see: (a) Bergbreiter, D. E.; Chen, B. *J. Chem. Soc., Chem. Commun.* **1983** 1238–1239. (b) Felpin, F.-X.; Landais, Y. *J. Org. Chem.* **2005**, 70, 6441–6446.

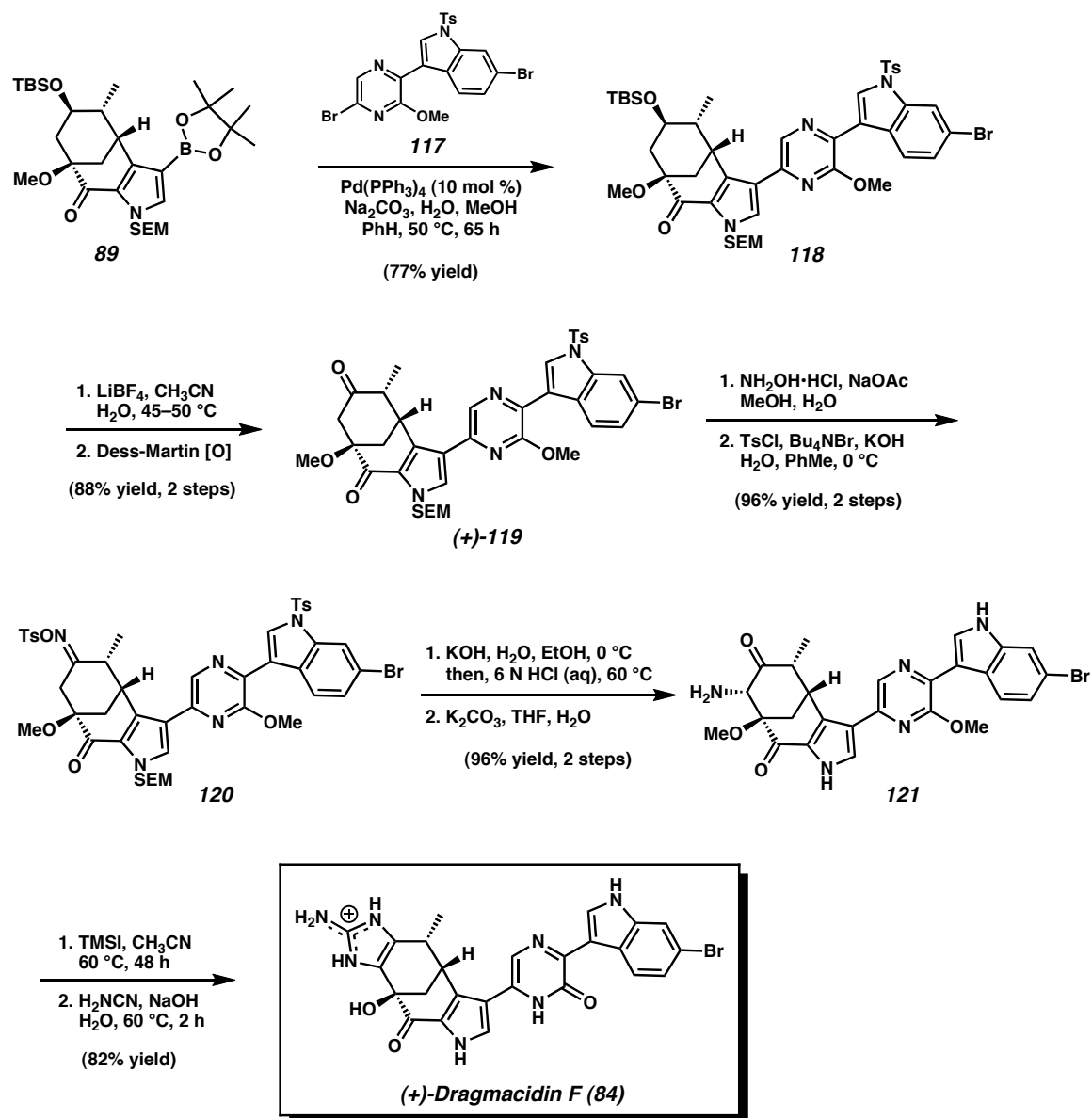
- (62) (a) Sajiki, H.; Kume, A.; Hattori, K.; Hirota, K. *Tetrahedron Lett.* **2002**, 43, 7247–7250. (b) Ishizaki, M.; Yamada, M.; Watanabe, S.-i.; Hoshino, O.; Nishitani, K.; Hayashida, M.; Tanaka, A.; Hara, H. *Tetrahedron* **2004**, 60, 7973–7981.
- (63) Simple control experiments suggest that the presence of TCNE does not prevent the direct reduction of olefins from occurring.
- (64) With the exception of **138** (entry 10), all of the compounds in Table 3.4.1 are enantiopure.
- (65) The major product in this reaction resulted from direct hydrogenation of the olefin moiety and was formed as a mixture of diastereomers.
- (66) No reductive isomerization product could be isolated from this reaction.
- (67) The absolute stereochemistry of **138** (entry 10) depicted is shown by analogy to the other products in Table 3.4.1.
- (68) The three-dimensional conformations of **97** and **142** were ascertained by  $^1\text{H}$  NMR homonuclear decoupling and NOESY-1D experiments.
- (69) Brown, J. M. *Angew. Chem., Int. Ed. Engl.* **1987**, 26, 190–203.

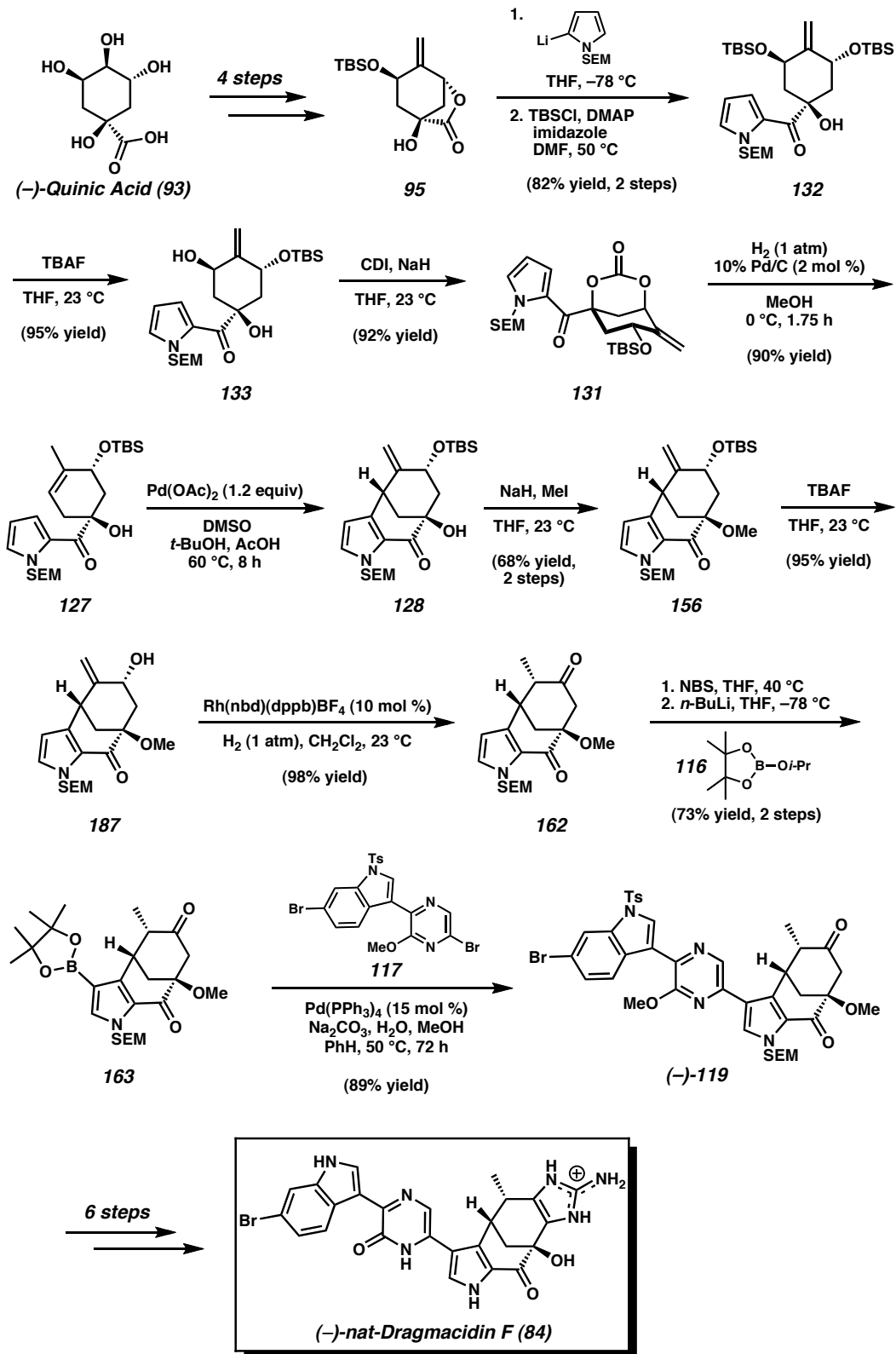
- (70) Bergens, S. H.; Bosnich, B. *J. Am. Chem. Soc.* **1991**, *113*, 958–967.
- (71) Xiao, W. *Huaxue Shiji* **1992**, *14*, 363–366.
- (72) Bailey, D. M.; Johnson, R. E. *J. Med. Chem.* **1973**, *16*, 1300–1302.
- (73) The synthesis of allylic alcohol **111** is described on p. 96.
- (74) (a) Liu, Y.; Gribble, G. W. *J. Nat. Prod.* **2002**, *65*, 748–749. (b) Bergman, J.; Venemalm, L. *J. Org. Chem.* **1992**, *57*, 2495–2497.
- (75) Claridge, T. D. W. in *High-Resolution NMR Techniques in Organic Chemistry*; Pergamon: Amsterdam, 1999; pp. 320–326.
- (76) The synthesis of acetoxycarbonate **144** is described on p. 96.
- (77) Tsuji, J.; Minami, I.; Shimizu, I. *Synthesis* **1986**, 623–627.

## **APPENDIX TWO**

### **Synthetic Summary for (+)- and (-)-Dragmacidin F (84)**

Scheme A2.1 The synthesis of boronic ester **89**

Scheme A2.2 The synthesis of (+)-dragmacidin F (**84**)

Scheme A2.3 The synthesis of (–)-dragmacidin F (**84**)



### **APPENDIX THREE**

#### **Spectra Relevant to Chapter Three:**

#### **The Total Syntheses of (+)- and (–)-Dragmacidin F**

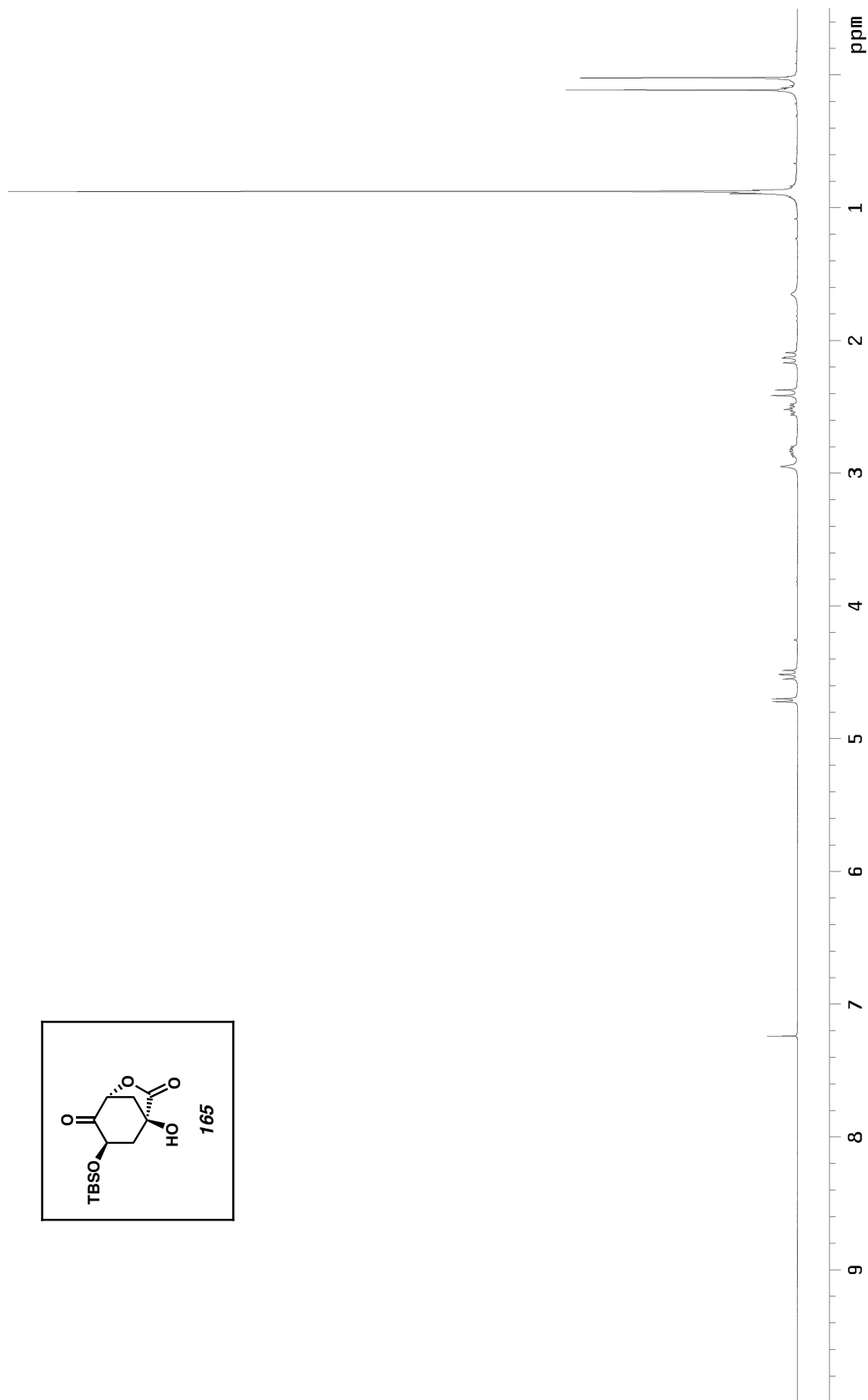
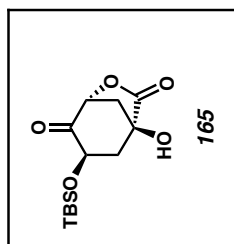
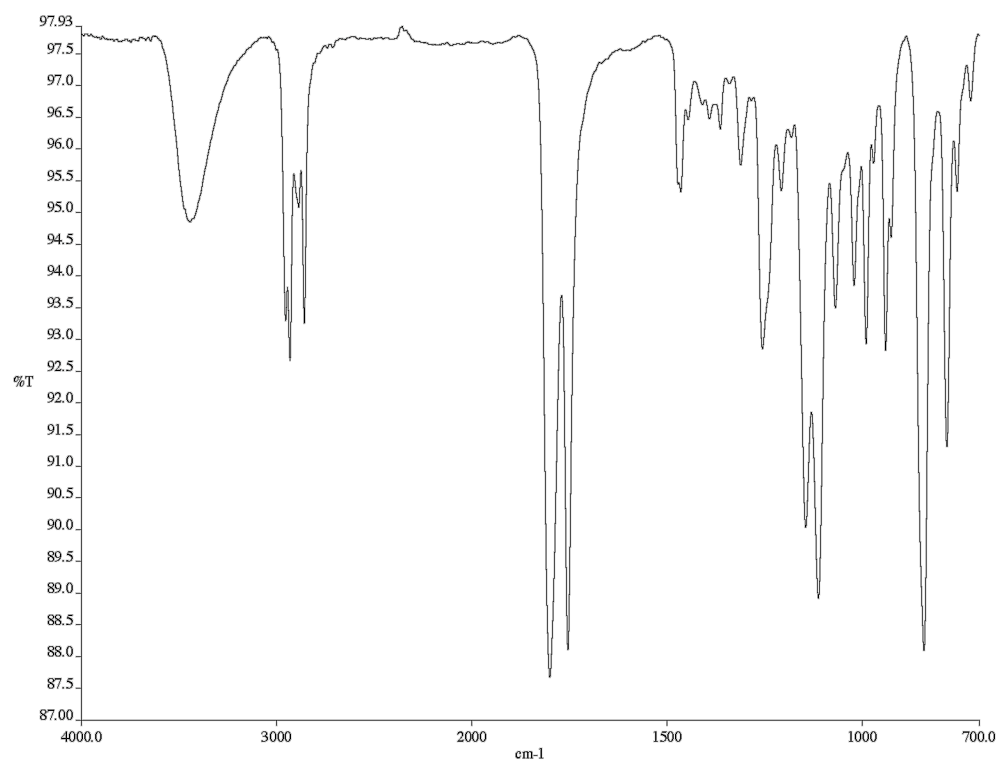
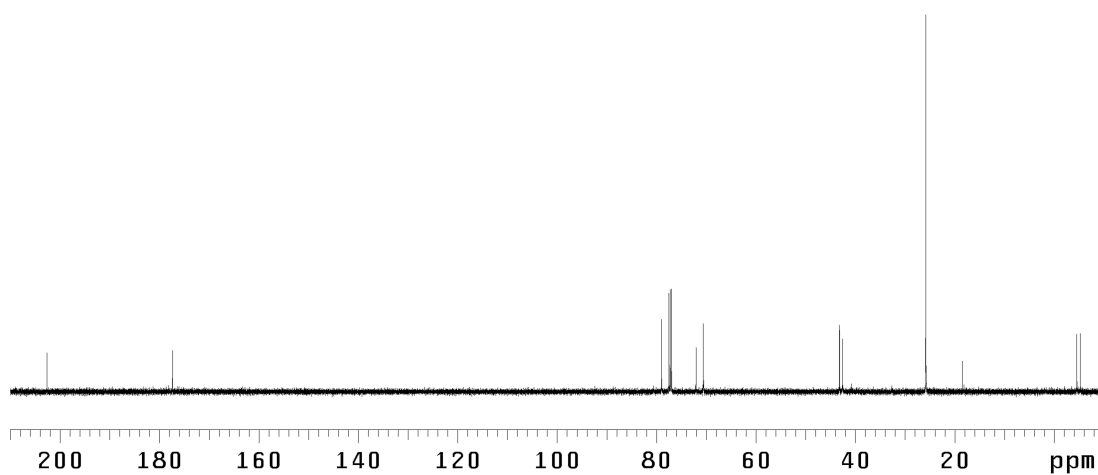


Figure A3.1  $^1\text{H}$  NMR (300 MHz,  $\text{CDCl}_3$ ) of compound **165**



*Figure A3.2* Infrared spectrum (thin film/NaCl) of compound **165**



*Figure A3.3* <sup>13</sup>C NMR (75 MHz, CDCl<sub>3</sub>) of compound **165**

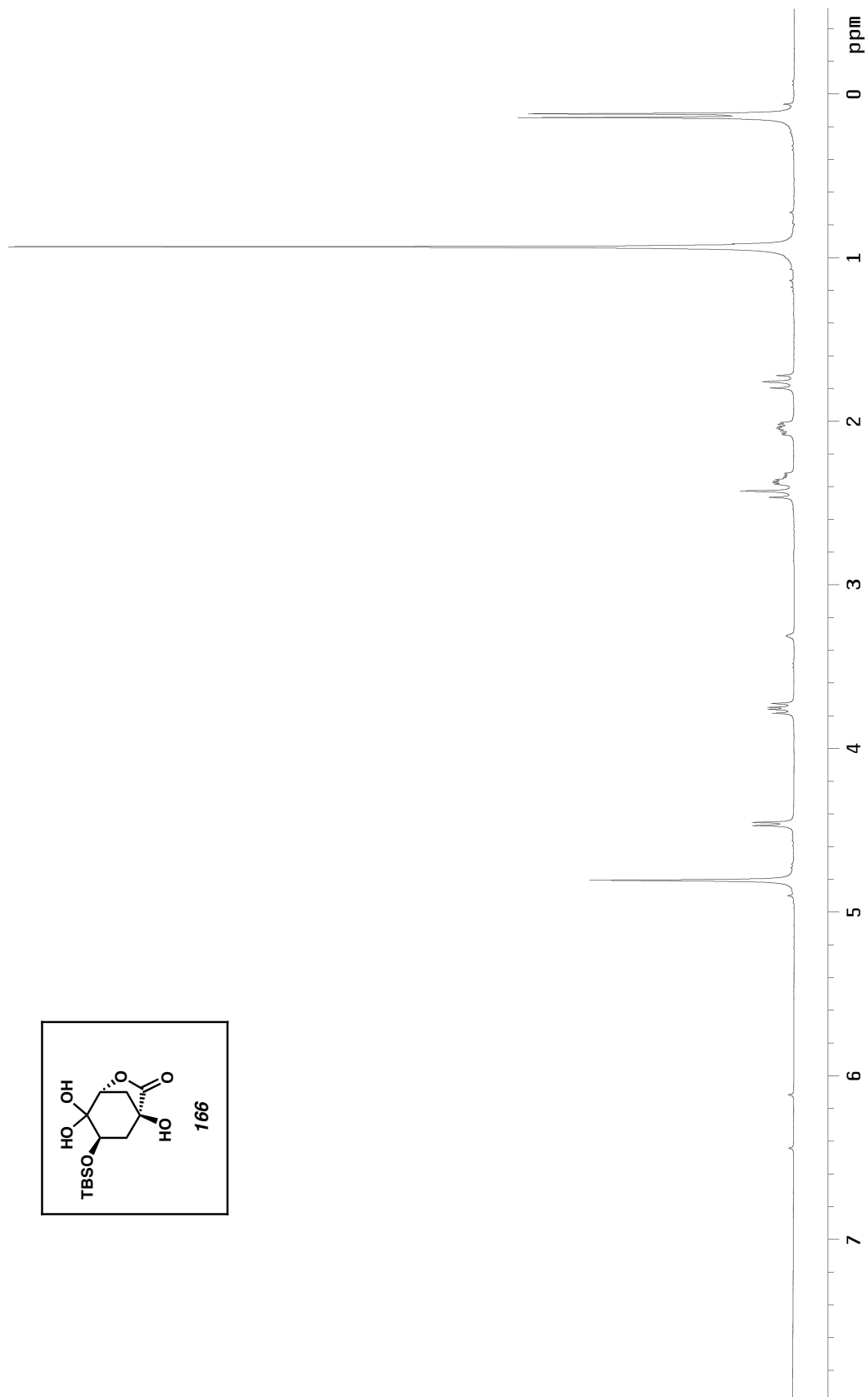


Figure A3.4  $^1\text{H}$  NMR (300 MHz,  $\text{CD}_3\text{OD}$ ) of compound **166**

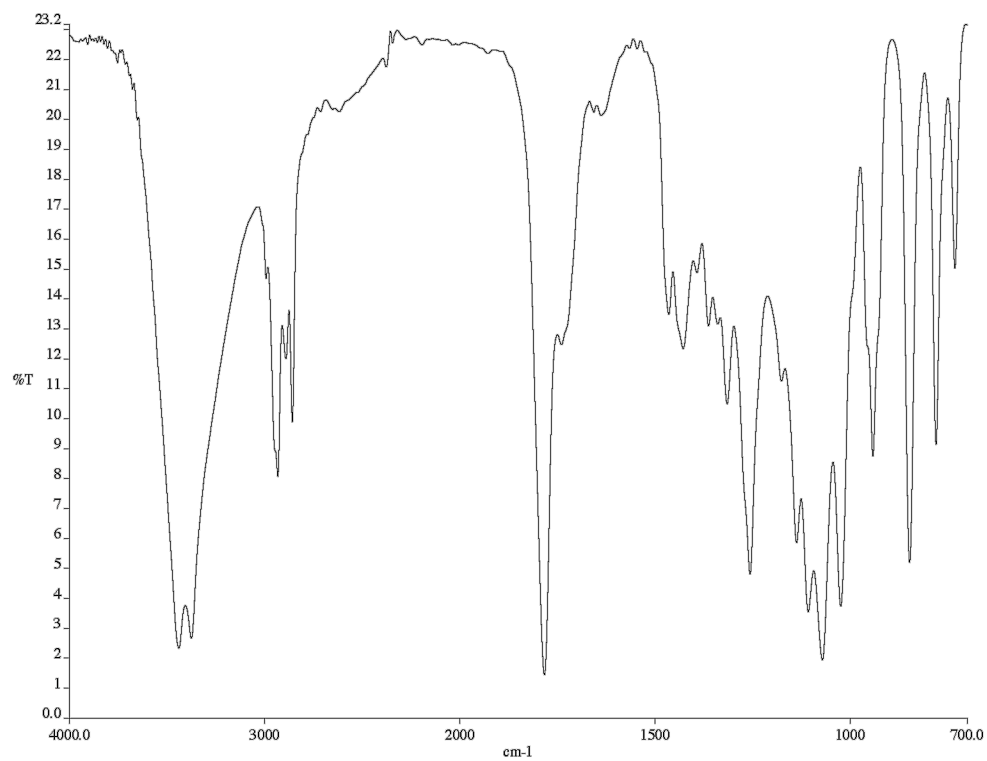


Figure A3.5 Infrared spectrum (KBr pellet) of compound **166**

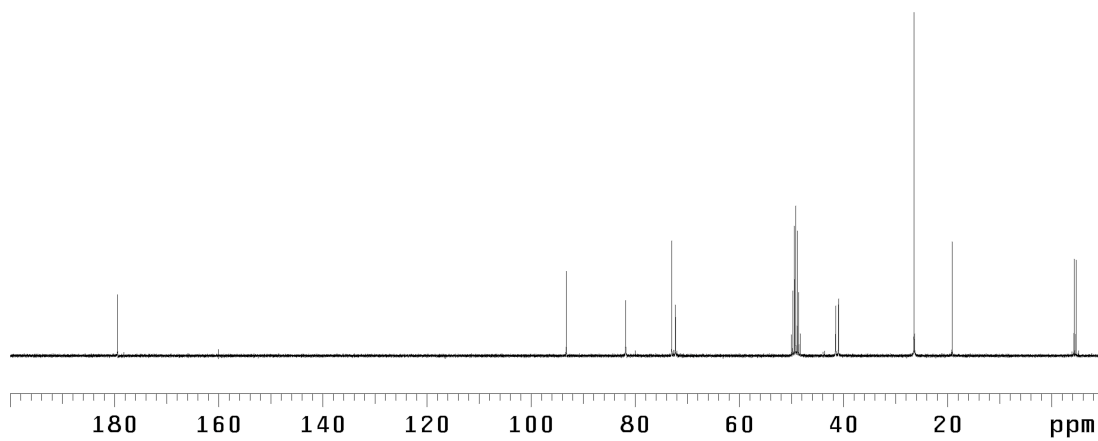


Figure A3.6  $^{13}\text{C}$  NMR (75 MHz,  $\text{CD}_3\text{OD}$ ) of compound **166**

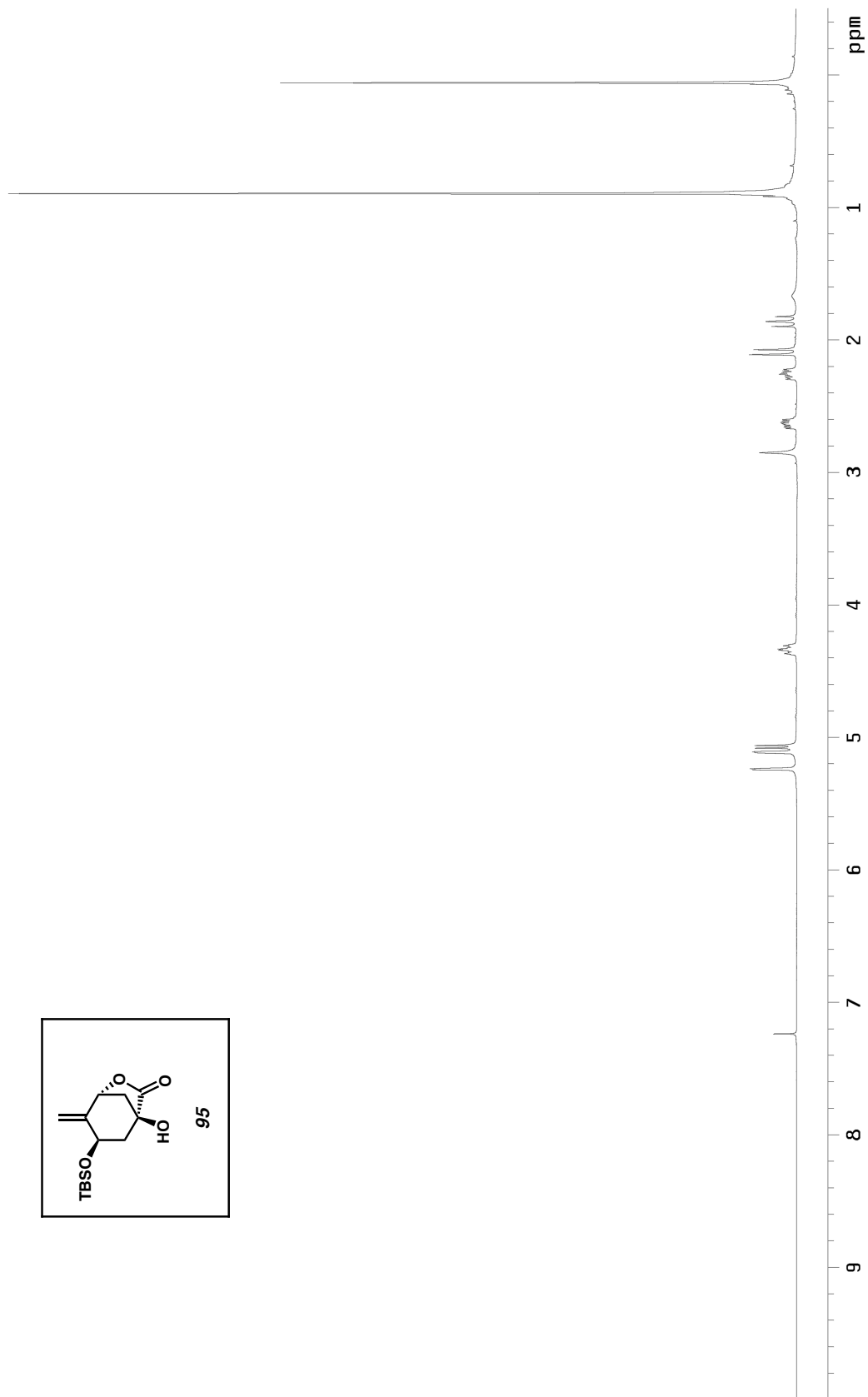
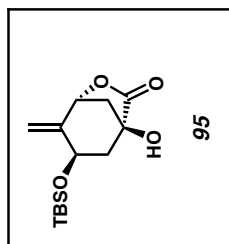
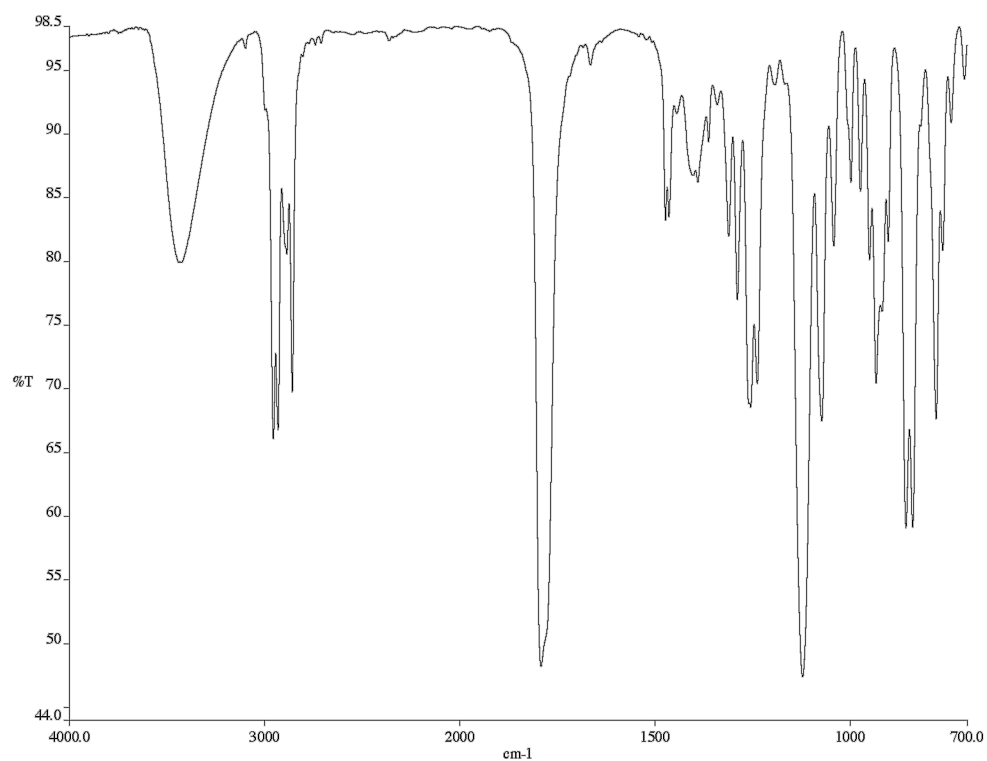
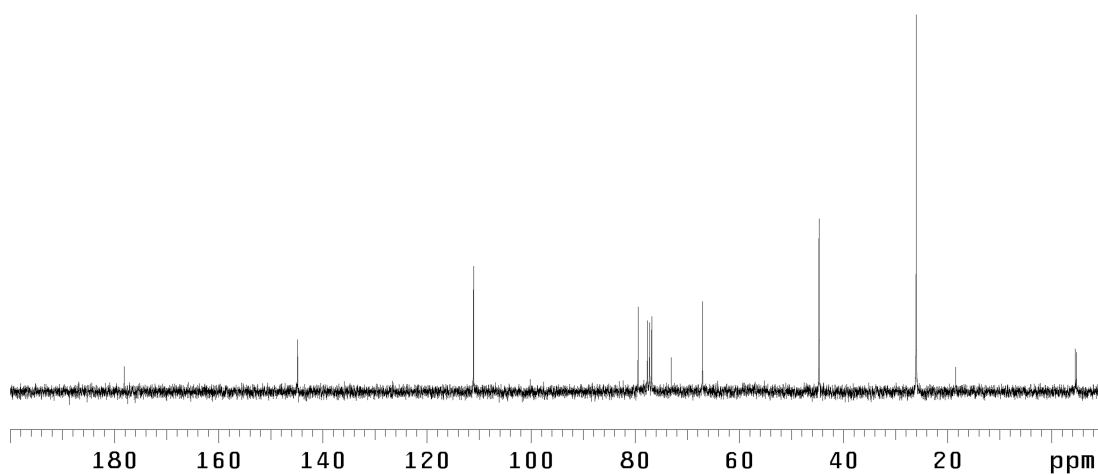


Figure A3.7  $^1\text{H}$  NMR (300 MHz,  $\text{CDCl}_3$ ) of compound **95**



*Figure A3.8* Infrared spectrum (thin film/NaCl) of compound **95**



*Figure A3.9* <sup>13</sup>C NMR (75 MHz, CDCl<sub>3</sub>) of compound **95**

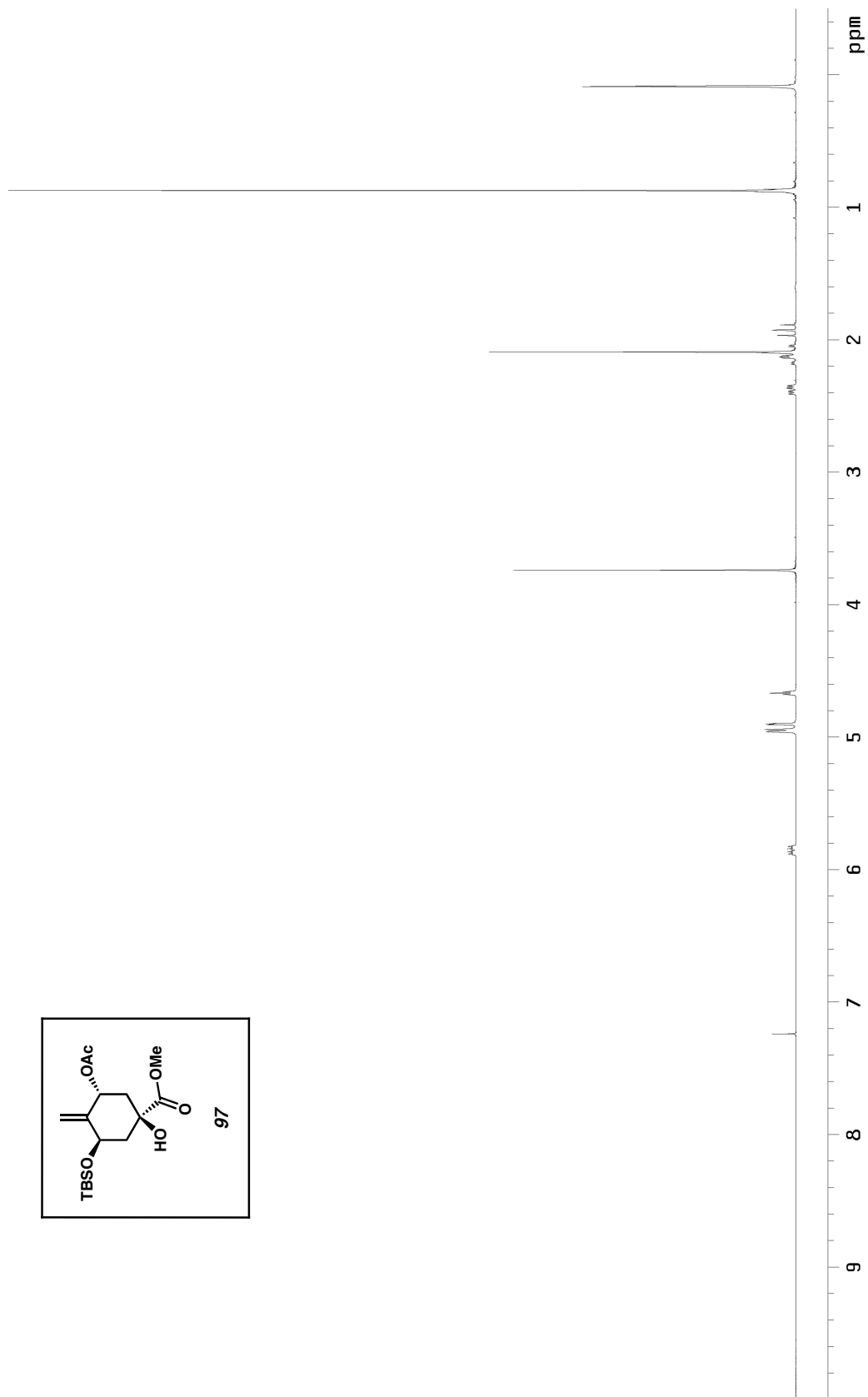


Figure A3.10  $^1\text{H}$  NMR (300 MHz,  $\text{CDCl}_3$ ) of compound **97**



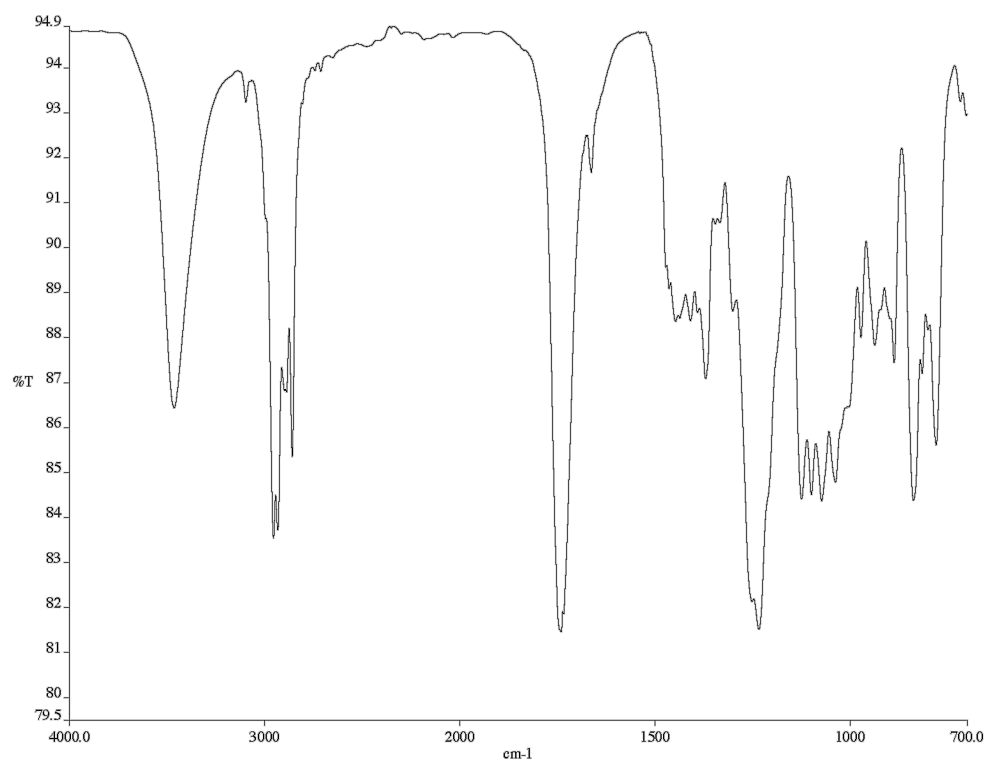


Figure A3.11 Infrared spectrum (thin film/NaCl) of compound **97**

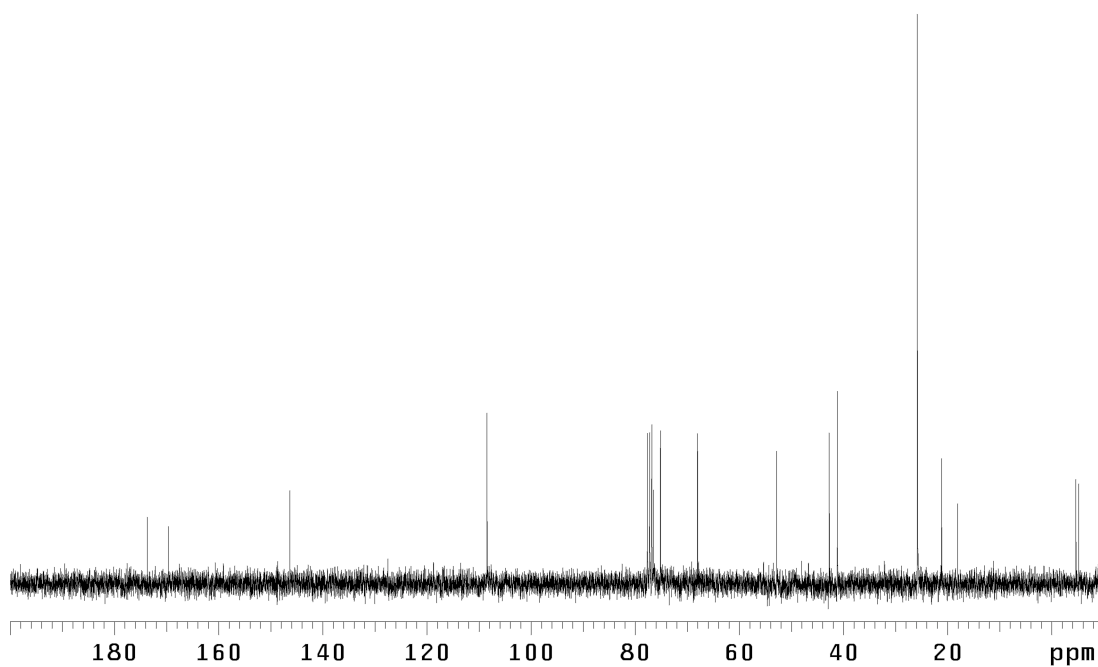


Figure A3.12 <sup>13</sup>C NMR (75 MHz, CDCl<sub>3</sub>) of compound **97**

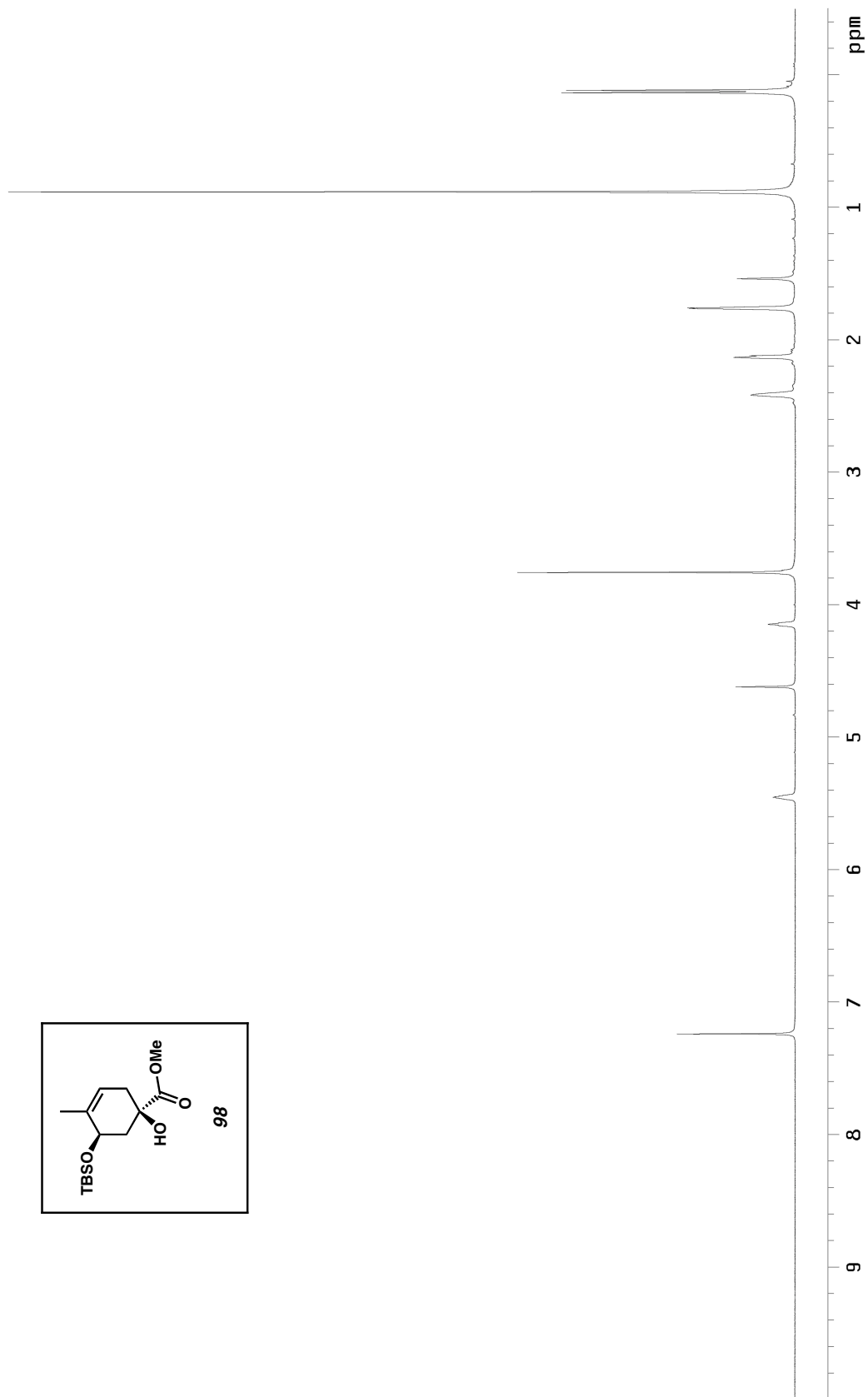


Figure A3.13  $^1\text{H}$  NMR (300 MHz,  $\text{CDCl}_3$ ) of compound **98**

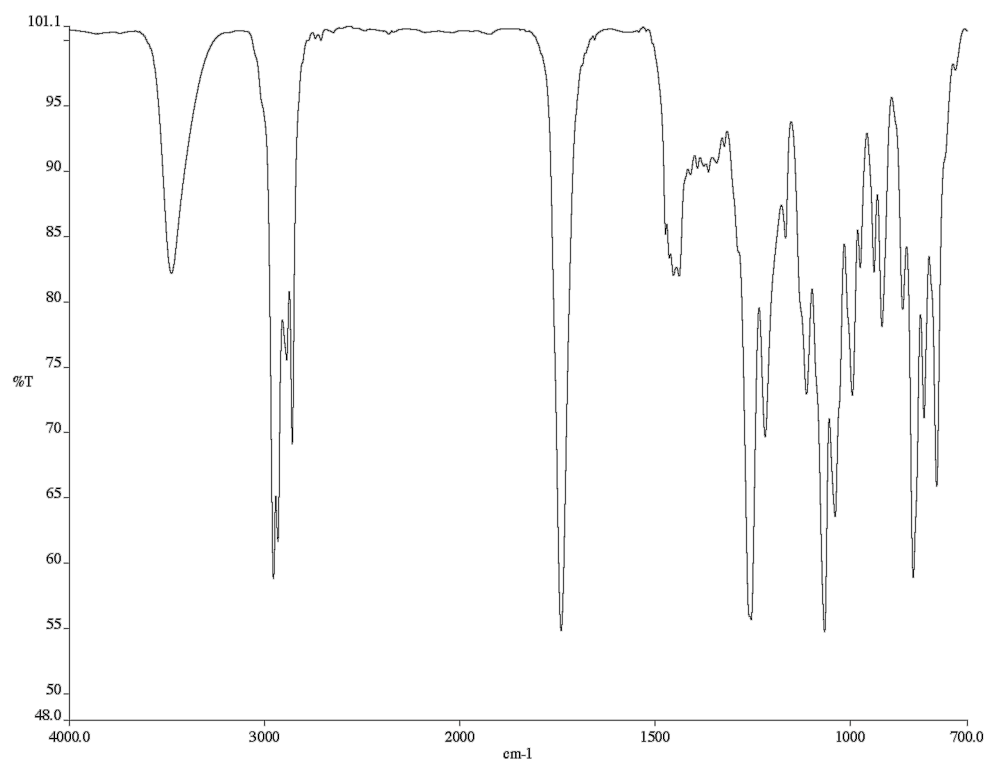


Figure A3.14 Infrared spectrum (thin film/NaCl) of compound **98**

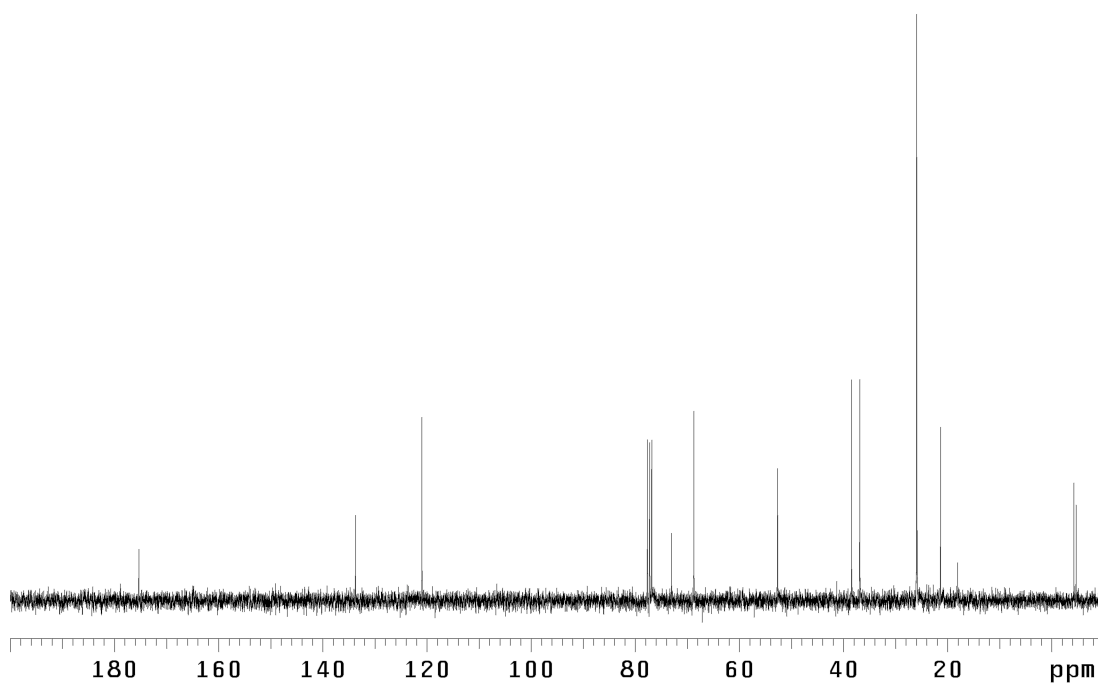


Figure A3.15 <sup>13</sup>C NMR (75 MHz, CDCl<sub>3</sub>) of compound **98**

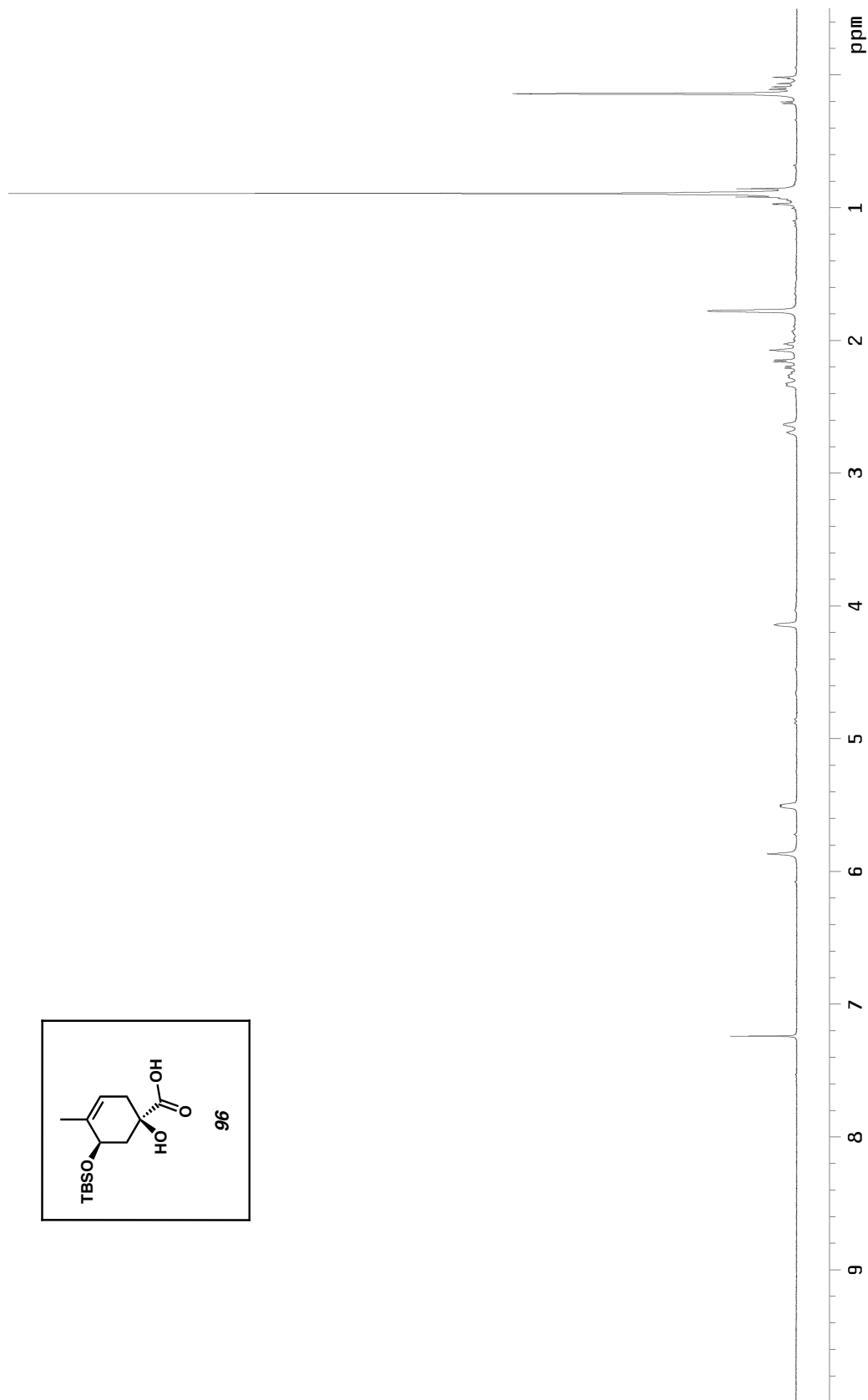
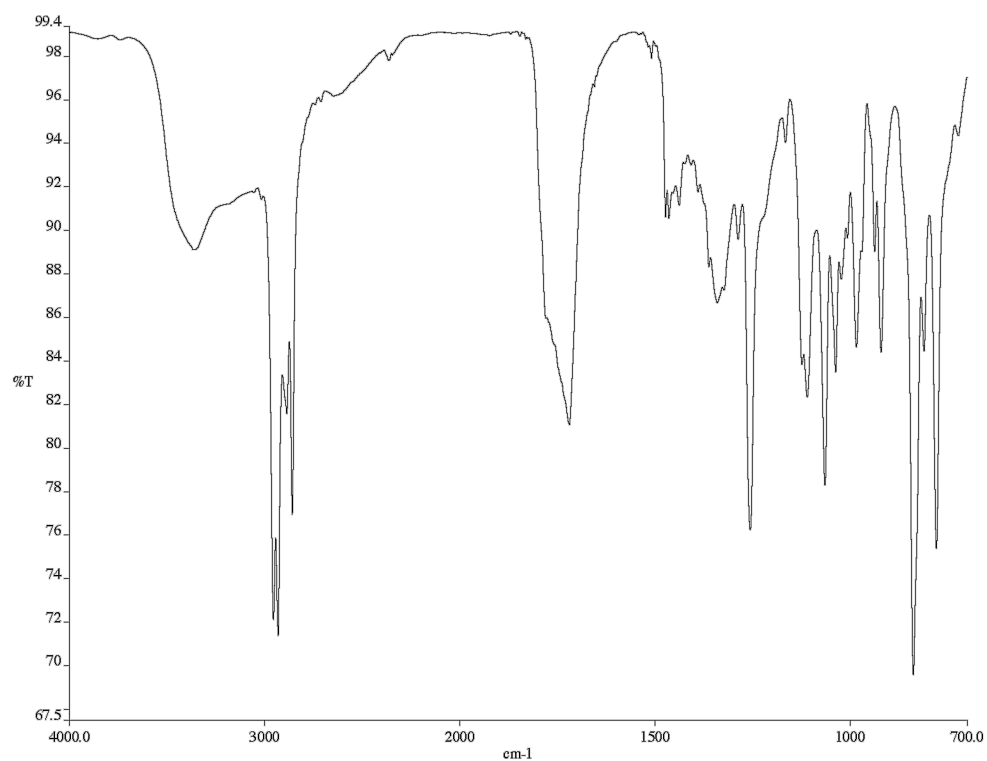
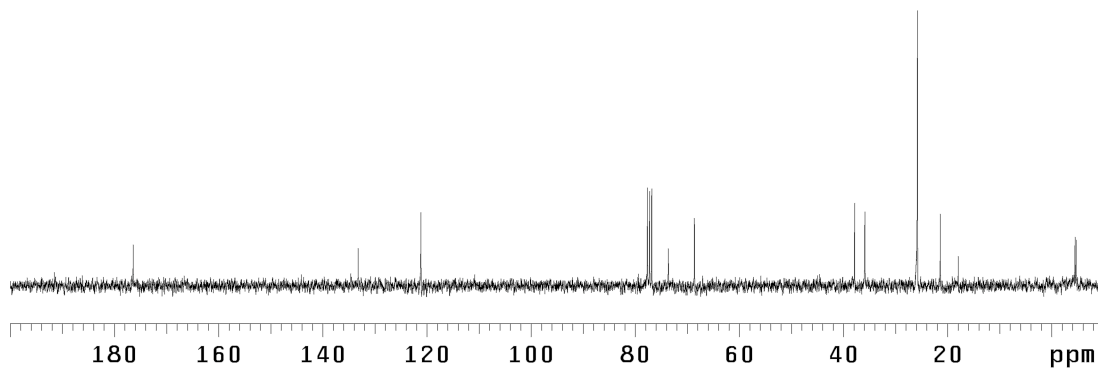


Figure A3.16  $^1\text{H}$  NMR (300 MHz,  $\text{CDCl}_3$ ) of compound **96**



*Figure A3.17* Infrared spectrum (thin film/NaCl) of compound **96**



*Figure A3.18* <sup>13</sup>C NMR (75 MHz, CDCl<sub>3</sub>) of compound **96**

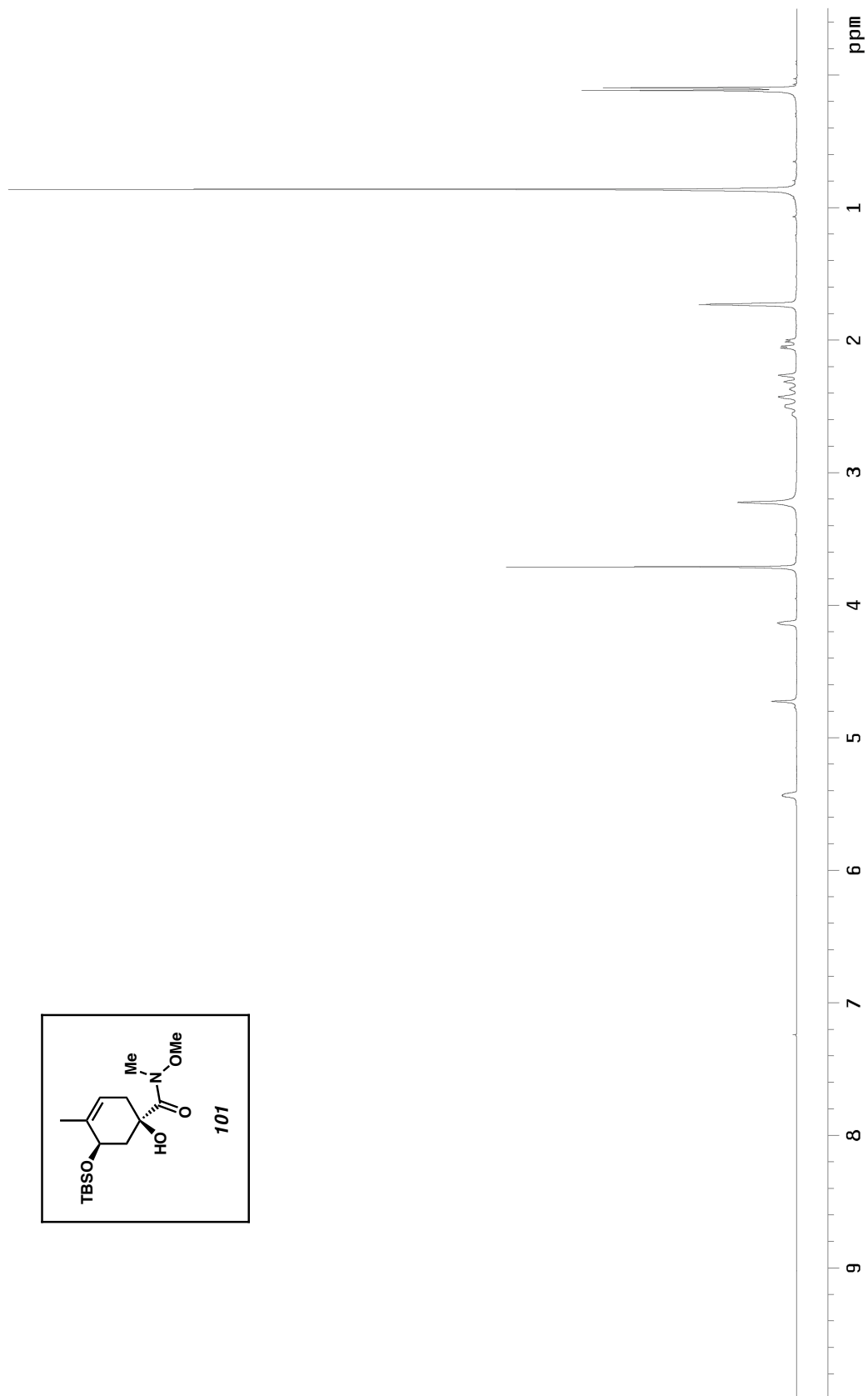
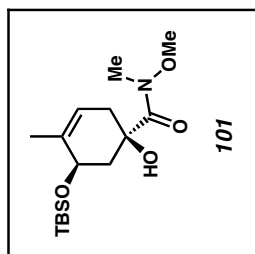
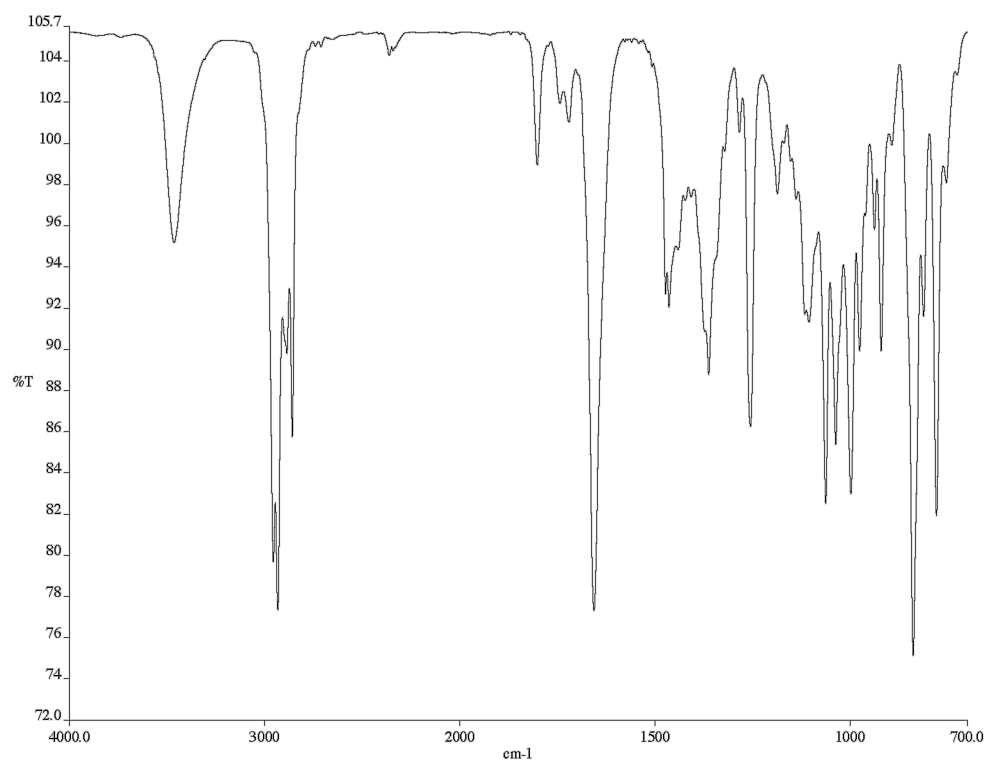
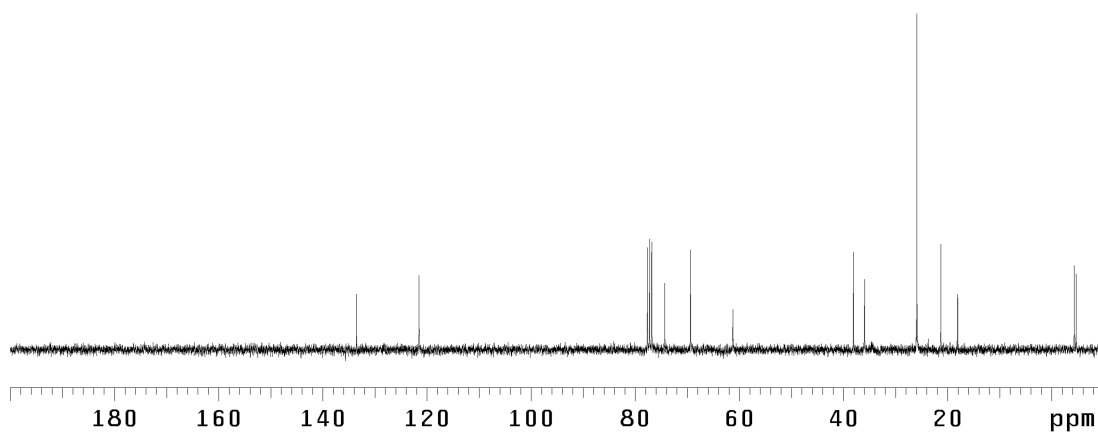


Figure A3.19  $^1\text{H}$  NMR (300 MHz,  $\text{CDCl}_3$ ) of compound **101**



*Figure A3.20* Infrared spectrum (thin film/NaCl) of compound **101**



*Figure A3.21* <sup>13</sup>C NMR (75 MHz, CDCl<sub>3</sub>) of compound **101**

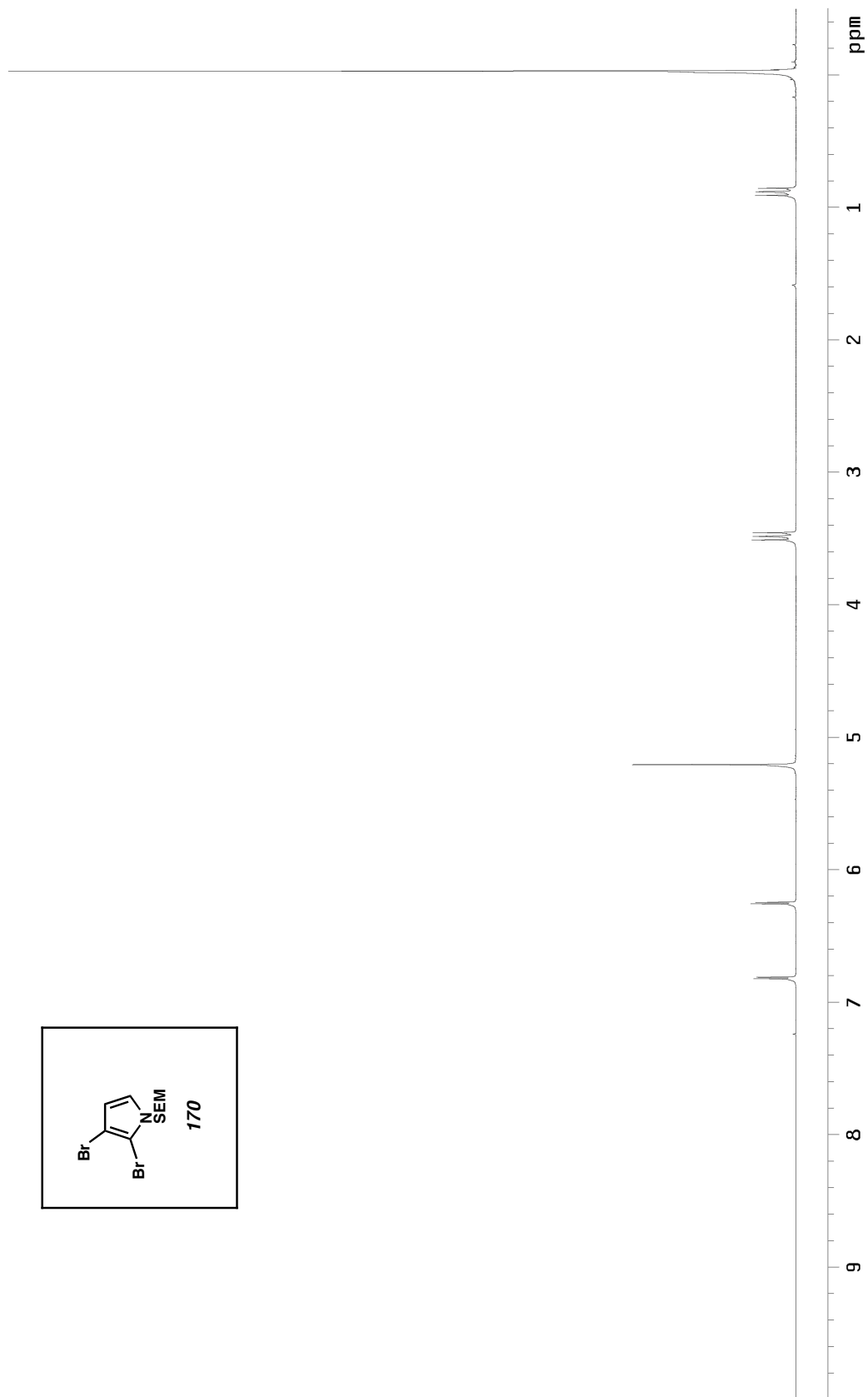
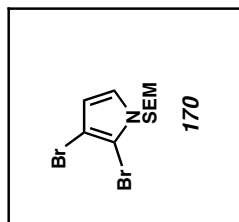


Figure A3.22  $^1\text{H}$  NMR (300 MHz,  $\text{CDCl}_3$ ) of compound **170**



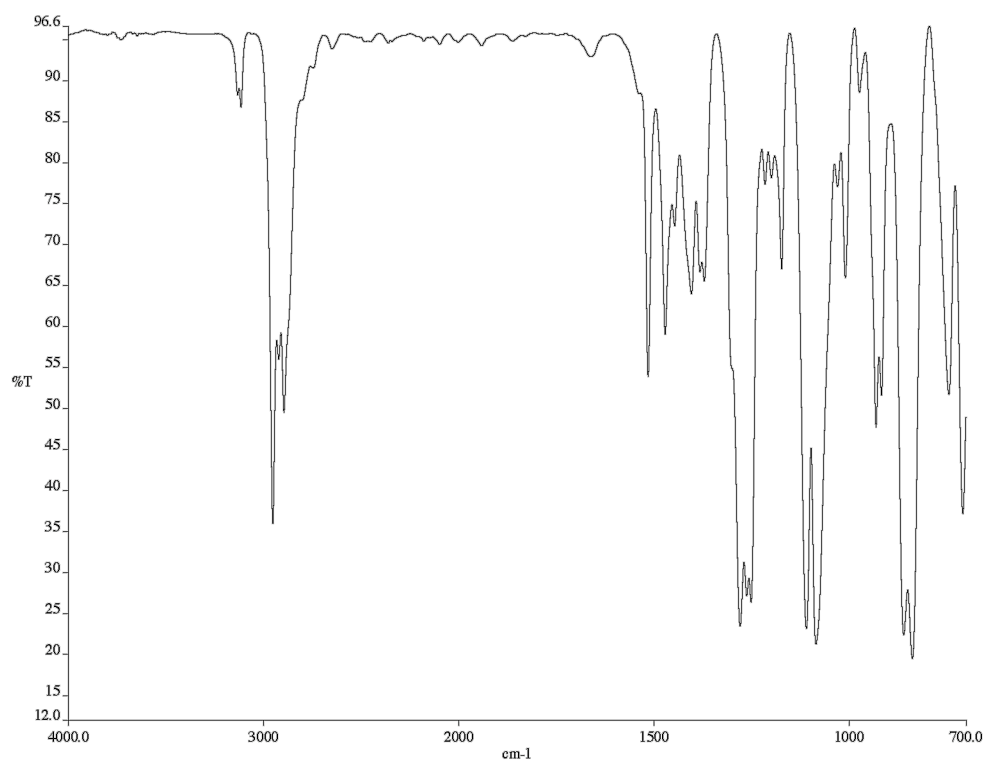


Figure A3.23 Infrared spectrum (thin film/NaCl) of compound **170**

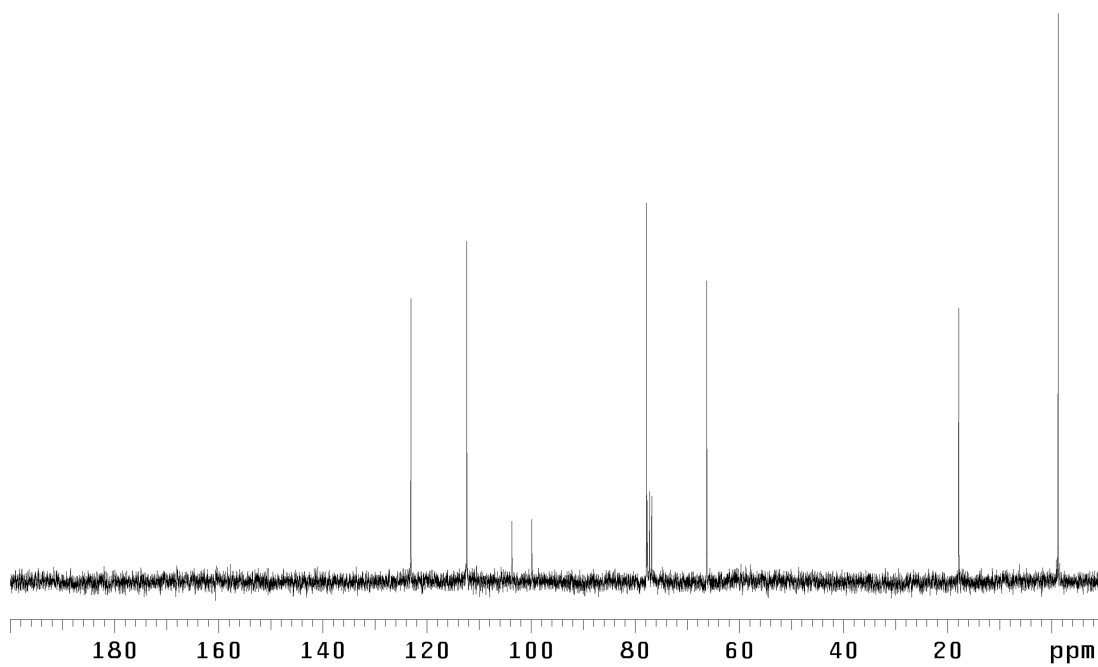


Figure A3.24 <sup>13</sup>C NMR (75 MHz, CDCl<sub>3</sub>) of compound **170**

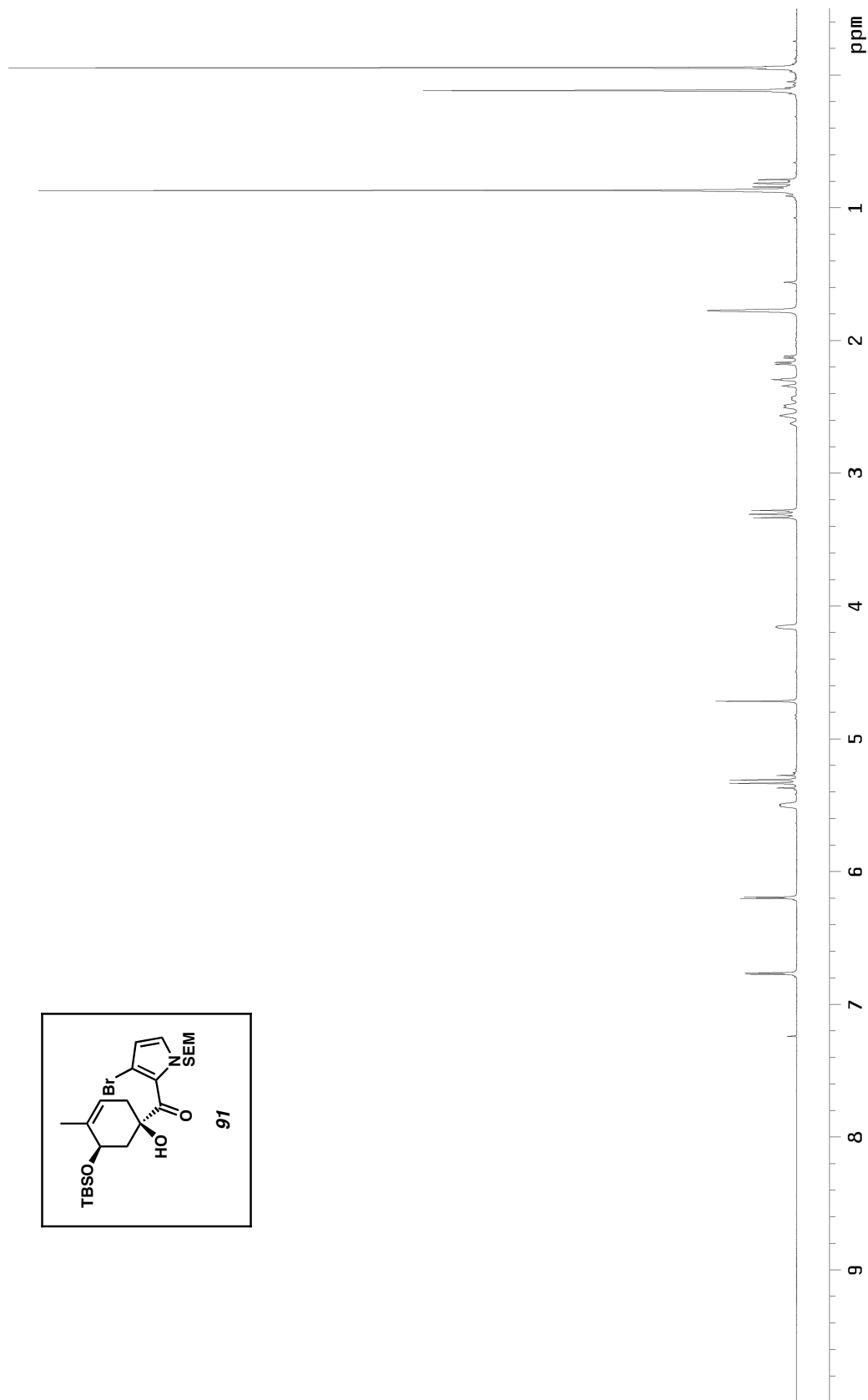


Figure A3.25  $^1\text{H}$  NMR (300 MHz,  $\text{CDCl}_3$ ) of compound **91**

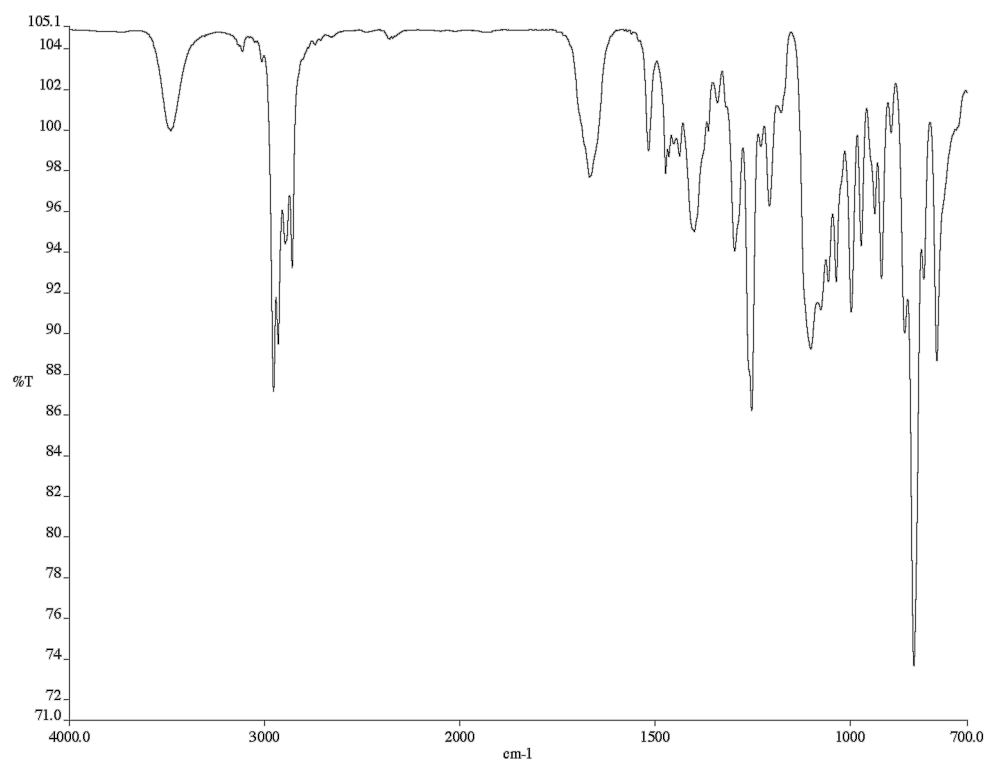


Figure A3.26 Infrared spectrum (thin film/NaCl) of compound **91**

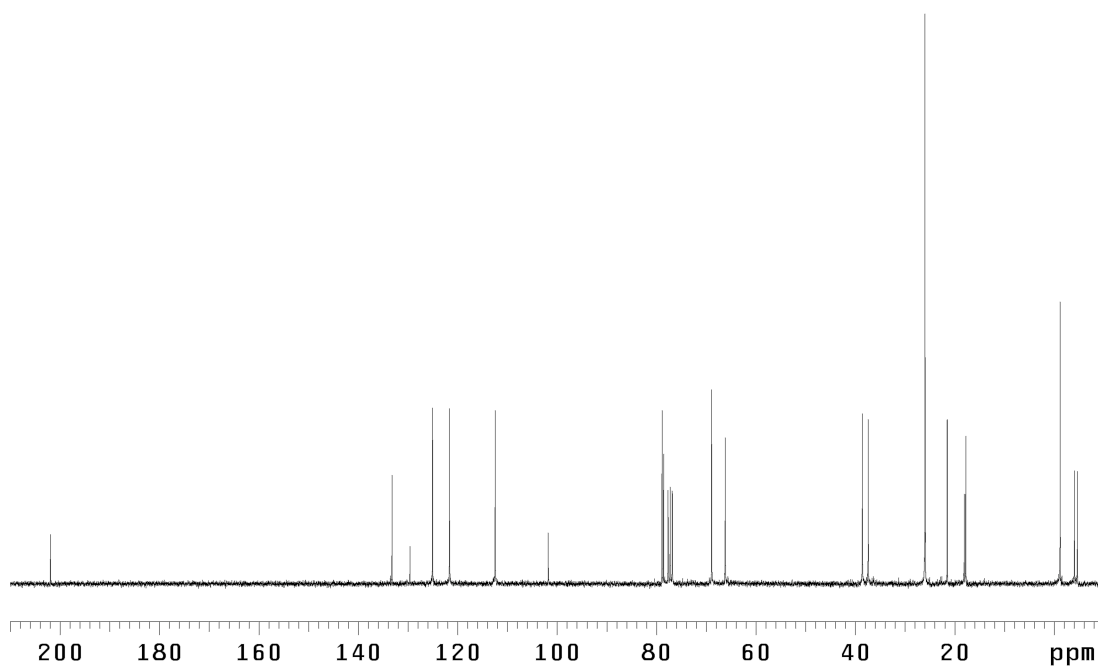
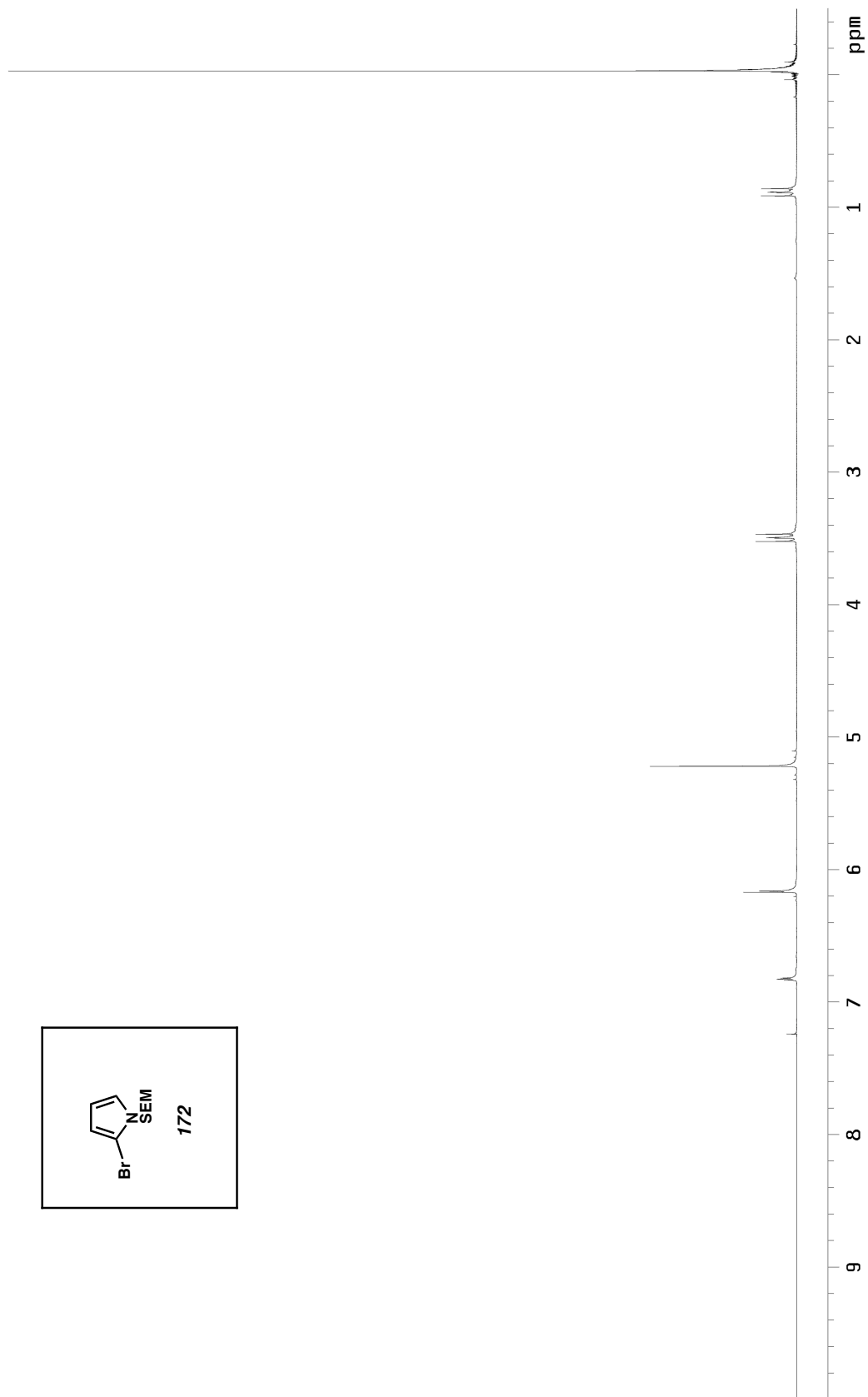
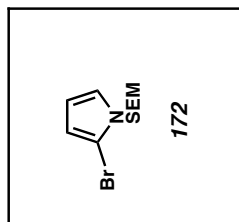


Figure A3.27 <sup>13</sup>C NMR (75 MHz, CDCl<sub>3</sub>) of compound **91**



*Figure A3.28*  $^1\text{H}$  NMR (300 MHz,  $\text{CDCl}_3$ ) of compound **172**

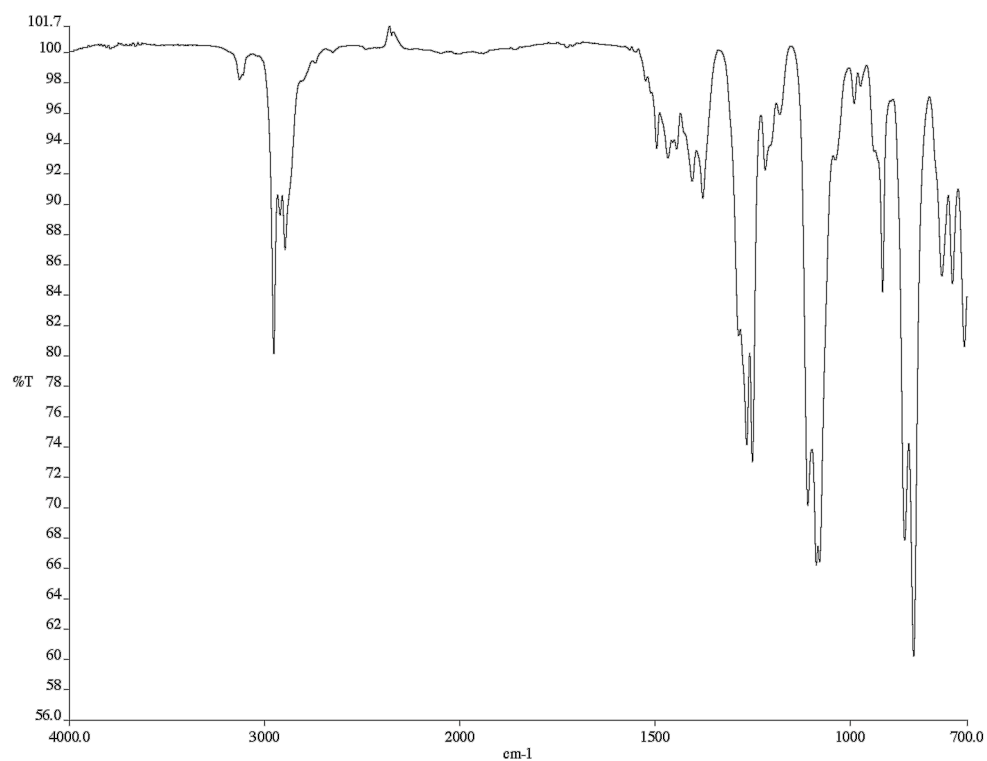


Figure A3.29 Infrared spectrum (thin film/NaCl) of compound **172**

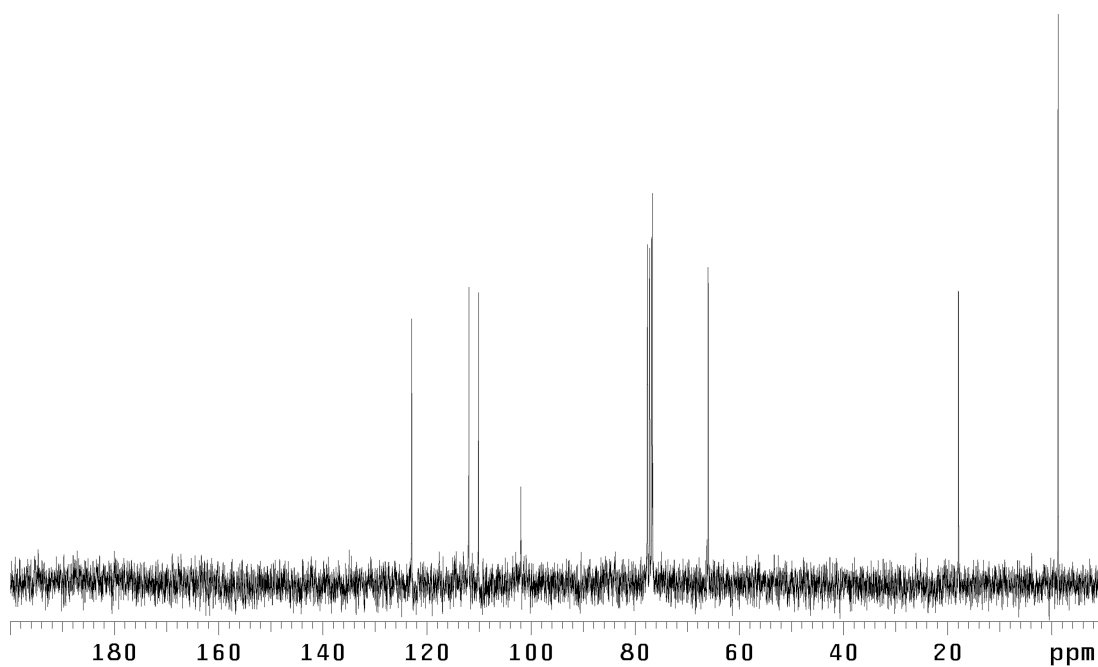


Figure A3.30 <sup>13</sup>C NMR (75 MHz, CDCl<sub>3</sub>) of compound **172**

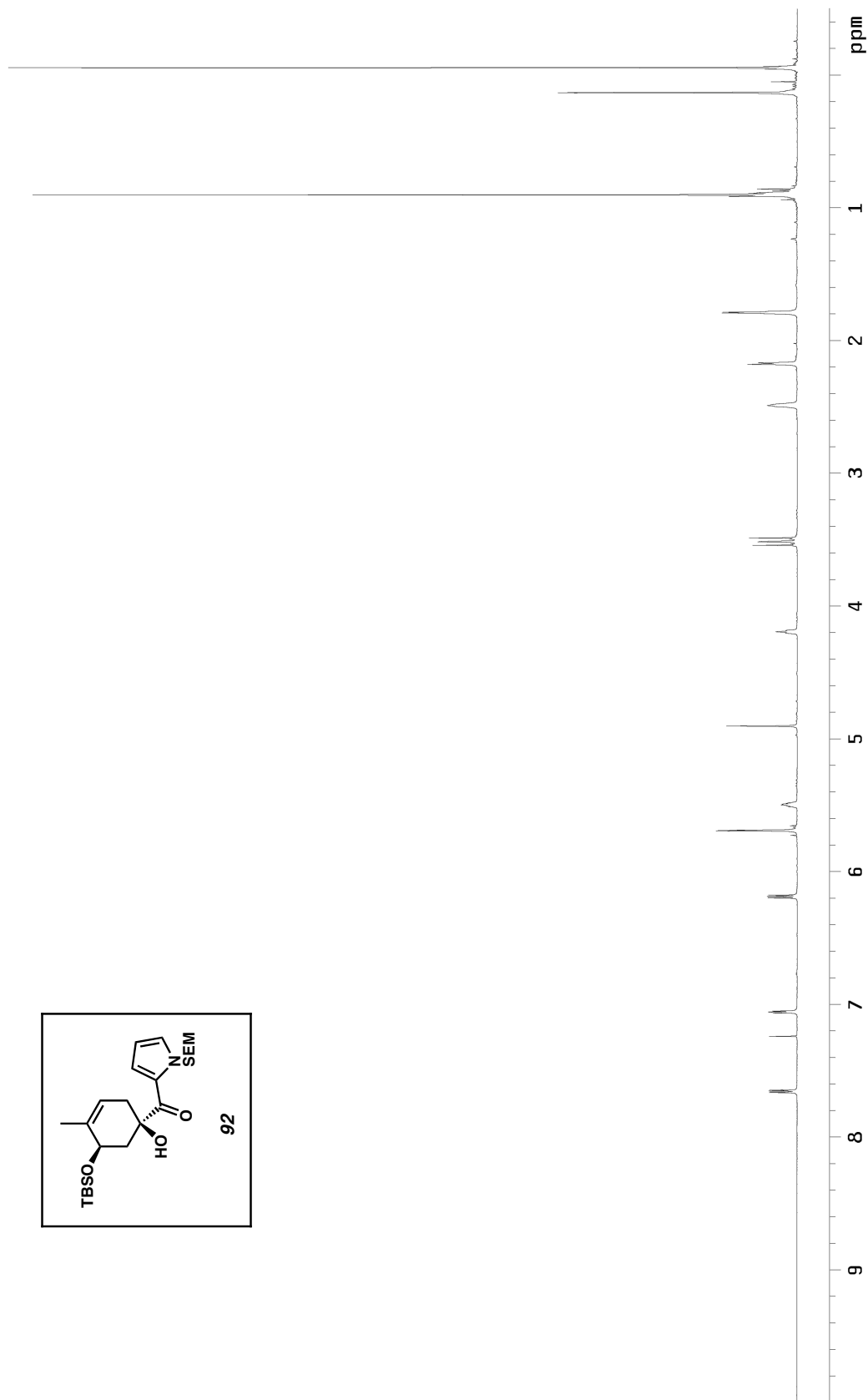
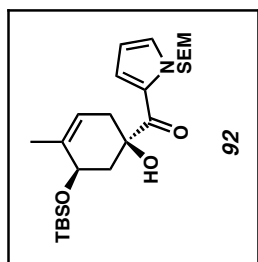
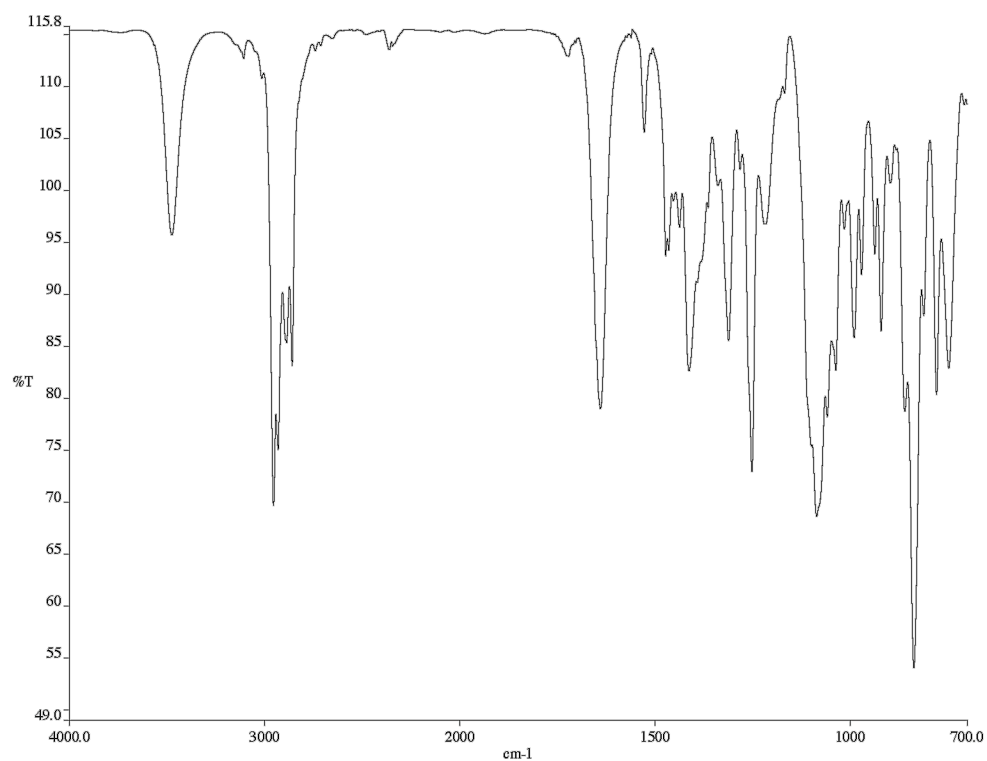
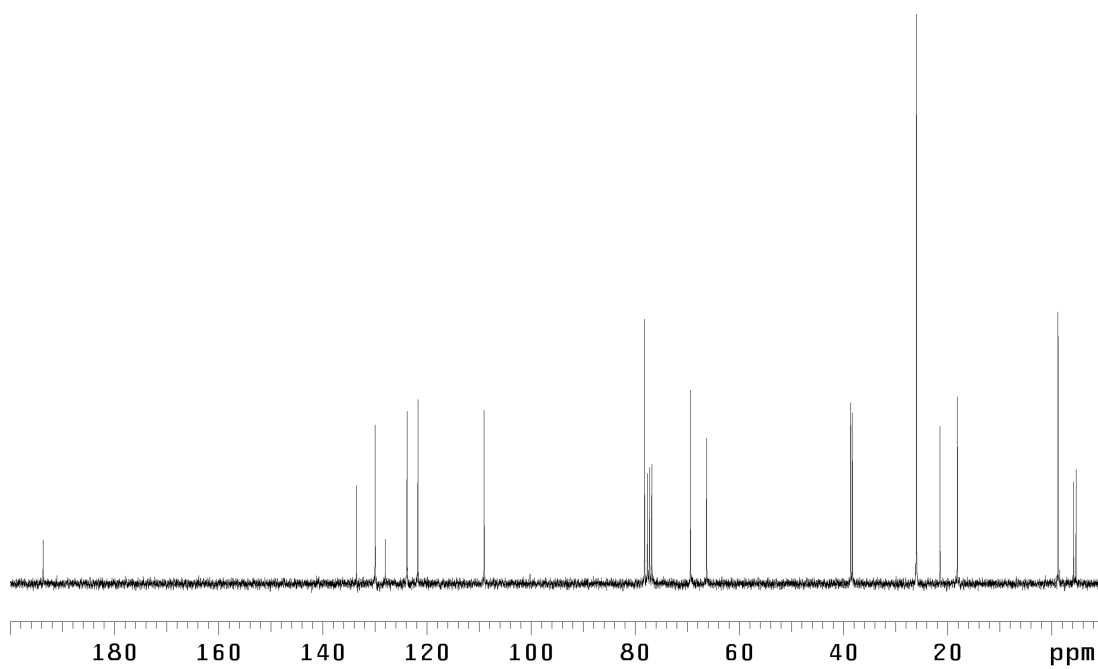


Figure A3.31 <sup>1</sup>H NMR (300 MHz, CDCl<sub>3</sub>) of compound **92**





*Figure A3.32* Infrared spectrum (thin film/NaCl) of compound **92**



*Figure A3.33* <sup>13</sup>C NMR (75 MHz, CDCl<sub>3</sub>) of compound **92**

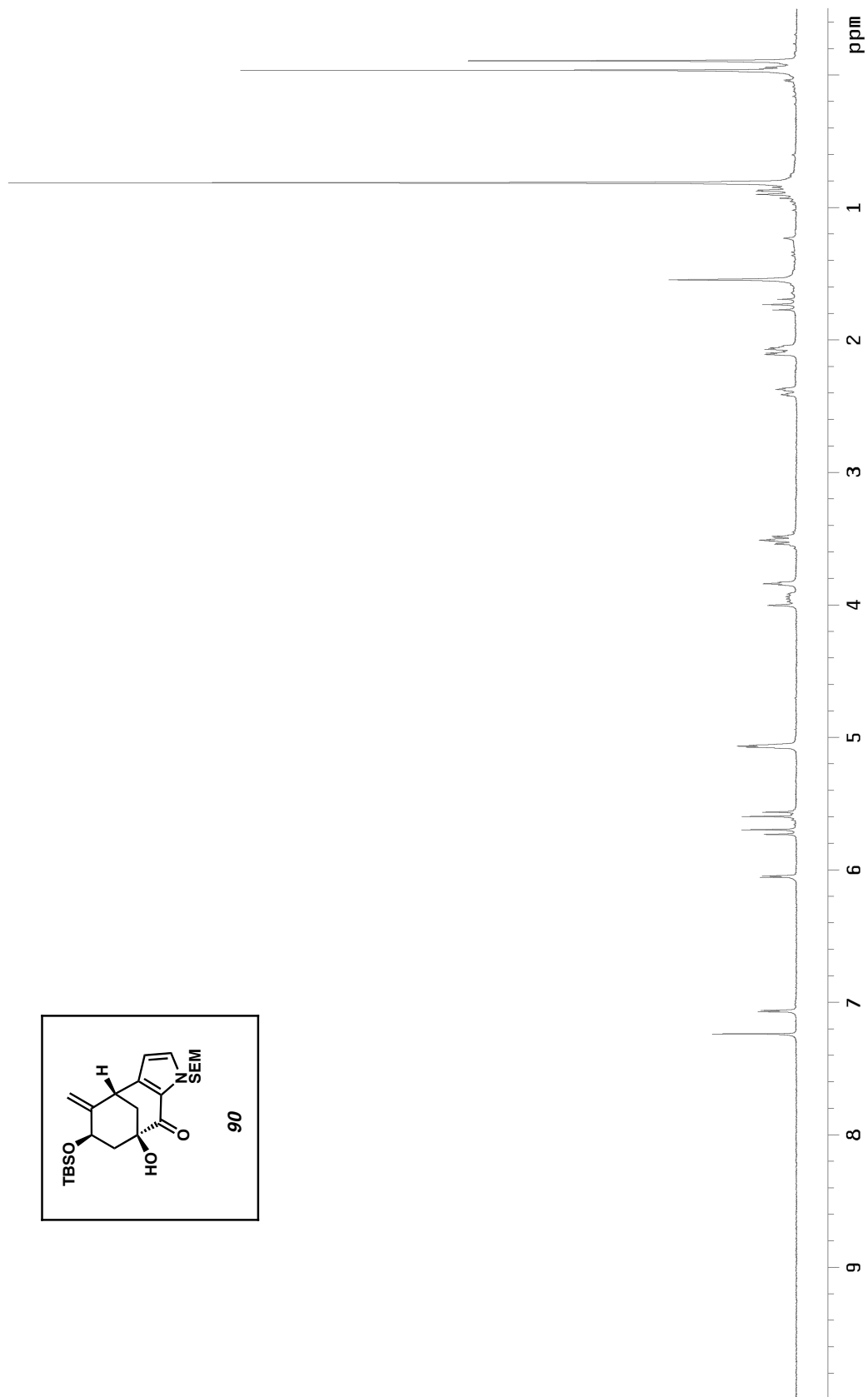
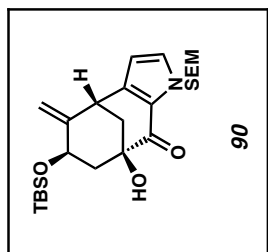


Figure A3.34  $^1\text{H}$  NMR (300 MHz,  $\text{CDCl}_3$ ) of compound **90**



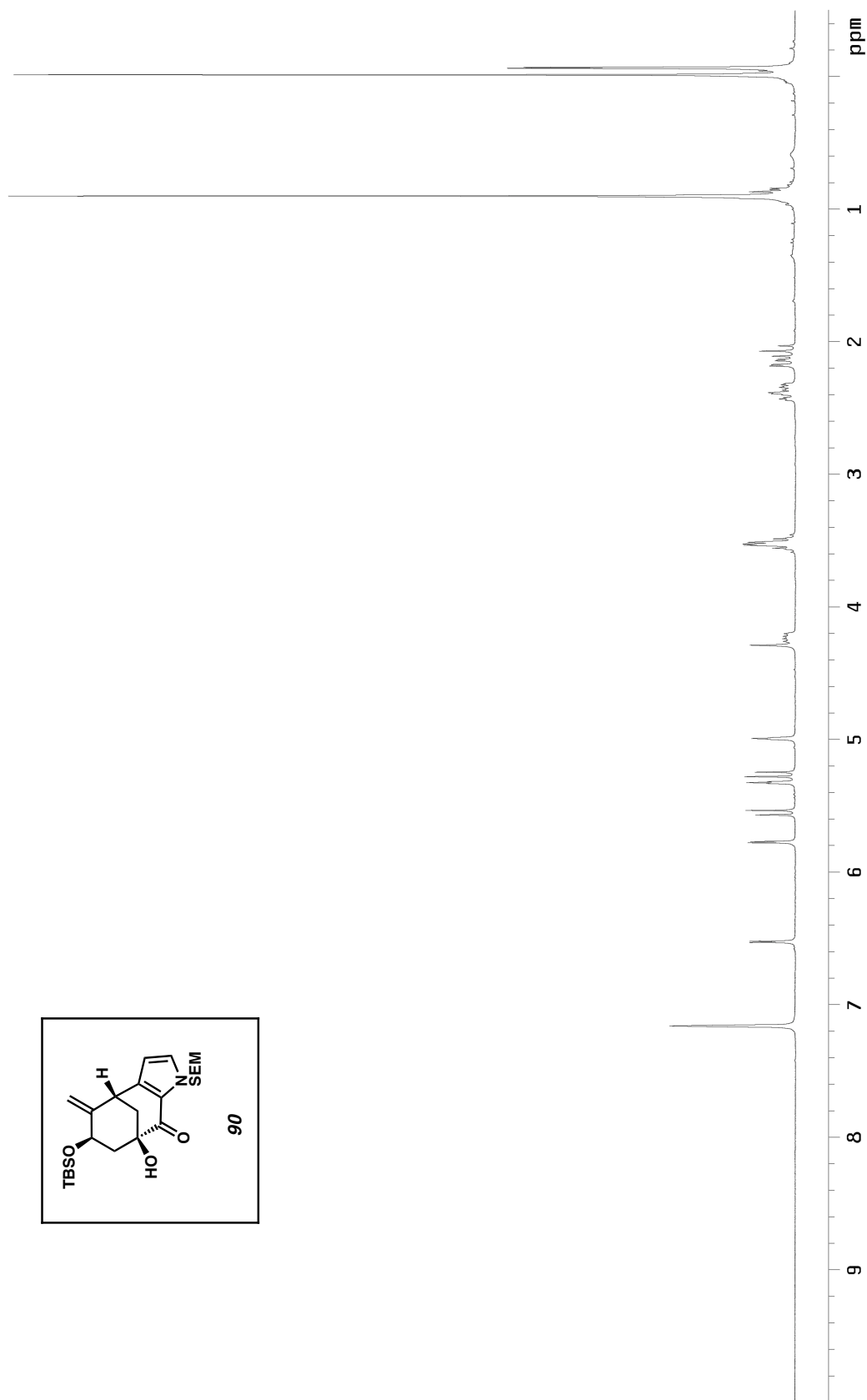
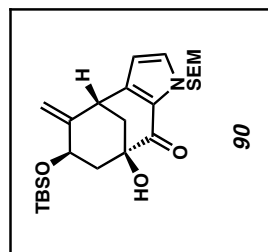


Figure A3.35  $^1\text{H}$  NMR (300 MHz,  $\text{C}_6\text{D}_6$ ) of compound **90**

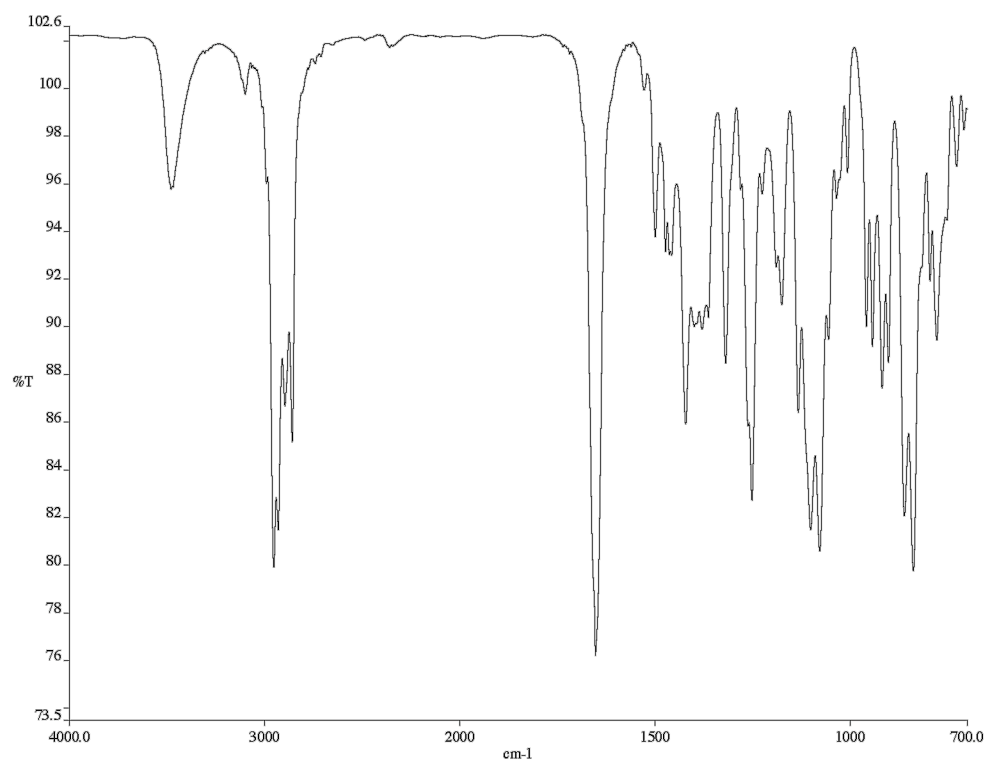


Figure A3.36 Infrared spectrum (thin film/NaCl) of compound **90**

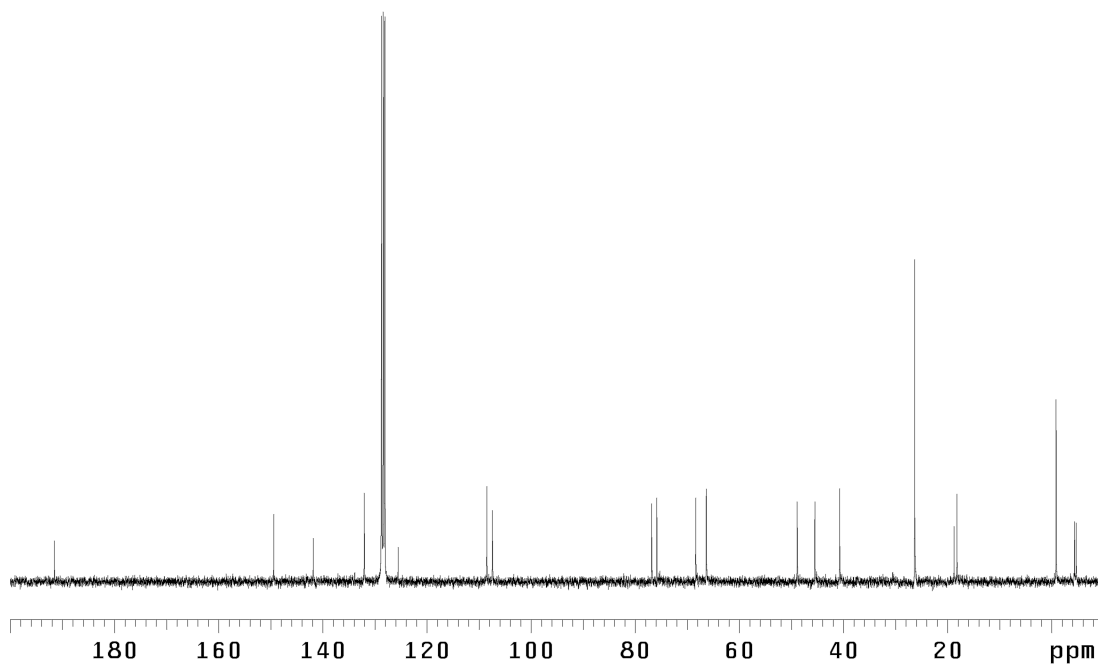


Figure A3.37 <sup>13</sup>C NMR (75 MHz, C<sub>6</sub>D<sub>6</sub>) of compound **90**

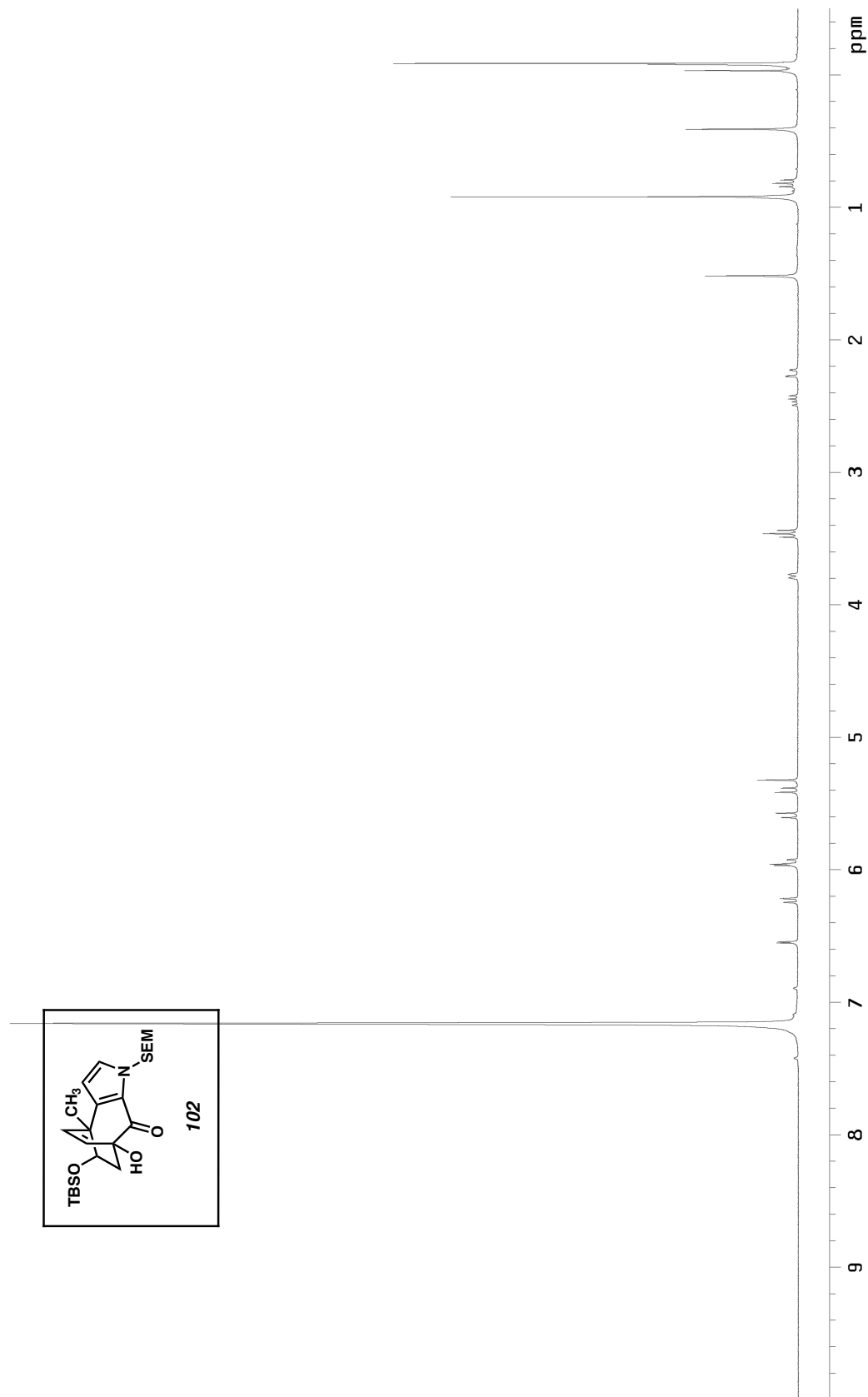


Figure A3.38  $^1\text{H}$  NMR (300 MHz,  $\text{C}_6\text{D}_6$ ) of compound **102**

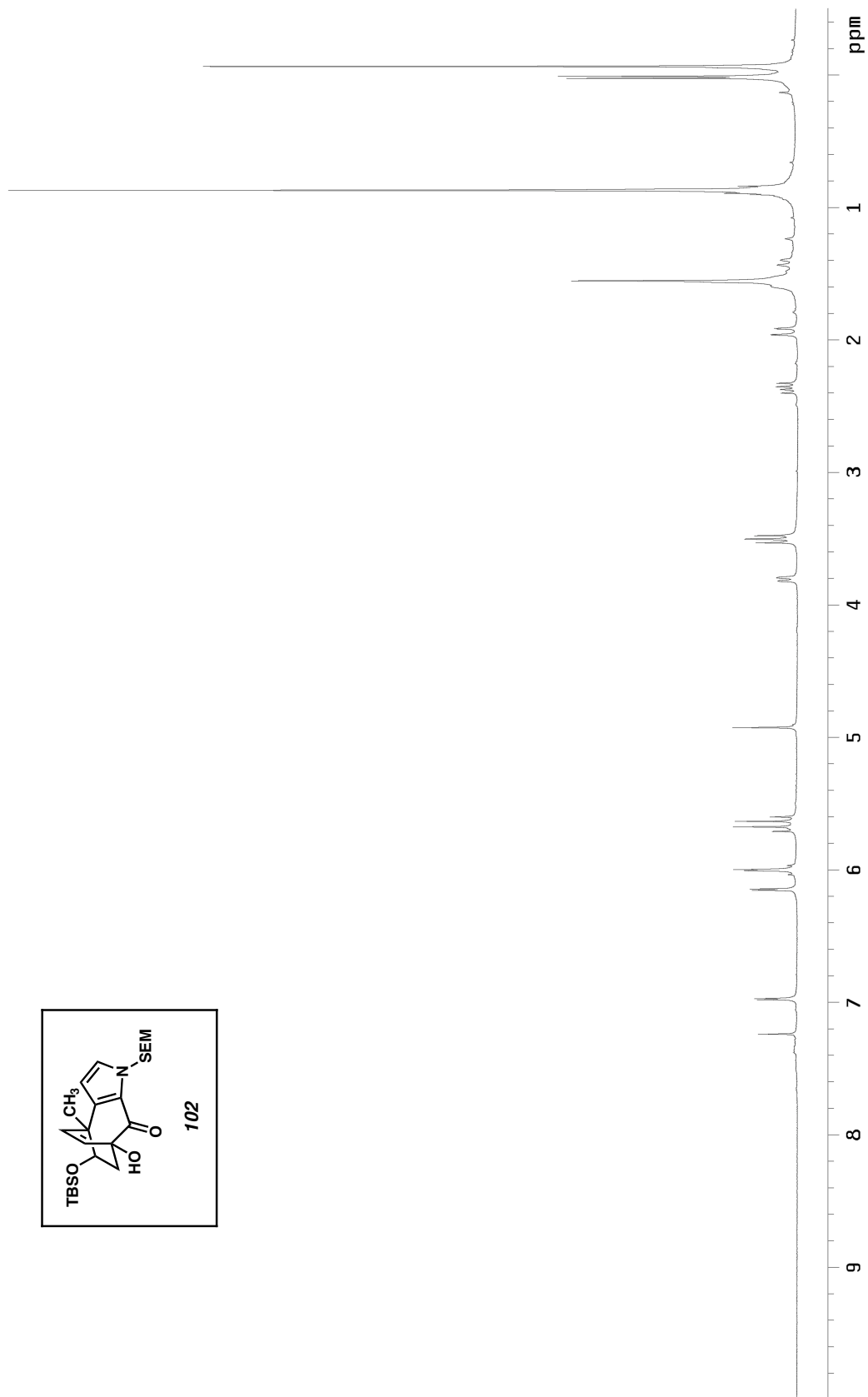
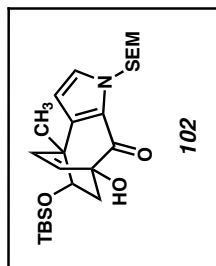


Figure A3.39 <sup>1</sup>H NMR (300 MHz, CDCl<sub>3</sub>) of compound **102**

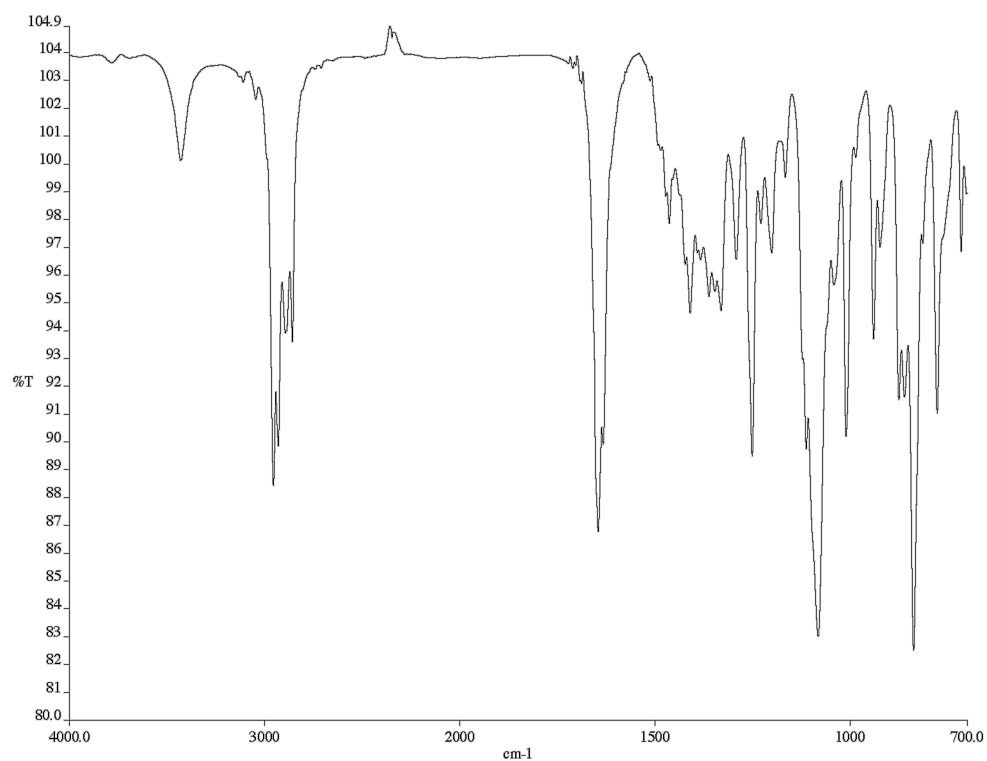


Figure A3.40 Infrared spectrum (thin film/NaCl) of compound **102**

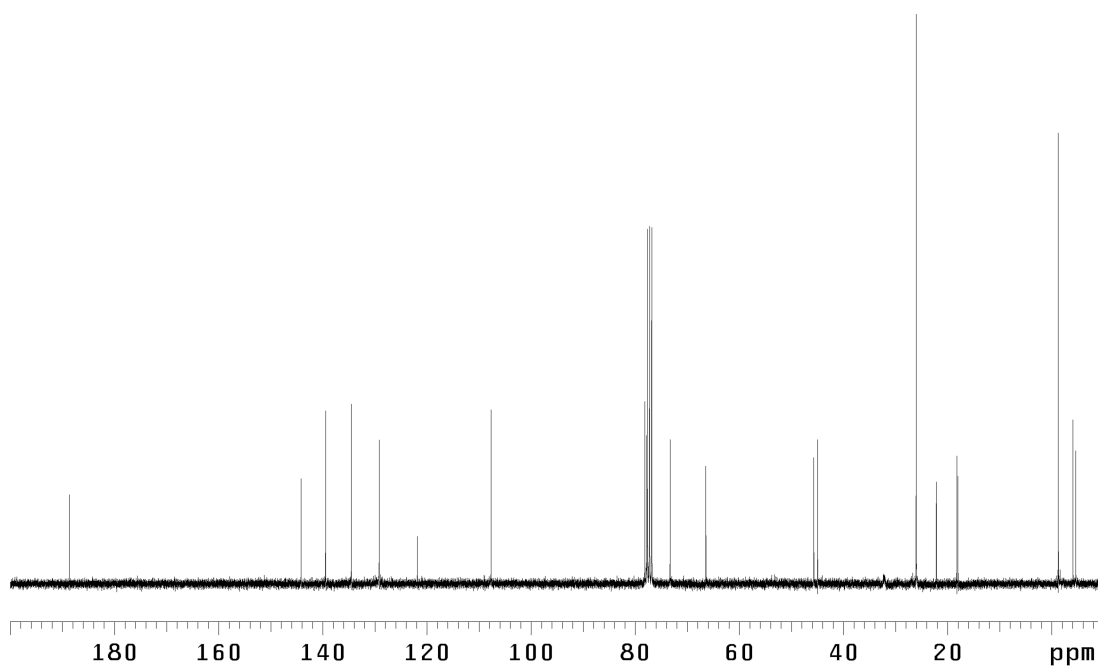


Figure A3.41 <sup>13</sup>C NMR (75 MHz, CDCl<sub>3</sub>) of compound **102**

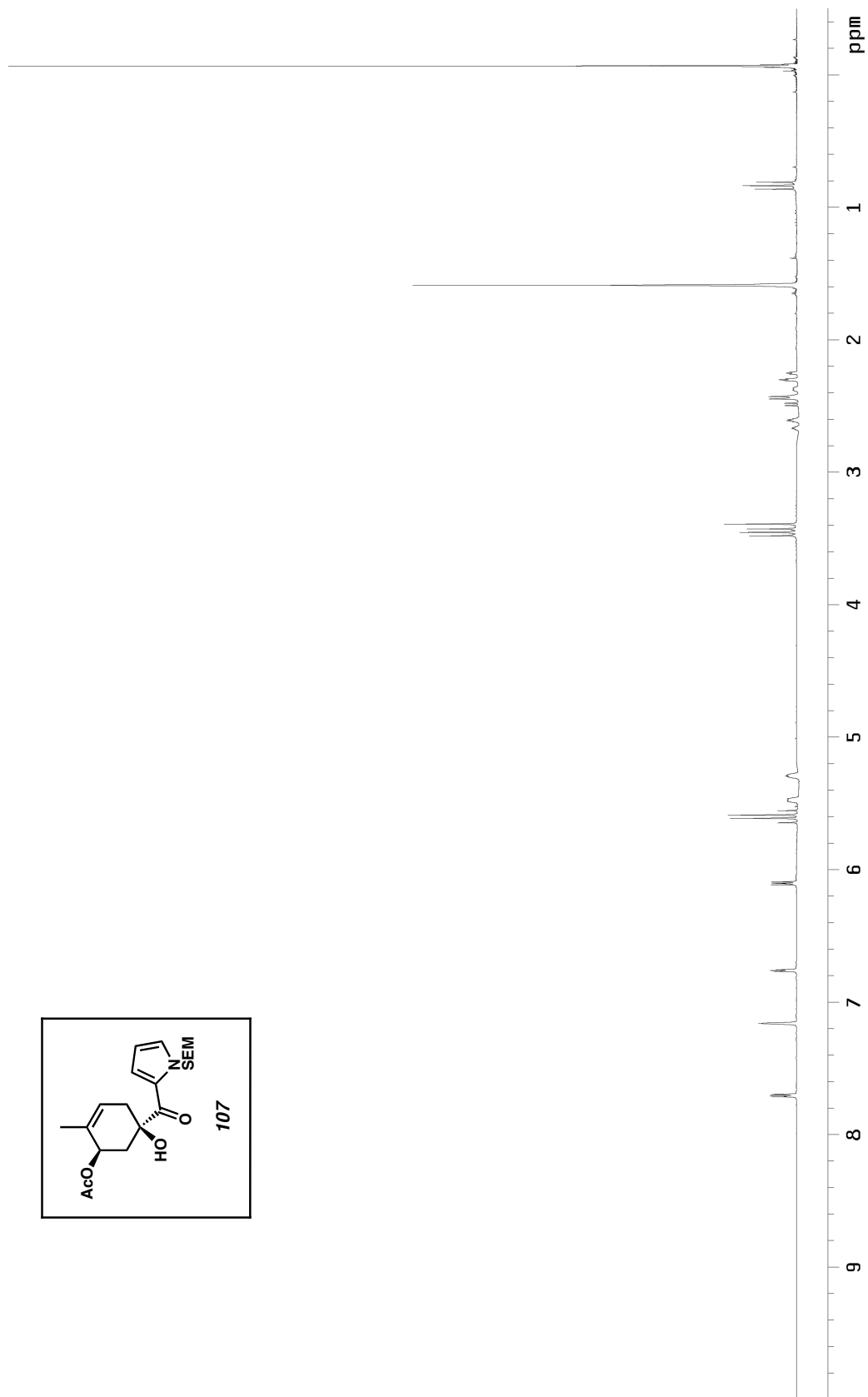
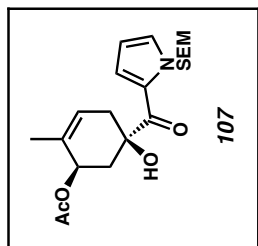


Figure A3.42  $^1\text{H}$  NMR (300 MHz,  $\text{C}_6\text{D}_6$ ) of compound **107**

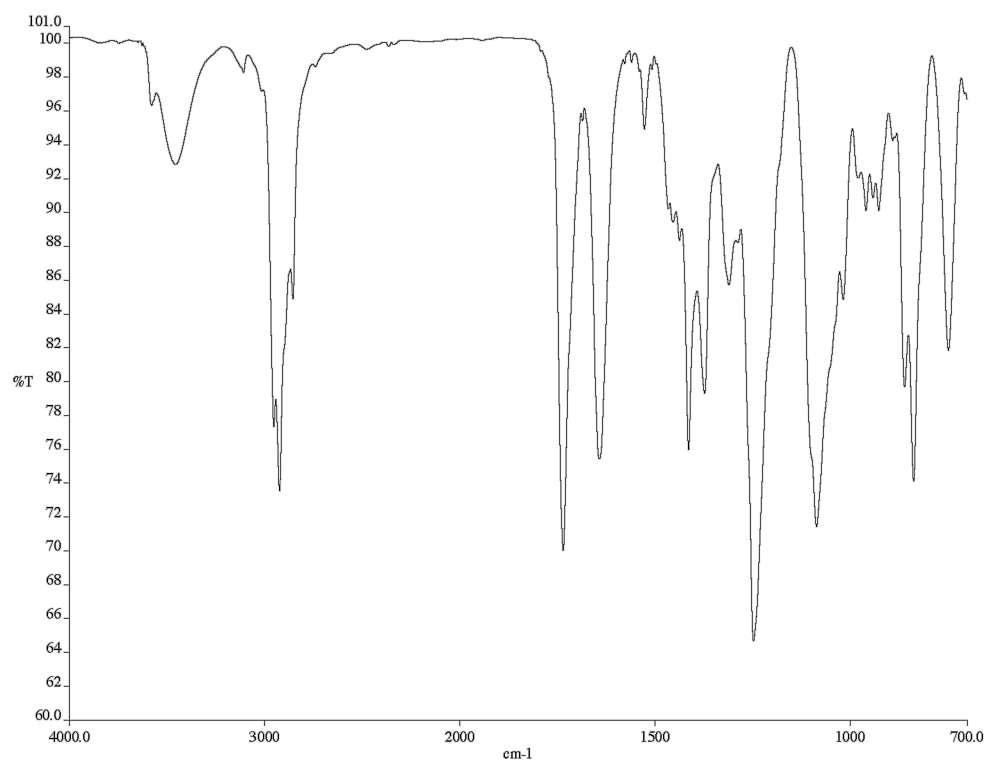


Figure A3.43 Infrared spectrum (thin film/NaCl) of compound **107**

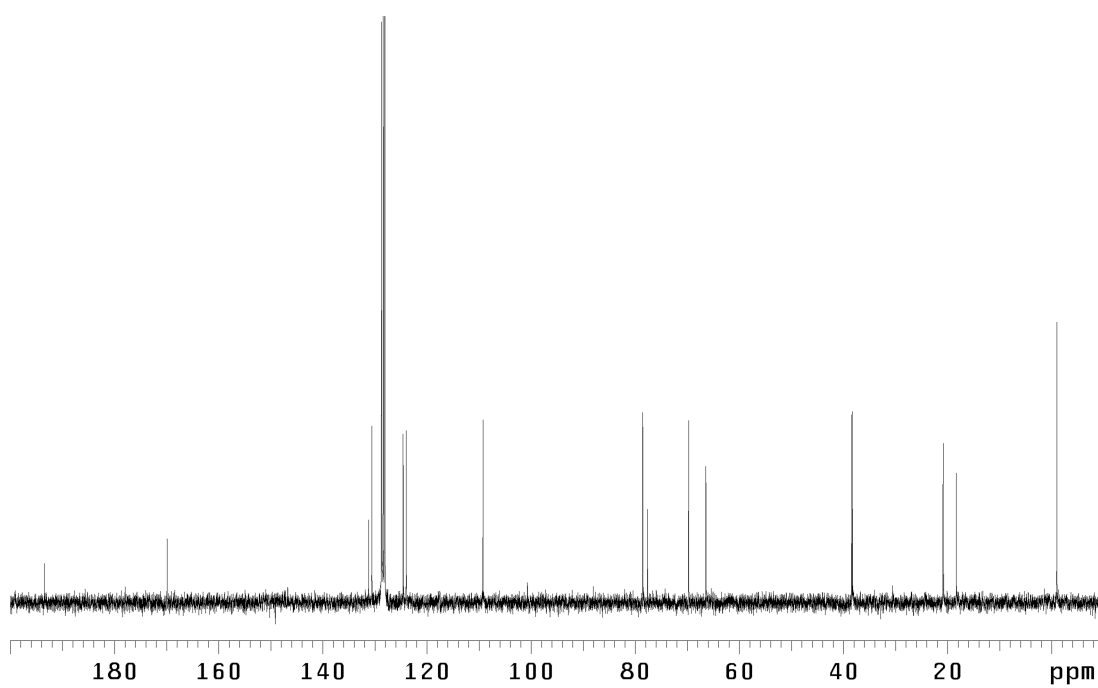


Figure A3.44 <sup>13</sup>C NMR (75 MHz, C<sub>6</sub>D<sub>6</sub>) of compound **107**

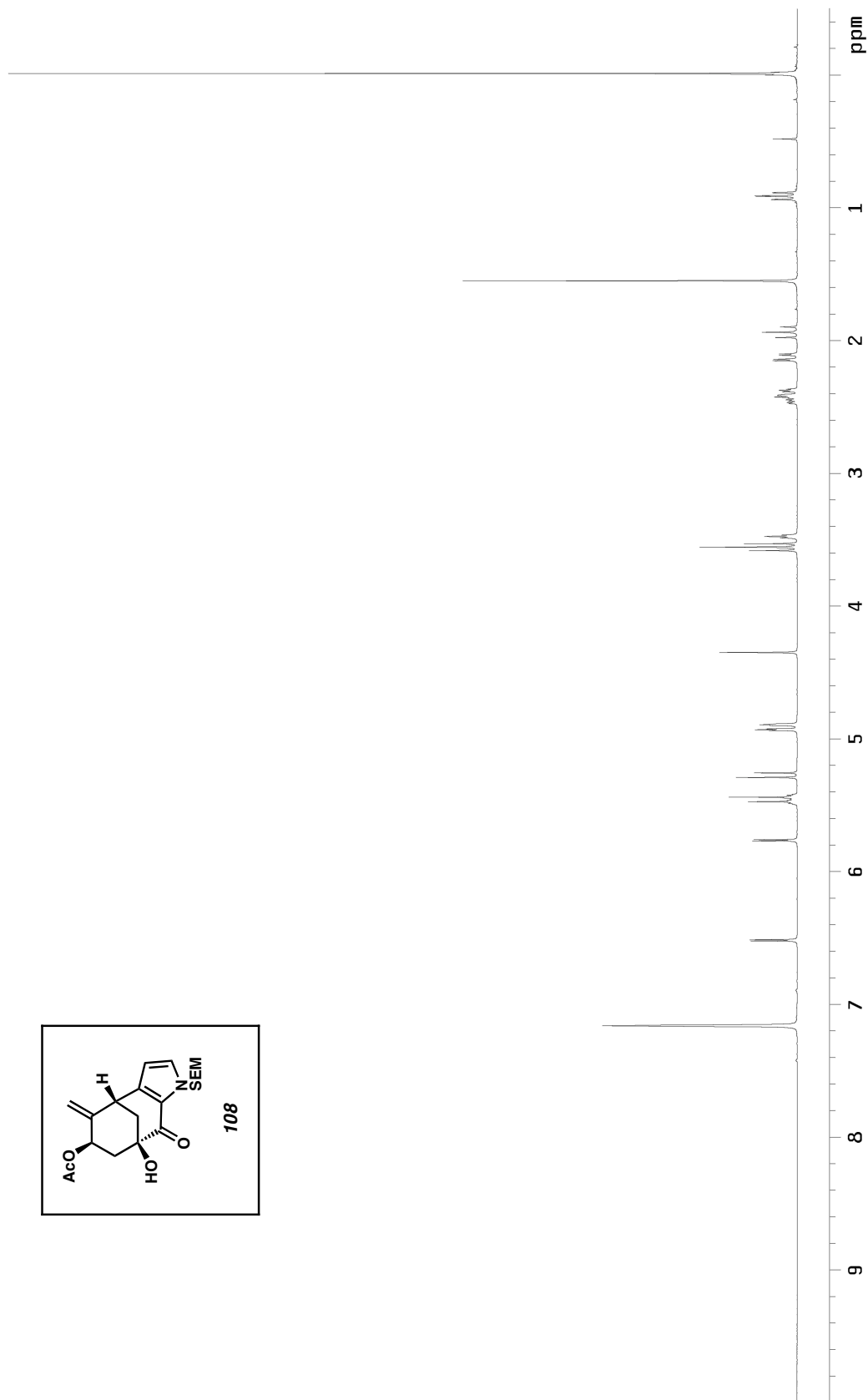


Figure A3.45  $^1\text{H}$  NMR (300 MHz,  $\text{C}_6\text{D}_6$ ) of compound **108**



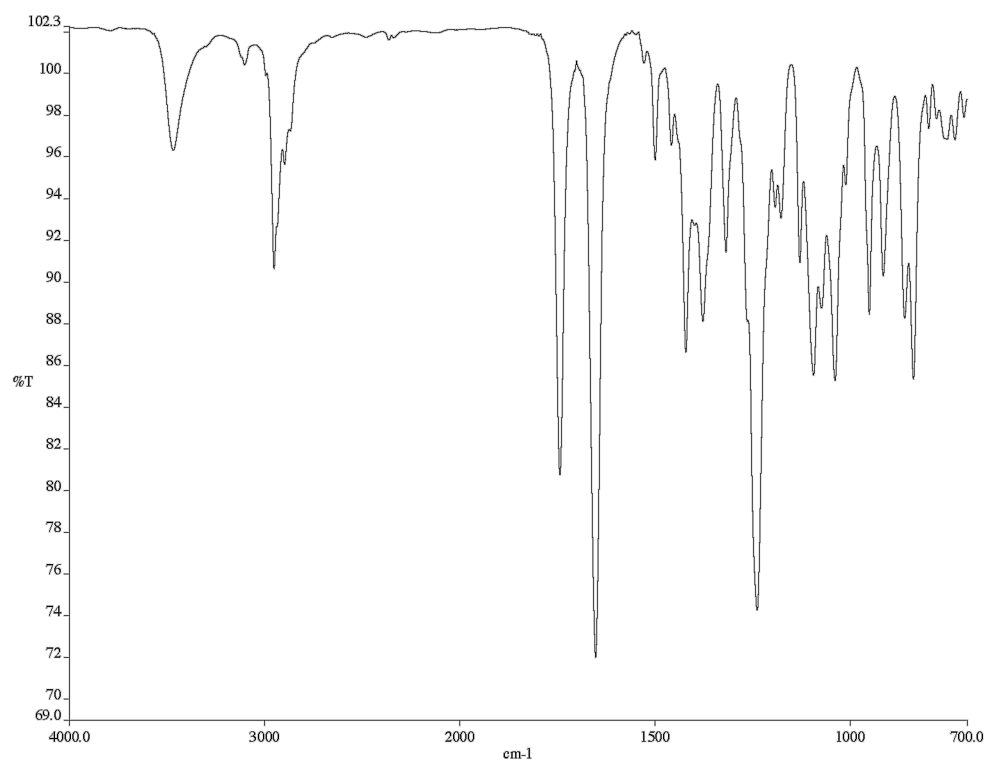


Figure A3.46 Infrared spectrum (thin film/NaCl) of compound **108**

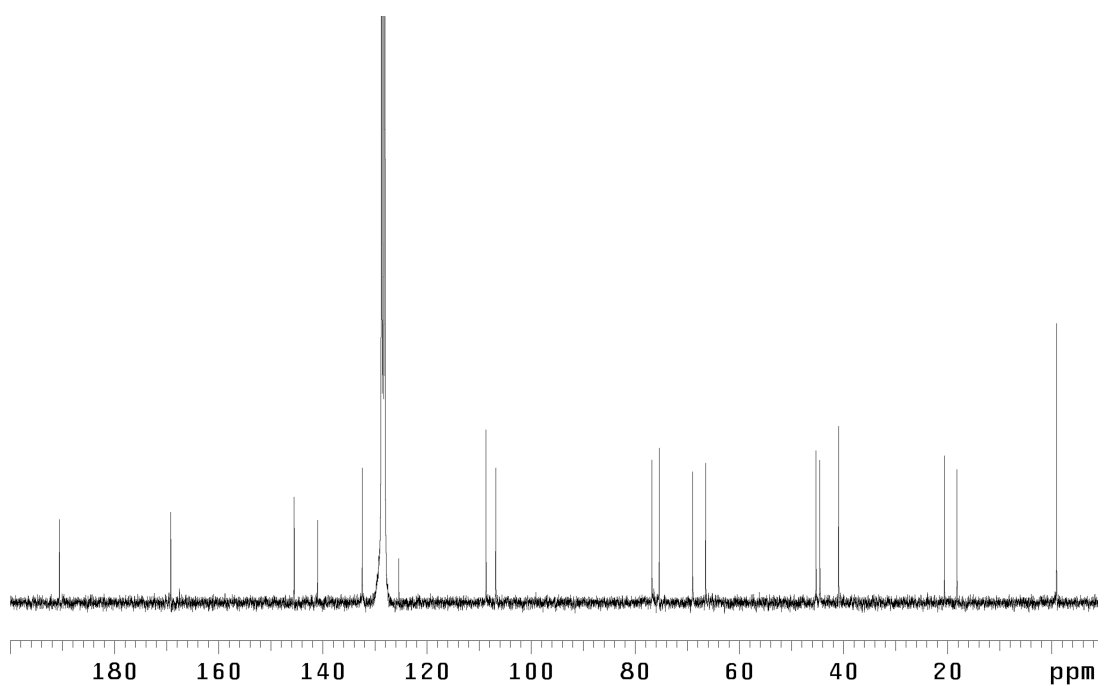


Figure A3.47 <sup>13</sup>C NMR (75 MHz, C<sub>6</sub>D<sub>6</sub>) of compound **108**

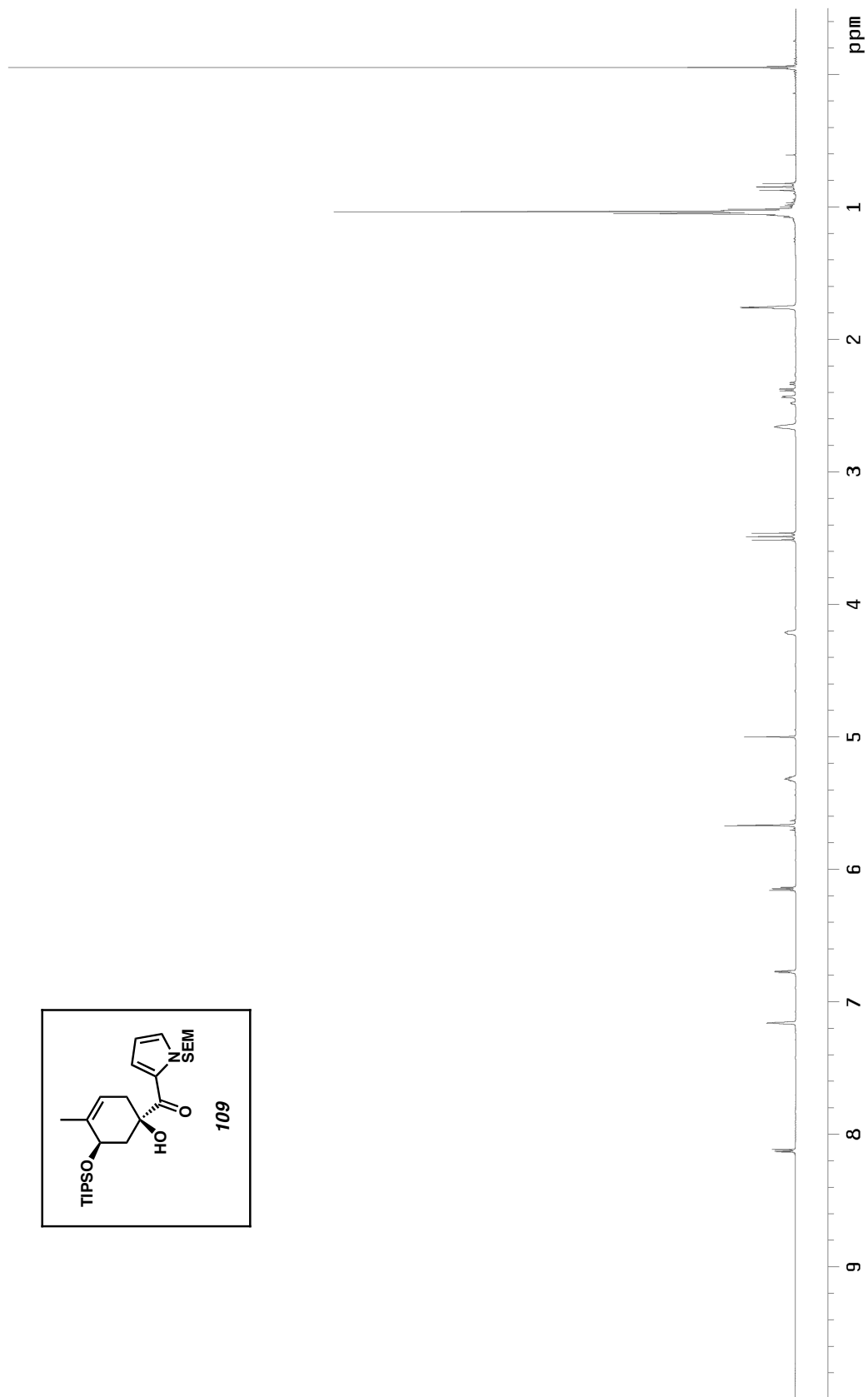
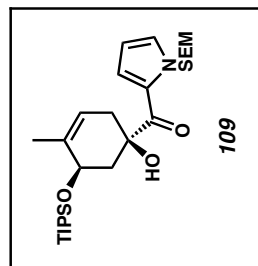


Figure A3.48  $^1\text{H}$  NMR (300 MHz,  $\text{C}_6\text{D}_6$ ) of compound **109**

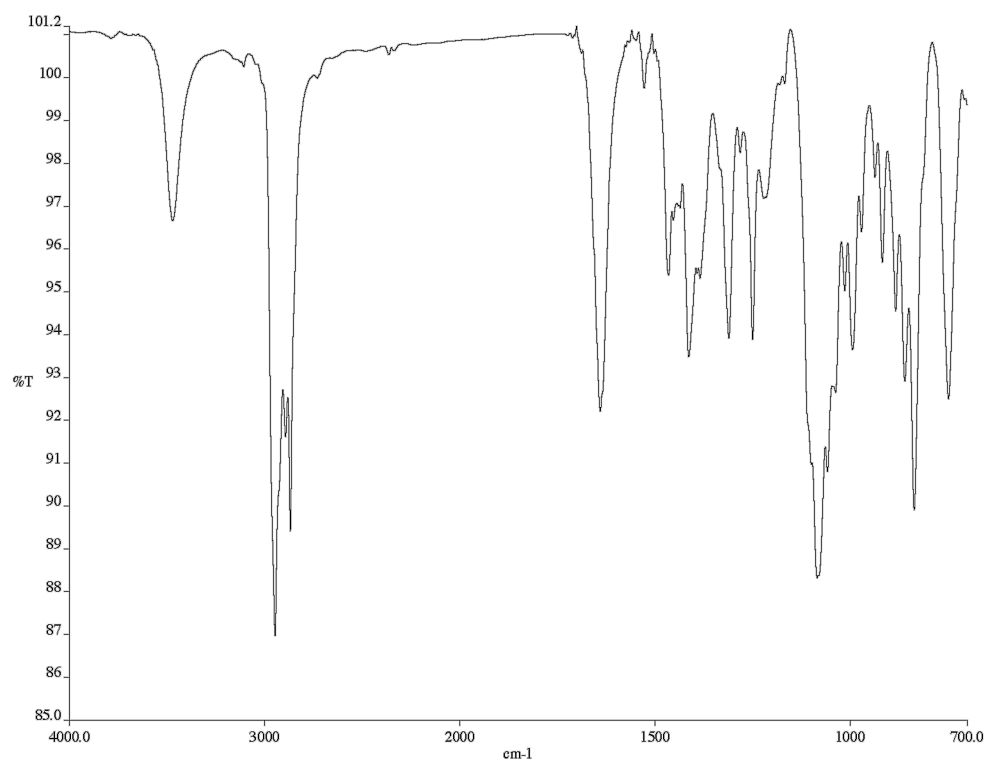


Figure A3.49 Infrared spectrum (thin film/NaCl) of compound **109**

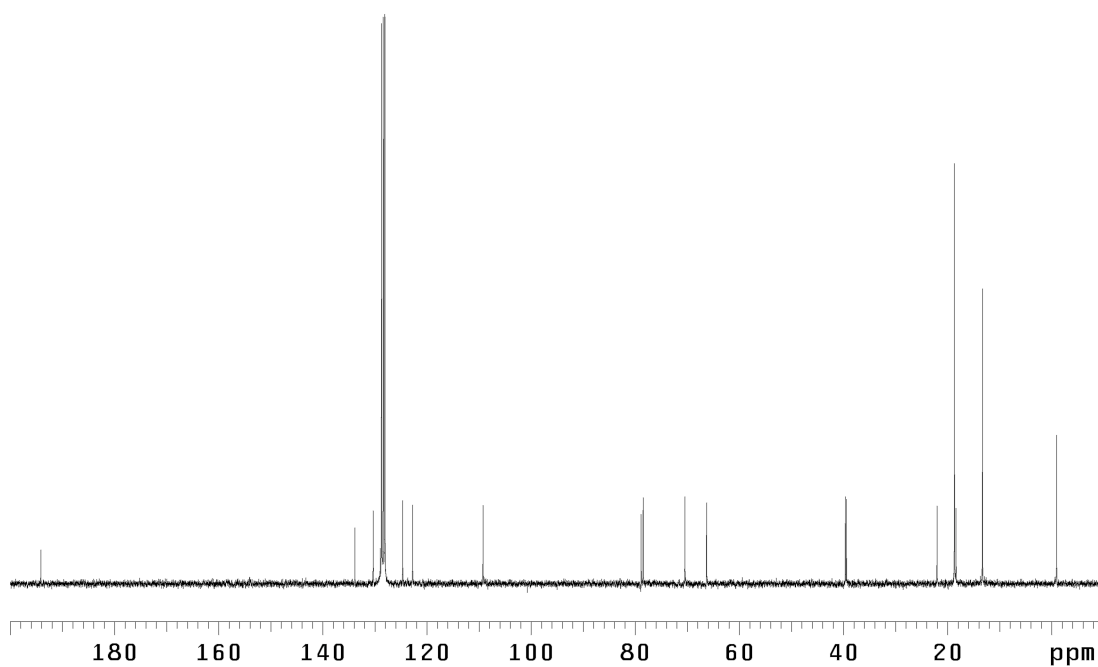


Figure A3.50 <sup>13</sup>C NMR (75 MHz, C<sub>6</sub>D<sub>6</sub>) of compound **109**

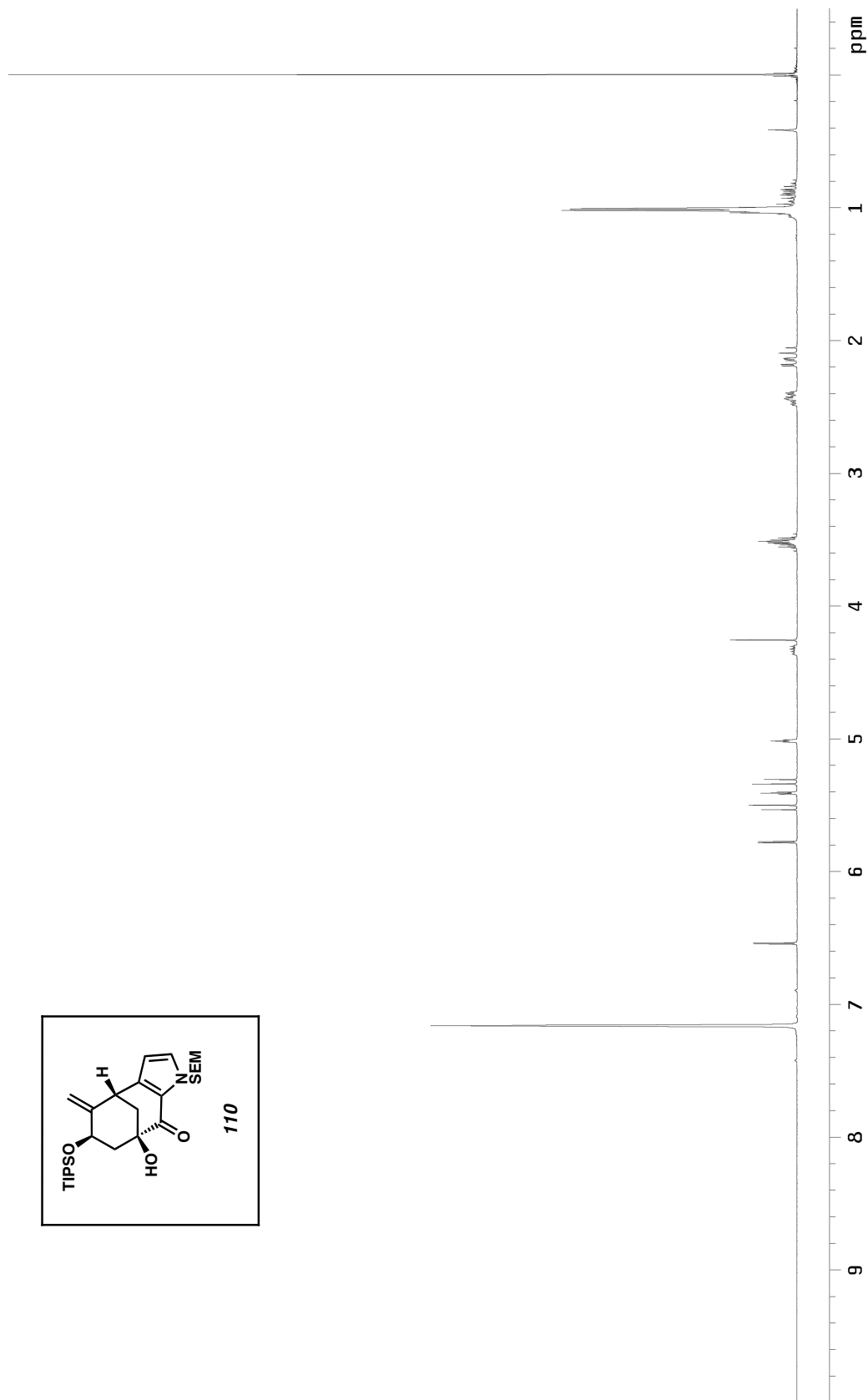
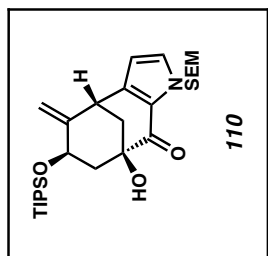


Figure A3.51 <sup>1</sup>H NMR (300 MHz, C<sub>6</sub>D<sub>6</sub>) of compound **110**



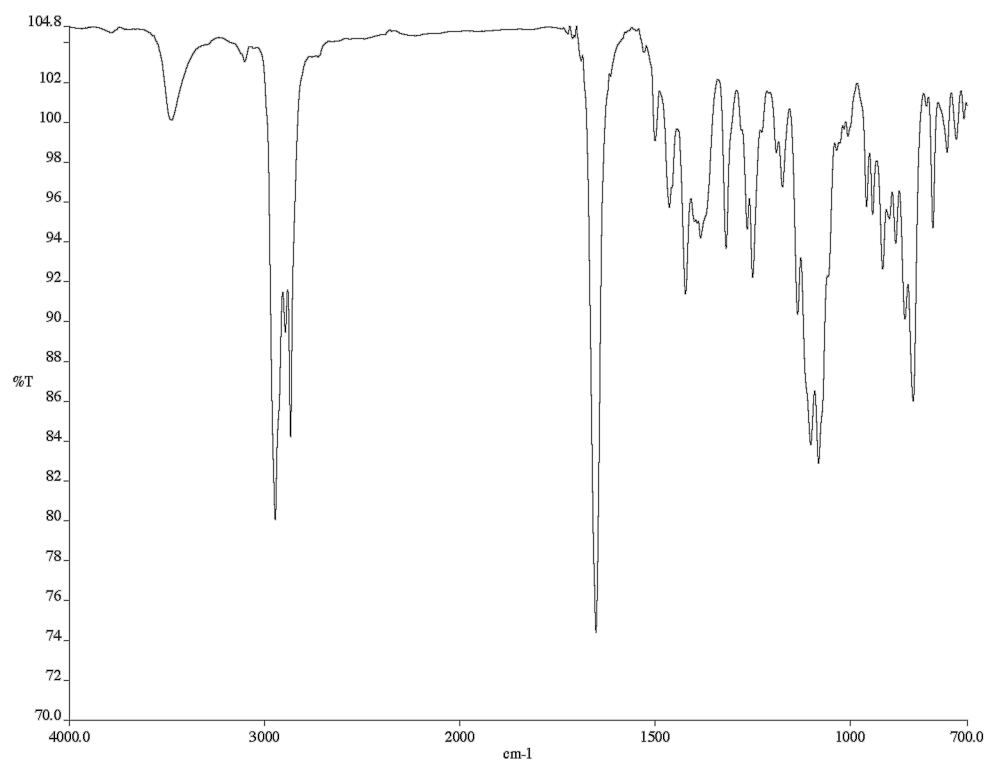


Figure A3.52 Infrared spectrum (thin film/NaCl) of compound **110**

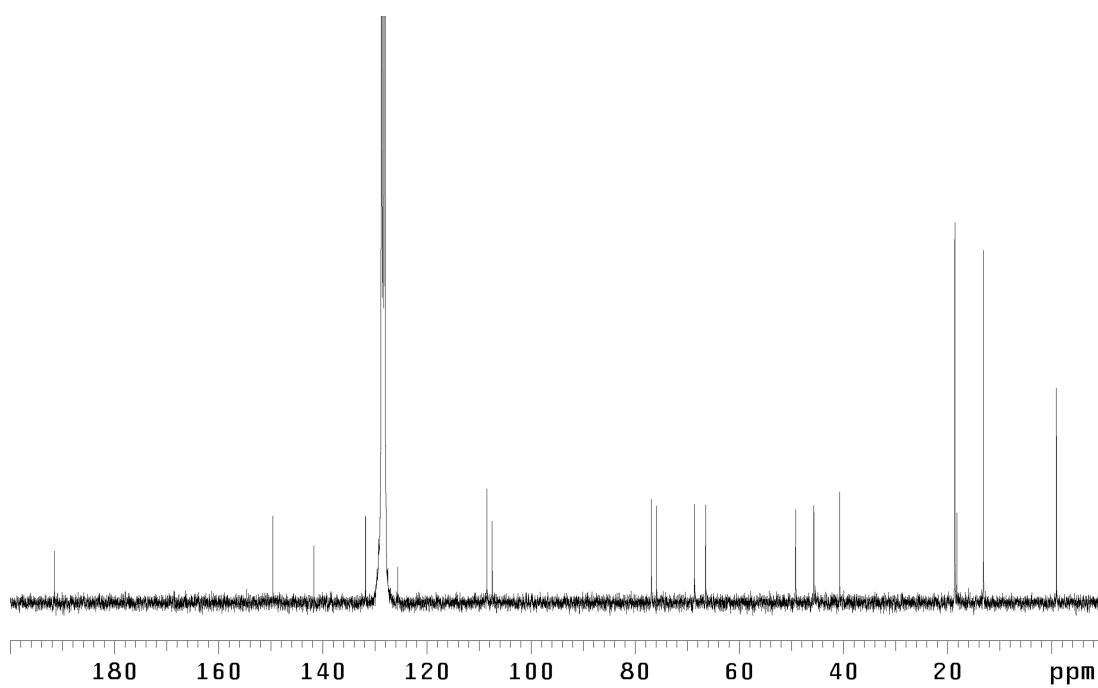


Figure A3.53 <sup>13</sup>C NMR (75 MHz, C<sub>6</sub>D<sub>6</sub>) of compound **110**

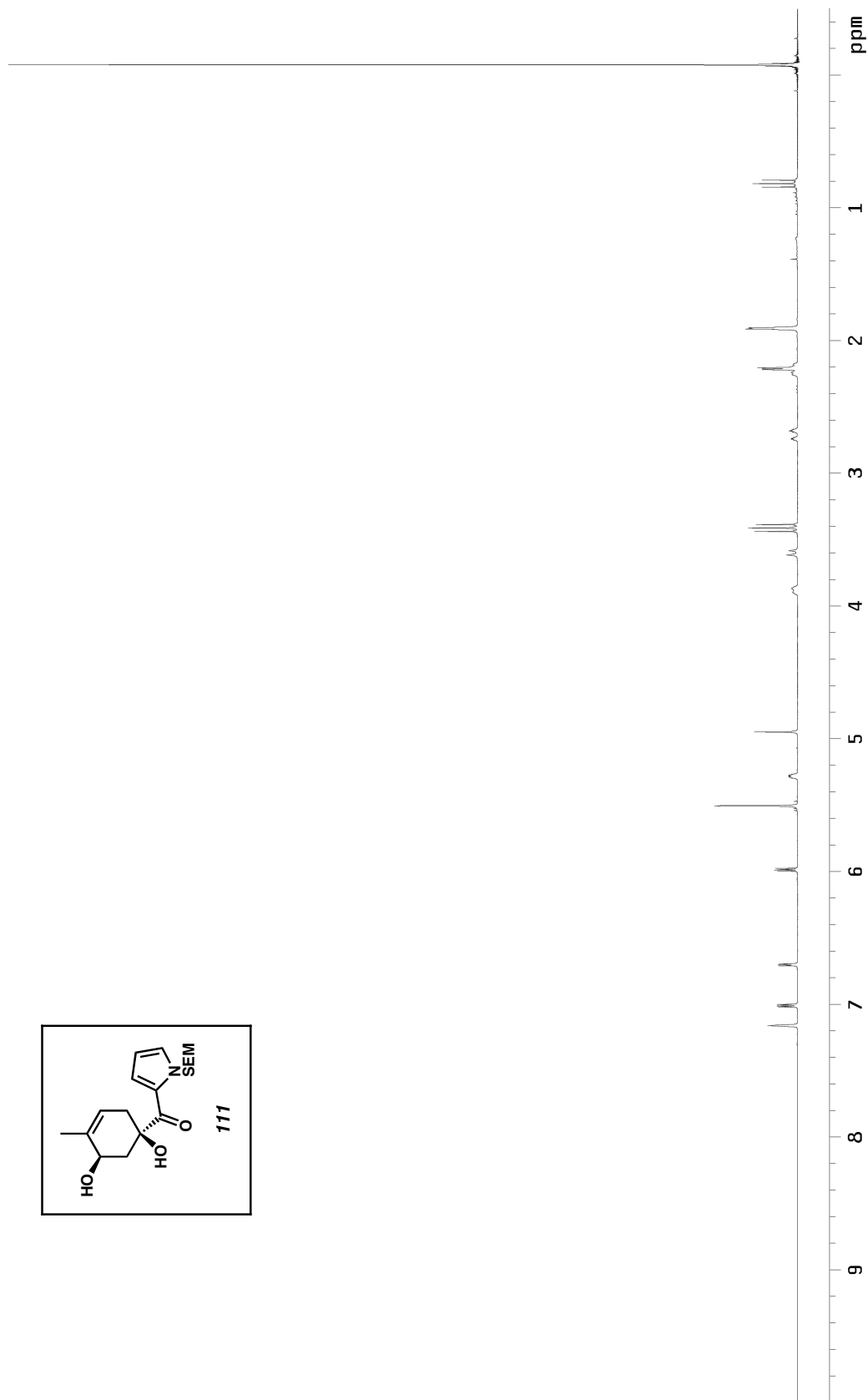


Figure A3.54  $^1\text{H}$  NMR (300 MHz,  $\text{C}_6\text{D}_6$ ) of compound **111**

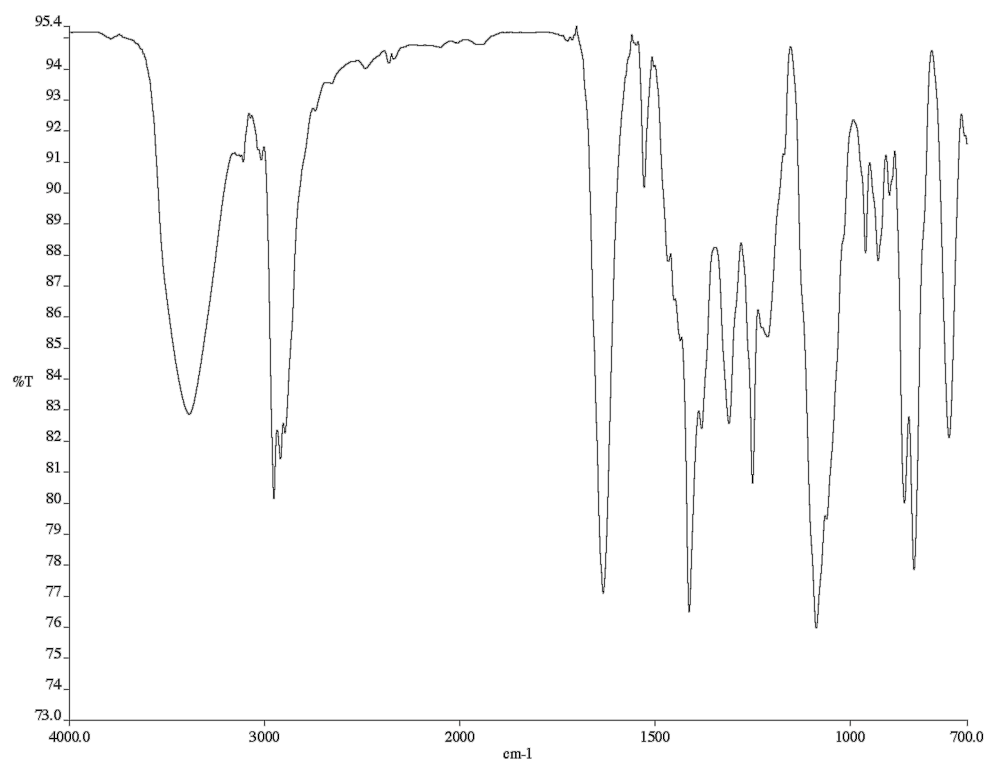


Figure A3.55 Infrared spectrum (thin film/NaCl) of compound **111**

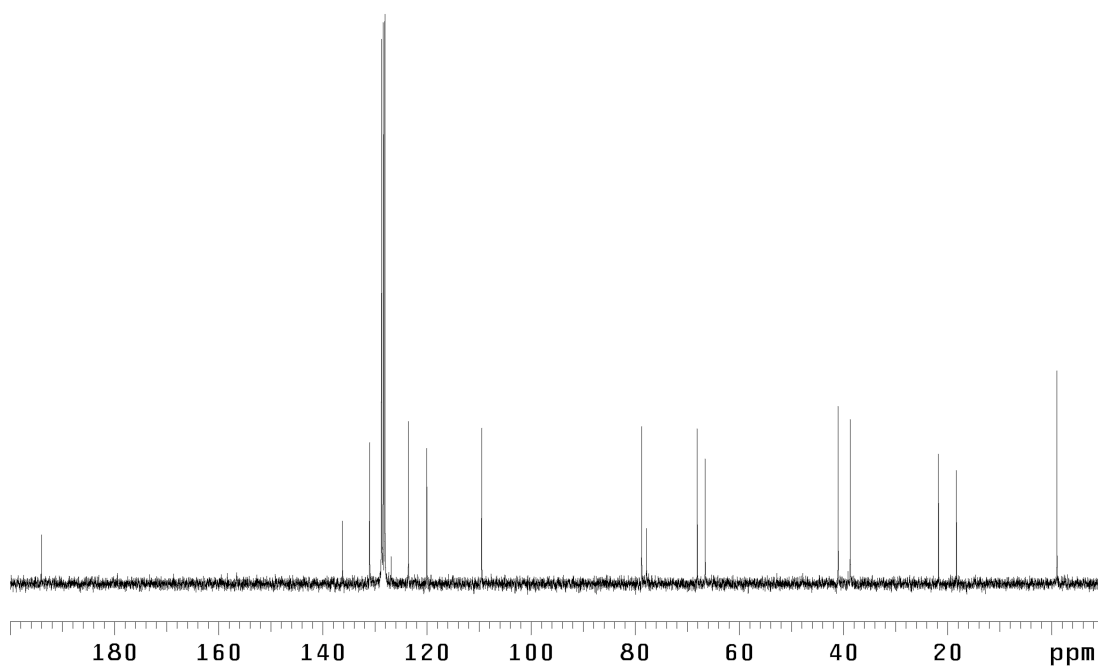


Figure A3.56 <sup>13</sup>C NMR (75 MHz, C<sub>6</sub>D<sub>6</sub>) of compound **111**

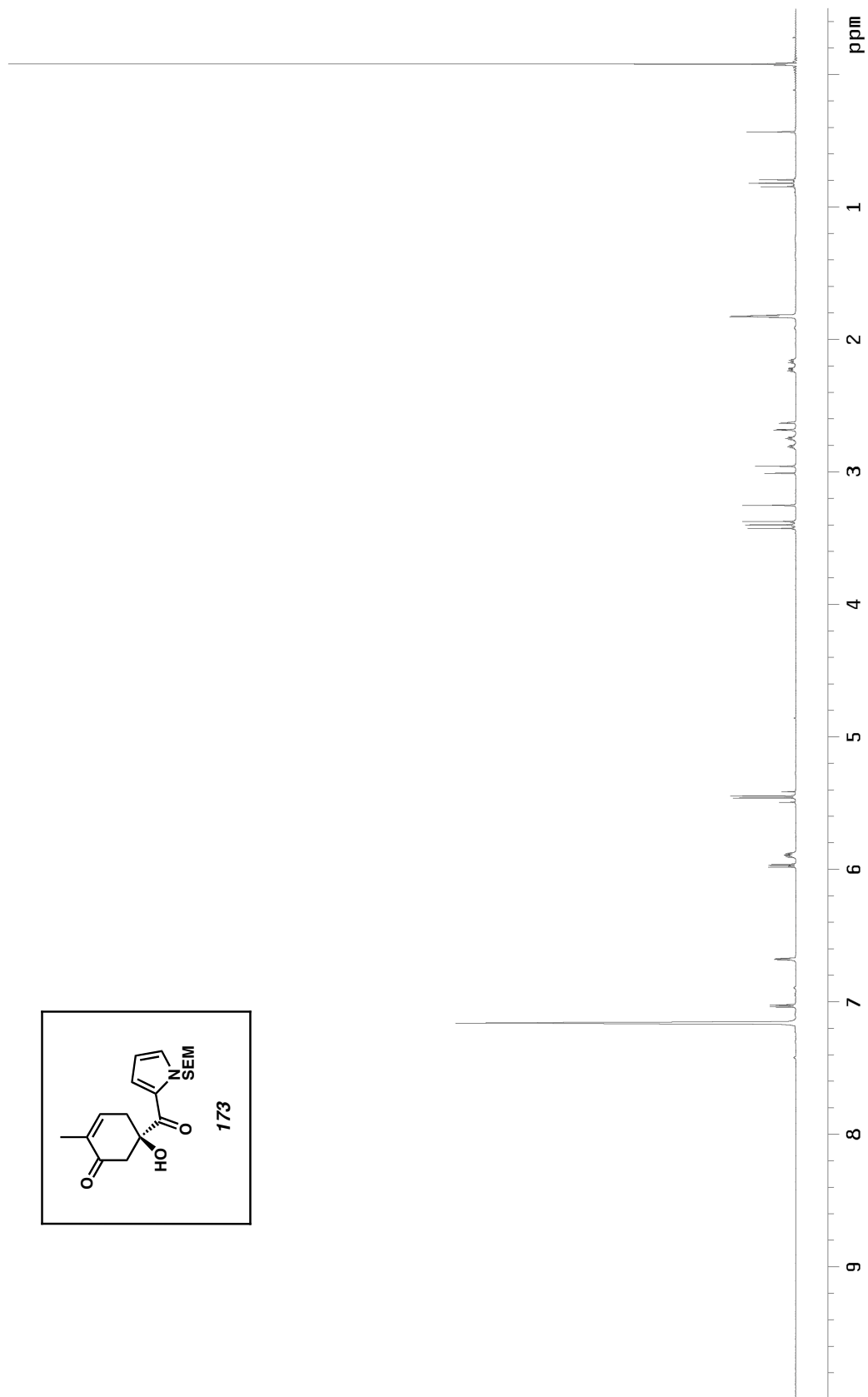


Figure A3.57  $^1\text{H}$  NMR (300 MHz,  $\text{CDCl}_3$ ) of compound **173**



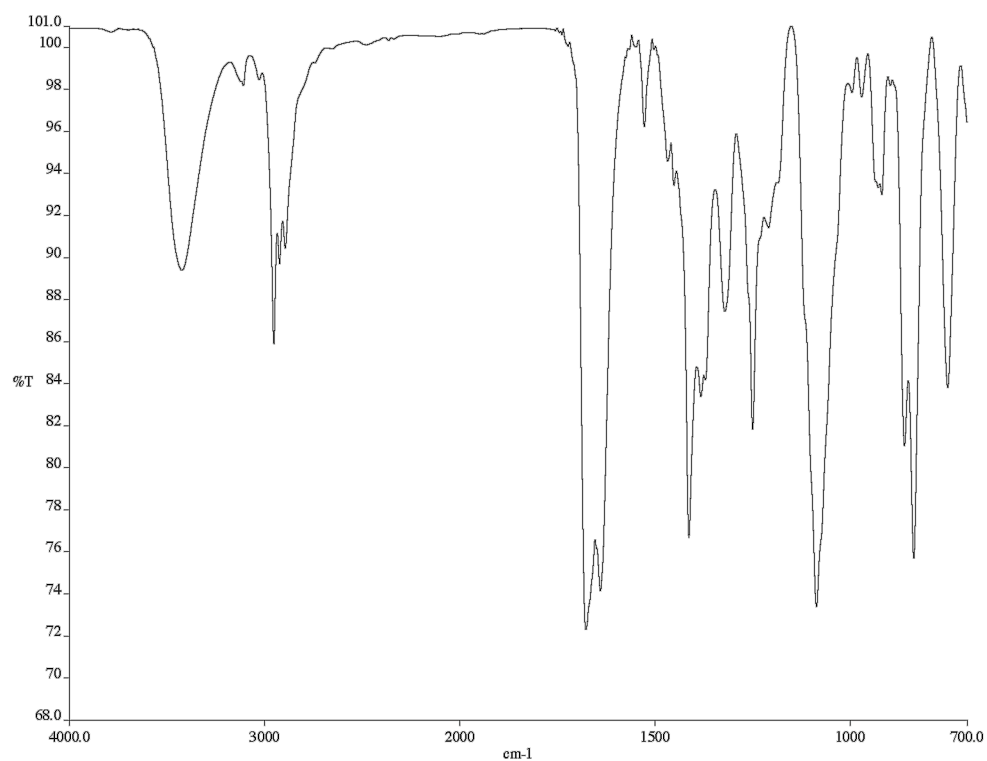


Figure A3.58 Infrared spectrum (thin film/NaCl) of compound **173**

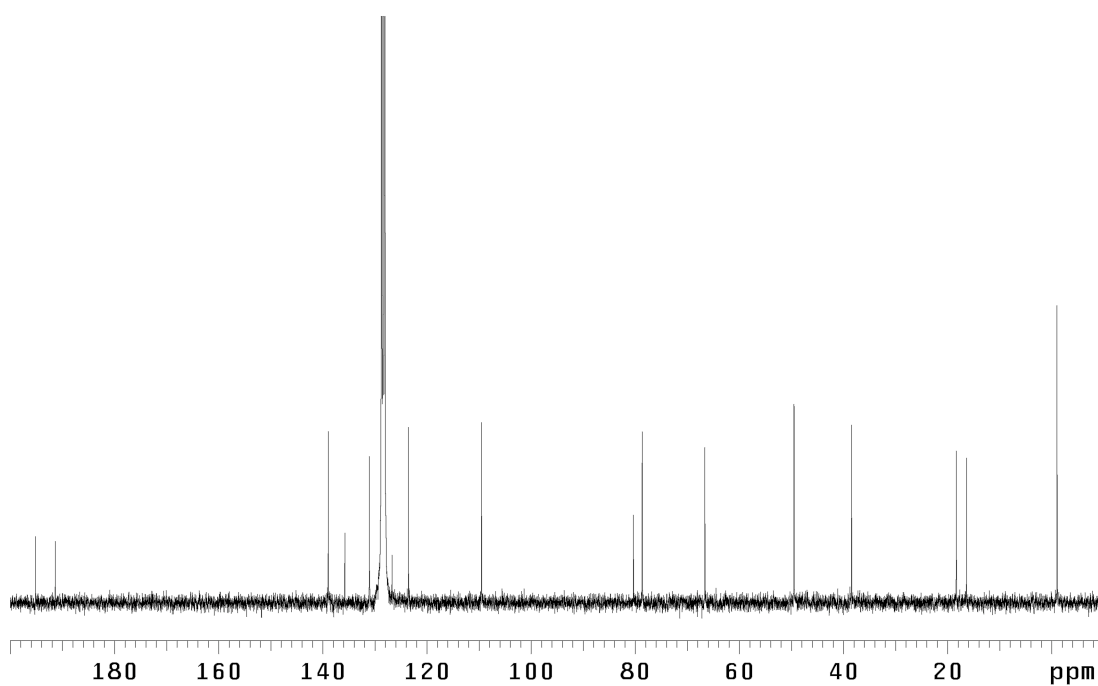


Figure A3.59 <sup>13</sup>C NMR (75 MHz, C<sub>6</sub>D<sub>6</sub>) of compound **173**

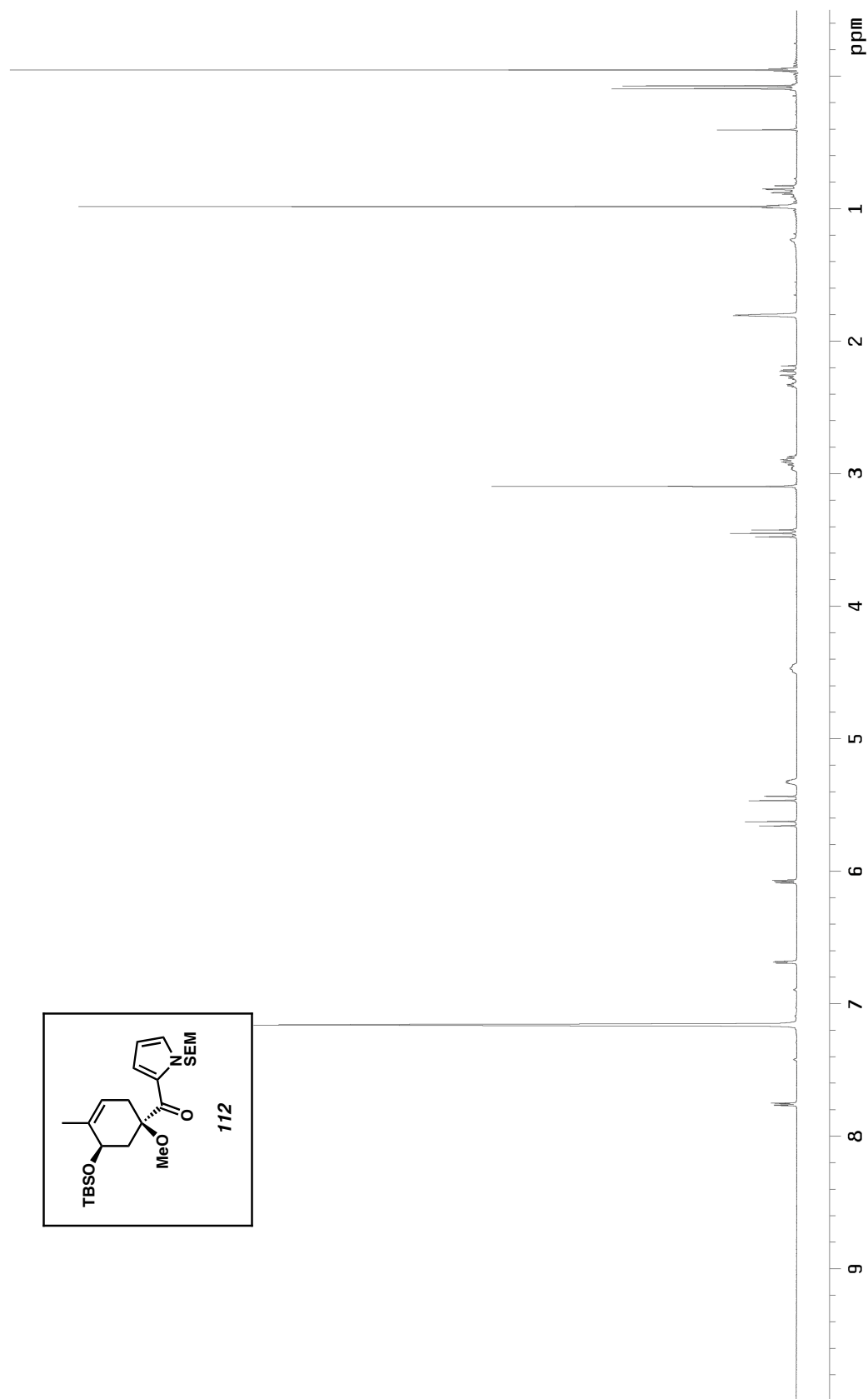


Figure A3.60  $^1\text{H}$  NMR (300 MHz,  $\text{CDCl}_3$ ) of compound **112**

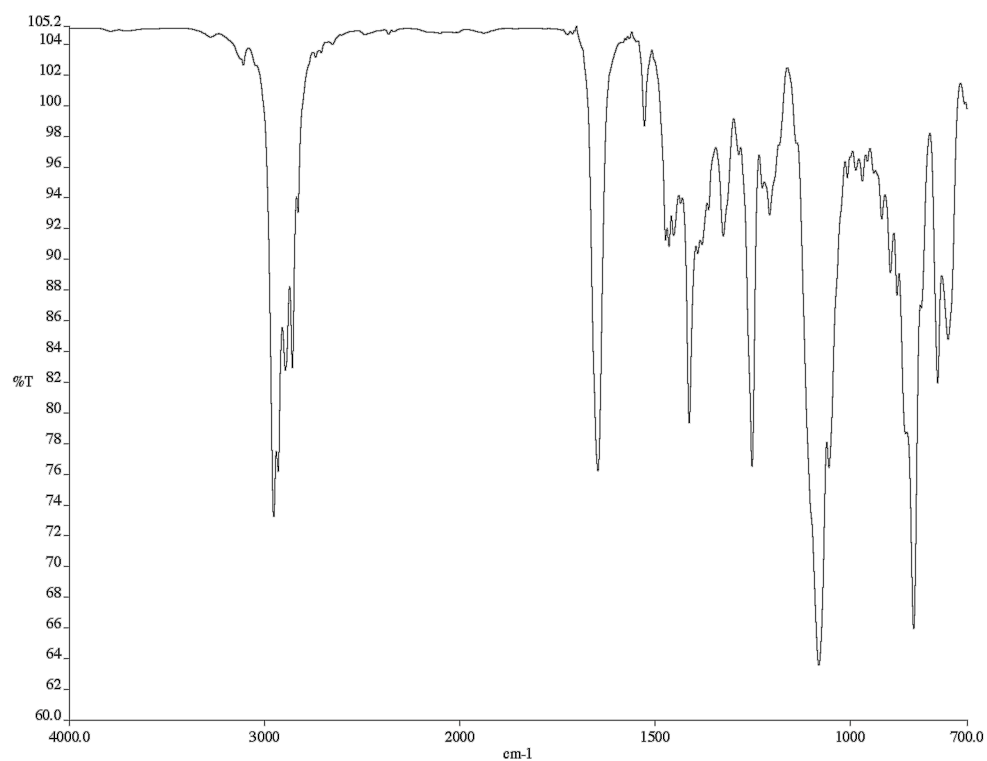


Figure A3.61 Infrared spectrum (thin film/NaCl) of compound **112**

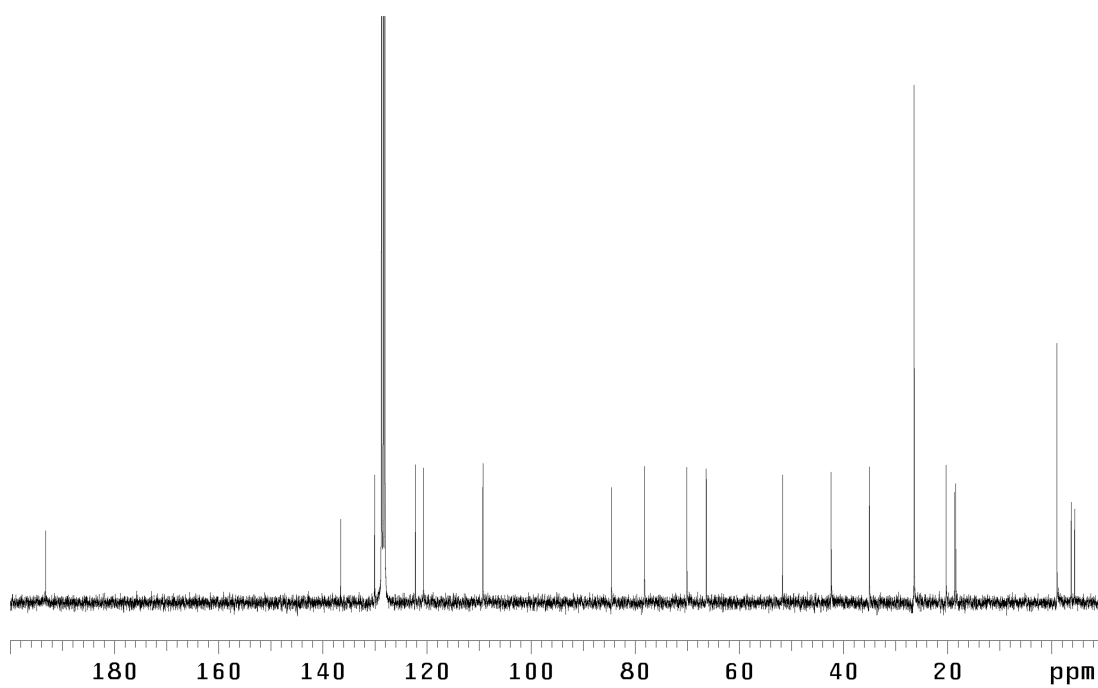


Figure A3.62 <sup>13</sup>C NMR (75 MHz, C<sub>6</sub>D<sub>6</sub>) of compound **112**

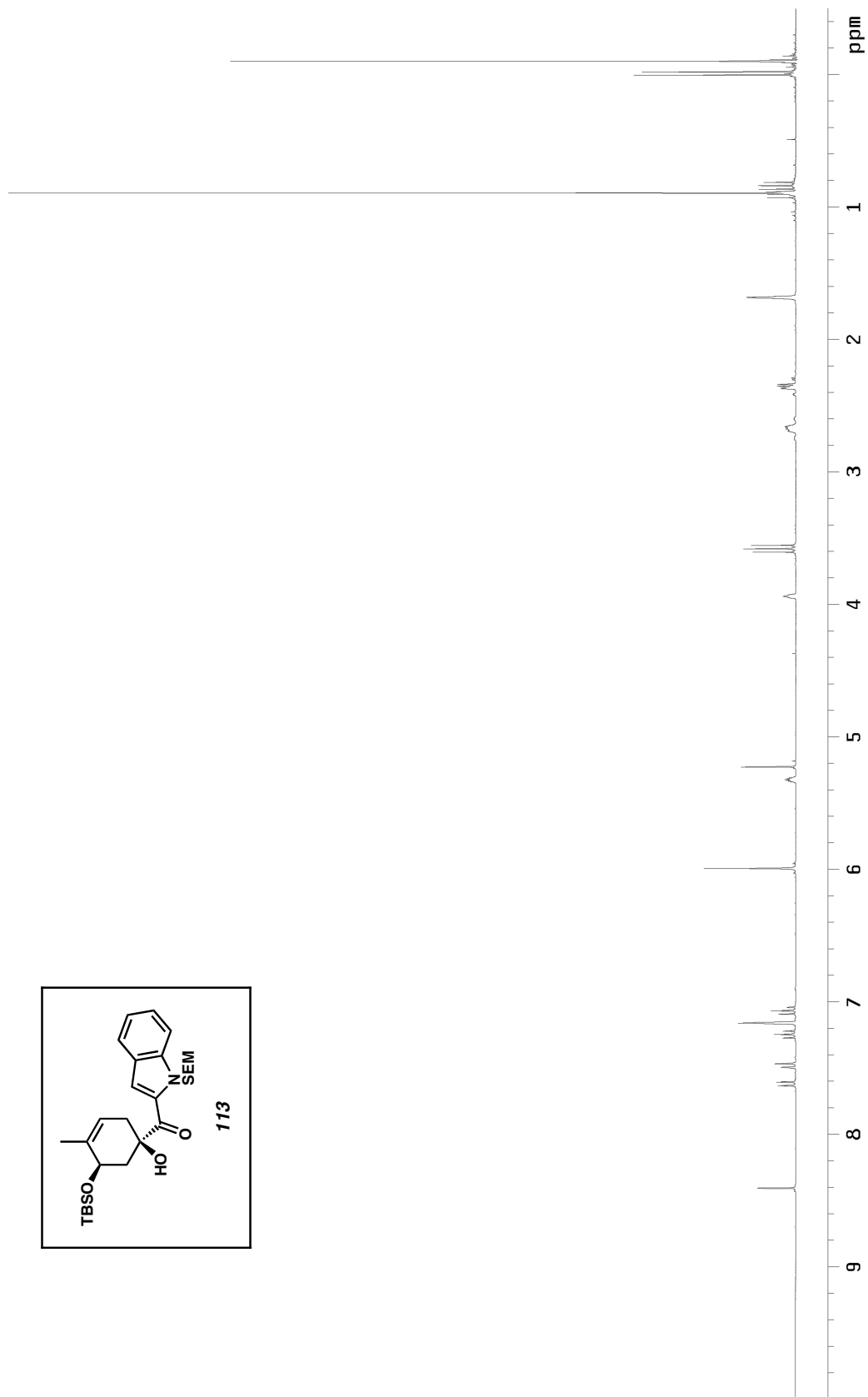


Figure A3.63  $^1\text{H}$  NMR (300 MHz,  $\text{C}_6\text{D}_6$ ) of compound **113**

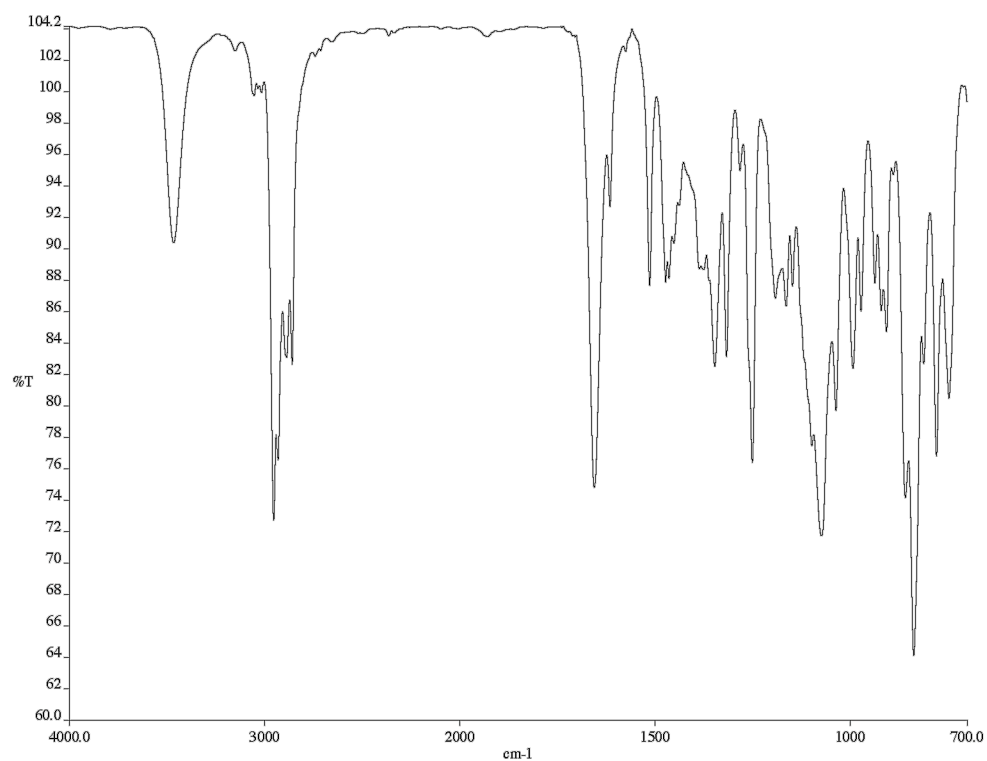


Figure A3.64 Infrared spectrum (thin film/NaCl) of compound **113**

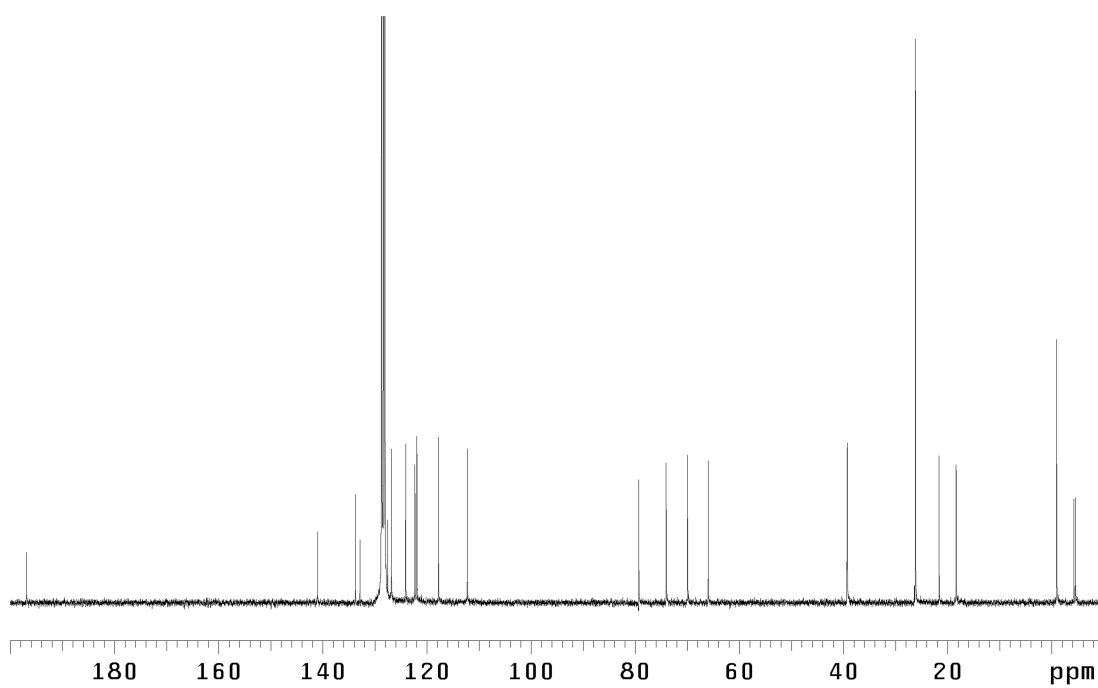


Figure A3.65  $^{13}\text{C}$  NMR (75 MHz,  $\text{C}_6\text{D}_6$ ) of compound **113**

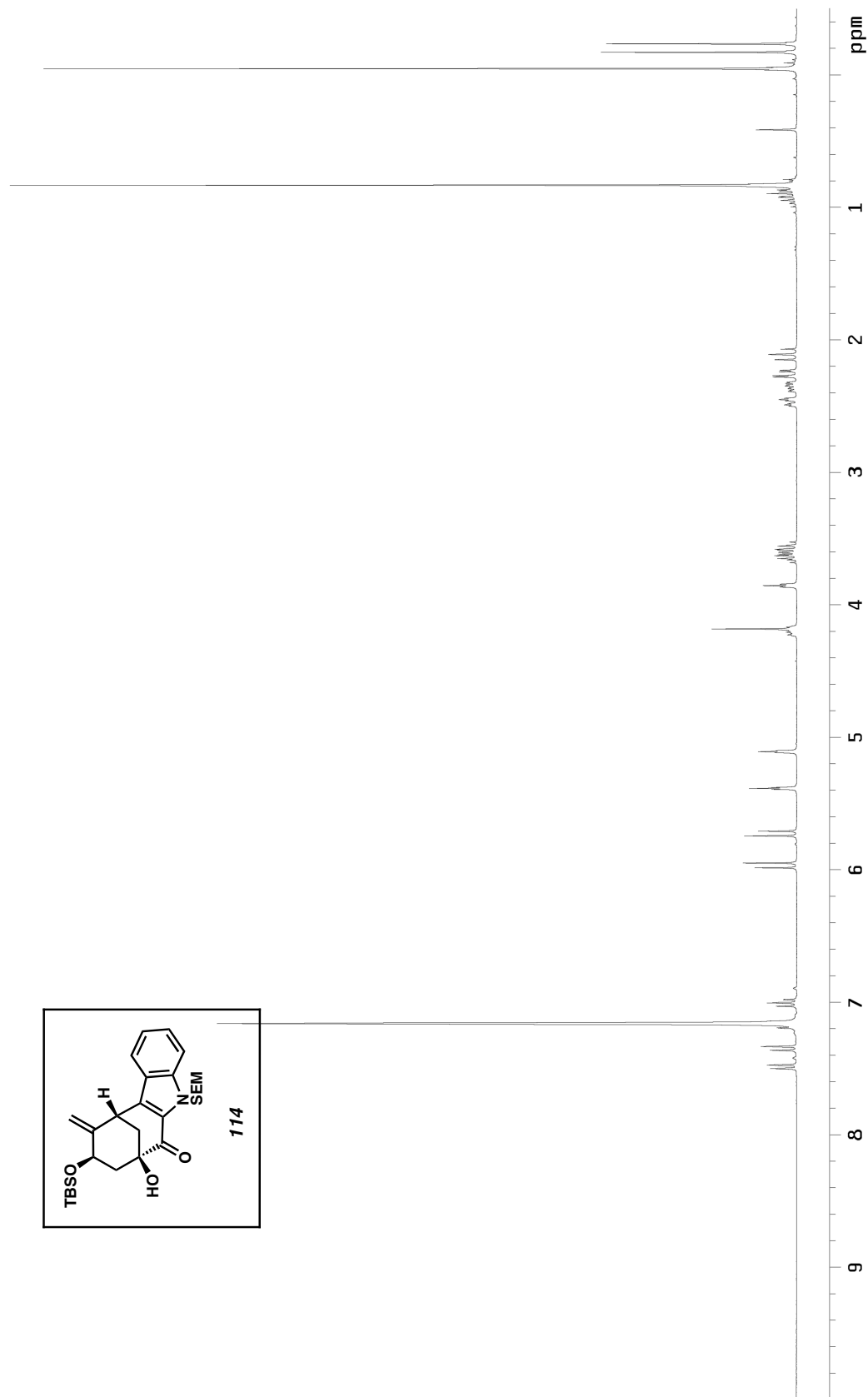


Figure A3.66  $^1\text{H}$  NMR (300 MHz,  $\text{C}_6\text{D}_6$ ) of compound **114**

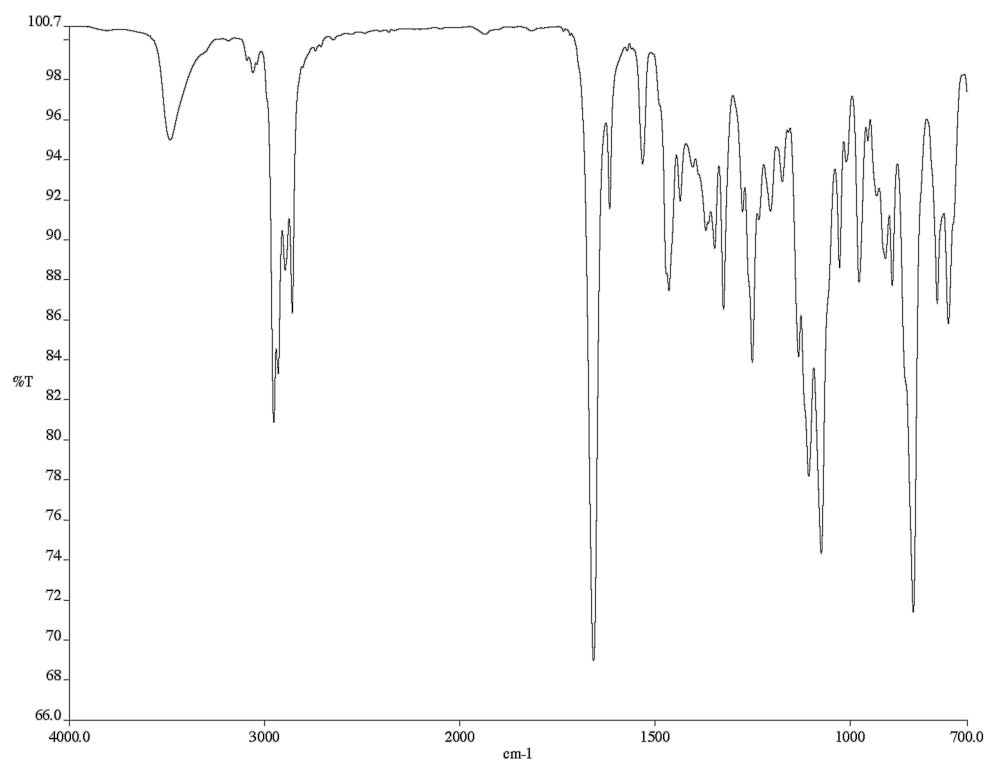


Figure A3.67 Infrared spectrum (thin film/NaCl) of compound **114**

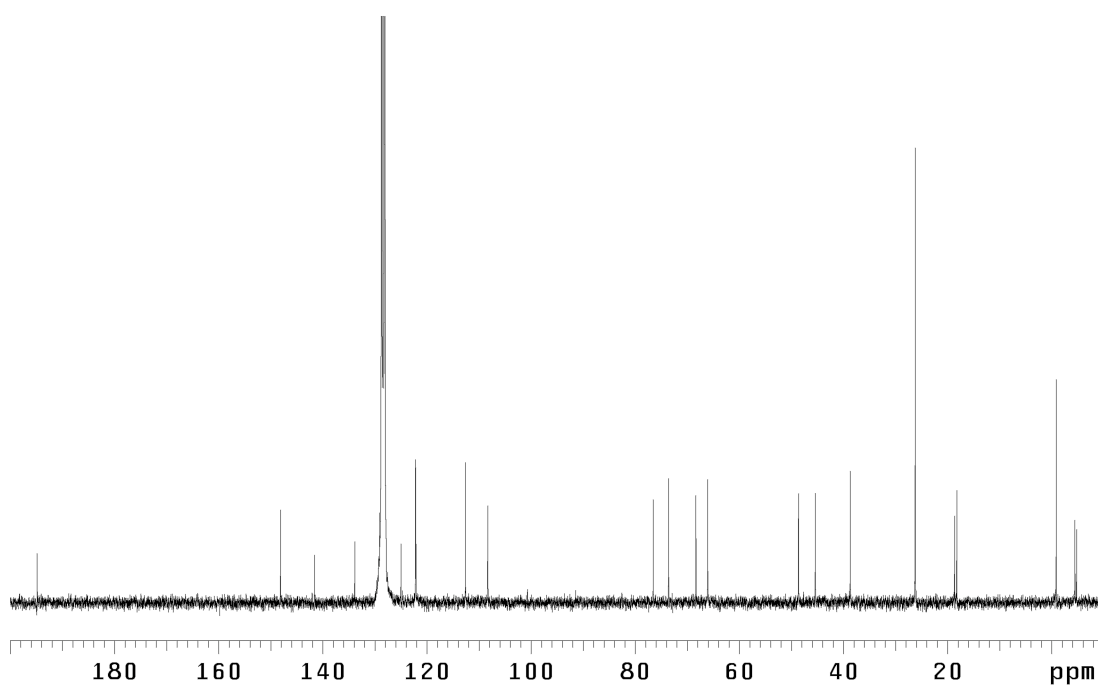


Figure A3.68 <sup>13</sup>C NMR (75 MHz, C<sub>6</sub>D<sub>6</sub>) of compound **114**

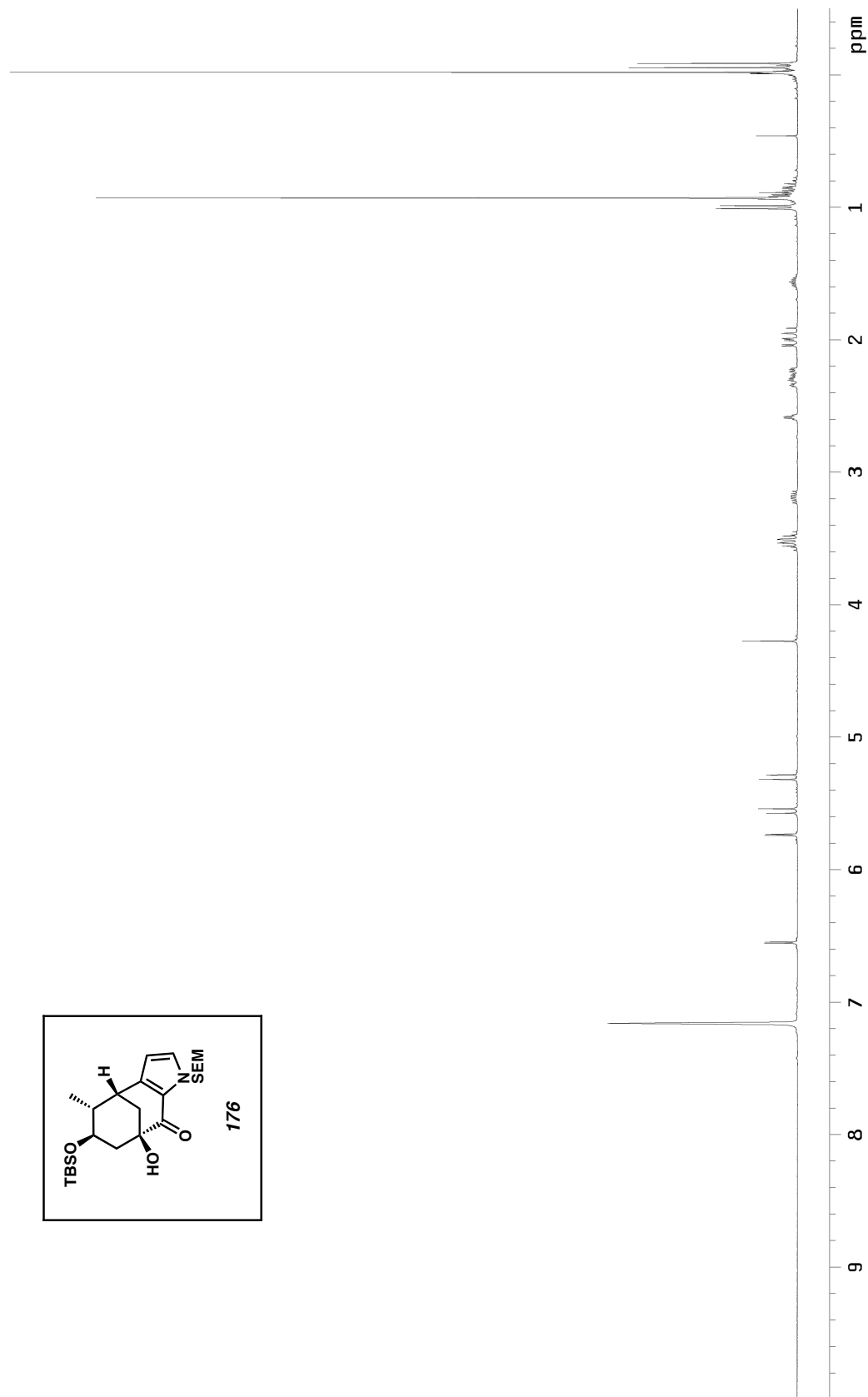


Figure A3.69  $^1\text{H}$  NMR (300 MHz,  $\text{C}_6\text{D}_6$ ) of compound **176**



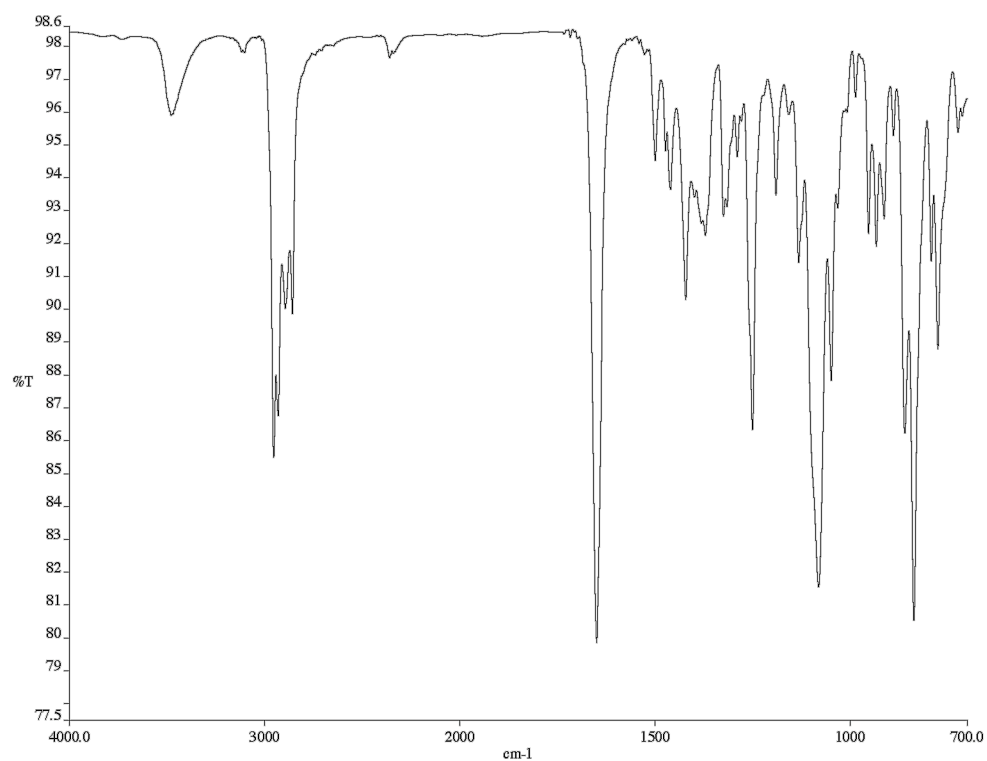


Figure A3.70 Infrared spectrum (thin film/NaCl) of compound **176**

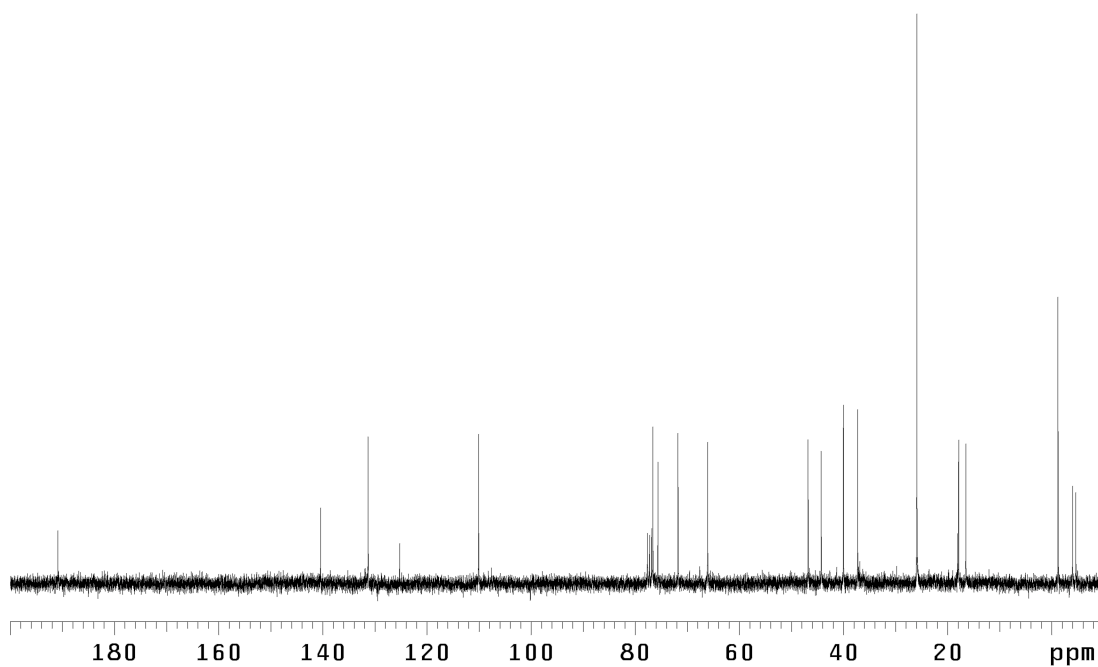


Figure A3.71 <sup>13</sup>C NMR (75 MHz, CDCl<sub>3</sub>) of compound **176**

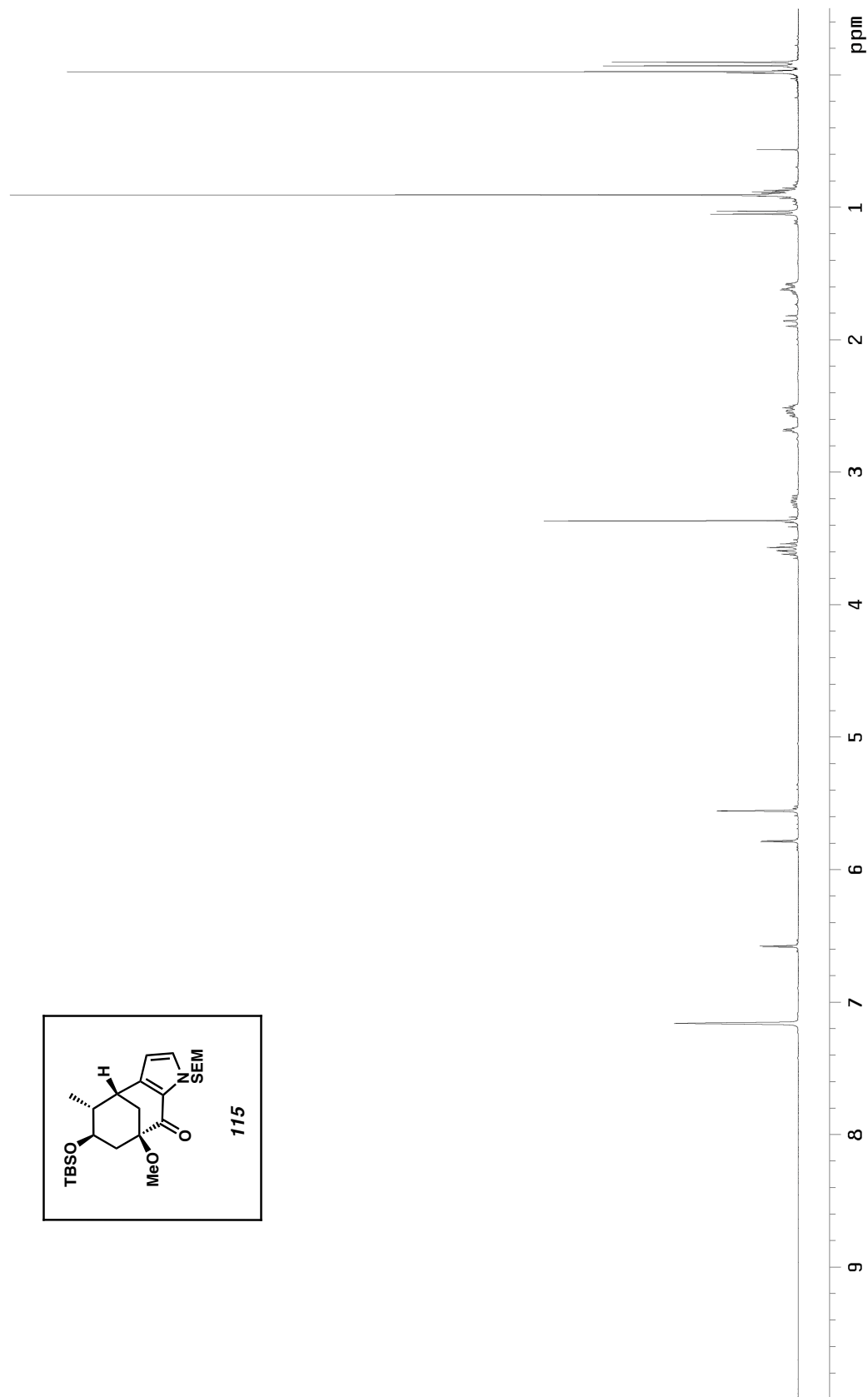


Figure A3.72  $^1\text{H}$  NMR (300 MHz,  $\text{C}_6\text{D}_6$ ) of compound **115**

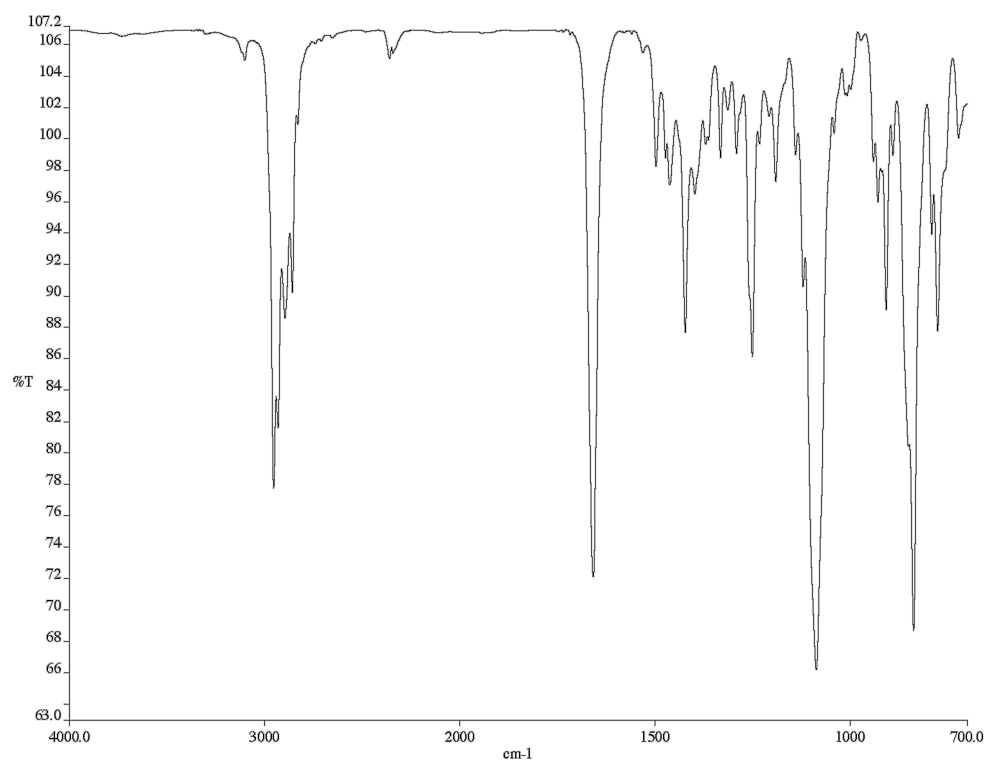


Figure A3.73 Infrared spectrum (thin film/NaCl) of compound **115**

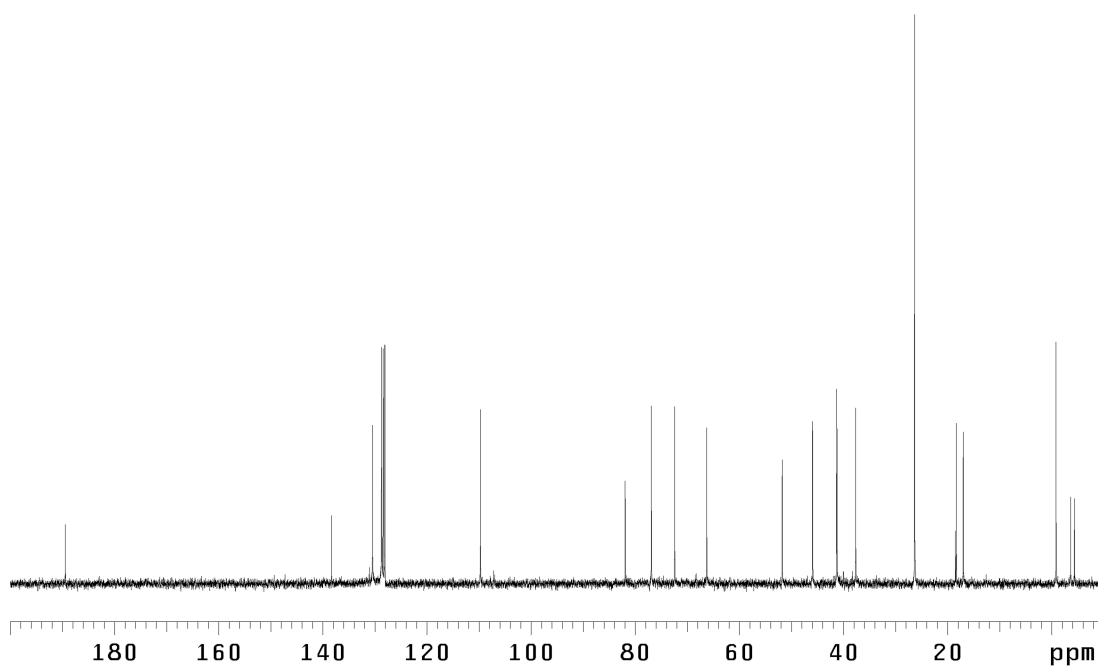


Figure A3.74 <sup>13</sup>C NMR (75 MHz, C<sub>6</sub>D<sub>6</sub>) of compound **115**

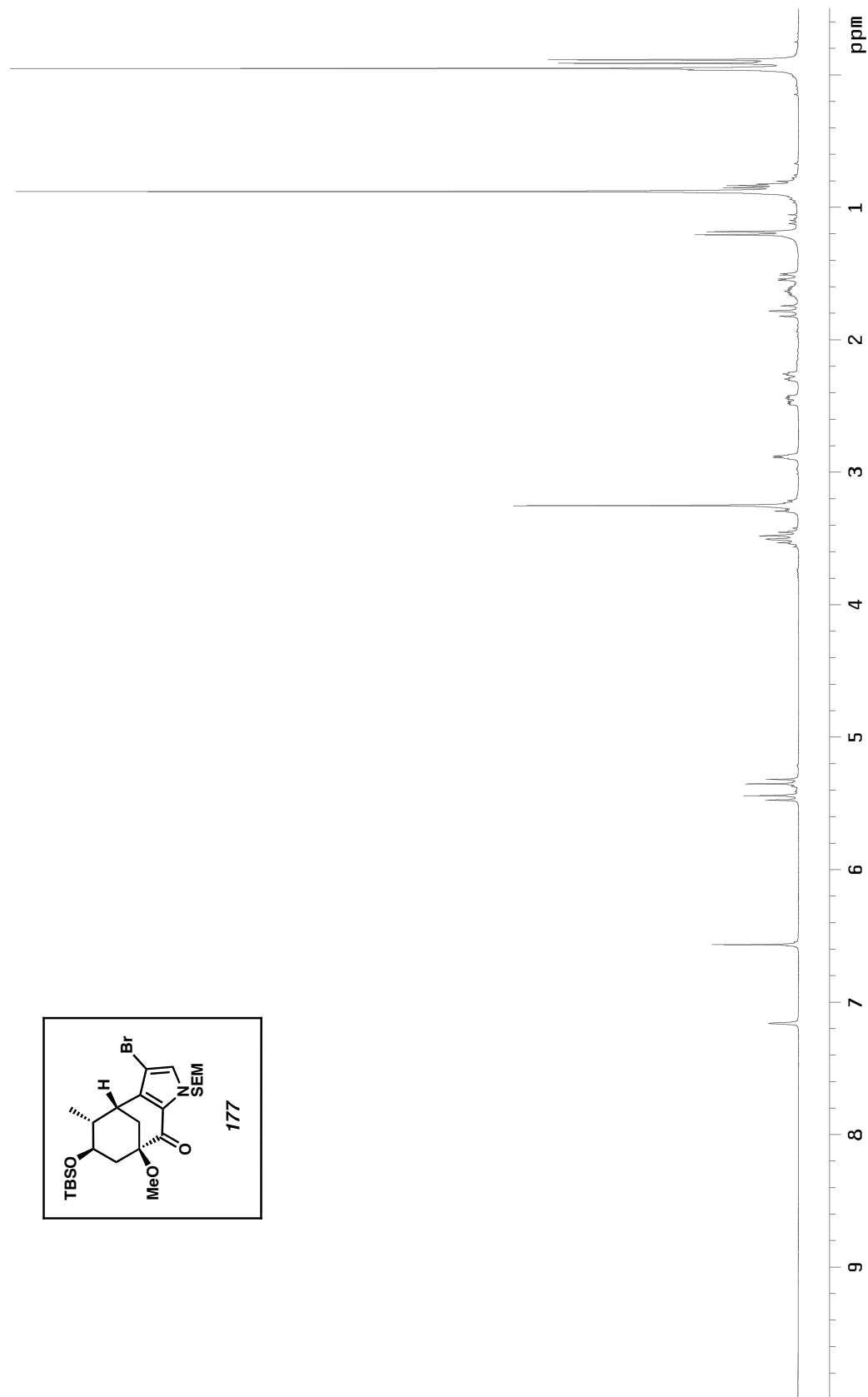


Figure A3.75  $^1\text{H}$  NMR (300 MHz,  $\text{C}_6\text{D}_6$ ) of compound **177**

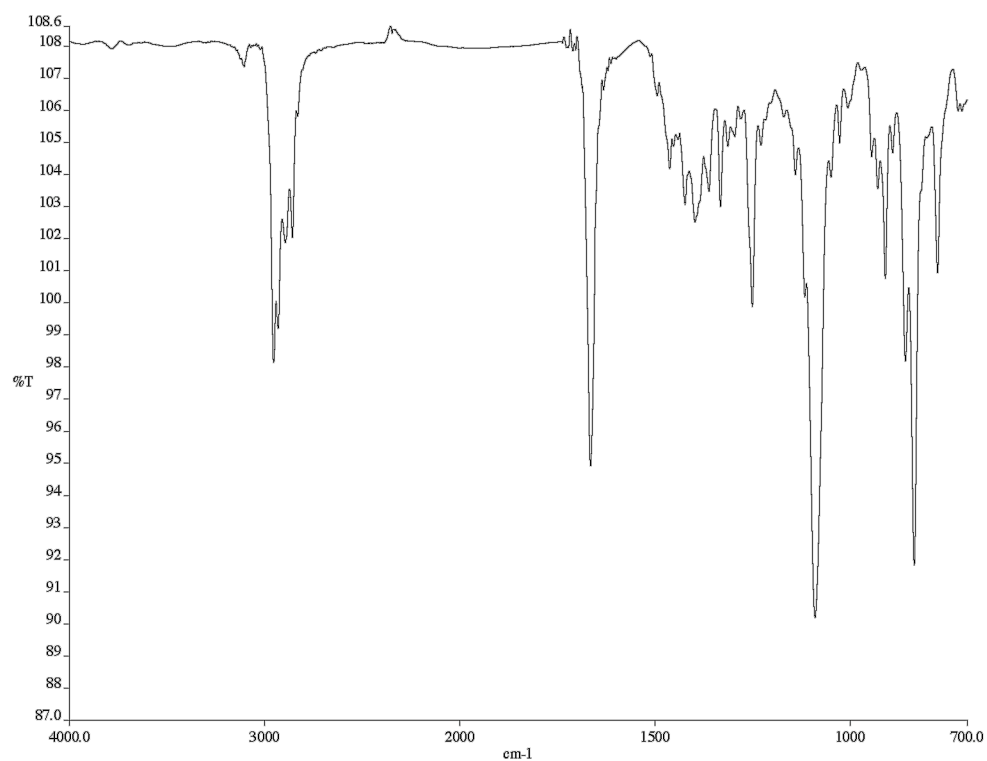


Figure A3.76 Infrared spectrum (thin film/NaCl) of compound **177**

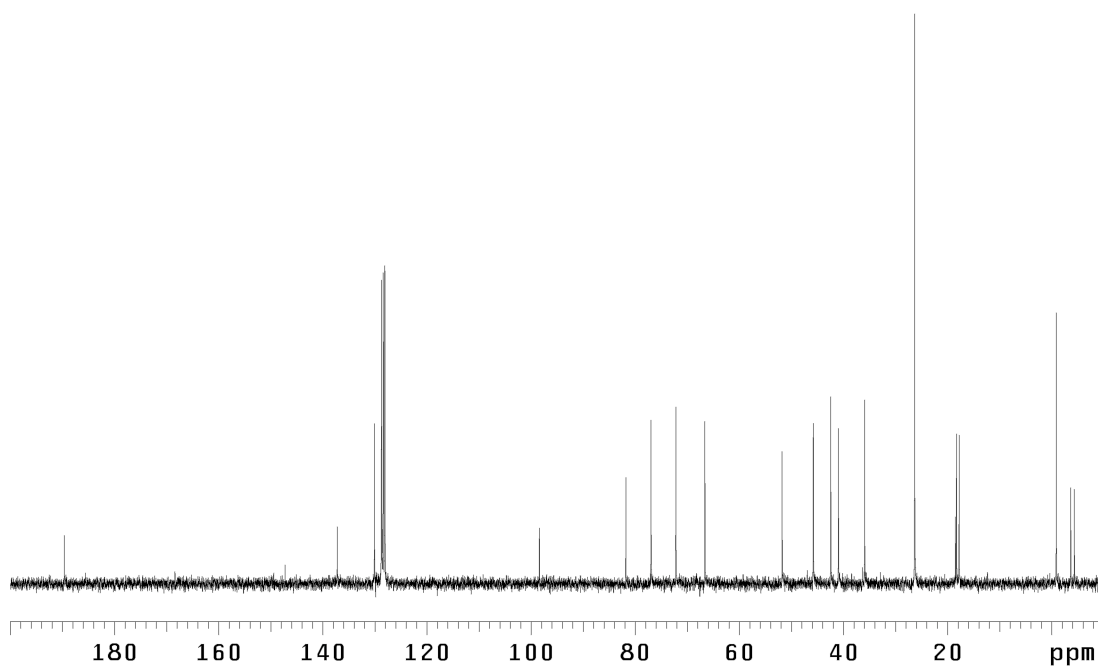


Figure A3.77  $^{13}\text{C}$  NMR (75 MHz,  $\text{C}_6\text{D}_6$ ) of compound **177**

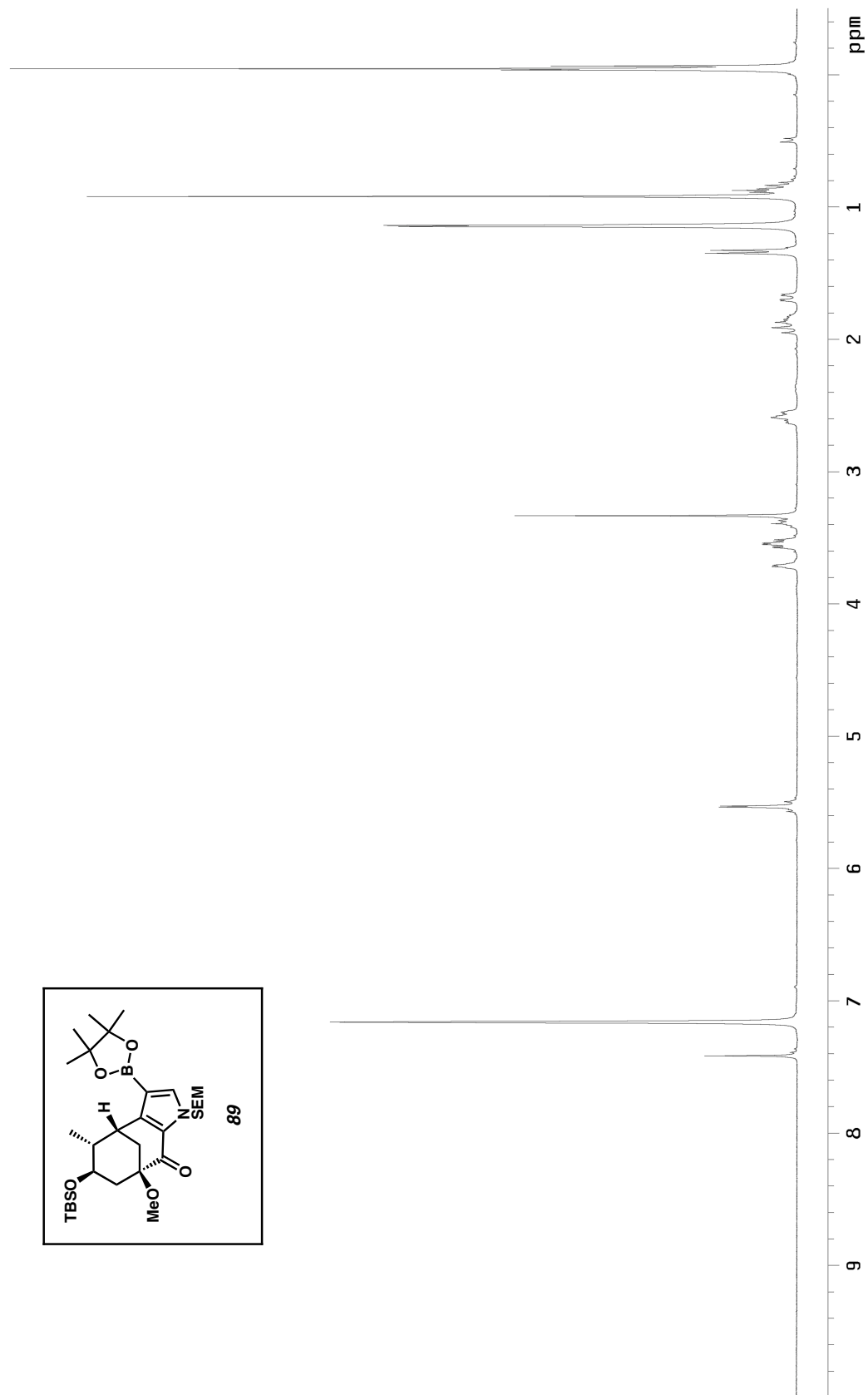


Figure A3.78  $^1\text{H}$  NMR (300 MHz,  $\text{CDCl}_3$ ) of compound **89**

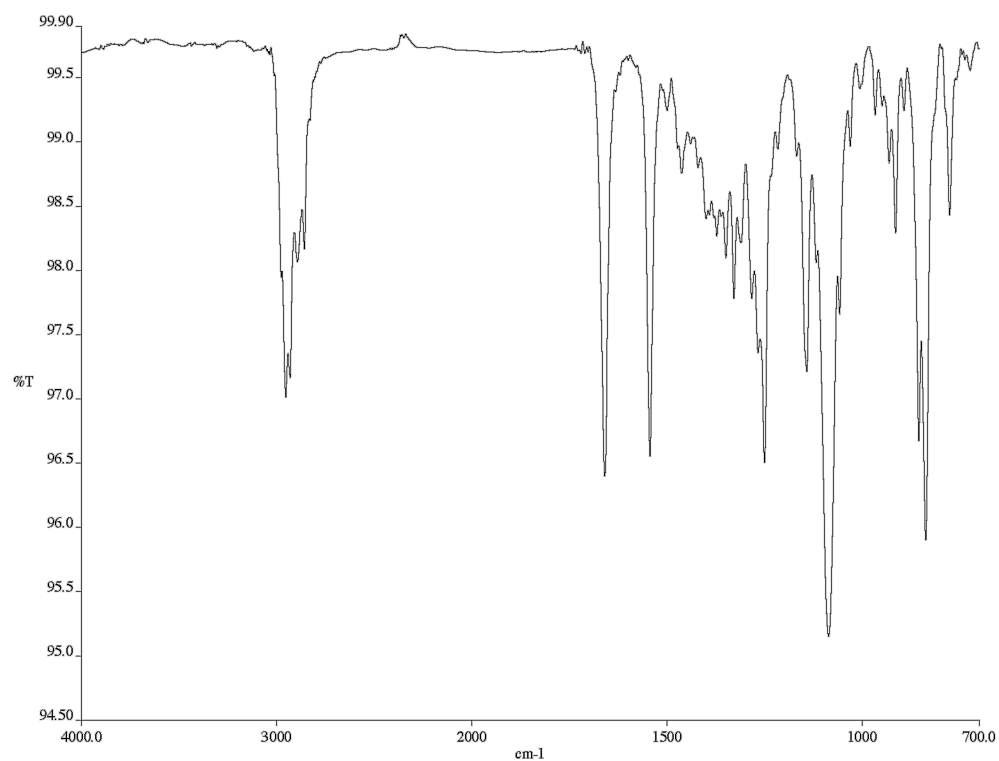


Figure A3.79 Infrared spectrum (thin film/NaCl) of compound **89**

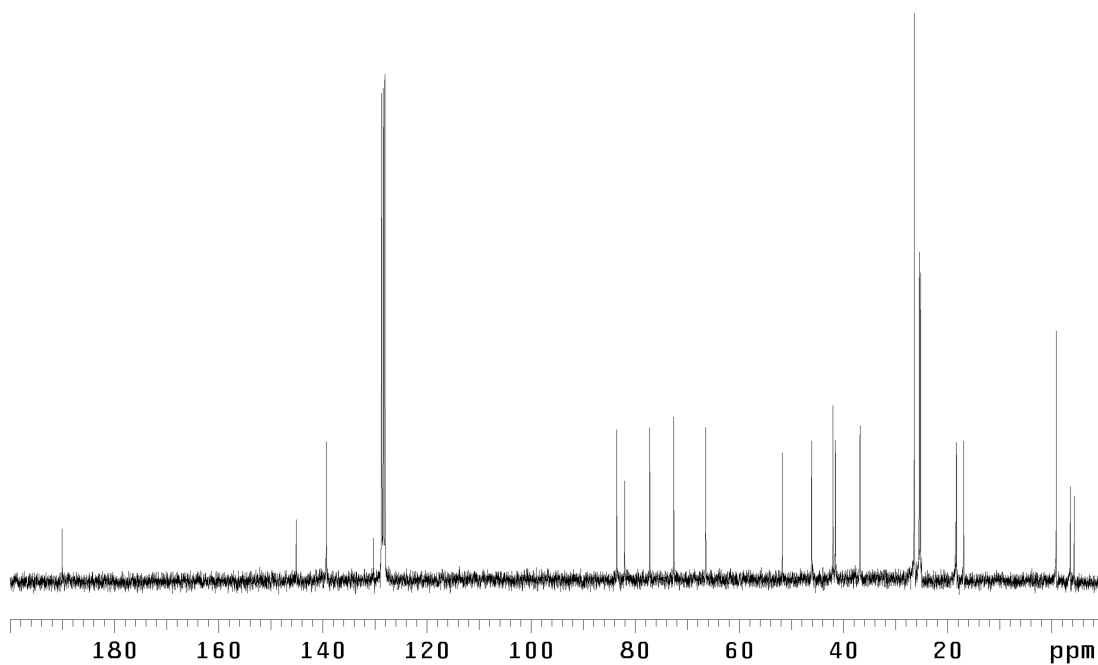


Figure A3.80 <sup>13</sup>C NMR (75 MHz, C<sub>6</sub>D<sub>6</sub>) of compound **89**

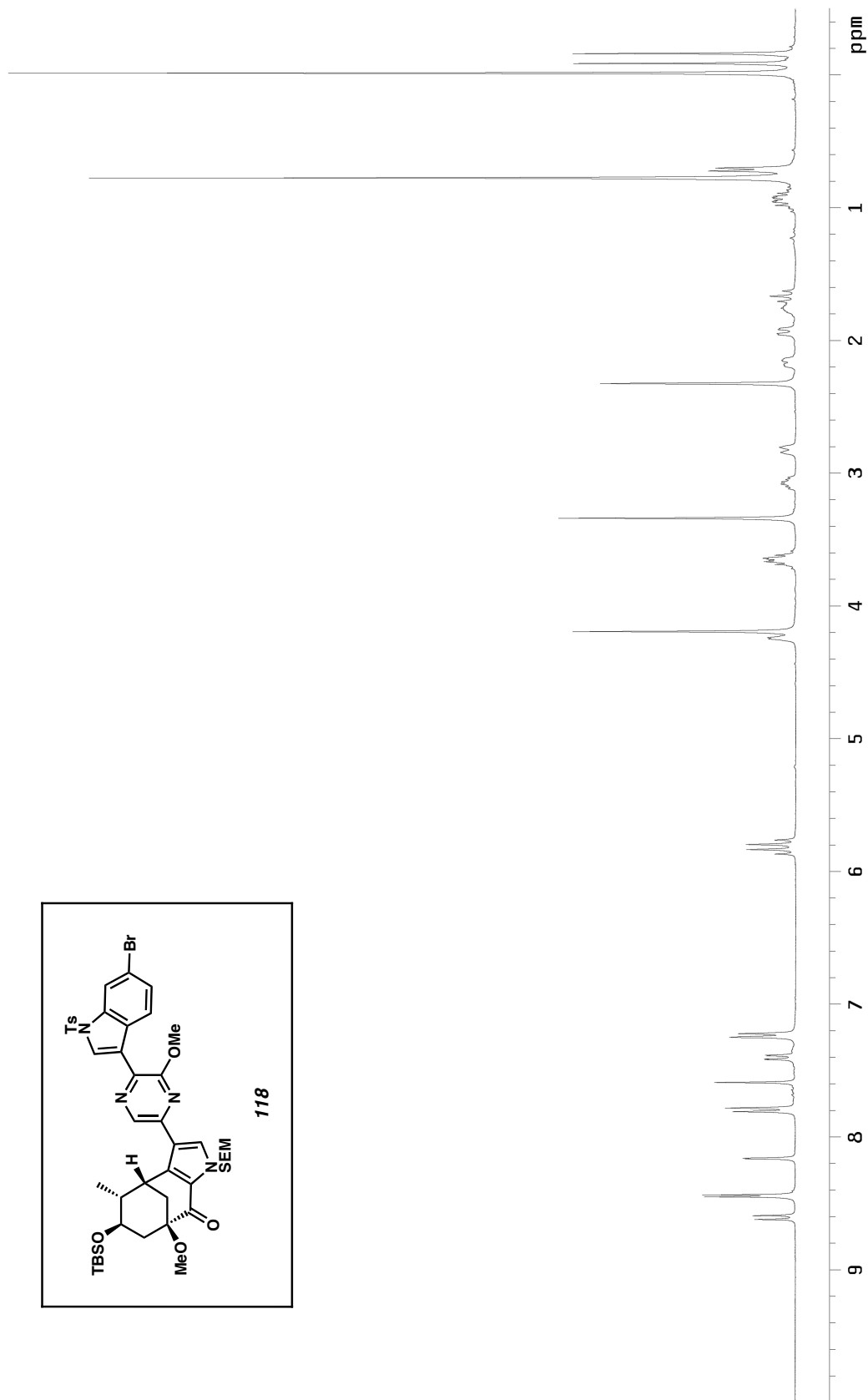


Figure A3.81  $^1\text{H}$  NMR (300 MHz,  $\text{CDCl}_3$ ) of compound **118**



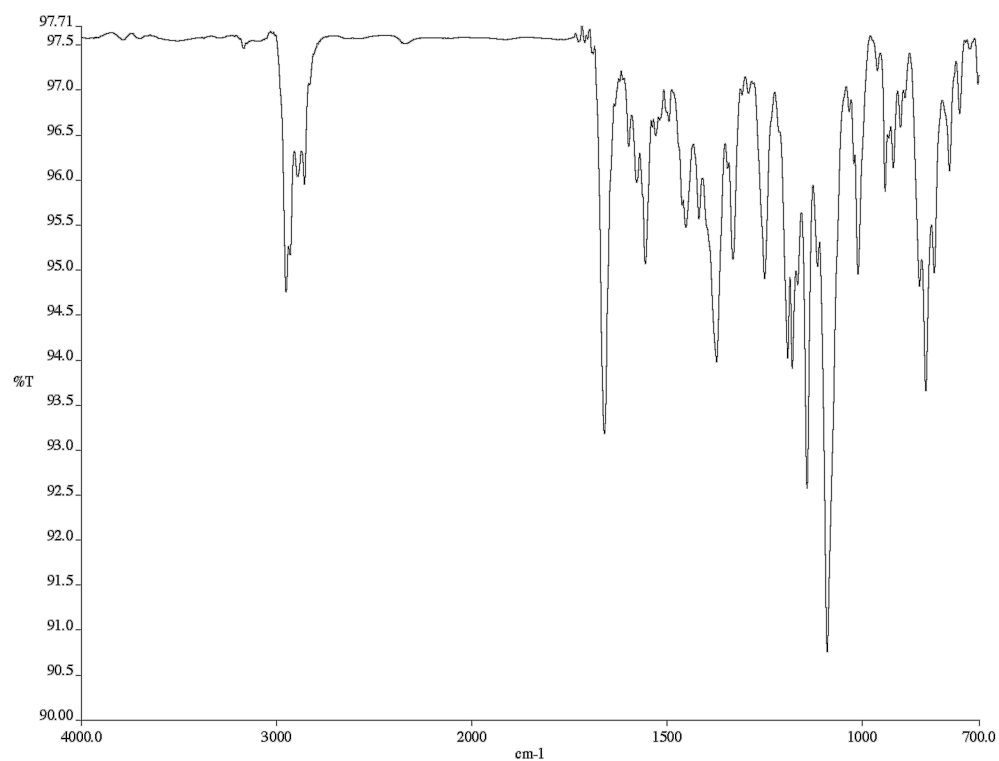


Figure A3.82 Infrared spectrum (thin film/NaCl) of compound **118**

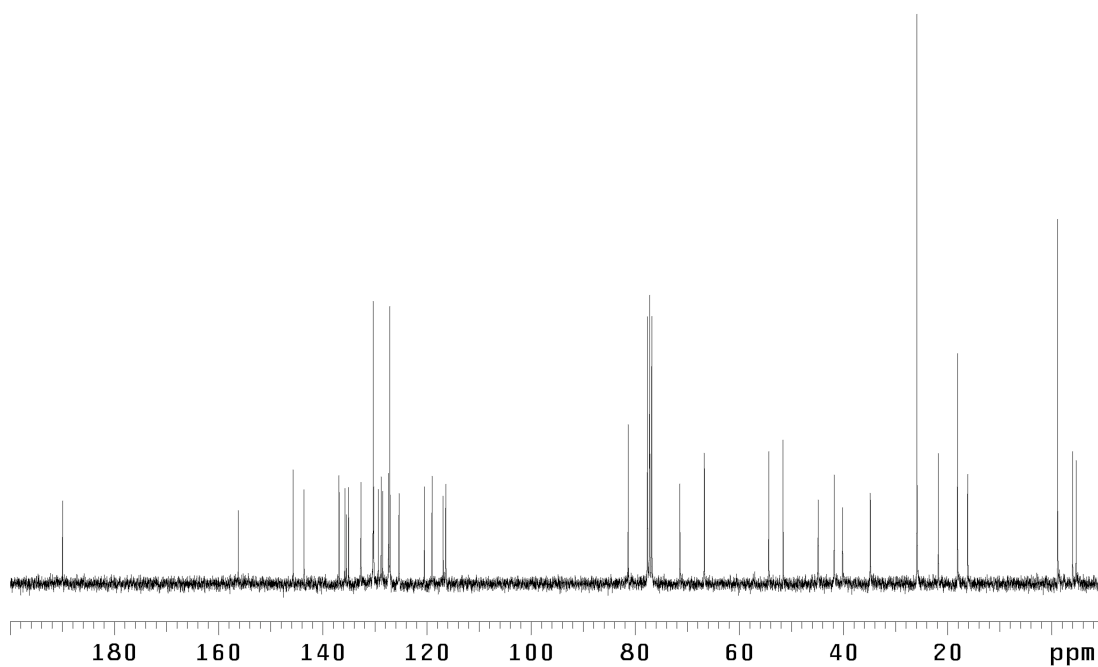


Figure A3.83 <sup>13</sup>C NMR (75 MHz, CDCl<sub>3</sub>) of compound **118**

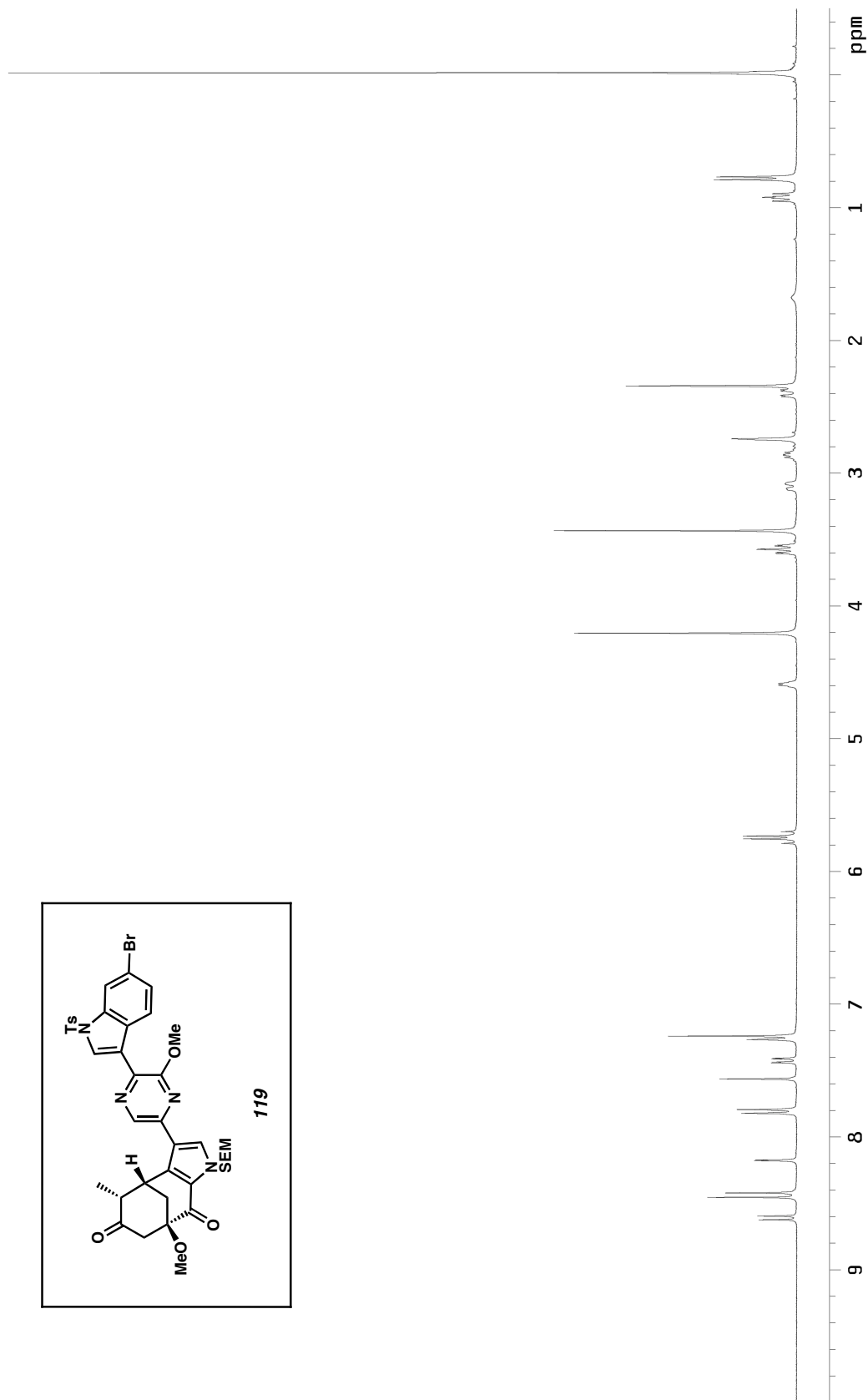


Figure A3.84  $^1\text{H}$  NMR (300 MHz,  $\text{CDCl}_3$ ) of compound **119**

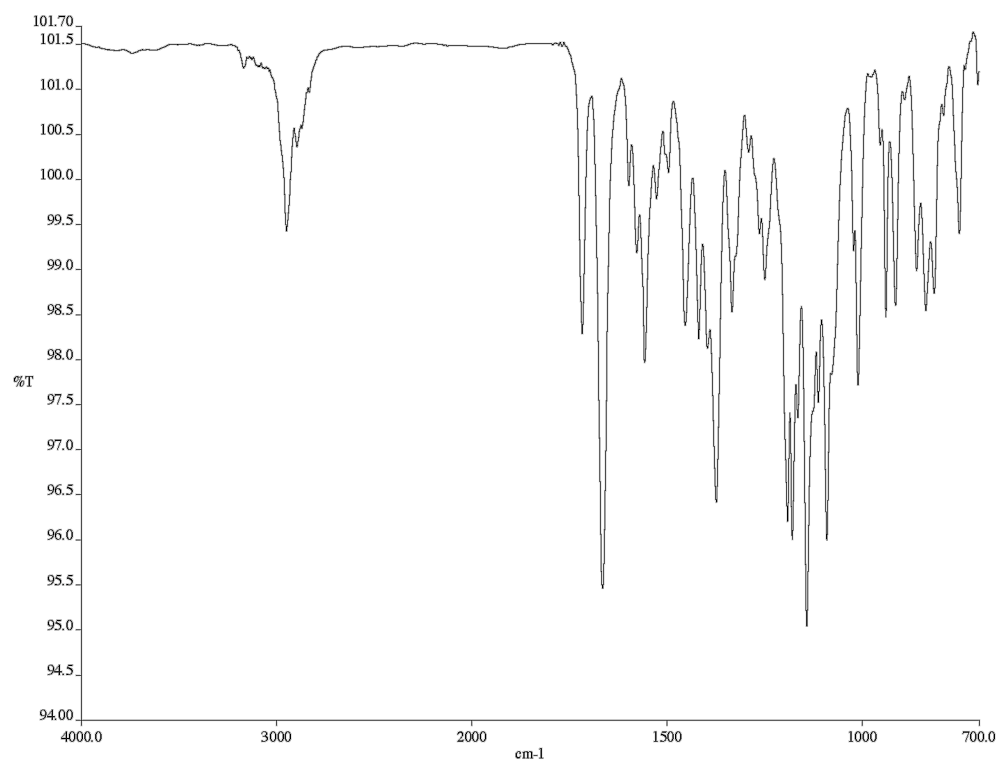


Figure A3.85 Infrared spectrum (thin film/NaCl) of compound **119**

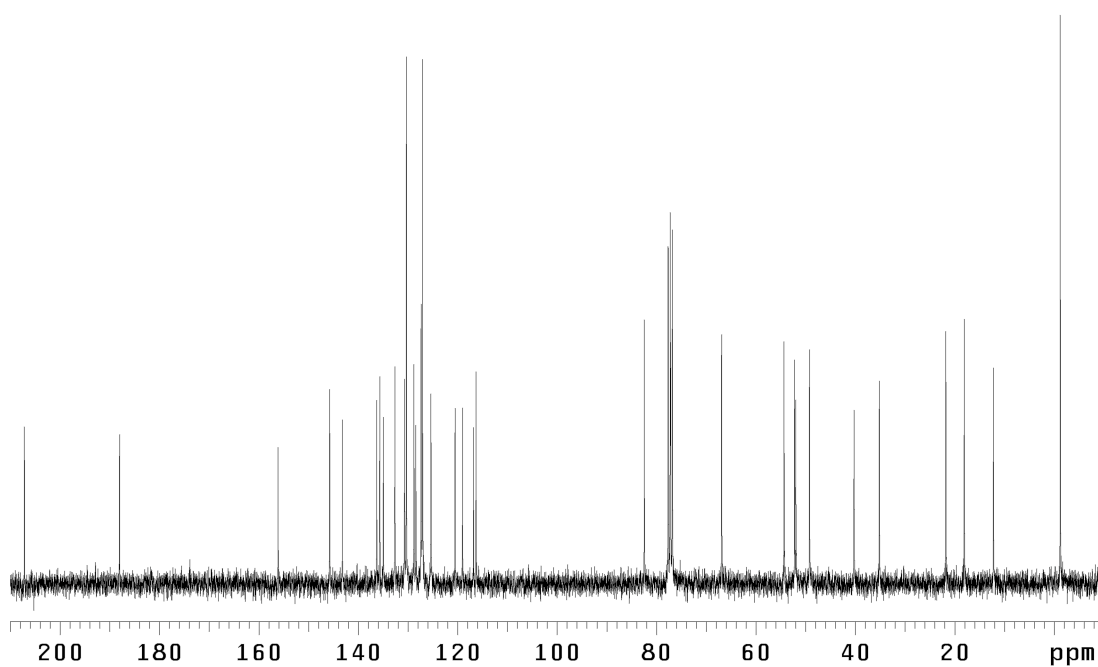


Figure A3.86 <sup>13</sup>C NMR (75 MHz, CDCl<sub>3</sub>) of compound **119**

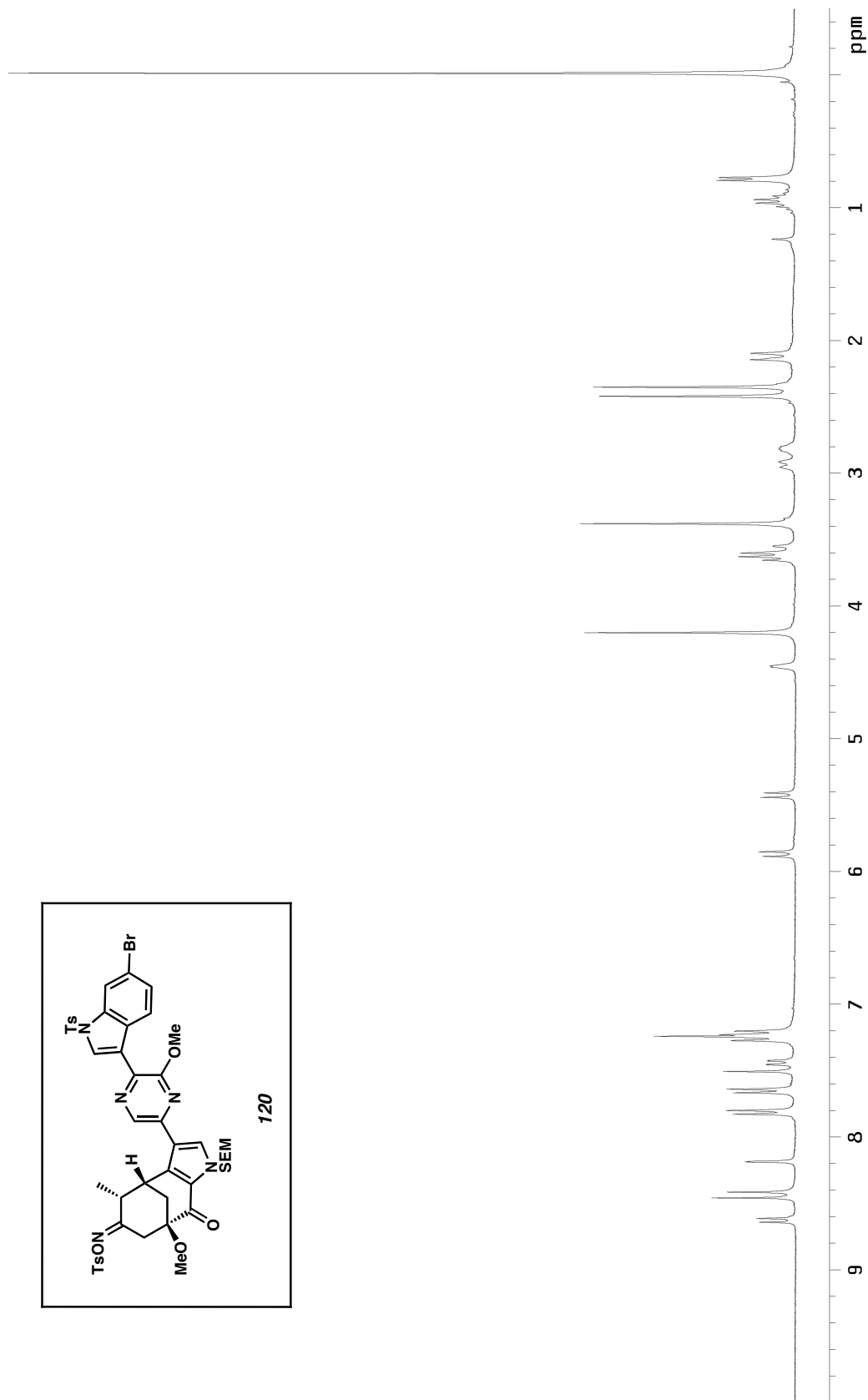


Figure A3.87  $^1\text{H}$  NMR (300 MHz,  $\text{CDCl}_3$ ) of compound **120**

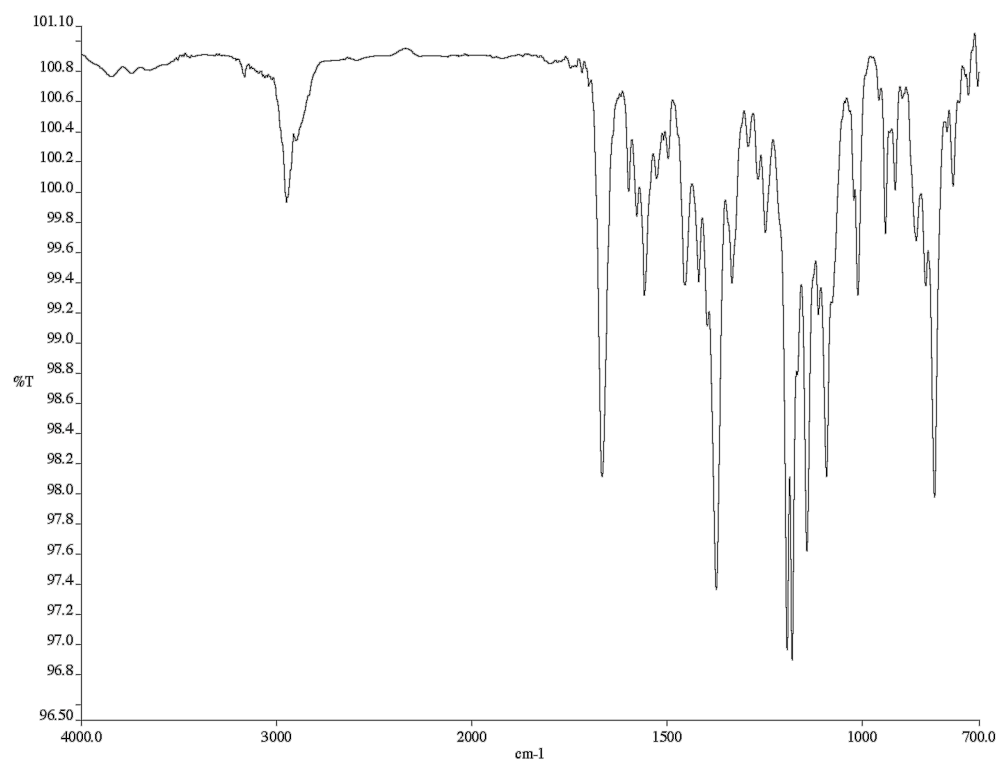


Figure A3.88 Infrared spectrum (thin film/NaCl) of compound **120**

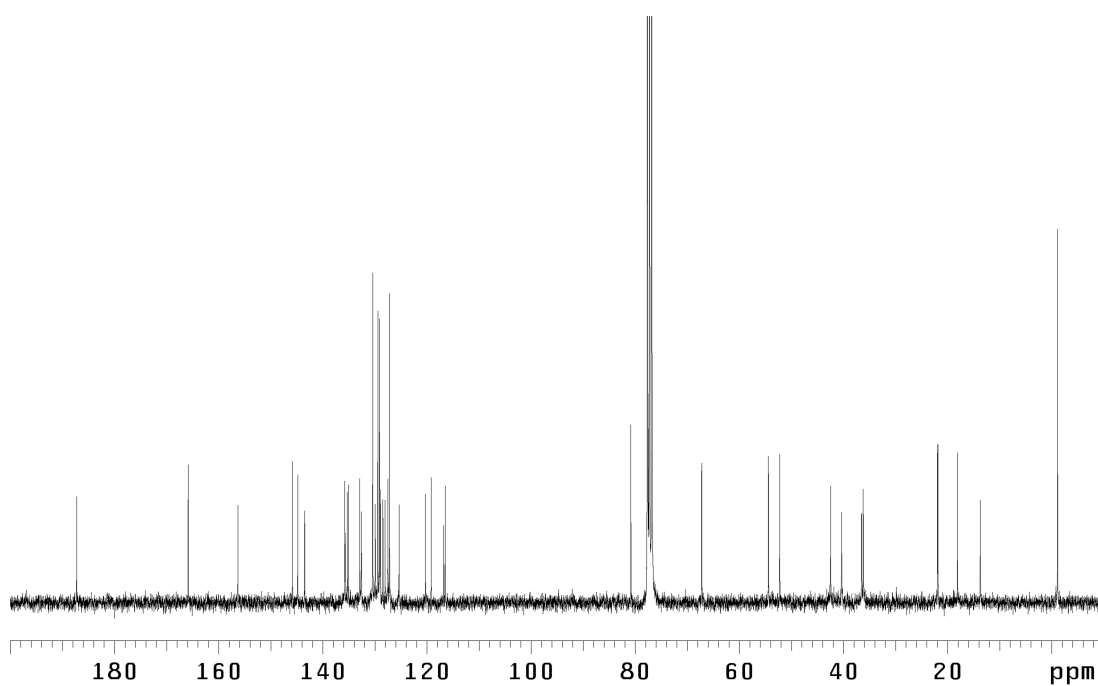


Figure A3.89 <sup>13</sup>C NMR (75 MHz, CDCl<sub>3</sub>) of compound **120**

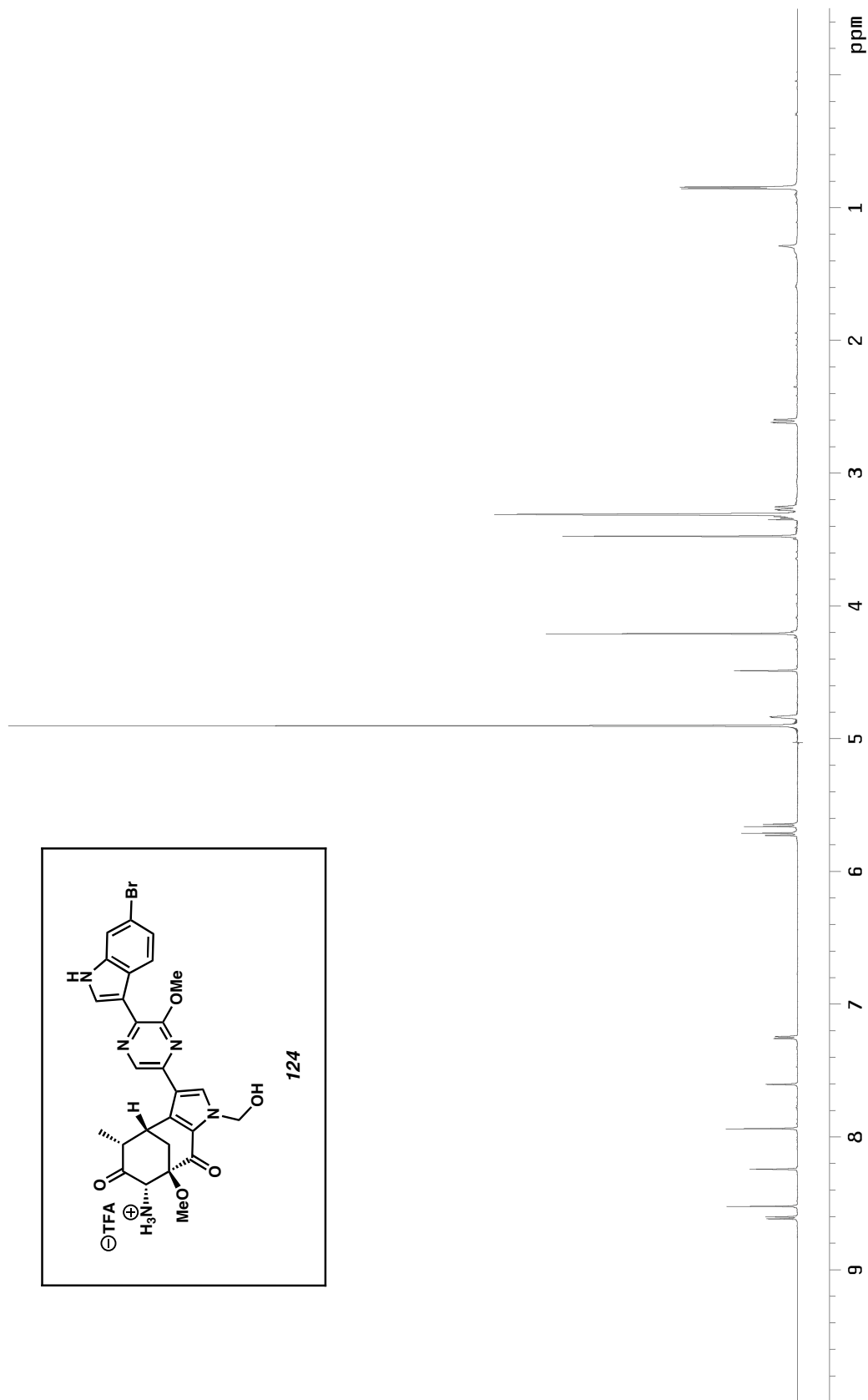


Figure A3.90 <sup>1</sup>H NMR (600 MHz, CD<sub>3</sub>OD) of compound **124**

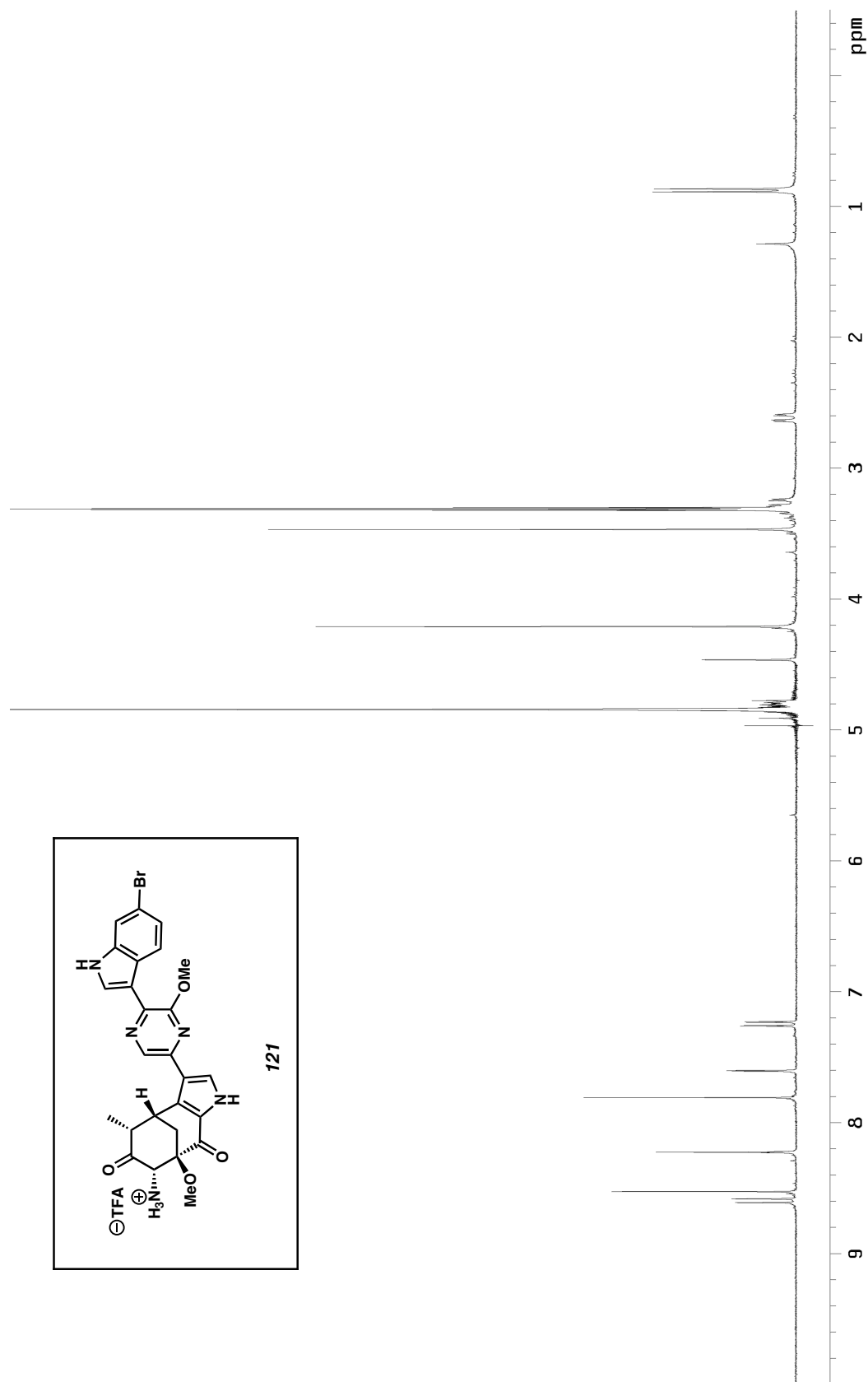


Figure A3.91 <sup>1</sup>H NMR (300 MHz, CD<sub>3</sub>OD) of compound **121**

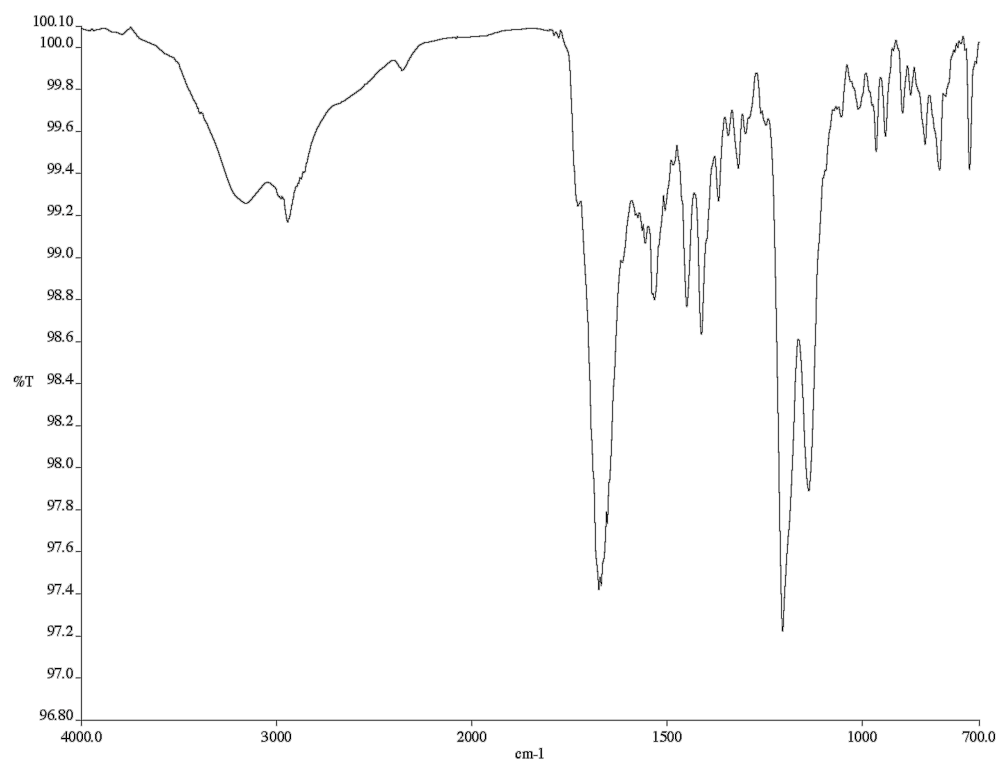


Figure A3.92 Infrared spectrum (thin film/NaCl) of compound **121**

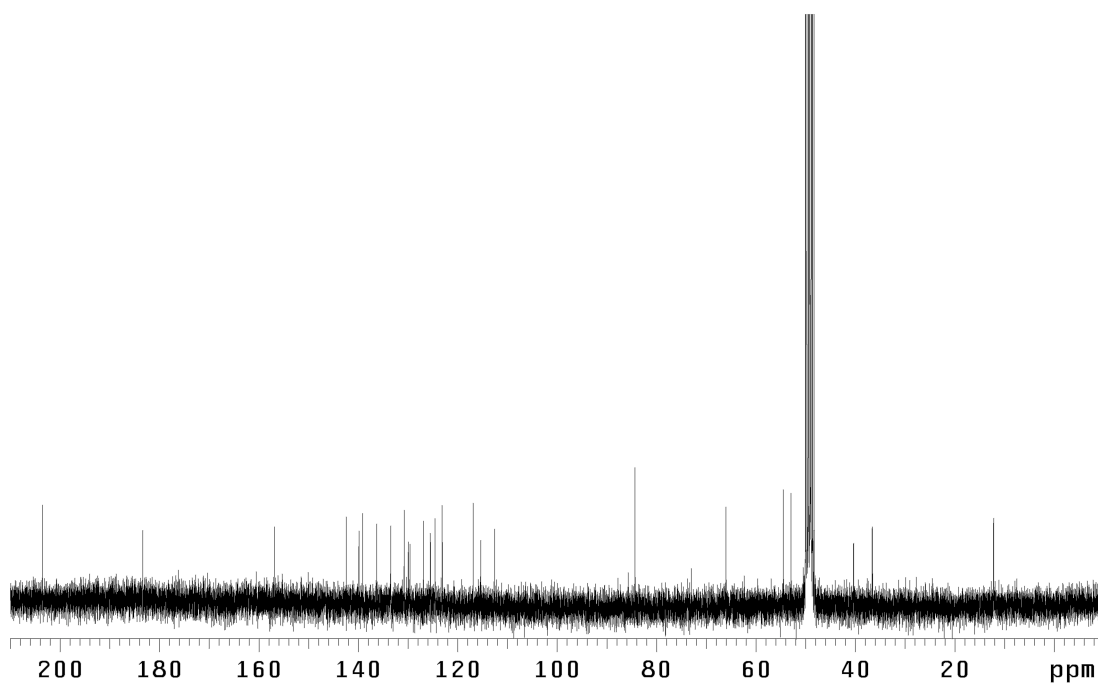


Figure A3.93 <sup>13</sup>C NMR (75 MHz, CD<sub>3</sub>OD) of compound **121**



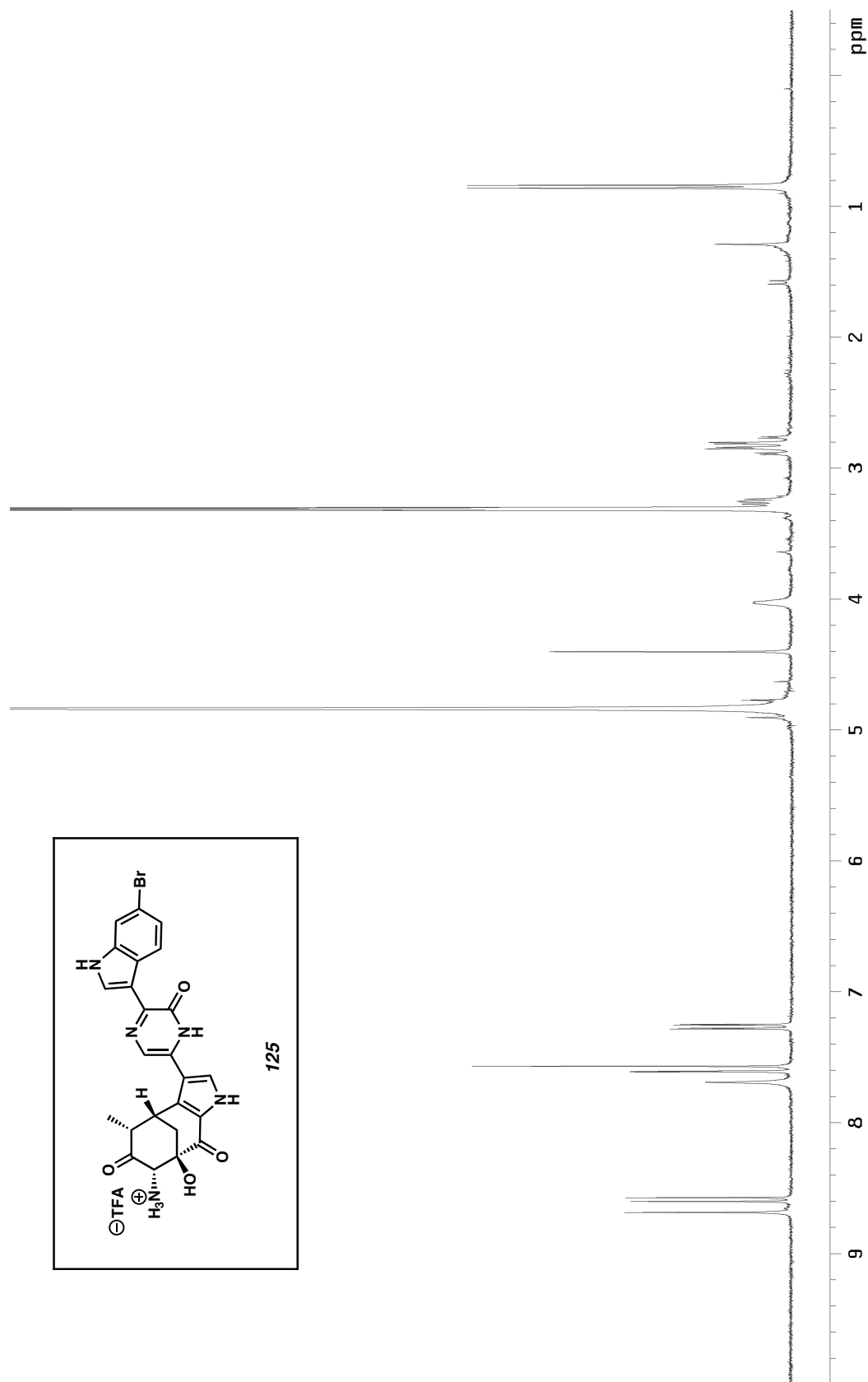


Figure A3.94  $^1\text{H}$  NMR (300 MHz,  $\text{CD}_3\text{OD}$ ) of compound **125**

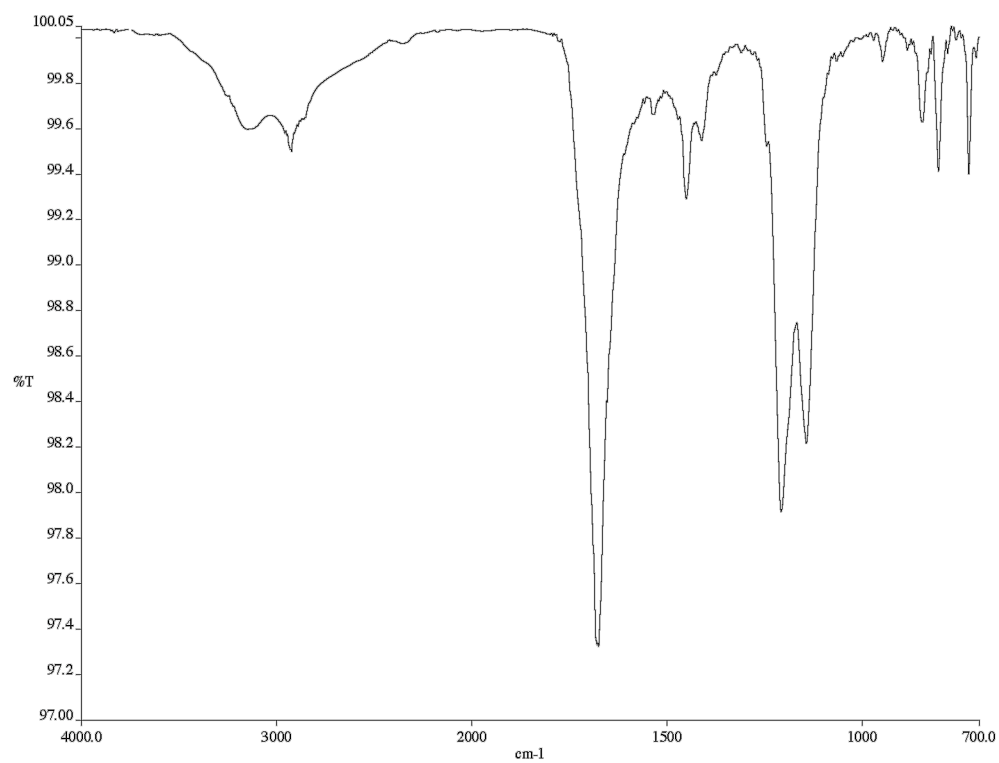


Figure A3.95 Infrared spectrum (thin film/NaCl) of compound **125**

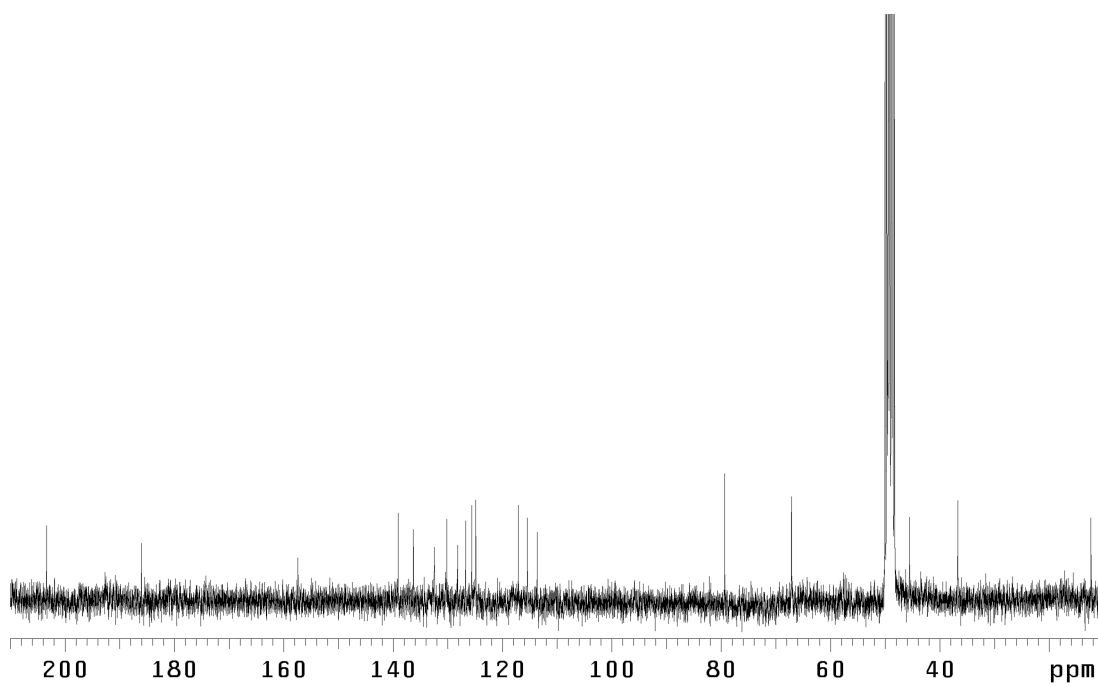


Figure A3.96 <sup>13</sup>C NMR (75 MHz, CD<sub>3</sub>OD) of compound **125**

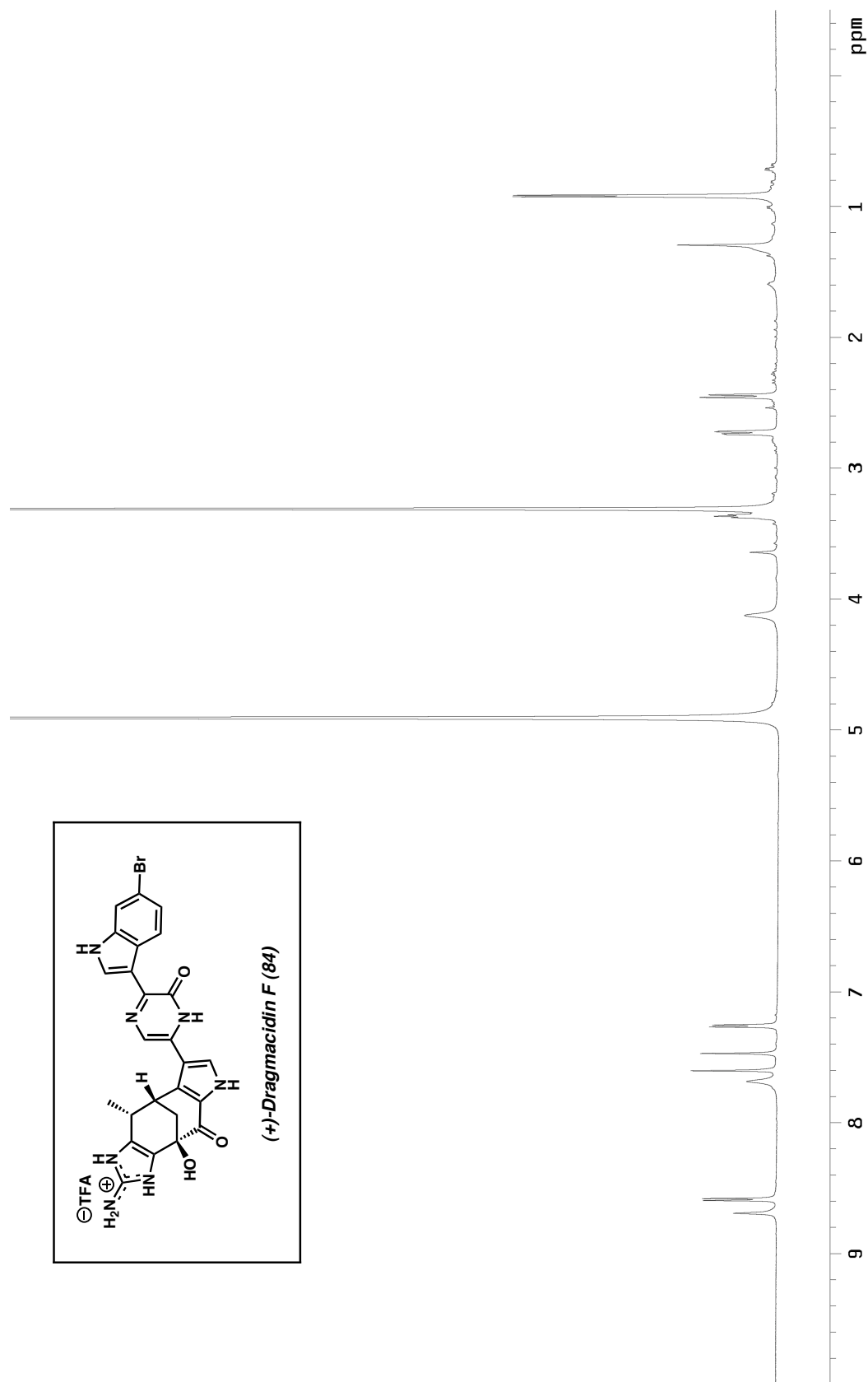


Figure A3.97  $^1\text{H}$  NMR (600 MHz,  $\text{CD}_3\text{OD}$ ) of (+)-dragmacidin F (84)

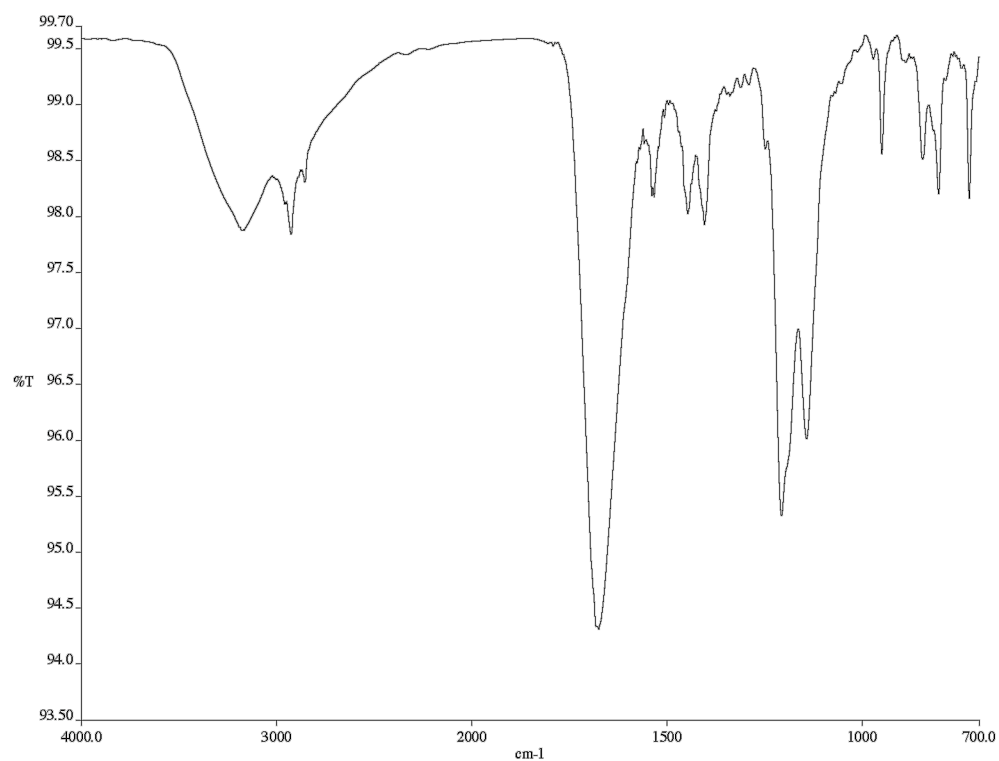


Figure A3.98 Infrared spectrum (thin film/NaCl) of (+)-dragmacidin F (**84**)

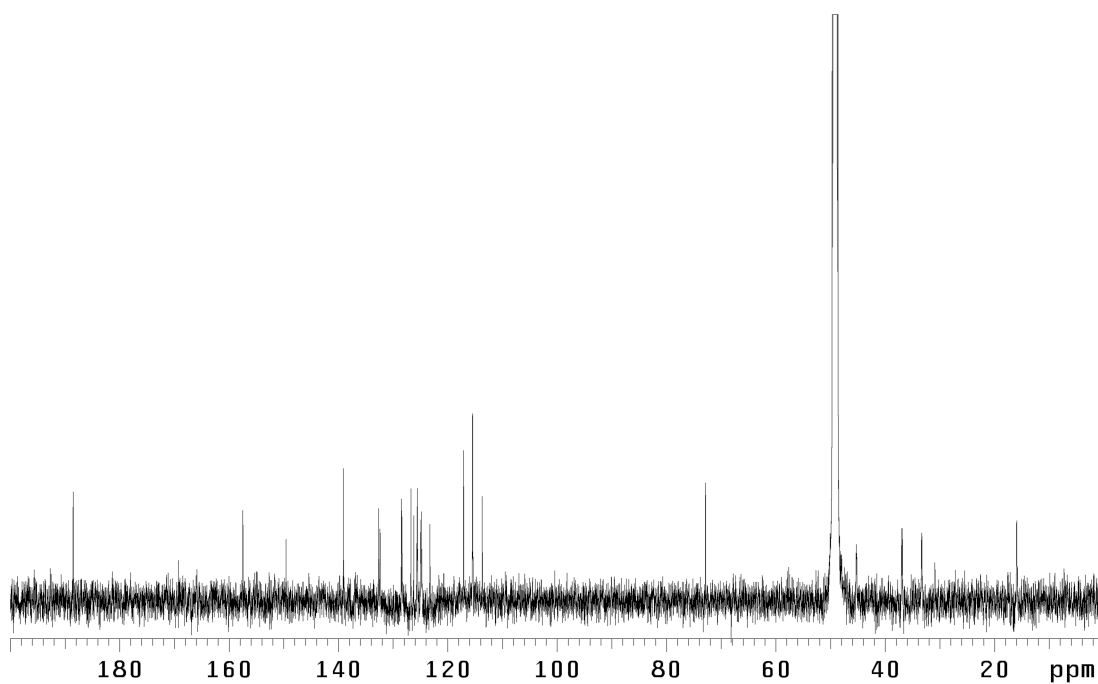


Figure A3.99 <sup>13</sup>C NMR (125 MHz, CD<sub>3</sub>OD) of (+)-dragmacidin F (**84**)

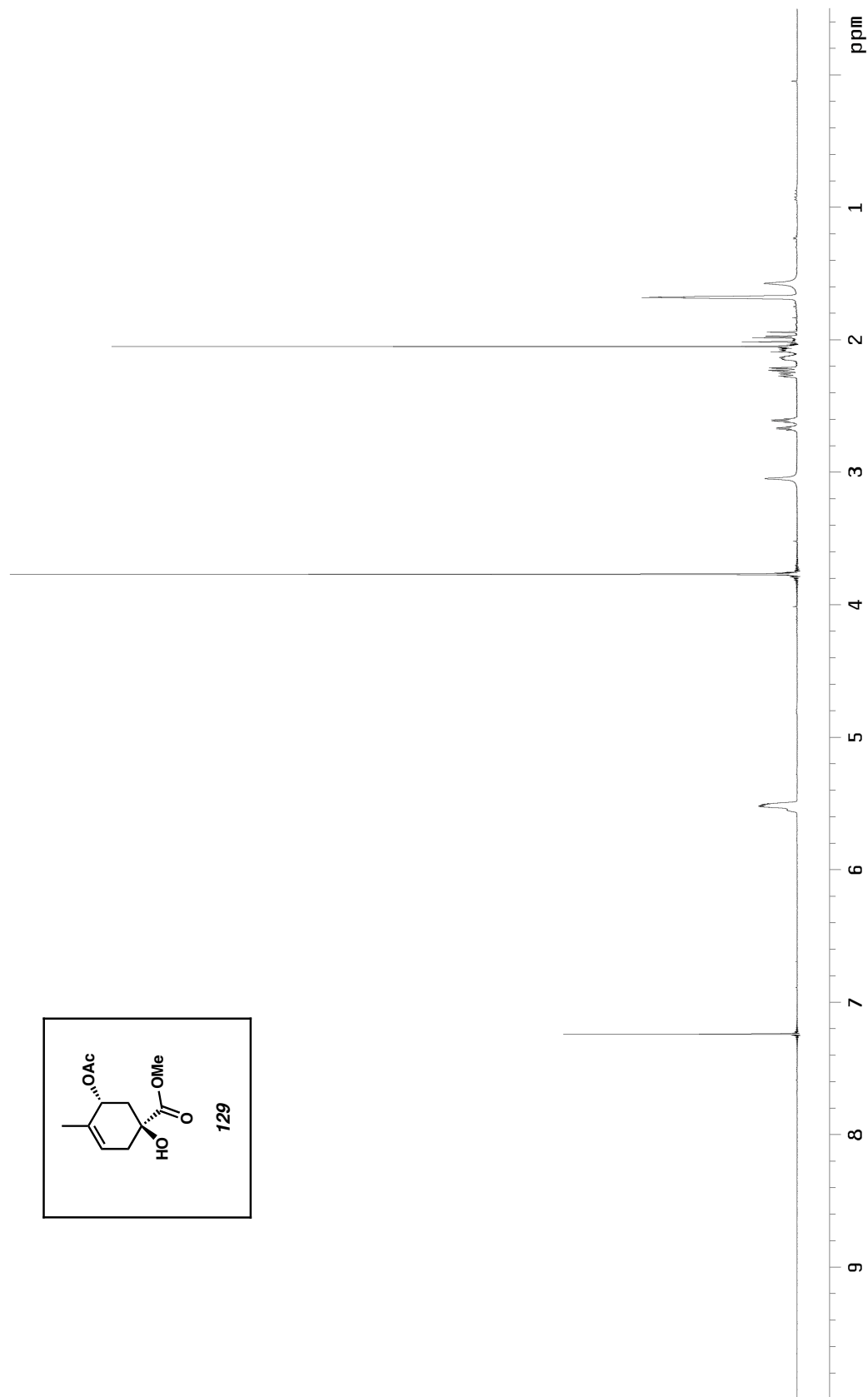


Figure A3.100  $^1\text{H}$  NMR (300 MHz,  $\text{CDCl}_3$ ) of compound **129**

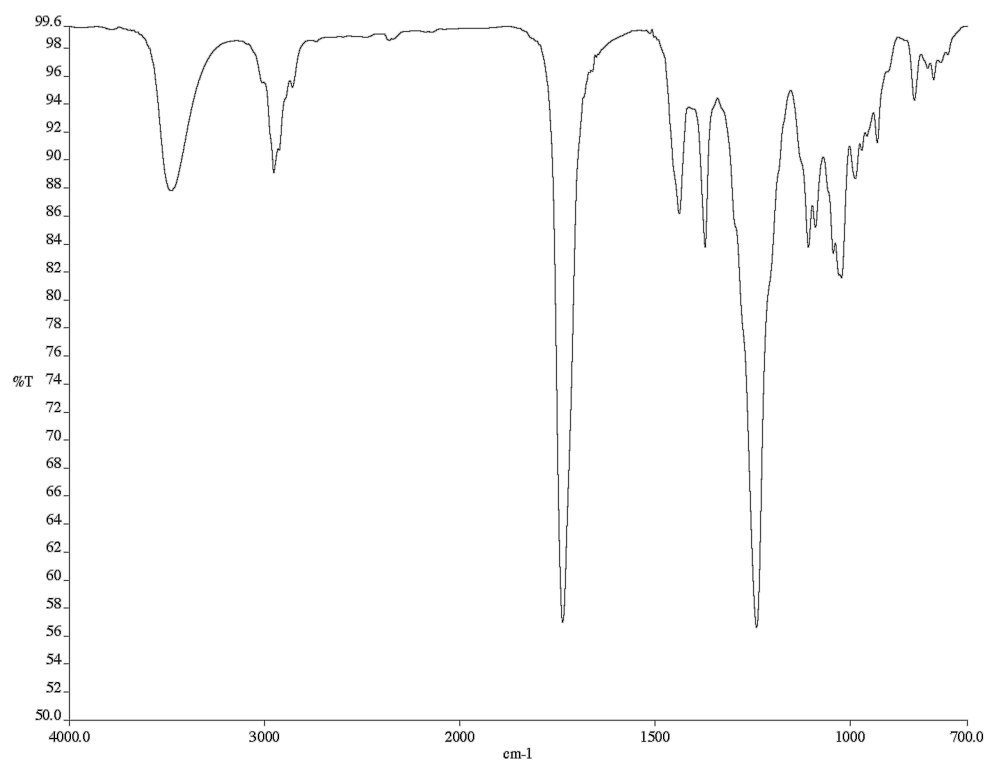


Figure A3.101 Infrared spectrum (thin film/NaCl) of compound **129**

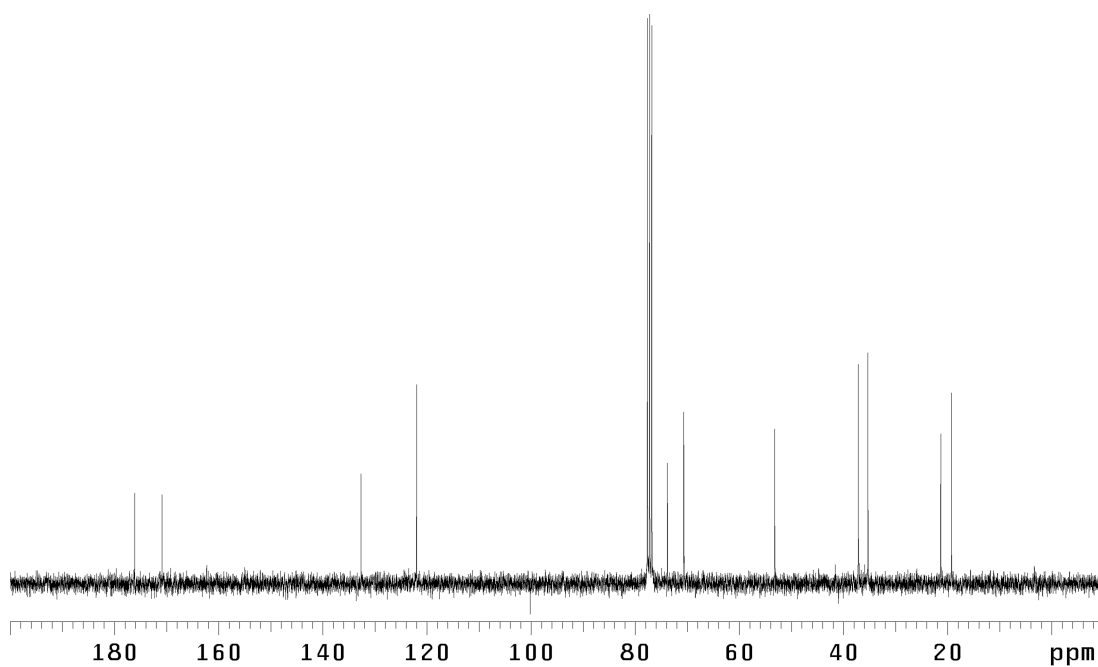


Figure A3.102 <sup>13</sup>C NMR (75 MHz, CDCl<sub>3</sub>) of compound **129**

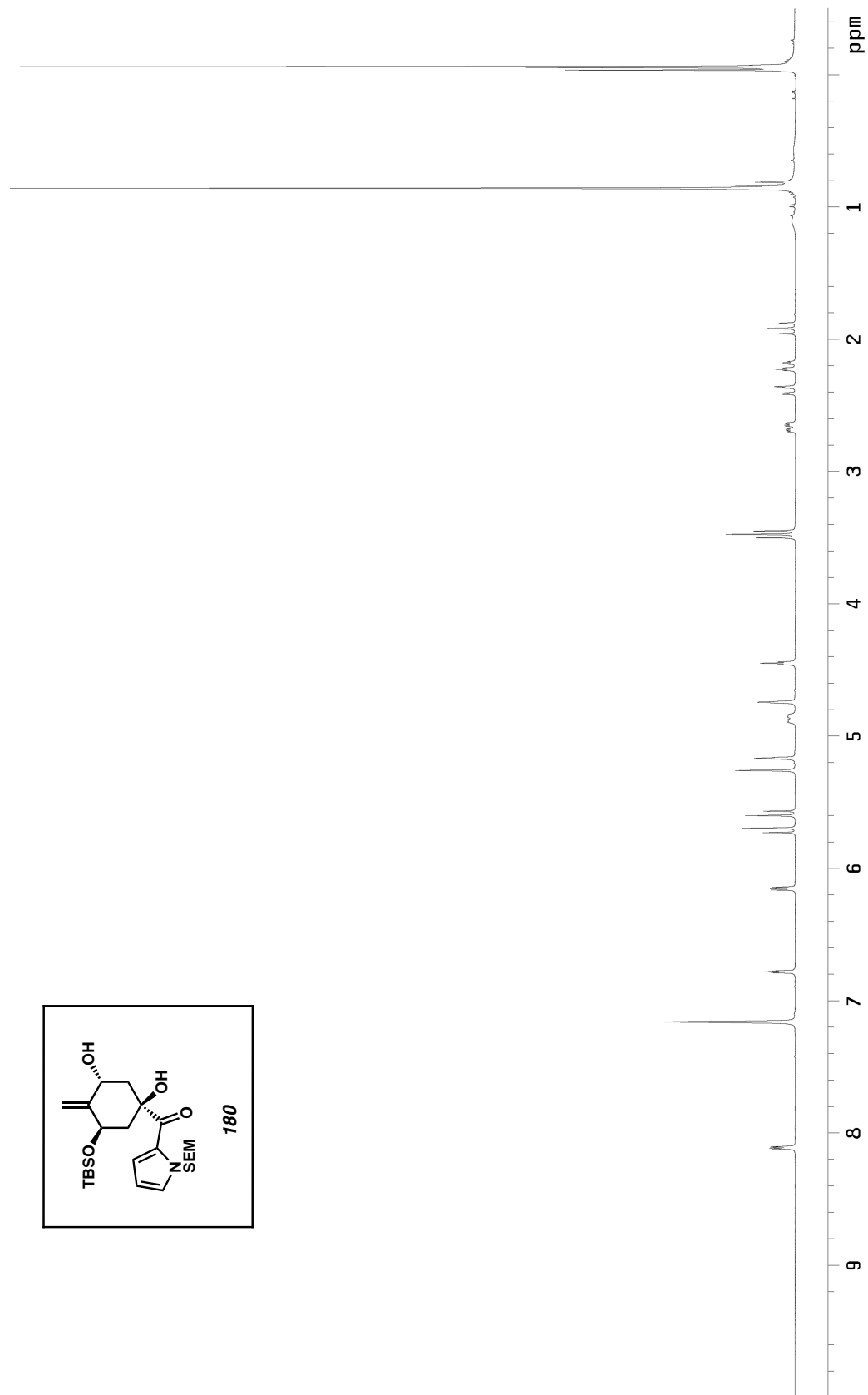
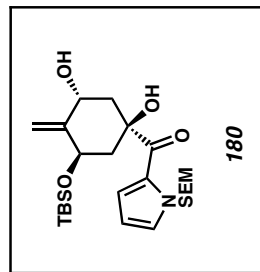


Figure A3.103  $^1\text{H}$  NMR (300 MHz,  $\text{C}_6\text{D}_6$ ) of compound **180**

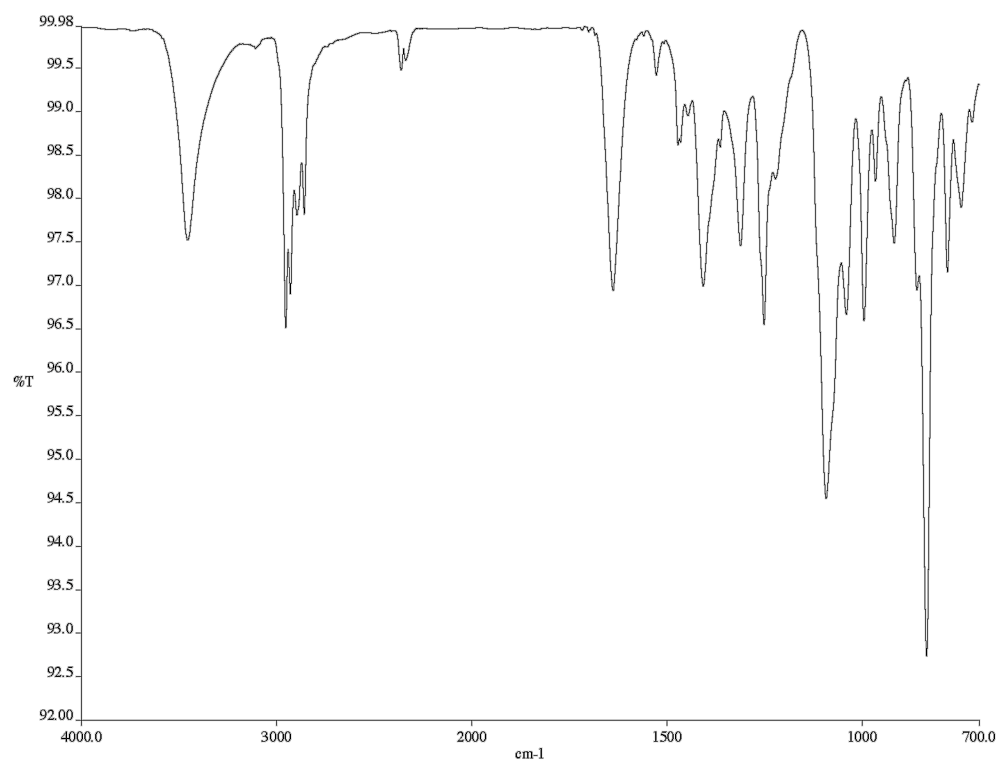


Figure A3.104 Infrared spectrum (thin film/NaCl) of compound **180**

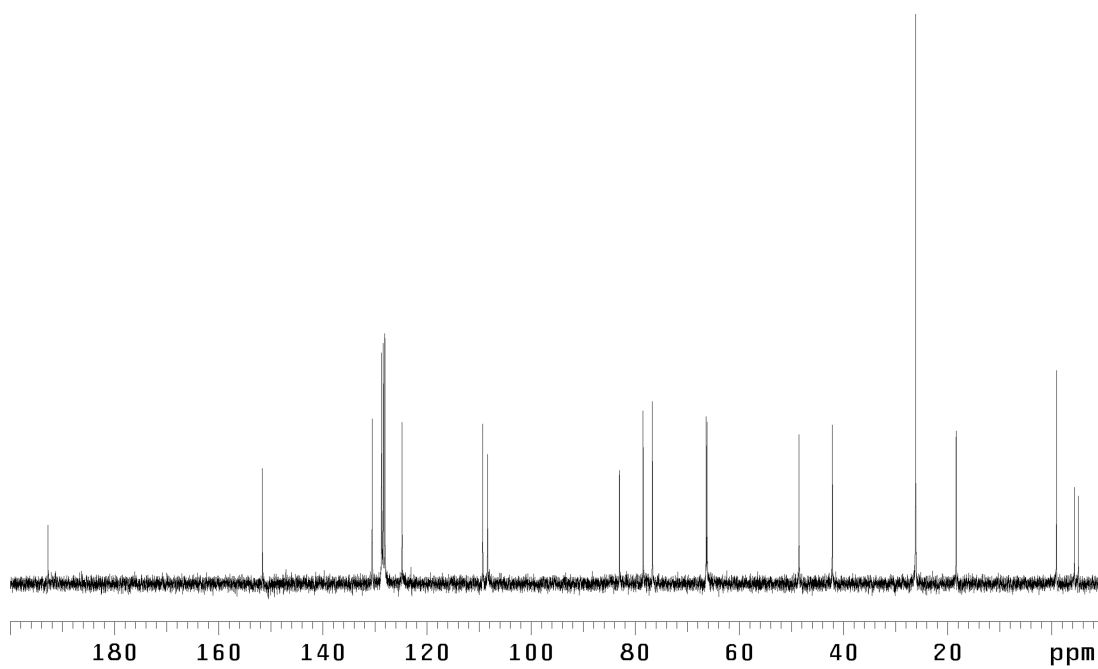


Figure A3.105 <sup>13</sup>C NMR (75 MHz, C<sub>6</sub>D<sub>6</sub>) of compound **180**



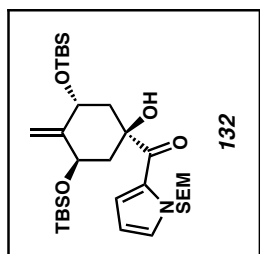
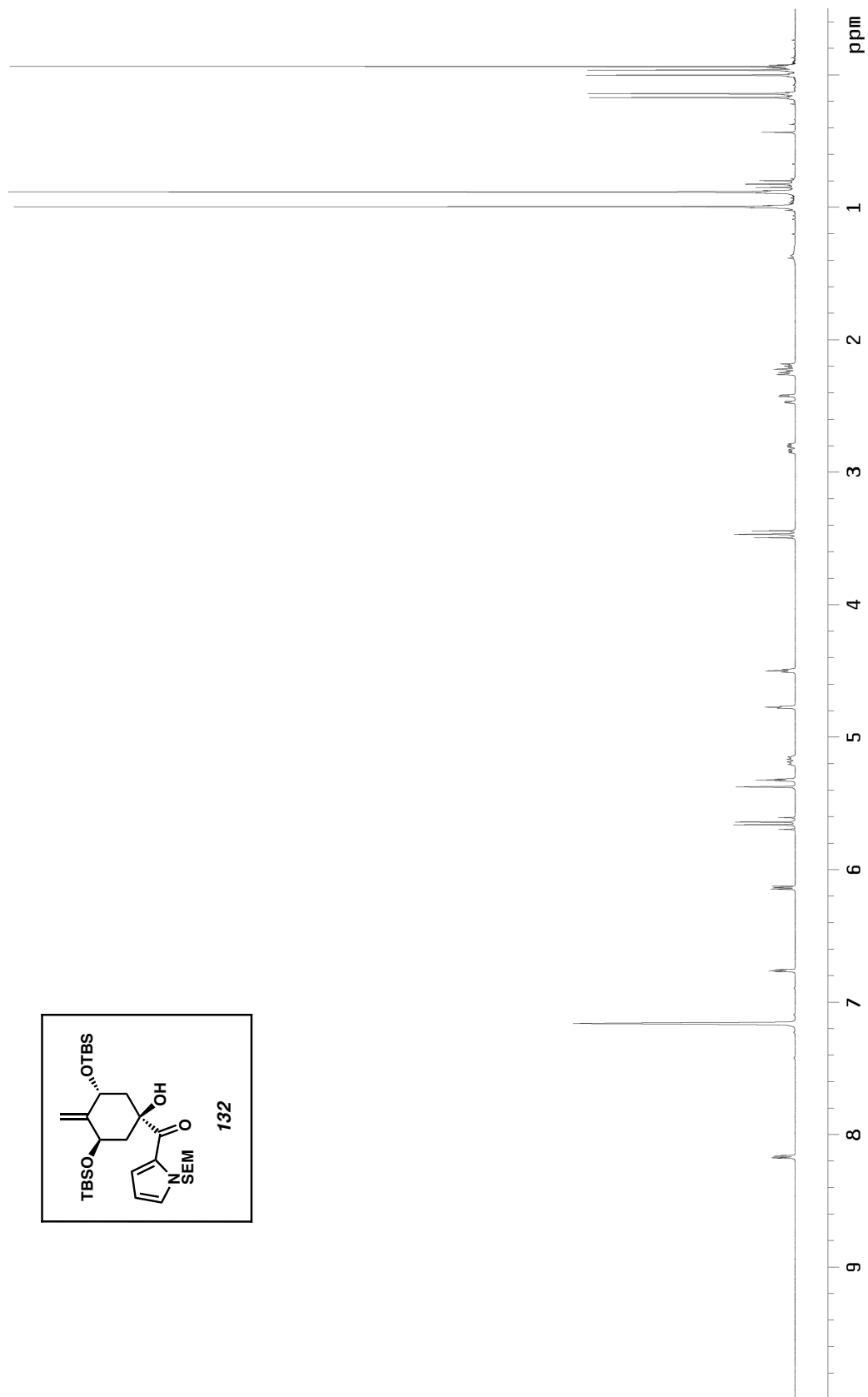


Figure A3.106 <sup>1</sup>H NMR (300 MHz, C<sub>6</sub>D<sub>6</sub>) of compound **132**

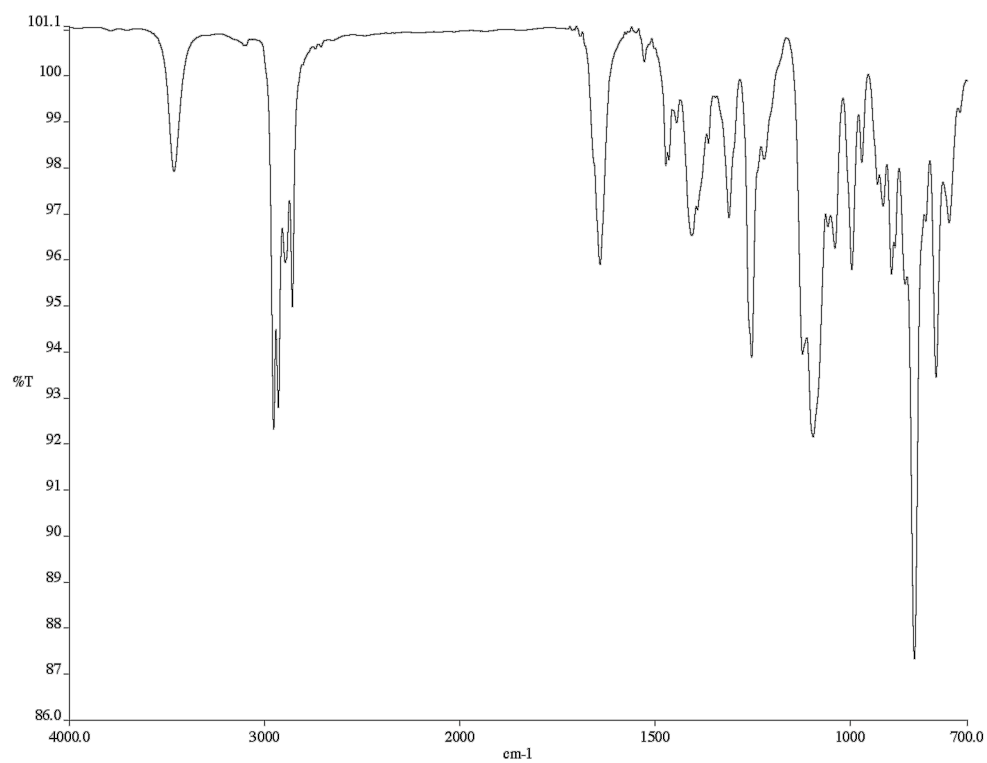


Figure A3.107 Infrared spectrum (thin film/NaCl) of compound **132**

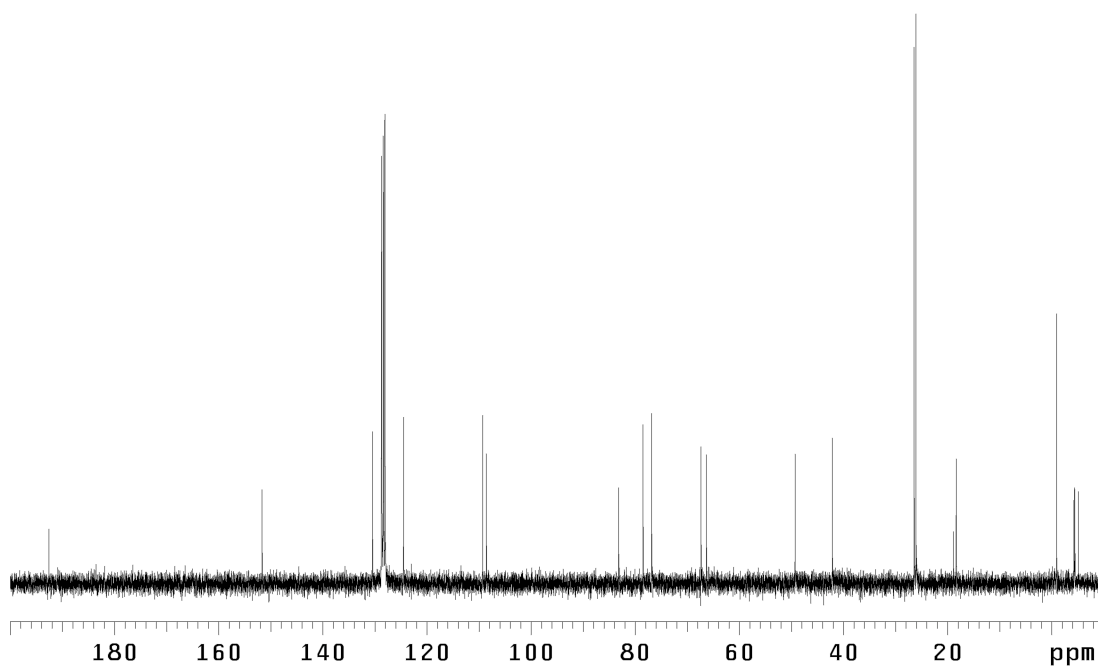


Figure A3.108 <sup>13</sup>C NMR (75 MHz, C<sub>6</sub>D<sub>6</sub>) of compound **132**

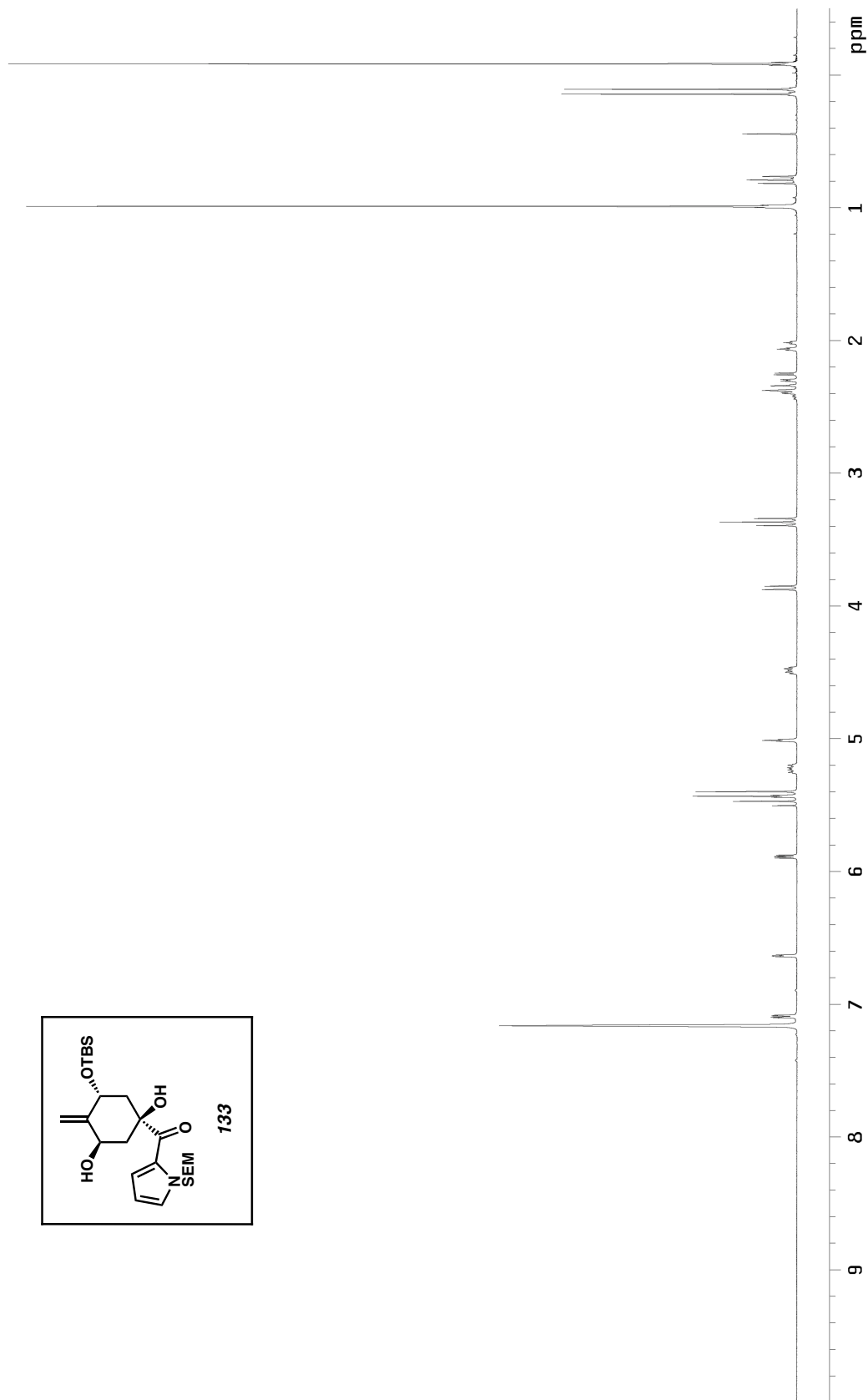
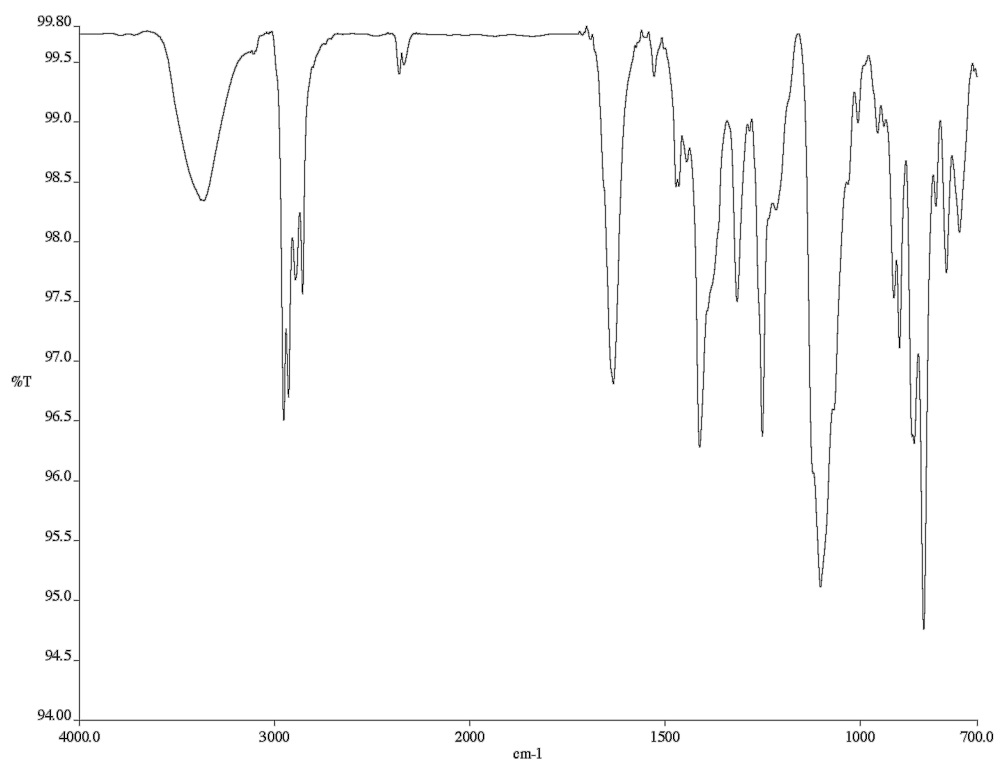
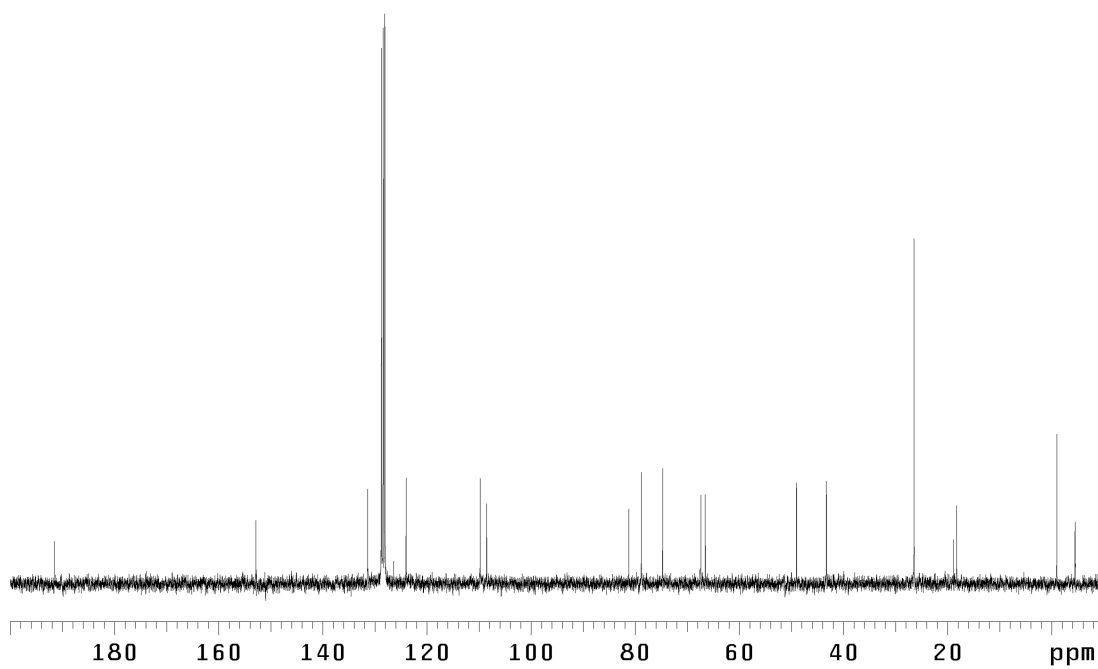


Figure A3.109  $^1\text{H}$  NMR (300 MHz,  $\text{C}_6\text{D}_6\text{O}$ ) of compound **133**



*Figure A3.110* Infrared spectrum (thin film/NaCl) of compound **133**



*Figure A3.111* <sup>13</sup>C NMR (75 MHz, C<sub>6</sub>D<sub>6</sub>) of compound **133**

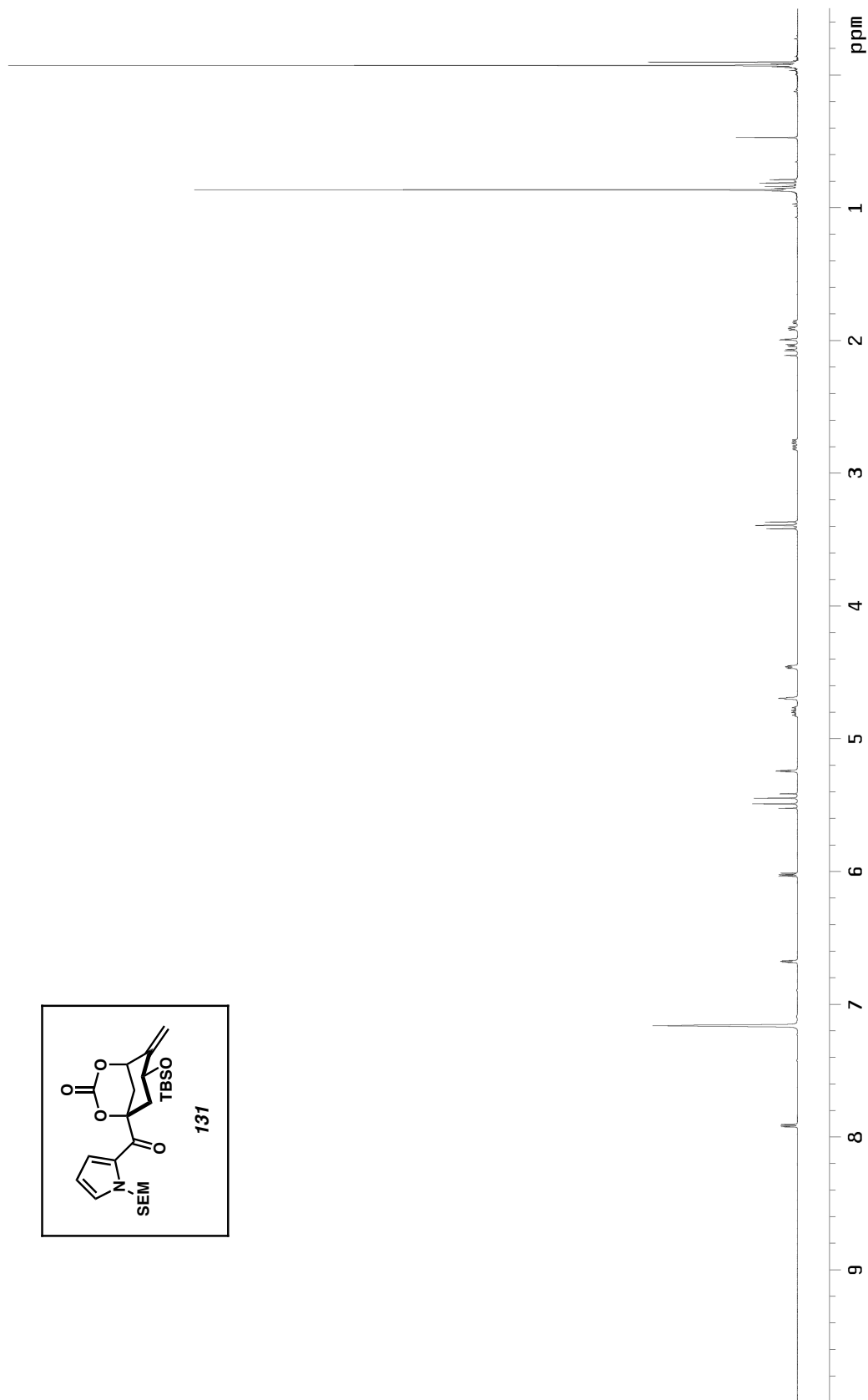
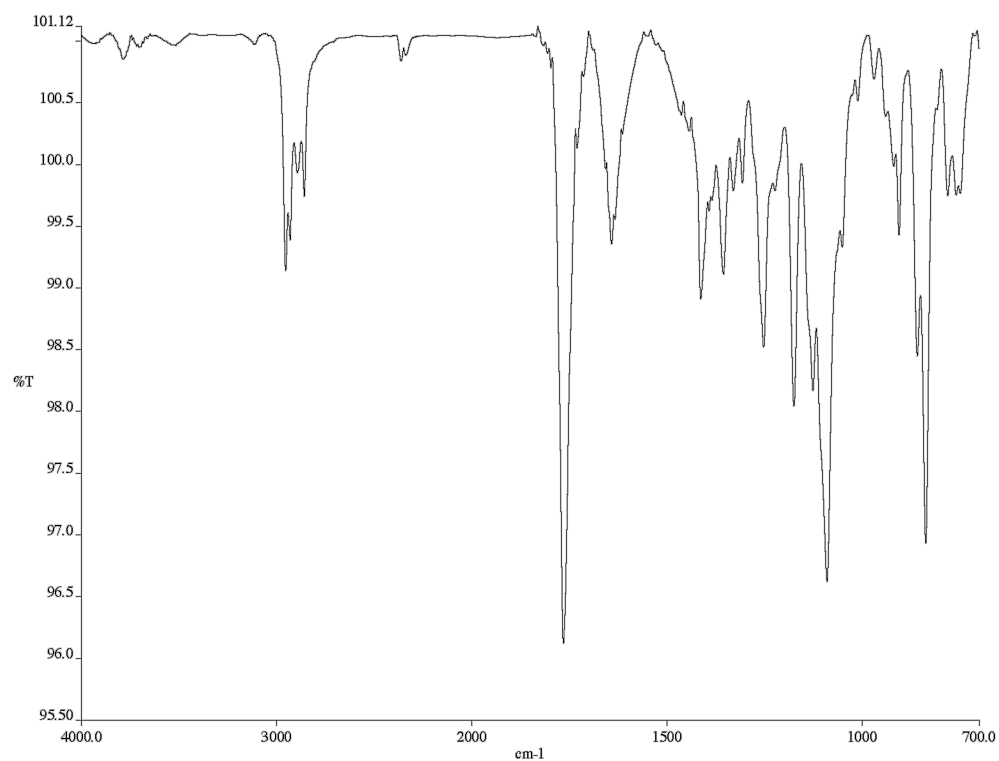
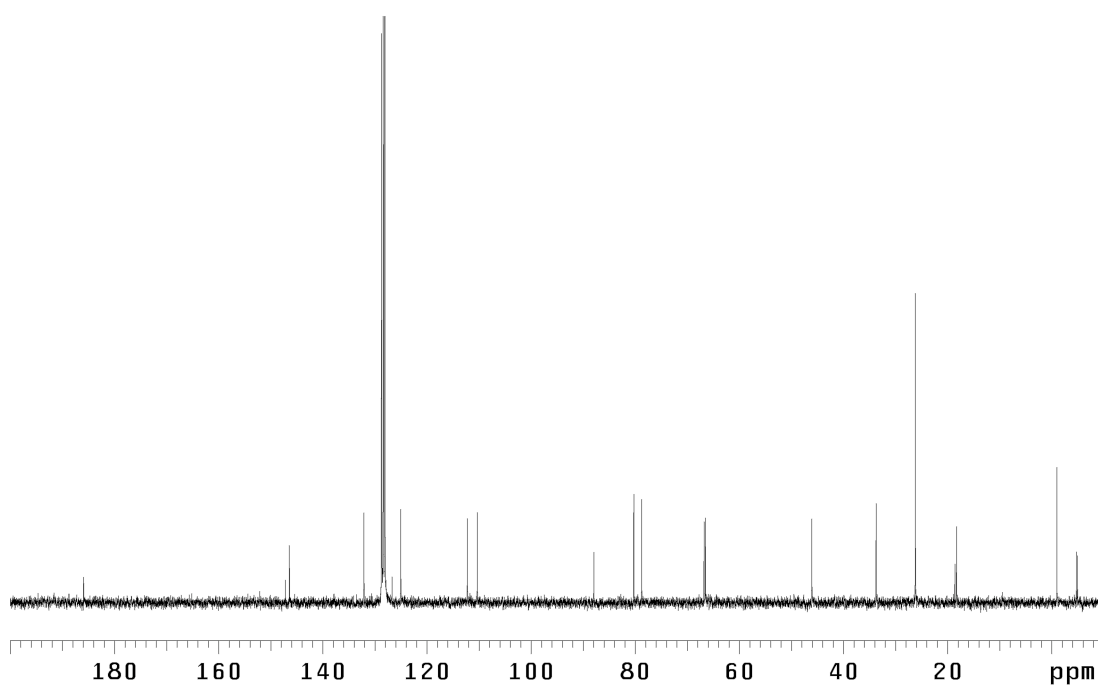


Figure A3.112  $^1\text{H}$  NMR (300 MHz,  $\text{C}_6\text{D}_6$ ) of compound **131**



*Figure A3.113* Infrared spectrum (thin film/NaCl) of compound **131**



*Figure A3.114* <sup>13</sup>C NMR (75 MHz, C<sub>6</sub>D<sub>6</sub>) of compound **131**

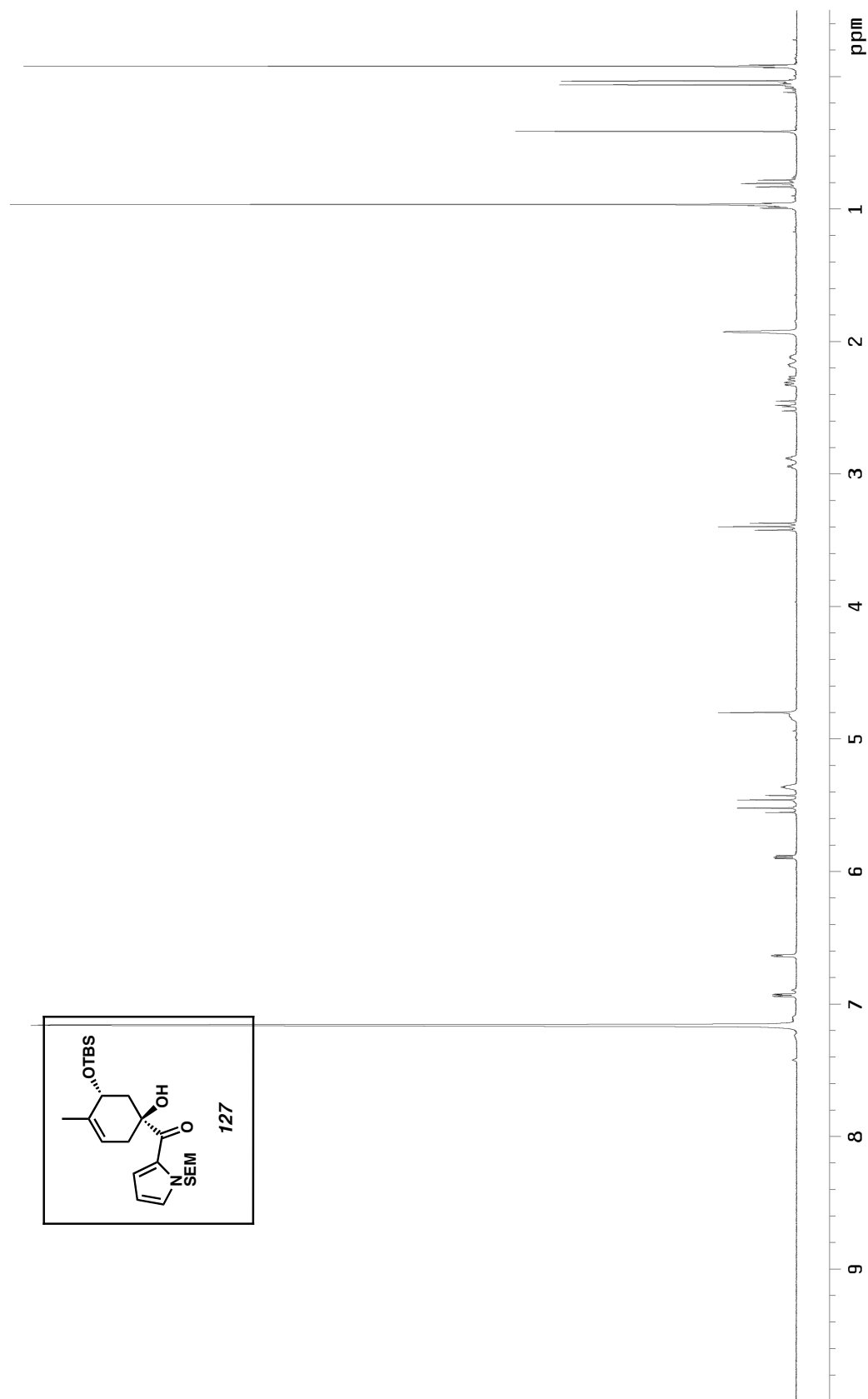


Figure A3.115  $^1\text{H}$  NMR (300 MHz,  $\text{CDCl}_3$ ) of compound **127**

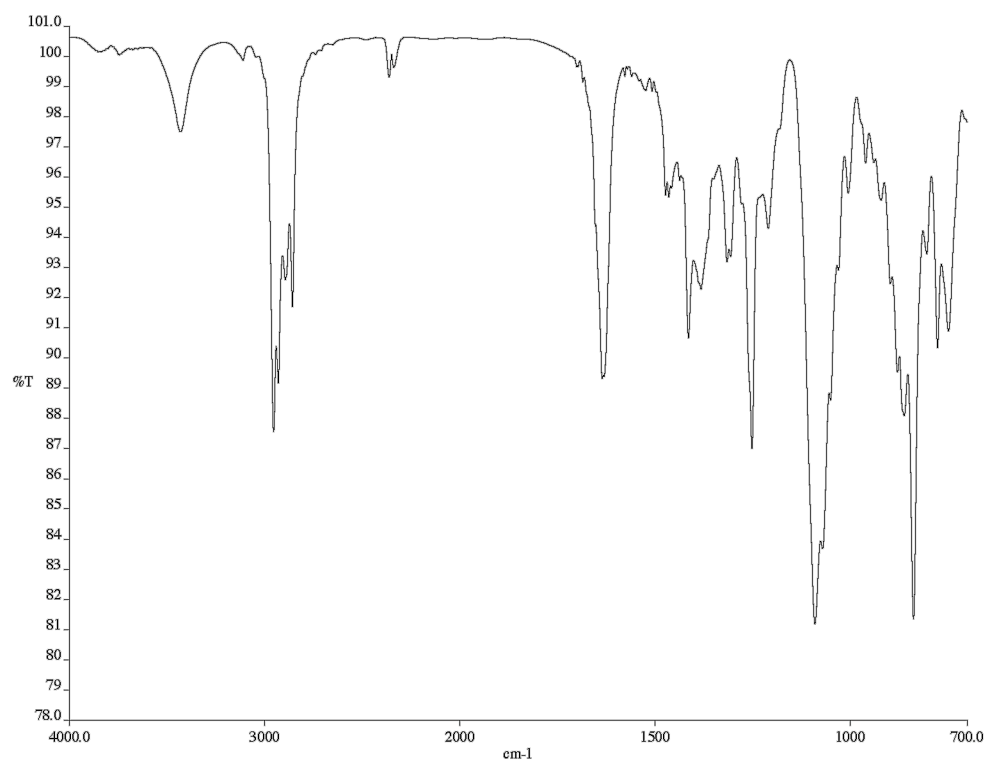


Figure A3.116 Infrared spectrum (thin film/NaCl) of compound **127**

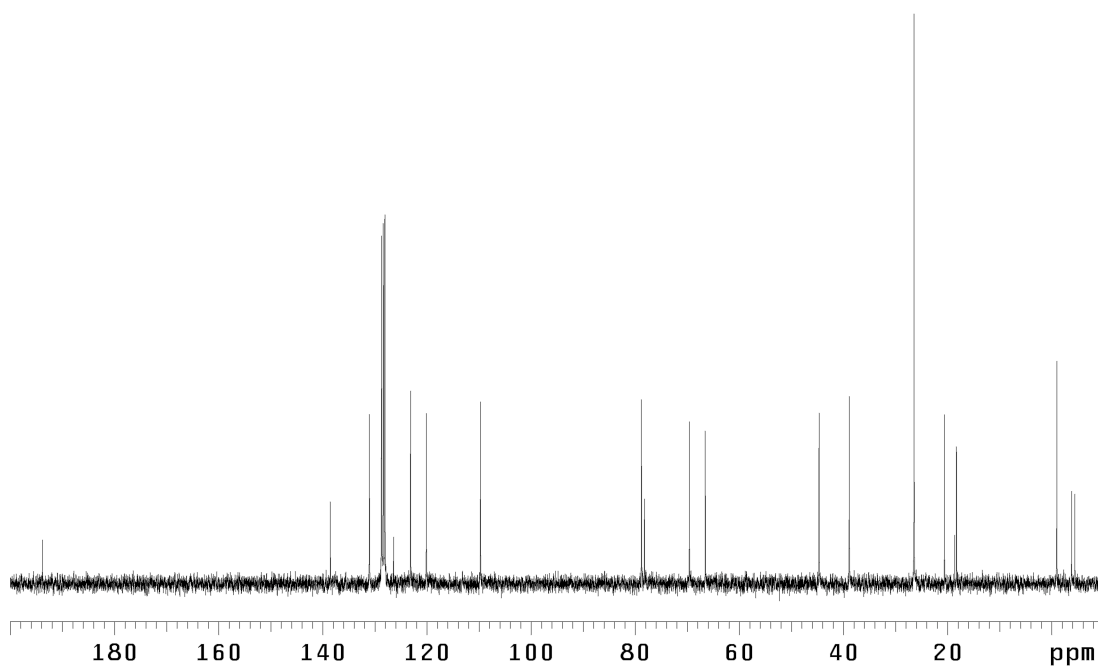


Figure A3.117 <sup>13</sup>C NMR (75 MHz, C<sub>6</sub>D<sub>6</sub>) of compound **127**



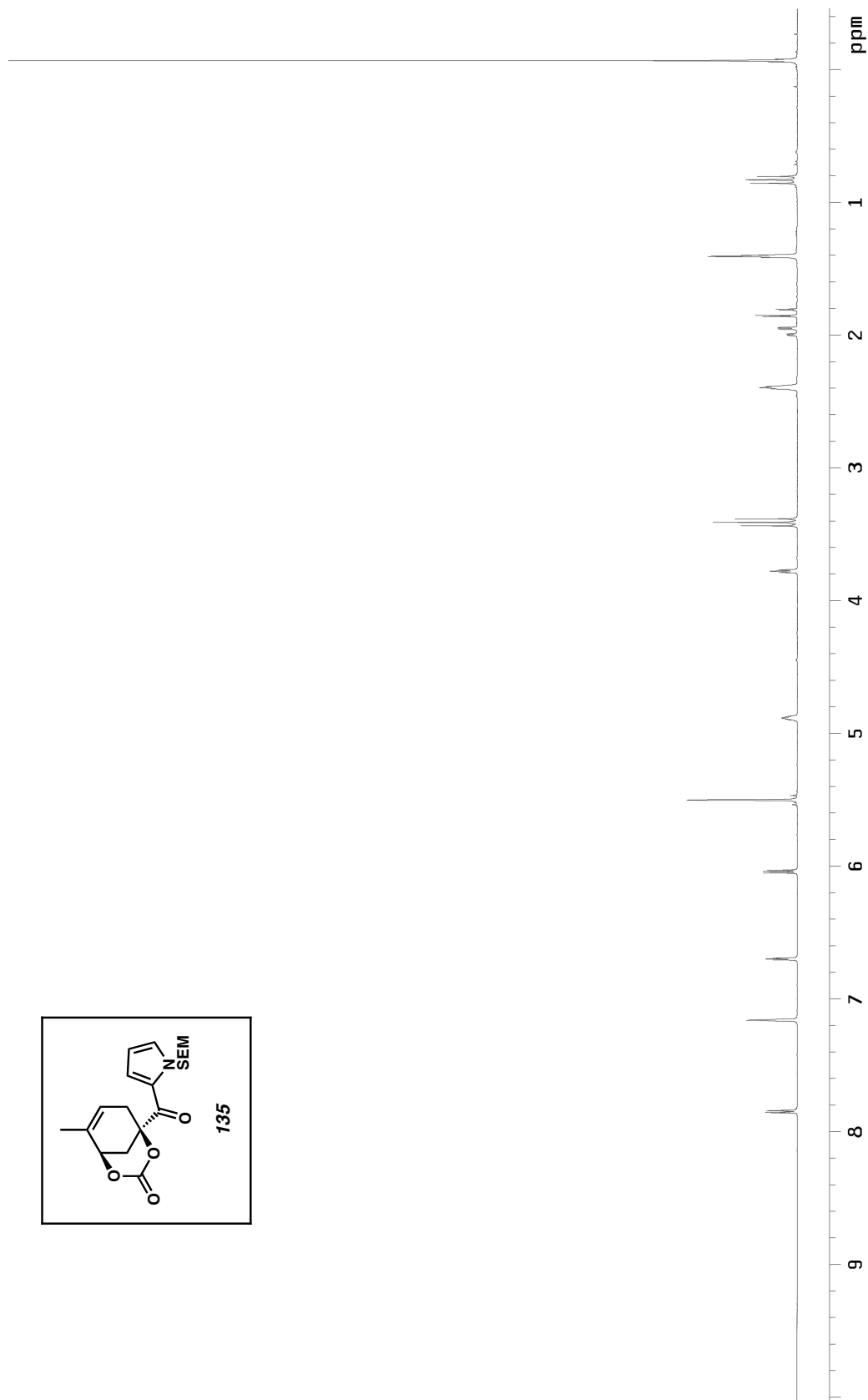
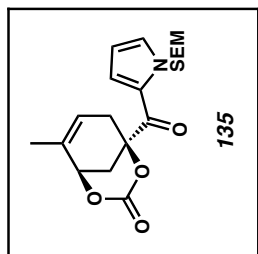


Figure A3.118 <sup>1</sup>H NMR (300 MHz, C<sub>6</sub>D<sub>6</sub>) of compound **135**

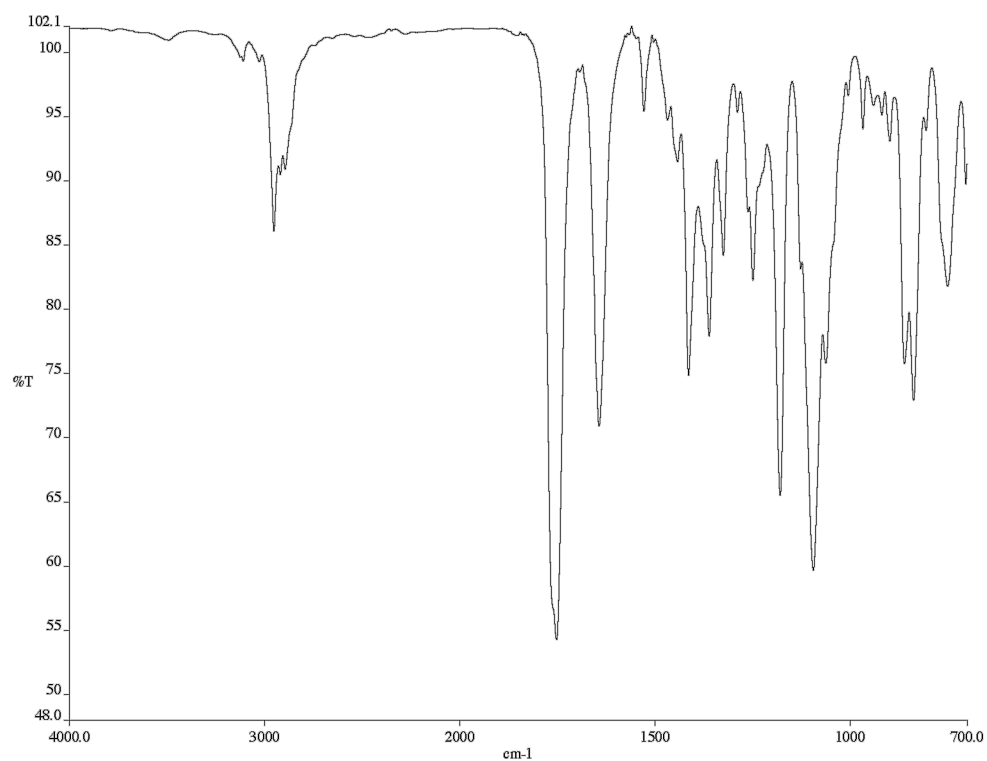


Figure A3.119 Infrared spectrum (thin film/NaCl) of compound **135**

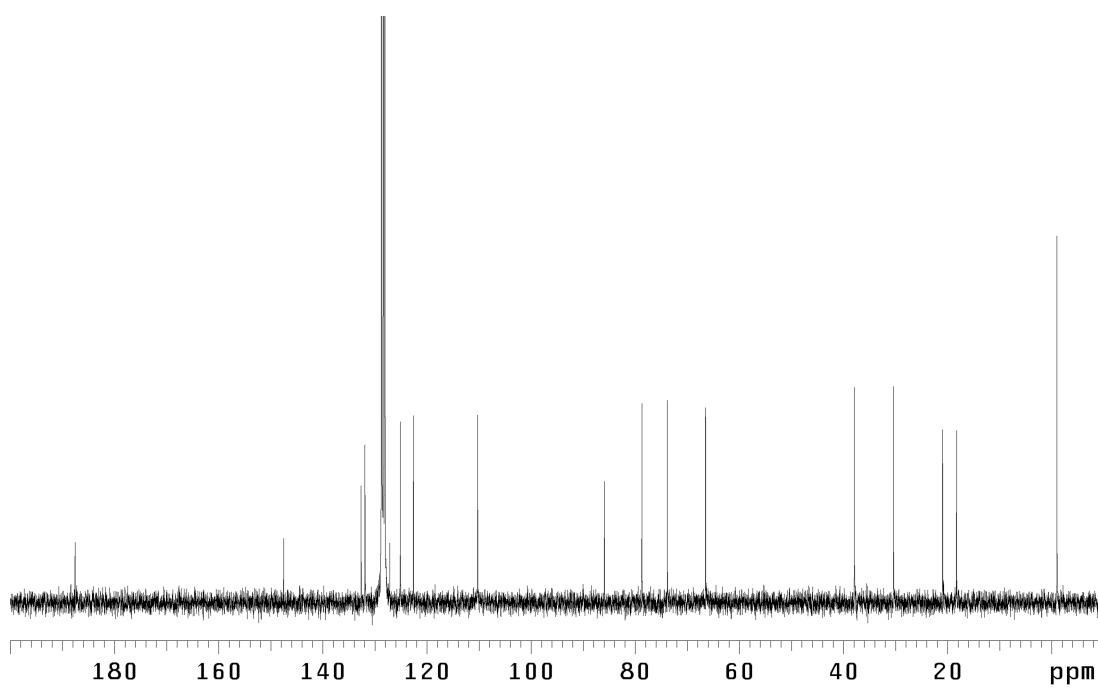


Figure A3.120 <sup>13</sup>C NMR (75 MHz, C<sub>6</sub>D<sub>6</sub>) of compound **135**

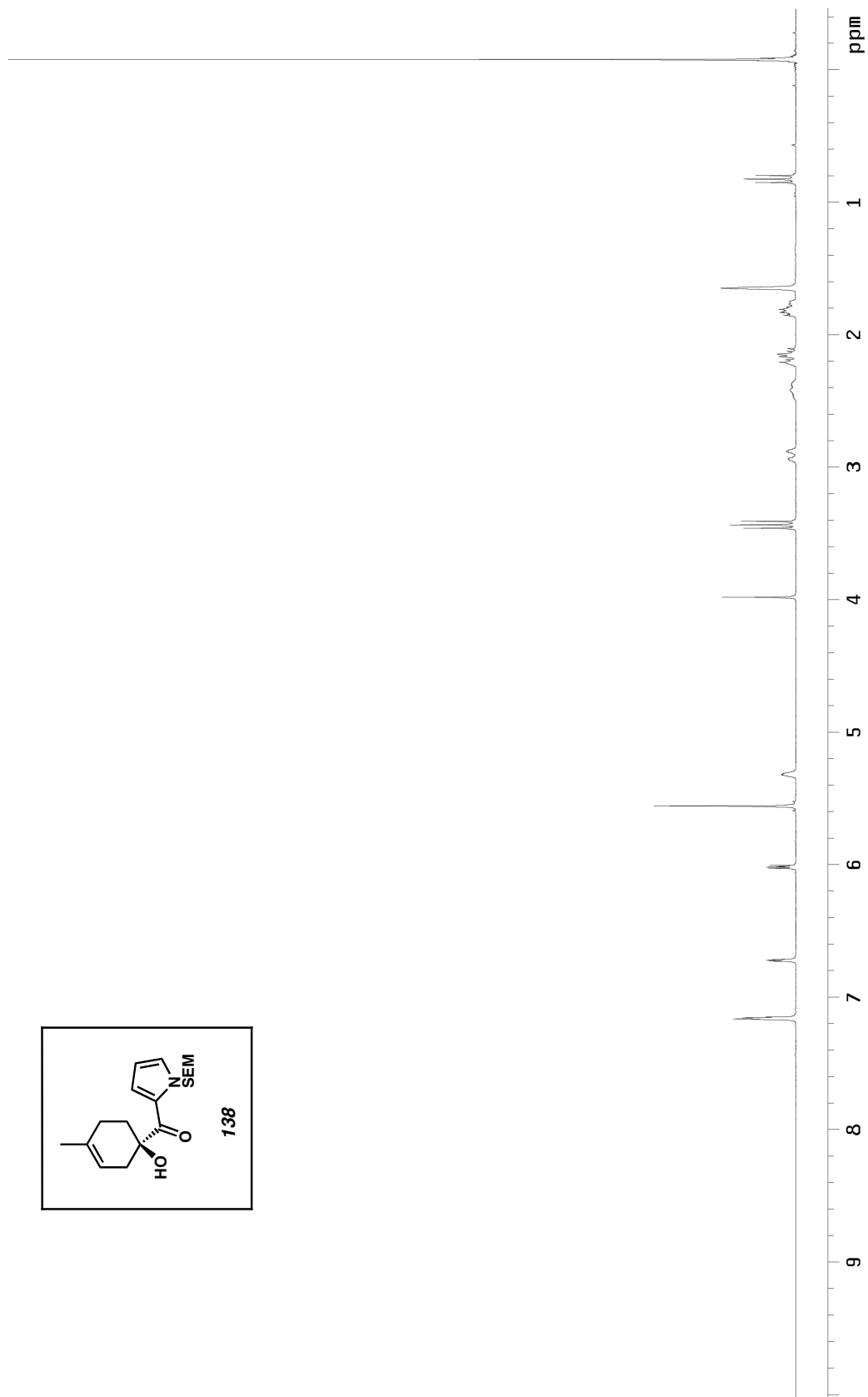
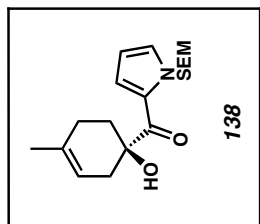


Figure A3.121  $^1\text{H}$  NMR (300 MHz,  $\text{C}_6\text{D}_6$ ) of compound **138**

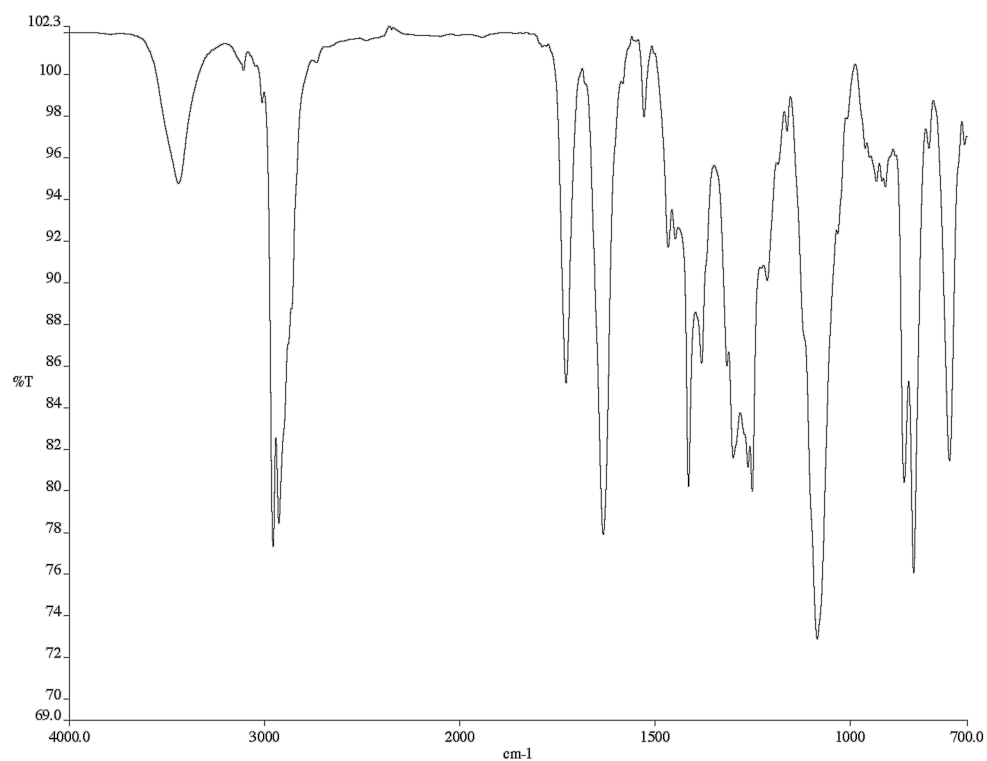


Figure A3.122 Infrared spectrum (thin film/NaCl) of compound **138**

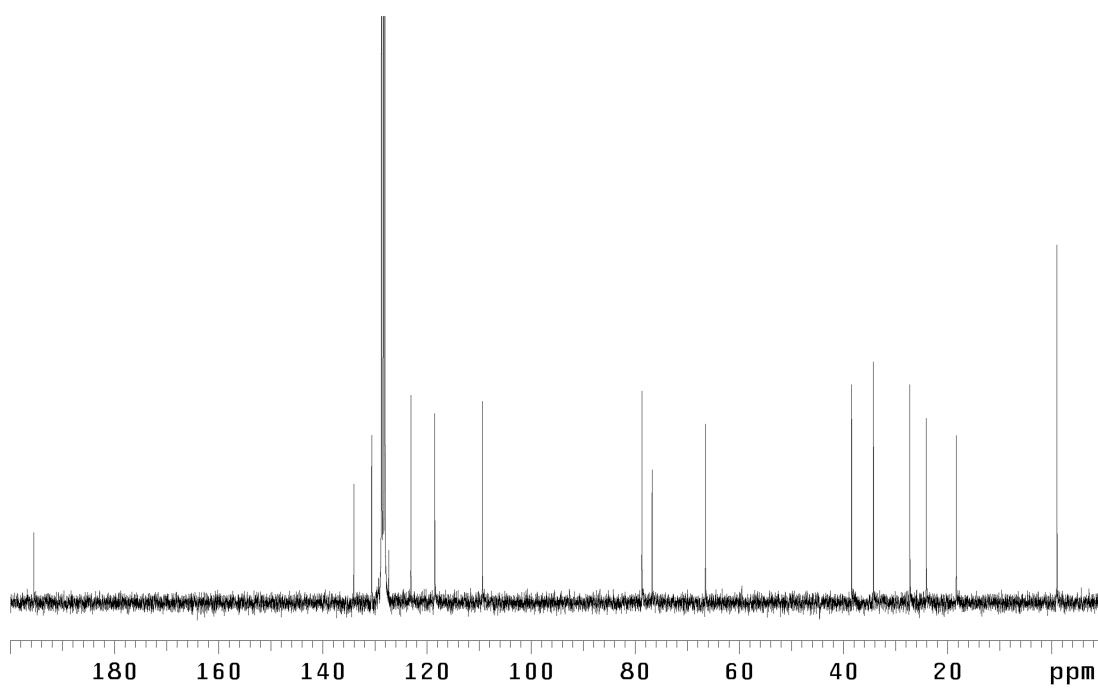


Figure A3.123 <sup>13</sup>C NMR (75 MHz, C<sub>6</sub>D<sub>6</sub>) of compound **138**

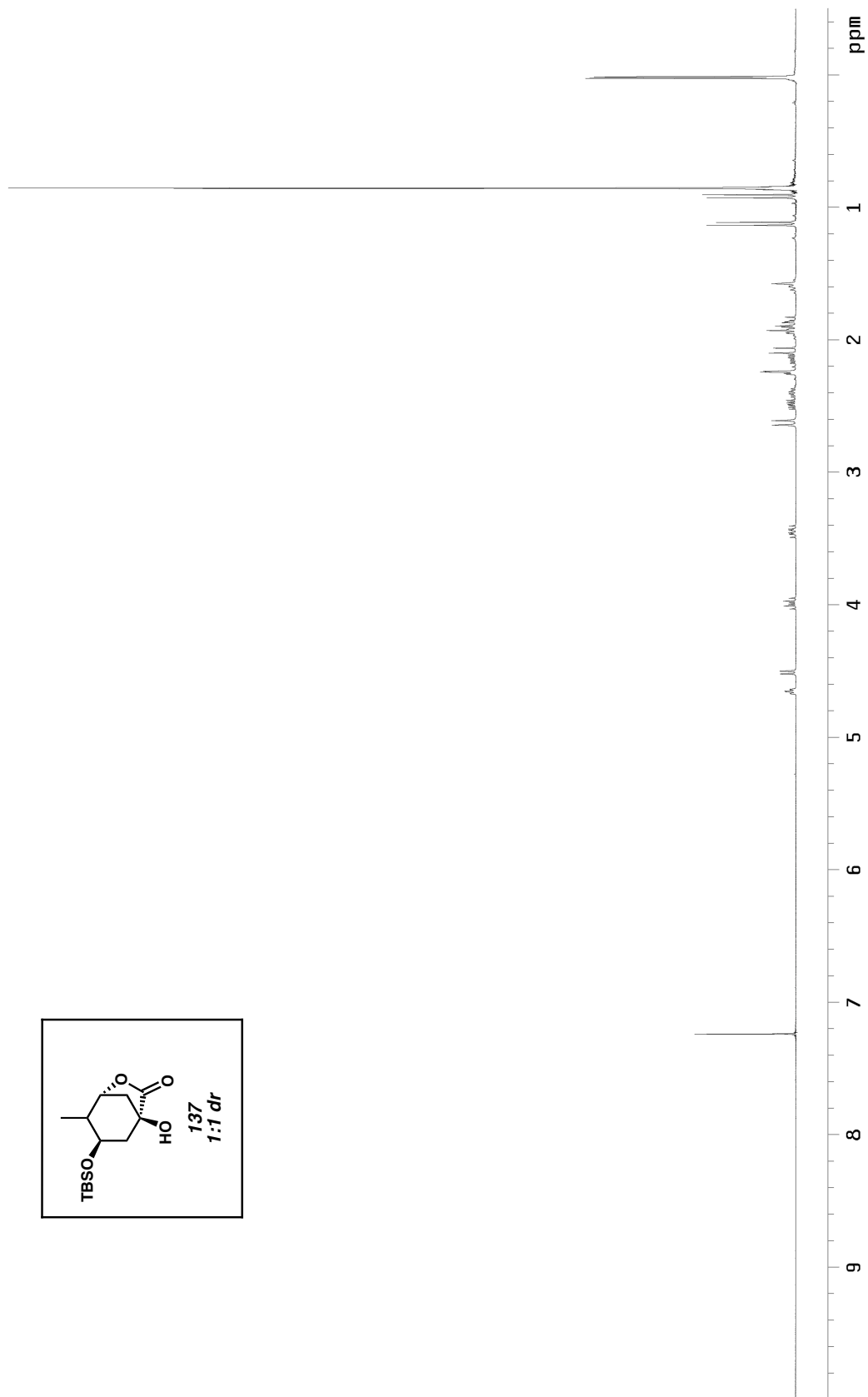
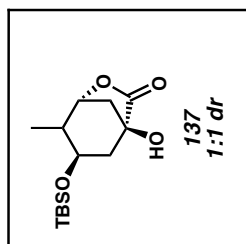


Figure A3.124 <sup>1</sup>H NMR (300 MHz, CDCl<sub>3</sub>) of compound **137**

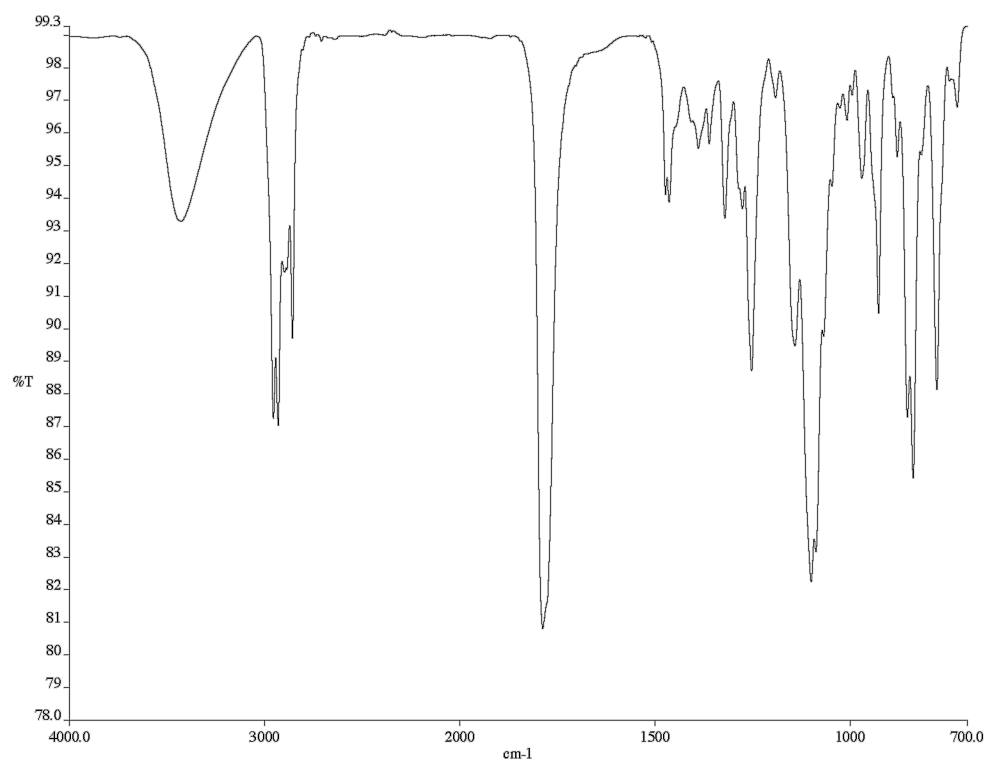


Figure A3.125 Infrared spectrum (thin film/NaCl) of compound **137**

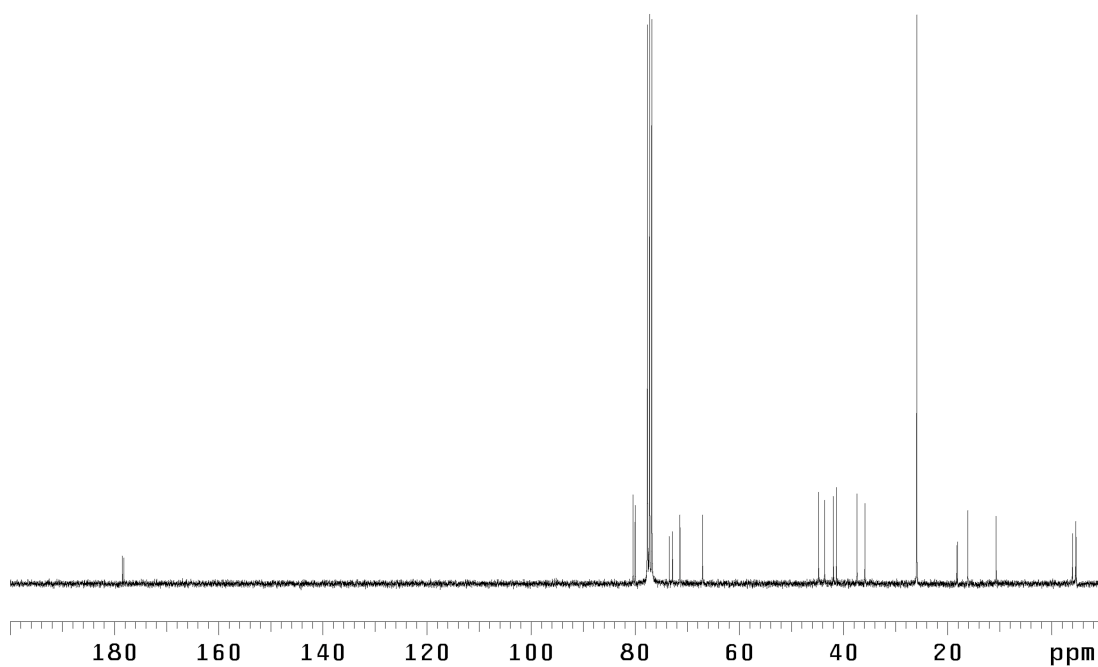


Figure A3.126 <sup>13</sup>C NMR (75 MHz, CDCl<sub>3</sub>) of compound **137**

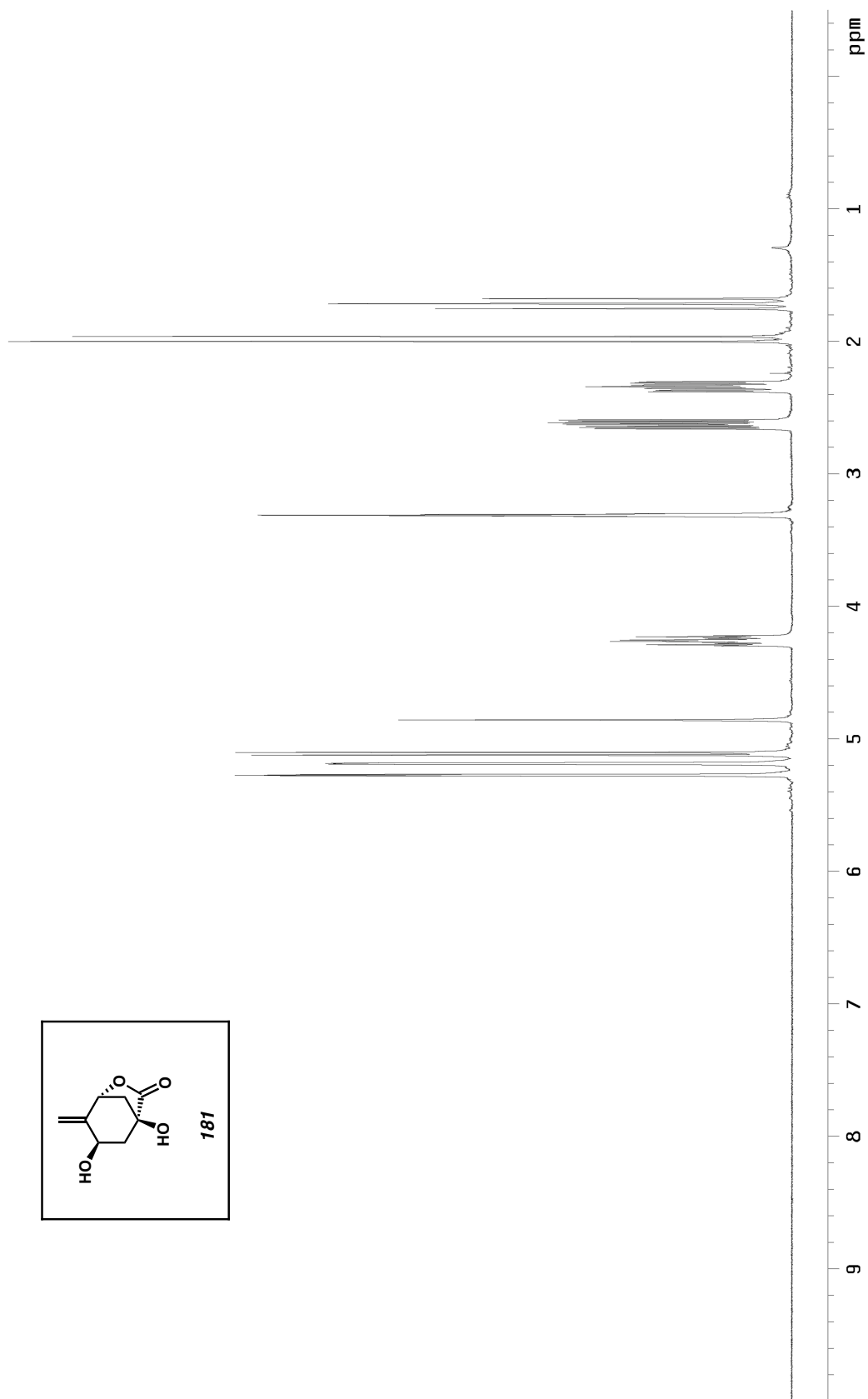
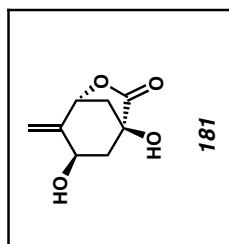


Figure A3.127  $^1\text{H}$  NMR (300 MHz,  $\text{CD}_3\text{OD}$ ) of compound **181**





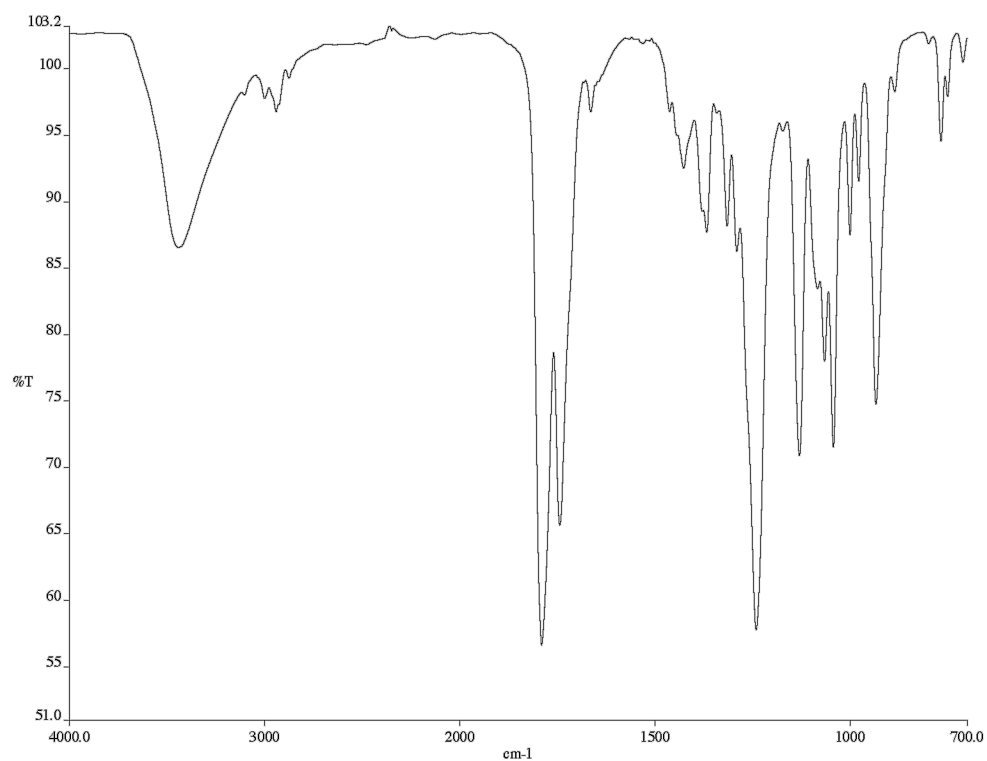


Figure A3.129 Infrared spectrum (thin film/NaCl) of compound **140**

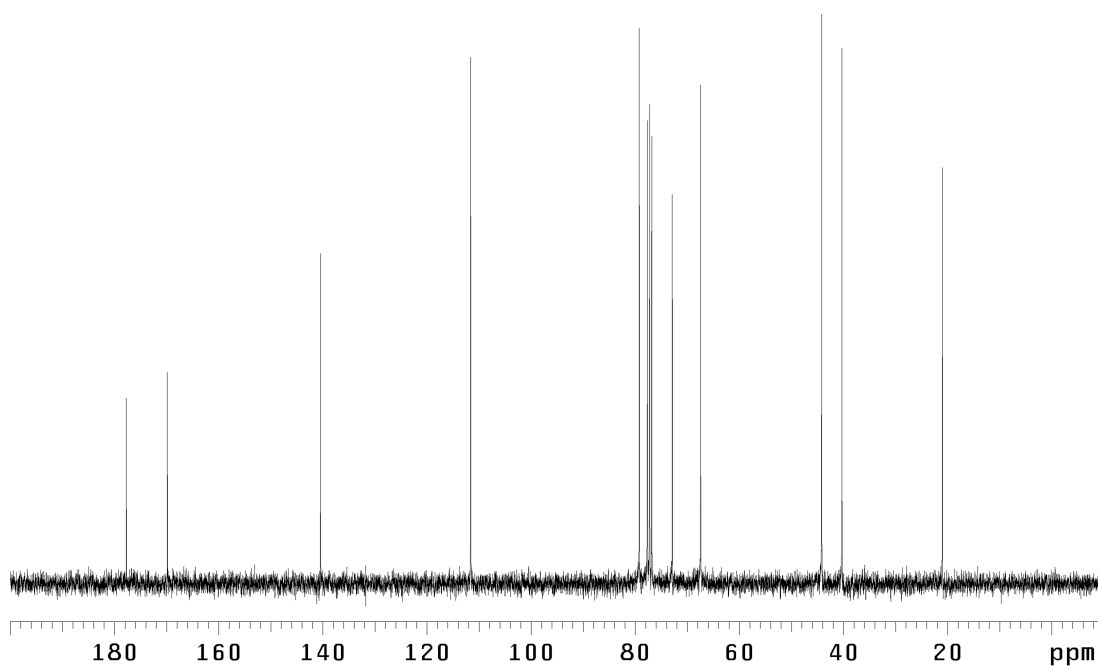


Figure A3.130 <sup>13</sup>C NMR (75 MHz, CDCl<sub>3</sub>) of compound **140**

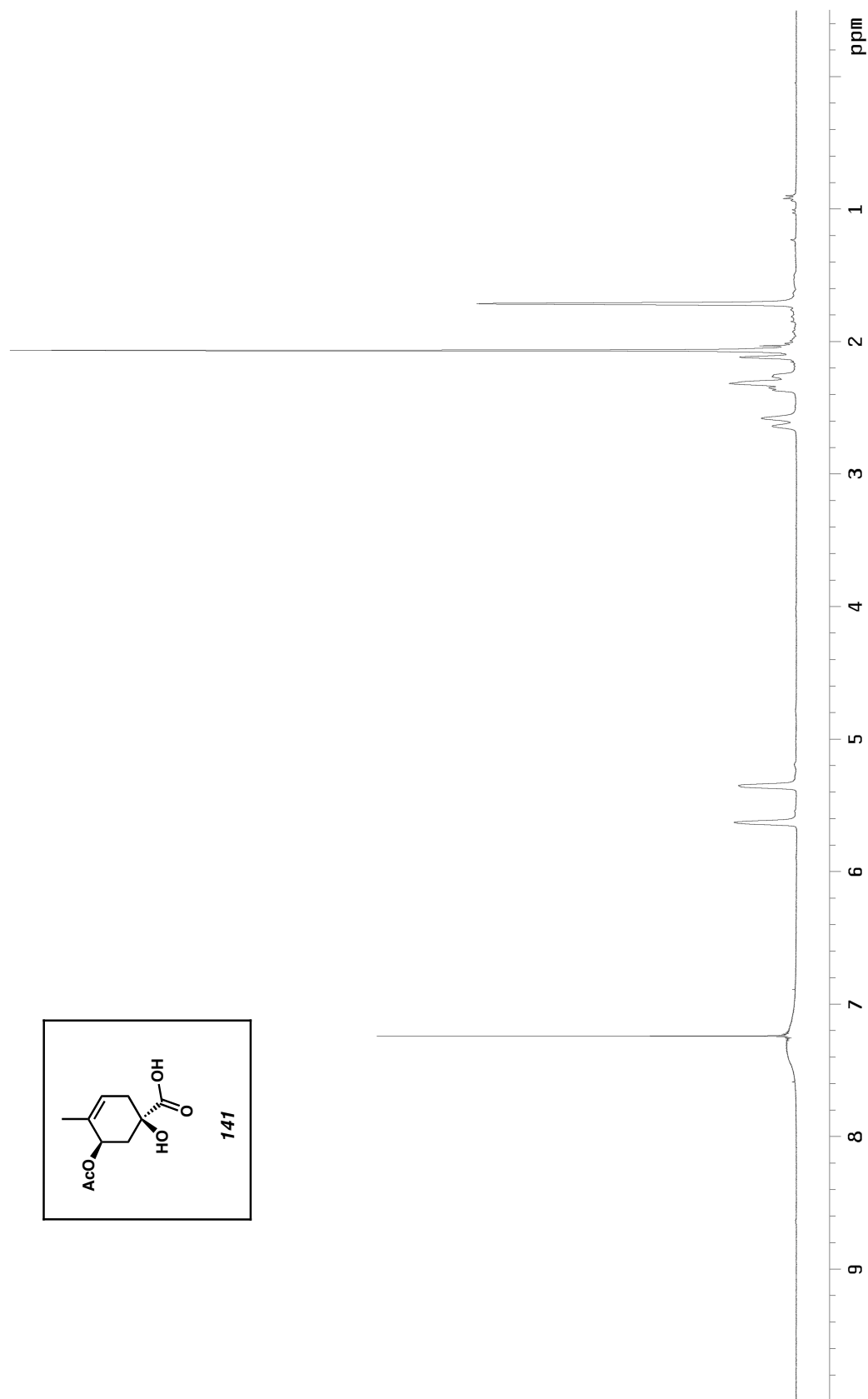


Figure A3.131  $^1\text{H}$  NMR (300 MHz,  $\text{CDCl}_3$ ) of compound **141**

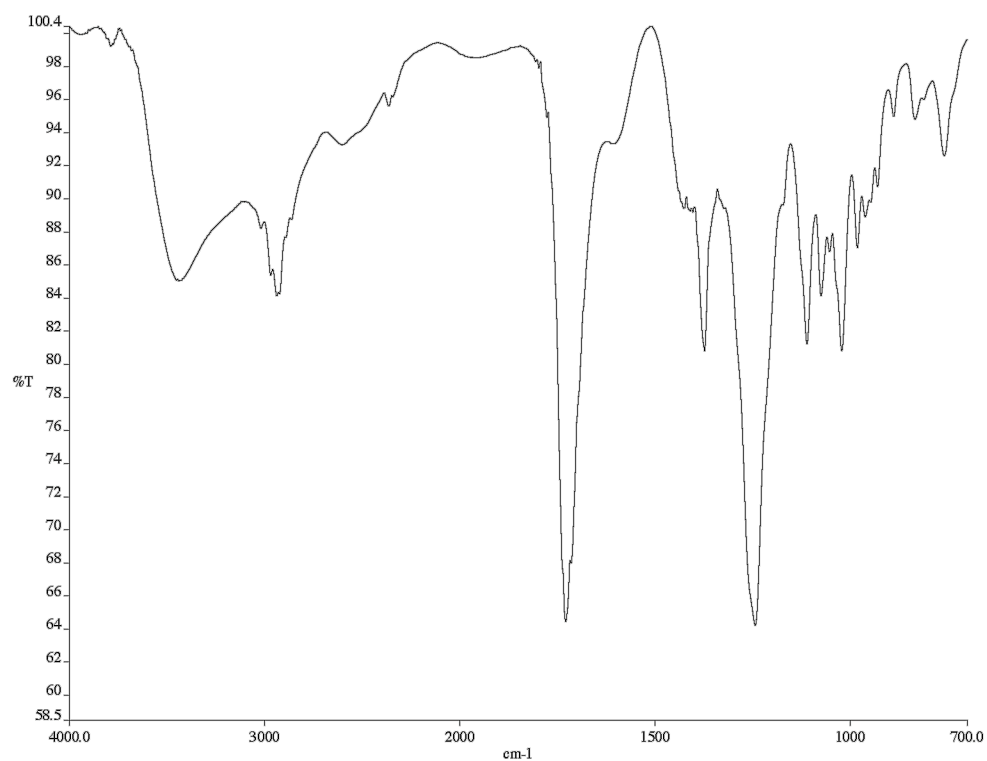


Figure A3.132 Infrared spectrum (thin film/NaCl) of compound **141**

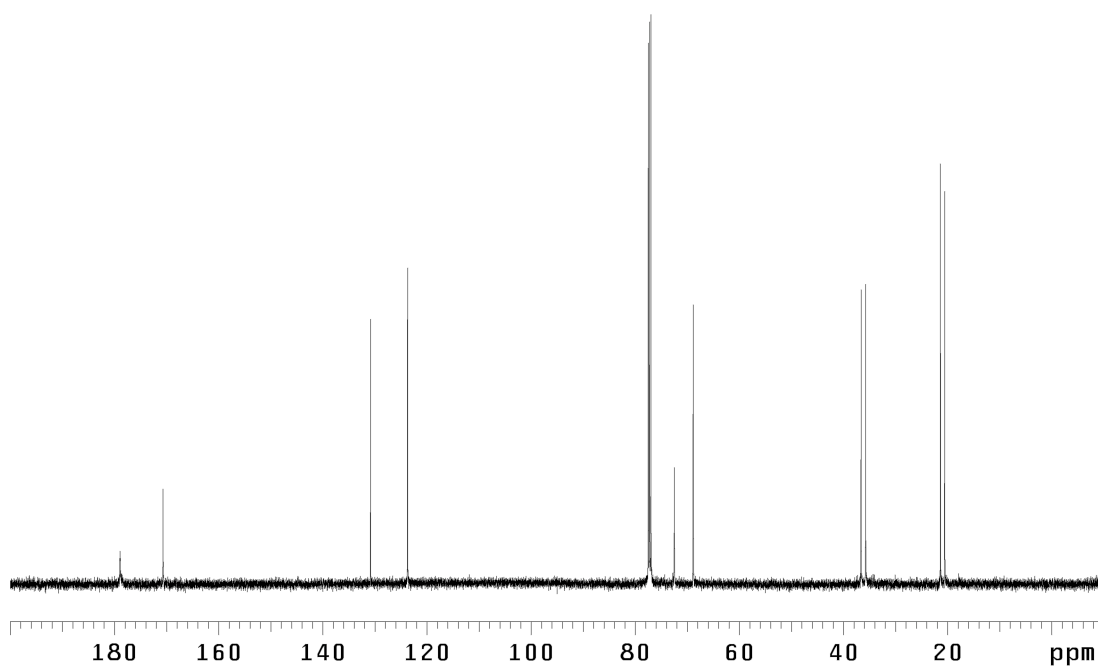


Figure A3.133 <sup>13</sup>C NMR (125 MHz, CDCl<sub>3</sub>) of compound **141**

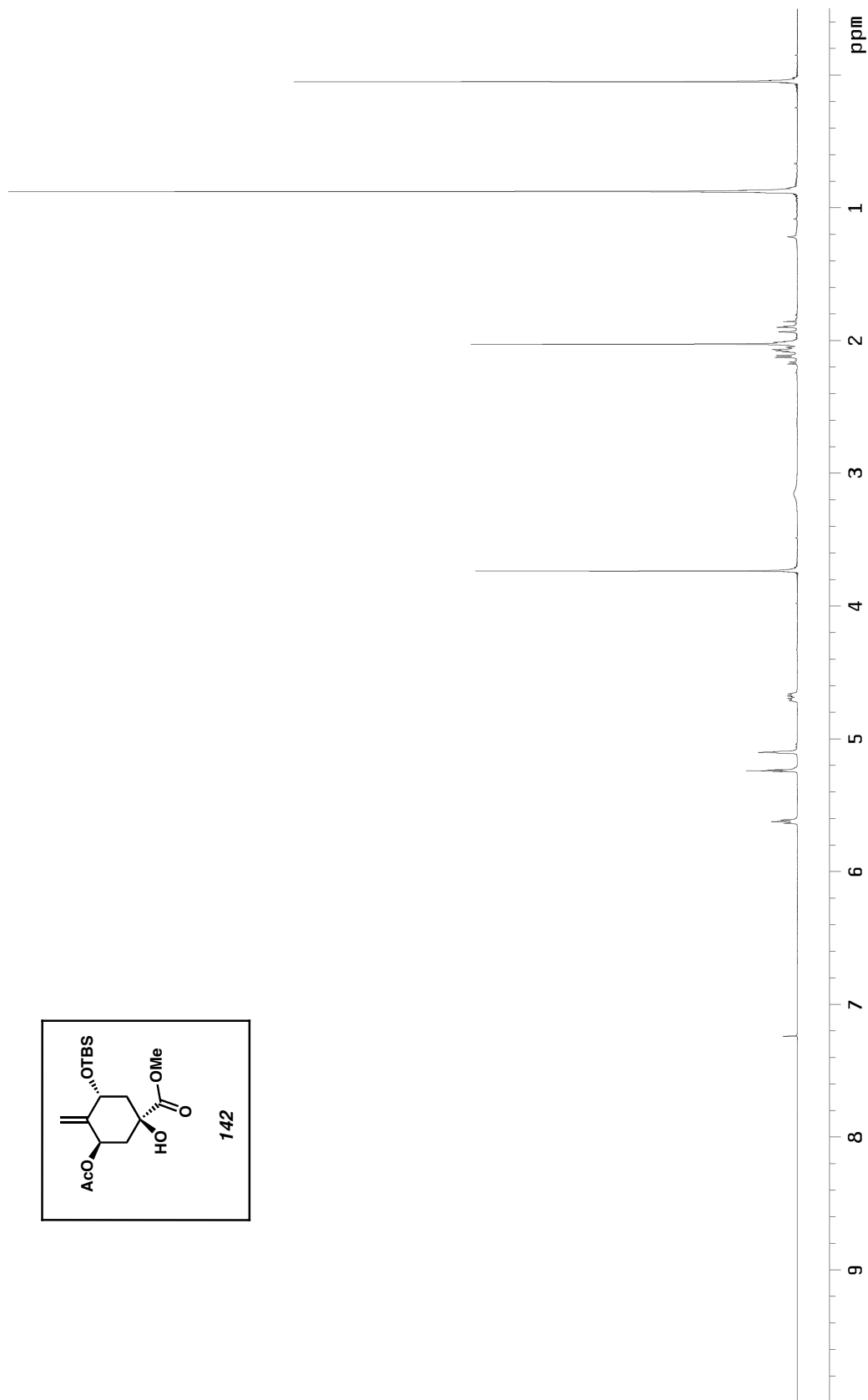


Figure A3.134  $^1\text{H}$  NMR (300 MHz,  $\text{CDCl}_3$ ) of compound **142**

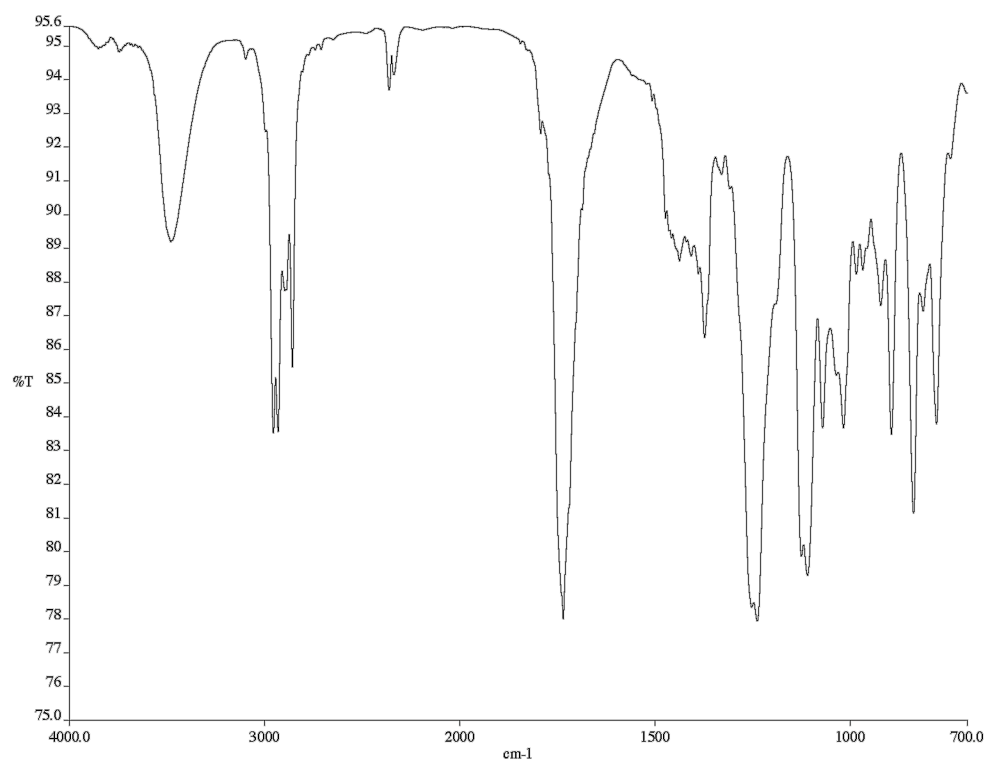


Figure A3.135 Infrared spectrum (thin film/NaCl) of compound **142**

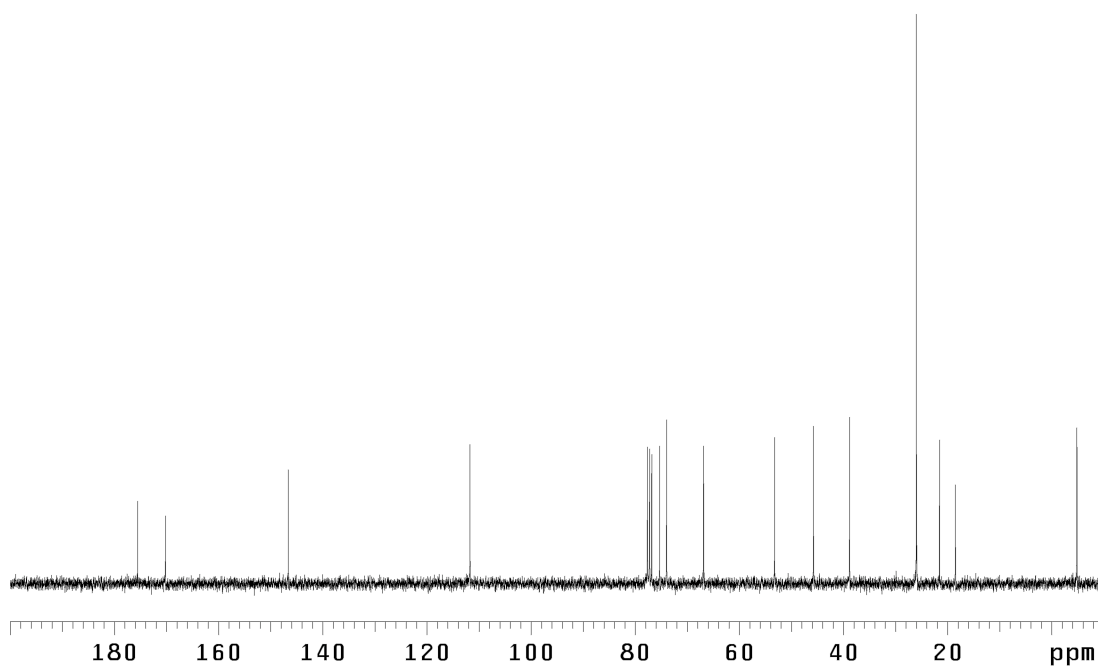


Figure A3.136 <sup>13</sup>C NMR (75 MHz, CDCl<sub>3</sub>) of compound **142**

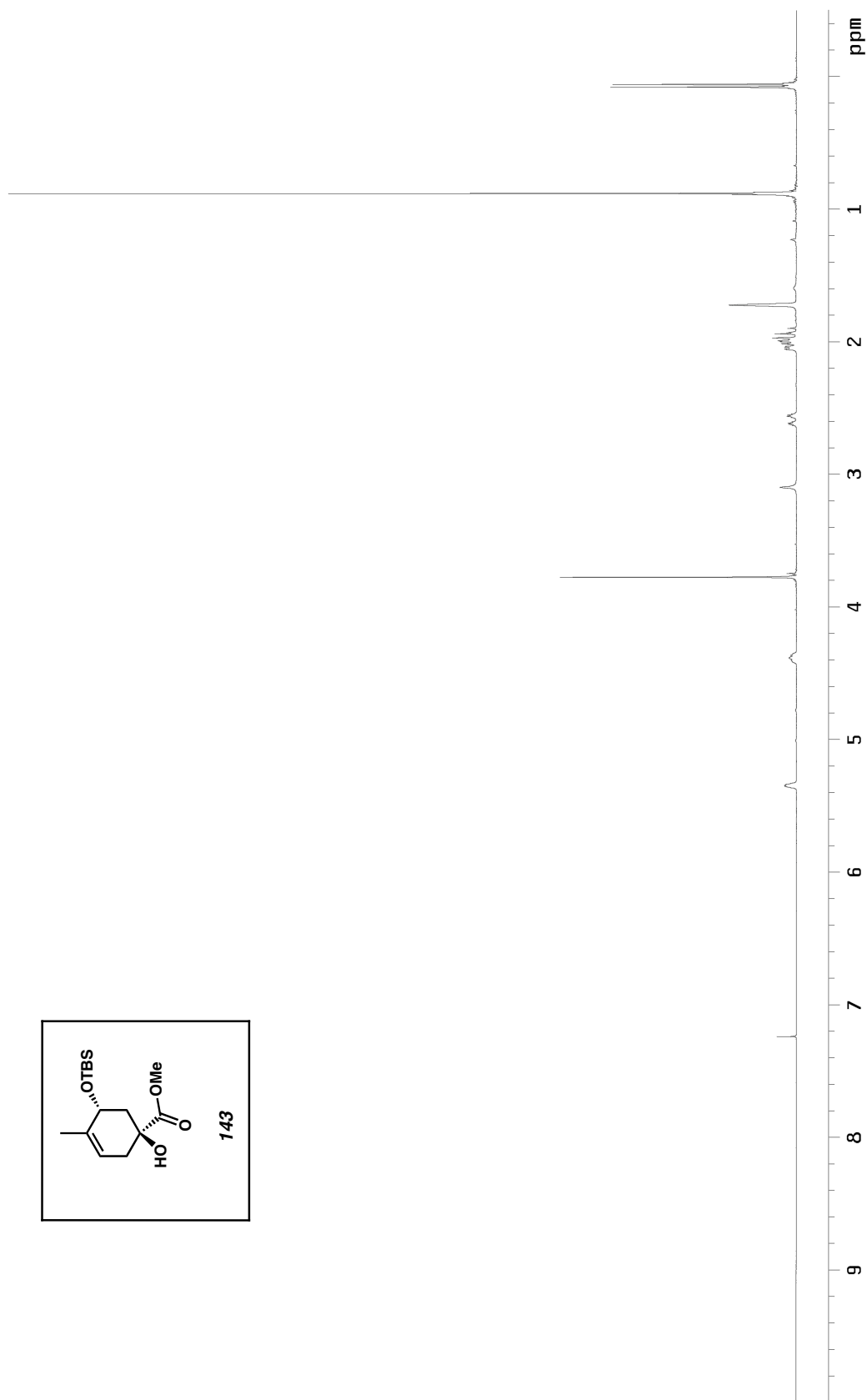
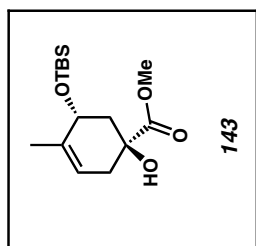


Figure A3.137 <sup>1</sup>H NMR (300 MHz, CDCl<sub>3</sub>) of compound **143**

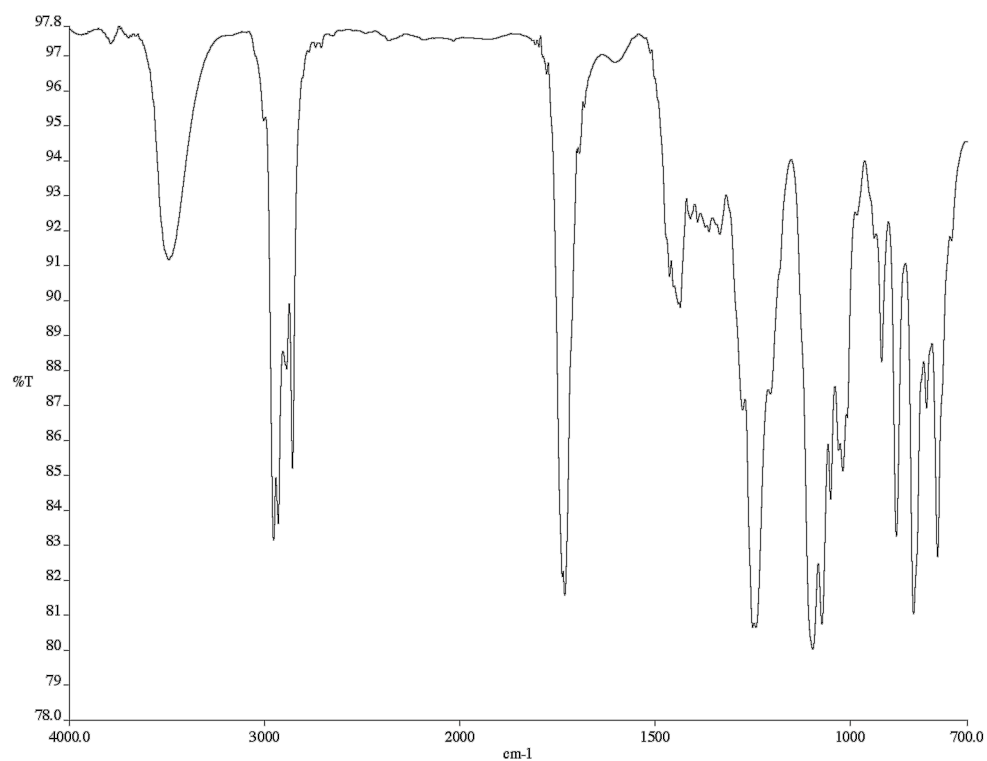


Figure A3.138 Infrared spectrum (thin film/NaCl) of compound **143**

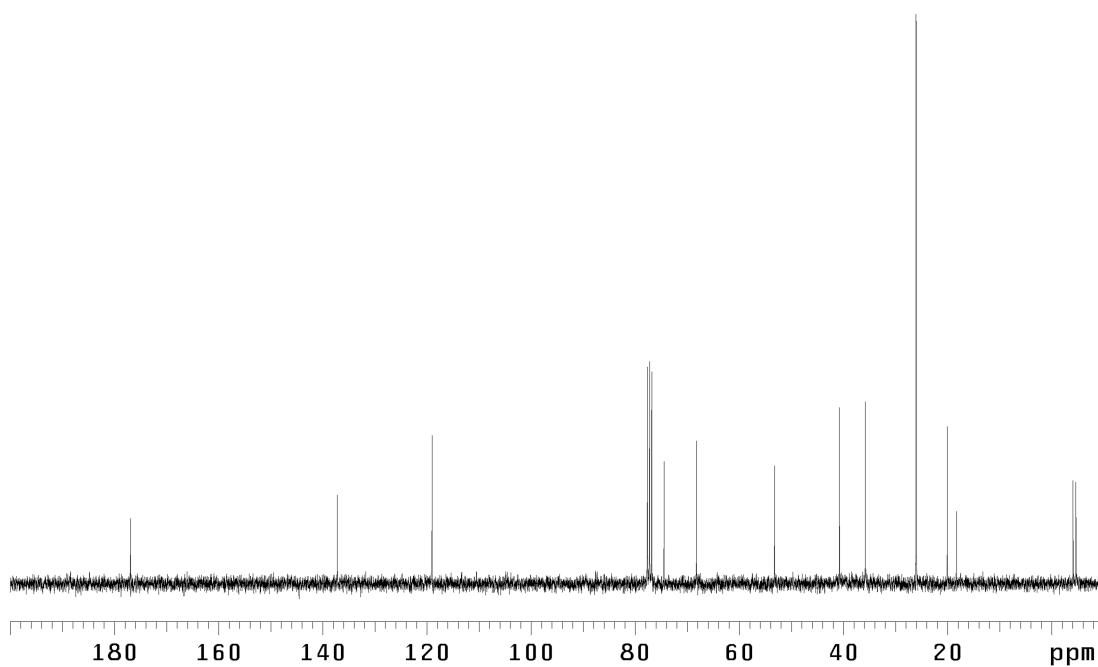


Figure A3.139 <sup>13</sup>C NMR (75 MHz, CDCl<sub>3</sub>) of compound **143**

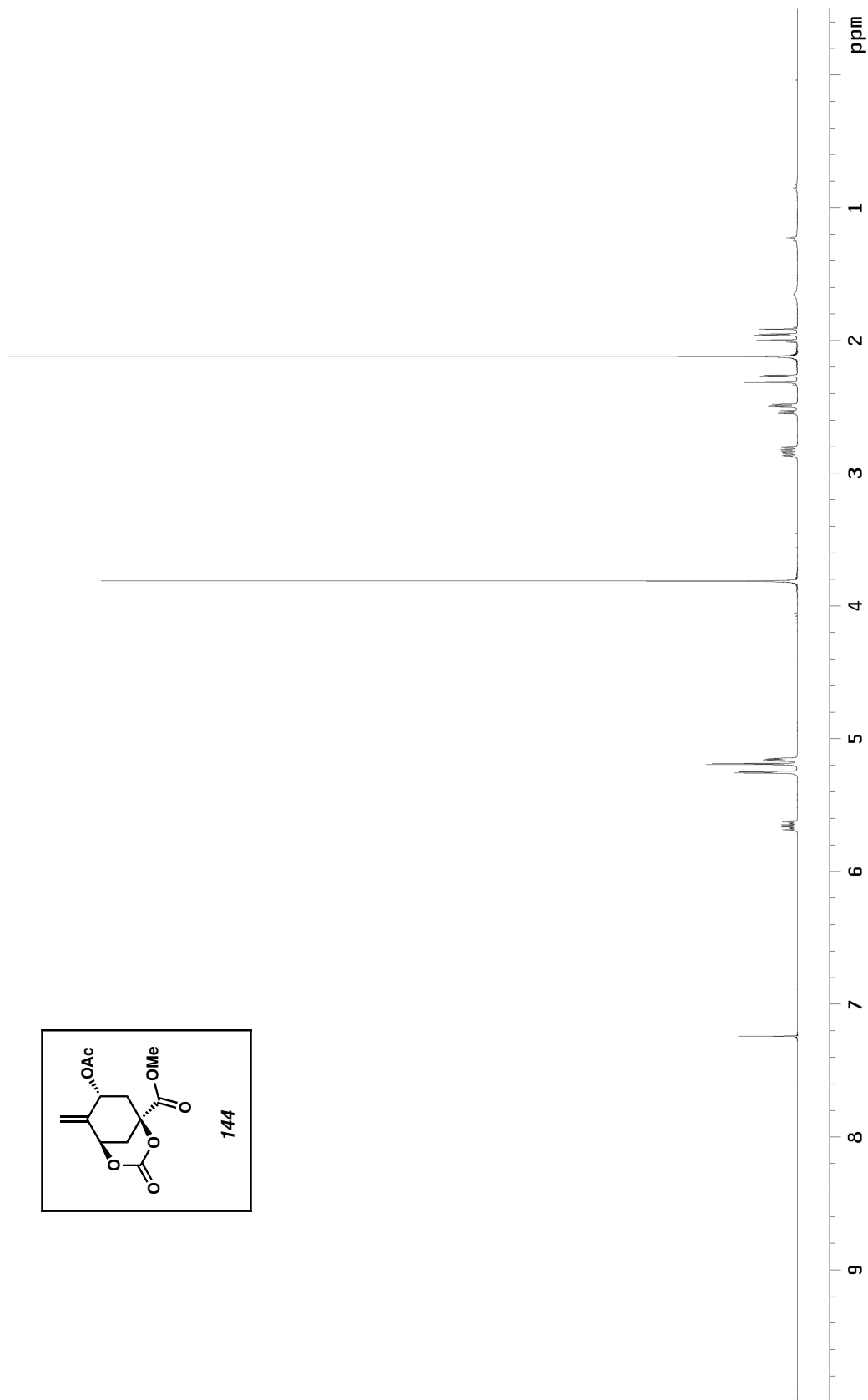


Figure A3.140  $^1\text{H}$  NMR (300 MHz,  $\text{CDCl}_3$ ) of compound **144**



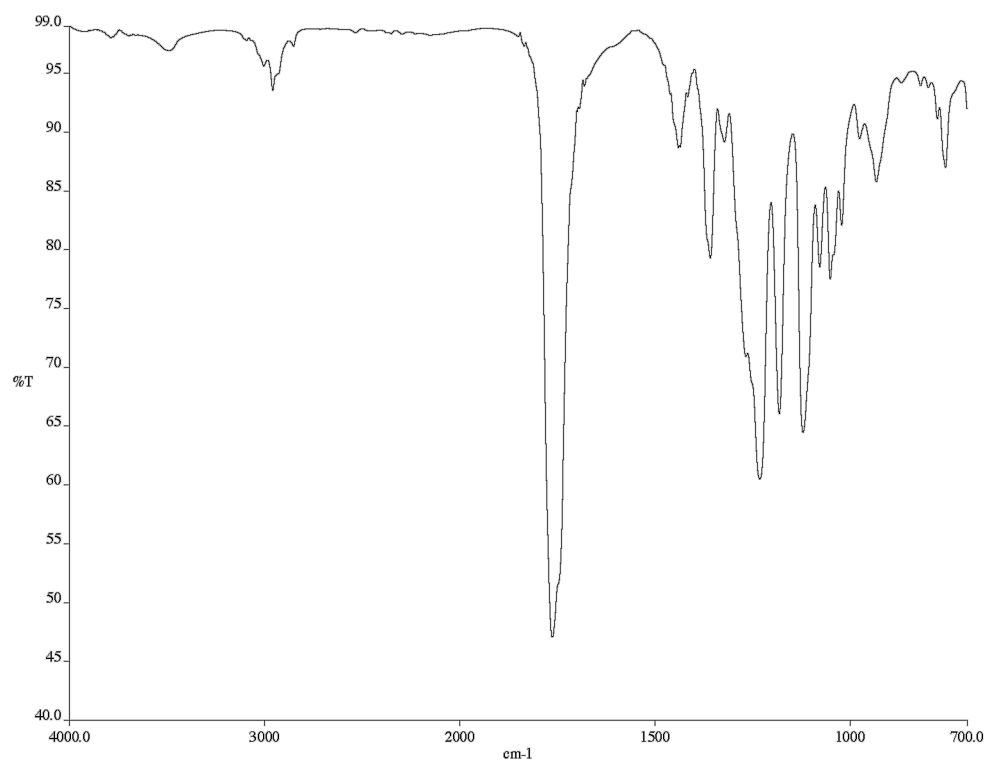


Figure A3.141 Infrared spectrum (thin film/NaCl) of compound **144**

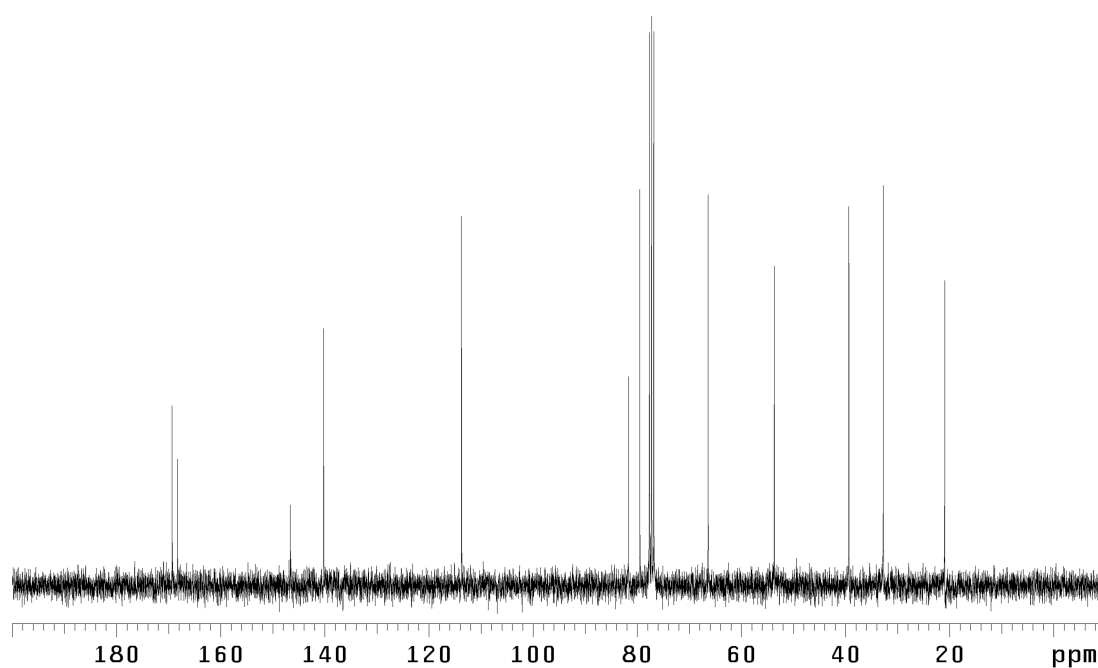


Figure A3.142 <sup>13</sup>C NMR (75 MHz, CDCl<sub>3</sub>) of compound **144**

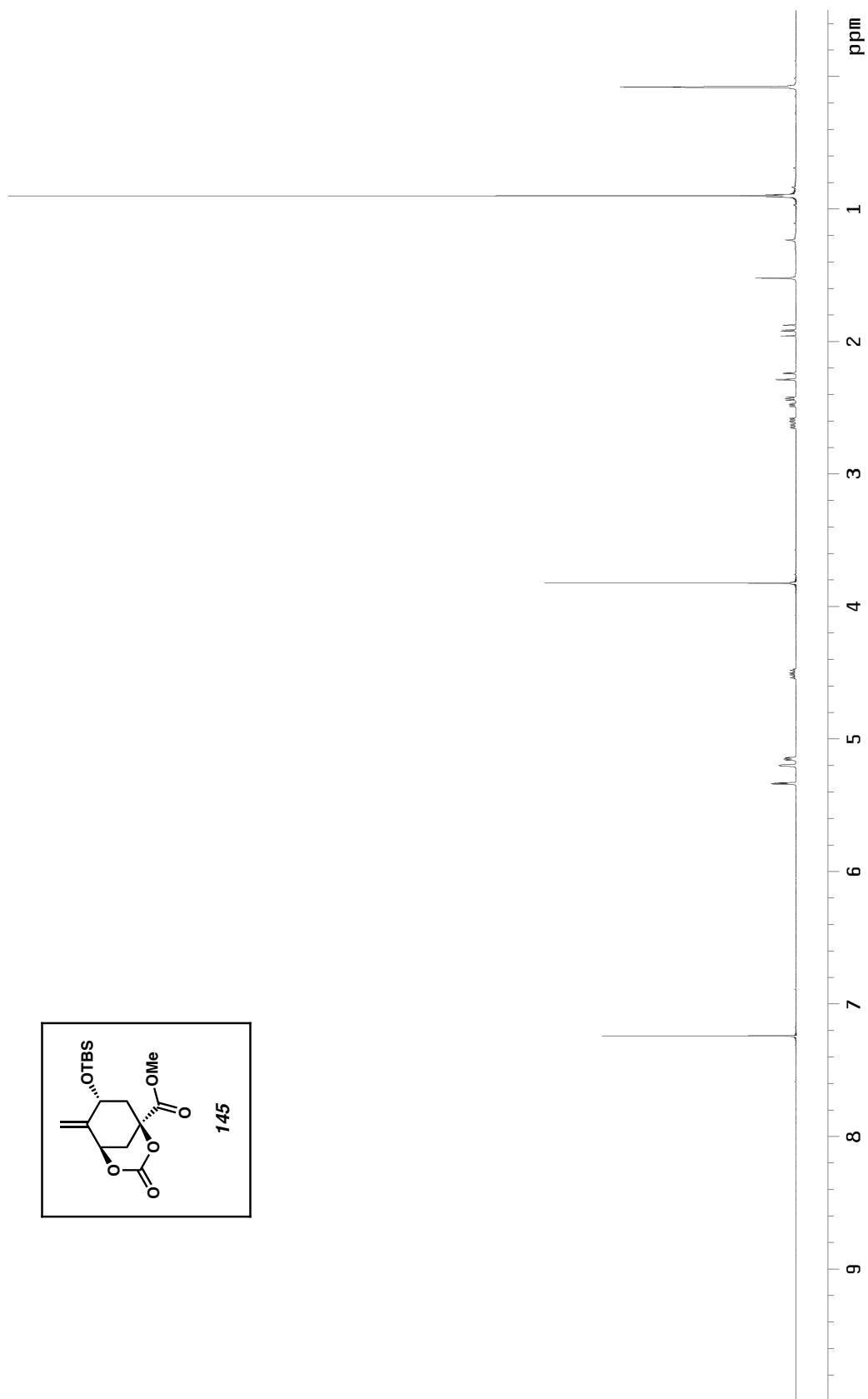


Figure A3.143  $^1\text{H}$  NMR (300 MHz,  $\text{CDCl}_3$ ) of compound **145**

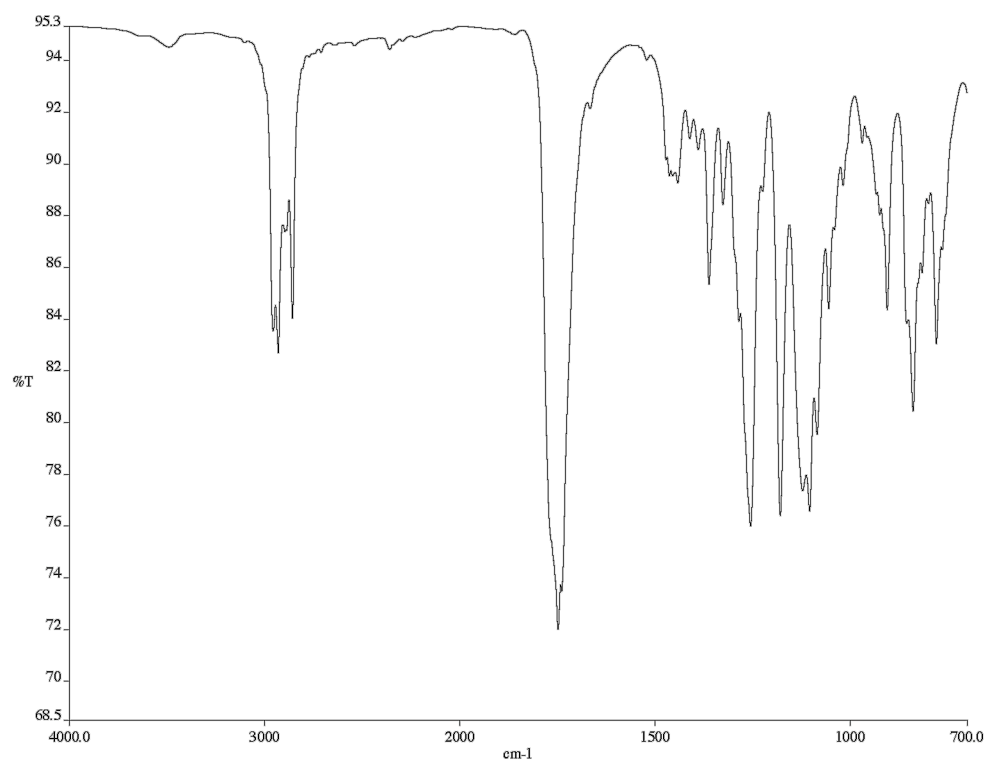


Figure A3.144 Infrared spectrum (thin film/NaCl) of compound **145**

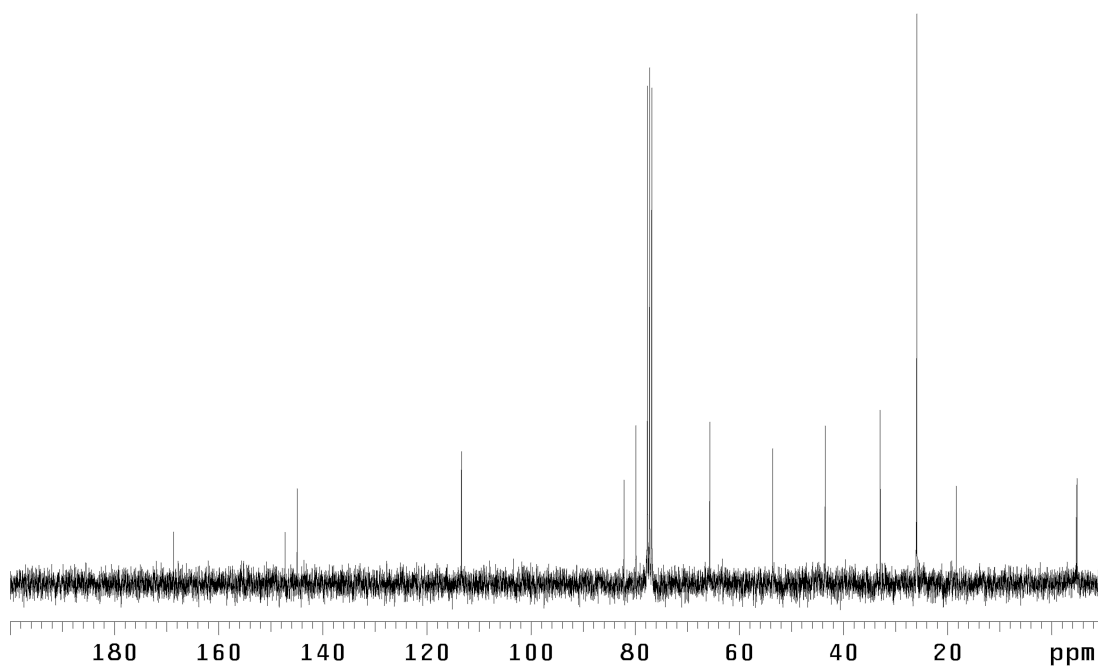


Figure A3.145 <sup>13</sup>C NMR (75 MHz, CDCl<sub>3</sub>) of compound **145**

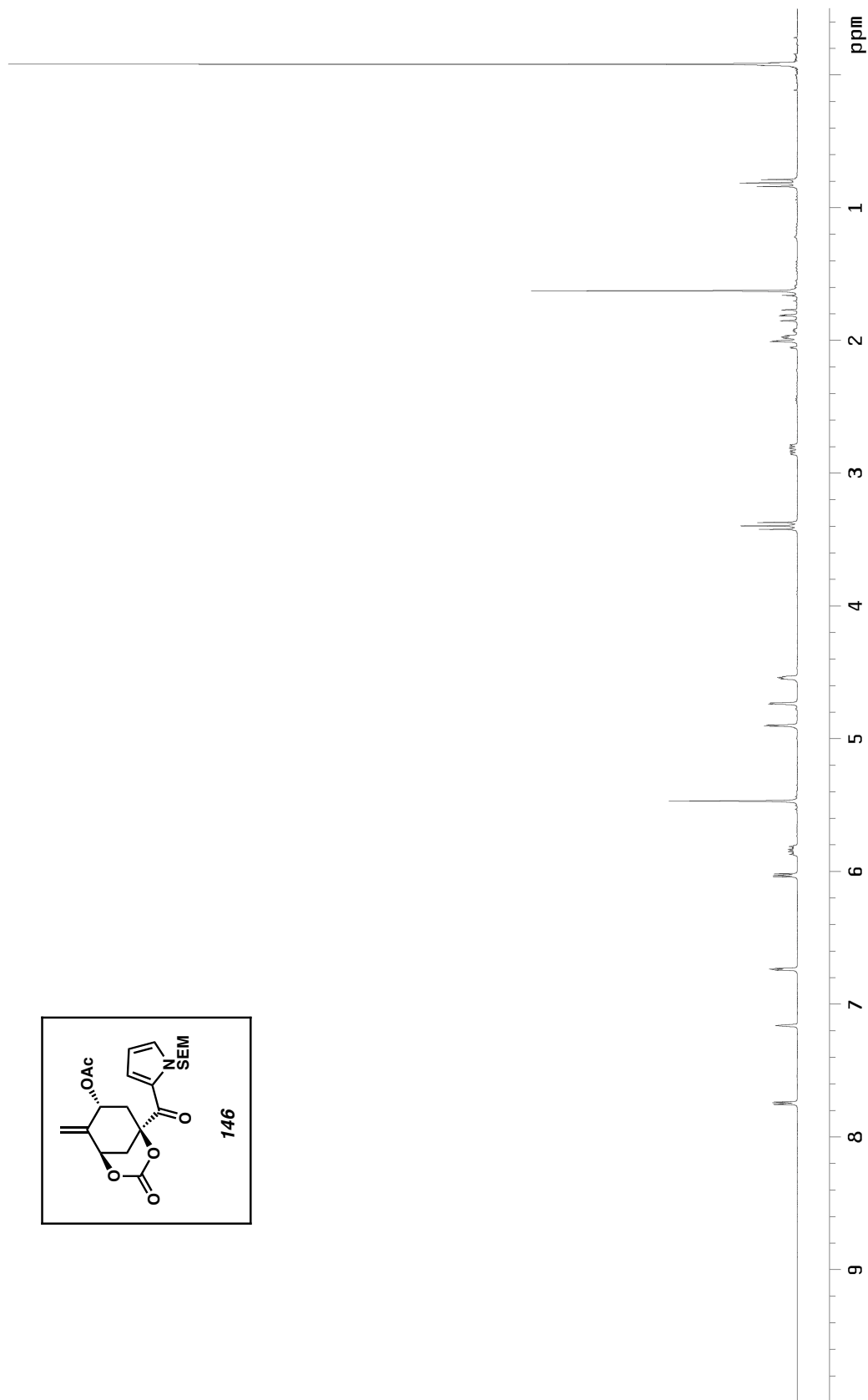


Figure A3.146 <sup>1</sup>H NMR (300 MHz, C<sub>6</sub>D<sub>6</sub>) of compound **146**

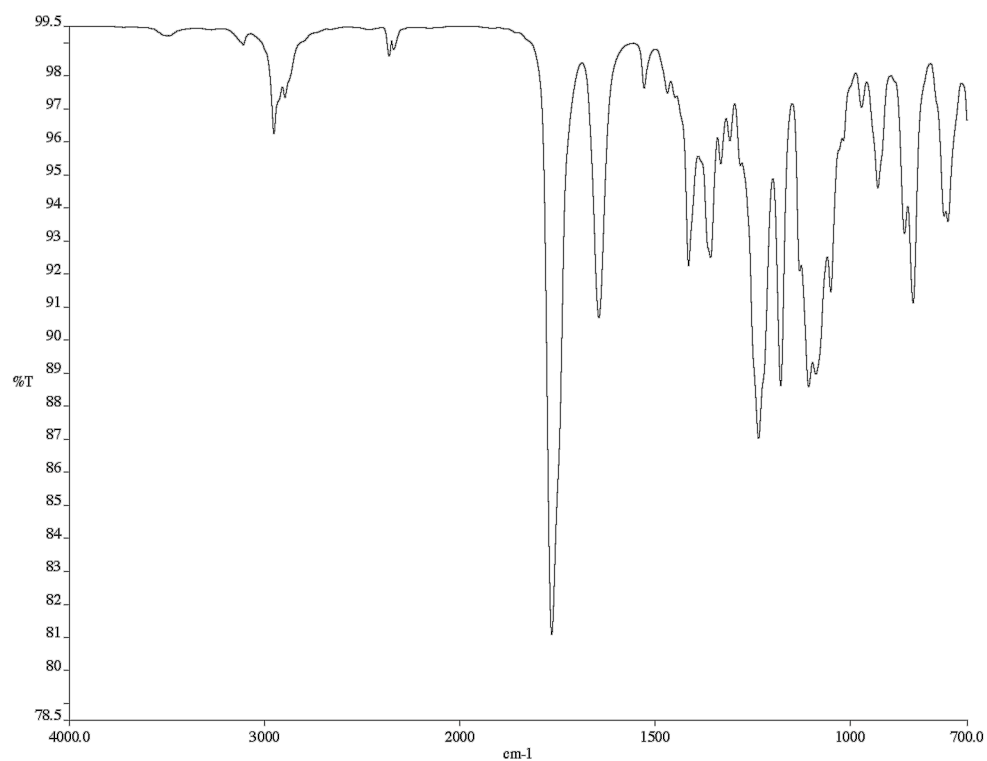


Figure A3.147 Infrared spectrum (thin film/NaCl) of compound **146**

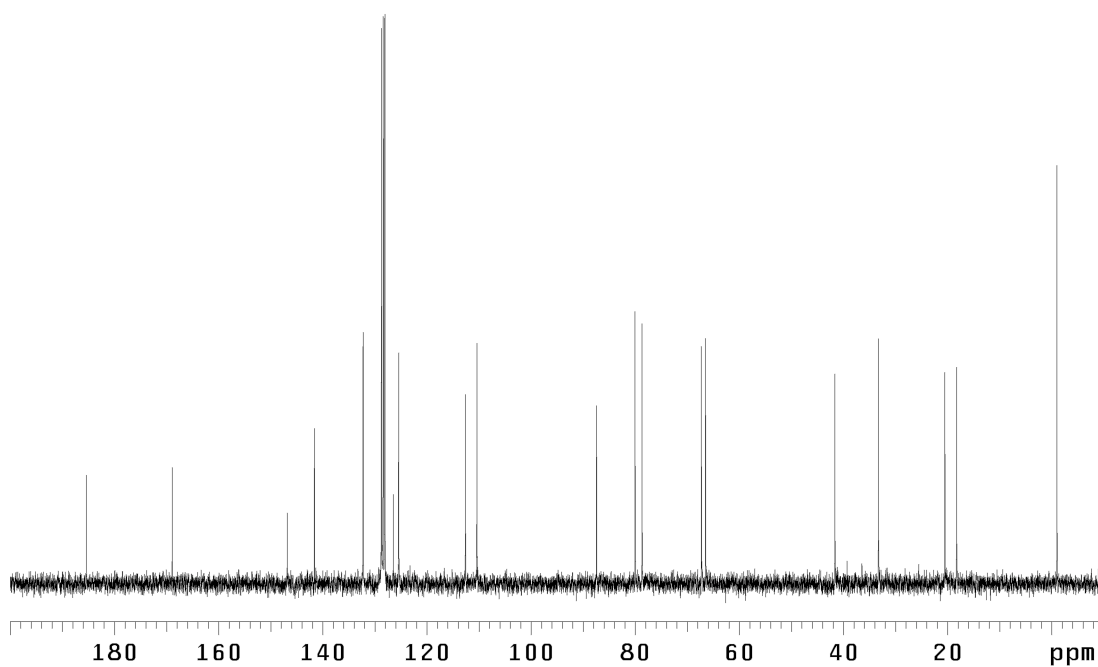


Figure A3.148 <sup>13</sup>C NMR (75 MHz, C<sub>6</sub>D<sub>6</sub>) of compound **146**

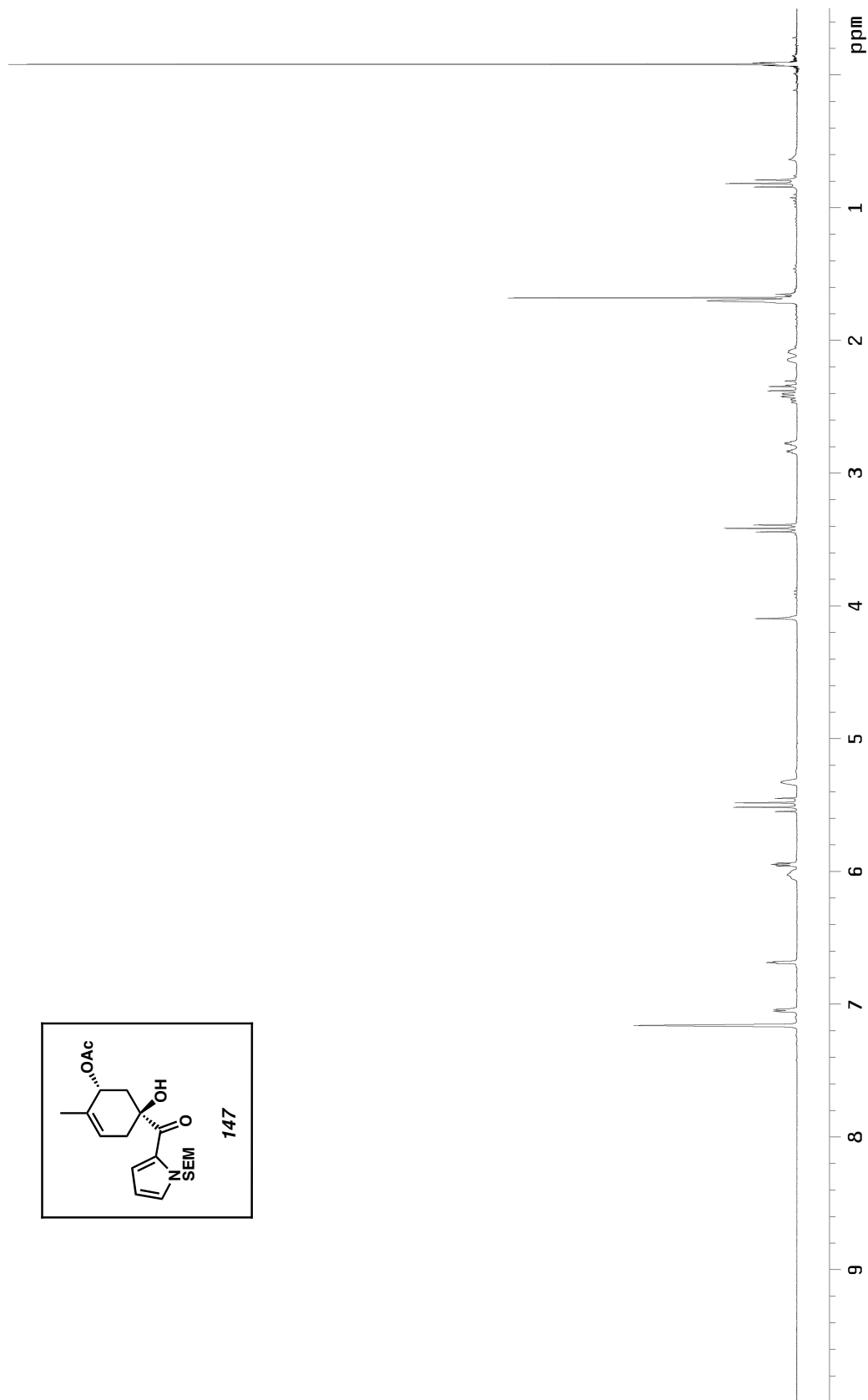


Figure A3.149 <sup>1</sup>H NMR (300 MHz, C<sub>6</sub>D<sub>6</sub>) of compound **147**

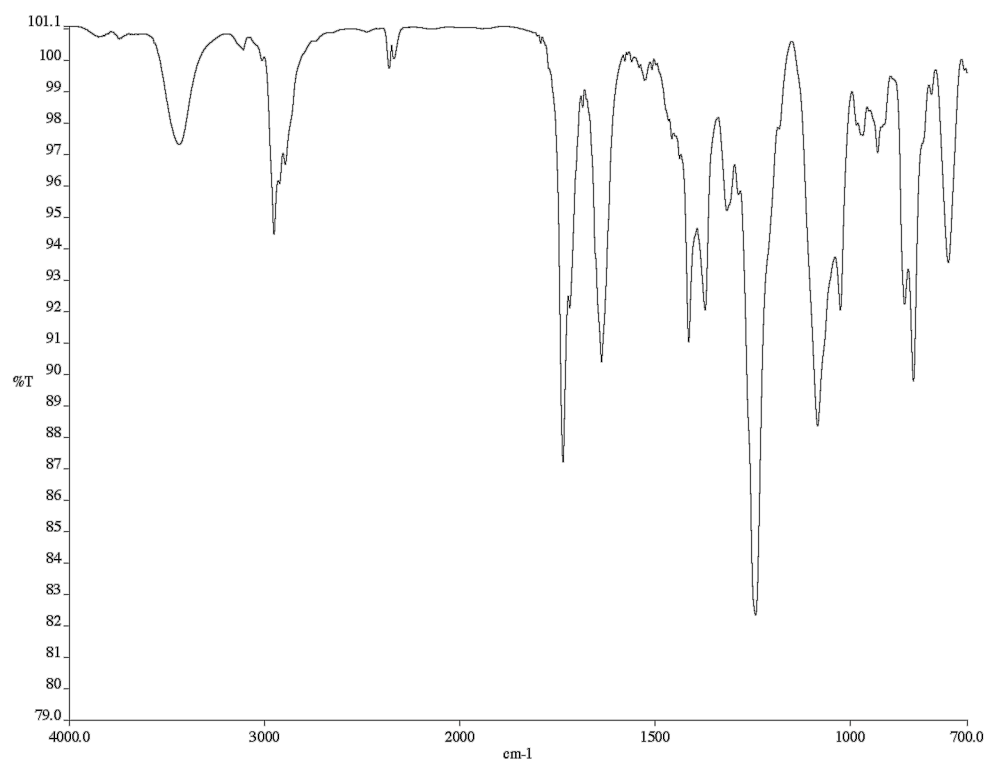


Figure A3.150 Infrared spectrum (thin film/NaCl) of compound **147**

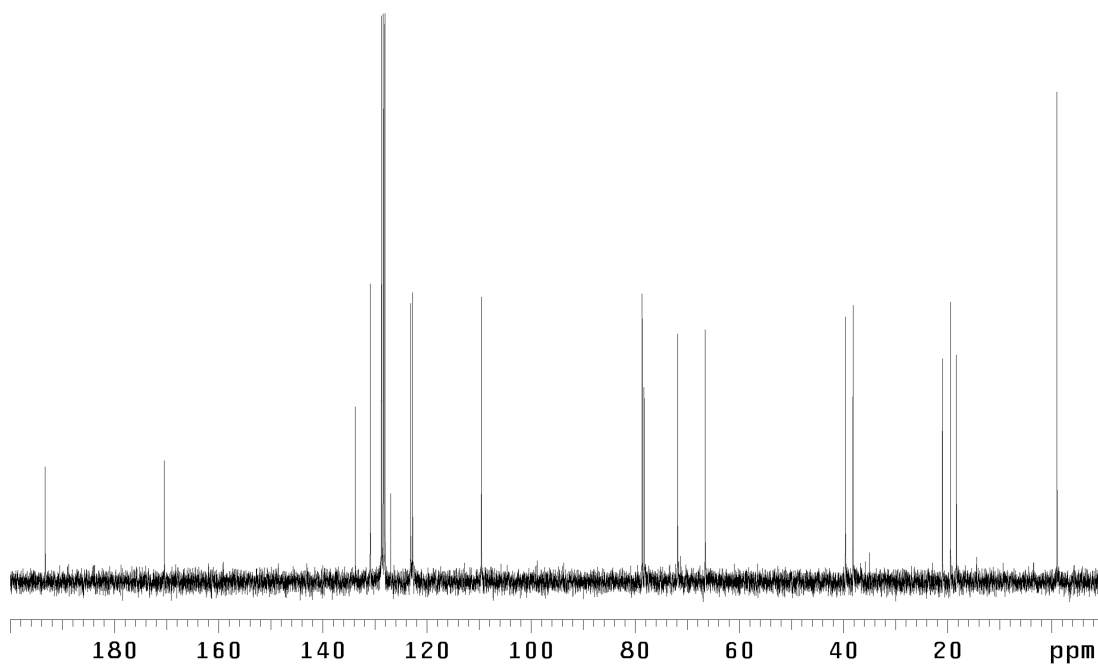
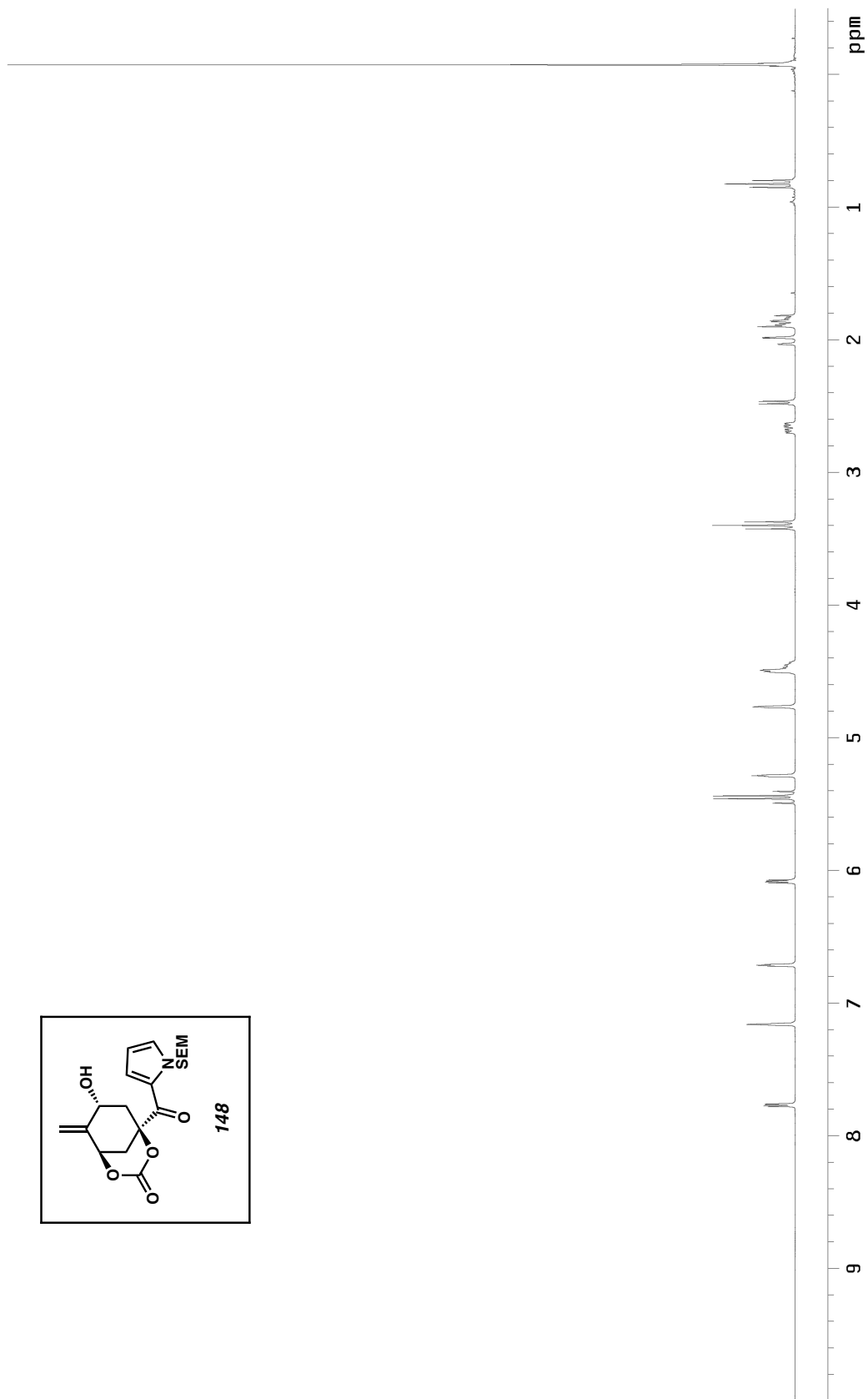
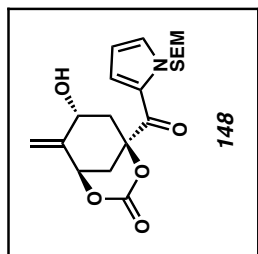


Figure A3.151 <sup>13</sup>C NMR (75 MHz, C<sub>6</sub>D<sub>6</sub>) of compound **147**



*Figure A3.152* <sup>1</sup>H NMR (300 MHz, C<sub>6</sub>D<sub>6</sub>) of compound **148**



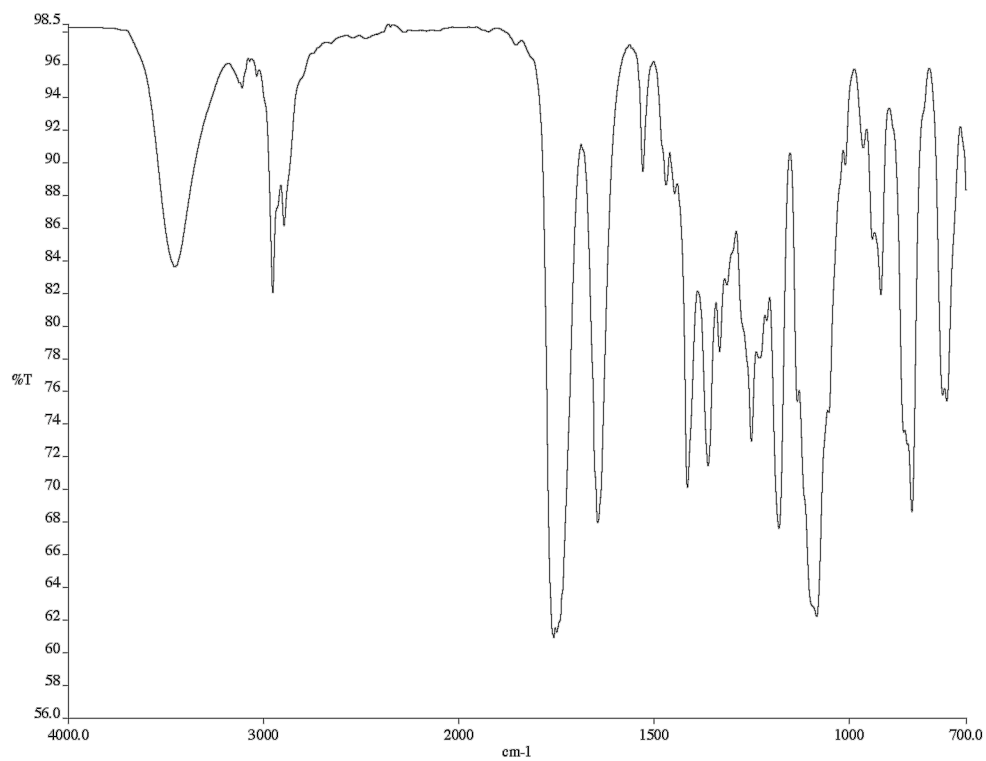


Figure A3.153 Infrared spectrum (thin film/NaCl) of compound **148**

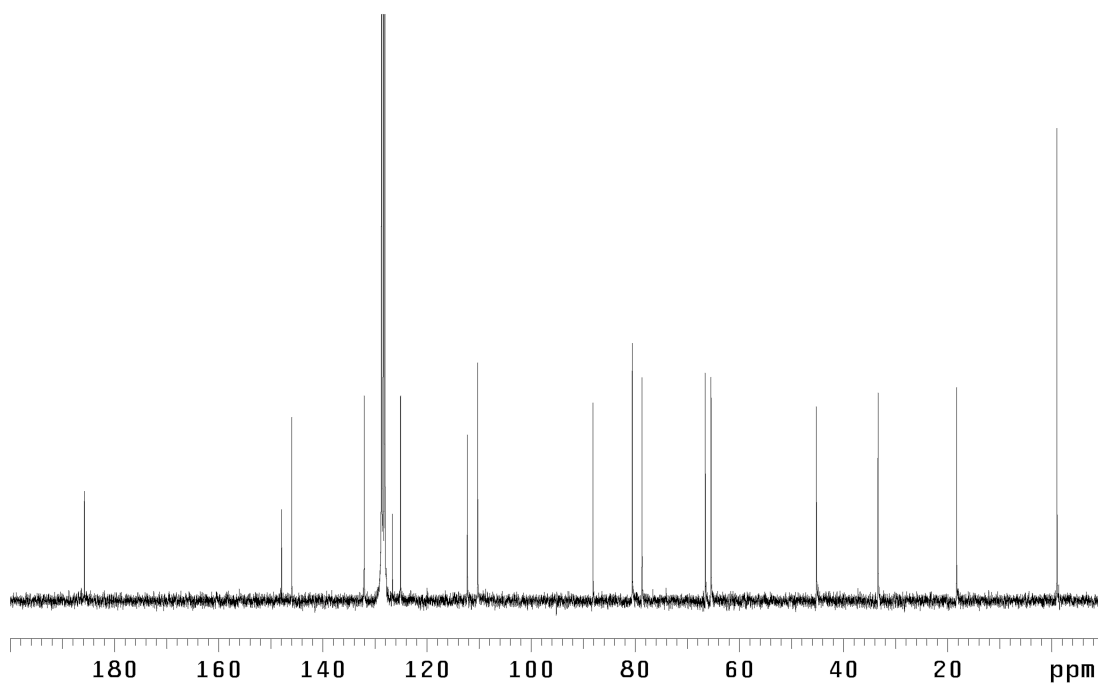


Figure A3.154 <sup>13</sup>C NMR (75 MHz, C<sub>6</sub>D<sub>6</sub>) of compound **148**

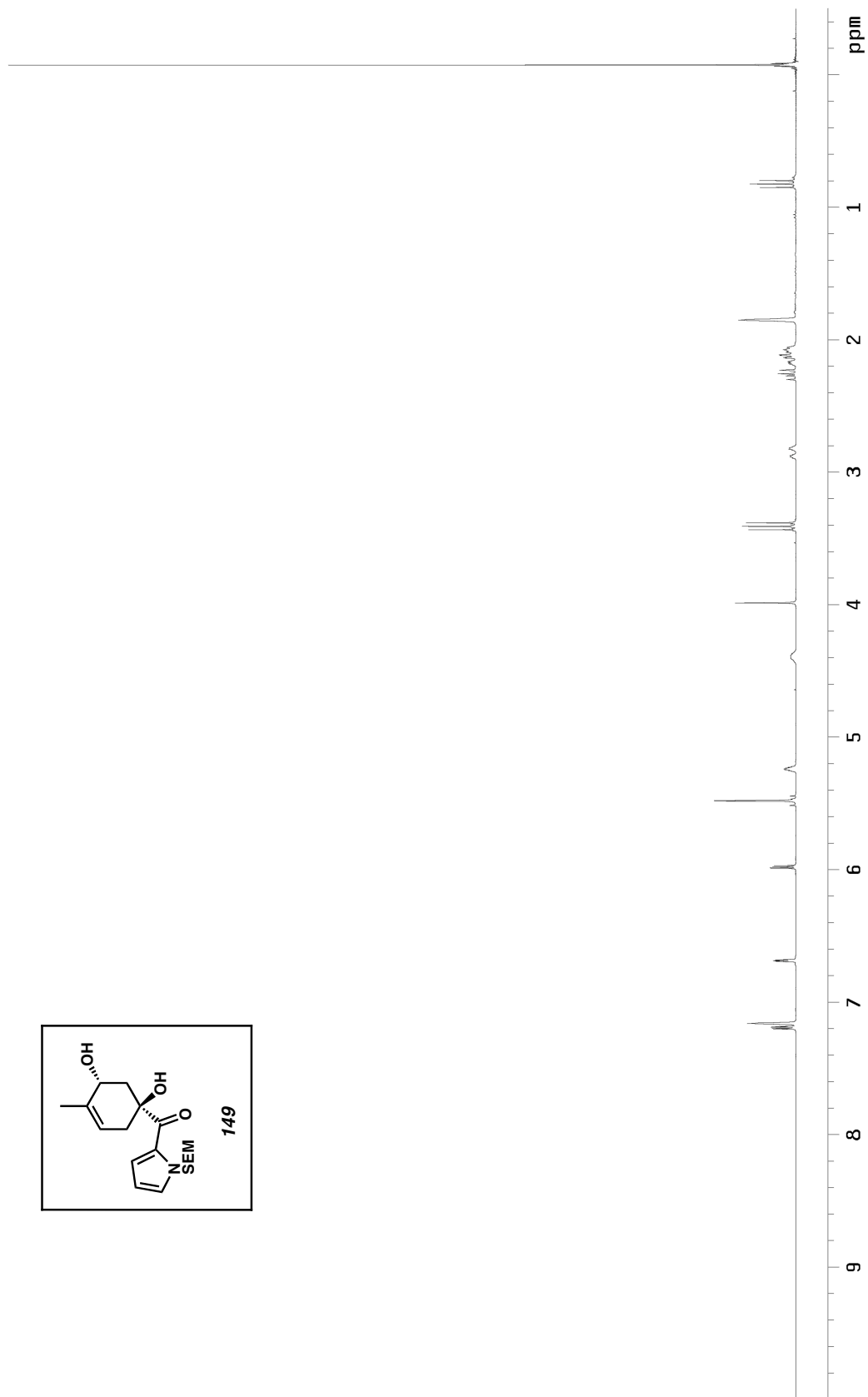
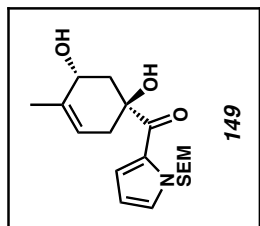


Figure A3.155  $^1\text{H}$  NMR (300 MHz,  $\text{C}_6\text{D}_6$ ) of compound **149**

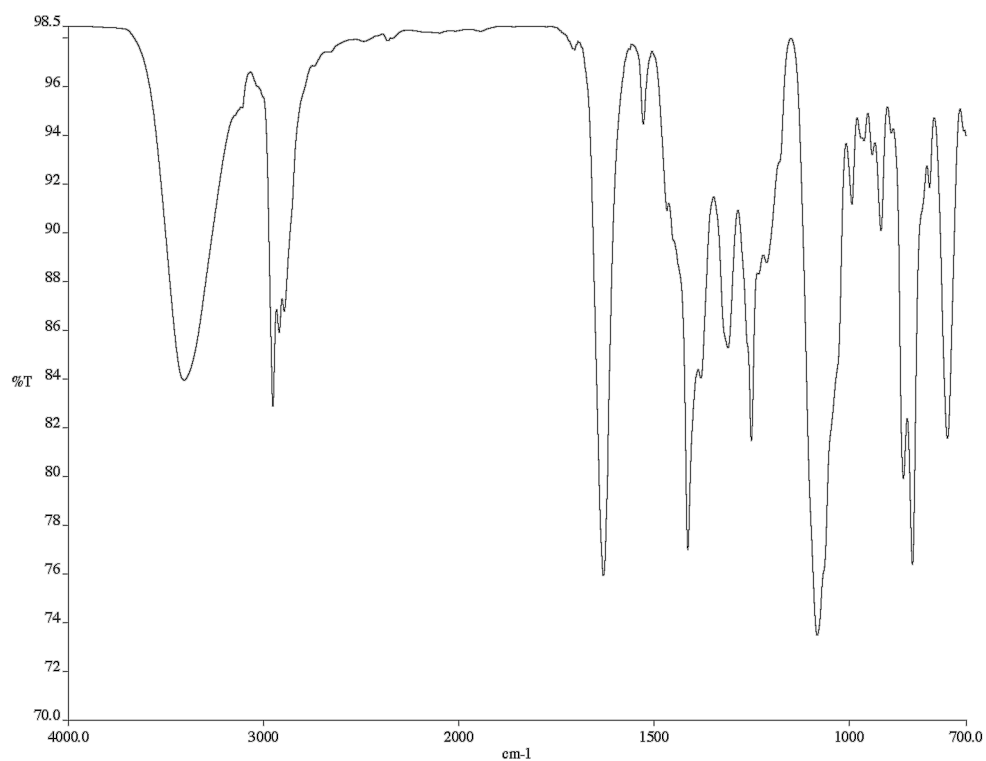


Figure A3.156 Infrared spectrum (thin film/NaCl) of compound **149**

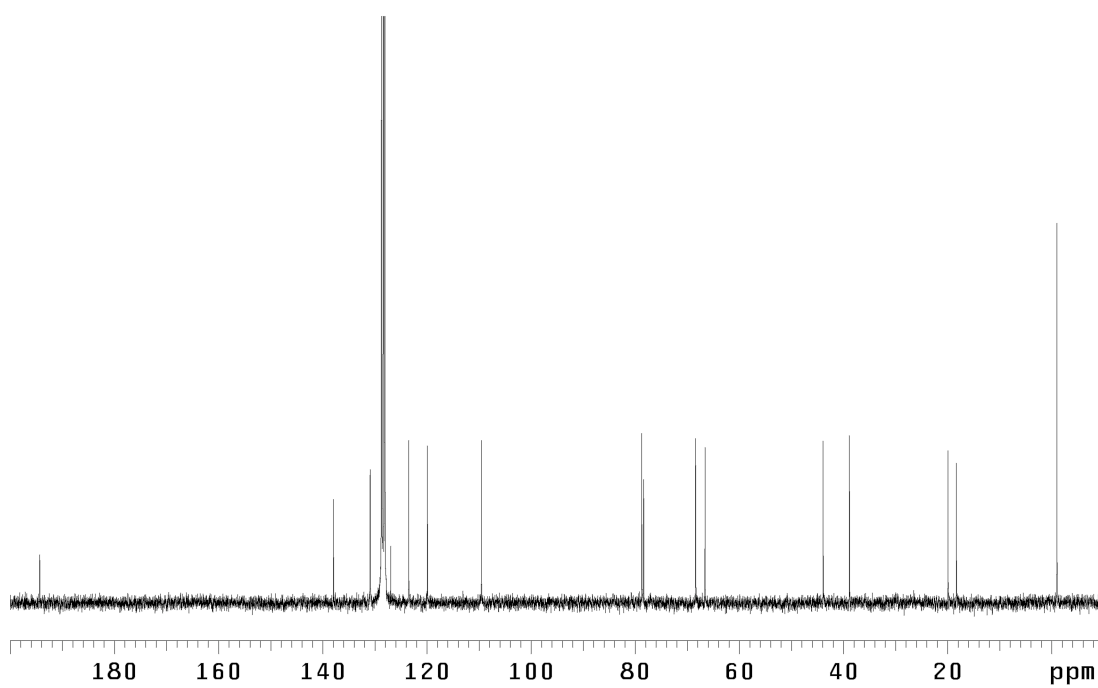


Figure A3.157 <sup>13</sup>C NMR (75 MHz, C<sub>6</sub>D<sub>6</sub>) of compound **149**

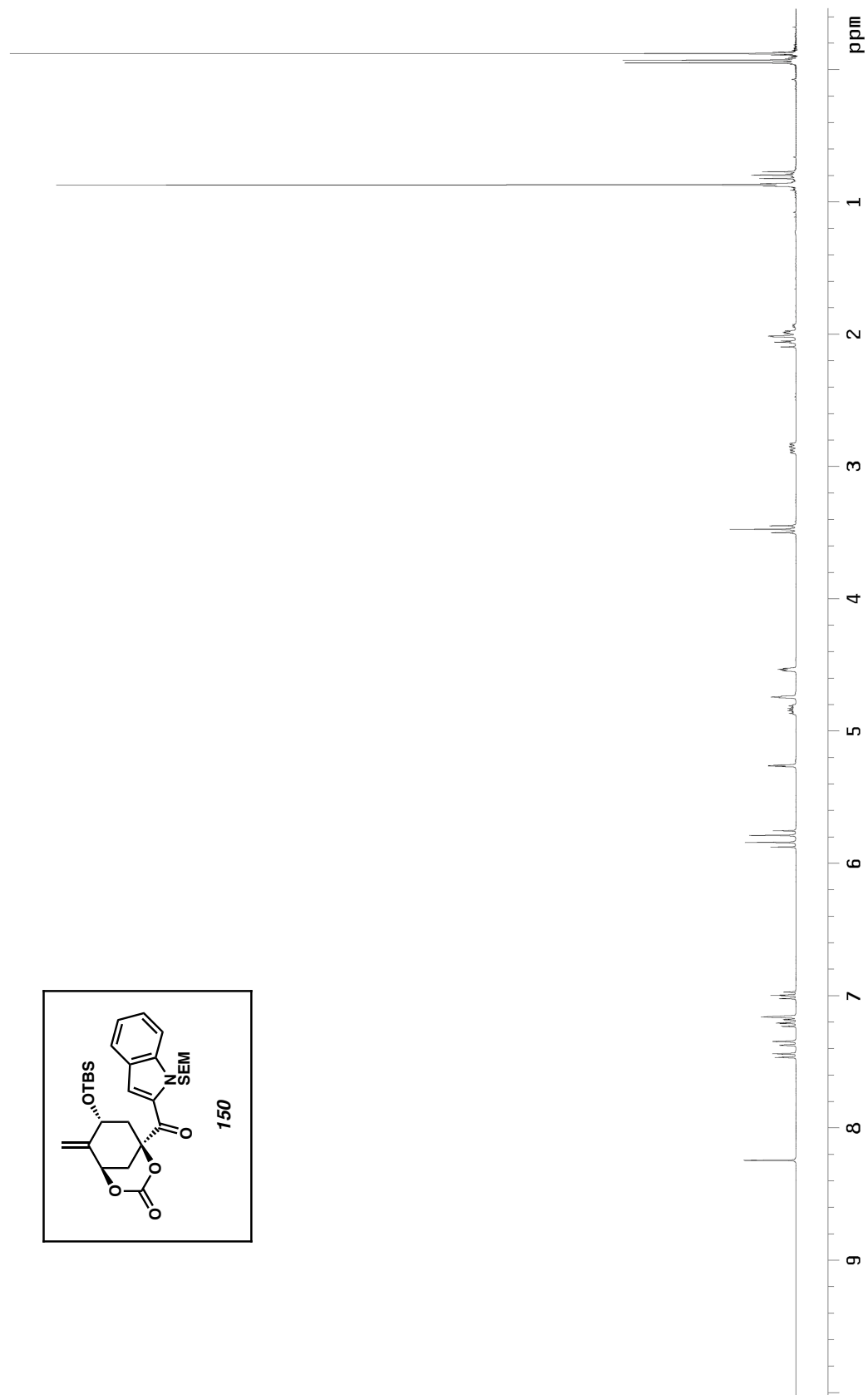
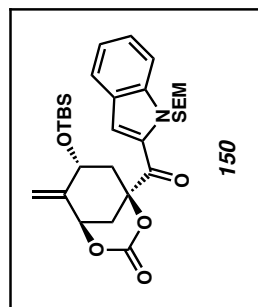


Figure A3.158  $^1\text{H}$  NMR (300 MHz,  $\text{C}_6\text{D}_6$ ) of compound **150**

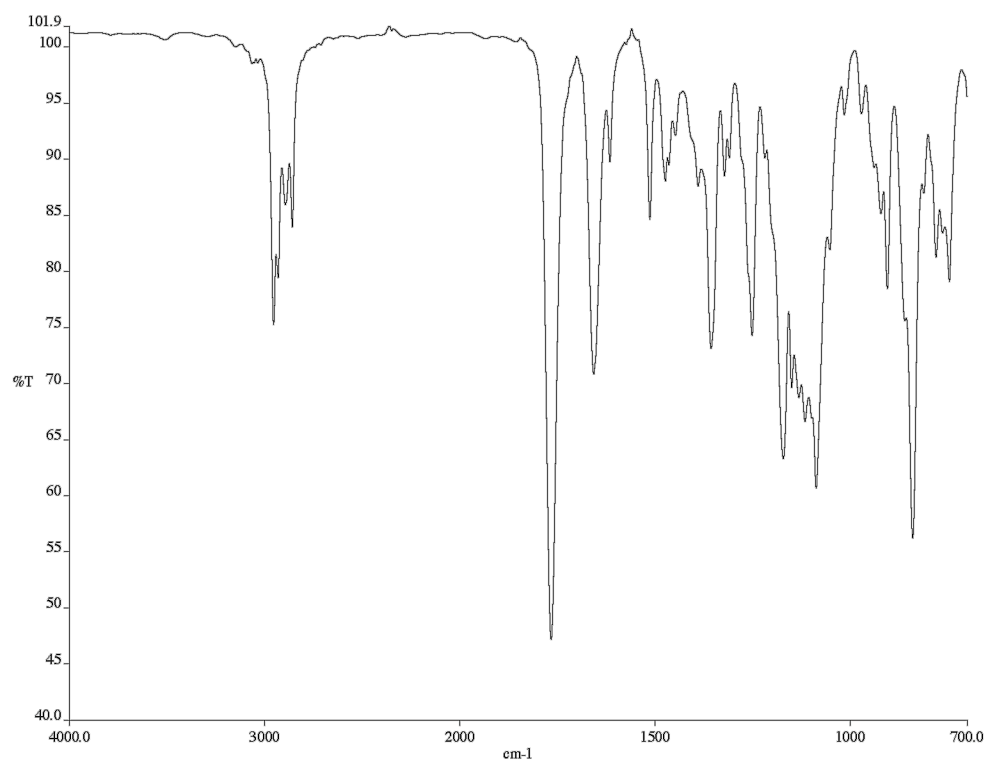


Figure A3.159 Infrared spectrum (thin film/NaCl) of compound **150**

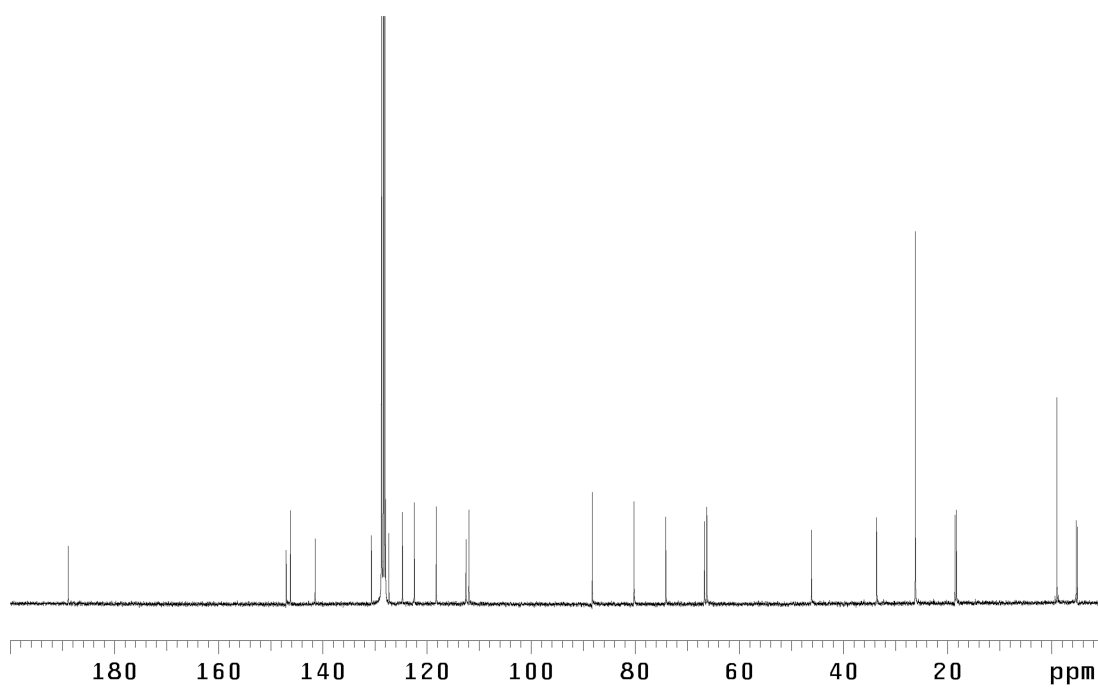


Figure A3.160 <sup>13</sup>C NMR (75 MHz, C<sub>6</sub>D<sub>6</sub>) of compound **150**

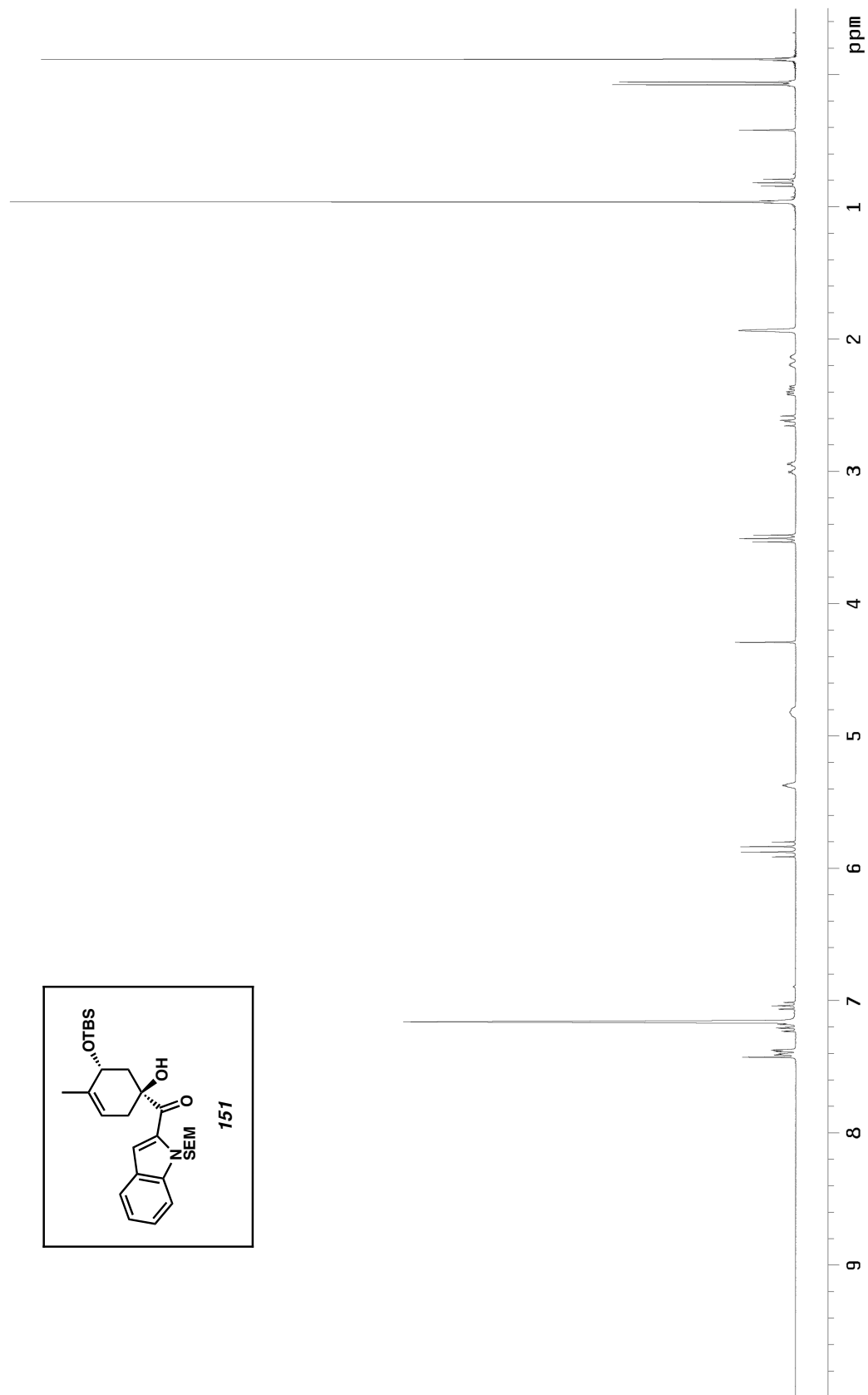
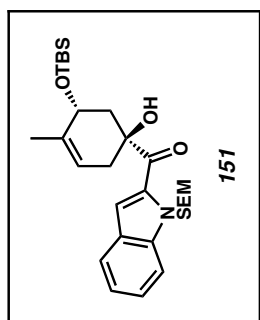


Figure A3.161 <sup>1</sup>H NMR (300 MHz, C<sub>6</sub>D<sub>6</sub>) of compound **151**



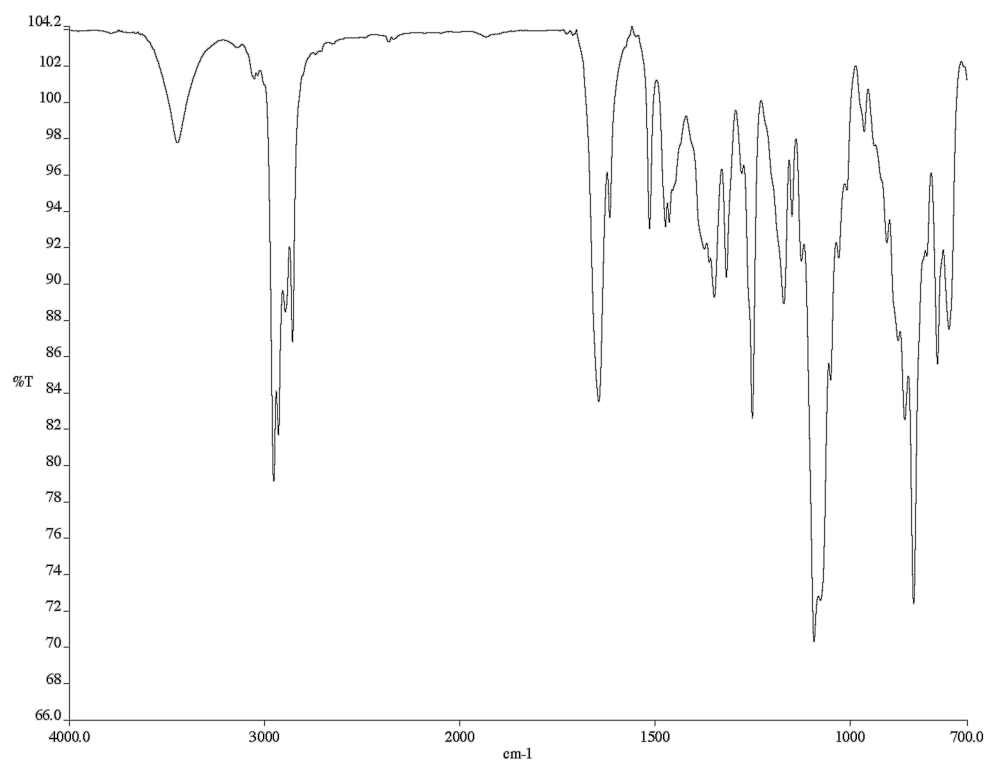


Figure A3.162 Infrared spectrum (thin film/NaCl) of compound **151**

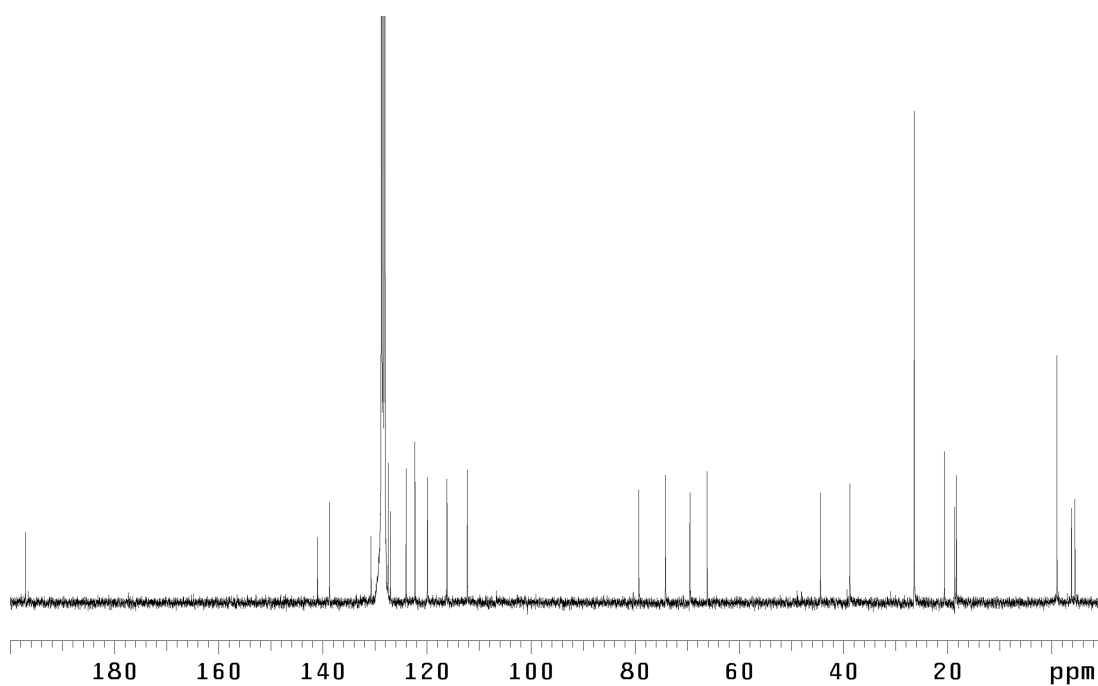


Figure A3.163 <sup>13</sup>C NMR (75 MHz, C<sub>6</sub>D<sub>6</sub>) of compound **151**

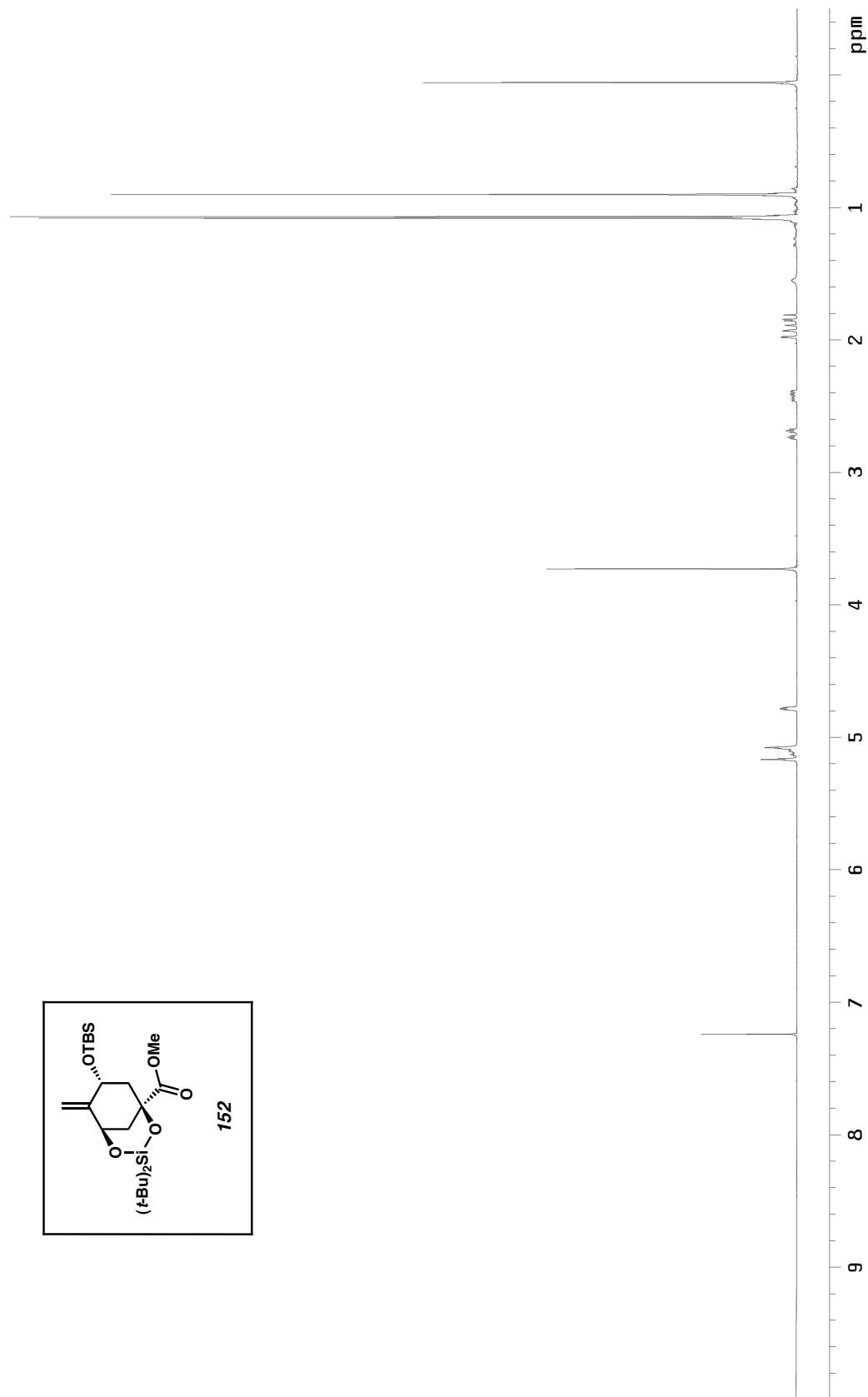


Figure A3.164  $^1\text{H}$  NMR (300 MHz,  $\text{CDCl}_3$ ) of compound **152**



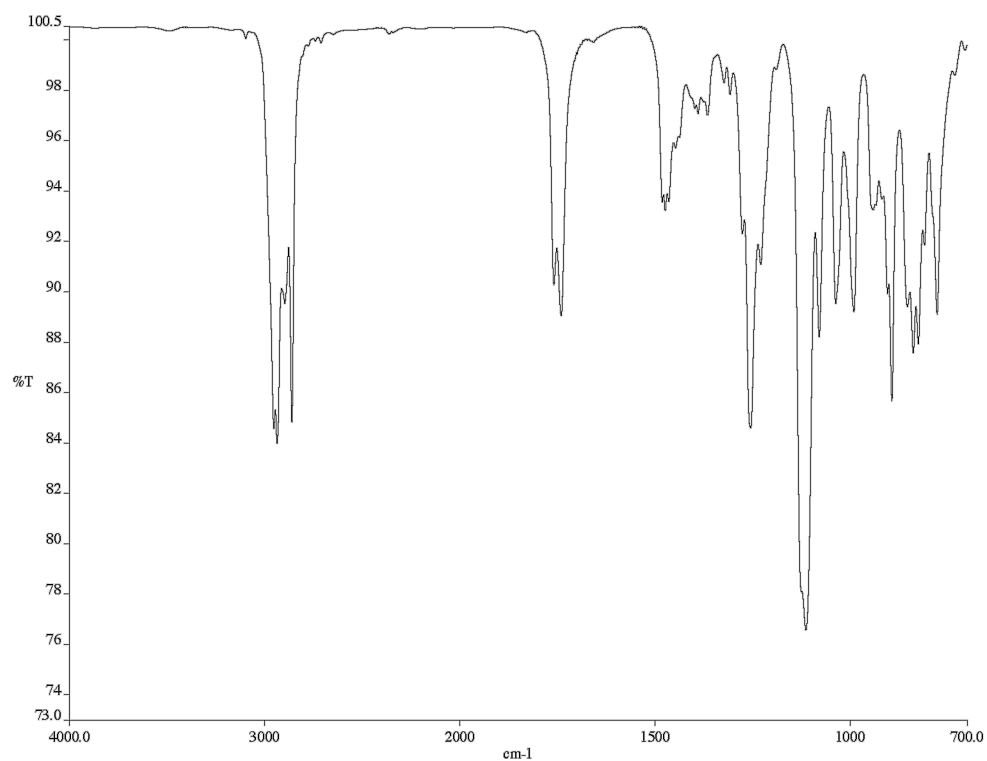


Figure A3.165 Infrared spectrum (thin film/NaCl) of compound **152**

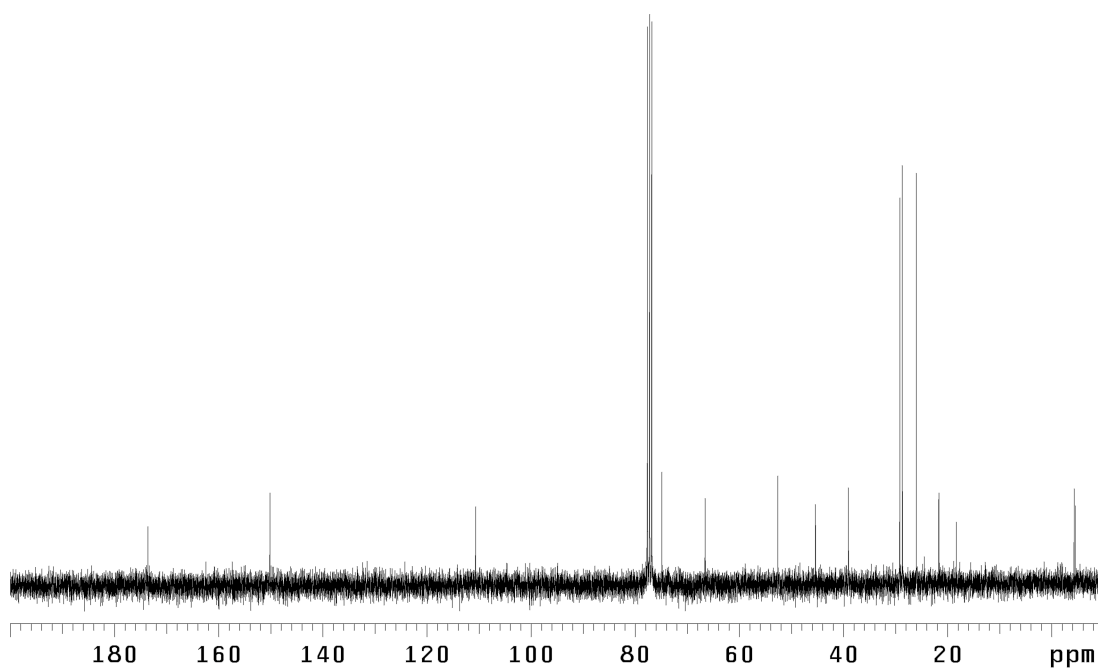


Figure A3.166 <sup>13</sup>C NMR (75 MHz, CDCl<sub>3</sub>) of compound **152**

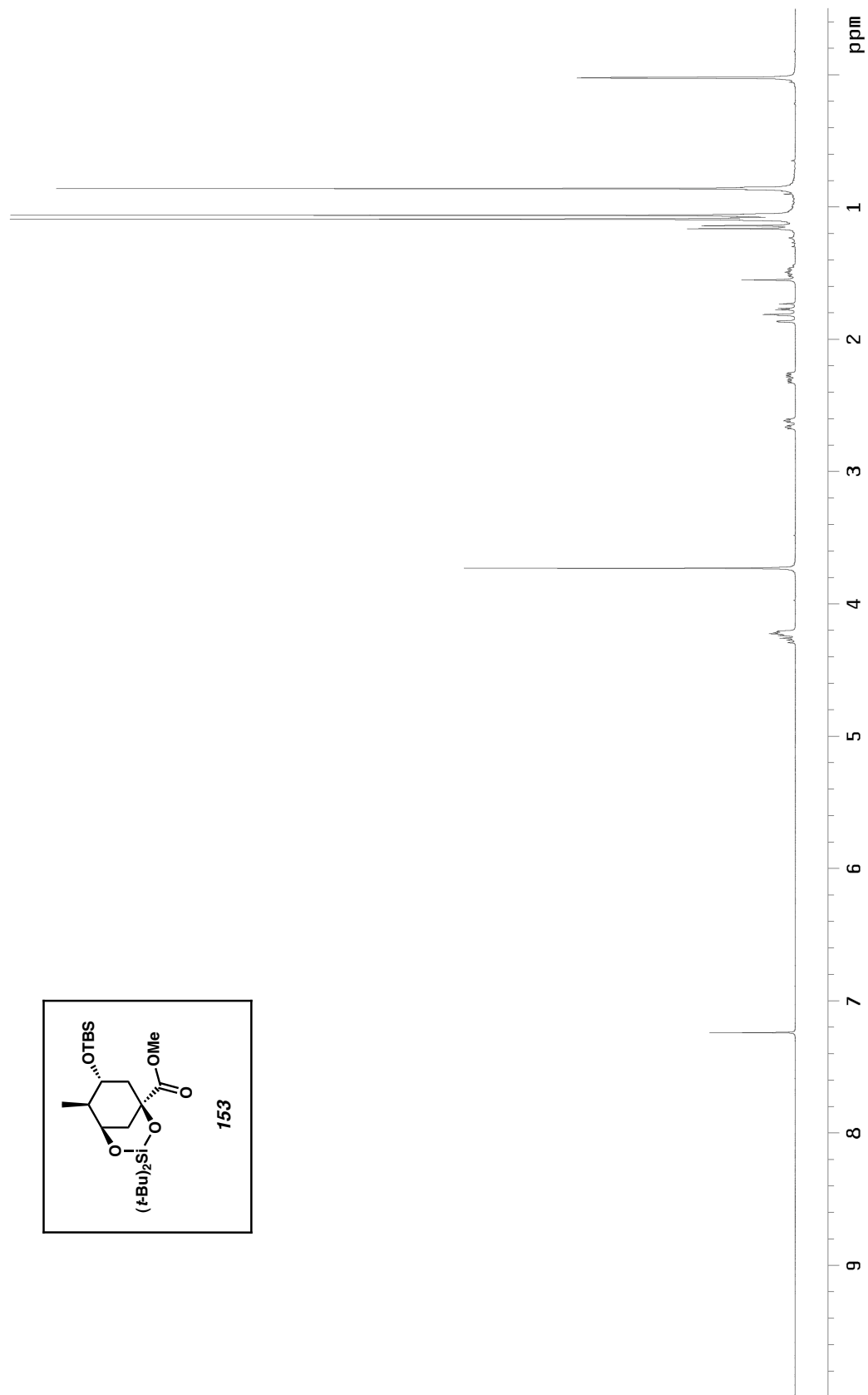
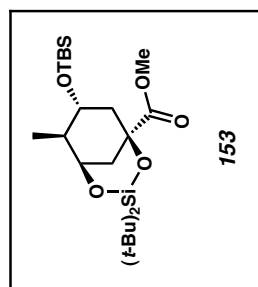


Figure A3.167 <sup>1</sup>H NMR (300 MHz, CDCl<sub>3</sub>) of compound **153**

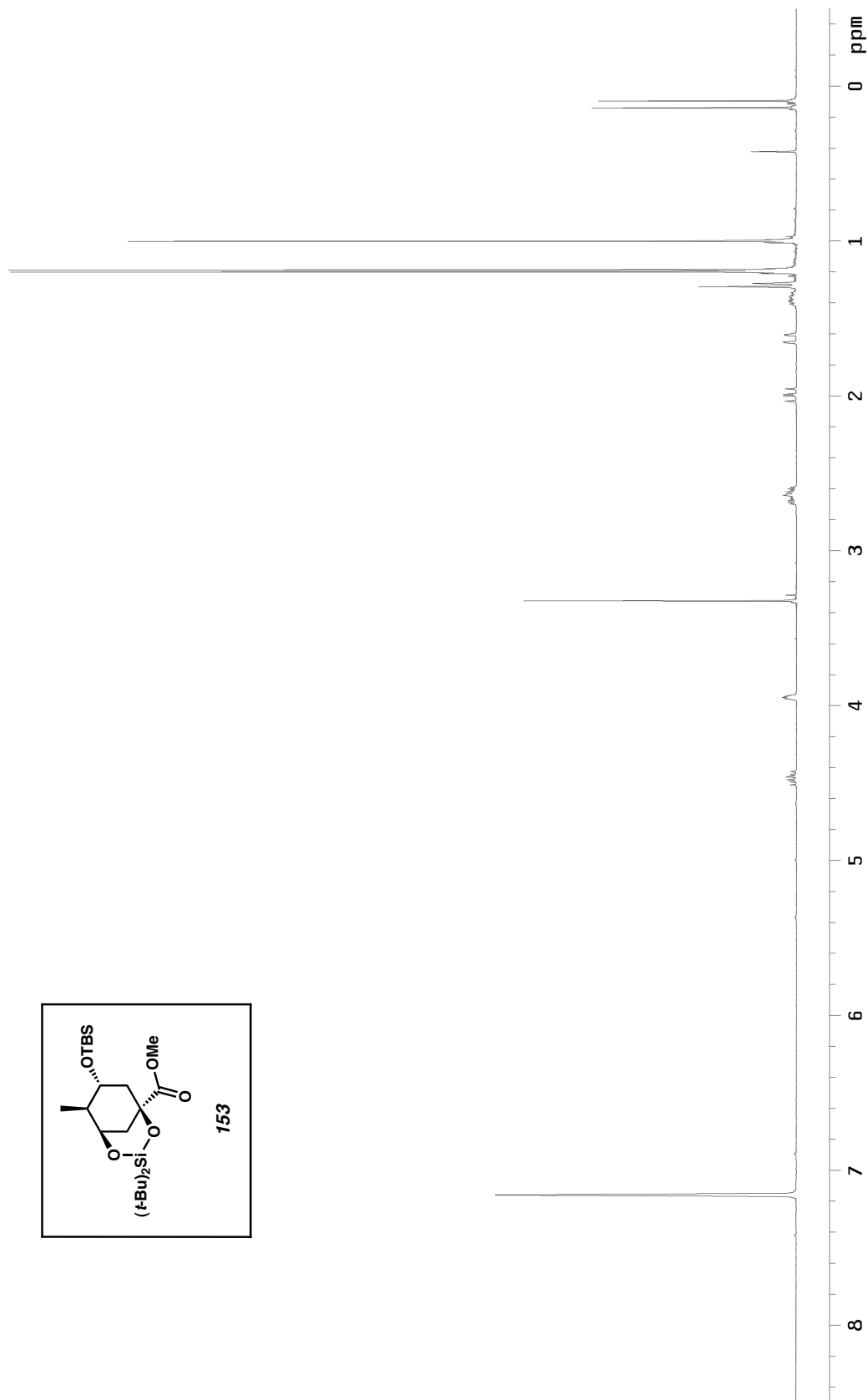
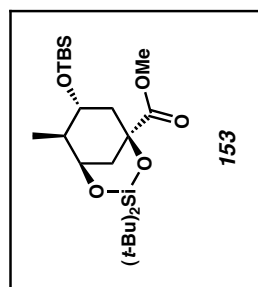


Figure A3.168  $^1\text{H}$  NMR (300 MHz,  $\text{C}_6\text{D}_6$ ) of compound **153**

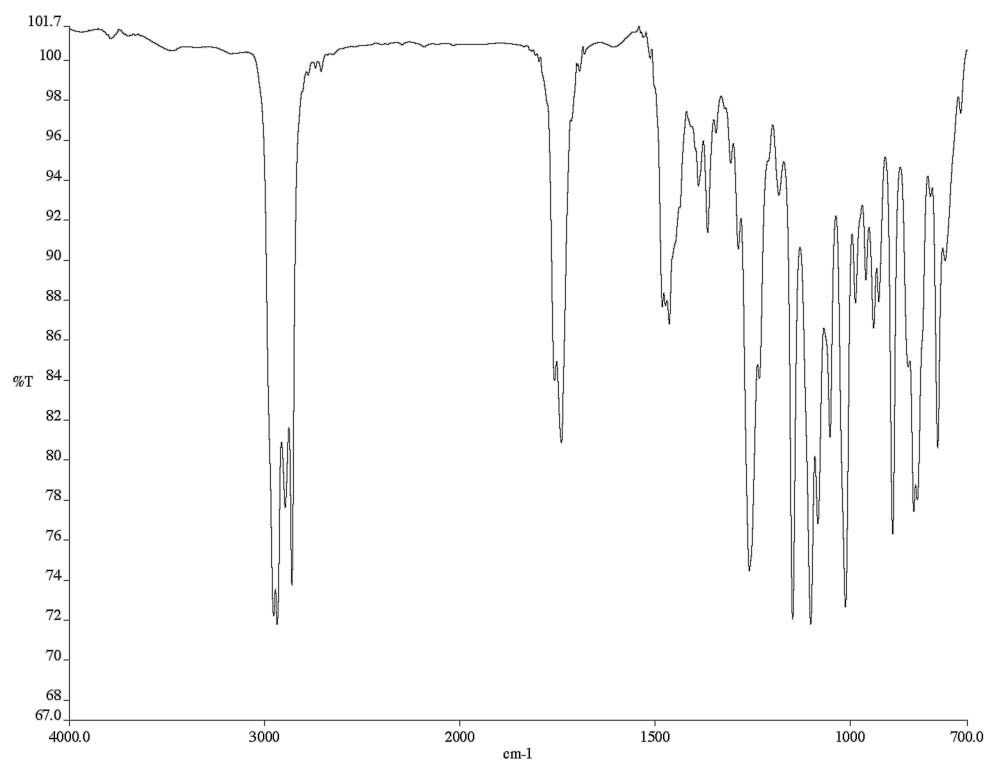


Figure A3.169 Infrared spectrum (thin film/NaCl) of compound **153**

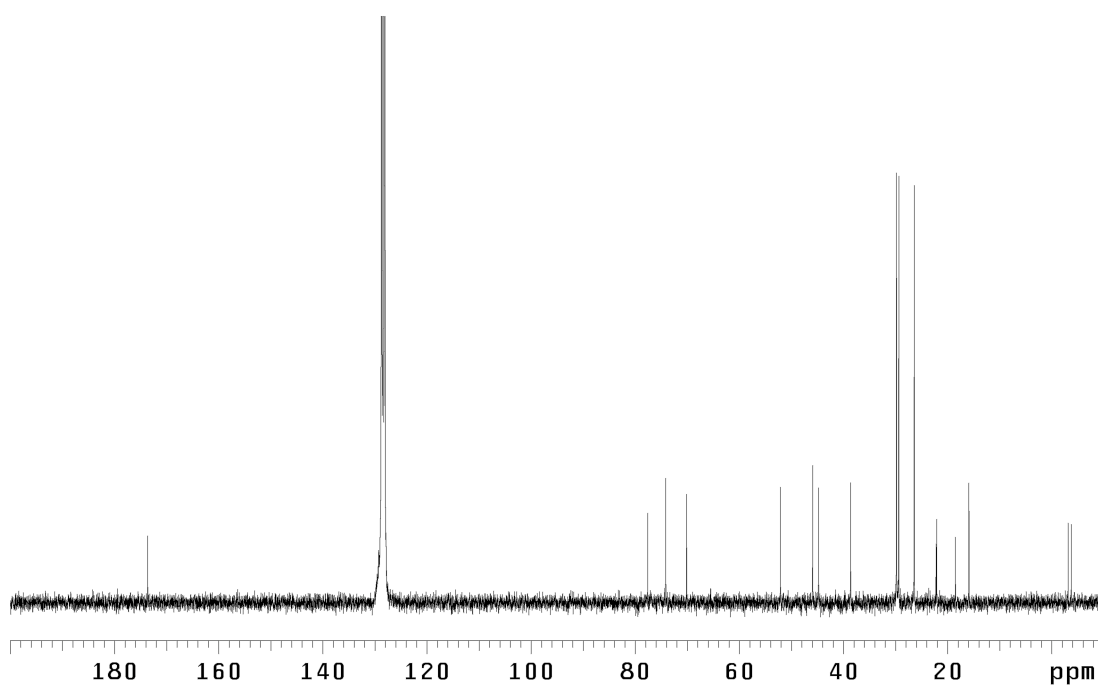


Figure A3.170 <sup>13</sup>C NMR (75 MHz, C<sub>6</sub>D<sub>6</sub>) of compound **153**

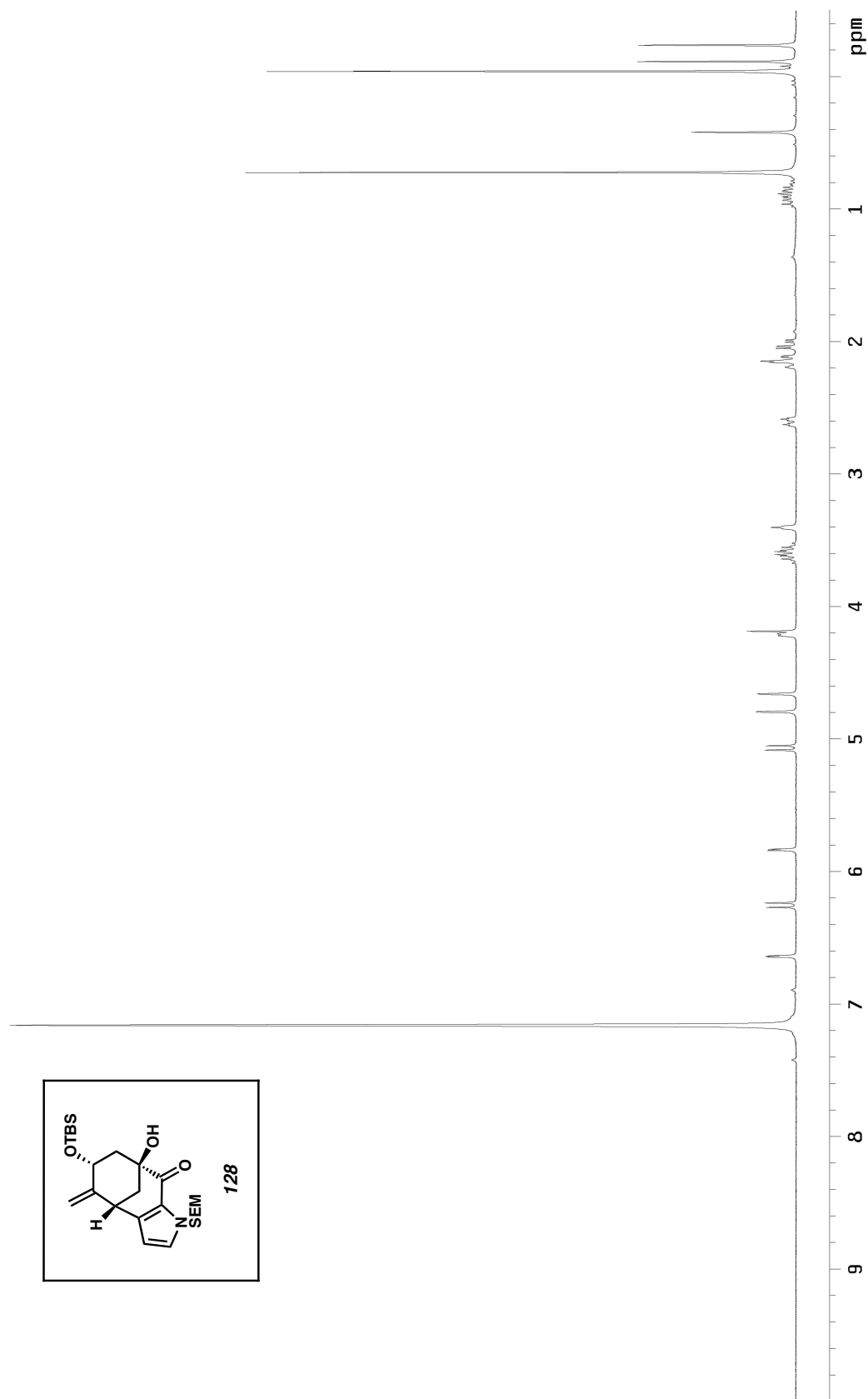


Figure A3.171  $^1\text{H}$  NMR (300 MHz,  $\text{C}_6\text{D}_6\text{O}$ ) of compound **128**

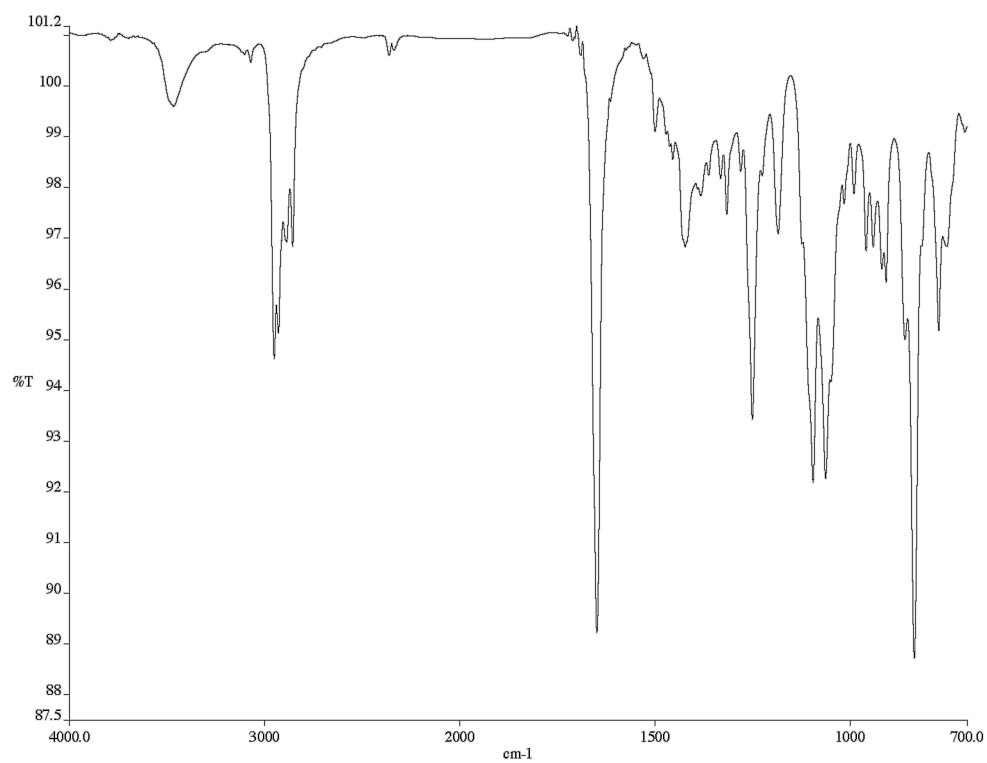


Figure A3.172 Infrared spectrum (thin film/NaCl) of compound **128**

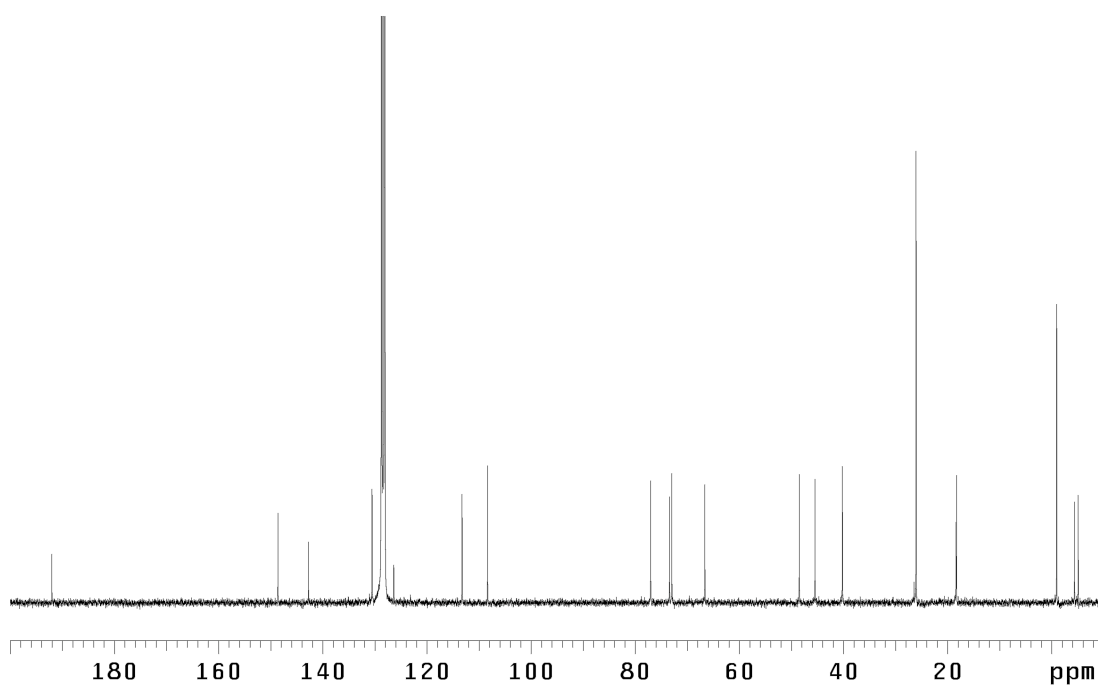


Figure A3.173 <sup>13</sup>C NMR (75 MHz, C<sub>6</sub>D<sub>6</sub>) of compound **128**

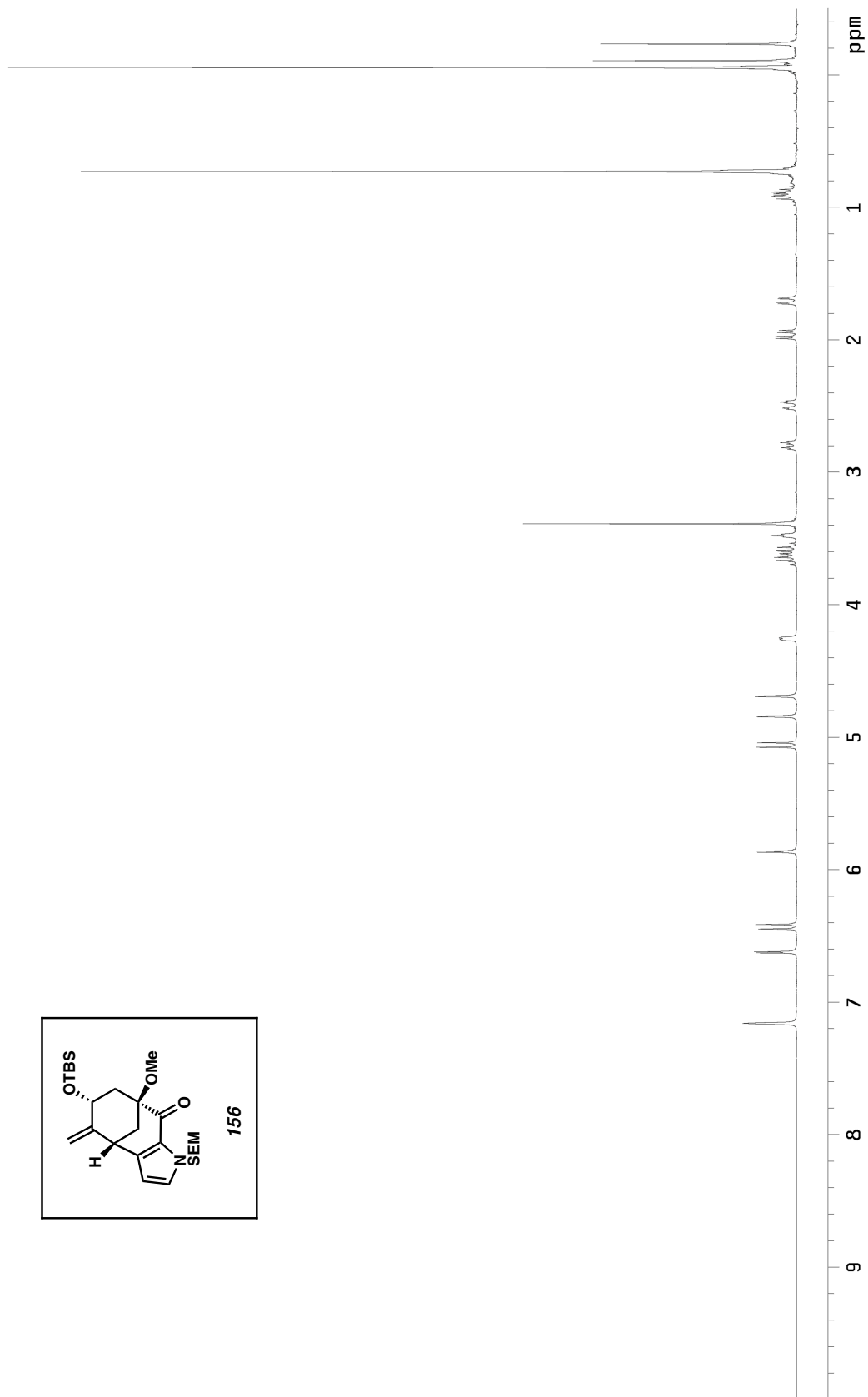
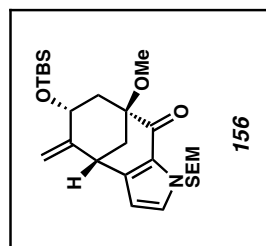


Figure A3.174  $^1\text{H}$  NMR (300 MHz,  $\text{C}_6\text{D}_6$ ) of compound **156**

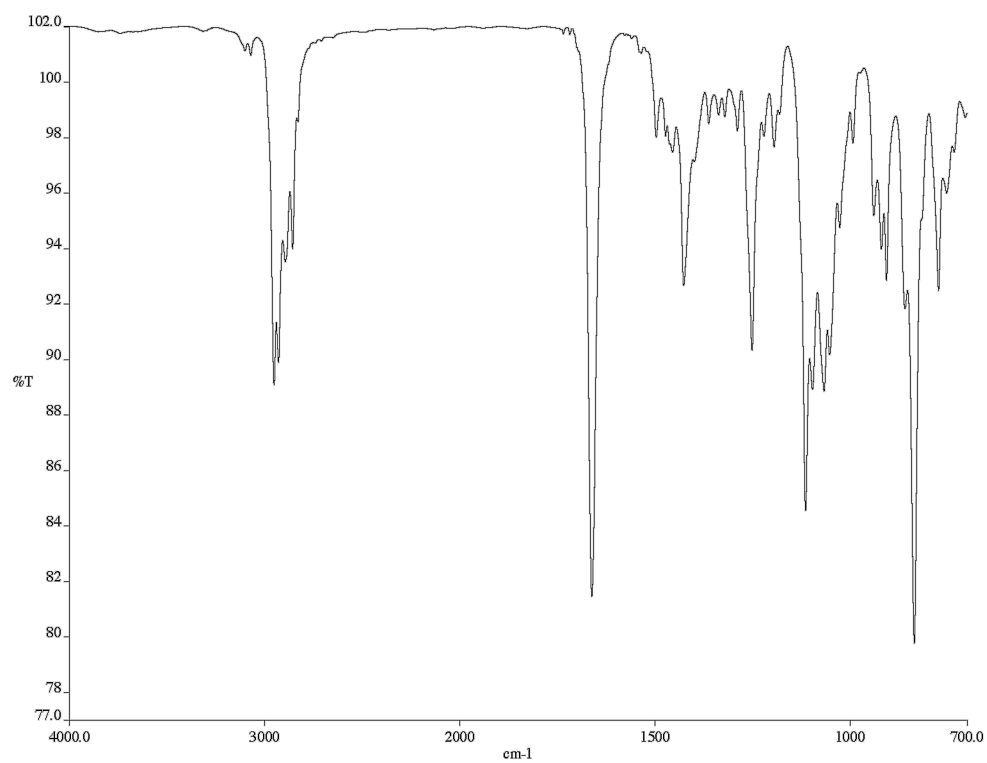


Figure A3.175 Infrared spectrum (thin film/NaCl) of compound **156**

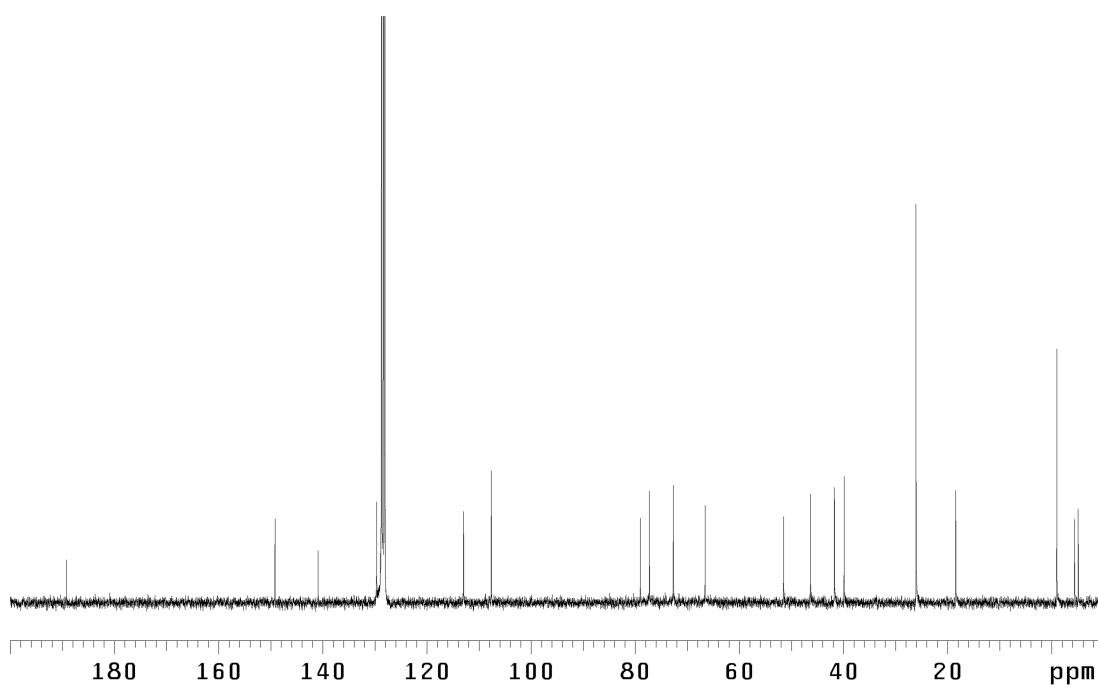


Figure A3.176 <sup>13</sup>C NMR (75 MHz, C<sub>6</sub>D<sub>6</sub>) of compound **156**



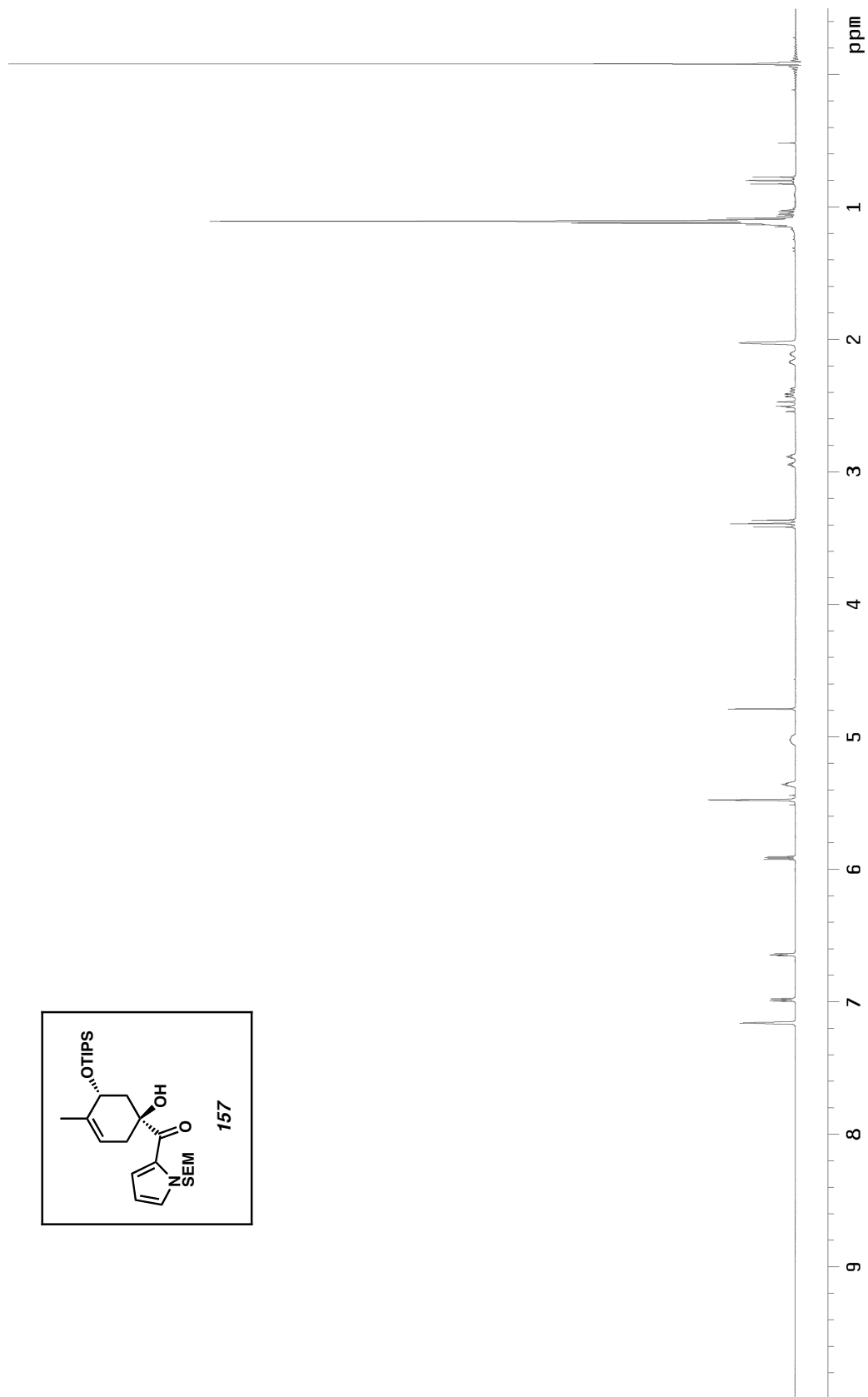
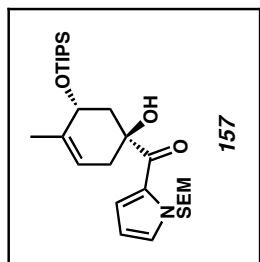


Figure A3.177  $^1\text{H}$  NMR (300 MHz,  $\text{C}_6\text{D}_6$ ) of compound **157**

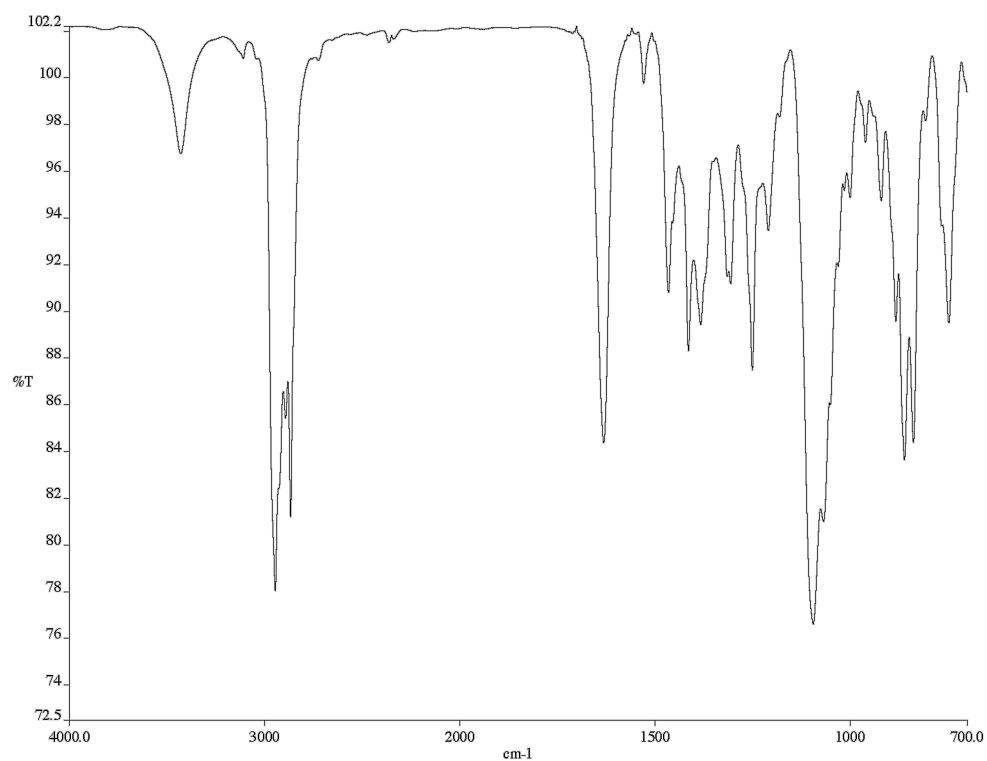


Figure A3.178 Infrared spectrum (thin film/NaCl) of compound **157**

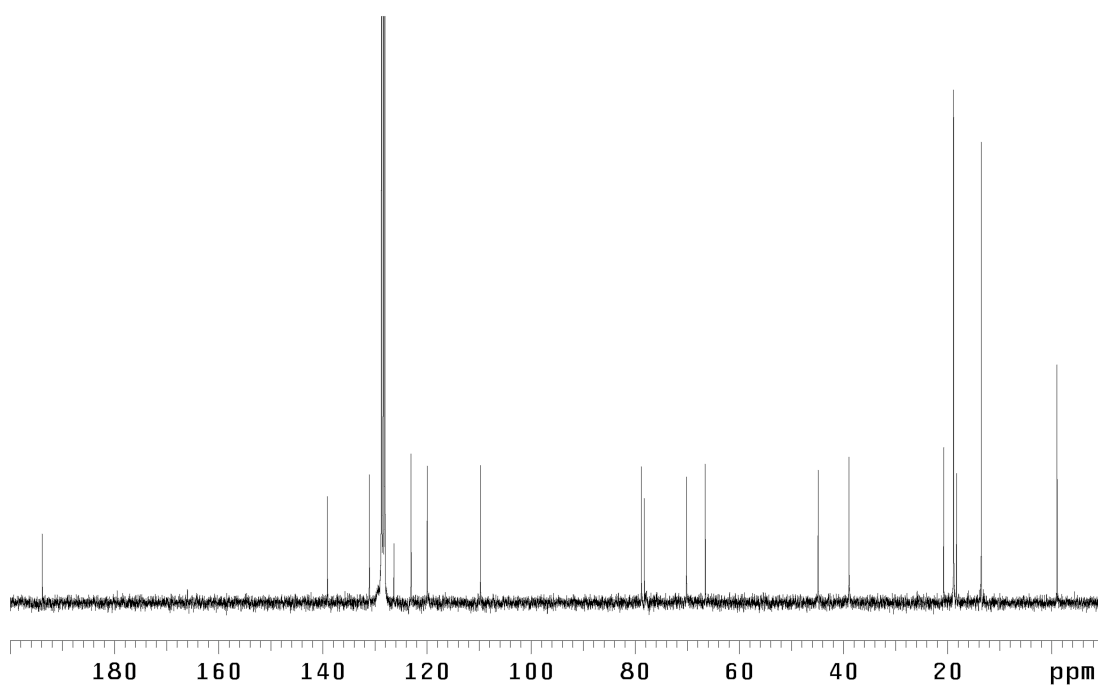


Figure A3.179 <sup>13</sup>C NMR (75 MHz, C<sub>6</sub>D<sub>6</sub>) of compound **157**

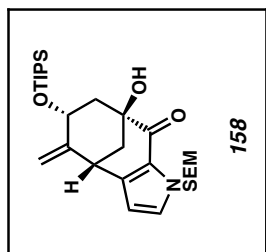
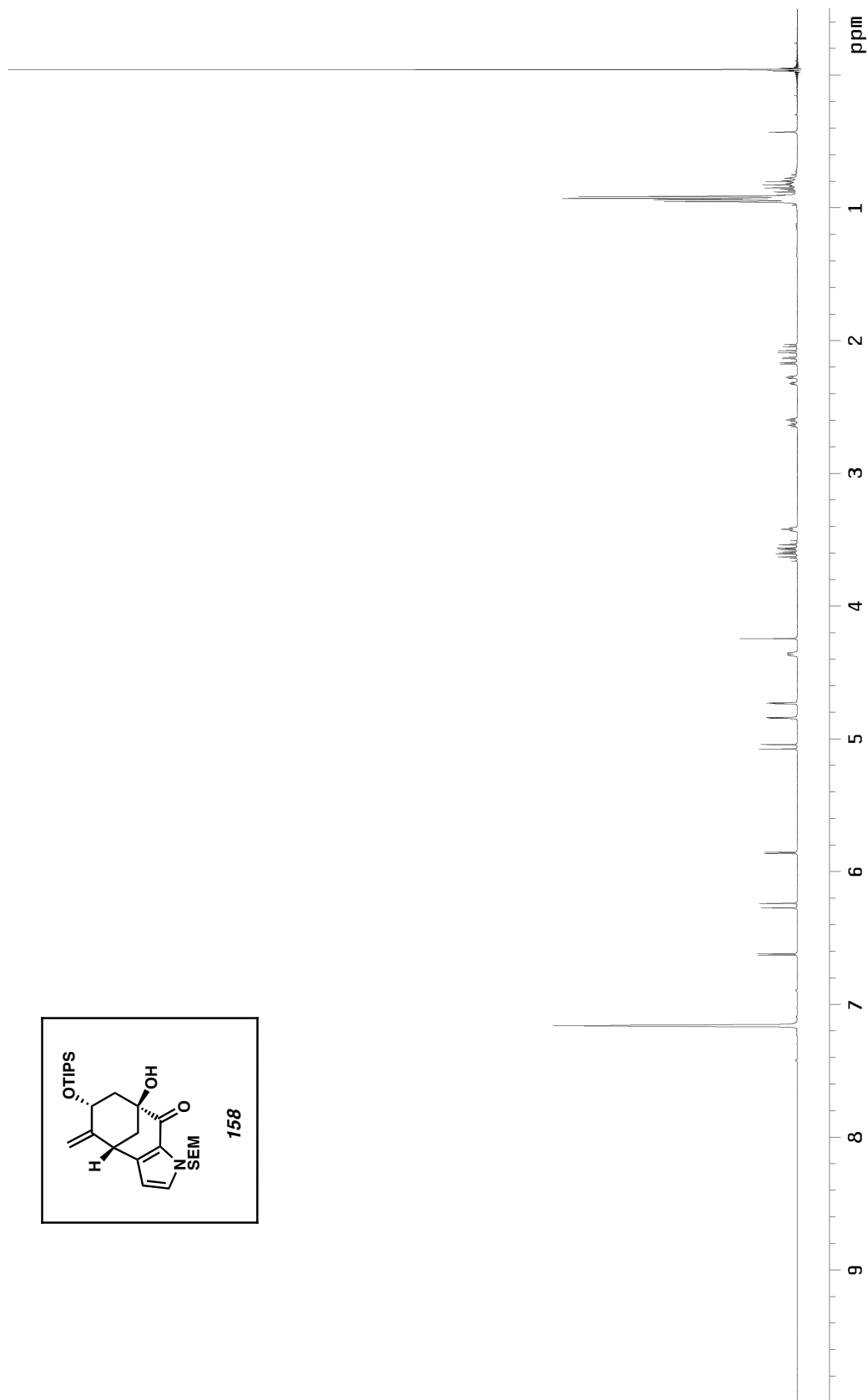
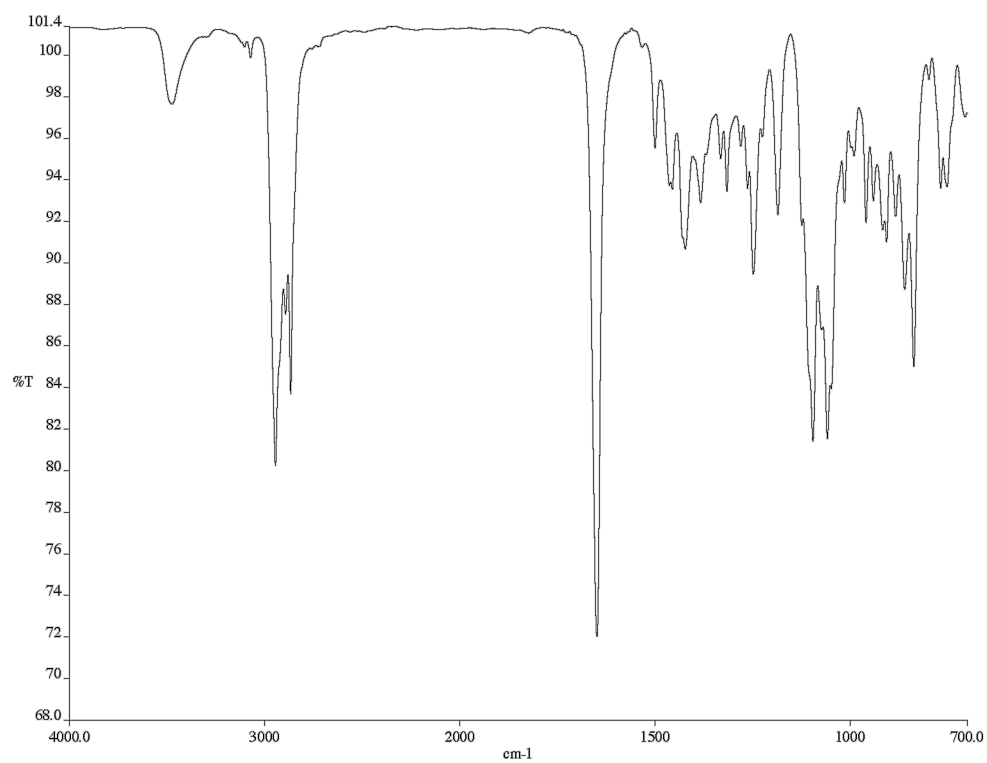
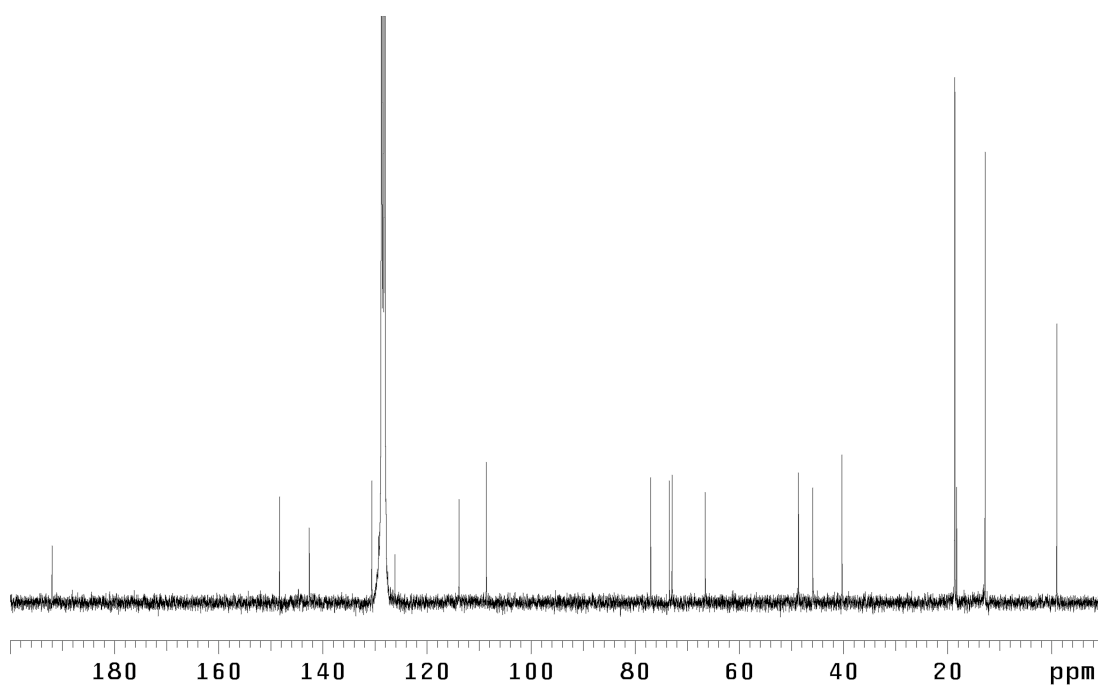


Figure A3.180 <sup>1</sup>H NMR (300 MHz, C<sub>6</sub>D<sub>6</sub>) of compound **158**



*Figure A3.181* Infrared spectrum (thin film/NaCl) of compound **158**



*Figure A3.182* <sup>13</sup>C NMR (75 MHz, C<sub>6</sub>D<sub>6</sub>) of compound **158**

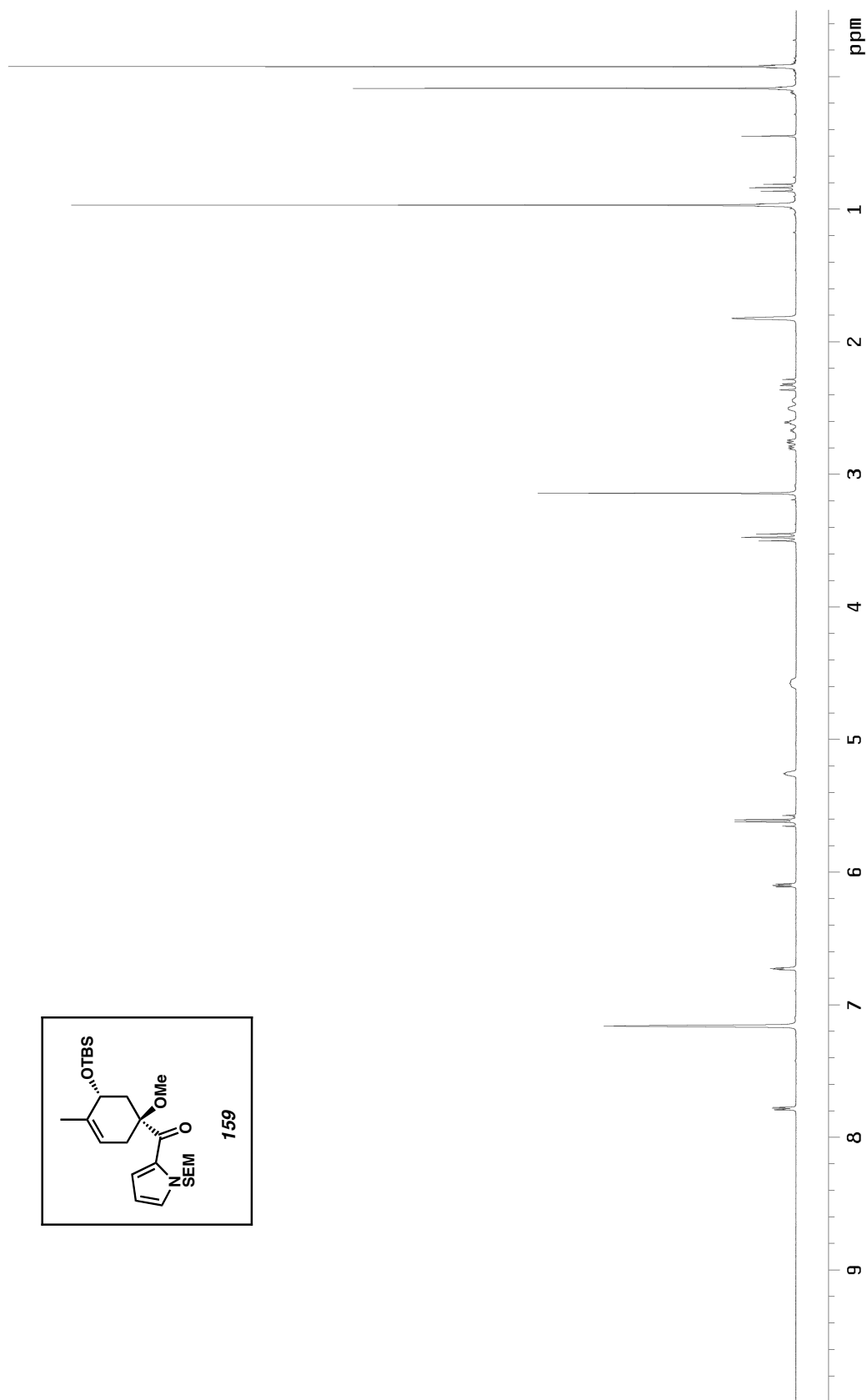
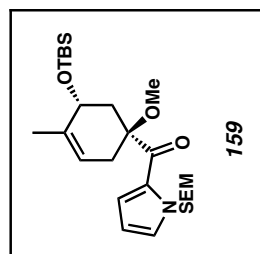


Figure A3.183  $^1\text{H}$  NMR (300 MHz,  $\text{C}_6\text{D}_6$ ) of compound **159**

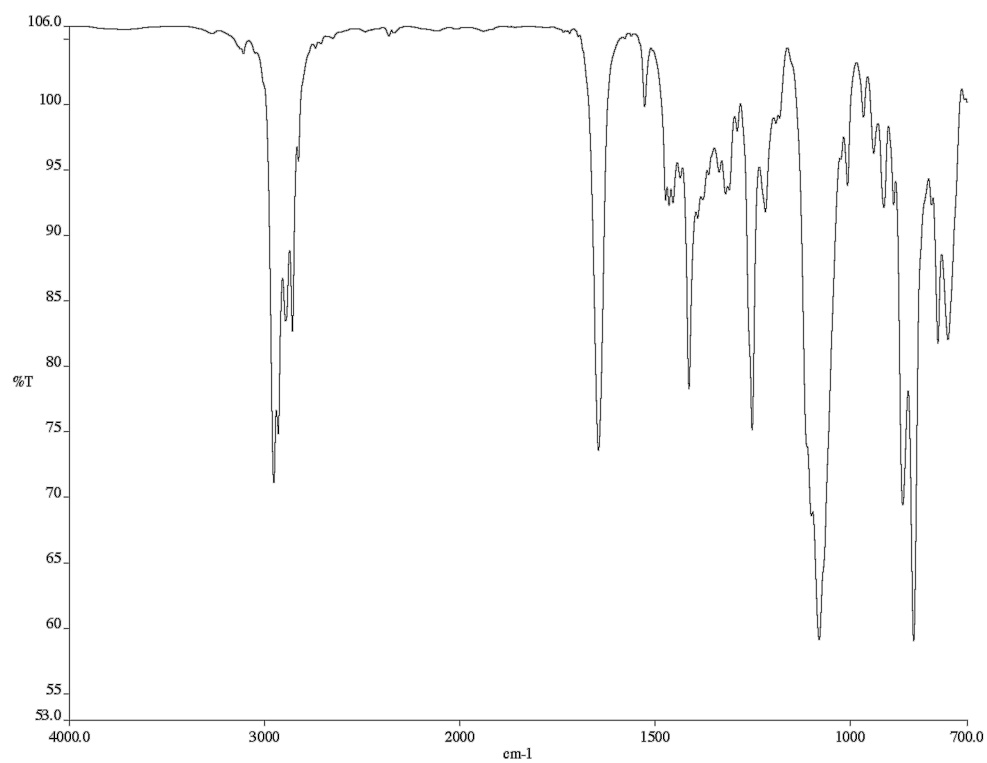


Figure A3.184 Infrared spectrum (thin film/NaCl) of compound **159**

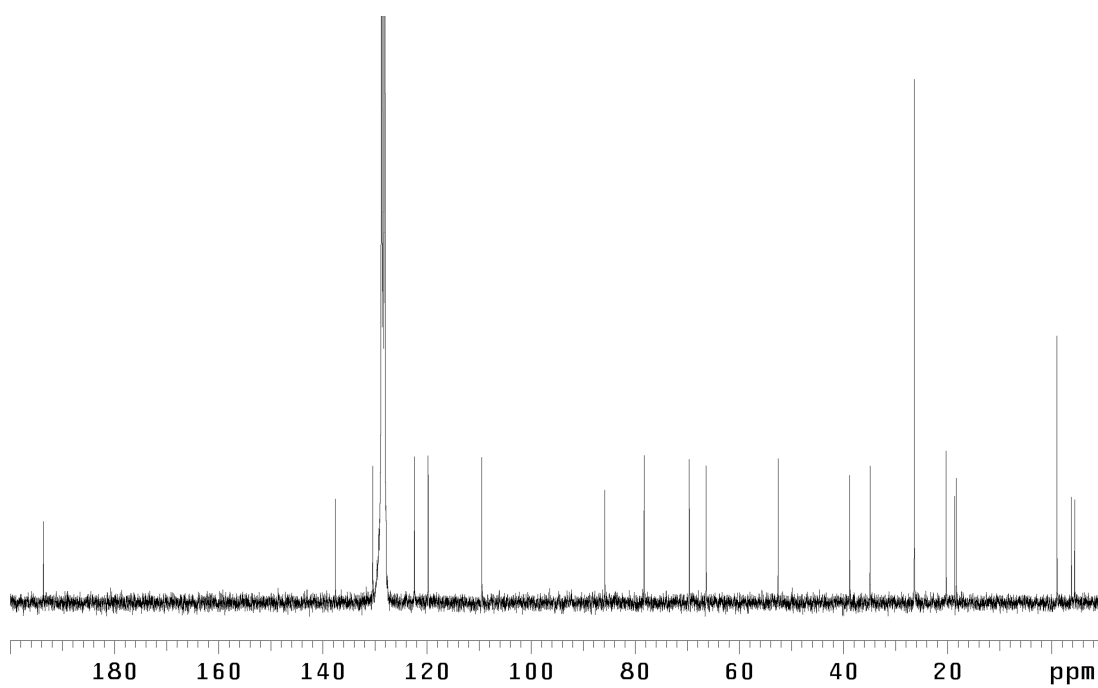


Figure A3.185 <sup>13</sup>C NMR (75 MHz, C<sub>6</sub>D<sub>6</sub>) of compound **159**

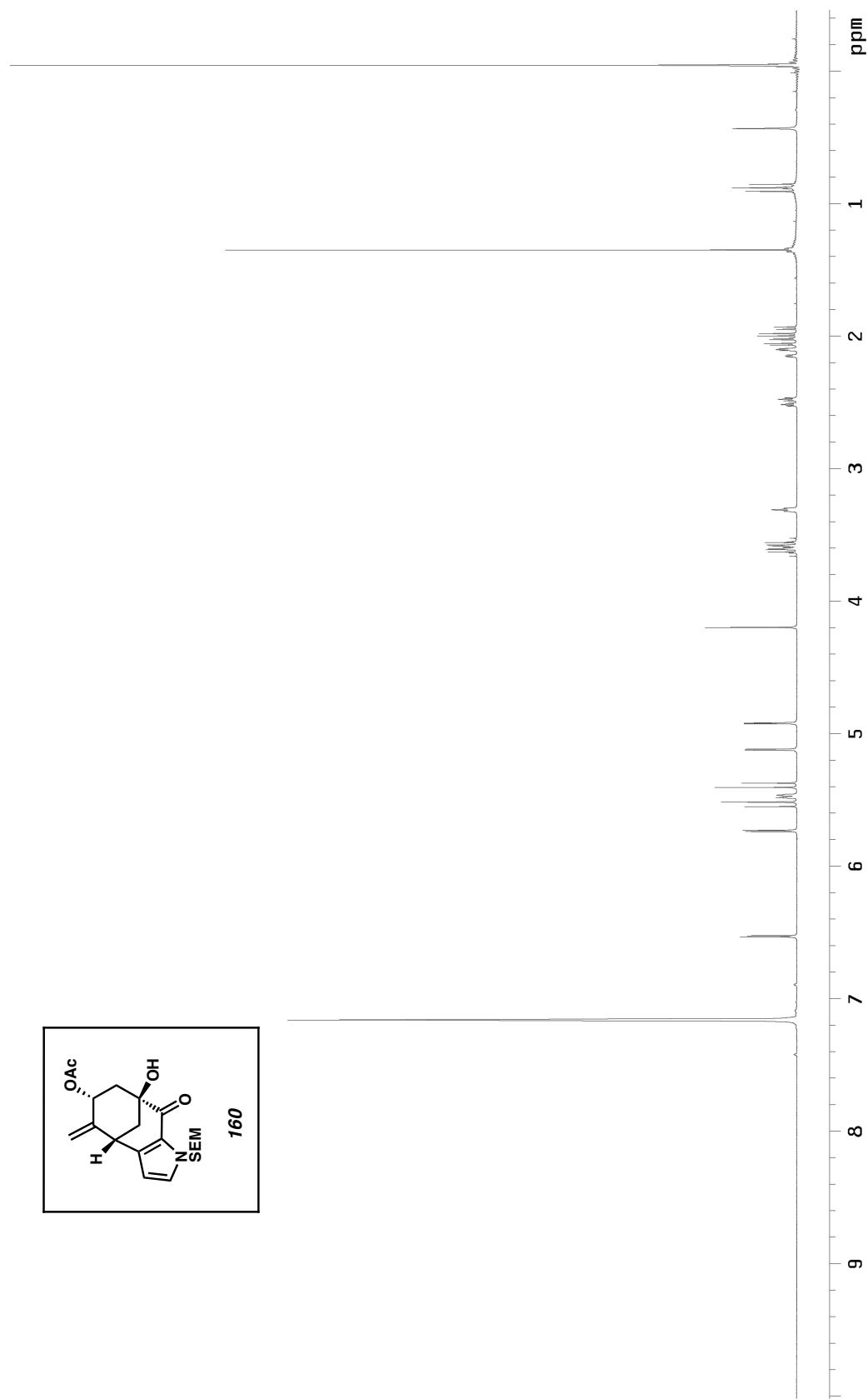


Figure A3.186  $^1\text{H}$  NMR (300 MHz,  $\text{C}_6\text{D}_6\text{O}$ ) of compound **160**

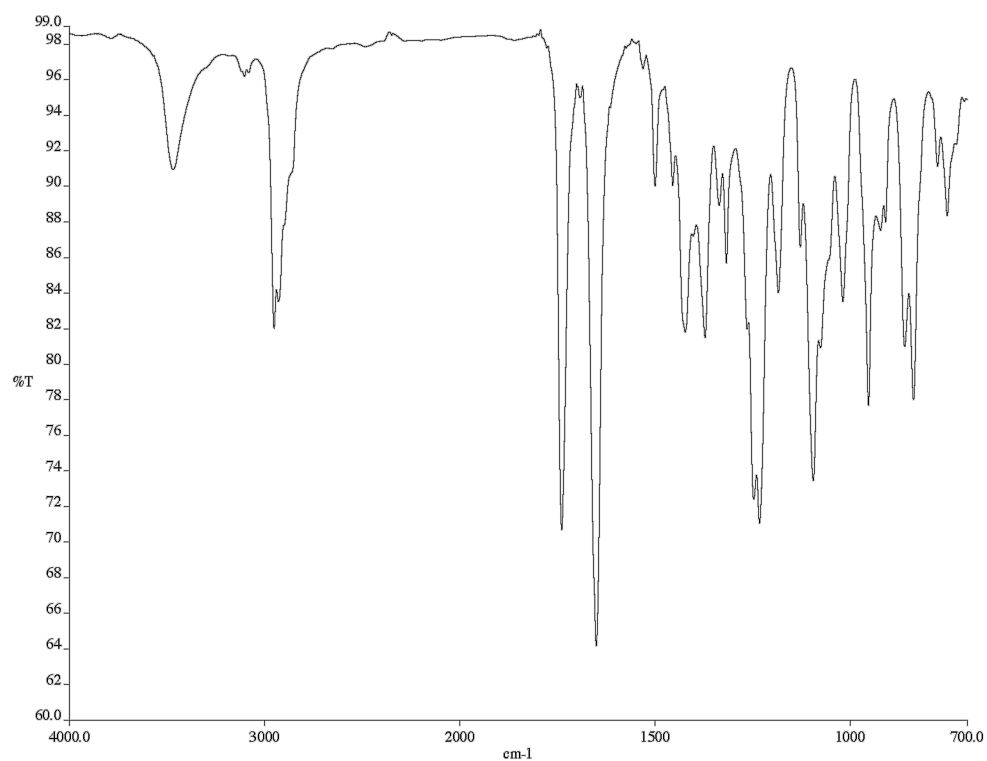


Figure A3.187 Infrared spectrum (thin film/NaCl) of compound **160**

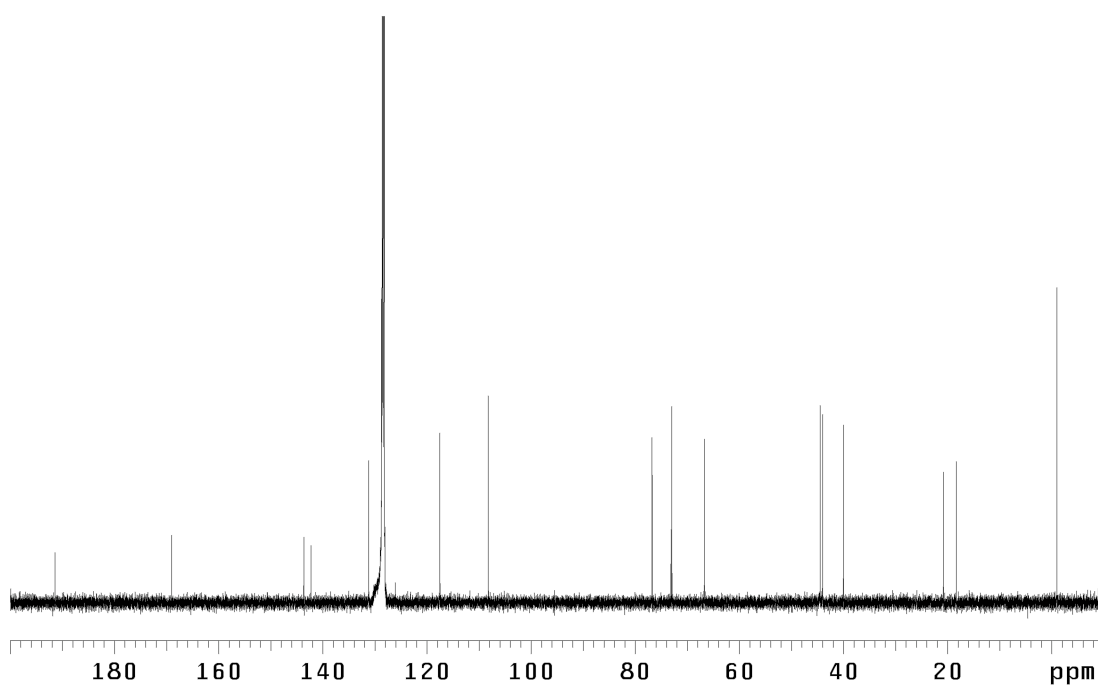


Figure A3.188 <sup>13</sup>C NMR (125 MHz, C<sub>6</sub>D<sub>6</sub>) of compound **160**



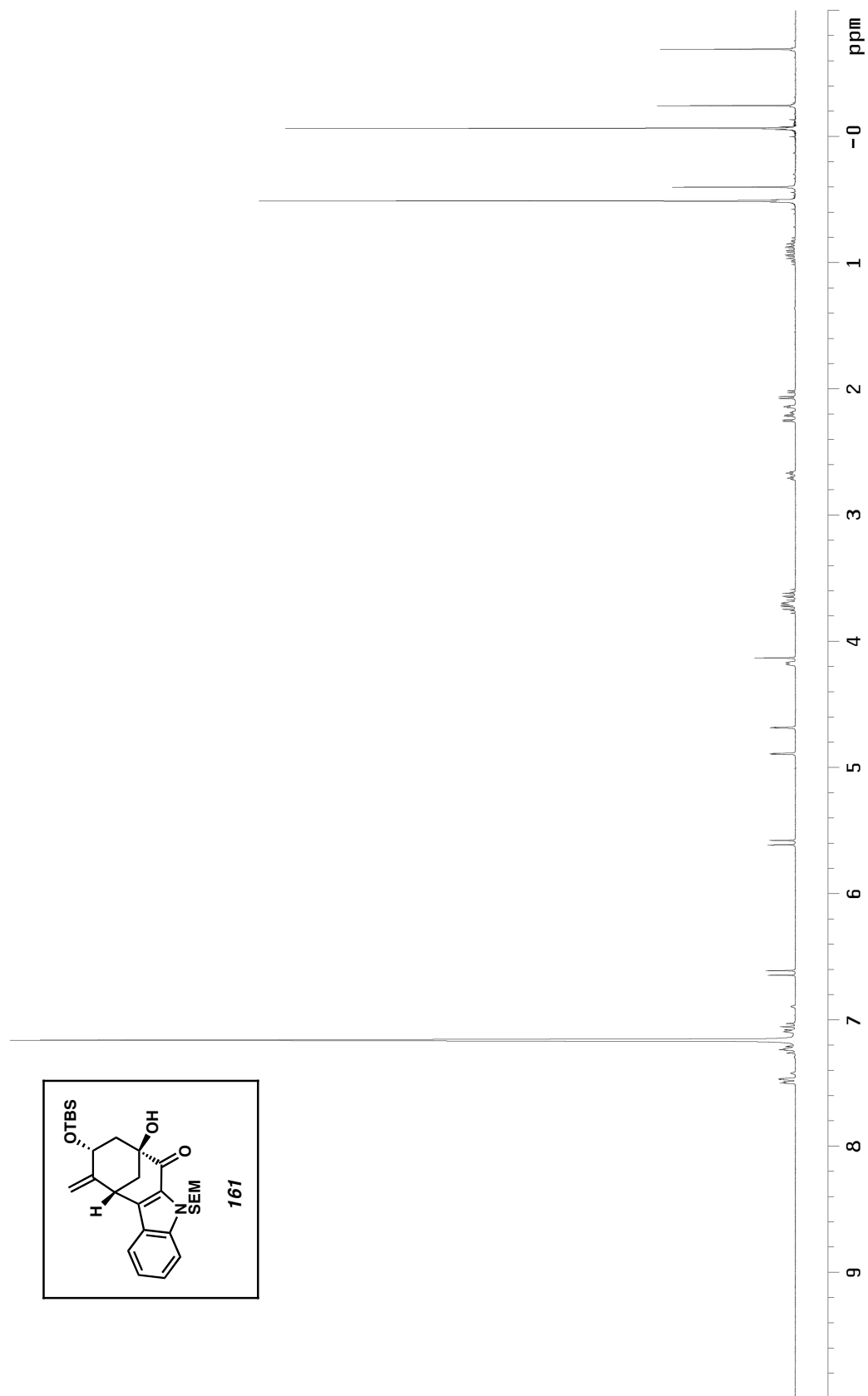


Figure A3.189 <sup>1</sup>H NMR (300 MHz, C<sub>6</sub>D<sub>6</sub>) of compound **161**

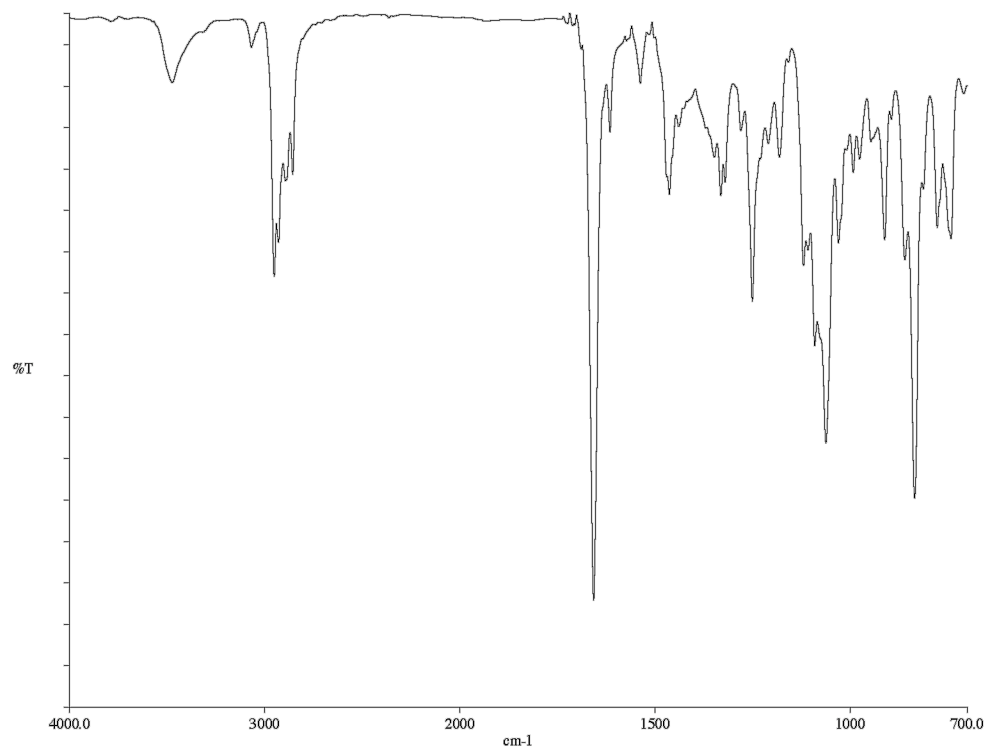


Figure A3.190 Infrared spectrum (thin film/NaCl) of compound **161**

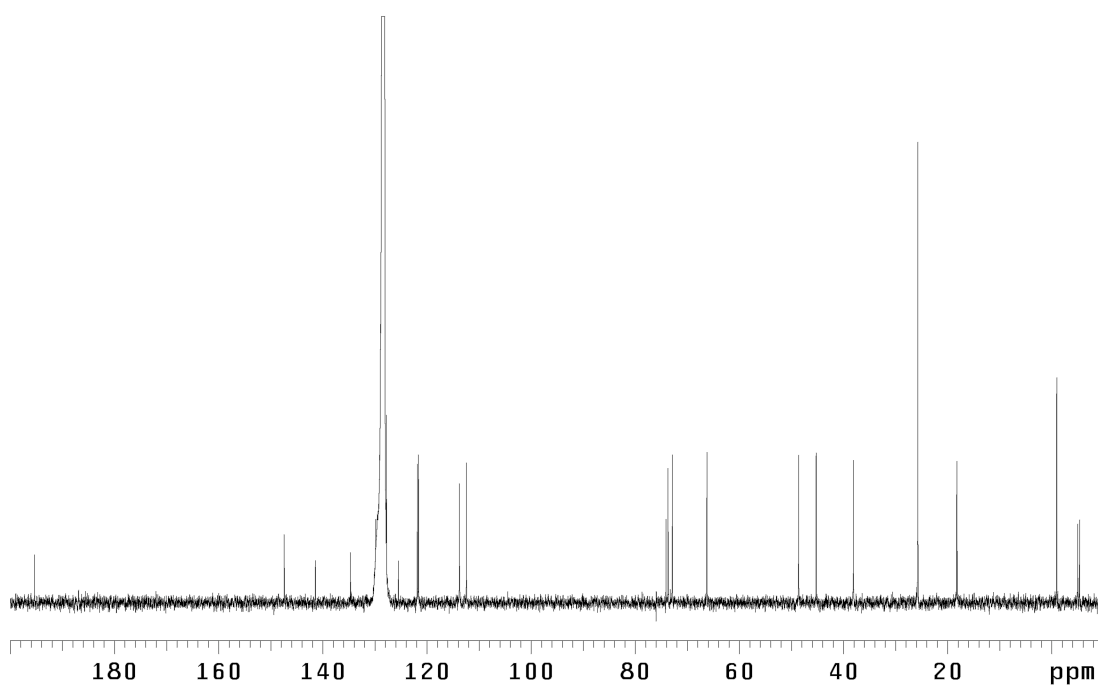


Figure A3.191 <sup>13</sup>C NMR (125 MHz, C<sub>6</sub>D<sub>6</sub>) of compound **161**

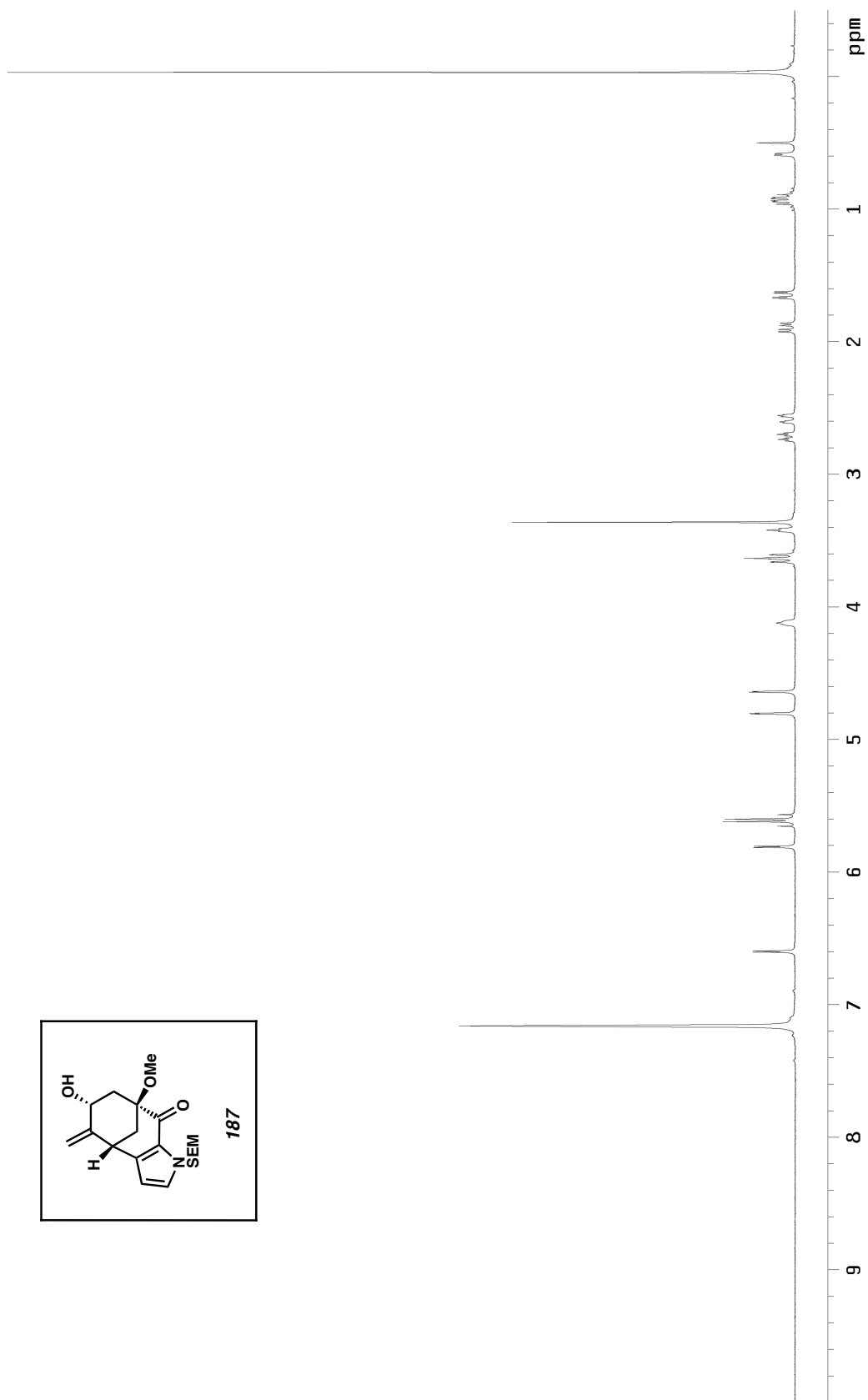
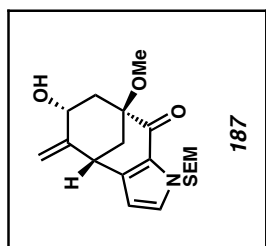


Figure A3.192  $^1\text{H}$  NMR (300 MHz,  $\text{C}_6\text{D}_6$ ) of compound **187**

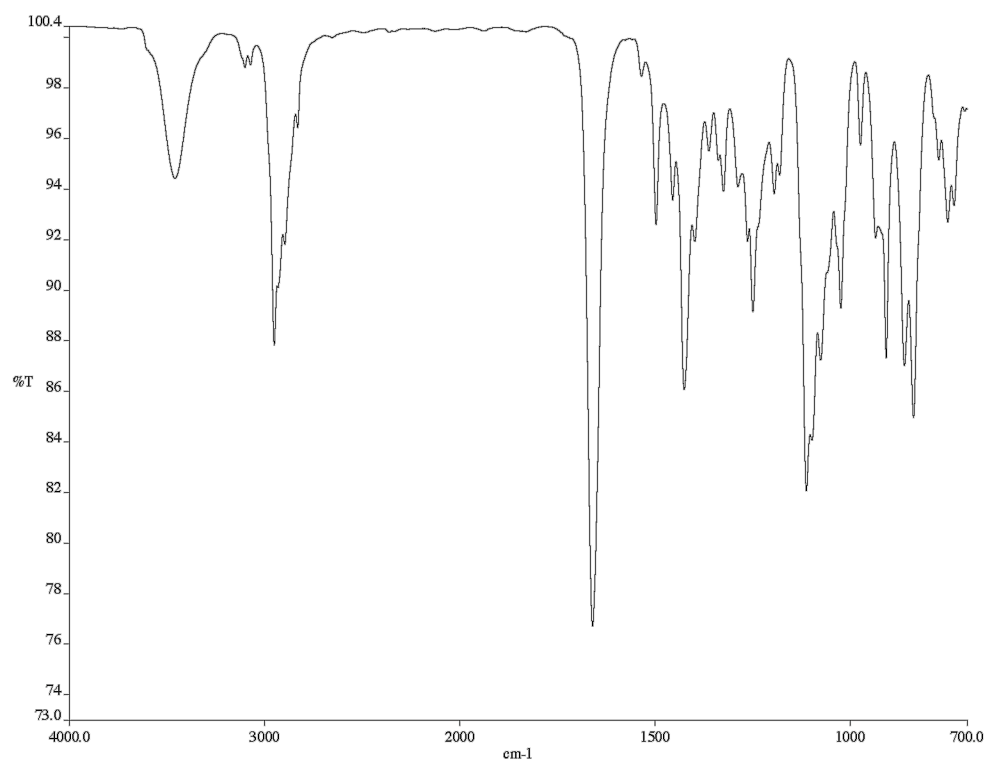


Figure A3.193 Infrared spectrum (thin film/NaCl) of compound **187**

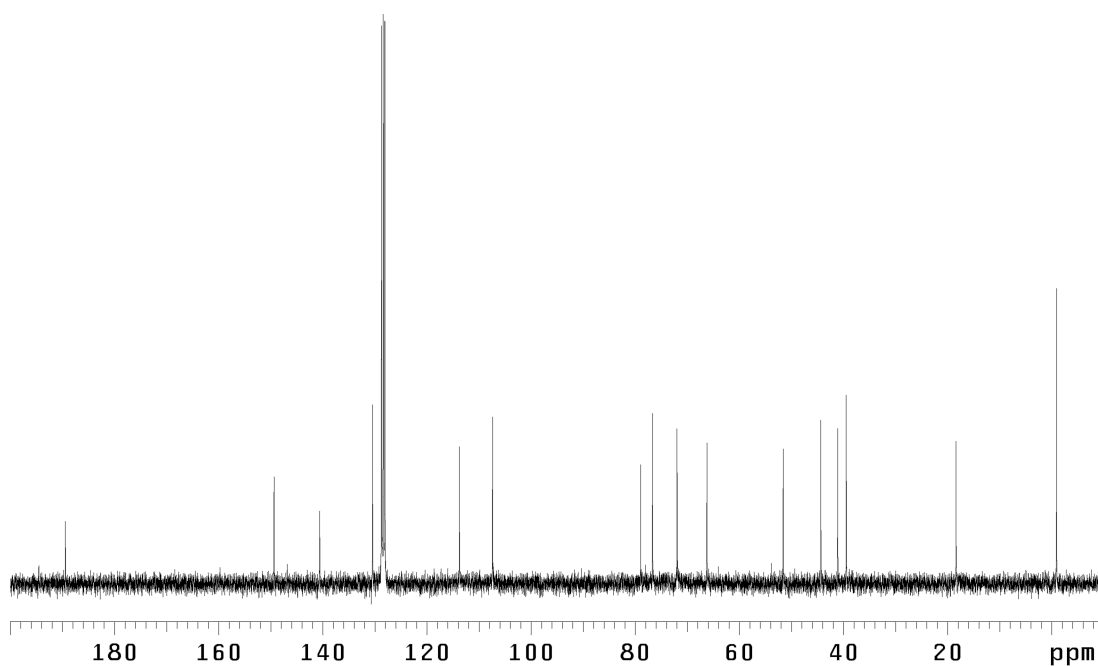


Figure A3.194 <sup>13</sup>C NMR (75 MHz, C<sub>6</sub>D<sub>6</sub>) of compound **187**

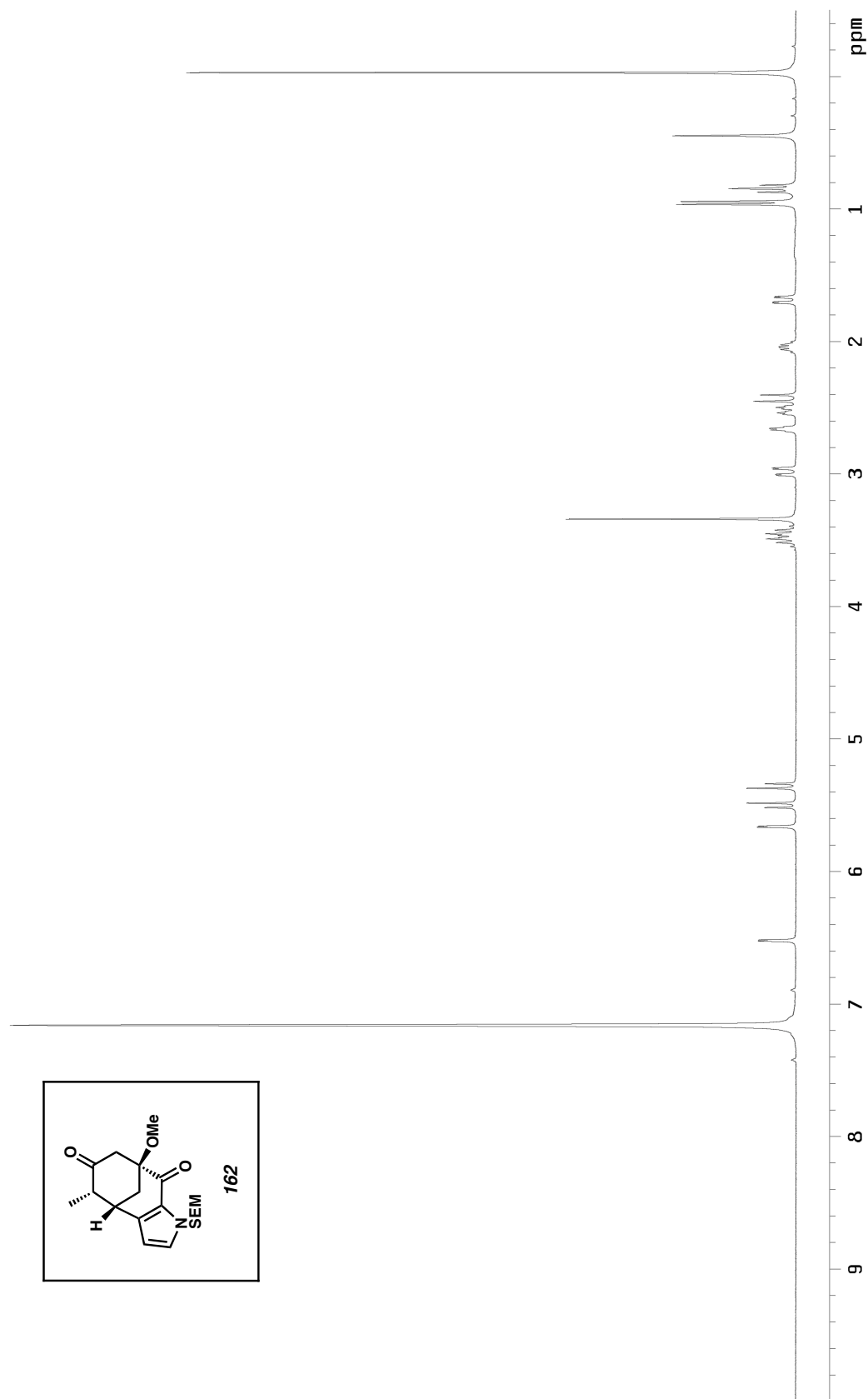


Figure A3.195  $^1\text{H}$  NMR (300 MHz,  $\text{CDCl}_3$ ) of compound **162**

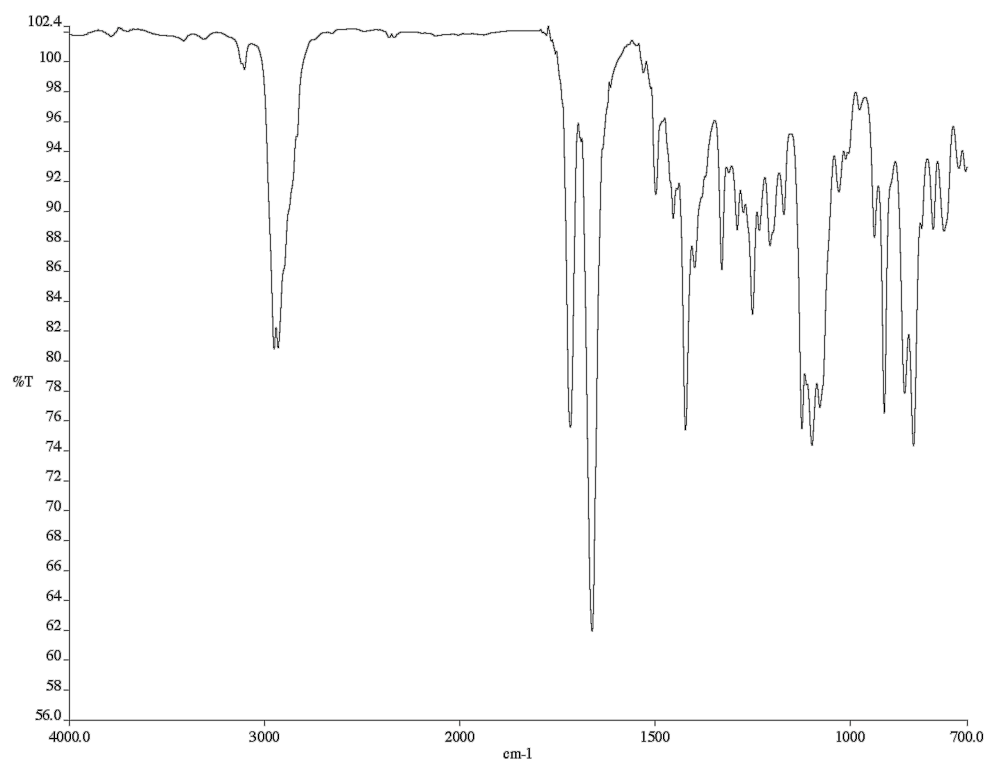


Figure A3.196 Infrared spectrum (thin film/NaCl) of compound **162**

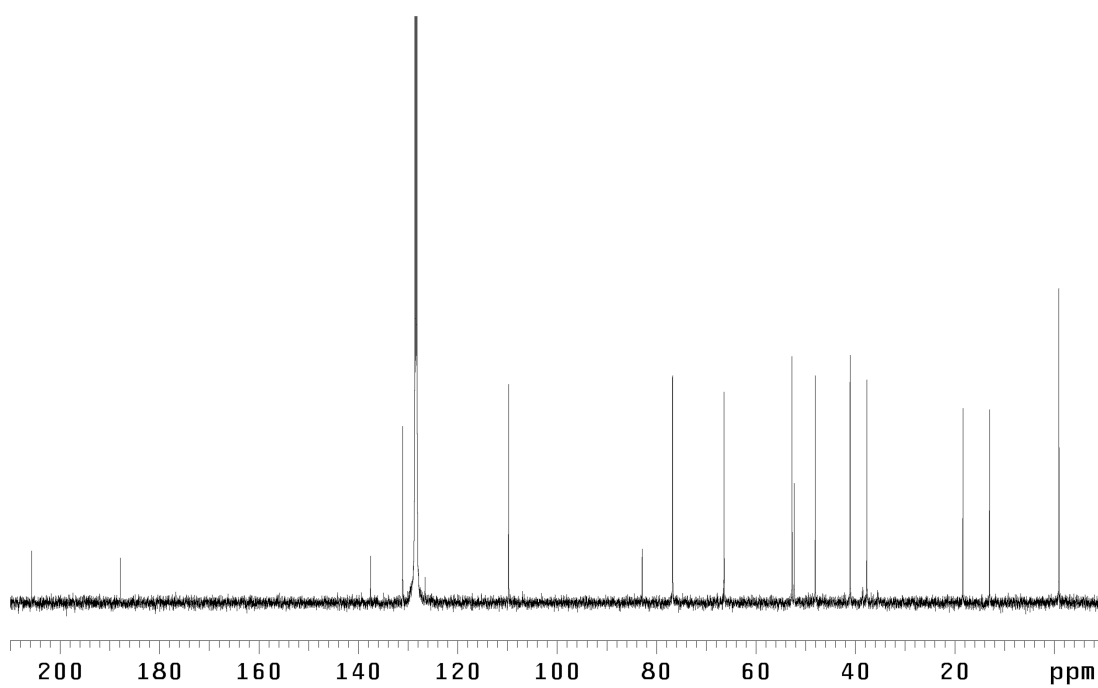


Figure A3.197 <sup>13</sup>C NMR (125 MHz, C<sub>6</sub>D<sub>6</sub>) of compound **162**

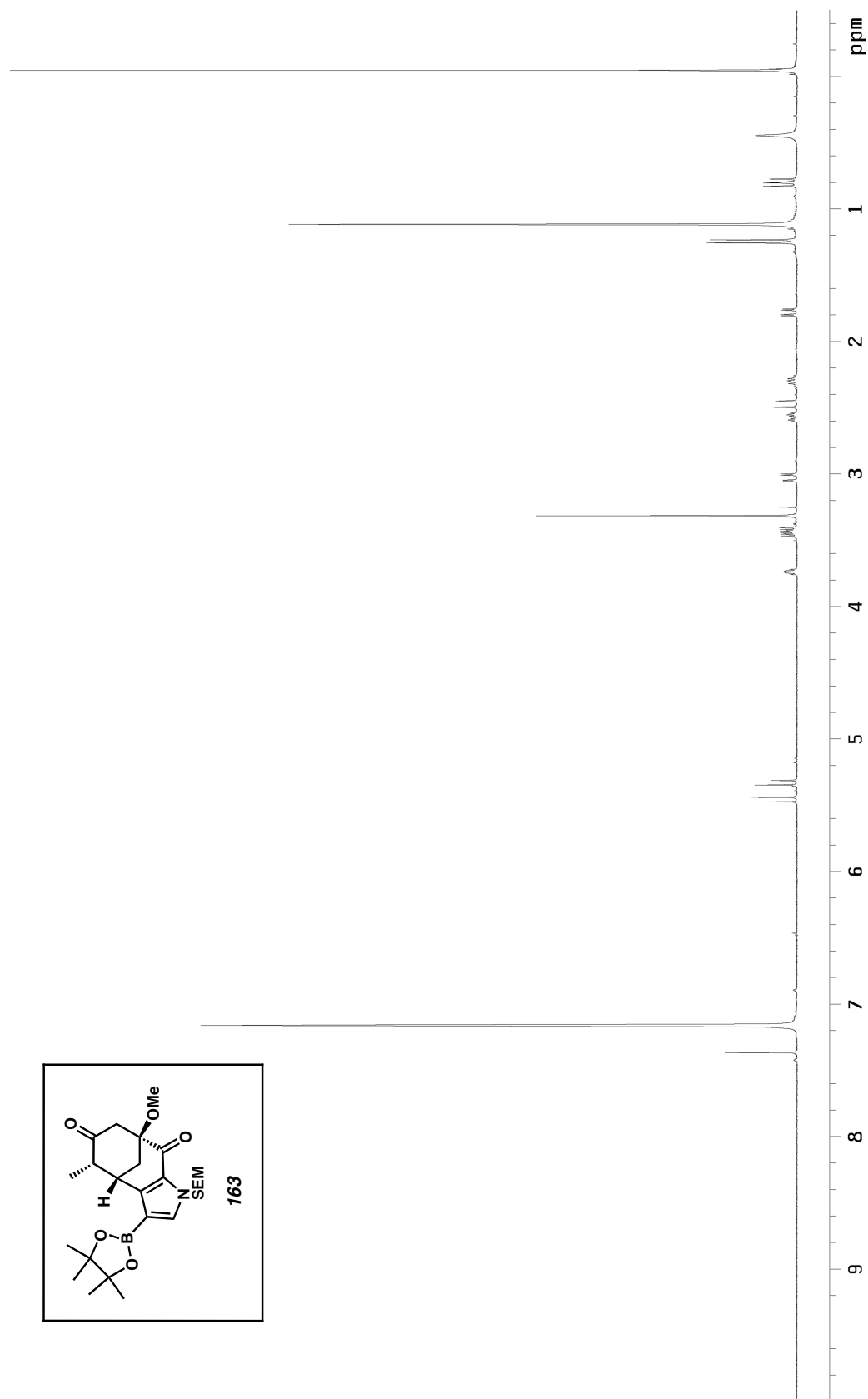
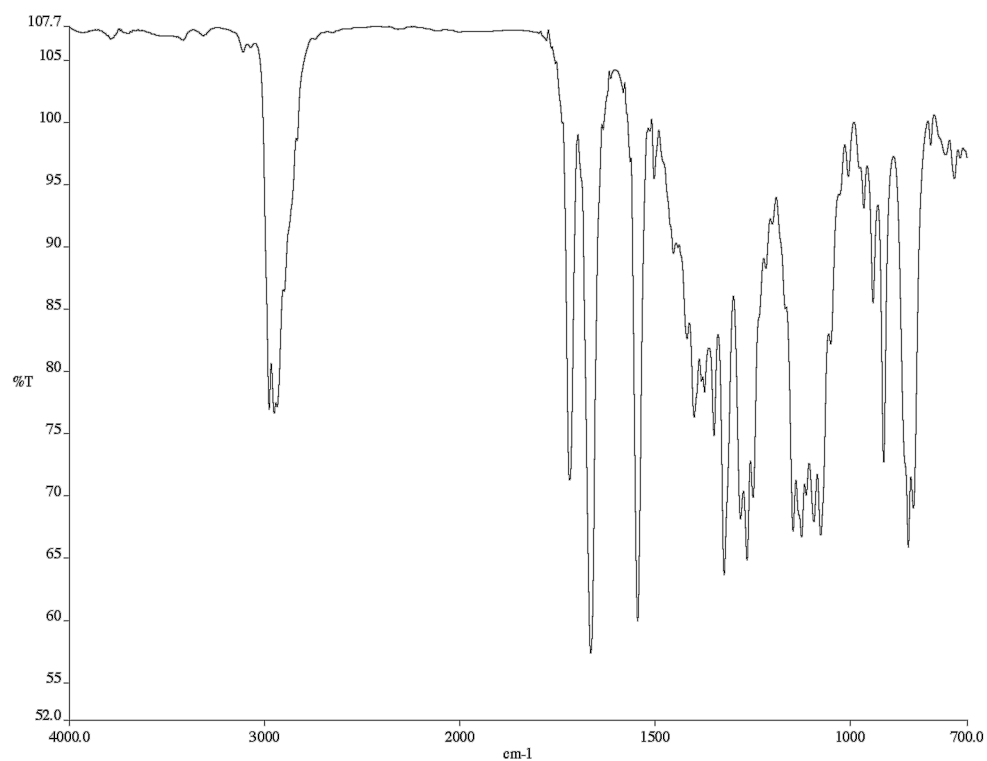
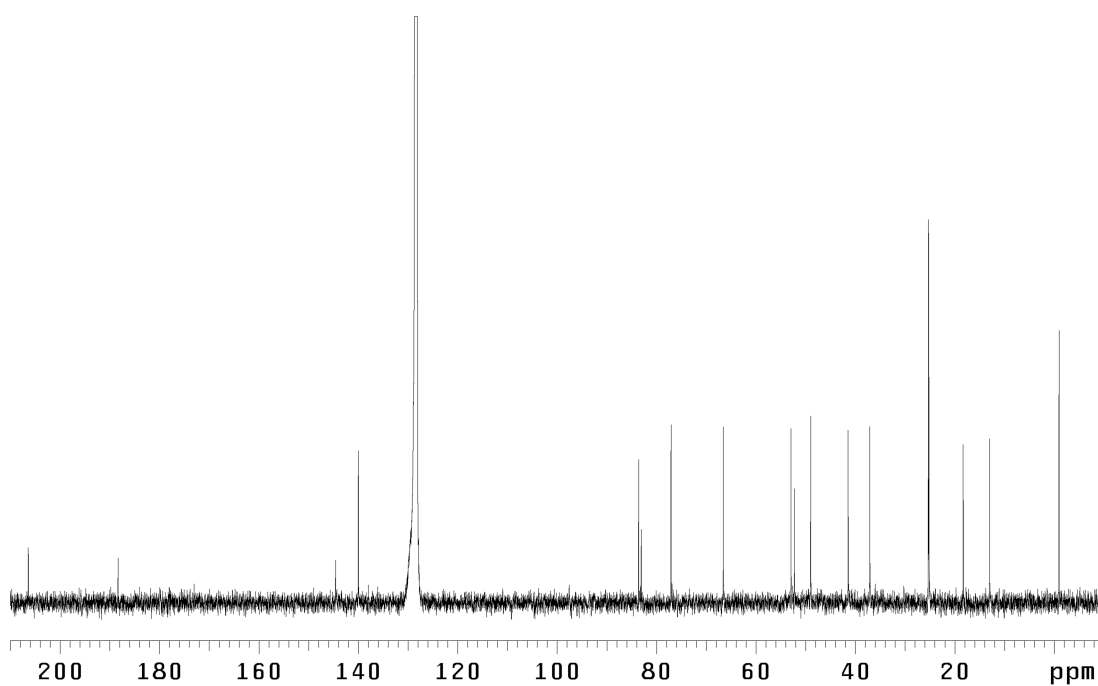


Figure A3.198  $^1\text{H}$  NMR (300 MHz,  $\text{CDCl}_3$ ) of compound **163**



*Figure A3.199* Infrared spectrum (thin film/NaCl) of compound **163**



*Figure A3.200* <sup>13</sup>C NMR (125 MHz, C<sub>6</sub>D<sub>6</sub>) of compound **163**



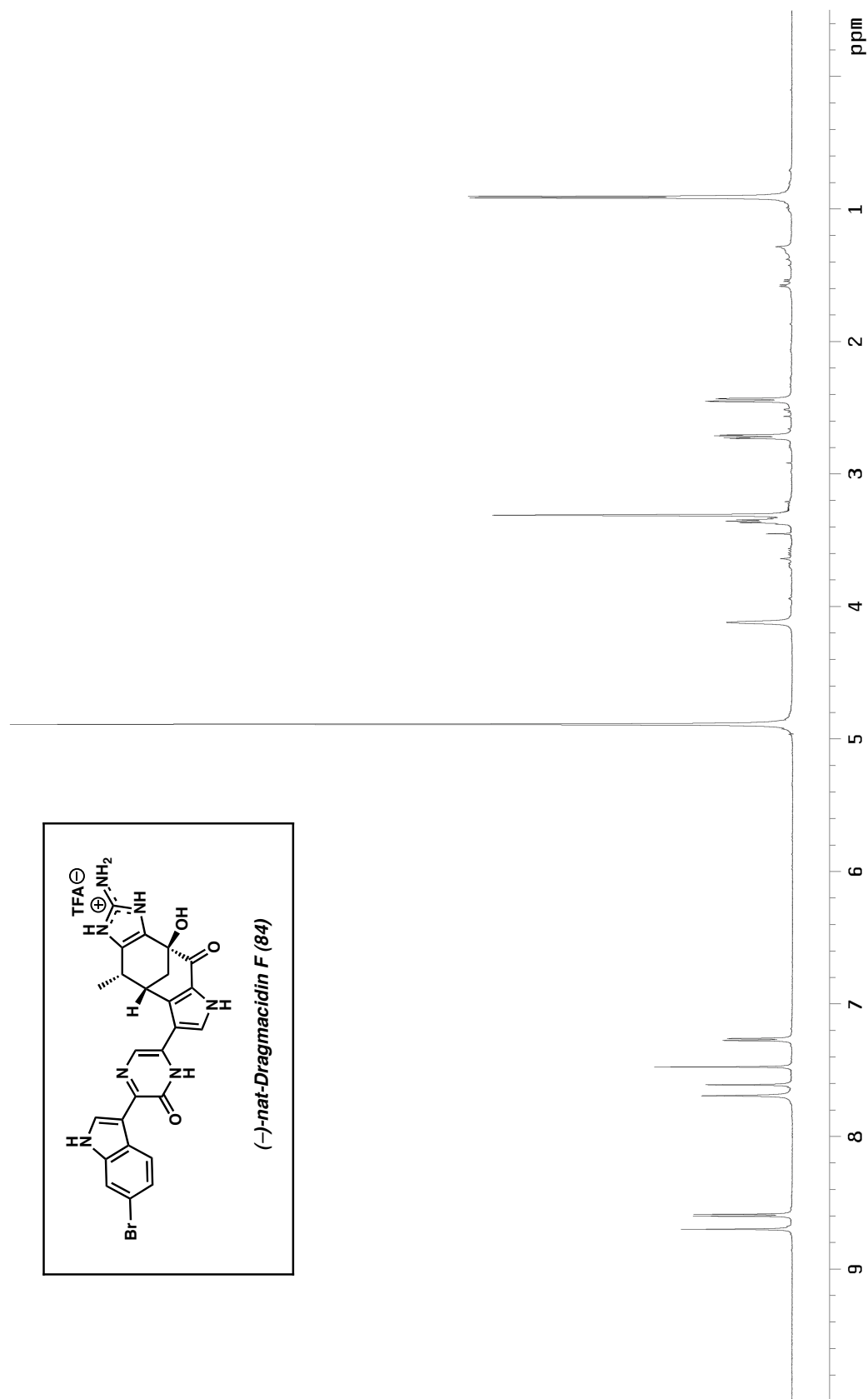


Figure A3.201  $^1\text{H}$  NMR (600 MHz,  $\text{CD}_3\text{OD}$ ) of (-)-dragnacidin F (84)

## CHAPTER FOUR

### Progress Toward The Total Synthesis of (*R*)-Telomestatin<sup>†</sup>

#### 4.1 Background

##### 4.1.1 Telomeres and Telomerase

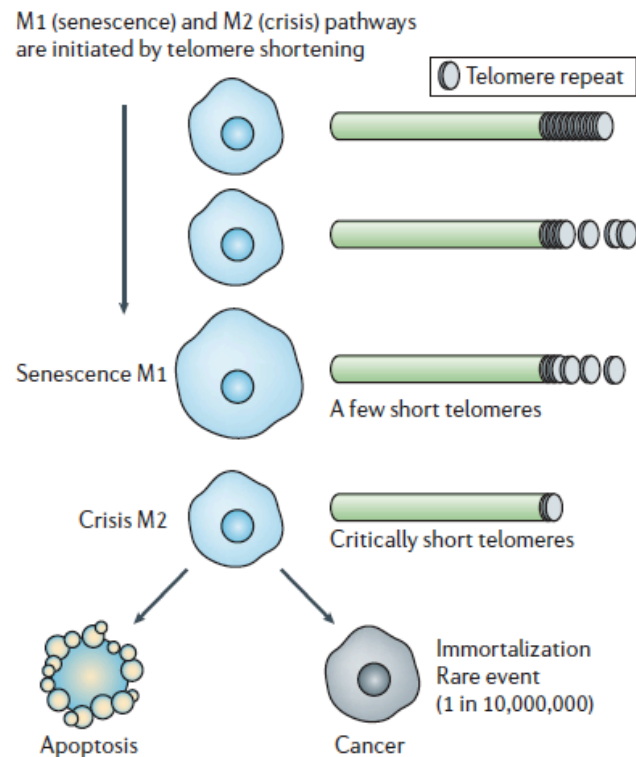
The ends of eukaryotic chromosomes consist of specialized DNA nucleoprotein complexes known as telomeres.<sup>1</sup> Telomeres safeguard the integrity of chromosomes and protect them from base-pair loss, comparable to the small plastic at the end of a shoelace that prevents the twine from unraveling. The human telomere is composed of tandem repeats of the guanine-rich hexanucleotide sequence d(TTAGGG). With the exception of the single-stranded 3' overhang, most telomeric DNA is double stranded.

In human cells, telomere length erodes naturally with each cell division cycle, since DNA polymerase is unable to fully replicate the ends – a phenomenon known as the “end replication problem”. Thus, telomeres are thought to effectively function as cellular clocks, keeping record of how many times a cell divides. Telomeres progressively shorten until a critically short length of telomeric DNA is reached, at which point cells undergo replicative senescence (mortality stage 1 (M1), see Figure 4.1.1), losing their ability to divide.<sup>1</sup> This can be followed by cell crisis (mortality stage 2 ((M2)) and apoptosis.

---

<sup>†</sup> This work was performed in collaboration with Dr. Haiming M. Zhang, a postdoctoral scholar in the Stoltz group, and Justin T. Mohr, a graduate student in the Stoltz group.

Figure 4.1.1 (reprinted with permission from (2); © 2006, Macmillan Publishers Ltd.)



A mechanism for telomere maintenance is provided by a specialized cellular ribonucleoprotein enzyme complex called telomerase.<sup>1,2,3,4,5</sup> Discovered by Carol Greider in 1984, telomerase is involved in telomere capping and in the DNA-damage response, and has been implicated in aging and genetic diseases.<sup>2,3</sup> In human cells, telomerase functions as a reverse transcriptase to add multiple copies of the TTAGGG motif to the end of the G-strand of the telomere. Telomerase activity is usually absent from normal cells; however, in the majority of tumor cells (85-90%) this enzyme is overexpressed, contributing to the immortalization of human tumor cells by protecting against telomere loss during replication.<sup>6</sup> Because telomerase is necessary for the immortality of so many cancer types, telomerase inhibition has become an important target for the development of new anticancer agents.<sup>3</sup>

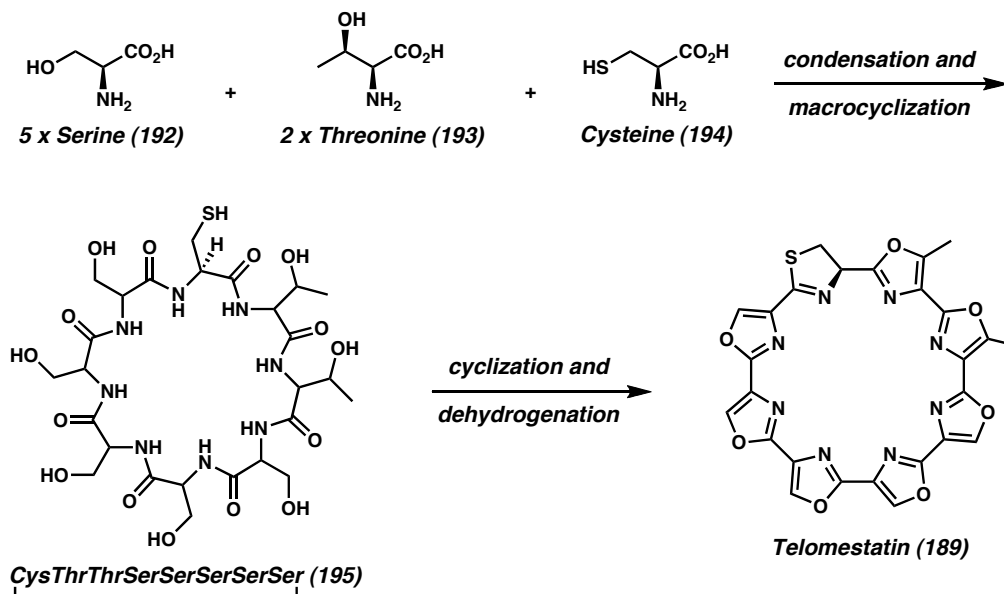


telomerase.<sup>13</sup> While direct catalytic inhibition of telomerase by telomestatin (**189**) cannot be ruled out, evidence suggests that telomestatin (**189**) facilitates the formation of or stabilizes G-quadruplex structures (e.g., **191**), thereby inhibiting telomerase activity indirectly.<sup>9b,14</sup> Indeed, modeling studies on the binding interactions of telomestatin (**189**) and the G-quadruplex (e.g., **191**) demonstrated that sources of stable interactions include hydrogen bonding between the nitrogens of the guanine bases and the oxygens of the oxazole rings, stacking interactions with the G-tetrad, as well as electrostatic interactions between the ring nitrogens and the guanine bases.<sup>9b</sup>

#### 4.1.3 Biosynthesis

The biosynthesis of telomestatin (**189**), although not yet reported in the literature, probably involves the intermediacy of octapeptide **195** generated from the condensation and macrocyclization of eight amino acids—five serine (**192**), two threonine (**193**), and one cysteine (**194**) (Scheme 4.1.1).<sup>15,16</sup> Cyclodehydration and oxidation of **195** would then generate the final product (**189**). Although telomestatin (**189**) is almost certainly derived from the abovementioned amino acids, there is no evidence to suggest that all of the peptide bonds must be formed prior to the heterocyclization steps.<sup>15a</sup>

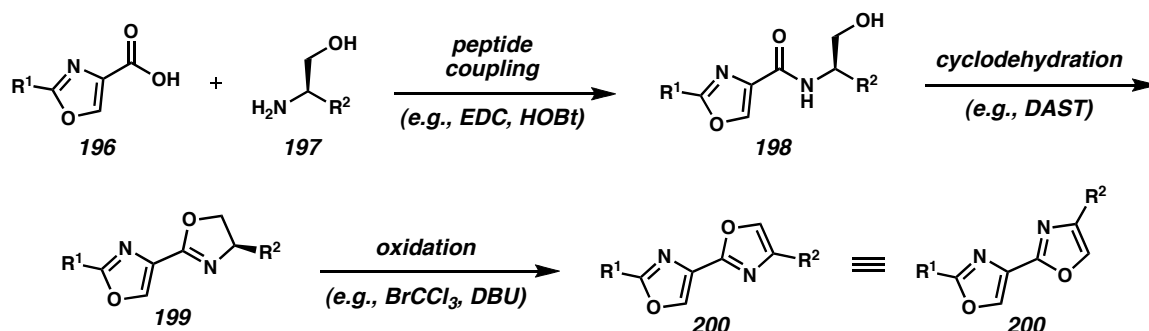
Scheme 4.1.1



#### 4.1.4 Previous Synthetic Studies

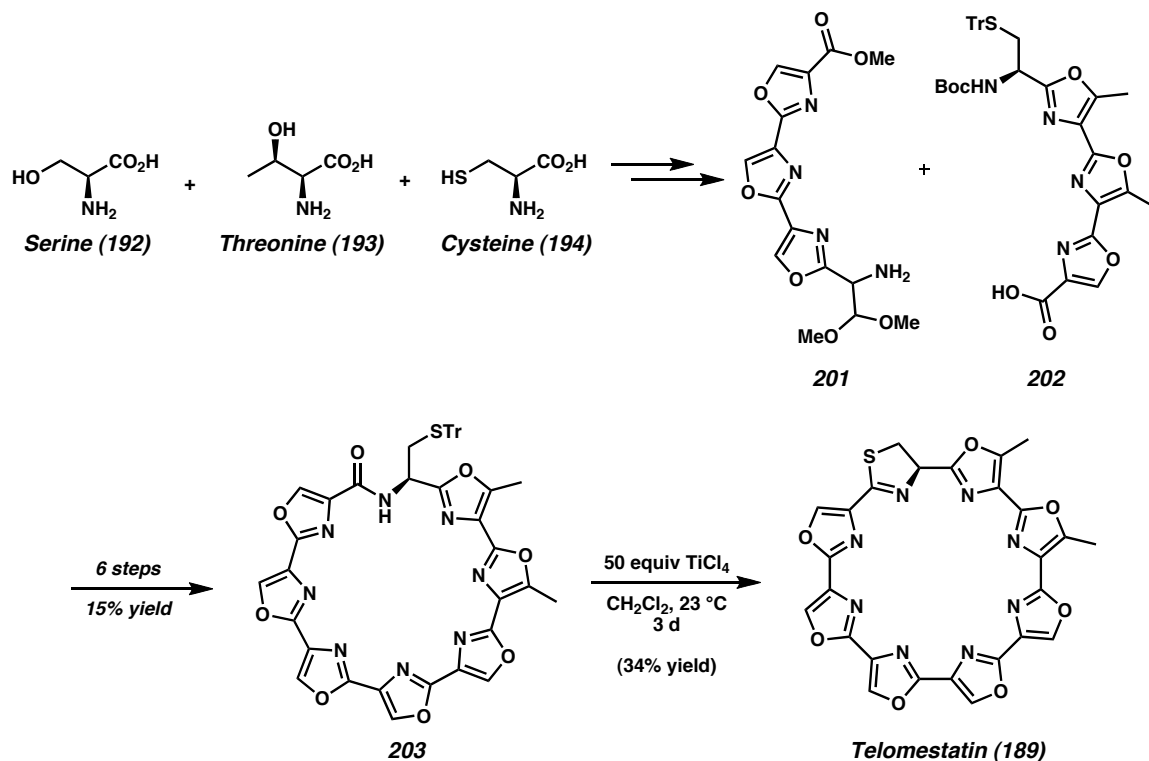
There are two published total syntheses of telomestatin (**189**) in the literature,<sup>17</sup> as well as a handful of syntheses en route to the natural product.<sup>10,18,19</sup> Despite the amount of synthetic attention that this molecule has garnered, however, every one of the reported approaches relies heavily on the use of amino acid precursors, as well as linear, repeated peptide-bond formation–cyclization–oxidation sequences to form the oxazole rings (**196** + **197** → **198** → **199** → **200**, Scheme 4.1.2). In fact, this sequence bears resemblance to the proposed telomestatin (**189**) biosynthesis (Scheme 4.1.1, *vide infra*). Not surprisingly, the use of these methods typically also requires multiple protection and deprotection steps. While the described routes are usually reasonably convergent, the use of this inefficient design strategy (i.e., Scheme 4.1.2) renders them lengthy and impractical—especially for analog synthesis.

Scheme 4.1.2



The first total synthesis of telomestatin (**189**) appeared in the literature in a 2002 patent reported by the Japanese company Taiho Pharmaceutical (Scheme 4.1.3).<sup>17a</sup> While experimental details are limited, they achieved the synthesis of **201** and **202** in unreported yields via the use of peptide bond formation–cyclization–oxidation sequences beginning from amino acid precursors (**192–194**, see Scheme 4.1.2, *vide infra*). Trisoxazole ester **201** and trisoxazole acid **202** were then stitched together in a similar manner over 6 steps to form **203**, and TiCl<sub>4</sub>-mediated thiazoline closure produced the natural product (**189**). Advancing the two key trisoxazole fragments (**201** and **202**) to the end required 7 total steps in 5% overall yield, with 10 mg of the natural product reported.

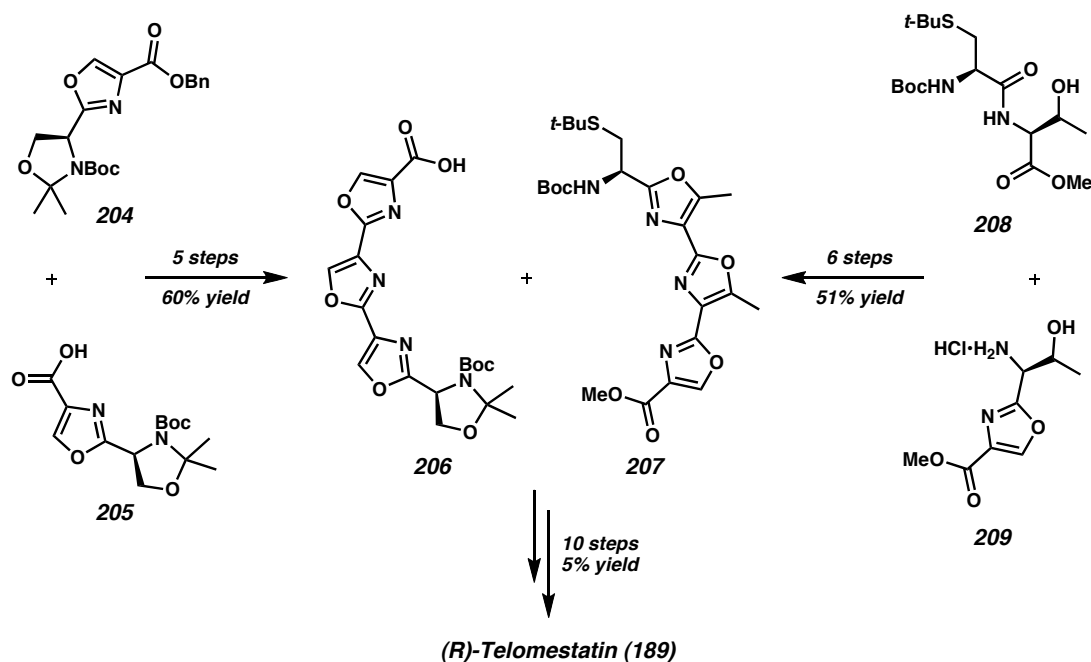
Scheme 4.1.3



During the course of our synthetic endeavors, a Japanese group led by Doi and Takahashi also reported a total synthesis of telomestatin (**189**), and definitively confirmed the absolute stereochemistry of the natural product as (*R*)-telomestatin (**189**).<sup>17b</sup> Although the details of the Taiho Pharmaceutical synthesis are incomplete,<sup>17a</sup> both of these routes appear to be fundamentally similar (Scheme 4.1.4). Amino-acid-derived building blocks **204**, **205**, **208**, and **209** were readily available in less than 5 steps, and could be advanced to key trisoxazole fragments **206** and **207** using the cyclization protocol previously described (see Scheme 4.1.2, *vide infra*). These two key fragments (**206** and **207**) were then advanced over 10 subsequent steps to provide the natural product in 5% overall yield from these intermediates.



Scheme 4.1.4



In addition to the aforementioned synthetic efforts, a handful of novel poly-oxazole methodologies have also been published. These methods include a two-stage iterative oxazole synthesis by Vedejs,<sup>20a</sup> as well as a series of palladium-catalyzed Suzuki coupling approaches by Greaney and Inoue.<sup>20b-d</sup> While these approaches seem promising, to date they have not been resulted in a completed total synthesis of telomestatin (**189**).

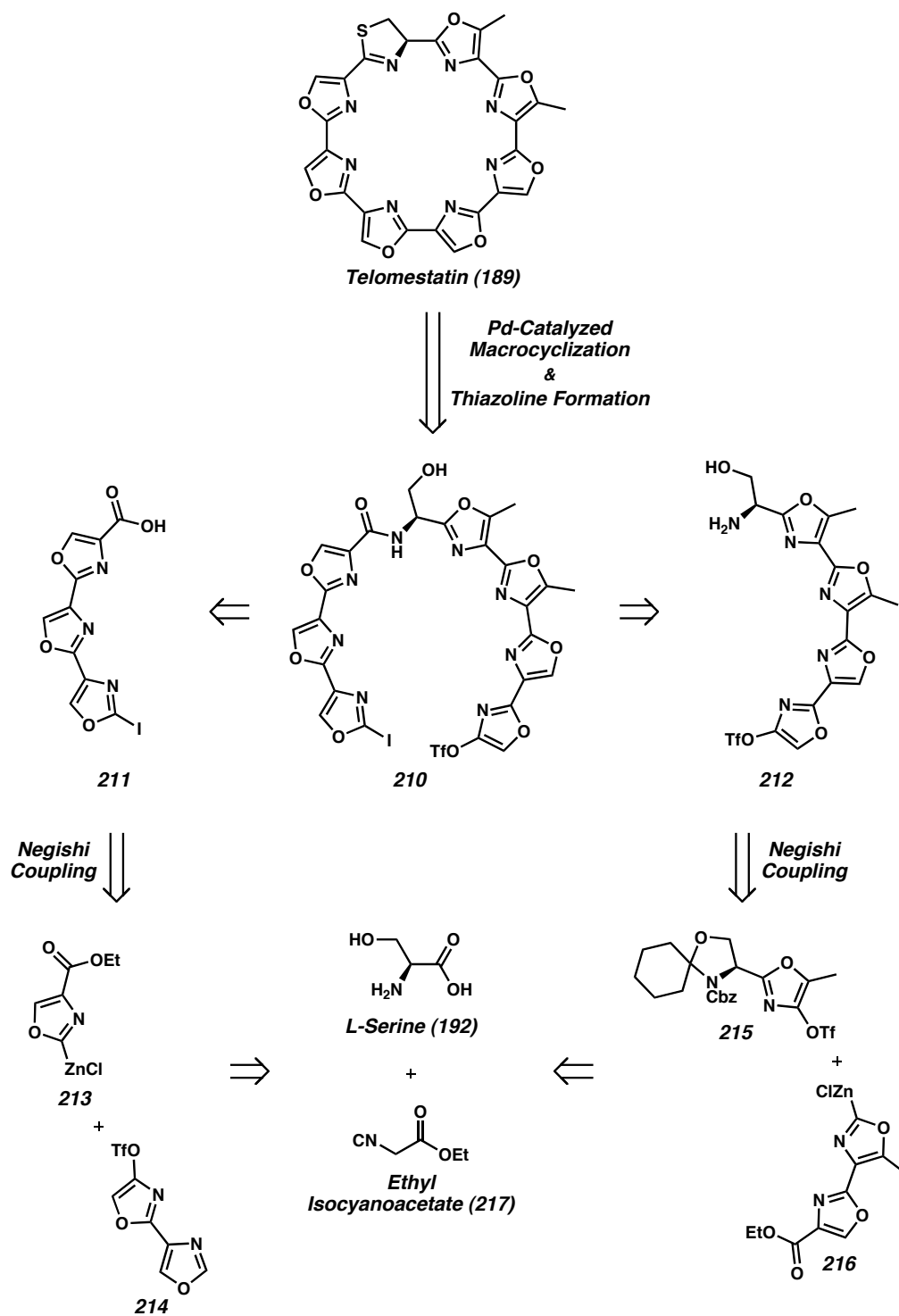
Given the significant anticancer therapeutic potential of telomestatin (**189**),<sup>9,10</sup> as well as the lengthy and low-yielding preparations to date,<sup>17</sup> a successful synthesis of this molecule would not only deliver the natural product in an efficient manner, but would also be readily amenable to analog synthesis for further biological testing.

#### 4.1.5 Retrosynthetic Analysis of Telomestatin

Our retrosynthetic analysis for telomestatin (**189**) is shown in Scheme 4.1.5. On the basis of the reported telomestatin (**189**) syntheses,<sup>17</sup> as well as the potential for sulfur to oxidize or poison metal catalysts, we envisioned a late-stage installation of the sulfur moiety and the thiazoline ring. Additionally, in order to maximize synthetic efficiency, we sought to complete the final aryl–aryl linkage of **210** and induce macrocyclization using a palladium-catalyzed cross-coupling.<sup>21,22</sup> This maneuver would also allow for a high degree of convergency by dividing the molecule into two roughly equal halves.<sup>23</sup> Disconnection across the amide bond in **210** then reveals trisoxazole iodo acid **211** and tetrakisoxazole amino alcohol **212**.

Iodo acid **211** would be targeted by way of a palladium-catalyzed Negishi cross-coupling between zinc reagent **213** and bisoxazole triflate **214**. Amino alcohol **212**, in turn, would also be assembled using a Negishi cross-coupling between triflate **215** and zinc reagent **216**. All of the achiral oxazole building blocks (**213**, **214**, **216**) would be obtained from ethyl isocyanoacetate (**217**), and chiral triflate **215** would be derived from the natural amino acid *L*-serine (**192**).

Scheme 4.1.5

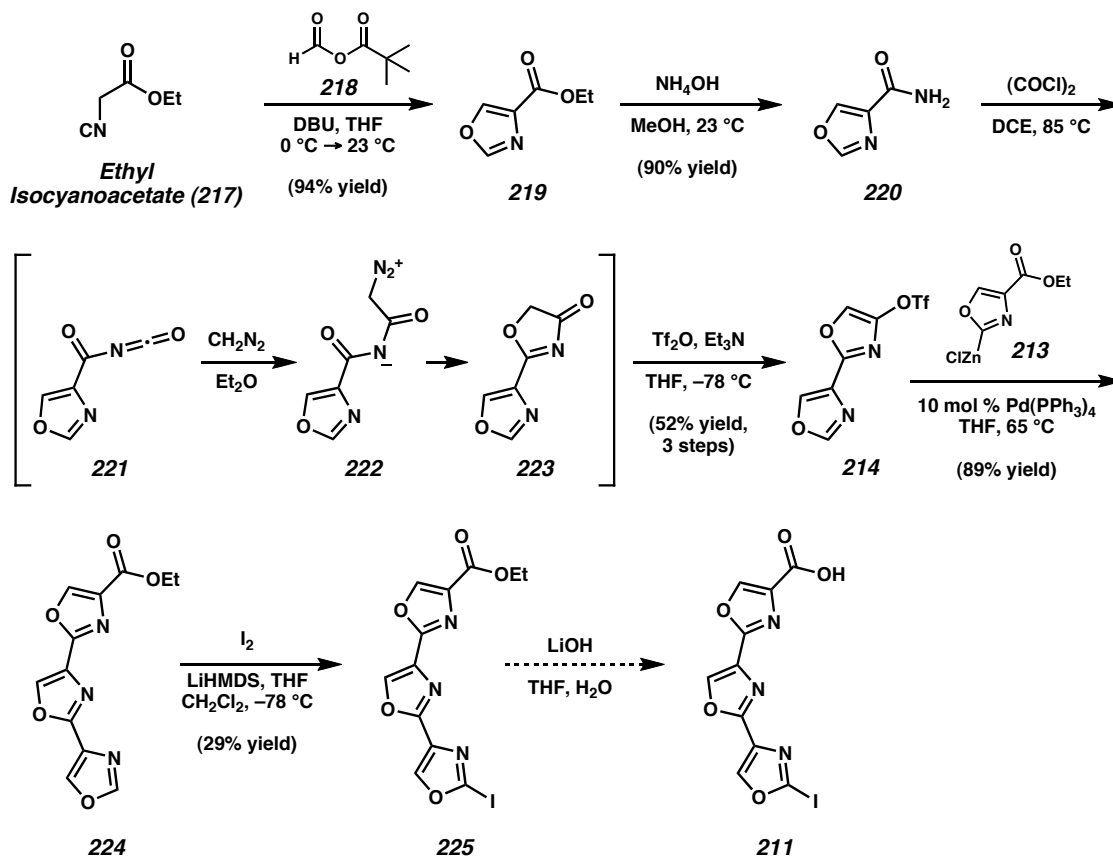


## 4.2 Progress Toward The Total Synthesis of Telomestatin

### 4.2.1 Synthesis of Left-hand Trisoxazole Iodo Acid

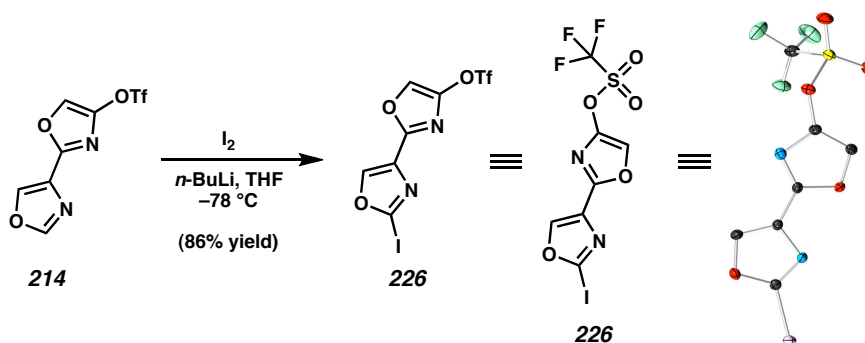
Our synthesis of the left-hand trisoxazole portion (**211**) of telomestatin (**189**) began with the preparation of known oxazole ester **219**. Exposure of ethyl isocyanoacetate (**217**) to mixed anhydride **218**<sup>24</sup> and DBU led to a high yield of oxazole ester **219**,<sup>25</sup> which was smoothly converted to amide **220** by the action of aqueous ammonia in methanol (Scheme 4.2.1). Conversion to bisoxazole triflate **214** was achieved by means of a three-step sequence, which commenced by heating amide **220** in the presence of oxalyl chloride to give rise to acyl isocyanate **221**.

Scheme 4.2.1



Subjection of acyl isocyanate **221** to anhydrous, alcohol-free diazomethane dried over sodium metal<sup>26</sup> led to in situ production of **222**, which rapidly cyclized with loss of nitrogen to form oxazolone **223**.<sup>27</sup> Treatment of this intermediate with  $\text{Ti}_2\text{O}$  and amine base produced bisoxazole triflate **214** in 52% yield over 3 steps.<sup>28</sup> Although NMR techniques were initially used for characterization, further confirmation of the structural identity was achieved by single crystal X-ray diffraction upon conversion to the iodo derivative (**214**  $\rightarrow$  **226**, Scheme 4.2.2).<sup>29</sup>

Scheme 4.2.2



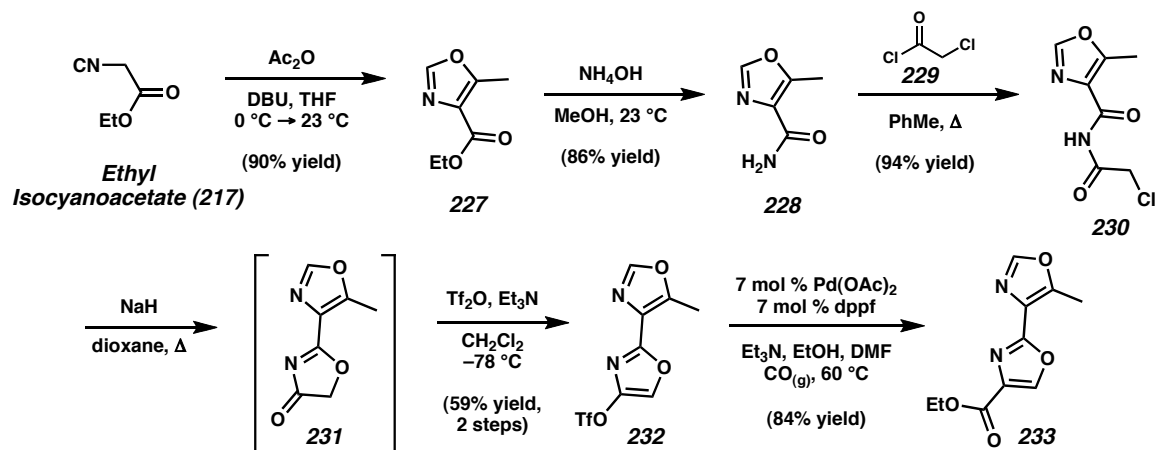
A wide range of cross-couplings of appropriate mono and bisoxazole subunits were investigated to prepare the desired trisoxazole fragment (**224**), including Stille, Suzuki, and Negishi protocols.<sup>30,31</sup> Ultimately, the Negishi approach proved to be the most robust to accomplish this union.<sup>30</sup> The necessary zinc reagent (**213**) for this reaction could be prepared from **219** via a deprotonation/quenching event with LiHMDS and  $\text{ZnCl}_2$ , furnishing trisoxazole **224** after successful aryl fusion with bisoxazole **214**.<sup>32</sup> Installation of the heteroaryl iodide could be realized at this juncture, since incorporating the iodide earlier in the synthesis would likely interfere with the Negishi cross-coupling

of **214** + **213**.<sup>33</sup> Deprotonation of trisoxazole **224** using LiHMDS, in an optimized solvent mixture of THF and dichloromethane,<sup>34</sup> followed by quenching with iodine produced **225**.<sup>32</sup> Finally, it is anticipated that hydrolysis of ester **225** would lead to the desired acid (**211**).

#### 4.2.2 Synthesis of Right-hand Tetrakisoxazole Amino Alcohol

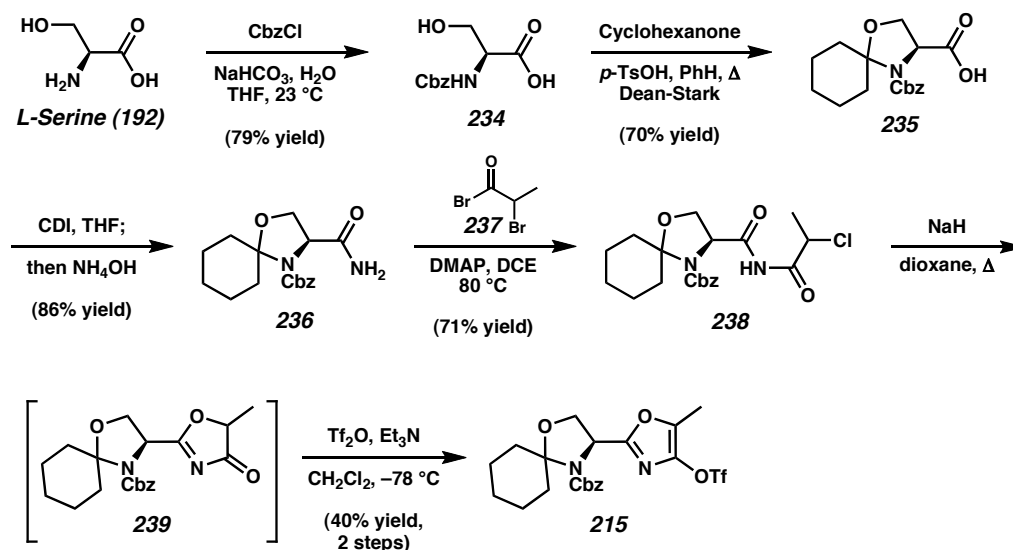
Assembly of the tetrakisoxazole amino alcohol subunit (**212**) begins with the preparation of methylbisoxazole ester **233**. The synthesis of this fragment is adapted from the route to bisoxazole triflate **214** (see Scheme 4.2.1, *vide infra*). Following a reported two-step procedure, mixing ethyl isocyanoacetate (**217**) with acetic anhydride and DBU led to the formation of methyloxazole ester **227**,<sup>35</sup> which was treated with ammonium hydroxide to generate amide **228** (Scheme 4.2.3). Acetylation with chloroacetyl chloride (**229**) gave rise to imide **230**, which could be converted to triflate **232** via oxazolone **231**. A Pd-catalyzed carbonylation reaction of triflate **232** with ethanol led to the production of desired ester **233** in 84% yield.

Scheme 4.2.3



With ester **233** now in hand, preparation of the triflate coupling partner (**215**) could proceed. Protection of *L*-serine (**192**) as the *N*-Cbz carbamate (**234**) was accomplished using published procedures (Scheme 4.2.4).<sup>36</sup> Refluxing **234** under Dean-Stark conditions with cyclohexanone and a catalytic amount of *p*-toluenesulfonic acid afforded cyclohexylidene **235**.<sup>37</sup> Acid **235** was then activated with CDI, and displaced with NH<sub>4</sub>OH to produce amide **236**. Reaction of amide **236** with **237** led to imide cyclization precursor **238**, which was treated with NaH to form oxazolone **239**. Finally, oxazole triflate **215** was accessed from oxazolone **239** via triflation.

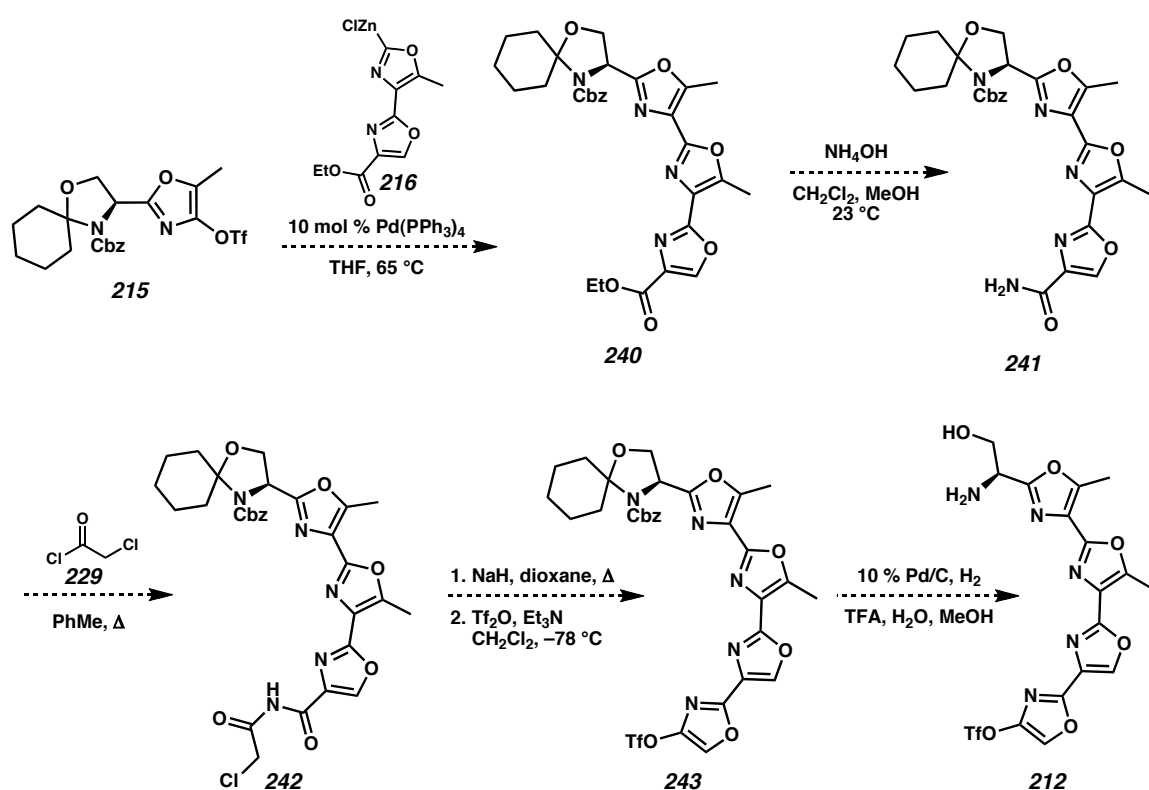
Scheme 4.2.4



With the ready availability of the key coupling partners (**215** and **233**), the Negishi cross-coupling was attempted. It is anticipated that exposure of triflate **215** to the Negishi reagent (**216**) of ester **233** under palladium catalysis would lead to the assembly of trisoxazole **240** (Scheme 4.2.5).<sup>38</sup> Installation of the final oxazole ring present in

desired tetrakisoxazole **212** could then be initiated via conversion to amide **241**. Acylation of amide **241** would then be executed to prepare imide **242**, which could be cyclized and treated with  $\text{Trf}_2\text{O}$  to furnish tetrakisoxazole triflate **243**.<sup>39</sup> Cleavage of both the benzyl carbamate and cyclohexylidene protecting groups would then occur under the action of  $\text{Pd/C}$ ,  $\text{H}_2$ , and  $\text{TFA}$  in wet methanol, ultimately affording amino alcohol **212**.<sup>40</sup>

Scheme 4.2.5



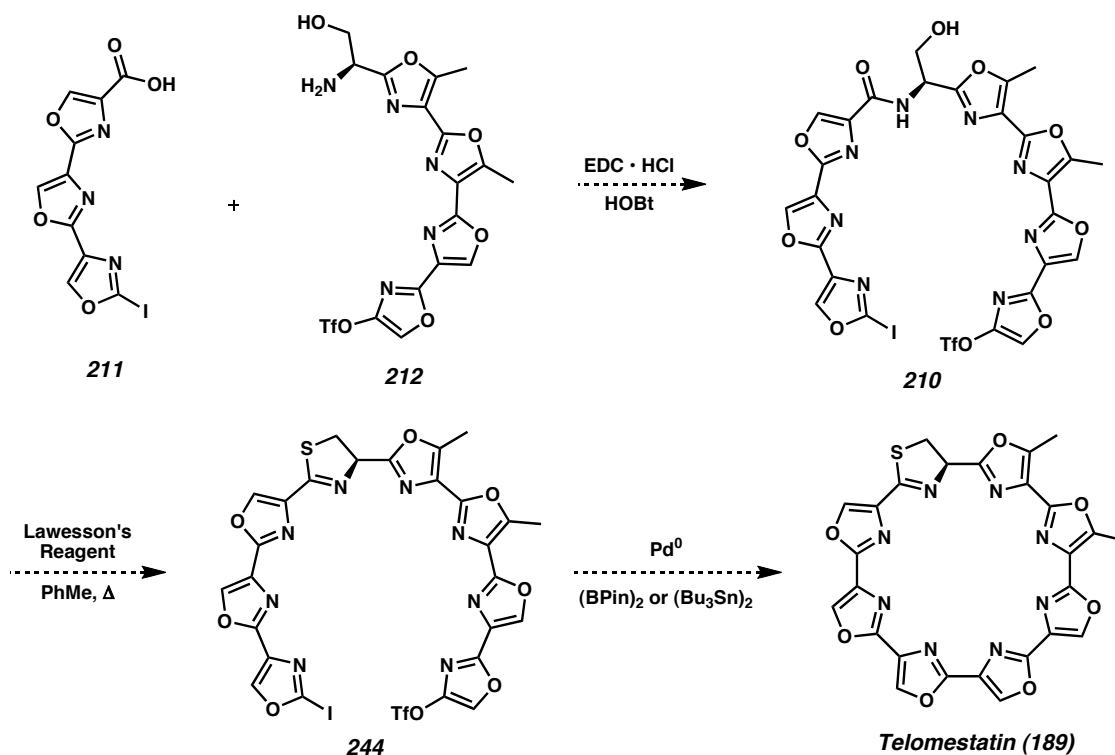
#### 4.2.3 Late-Stage and Proposed Endgame

With the assembly of the two major fragments completed (**211** and **212**), amide bond formation would then be initiated (Scheme 4.2.6). Successful coupling of these two partners would afford hydroxyamide **210**. Treatment of **210** with Lawesson's reagent is



then anticipated to lead to closure of the thiazoline ring to form **244**.<sup>41</sup> Finally, an intramolecular Pd-catalyzed cross-coupling of the iodide and triflate moieties of **244** would complete the macrocycle, as well as the total synthesis of telomestatin (**189**).<sup>21,42,43,44</sup>

Scheme 4.2.6



### 4.3 Conclusion

In conclusion, we have developed an extremely promising route to deliver the potent telomerase inhibitor (*R*)-telomestatin (**189**) from readily available ethyl isocyanoacetate (**217**) and *L*-serine (**192**). Our convergent synthesis employs palladium-mediated cross-coupling reactions to assemble oligooxazole intermediates from oxazole

building blocks. Additionally, this strategy utilizes a minimum number of protecting groups, and proposes a unique aryl–aryl macrocyclization as the last step of the synthesis.

In addition to the biological relevance of the desired target, a successful total synthesis of telomestatin using our approach would also enable rapid access to the preparation of telomestatin analogs. This would allow for the investigation of key interactions between telomestatin and the G-quadruplex, as well as the examination of the predictions generated by previous computer modeling studies, especially the still unresolved question of whether telomestatin actually facilitates the formation of the G-quadruplex, stabilizes the G-quadruplex, or does both.

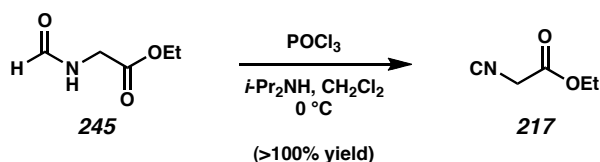
## 4.4 Experimental Section

### 4.4.1 Materials and Methods

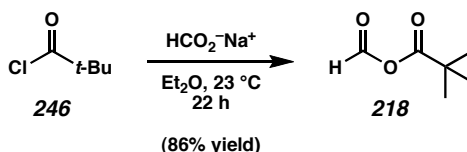
Unless stated otherwise, reactions were conducted in flame-dried glassware under an atmosphere of nitrogen using anhydrous solvents (either freshly distilled or passed through activated alumina columns). All commercially obtained reagents were used as received. Reaction temperatures were controlled using an IKAmag temperature modulator. Thin-layer chromatography (TLC) was conducted with E. Merck silica gel 60 F254 pre-coated plates (0.25 mm) and visualized using a combination of UV, anisaldehyde, ceric ammonium molybdate, and potassium permanganate staining. ICN silica gel (particle size 0.032–0.063 mm) or SiliCycle SiliaFlash P60 Academic silica gel (particle size 0.040–0.063 mm; pore diameter 60 Å) was used for flash column chromatography.  $^1\text{H}$  NMR spectra were recorded on a Varian Mercury 300 (at 300 MHz), or a Varian Inova 500 (at 500 MHz) and are reported relative to  $\text{Me}_4\text{Si}$  ( $\delta$  0.0). Data for  $^1\text{H}$  NMR spectra are reported as follows: chemical shift ( $\delta$  ppm), multiplicity, coupling constant (Hz), and integration.  $^{13}\text{C}$  NMR spectra were recorded on a Varian Mercury 300 (at 75 MHz), or a Varian Inova 500 (at 125 MHz) and are reported relative to  $\text{Me}_4\text{Si}$  ( $\delta$  0.0). Data for  $^{13}\text{C}$  NMR spectra are reported in terms of chemical shift ( $\delta$  ppm) and coupling constant ( $^{19}\text{F}$ , Hz).  $^{19}\text{F}$  NMR spectra were recorded on a Varian Mercury 300 (at 282 MHz) and are reported relative to external  $\text{F}_3\text{CCO}_2\text{H}$  standard ( $\delta$  –76.53). Data for  $^{19}\text{F}$  NMR spectra are reported in terms of chemical shift ( $\delta$  ppm). IR spectra were recorded on a Perkin Elmer Paragon 1000 spectrometer or a Perkin Elmer Spectrum BXII spectrometer and are reported in frequency of absorption ( $\text{cm}^{-1}$ ). Optical rotations were measured with a Jasco P-1010 polarimeter. High-resolution mass spectra were obtained

from the California Institute of Technology Mass Spectral Facility. X-Ray crystallographic data were obtained from the California Institute of Technology Beckman Institute X-Ray Crystallography Laboratory.

#### 4.4.2 Preparative Procedures

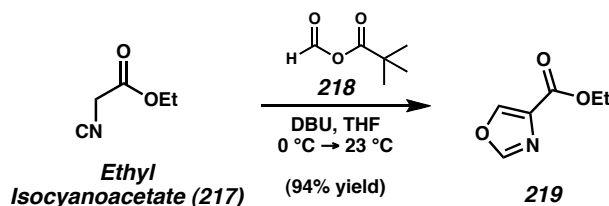


**Ethyl Isocyanoacetate (217).** To a solution of *N*-formylglycine ethyl ester (**245**, 52.9 mL, 403.4 mmol) in  $\text{CH}_2\text{Cl}_2$  (330 mL) at 0 °C was added *i*-Pr<sub>2</sub>NH (142 mL, 1.013 mol).  $\text{POCl}_3$  (41.0 mL, 447.9 mmol) was added dropwise over 1 h (1 drop/s addition rate). The reaction was stirred for 3 h at 0 °C, then quenched by slow addition of  $\text{Na}_2\text{CO}_3$  (90.0 g in 400 mL  $\text{H}_2\text{O}$ ), keeping the internal temperature below 15 °C. After the addition was complete, the reaction was stirred for 2 h at 23 °C.  $\text{CH}_2\text{Cl}_2$  (500 mL) and  $\text{H}_2\text{O}$  (400 mL) were added, and the phases were partitioned. The aqueous layer was further extracted with  $\text{CH}_2\text{Cl}_2$  (2 x 250 mL). The organic layers were combined, washed with  $\text{H}_2\text{O}$  (200 mL), dried over  $\text{MgSO}_4$ , filtered, and evaporated in vacuo to furnish ethyl isocyanoacetate (**217**, 46.2 g, 45.6 g theoretical, >100% yield) as an orange oil. This crude material was used without any further purification.  $R_f$  0.61 (1:1 hexanes:EtOAc);  $^1\text{H}$  NMR (300 MHz,  $\text{CDCl}_3$ )  $\delta$  4.27 (q,  $J$  = 7.1 Hz, 2H), 4.20 (s, 2H), 1.31 (t,  $J$  = 7.2 Hz, 3H). This compound is also commercially available from Aldrich (226319).



**Mixed Anhydride 218.**<sup>24</sup> To a suspension of finely powdered oven-dried sodium formate (63.78 g, 937.9 mmol) in Et<sub>2</sub>O (590 mL) was added pivaloyl chloride (**246**, 57.7 mL, 468.7 mmol) over 2 min. The suspension was vigorously stirred at 23 °C for 22 h. The solid was removed by filtration, and the filtrate was evaporated in vacuo at 0 °C, affording mixed anhydride **218** (52.3 g, 86% yield) as a volatile, colorless oil. This material was immediately used in the next step without further purification. Characterization data for this compound have been previously reported.<sup>24</sup>

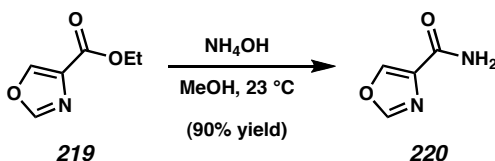
*NOTE: The rate of this heterogeneous reaction seems to be dependent on the particle size of sodium formate as well as the stirring rate. It is highly advised to monitor the reaction by <sup>1</sup>H NMR until the pivaloyl chloride (**246**) is consumed.*



**Oxazole Ester 219.**<sup>25</sup> To a stirring solution of ethyl isocyanoacetate (**217**, 5.74 g, 5.54 mL, 50.7 mmol) in THF (60 mL) at 0 °C was added DBU (15.2 mL, 101.6 mmol), followed by a solution of mixed anhydride **218** (13.2 g, 101.4 mmol) in THF (40 mL) added over 5 min. The mixture was stirred at 0 °C for 30 min, and then at 23 °C for 15 h. The reaction mixture was concentrated, and the crude product was filtered over a plug of silica gel (1:1 hexanes:EtOAc eluent). The solvent was evaporated under reduced

pressure, and the residue was purified by flash chromatography (3:2 hexanes:EtOAc eluent) to afford oxazole ester **219** (6.44 g, 90% yield) as a yellow oil, which solidified upon refrigeration.

*Alternate Procedure.* To a solution of ethyl isocyanoacetate (**217**, 22.4 g, 197.6 mmol) in THF (221 mL) at 0 °C was added DBU (60.0 mL, 401.2 mmol), followed by additional THF (30 mL). To this solution was added freshly prepared mixed anhydride **218** (51.7 g, 397.5 mmol) in THF (120 mL) via cannula over 25 min at 0 °C, followed by additional THF (40 mL). The reaction was stirred for 4 h, and the temperature was allowed to increase gradually from 0 °C → 23 °C. EtOAc (255 mL) and H<sub>2</sub>O (130 mL) were added, and the phases were partitioned. The aqueous layer was further extracted with EtOAc (3 x 250 mL). The organic layers were combined and washed with 0.5 M HCl (2 x 100 mL), saturated aq. Na<sub>2</sub>CO<sub>3</sub> (100 mL), H<sub>2</sub>O (100 mL), and brine (100 mL). The combined organic layers were dried over MgSO<sub>4</sub>, filtered, and evaporated to yield a dark, orange oil. The crude product was purified by passage over a plug of silica gel (1:1 hexanes:EtOAc eluent) to provide oxazole ester **219** (14.80 g, 53% yield) as a yellow oil. *R*<sub>f</sub> 0.43 (1:1 hexanes:EtOAc); <sup>1</sup>H NMR (300 MHz, CDCl<sub>3</sub>) δ 8.25 (d, *J* = 0.8 Hz, 1H), 7.91 (d, *J* = 0.8 Hz, 1H), 4.38 (q, *J* = 7.2 Hz, 2H), 1.37 (t, *J* = 7.2 Hz, 3H); <sup>13</sup>C NMR (75 MHz, CDCl<sub>3</sub>) δ 161.2, 151.6, 144.2, 133.6, 61.5, 14.5; IR (film) 3131, 2983, 1740, 1312, 1148, 1102 cm<sup>-1</sup>; HRMS-EI (*m/z*): [M]<sup>+</sup> calc'd for C<sub>6</sub>H<sub>7</sub>NO<sub>3</sub>, 141.0426; found, 141.0423.

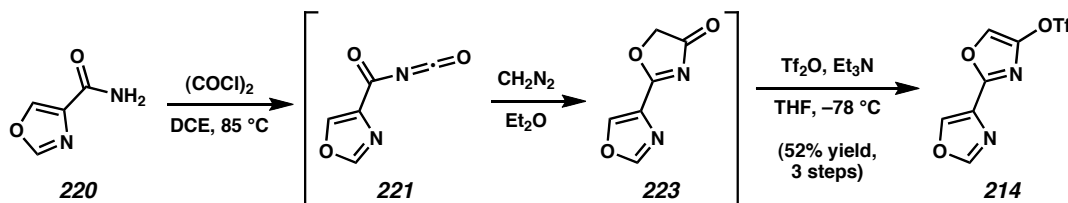


**Oxazole Amide 220.** To a solution of oxazole ester **219** (1.41 g, 10.0 mmol) in MeOH (25 mL) was added concentrated ammonium hydroxide (28.0–30.0% in H<sub>2</sub>O, 25 mL) in one portion at 23 °C. After stirring at 23 °C for 3 h, the solvent was evaporated in vacuo. The crude product was adsorbed onto silica gel using MeOH as solvent, and purified by flash chromatography (10:1 CHCl<sub>3</sub>:MeOH eluent) to furnish amide **220** (1.02 g, 90% yield) as a white solid.

*Alternate Procedure.* To a solution of oxazole ester **219** (28.92 g, 204.9 mmol) in MeOH (134 mL) was added concentrated ammonium hydroxide (28–30%, 127 mL) in one portion at 23 °C. The reaction was stirred for 11 h at 23 °C, and then the solvent was evaporated in vacuo. Following further coevaporation under reduced pressure with acetonitrile (3 x 150 mL), the crude product was dissolved in boiling EtOAc (750 mL). Solid impurities were removed by decantation, and the solution was allowed to cool to 23 °C. Hexanes (1 L) was added, and the solution was cooled to 12 °C and allowed to crystallize. The product was collected by vacuum filtration and dried further under high vac to yield oxazole amide **220** (14.30 g, 62% yield) as a pale yellow solid. The filtrate was concentrated, and the crystallization procedure was repeated to afford a second batch of **220** (3.59 g), which was combined with the first batch to provide oxazole amide **220** (17.89 g, 78% combined yield) as a pale yellow solid. *R*<sub>f</sub> 0.35 (10:1 CHCl<sub>3</sub>:MeOH); mp 156–158 °C; <sup>1</sup>H NMR (300 MHz, DMSO-*d*<sub>6</sub>) δ 8.56 (d, *J* = 1.1 Hz, 1H), 8.48 (d, *J* = 1.1 Hz, 1H), 7.66 (br s, 1H), 7.51 (br s, 1H); <sup>13</sup>C NMR (75 MHz, DMSO-*d*<sub>6</sub>) δ 161.8, 152.2,



142.0, 135.8; IR (KBr) 3379, 3154, 3111, 1664 (br), 1413, 1111  $\text{cm}^{-1}$ ; HRMS-EI ( $m/z$ ):  $[\text{M}]^+$  calc'd for  $\text{C}_4\text{H}_4\text{N}_2\text{O}_2$ , 112.0273; found, 112.0271.



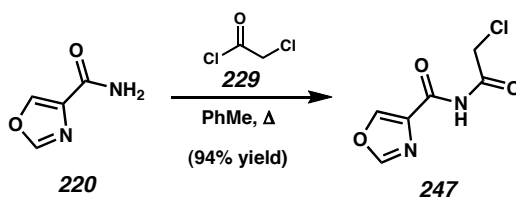
**Bisoxazole Triflate 214.** To oxazole amide **220** (224.0 mg, 2.0 mmol) and 1,2-dichloroethane (20 mL) in a Schlenk flask at  $23\text{ }^\circ\text{C}$  was added  $(\text{COCl})_2$  (0.720 mL, 8.25 mmol) in a rapid dropwise fashion. The flask was sealed, and the mixture was heated at  $85\text{ }^\circ\text{C}$  for 2 h. The reaction was allowed to cool to  $23\text{ }^\circ\text{C}$ , and the solvent was carefully evaporated in vacuo under an inert atmosphere to afford **221** as a pale yellow solid, which was immediately used in the subsequent reaction without further purification.

To crude acylisocyanate **221** dissolved in  $\text{Et}_2\text{O}$  (20 mL) was added a sodium-dried ethanol-free solution of freshly prepared  $\text{CH}_2\text{N}_2$  in  $\text{Et}_2\text{O}$ <sup>26</sup> (20 mL) in a rapid dropwise fashion. When bubbling ceased, and the solution turned pale yellow, the solvent was carefully concentrated in vacuo under an inert atmosphere to afford crude oxazolone **223** as a yellow solid, which was directly used in the following step.

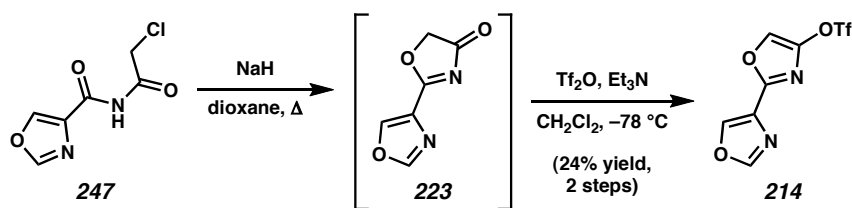
To oxazolone **223** in THF (30 mL) at  $-78\text{ }^\circ\text{C}$  was added  $\text{Et}_3\text{N}$  (0.700 mL, 5.02 mmol), followed by dropwise addition of  $\text{Tf}_2\text{O}$  (0.512 mL, 3.04 mmol). The reaction was stirred at  $-78\text{ }^\circ\text{C}$  for 1 h, and allowed to thaw at  $23\text{ }^\circ\text{C}$  for 30 min.  $\text{Et}_2\text{O}$  (30 mL) was then added, and the precipitates were removed by vacuum filtration. The filtrate was concentrated in vacuo, and the residue was purified by flash chromatography (2:1 hexanes: $\text{EtOAc}$  eluent) to afford bisoxazole triflate **214** (298.0 mg, 52% yield, 3 steps) as

a yellow oil, which solidified upon refrigeration.  $R_f$  0.64 (1:1 hexanes:EtOAc);  $^1\text{H}$  NMR (300 MHz,  $\text{CDCl}_3$ )  $\delta$  8.30 (d,  $J = 0.8$  Hz, 1H), 8.00 (d,  $J = 0.8$  Hz, 1H), 7.75 (s, 1H);  $^{13}\text{C}$  NMR (75 MHz,  $\text{CDCl}_3$ )  $\delta$  153.1, 152.3, 145.8, 140.0, 129.7, 126.9, 118.8 (q,  $J_{\text{CF}} = 320$  Hz);  $^{19}\text{F}$  NMR (282 MHz,  $\text{CDCl}_3$ )  $\delta$  -73.2; IR (film) 3133, 1585, 1429, 1215, 1131  $\text{cm}^{-1}$ ; HRMS-EI ( $m/z$ ):  $[\text{M}]^+$  calc'd for  $\text{C}_7\text{H}_3\text{N}_2\text{O}_3\text{F}_3\text{S}$ , 283.9715; found, 283.9707.

*Alternate procedure for the preparation of 214:*



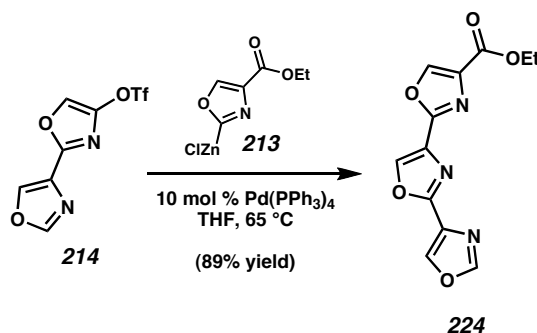
**Oxazole Chloro Imide 247.** To a suspension of oxazole amide **220** (3.20 g, 28.6 mmol) in toluene (30 mL) was added chloroacetyl chloride (**229**, 3.0 mL, 37.7 mmol) over 30 sec at 23 °C. The flask was fitted with reflux condenser and a drying tube containing Drierite<sup>®</sup>, and the reaction mixture was heated at 115 °C for 4.5 h under gentle reflux. The reaction was allowed to cool to 23 °C, and hexanes (150 mL) was added. After cooling to 0 °C, the product was collected by vacuum filtration, washed with hexanes (3 x 30 mL), and further dried under high vac to furnish oxazole imide **247** (5.04 g, 94% yield) as a light brown powder.  $R_f$  0.33 (1:1 hexanes:EtOAc); mp 126–128 °C;  $^1\text{H}$ -NMR (300 MHz,  $\text{DMSO}-d_6$ )  $\delta$  11.06 (br s, 1H), 8.97 (d,  $J = 1.1$  Hz, 1H), 8.62 (d,  $J = 1.1$  Hz, 1H), 4.73 (s, 2H);  $^{13}\text{C}$  NMR (75 MHz,  $\text{DMSO}-d_6$ )  $\delta$  167.5, 158.9, 152.8, 144.9, 133.9, 45.5; IR (KBr) 3307, 3139, 1734, 1700, 1578, 1471, 1287, 1188, 1095, 1050  $\text{cm}^{-1}$ ; HRMS-EI ( $m/z$ ):  $[\text{M}]^+$  calc'd for  $\text{C}_6\text{H}_5\text{N}_2\text{O}_3\text{Cl}$ , 187.9989; found, 187.9992.



**Bisoxazole Triflate 214.** To a whipped suspension of NaH (60% dispersion in mineral oil, 1.81 g, 45.3 mmol) in dioxane (725 mL) at 23 °C was added oxazole imide **247** (8.00 g, 42.4 mmol) portionwise over 1 min. The mixture was stirred at 23 °C for 15 min and then was heated at 110 °C for 40 min. After cooling to 23 °C over 1 h, the reaction mixture was filtered over a pad of Celite<sup>®</sup> ( $\text{ Et}_2\text{O}$  eluent). The filtrate was coevaporated under reduced pressure with heptane (3 x 500 mL) and benzene (300 mL), and was further dried under high vac to provide oxazolone **223** as an orange solid. This material was immediately carried to the subsequent step without further purification. Although oxazolone **223** is typically used in crude form, it has been observed by  $^1\text{H}$  NMR.  $^1\text{H}$  NMR (300 MHz,  $\text{ DMSO-}d_6$ )  $\delta$  (9.31,  $J$  = 0.9 Hz, 1H), 8.75 (d,  $J$  = 0.9 Hz, 1H), 4.91 (s, 2H).

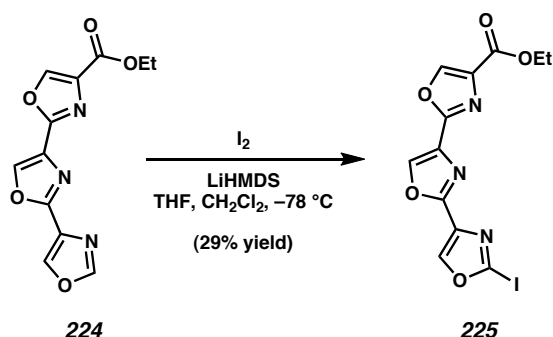
To oxazolone **223** dissolved in  $\text{ CH}_2\text{Cl}_2$  (230 mL) at  $-78\text{ }^\circ\text{C}$  was added  $\text{ Et}_3\text{N}$  (12.0 mL, 86.1 mmol) over 1 min, followed by dropwise addition of freshly prepared  $\text{ Tf}_2\text{O}$  (8.6 mL, 51.1 mmol) over 2 min. The reaction was held at  $-78\text{ }^\circ\text{C}$  for 45 min, and was then immediately warmed to 0 °C for 15 min.  $\text{ H}_2\text{O}$  (100 mL) was added, and the phases were partitioned. The aqueous phase was further extracted with  $\text{ CH}_2\text{Cl}_2$  (2 x 300 mL), and the combined organics were dried over  $\text{ MgSO}_4$  and concentrated under reduced pressure to afford a dark colored syrup. The residue was purified by flash chromatography (7:3 hexanes: $\text{ CH}_2\text{Cl}_2 \rightarrow$  1:1 hexanes: $\text{ CH}_2\text{Cl}_2$  eluent), and the product-containing fractions were collected and concentrated in vacuo. The crude product was further purified by flash

chromatography (4:1 hexanes:EtOAc eluent) to afford bisoxazole triflate **214** (2.927 g, 24% yield, 2 steps) as an off-white solid.



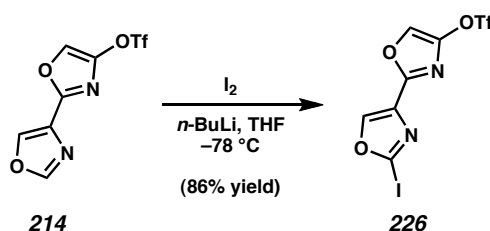
**Trisoxazole Ester 224.** To oxazole ester **219** (155.2 mg, 1.10 mmol) in THF (9.5 mL) at  $-78\text{ }^{\circ}\text{C}$  was added LiHMDS (1.0 M in THF, 1.23 mL, 1.23 mmol) in a dropwise fashion. The reaction was stirred at  $-78\text{ }^{\circ}\text{C}$  for 30 min, and then  $\text{ZnCl}_2$  (0.5 M in THF, 6.70 mL, 3.35 mmol) was added over 3 min. The solution was kept at  $-78\text{ }^{\circ}\text{C}$  for an additional 5 min and was then held at  $0\text{ }^{\circ}\text{C}$  for 2.5 h to deliver Negishi reagent **213**. In a separate flask was prepared a solution of bisoxazole triflate **214** (267.8 mg, 0.94 mmol),  $\text{Pd}(\text{PPh}_3)_4$  (109.5 mg, 0.09 mmol), and THF (9.5 mL). This freshly prepared solution was then transferred into the flask containing Negishi reagent **213** via cannula, and the resulting mixture was heated at  $65\text{ }^{\circ}\text{C}$  for 1.5 h. After cooling to  $23\text{ }^{\circ}\text{C}$ , the reaction mixture was diluted with  $\text{CH}_2\text{Cl}_2$  (30 mL) and filtered over a plug of silica gel (1:1 hexanes:EtOAc  $\rightarrow$  EtOAc eluent). The product containing-fractions were concentrated under reduced pressure, adsorbed onto silica gel using a 1:1 mixture of THF: $\text{CH}_2\text{Cl}_2$  as solvent, and purified further by flash chromatography (3:1 hexanes:EtOAc  $\rightarrow$  EtOAc eluent). The product-containing fractions were concentrated in vacuo and redissolved in a minimum of hot  $\text{CH}_2\text{Cl}_2$ :THF (1:1, 4 mL). Hexanes (12 mL) was added, and the

suspension was stirred for 2 h. The solvent was carefully removed, and the solid was triturated with hexanes (2 x 10 mL). The solid was dried under high vac to provide trisoxazole ester **224** (230.4 mg, 89% yield) as a fluffy, white solid.  $R_f$  0.31 (3:1 EtOAc:hexanes);  $^1\text{H}$  NMR (300 MHz,  $\text{DMSO}-d_6$ )  $\delta$  9.10 (s, 1H), 9.05 (d,  $J = 1.1$  Hz, 1H), 8.99 (s, 1H), 8.68 (d,  $J = 0.8$  Hz, 1H), 4.32 (q,  $J = 7.2$  Hz, 2H), 1.31 (t,  $J = 7.0$  Hz, 3H);  $^{13}\text{C}$  NMR (125 MHz,  $\text{DMSO}-d_6$ )  $\delta$  160.4, 155.6, 154.9, 153.6, 145.6, 141.1, 141.0, 133.5, 130.0, 128.5, 60.8, 14.1; IR (film) 3136, 1721, 1277, 1164  $\text{cm}^{-1}$ ; HRMS-FAB ( $m/z$ ):  $[\text{M} + \text{H}]^+$  calc'd for  $\text{C}_{12}\text{H}_{10}\text{N}_3\text{O}_5$ , 276.0620; found, 276.0629.



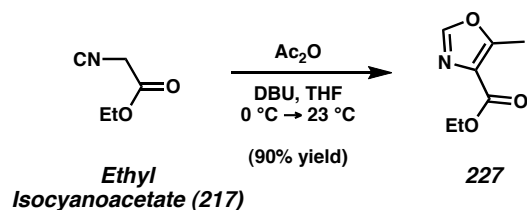
**Trisoxazole Iodo Ester 225.** To trisoxazole ester **224** (100.1 mg, 0.37 mmol) in THF (24 mL) and  $\text{CH}_2\text{Cl}_2$  (13 mL) at  $-78\text{ }^\circ\text{C}$  was added LiHMDS (1.0 M in THF, 440  $\mu\text{L}$ , 0.44 mmol) dropwise. The reaction was stirred for 30 min at  $-78\text{ }^\circ\text{C}$ , and then a solution of  $\text{I}_2$  (138.6 mg, 0.55 mmol) in THF (2.0 mL) was added in a rapid dropwise fashion. The solution was allowed to warm slowly to  $23\text{ }^\circ\text{C}$  over 3 h and then was concentrated in vacuo. The residue was dissolved in a minimum of THF: $\text{CH}_2\text{Cl}_2$  (1:1, 7 mL) and was filtered over a plug of silica gel (1:1 EtOAc: $\text{CH}_2\text{Cl}_2$  eluent). The product-containing fractions were concentrated and purified by flash chromatography (6:4  $\text{CH}_2\text{Cl}_2$ :EtOAc eluent). The solid residue was suspended in THF: $\text{CH}_2\text{Cl}_2$  (1:1, 4 mL) and

hexanes (10 mL) and vigorously triturated. Further trituration with hexanes (2 x 10 mL) and drying under high vac afforded trisoxazole iodo ester **225** (42.3 mg, 29% yield) as a yellow solid.  $R_f$  0.35 (1:1 hexanes:EtOAc);  $^1\text{H}$  NMR (300 MHz,  $\text{DMSO}-d_6$ )  $\delta$  9.12 (s, 1H), 9.10 (s, 1H), 9.00 (s, 1H), 4.32 (q,  $J = 7.1$  Hz, 2H), 1.31 (t,  $J = 7.0$  Hz, 3H);  $^{13}\text{C}$  NMR (75 MHz,  $\text{DMSO}-d_6$ )  $\delta$  160.4, 154.8, 154.7, 146.2, 145.6, 141.1, 133.5, 131.5, 130.0, 109.3, 60.8, 14.1; IR (film) 3132, 1720, 1133  $\text{cm}^{-1}$ ; HRMS-EI ( $m/z$ ):  $[\text{M}]^+$  calc'd for  $\text{C}_{12}\text{H}_8\text{N}_3\text{O}_5\text{I}$ , 409.9509; found, 409.9500.

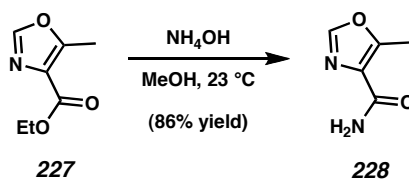


**Bisoxazole Iodo Triflate 226.** To bisoxazole triflate **214** (41.3 mg, 0.15 mmol) in THF (3.0 mL) at  $-78^\circ\text{C}$  was added  $n\text{-BuLi}$  (2.5 M in hexanes, 65  $\mu\text{L}$ , 0.16 mmol) in a dropwise fashion. After stirring at  $-78^\circ\text{C}$  for 30 min, a separate solution of  $\text{I}_2$  (43.9 mg, 0.17 mmol) in THF (1.0 mL) cooled to  $-78^\circ\text{C}$  was added via cannula. Additional THF (0.5 mL) was used to rinse the cannula, which was added to the reaction mixture. The reaction was stirred at  $-78^\circ\text{C}$  for 1.5 h, allowed to thaw to  $23^\circ\text{C}$ , and concentrated in vacuo. The residue was purified directly by flash chromatography (3:1 hexanes:EtOAc eluent) to provide bisoxazole iodo triflate **226** (51.5 mg, 86% yield) as a yellow solid. Suitable crystals for X-ray diffraction were obtained by vapor diffusion of heptane into an EtOAc solution of **226** at  $23^\circ\text{C}$ .  $R_f$  0.30 (4:1 hexanes:EtOAc); mp  $96\text{--}98^\circ\text{C}$ ;  $^1\text{H}$  NMR (300 MHz,  $\text{CDCl}_3$ )  $\delta$  8.33 (s, 1H), 7.74 (s, 1H), 7.75 (s, 1H);  $^{13}\text{C}$  NMR (75 MHz,  $\text{CDCl}_3$ )  $\delta$  152.0, 145.8, 145.1, 132.9, 127.1, 118.8 (q,  $J_{\text{CF}} = 320$  Hz), 103.4;  $^{19}\text{F}$  NMR (282 MHz,

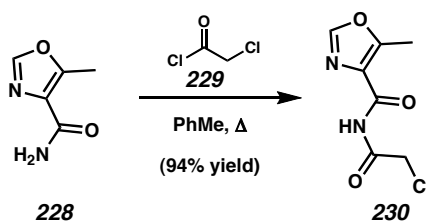
$\text{CDCl}_3$ )  $\delta$   $-73.2$ ; IR (film)  $3451$  (br),  $1585$ ,  $1430$ ,  $1221$   $\text{cm}^{-1}$ ; HRMS-EI ( $m/z$ ):  $[\text{M}]^+$  calc'd for  $\text{C}_7\text{H}_2\text{F}_3\text{IN}_2\text{O}_5\text{S}$ ,  $409.8681$ ; found,  $409.8693$ .



**Methyl Oxazole Ethyl Ester 227.**<sup>35</sup> To a solution of ethyl isocyanoacetate (**217**,  $1.13$  g,  $10.0$  mmol) in THF ( $12$  mL) at  $0^\circ\text{C}$  was added DBU ( $3.0$  mL,  $20.0$  mmol), followed by dropwise addition of a solution of acetic anhydride ( $1.89$  mL,  $20.0$  mmol) in THF ( $8$  mL). The mixture was stirred at  $0^\circ\text{C}$  for  $30$  min and then at  $23^\circ\text{C}$  for  $12$  h. The reaction mixture was concentrated under reduced pressure, and the residue was purified by flash column chromatography ( $3:2$  hexanes:EtOAc eluent) to give methyl oxazole ethyl ester **227** ( $1.54$  g,  $90\%$  yield) as a yellow oil. Characterization data for this compound have been reported previously.<sup>35</sup>  $R_f$   $0.47$  ( $1:1$  hexanes:EtOAc);  $^1\text{H}$  NMR ( $300$  MHz,  $\text{CDCl}_3$ )  $\delta$   $7.71$  (s,  $1\text{H}$ ),  $4.36$  (q,  $J = 7.1$  Hz,  $2\text{H}$ ),  $2.62$  (s,  $3\text{H}$ ),  $1.37$  (t,  $J = 7.2$  Hz,  $3\text{H}$ );  $^{13}\text{C}$  NMR ( $75$  MHz,  $\text{CDCl}_3$ )  $\delta$   $162.4$ ,  $156.6$ ,  $149.0$ ,  $127.5$ ,  $61.2$ ,  $14.5$ ,  $12.1$ ; IR (film)  $3129$ ,  $2983$ ,  $1716$ ,  $1615$ ,  $1105$   $\text{cm}^{-1}$ ; HRMS-EI ( $m/z$ ):  $[\text{M}]^+$  calc'd for  $\text{C}_7\text{H}_9\text{NO}_3$ ,  $155.0582$ ; found,  $155.0585$ .



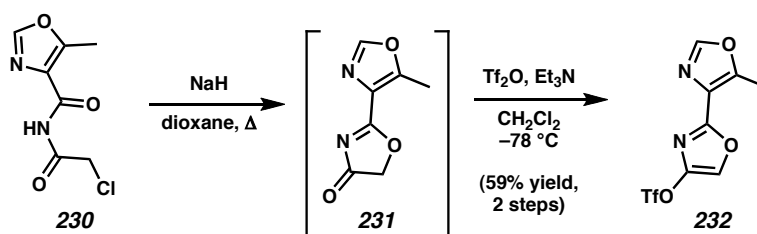
**Methyl Oxazole Amide 228.** To a solution of methyl oxazole ester **227** (1.55 g, 10 mmol) in MeOH (25 mL) was added concentrated ammonium hydroxide (28–30%, 25 mL) in one portion at 23 °C. The reaction mixture was stirred at 23 °C for 66 h, and then the solvent was evaporated under reduced pressure. The crude product was adsorbed onto silica gel using MeOH as solvent, and purified by flash chromatography (12:1 CHCl<sub>3</sub>:MeOH eluent) to yield methyl oxazole amide **228** (1.07 g, 86% yield) as a white solid. *R<sub>f</sub>* 0.41 (10:1 CHCl<sub>3</sub>:MeOH); <sup>1</sup>H NMR (300 MHz, DMSO-*d*<sub>6</sub>) δ 8.29 (s, 1H), 7.48 (br s, 1H), 7.40 (br s, 1H), 2.55 (s, 3H); <sup>13</sup>C NMR (75 MHz, DMSO-*d*<sub>6</sub>) δ 163.1, 152.4, 149.4, 128.6, 11.2; IR (KBr) 3391, 3154, 1690, 1621, 1193, 1121 cm<sup>-1</sup>; HRMS-EI (*m/z*): [M]<sup>+</sup> calc'd for C<sub>5</sub>H<sub>6</sub>N<sub>2</sub>O<sub>2</sub>, 126.0429; found, 126.0435.



**Methyl Oxazole Chloro Imide 230.** To methyl oxazole amide **228** (732.6 mg, 5.81 mmol) in toluene (6 mL) was added chloroacetyl chloride (**229**, 650 μL, 8.17 mmol) over 30 sec at 23 °C. The flask was fitted with reflux condenser and a drying tube containing Drierite<sup>®</sup>, and the reaction mixture was heated at 115 °C for 9 h under gentle reflux. The reaction was allowed to cool to 23 °C, and hexanes (50 mL) was added. The suspension was vigorously stirred for 2 h at 23 °C. The product was collected by vacuum



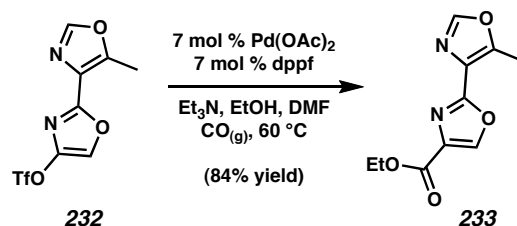
filtration, rinsed with hexanes (3 x 10 mL), and further dried under high vac to afford methyl oxazole chloro imide **230** (1.10 g, 94% yield) as a white solid.  $R_f$  0.50 (1:1 hexanes:EtOAc);  $^1\text{H}$  NMR (300 MHz, DMSO- $d_6$ ):  $\delta$  10.64 (br s, 1H), 8.48 (s, 1H), 4.70 (s, 2H), 2.61 (s, 3H);  $^{13}\text{C}$  NMR (300 MHz, DMSO- $d_6$ )  $\delta$  166.8, 159.9, 156.3, 150.0, 127.3, 45.0, 11.5; IR (film) 3261, 1732, 1724, 1704, 1614, 1482, 1180  $\text{cm}^{-1}$ ; HRMS-EI ( $m/z$ ):  $[\text{M}]^+$  calc'd for  $\text{C}_7\text{H}_7\text{N}_2\text{O}_3\text{Cl}$ , 202.0145; found, 202.0142.



**Methyl Bisoxazole Triflate 232.** To a well-stirred suspension of NaH (60% dispersion in mineral oil, 251.2 mg, 6.28 mmol) in dioxane (90 mL) was slowly added chloro imide **230** (1.096 g, 5.41 mmol) over 1 min at 23 °C. After stirring 15 min at this temperature, the reaction was heated at 110 °C for 40 min and then allowed to cool at 23 °C for 20 min, and then at 10 °C for 30 min. The mixture was filtered over a pad of Celite<sup>®</sup> (Et<sub>2</sub>O eluent), and then evaporated in vacuo, coevaporating with heptane (3 x 100 mL) and benzene (50 mL). Trace volatiles were removed by high vac to afford oxazolone **231**, which was immediately used in the subsequent reaction.

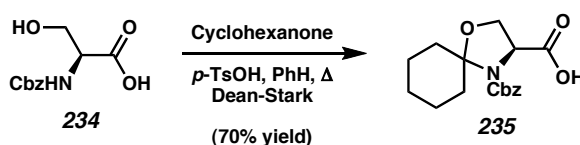
To a solution of oxazolone **231** in CH<sub>2</sub>Cl<sub>2</sub> (30 mL) at -78 °C was added Et<sub>3</sub>N (1.5 mL, 10.8 mmol) dropwise over 1 min. Freshly prepared Tf<sub>2</sub>O (1.1 mL, 6.5 mmol) was then added dropwise over 2 min. After stirring for 45 min at -78 °C, the reaction was immersed in a 0 °C bath for 15 min. The reaction was quenched at 0 °C by the addition of H<sub>2</sub>O (100 mL), and the phases were partitioned. The aqueous phase was further extracted

with  $\text{CH}_2\text{Cl}_2$  (3 x 100 mL). The combined organics were washed with brine (30 mL), dried over  $\text{MgSO}_4$ , and evaporated in vacuo. The crude product was purified by flash chromatography (4:1 hexanes:EtOAc eluent) to afford methyl bisoxazole triflate **232** (955.6 mg, 59% yield, 2 steps) as an orange solid.  $R_f$  0.19 (4:1 hexanes:EtOAc);  $^1\text{H}$  NMR (300 MHz,  $\text{CDCl}_3$ )  $\delta$  7.82 (s, 1H), 7.73 (s, 1H), 2.68 (s, 3H);  $^{13}\text{C}$  NMR (75 MHz,  $\text{CDCl}_3$ )  $\delta$  154.0, 152.2, 150.3, 145.9, 126.3, 124.4, 118.8 (q,  $J_{CF} = 321$  Hz), 11.7;  $^{19}\text{F}$  NMR (282 MHz,  $\text{CDCl}_3$ )  $\delta$  -73.2; IR (film) 3133, 1647, 1589, 1435, 1229, 1137  $\text{cm}^{-1}$ ; HRMS-EI ( $m/z$ ):  $[\text{M}]^+$  calc'd for  $\text{C}_8\text{H}_5\text{N}_2\text{O}_5\text{F}_3\text{S}$ , 297.9871; found, 297.9862.



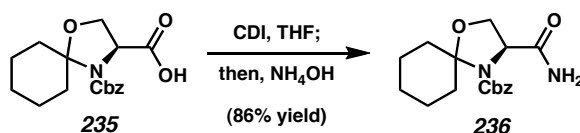
**Methyl Bisoxazole Ethyl Ester 233.** Methyl bisoxazole triflate **232** (1.46 g, 4.90 mmol),  $\text{Pd}(\text{OAc})_2$  (77.2 mg, 0.34 mmol), 1,1'-bis(diphenylphosphino)ferrocene (190.9 mg, 0.34 mmol), and DMF (27 mL) were combined in a 250 mL sealable Schlenk flask. EtOH (5.8 mL, 99.3 mmol) and  $\text{Et}_3\text{N}$  (1.9 mL, 13.6 mmol) were rapidly added, and the solution was sparged with carbon monoxide gas for 15 min. The flask was sealed and heated at  $60^\circ\text{C}$  for 12 h. The solution was allowed to cool to  $23^\circ\text{C}$ , and was sparged with argon for 15 min (*Caution: CO gas!*). EtOAc (300 mL) and  $\text{H}_2\text{O}$  (100 mL) were added, and the phases were separated. The aqueous layer was further extracted with EtOAc (2 x 200 mL). The combined organics were washed with 0.1 M HCl (50 mL),  $\text{H}_2\text{O}$  (50 mL), and brine (50 mL), dried over  $\text{MgSO}_4$ , and evaporated in vacuo. Purification by flash chromatography (7:1  $\text{CH}_2\text{Cl}_2$ :EtOAc eluent) furnished methyl

bisoxazole ethyl ester **233** (913.5 mg, 84% yield) as a brown-tan solid.  $R_f$  0.35 (1:1 hexanes:EtOAc);  $^1\text{H}$  NMR (300 MHz,  $\text{CDCl}_3$ )  $\delta$  8.25 (s, 1H), 7.82 (s, 1H), 4.38 (q,  $J$  = 7.1 Hz, 2H), 2.74 (s, 3H), 1.38 (t,  $J$  = 7.2 Hz, 3H);  $^{13}\text{C}$  NMR (75 MHz,  $\text{CDCl}_3$ )  $\delta$  161.3, 156.7, 151.7, 149.9, 143.5, 134.7, 124.5, 61.5, 14.5, 11.9; IR (film) 3127, 2983, 1739, 1720, 1576, 1316, 1113  $\text{cm}^{-1}$ ; HRMS-EI ( $m/z$ ):  $[\text{M}]^+$  calc'd for  $\text{C}_{10}\text{H}_{10}\text{N}_2\text{O}_4$ , 222.0641; found, 222.0648.

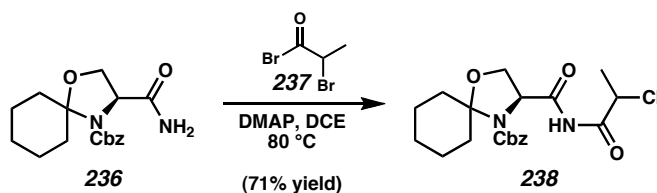


**Acid 235.** To *N*-Cbz-serine<sup>36</sup> (**234**, 5.0 g, 20.9 mmol) in benzene (150 mL) was added cyclohexanone (3.0 mL, 28.9 mmol) and *p*-toluenesulfonic acid (420 mg, 2.2 mmol). The mixture was heated to reflux under a Dean-Stark trap for 18 h and then was allowed to cool to 23 °C. The reaction mixture was poured over saturated aq.  $\text{NaHCO}_3$  (100 mL), and the phases were partitioned. The aqueous phase was further extracted with  $\text{Et}_2\text{O}$  (2 x 100 mL), and the combined organics were extracted with saturated aq.  $\text{NaHCO}_3$  (2 x 100 mL). The aqueous phases were all combined, acidified to pH = 2 using 3 M HCl, and extracted with EtOAc (2 x 150 mL). The combined EtOAc extracts were washed with 1 N HCl (40 mL) and brine (40 mL), dried over  $\text{MgSO}_4$ , and concentrated in vacuo to provide acid **235** (4.64 g, 70% yield) as an off-white foam.  $R_f$  0.24 (1:1 hexanes:EtOAc; 1% acetic acid);  $^1\text{H}$  NMR (500 MHz,  $\text{C}_6\text{D}_6$ , 70 °C, mixture of rotamers)  $\delta$  7.24–7.03 (comp. m, 5H), 5.09 (d,  $J$  = 12.7 Hz, 1H), 5.02 (d,  $J$  = 12.4 Hz, 1H), 4.31–4.24 (m, 1H), 3.95–3.80 (m, 1H), 3.65–3.58 (m, 1H), 2.83–1.00 (comp. m, 10H);  $^{13}\text{C}$  NMR (125 MHz,  $\text{CDCl}_3$ , major rotamer)  $\delta$  177.0, 152.0, 136.5, 128.7 (2C), 128.2,

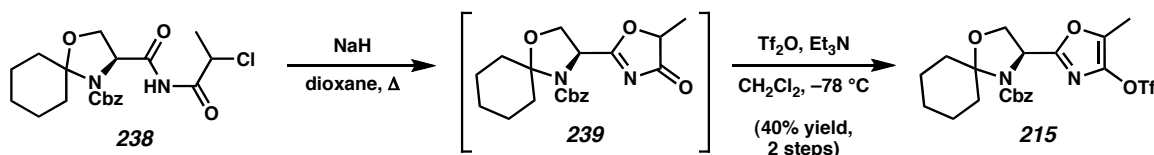
127.9 (2C), 97.2, 67.1, 66.6, 58.8, 33.5, 31.6, 24.8, 23.5, 23.4; IR (film) 2935 (br), 1713 (br), 1415, 1351, 1211, 1085  $\text{cm}^{-1}$ ; HRMS-EI ( $m/z$ ):  $[\text{M}]^+$  calc'd for  $\text{C}_{17}\text{H}_{21}\text{O}_5\text{N}$ , 319.1240; found, 319.1435;  $[\alpha]_{\text{D}}^{20} -26.99^\circ$  ( $c$  1.0, MeOH).



**Amide 236.** To acid **235** (6.12 g, 19.2 mmol) in THF (80 mL) at 23 °C was added 1,1'-carbonyldiimidazole (6.15 g, 37.9 mmol) in one portion. The reaction was stirred for 15 min, then concentrated ammonium hydroxide (28.0–30.0% in  $\text{H}_2\text{O}$ , 20 mL) was added in a steady stream. After 3 h of additional stirring at 23 °C, the reaction mixture was poured over EtOAc (200 mL) and 10% aq. citric acid (100 mL). The phases were partitioned, and the organic extract was washed with 1 M HCl (5 x 50 mL) until the pH of the aqueous phase was less than 2. The organic phase was further washed with saturated aq.  $\text{NaHCO}_3$  (50 mL) and brine (50 mL), dried over  $\text{MgSO}_4$ , and concentrated in vacuo to yield amide **236** (5.24 g, 86% yield) as a white foam.  $R_f$  0.42 (3:1 EtOAc:hexanes);  $^1\text{H}$  NMR (500 MHz,  $\text{CDCl}_3$ , 50 °C, mixture of rotamers)  $\delta$  7.37–7.27 (comp. m, 5H), 6.02 (br s, 1H), 5.31 (br s, 1H), 5.18 (d,  $J = 12.2$  Hz, 1H), 5.13 (d,  $J = 12.4$  Hz, 1H), 4.40 (app. d,  $J = 6.6$  Hz, 1H), 4.31–4.20 (m, 1H), 2.05 (app. t,  $J = 7.9$  Hz), 2.51–2.33 (m, 1H), 2.24–2.11 (m, 1H), 1.72–1.45 (comp. m, 7H), 1.28–1.10 (m, 1H);  $^{13}\text{C}$  NMR (125 MHz,  $\text{CDCl}_3$ , mixture of rotamers)  $\delta$  173.8 (br), 136.1, 128.8 (2C), 128.5, 128.1 (2C), 97.1, 67.4 (br), 67.2 (br), 60.4, 35.4 (br), 29.9 (br), 24.8, 23.5, 23.3; IR (film) 3335, 3197, 2934, 1694 (br), 1410, 1349, 1084  $\text{cm}^{-1}$ ; HRMS-EI ( $m/z$ ):  $[\text{M}]^+$  calc'd for  $\text{C}_{17}\text{H}_{22}\text{N}_2\text{O}_4$ , 319.1580; found, 318.1584;  $[\alpha]_{\text{D}}^{19} -19.56^\circ$  ( $c$  0.5, MeOH).



**Chloroimide 238.** To amide **236** (0.80 g, 2.51 mmol) in 1,2-dichloroethane (17 mL) at 23 °C was added DMAP (590.9 mg, 4.84 mmol), followed by dropwise addition of 2-bromopropionyl bromide (**237**, 470  $\mu\text{L}$ , 4.49 mmol). The solution was heated at 80 °C for 3 h and was then allowed to cool to 23 °C. The reaction mixture was purified directly by flash chromatography (7:1 hexanes:EtOAc  $\rightarrow$  4:1 hexanes:EtOAc eluent) to afford chloroimide **238** (0.73 g, 71% yield) as a colorless oil.  $R_f$  0.20 (4:1 hexanes:EtOAc);  $^1\text{H}$  NMR (500 MHz,  $\text{CDCl}_3$ , 50 °C, mixture of rotamers)  $\delta$  8.86 (br s, 1H), 7.36–7.26 (comp. m, 5H), 5.20–5.05 (m, 2H), 4.92–4.87 (m, 1H), 4.61–4.47 (m, 1H), 4.24–4.08 (comp. m, 2H), 2.55–1.10 (comp. m, 13H);  $^{13}\text{C}$  NMR (75 MHz,  $\text{CDCl}_3$ , mixture of rotamers)  $\delta$  171.0 (br), 169.2, 136.1, 128.8 (2C), 128.4, 128.1, 128.0, 97.4 (br), 67.4 (br), 61.5 (br), 54.9, 54.7, 34.3 (br), 31.0 (br), 24.8, 23.5, 21.6, 21.5; IR (film) 3275, 3208, 2936, 1743, 1715, 1413, 1348, 1204  $\text{cm}^{-1}$ ; HRMS-FAB ( $m/z$ ):  $[\text{M} + \text{H}]^+$  calc'd for  $\text{C}_{20}\text{H}_{26}\text{N}_2\text{ClO}_5$ , 409.1530; found, 409.1525;  $[\alpha]_D^{20}$   $-44.89^\circ$  (c 1.0, MeOH).



**Methyl Oxazole Triflate 215.** To a slurry of NaH (60% dispersion in mineral oil, 105.9 mg, 2.65 mmol) in dioxane (24 mL) at 23 °C was added a solution of chloroimide **238** (1.00 g, 2.45 mmol) in dioxane (13 mL) in a steady stream. Immediately after the

addition, the flask was fitted with a reflux condenser and was heated at 110 °C for 1 h. The flask was then allowed to cool to 23 °C over 2 h and was filtered over a pad of Celite® (CH<sub>2</sub>Cl<sub>2</sub> eluent). The filtrate was concentrated to a viscous, colorless oil. Benzene (10 mL) was added, and the volatiles were further evaporated in vacuo to afford oxazolone **239** as a white foam. This crude material was immediately carried to the subsequent step without further purification.

Crude oxazolone **239** was dissolved in CH<sub>2</sub>Cl<sub>2</sub> (14 mL), and the resulting colorless solution was cooled to –78 °C. Et<sub>3</sub>N (615 µL, 4.41 mmol) was added, followed by dropwise addition of Tf<sub>2</sub>O (445 µL, 2.65 mmol). The solution was maintained at –78 °C for 2.5 h, quenched by addition of H<sub>2</sub>O (1 mL), and allowed to thaw to 23 °C. Additional H<sub>2</sub>O (10 mL) was added, and the phases were separated. The aqueous layer was further extracted with CH<sub>2</sub>Cl<sub>2</sub> (5 x 5 mL), and the combined organics were dried over MgSO<sub>4</sub>, and concentrated to a brown oil. Purification of the crude product by flash chromatography (19:1 hexanes:EtOAc eluent) gave methyl oxazole triflate **215** (499.1 mg, 40% yield, 2 steps) as a white solid. *R<sub>f</sub>* 0.37 (4:1 hexanes:EtOAc); <sup>1</sup>H NMR (500 MHz, CDCl<sub>3</sub>, mixture of rotamers) δ 7.40–7.12 (comp. m, 5H), 5.20–4.90 (comp. m, 3H), 4.19–4.05 (comp. m, 2H), 2.49–1.04 (comp. m, 10H), 2.19 (s, 3H); <sup>13</sup>C NMR (75 MHz, CDCl<sub>3</sub>, major rotamer) δ 158.8, 151.9, 140.6, 138.1, 136.3, 128.6 (2C), 128.3, 128.1 (2C), 118.7 (q, *J<sub>CF</sub>* = 321 Hz), 97.2, 67.7, 67.1, 55.1, 33.7, 31.4, 24.7, 23.5, 23.5, 9.5; <sup>19</sup>F NMR (282 MHz, CDCl<sub>3</sub>) δ –73.5; IR (film) 2937, 1715, 1430, 1348, 1226, 1135 cm<sup>–1</sup>; HRMS-FAB (*m/z*): [M + H]<sup>+</sup> calc'd for C<sub>21</sub>H<sub>24</sub>SN<sub>2</sub>O<sub>7</sub>F<sub>3</sub>, 505.1256; found, 505.1232; [α]<sub>D</sub><sup>20</sup> –1.03° (*c* 1.0, MeOH).

#### 4.5 Notes and References

- (1) For a recent historical commentary regarding telomeres and telomerase, see: Blackburn, E. H.; Greider, C. W.; Szostak, J. W. *Nature Med.* **2006**, *12*, 1133–1138.
  
- (2) Reprinted, with permission, from: Shay, J. W.; Wright, W. E. *Nat. Rev. Drug Discovery* **2006**, *5*, 577–584 (Copyright 2006 Macmillan Publishers Ltd).
  
- (3) For recent reviews regarding telomerase and cancer therapeutics, see: (a) Incles, C. M.; Schultes, C. M.; Neidle, S. *Curr. Opin. Investig. Drugs* **2003**, *7*, 675–685. (b) Kelland, L. R. *Eur. J. Cancer* **2005**, *41*, 971–979. (c) Olaussen, K. A.; Dubrana, K.; Dornont, J.; Spano, J. P.; Sabatier, L.; Soria, J. C. *Crit. Rev. Oncol. Hematol.* **2006**, *57*, 191–214. (d) Pendino, F.; Tarkanyi, I.; Dudognon, C.; Hillion, J.; Lanotte, M.; Aradi, J.; Segal-Bendirdjian, E. *Curr. Cancer Drug Targets* **2006**, *6*, 147–180. (e) Artandi, S. E. *N. Engl. J. Med.* **2006**, *355*, 1195–1197. (f) Cian, A. D.; Lacroix, L.; Douarre, C.; Temine-Smalli, N.; Trentesaux, C.; Riou, J.-F.; Mergny, J.-L. *Biochimie* **2008**, *90*, 131–155.
  
- (4) The composition of human telomerase has recently been reported, see: Cohen, S.; Graham, M.; Lovrecz, G.; Bache, N.; Robinson, P.; Reddel, R. *Science* **2007**, *315*, 1850–1853.

- (5) An X-ray structure of the *N*-terminal domain of telomerase has recently been isolated. See: Jacobs, S. A.; Podell, E. R.; Cech, T. R. *Nat. Struct. Biol.* **2006**, *13*, 218–225.
- (6) Kim, N. W.; Piatyszek, M. A.; Prowse, K. R.; Harley, C. B.; West, M. D.; Ho, P. L. C.; Coviello, G. M.; Wright, W. E.; Weinrich, S. L.; Shay, J. W. *Science* **1994**, *266*, 2011–2015.
- (7) Shin-ya, K.; Wierzba, K.; Matsuo, K.; Ohtani, T.; Yamada, Y.; Furihata, K.; Hayakawa, Y.; Seto, H. *J. Am. Chem. Soc.* **2001**, *123*, 1262–1263.
- (8) For a review on directly linked polyazoles, see: (a) Riego, E.; Hernández, D.; Albericio, F.; Álvarez, M. *Synthesis* **2005**, 1907–1922. For a review on oxazole-containing natural products, see: (b) Yeh, V. S. C. *Tetrahedron* **2004**, *60*, 11995–12042.
- (9) For biological studies involving telomestatin, see: (a) Tauchi, T.; Sumi, M.; Nakajima, A.; Sashida, G.; Goto, A.; Ohyashiki, J. H.; Shin-ya, K.; Ohyashiki, K. *Blood* **2001**, *98*, 616A. (b) Kim, M.-Y.; Vankayalapati, H.; Kazuo, S.; Wierzba, K.; Hurley, L. H. *J. Am. Chem. Soc.* **2002**, *124*, 2098–2099. (c) Rosu, F.; Gabelica, V.; Shin-ya, K.; De Pauw, E. *Chem. Commun.* **2003**, 2702–2703. (d) Tauchi, T.; Shin-ya, K.; Sashida, G.; Sumi, M.; Nakajima, A.; Shimamoto, T.; Ohyashiki, J. H.;



Ohyashiki, K. *Oncogene* **2003**, *22*, 5338–5347. (e) Kim, M.-Y.; Guzman-Gleason, M.; Izbiccka, E.; Nishioka, D.; Hurley, L. H. *Cancer Res.* **2003**, *67*, 3247–3256. (f) Sumi, M.; Tauchi, T.; Sashida, G.; Nakajima, A.; Gotoh, A.; Shin-Ya, K.; Ohyashiki, J. H.; Ohyashiki, K. *Int. J. Oncol.* **2004**, *24*, 1481–1487. (g) Tauchi, T.; Shin-Ya, K.; Sashida, G.; Sumi, M.; Nakajima, A.; Ohyashiki, J. H.; Ohyashiki, K. *Blood* **2004**, *104*, 925A–926A. (h) Gomez, D.; Paterski, R.; Lemarteleur, T.; Shin-ya, K.; Mergny, J. L.; Riou, J. F. *J. Biol. Chem.* **2004**, *279*, 41487–41494. (i) Binz, N.; Shalaby, T.; Rivera, P.; Shin-Ya, K.; Grotzer, M. A. *Eur. J. Cancer* **2005**, *41*, 2873–2881. (j) Rezler, E. M.; Seenisamy, J.; Bashyam, S.; Kim, M. Y.; White, E.; Wilson, W. D.; Hurley, L. H. *J. Am. Chem. Soc.* **2005**, *127*, 9439–9447. (k) Tauchi, T.; Shin-ya, K.; Sashida, G.; Sumi, M.; Okabe, S.; Ohyashiki, J. H.; Ohyashiki, K. *Oncogene* **2006**, *25*, 5719–5725. (l) Gomez, D.; Wenner, T.; Brassart, B.; Douarre, C.; O'Donohue, M. F.; Khoury, V. E.; Shin-Ya, K.; Morjani, H.; Trentesaux, C.; Riou, J. F. *J. Biol. Chem.* **2006**, *281*, 38721–38729. (m) Gomez, D.; O'Donohue, M. F.; Wenner, T.; Douarre, C.; Macadre, J.; Koebel, P.; Giraud-Panis, M. J.; Kaplan, H.; Kolkes, A.; Shin-Ya, K.; Riou, J. F. *Cancer Res.* **2006**, *66*, 6908–6912. (n) Tahara, H.; Shin-ya, K.; Seimiya, H.; Yamada, H.; Tsuruo, T.; Ide, T. *Oncogene* **2006**, *25*, 1955–1966. (o) Zhang, L. L.; Tamura, K.; Shin-ya, K.; Takahashi, H. *Biochim. Biophys. Acta—Mol. Cell Res.* **2006**, *1763*, 39–44.

- (10) For biological studies of telomestatin derivatives, see: (a) Barbieri, C. M.; Srinivasan, A. R.; Rzuczek, S. G.; Rice, J. E.; LaVoie, E. J.; Pilch, D. S. *Nucleic*

*Acids Res.* **2007**, *35*, 3272–3286. (b) Minhas, G. S.; Pilch, D. S.; Kerrigan, J. E.; LaVoie, E. J.; Rice, J. E. *Bioorg. Med. Chem. Lett.* **2006**, *16*, 3891–3895. (c) Tera, M.; Sohtome, Y.; Ishizuka, H.; Doi, T.; Takagi, M.; Kazuo, S. Y.; Nagasawa, K. *Heterocycles* **2006**, *69*, 505–514. (d) Jantos, K.; Rodriguez, R.; Ladame, S.; Shirude, P. S.; Balasubramanian, S. *J. Am. Chem. Soc.* **2006**, *128*, 13662–13663.

- (11) A number of structurally-related compounds have been reported. See: (a) Gebhardt, K.; Schimana, J.; Krastel, P.; Dettner, K.; Rheinheimer, J.; Zeeck, A.; Fiedler, H. P. *J. Antibiot.* **2002**, *55*, 794–800. (b) Sohda, K. Y.; Nagai, K.; Yamori, T.; Suzuki, K. I.; Tanaka, A. *J. Antibiot.* **2005**, *58*, 27–31. (c) Sohda, K. Y.; Hiramoto, M.; Suzumura, K. I.; Takebayashi, Y.; Suzuki, K. I.; Tanaka, A. *J. Antibiot.* **2005**, *58*, 32–36. (d) Kanoh, K.; Matsuo, Y.; Adachi, K.; Imagawa, H.; Nishizawa, M.; Shizuri, Y. *J. Antibiot.* **2005**, *58*, 289–292. (e) Matsuo, Y.; Kanoh, K.; Yamori, T.; Kasai, H.; Katsuta, A.; Adachi, K.; Shin-ya, K.; Shizuri, Y. *J. Antibiot.* **2007**, *60*, 251–255. (f) Matsuo, Y.; Kanoh, K.; Imagawa, H.; Adachi, K.; Nishizawa, M.; Shizuri, Y. *J. Antibiot.* **2007**, *60*, 256–260.

- (12) Oganessian, L.; Bryan, T. M. *Bioessays* **2007**, *29*, 155–165.

- (13) Zahler, A. M.; Williamson, J. R.; Cech, T. R.; Prescott, D. M. *Nature* **1991**, *350*, 718–720.

- (14) Telomestatin (**189**) interacts preferentially with the intramolecular basket-type G-quadruplex conformation (**191**). See references 9b and j.
- (15) For biosynthetic proposals, see: (a) Hughes, R. A.; Moody, C. J. *Angew. Chem., Int. Ed.* **2007**, *46*, 7930–7954. (b) Kopp, F.; Maraheil, M. A. *Nat. Prod. Rep.* **2007**, *24*, 735–749.
- (16) Clardy, J.; Walsh, C. *Nature* **2004**, *432*, 829–837.
- (17) (a) Yamada, S.; Shigeno, K.; Kitagawa, K.; Okajima, S.; Asao, T. (Taiho Pharmaceutical Co. Ltd., Sosei Co. Ltd.). WO2002048153; *Chem. Abstr.* **2002**, *137*, 47050. (b) Doi, T.; Yoshida, M.; Shin-ya, K.; Takahashi, T. *Org. Lett.* **2006**, *8*, 4165–4167.
- (18) (a) Endoh, N.; Tsuboi, K.; Kim, R.; Yonezawa, Y.; Shin, C. *Heterocycles* **2003**, *60*, 1567–1572. (b) Chattopadhyay, S. K.; Biswas, S. *Tetrahedron Lett.* **2006**, *47*, 7897–7900. (c) Chattopadhyay, S. K.; Biswas, S.; Pal, B. K. *Synthesis* **2006**, 1289–1294. (d) Marson, C. M.; Saadi, M. *Org. Biomol. Chem.* **2006**, *4*, 3892–3893.
- (19) For syntheses of telomestatin-like compounds, see: (a) Deeley, J.; Pattenden, G. *Chem. Commun.* **2005**, 797–799. (b) Hernández, D.; Vilar, G.; Riego, E.; Cañedo, L. M.; Cuevas, C.; Albericio, F.; Álvarez, M. *Org. Lett.* **2007**, *9*, 809–811. (c)

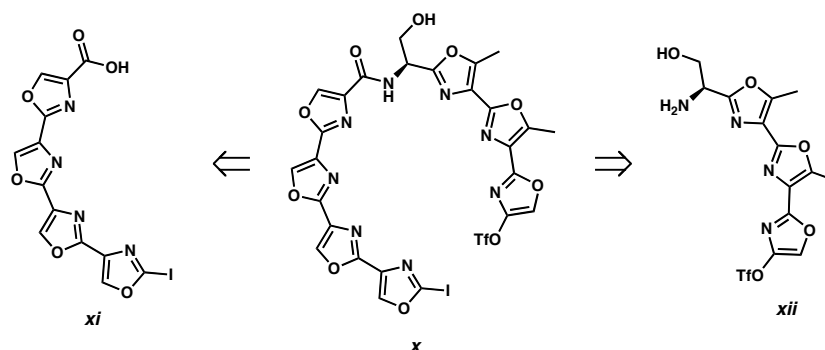
Hernández, D.; Riego, E.; Francesch, A.; Cuevas, C.; Albericio, F.; Álvarez, M. *Tetrahedron* **2007**, *63*, 9862–9870.

(20) (a) Atkins, J. M.; Vedejs, E. *Org. Lett.* **2005**, *7*, 3351–3354. (b) Araki, H.; Katoh, T.; Inoue, M. *Synlett* **2006**, 555–558. (c) Flegeau, E. F.; Popkin, M. E.; Greaney, M. F. *Org. Lett.* **2006**, *8*, 2495–2498. (d) Araki, H.; Katoh, T.; Inoue, M. *Tetrahedron Lett.* **2007**, *48*, 3713–3717.

(21) For examples of palladium-catalyzed biaryl formation for macrocyclization, see: (a) Patel, H. K.; Kilburn, J. D.; Langley, G. J.; Edwards, P. D.; Mitchell, T.; Southgate, R. *Tetrahedron Lett.* **1994**, *35*, 481–484. (b) Carbonnelle, A.-C.; Zhu, J. *Org. Lett.* **2000**, *2*, 3477–3480. (c) Nicolaou, K. C.; Bulger, P. G.; Sarlah, D. *Angew. Chem., Int. Ed.* **2005**, *44*, 4442–4489. (d) Blankenstein, J.; Zhu, J. *Eur. J. Org. Chem.* **2005**, 1949–1964.

(22) Heteroaryl–heteroaryl cross-couplings, especially those containing nitrogen heterocycles, are still in need of a universal method since they often exhibit poor reactivity. For relevant discussions, see: (a) Kudo, N.; Perseghini, M.; Fu, G. C. *Angew. Chem., Int. Ed.* **2006**, *45*, 1282–1284 and references therein. (b) Billingsley, K. L.; Anderson, K. W.; Buchwald, S. L. *Angew. Chem., Int. Ed.* **2006**, *45*, 3484–3488 and references therein.

- (23) Our initial retrosynthetic approach fragmented telomestatin (**189** → **x**) into tetrakisoxazole acid **xi** and a trisoxazole amino alcohol **xii**. Problems arising because of poor solubility of the tetrakisoxazole portion (**xi**) and intermediates en route led us to abandon this strategy.



- (24) (a) Behforouz, M.; Haddad, J.; Cai, W.; Arnold, M. B.; Farahnaz, M.; Sousa, A. C.; Horn, M. A. *J. Org. Chem.* **1996**, *61*, 6552–6555. (b) Fife, W. K.; Zhang, Z.-d. *J. Org. Chem.* **1986**, *51*, 3744–3746. (c) Hutchinson, C. R.; Harmon, A. D. *J. Org. Chem.* **1975**, *40*, 3474–3480.

- (25) Shafer, C. M.; Molinski, T. F. *Heterocycles* **2000**, *53*, 1167–1170.

- (26) de Boer, T. J.; Backer, H. *J. Org. Synth.* **1956**, *36*, 16–19.

- (27) For the synthesis of oxazolones and oxazole triflates, see references 20b–d, and see: (a) Sheehan, J. C.; Izzo, P. T. *J. Am. Chem. Soc.* **1949**, *71*, 4059–4062. (b) Rao, Y. S.; Filler, R. *Chem. Commun.* **1970**, 1622. (c) Rodehorst, R. M.; Koch, T. H. *J. Am. Chem. Soc.* **1975**, *97*, 7298–7304. (d) Kelly, T. R.; Lang, F. *Tetrahedron Lett.* **1995**,

36, 5139–5322. (e) Schaus, J. V.; Panek, J. S. *Org. Lett.* **2000**, 2, 469–471. (f) Smith, A. B., III; Minbirole, K. P.; Freeze, S. *Synlett* **2001**, 1739–1742. (g) Smith, A. B., III; Minbirole, K. P.; Verhoest, P. R.; Schelhaas, M. *J. Am. Chem. Soc.* **2001**, 123, 4834–4836. (h) Smith, A. B., III; Minbirole, K. P.; Verhoest, P. R.; Schelhaas, M. *J. Am. Chem. Soc.* **2001**, 123, 10942–10953. (i) Kelly, T. R.; Lang, F. *J. Org. Chem.* **1996**, 61, 4623–4633. (j) Langille, N. F.; Dakin, L. A.; Panek, J. S. *Org. Lett.* **2002**, 4, 2485–2488. (k) Trost, B. M.; Dogra, K.; Franzini, M. *J. Am. Chem. Soc.* **2004**, 126, 1944–1945. (l) Smith, A. B., III; Razler, T. M.; Pettit, G. R.; Chapuis, J.-C. *Org. Lett.* **2005**, 7, 4403–4406. (m) Smith, A. B., III; Razler, T. M.; Meis, R. M.; Pettit, G. R. *Org. Lett.* **2006**, 8, 797–799.

(28) Although no characterization data or experimental details were provided, the synthesis of compound **214** via a related route was recently reported. See reference 20d.

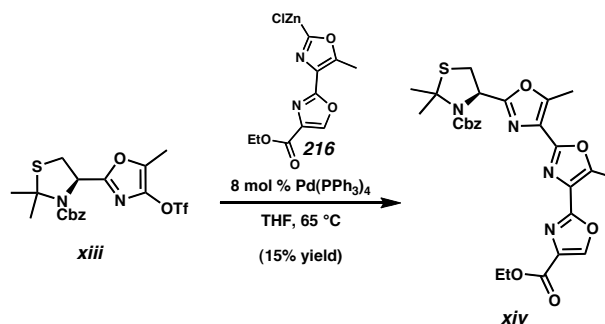
(29) (a) See Section 4.4 Experimental Section. (b) Iodobisoxazole triflate **226** is shown with 50% probability ellipsoids (Note: Only *Molecule A* is depicted). Crystallographic data have been deposited at the CCDC, 12 Union Road, Cambridge CB2 1EZ, UK, and copies can be obtained on request, free of charge, by quoting the publication citation and the deposition number 282586.

- (30) For useful reports of oxazole cross-couplings, see references 20b–d and references therein.
- (31) For Negishi cross-couplings of oxazoles, see: (a) Harn, N. K.; Gramer, C. J.; Anderson, B. A. *Tetrahedron Lett.* **1995**, 36, 9453–9456. (b) Anderson, B. A.; Harn, N. K. *Synthesis* **1996**, 583–585. (c) Anderson, B. A.; Becke, L. M.; Booher, R. N.; Flaugh, M. E.; Harn, N. K.; Kress, T. J.; Varie, D. L.; Wepsiec, J. P. *J. Org. Chem.* **1997**, 62, 8634–8639. (d) Vedejs, E.; Luchetta, L. M. *J. Org. Chem.* **1999**, 64, 1011–1014. (e) Reeder, M. R.; Gleaves, H. E.; Hoover, S. A.; Imbordino, H. R.; Pangborn, J. *J. Org. Process Res. Dev.* **2003**, 7, 696–699.
- (32) Although no characterization data or experimental details were provided, the syntheses of compounds **224** and **225** were recently reported. See reference 20d.
- (33) Handy, S. T.; Zhang, Y. *Chem. Commun.* **2006**, 299–301.
- (34) It was found that dichloromethane added sufficient solubility to aid with deprotonation.
- (35) Tormyshev, V. M.; Mikhalina, T. V.; Rogozhnikova, O. Y.; Troitskaya, T. Y.; Trukhin, D. V. *Russ. J. Org. Chem.* **2006**, 42, 1049–1053.

(36) (a) Lall, M. S.; Ramtohl, Y. K.; James, M. N. G.; Vederas, J. C. *J. Org. Chem.* **2002**, 67, 1536–1547. (b) Hwang, D.-R.; Helquist, P.; Shekhani, M. S. *J. Org. Chem.* **1985**, 50, 1264–1271. (c) Scheurer, A.; Mosset, P.; Bauer, W.; Saalfrank, R. W. *Eur. J. Org. Chem.* **2001**, 3067–3074.

(37) The acetonide protecting group was initially employed instead of a cyclohexylidene moiety, but it was found to be labile in later steps.

(38) Cross-coupling attempts using oxazole triflate **215** and a suitable trisoxazole partner to form tetrakisoxazole triflate **243** directly were not explored, due to the near certainty of competition between the various oxazole triflates. Cross-couplings in a related system to form ester **xiv** were met with limited success.



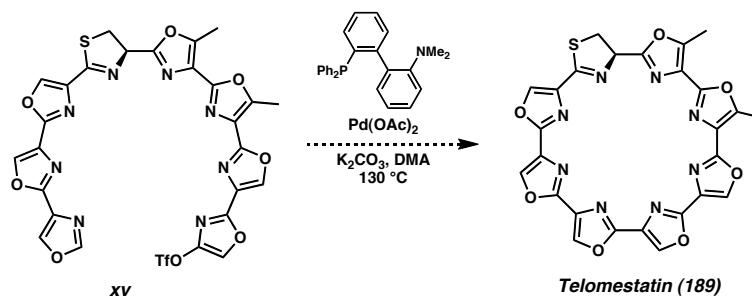
(39) Preliminary experiments have resulted in the preparation of milligram quantities of tetrakisoxazole triflate **243** using the described route.

(40) Altenbach, H.-J.; Himmeldirk, K. *Tetrahedron: Asymmetry* **1995**, 6, 1077–1080.



- (41) (a) Fincham, C. I.; Higginbottom, M.; Hill, D. R.; Horwell, D. C.; O'Toole, J. C.; Ratcliffe, G. S.; Rees, D. C.; Roberts, E. *J. Med. Chem.* **1992**, *35*, 1472–1484. (b) Pontillo, J.; Chen, C. *Bioorg. Med. Chem. Lett.* **2005**, *15*, 1407–1411.
- (42) Metal ions are known to promote intramolecular macrocyclizations via a templating effect, and may be useful for the final step. See: (a) Ercolani, G.; Mandolini, L.; Masci, B. *J. Am. Chem. Soc.* **1981**, *103*, 2780–2782. (b) Anderson, S.; Anderson, H. L.; Sanders, J. K. M. *Acc. Chem. Res.* **1993**, *26*, 469–475. (c) Blake, A. J.; Hannam, J. S.; Jolliffe, K. A.; Pattenden, G. *Synlett* **2000**, 1515–1518 and references therein. For a recent report, see: (d) Xu, Y.; Chen, L.; Ma, Y.; Li, J.; Cao, X. *Synlett* **2007**, 1901–1904 and references therein.

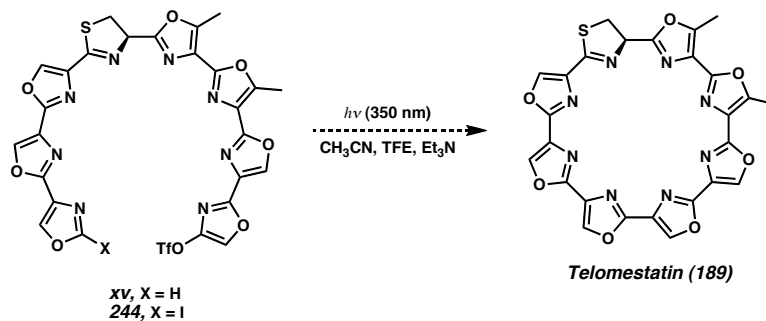
- (43) An alternate macrocyclization strategy via direct arylation may also be possible (i.e., **xv**  $\rightarrow$  **189**). For pertinent references, see: (a) Alberico, D.; Scott, M. E.; Lautens, M. *Chem. Rev.* **2007**, *107*, 174–238. (b) Campeau, L.-C.; Parisien, M.; Leblanc, M.; Fagnou, K. *J. Am. Chem. Soc.* **2004**, *126*, 9186–9187. (c) Campeau, L.-C.; Parisien, M.; Jean, A.; Fagnou, K. *J. Am. Chem. Soc.* **2006**, *128*, 581–590. (d) Miki, Y.; Shirokoshi, H.; Asai, M.; Aoki, Y.; Matsukida, H. *Heterocycles* **2003**, *60*, 2095–2101.



- (44) A final macrocyclization approach involving a Witkop photocyclization would be promising option as well (i.e., **244** or **xv**  $\rightarrow$  **189**). For relevant examples, see: (a) Fagnoni, M.; Albini, A. *Acc. Chem. Res.* **2005**, *38*, 713–721. (b) Burgett, A. W. G.; Li, Q.; Wei, Q.; Harran, P. G. *Angew. Chem., Int. Ed.* **2003**, *42*, 4961–4966. (c) De Carolis, M.; Protti, S.; Fagnoni, M.; Albini, A. *Angew. Chem., Int. Ed.* **2005**, *44*, 1232–1236. (d) Freccero, M.; Fagnoni, M.; Albini, A. *J. Am. Chem. Soc.* **2003**, *125*, 13182–13190. (e) Feldman, K. S.; Ngermmeesri, P. *Org. Lett.* **2005**, *7*, 5449–5452. (f) Mangion, I. K. "Development of Organocatalytic Direct Aldol Transformations, Total Syntheses of Brasoside and Littoralisone, and Progress Toward the Total

Synthesis of Diazonamide A." Ph.D. Thesis, California Institute of Technology,

2006. <http://resolver.caltech.edu/CaltechETD:etd-05232006-210214>



## **APPENDIX FOUR**

### **Spectra Relevant to Chapter Four:**

#### **Progress Toward The Total Synthesis of Telomestatin**

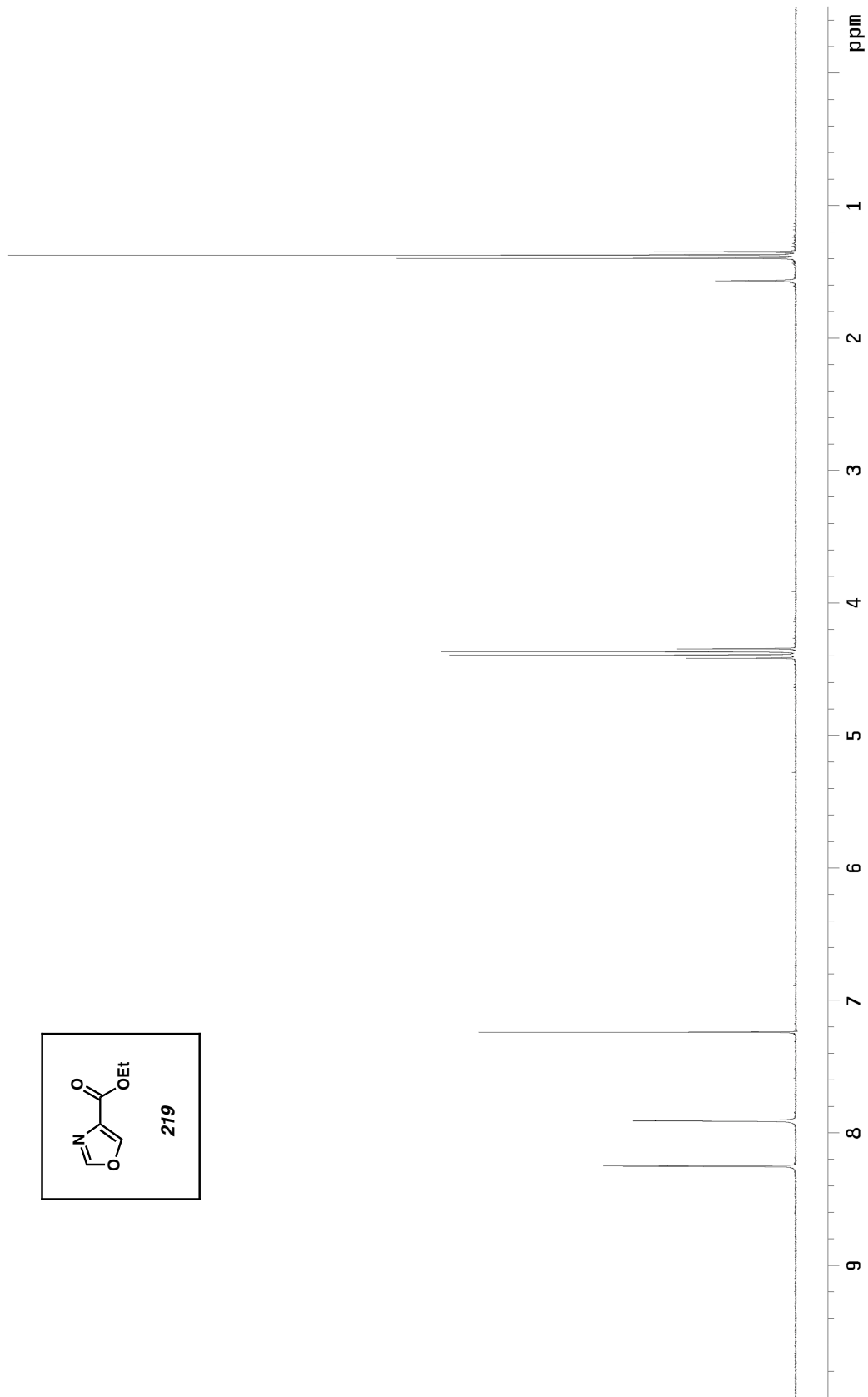
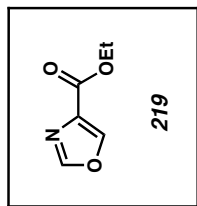


Figure A4.1  $^1\text{H}$  NMR (300 MHz,  $\text{CDCl}_3$ ) of compound **219**

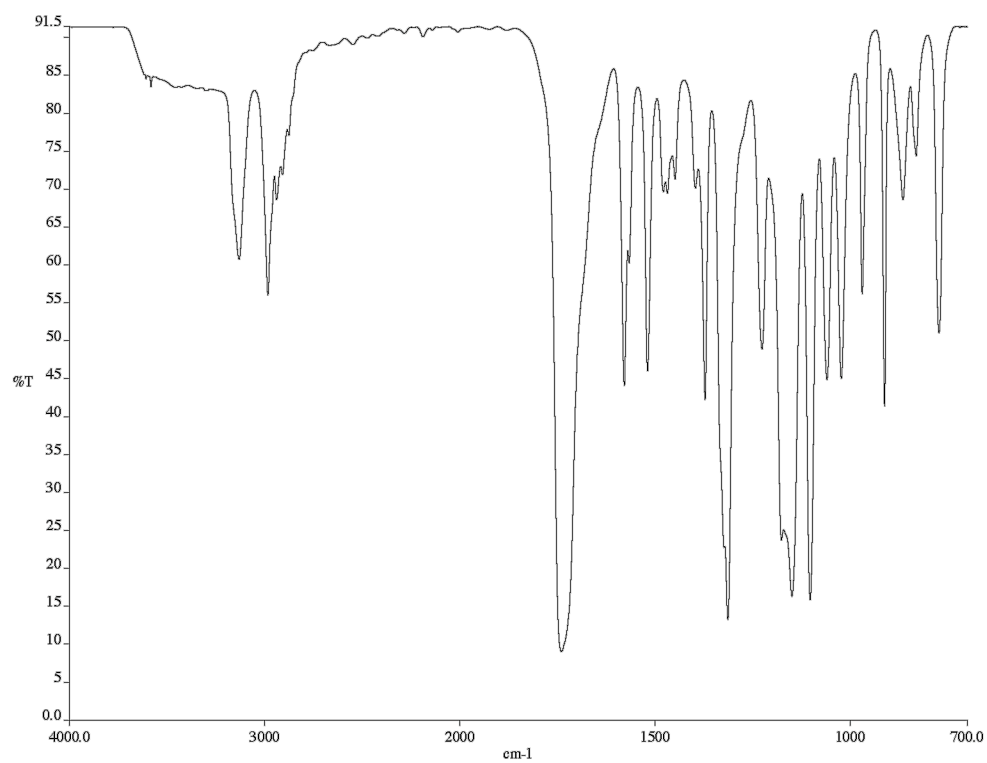


Figure A4.2 Infrared spectrum (thin film/NaCl) of compound **219**

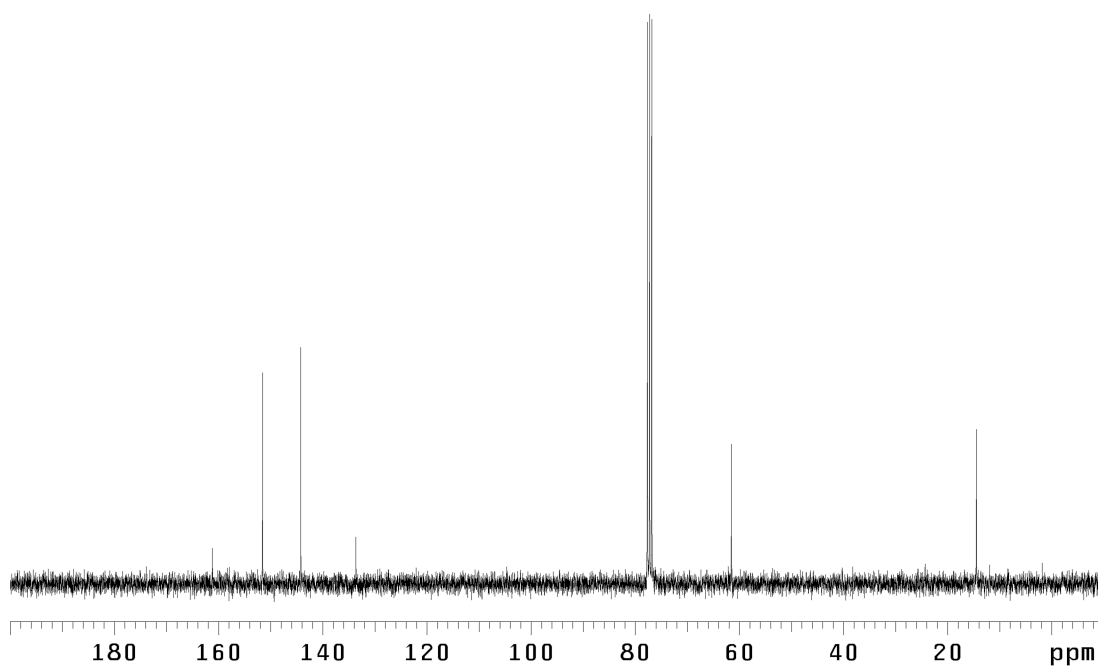


Figure A4.3 <sup>13</sup>C NMR (75 MHz, CDCl<sub>3</sub>) of compound **219**

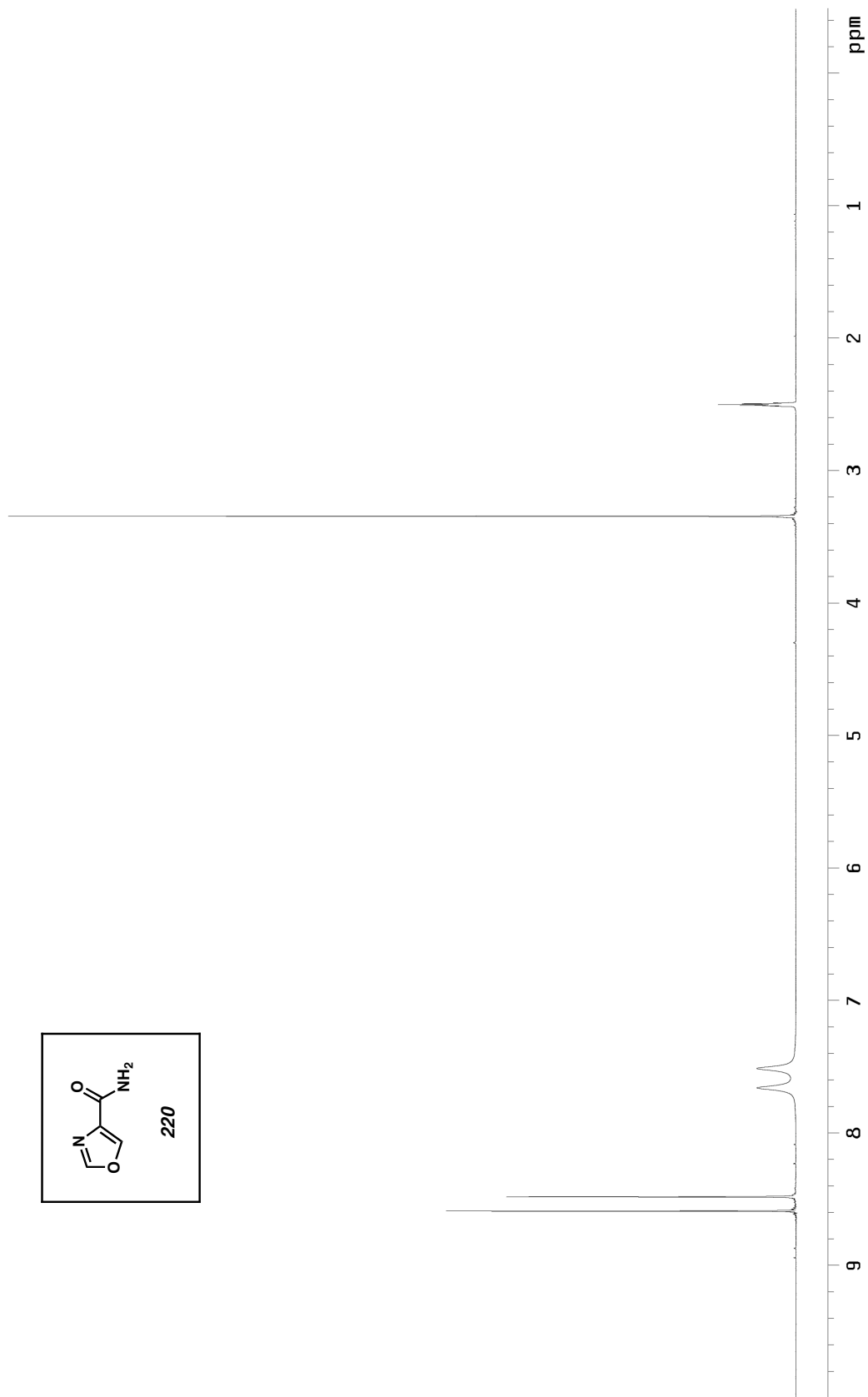
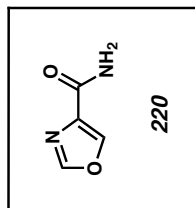


Figure A4.4 <sup>1</sup>H NMR (300 MHz, DMSO-*d*<sub>6</sub>) of compound 220

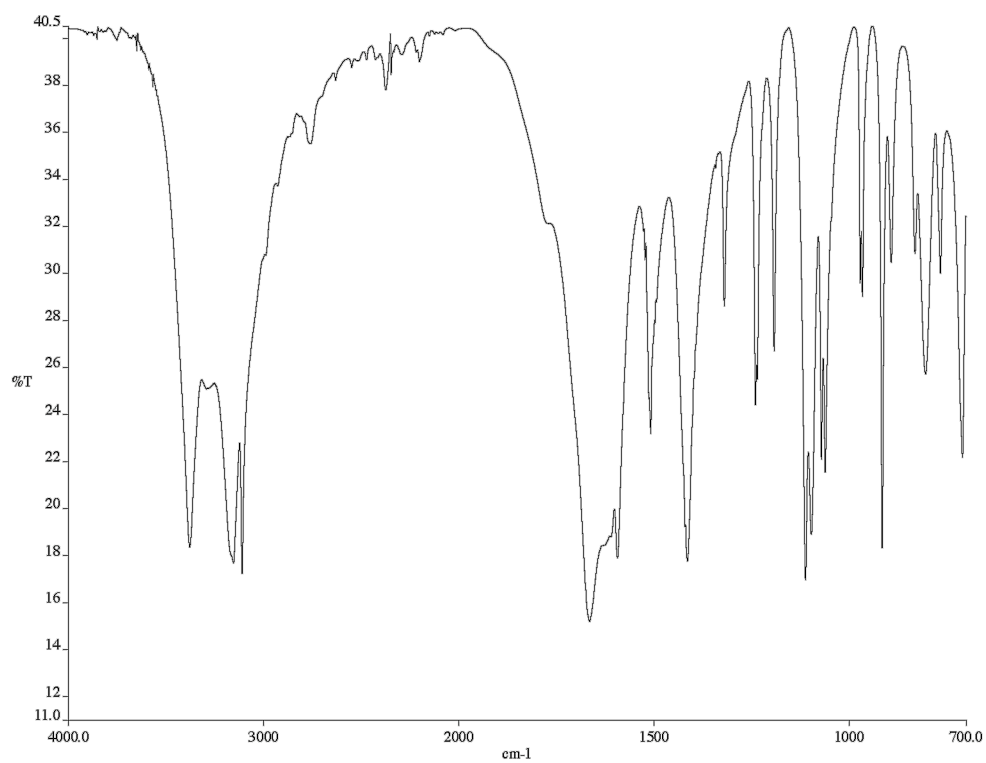


Figure A4.5 Infrared spectrum (KBr pellet) of compound **220**

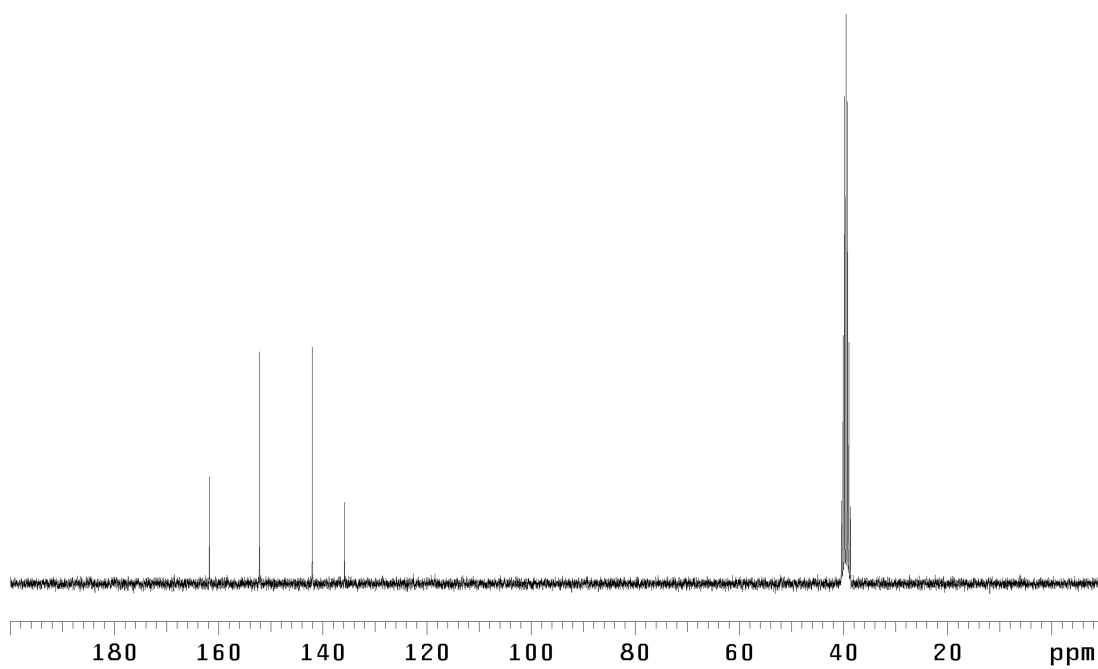


Figure A4.6  $^{13}\text{C}$  NMR (75 MHz,  $\text{DMSO}-d_6$ ) of compound **220**



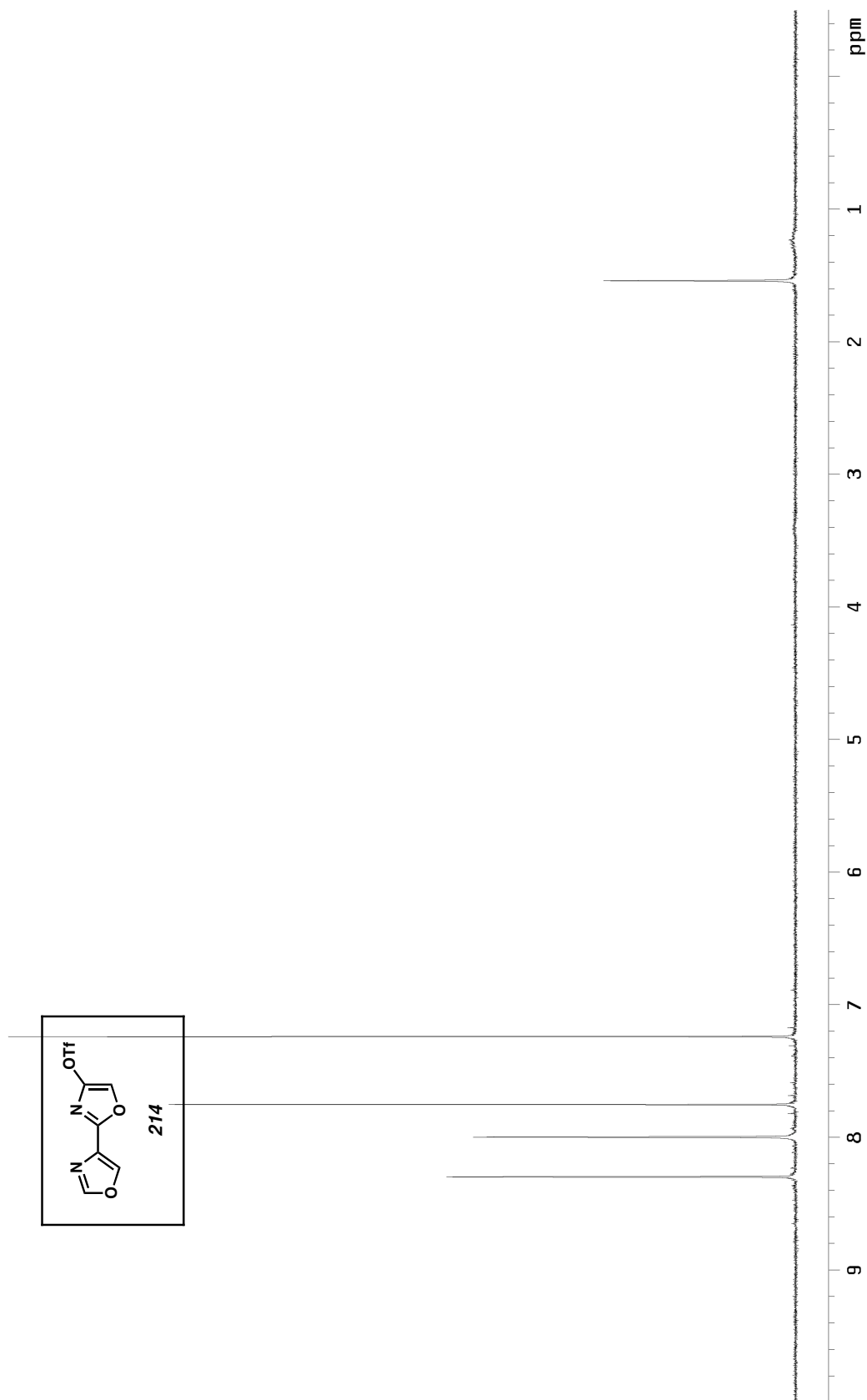


Figure A4.7 <sup>1</sup>H NMR (300 MHz, CDCl<sub>3</sub>) of compound **214**

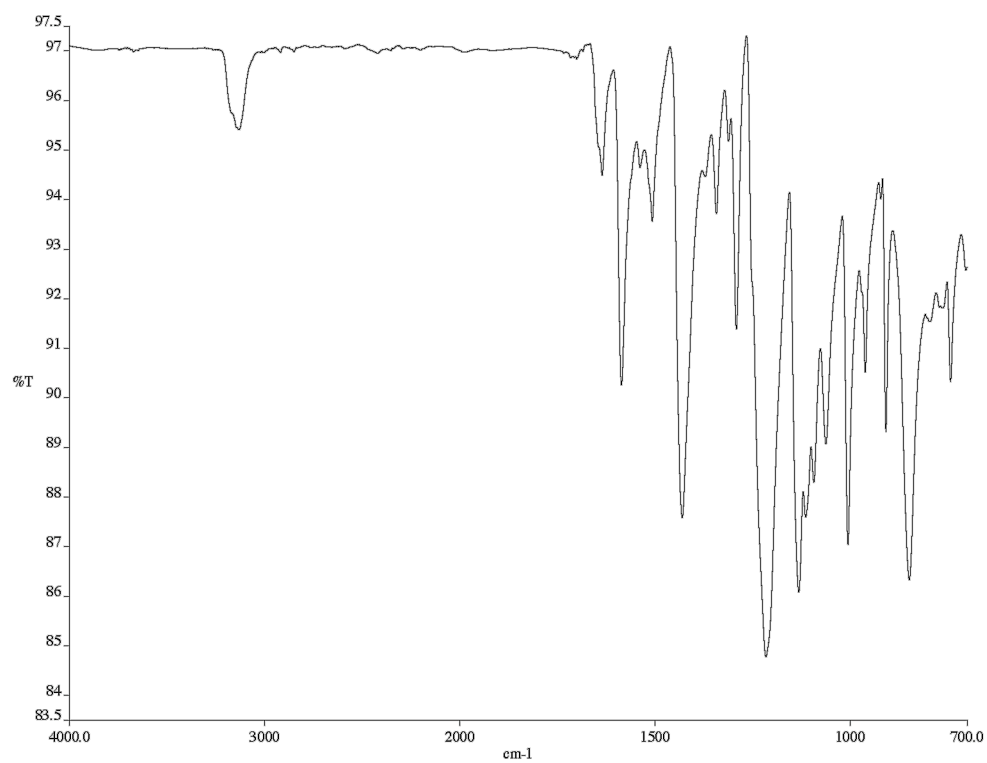


Figure A4.8 Infrared spectrum (thin film/NaCl) of compound **214**

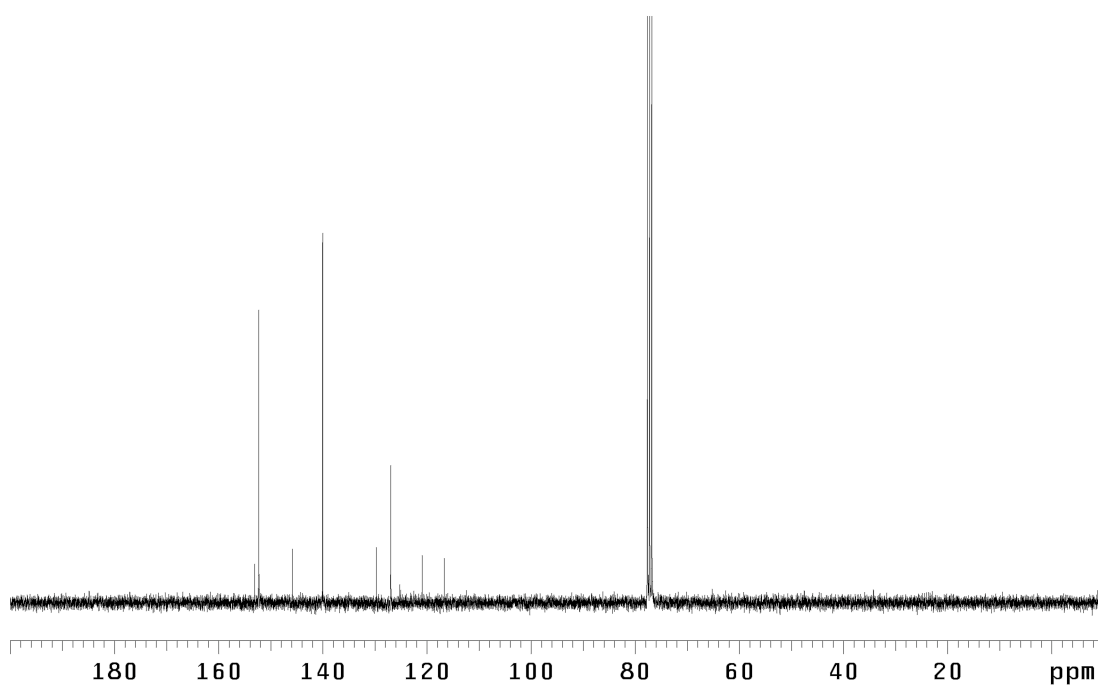


Figure A4.9 <sup>13</sup>C NMR (75 MHz, CDCl<sub>3</sub>) of compound **214**

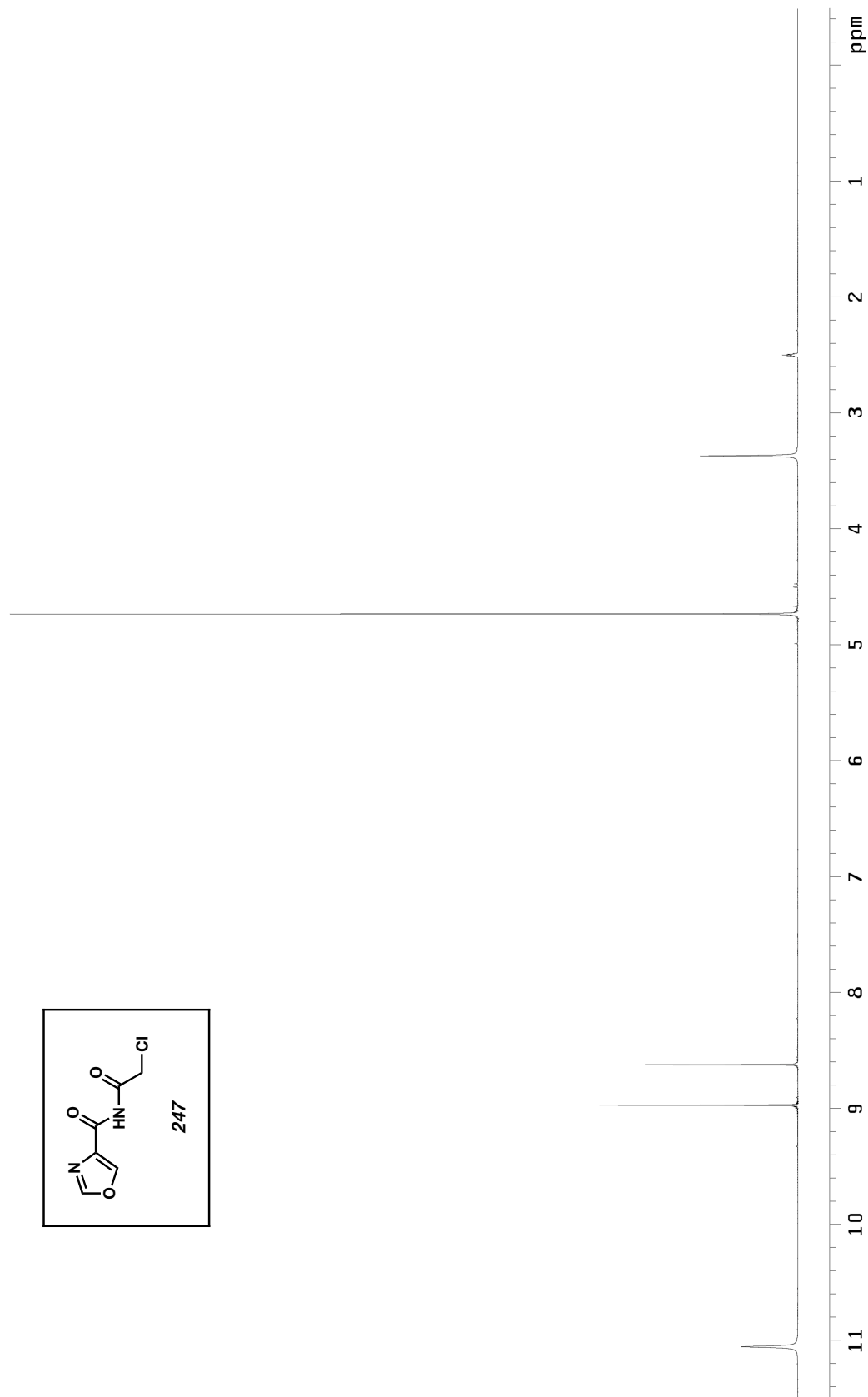


Figure A4.10  $^1\text{H}$  NMR (300 MHz,  $\text{DMSO-}d_6$ ) of compound **247**

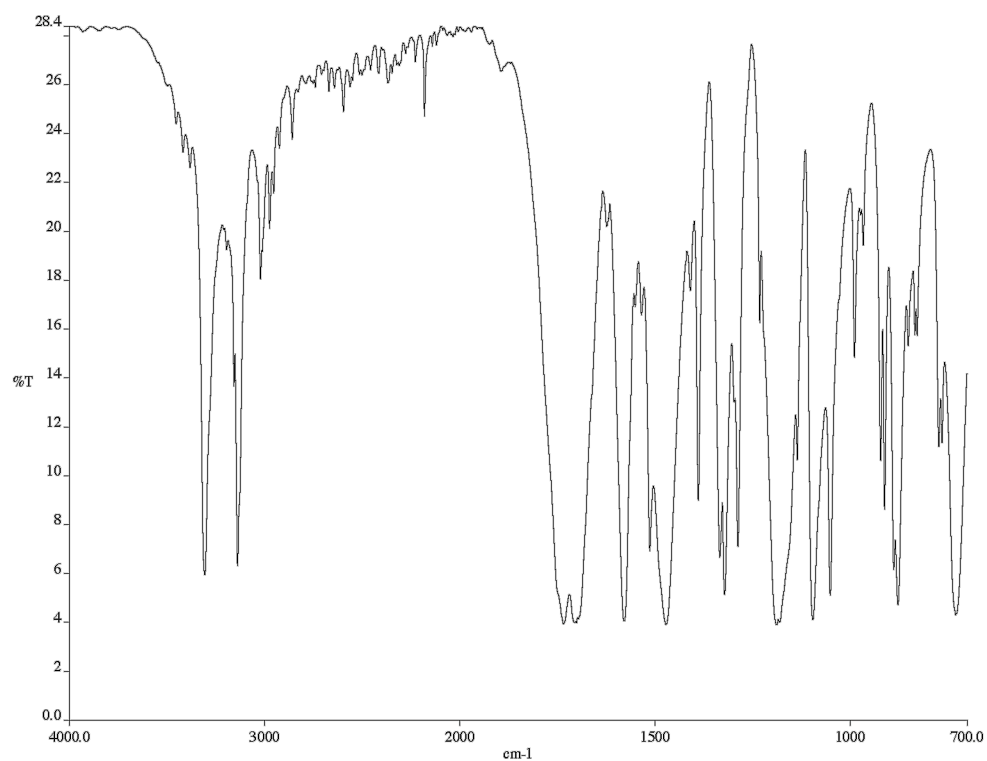


Figure A4.11 Infrared spectrum (KBr pellet) of compound **247**

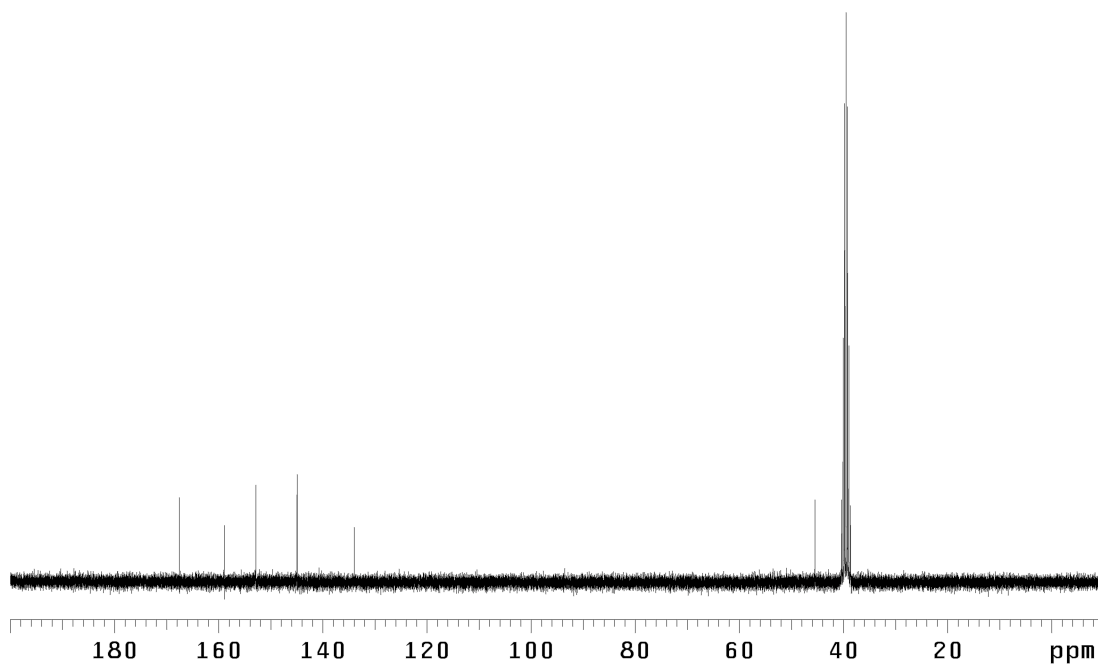


Figure A4.12  $^{13}\text{C}$  NMR (75 MHz,  $\text{DMSO}-d_6$ ) of compound **247**

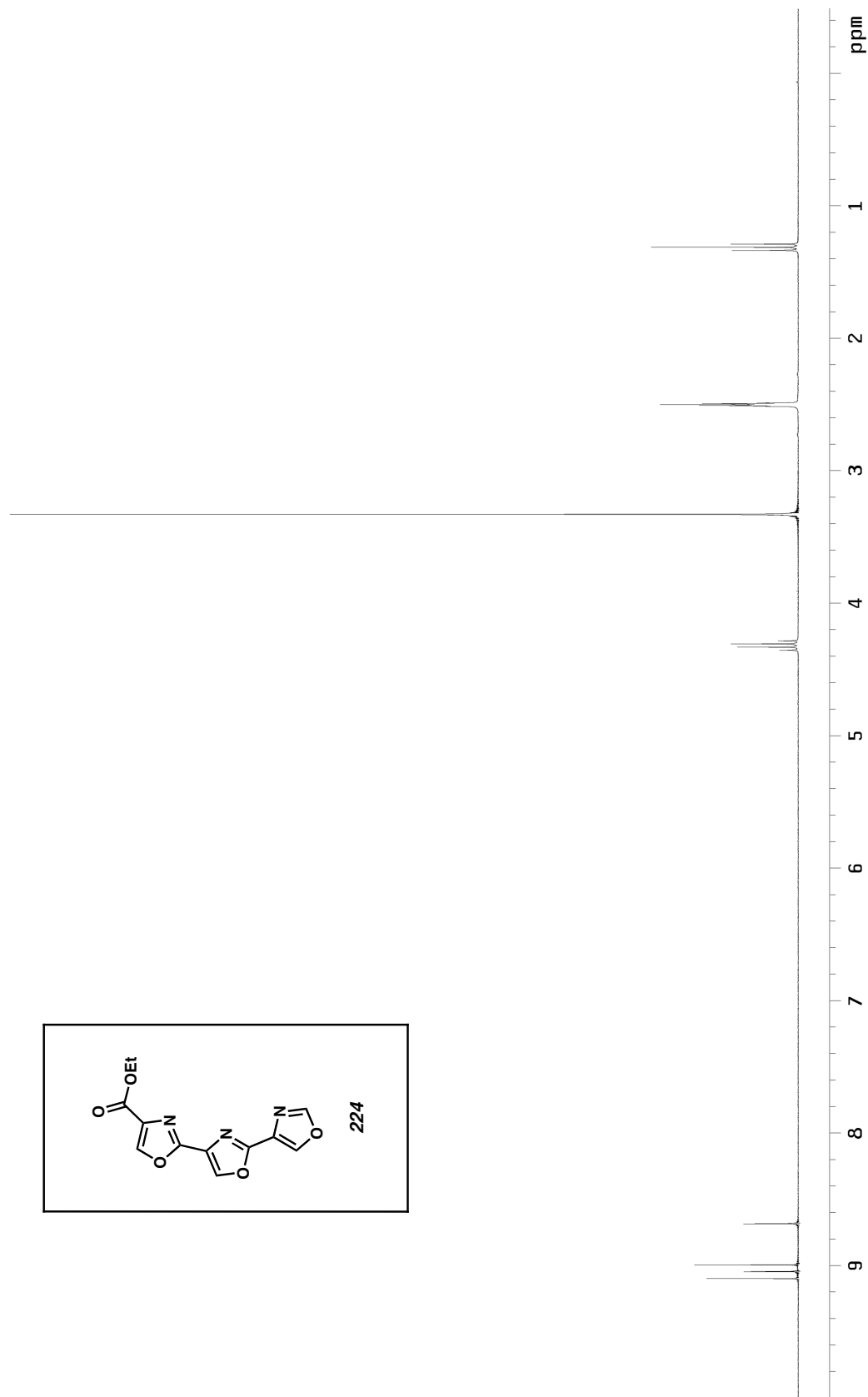


Figure A4.13  $^1\text{H}$  NMR (300 MHz,  $\text{DMSO}-d_6$ ) of compound **224**

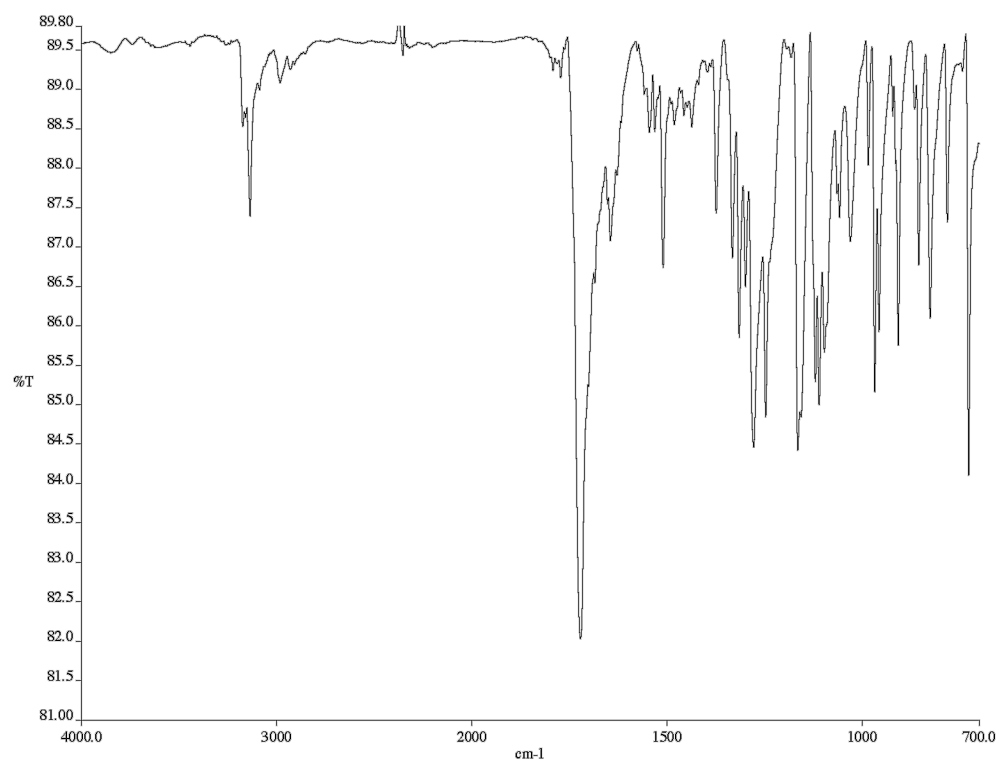


Figure A4.14 Infrared spectrum (thin film/NaCl) of compound **224**

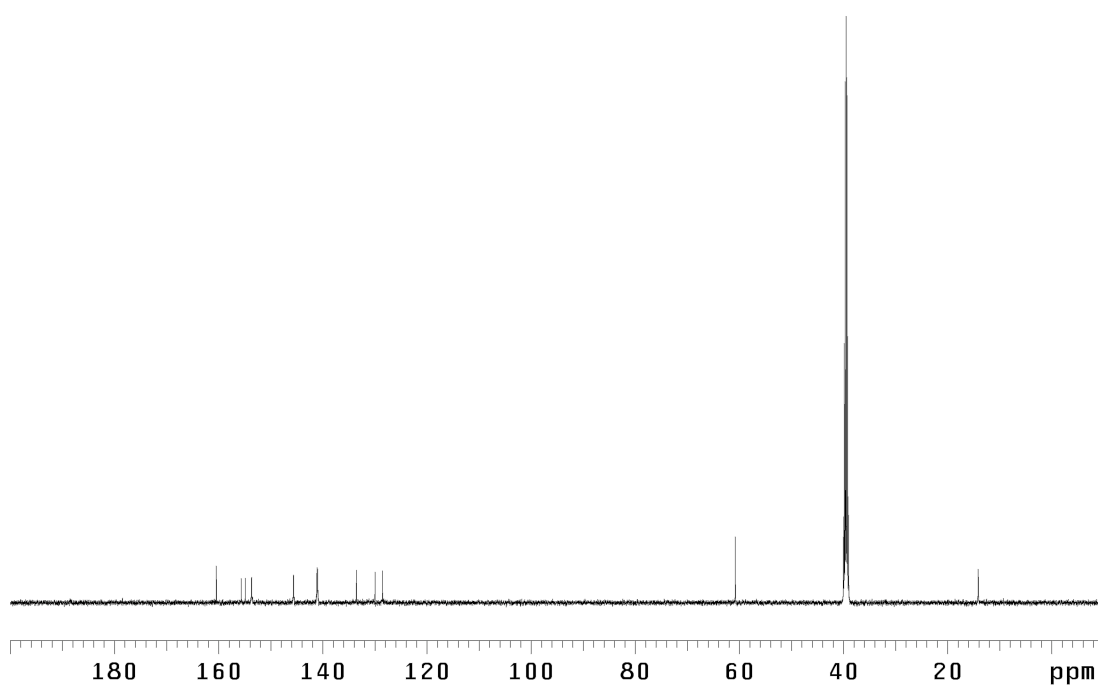


Figure A4.15 <sup>13</sup>C NMR (125 MHz, DMSO-*d*<sub>6</sub>) of compound **224**

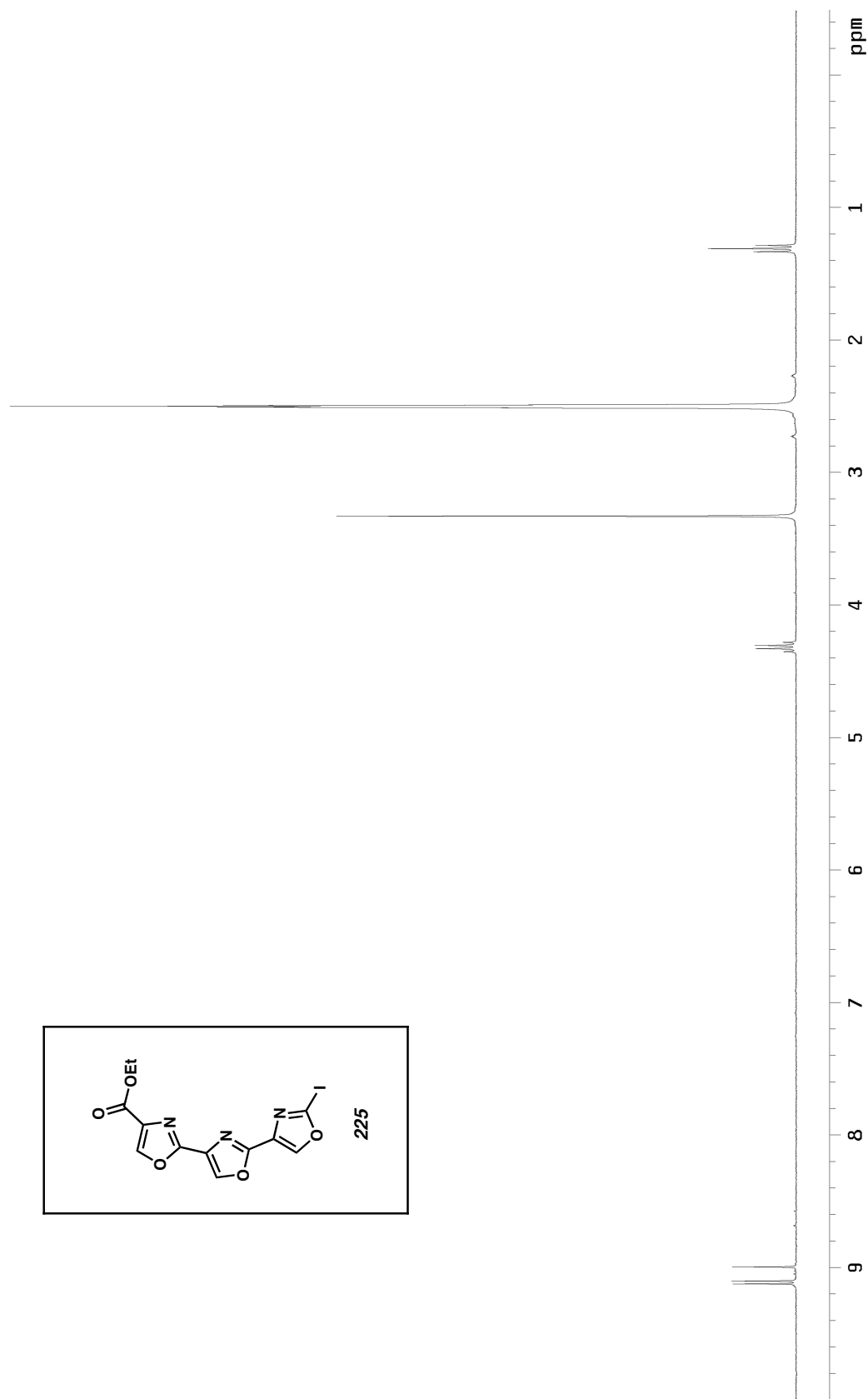


Figure A4.16  $^1\text{H}$  NMR (300 MHz,  $\text{DMSO}-d_6$ ) of compound **225**

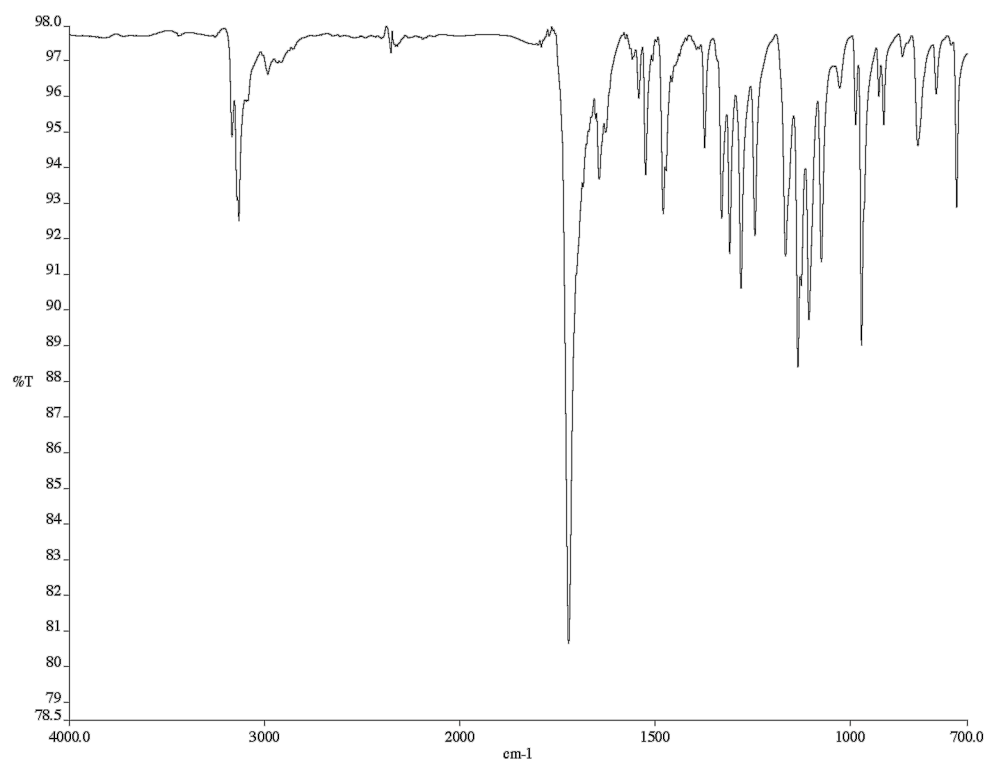


Figure A4.17 Infrared spectrum (thin film/NaCl) of compound **225**

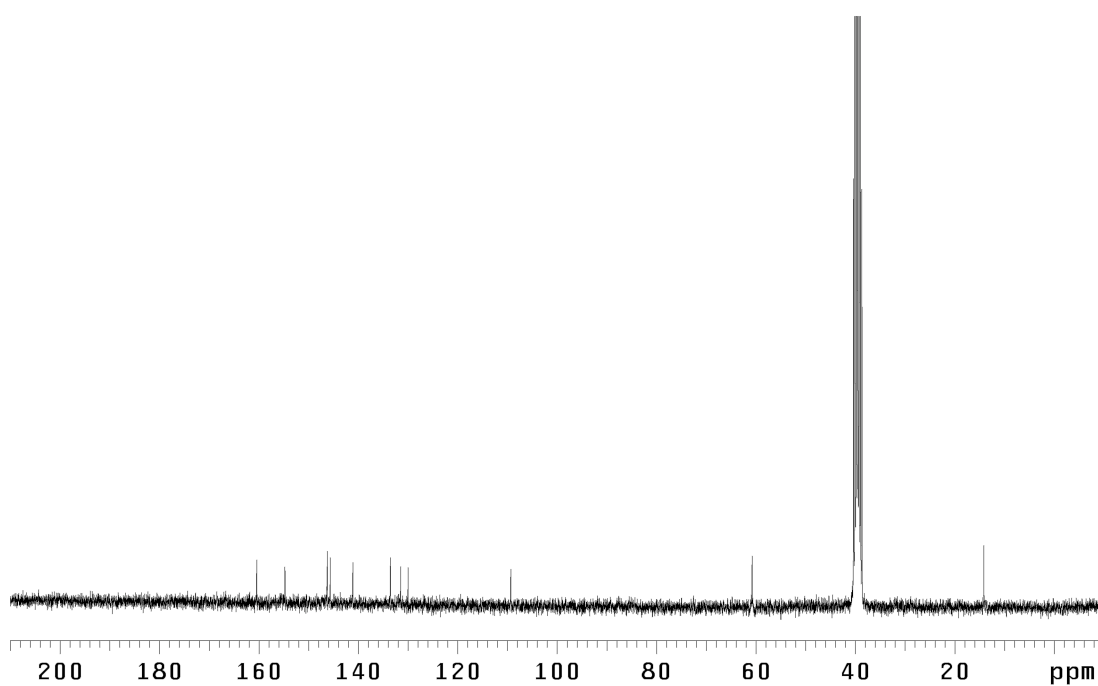


Figure A4.18 <sup>13</sup>C NMR (75 MHz, DMSO-*d*<sub>6</sub>) of compound **225**





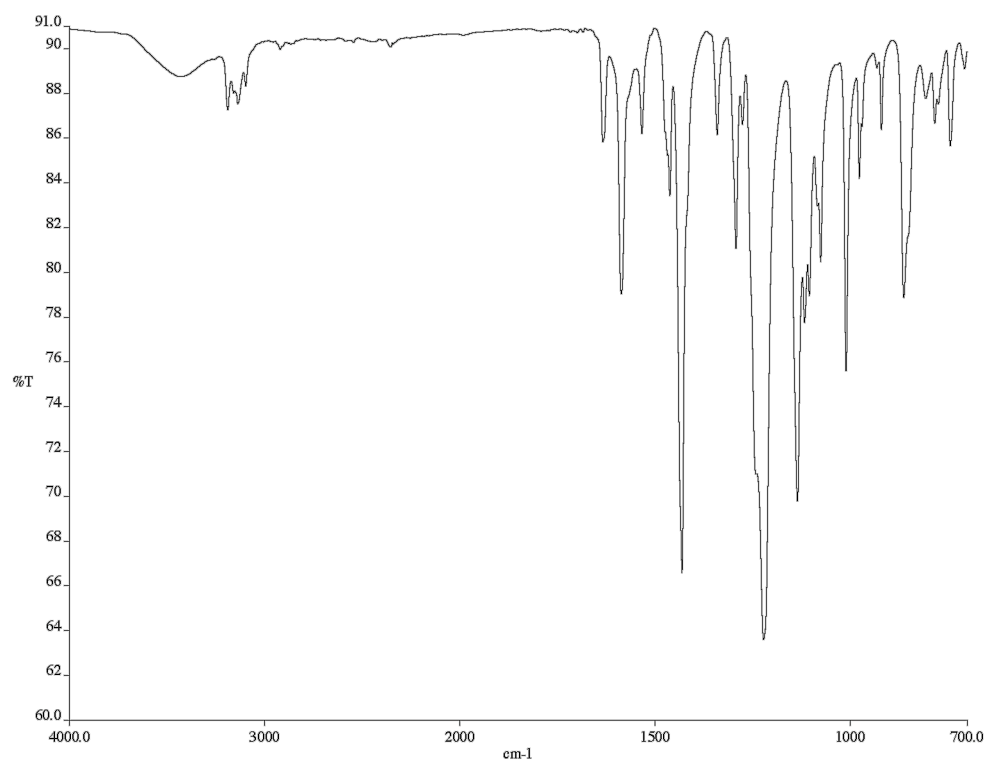


Figure A4.20 Infrared spectrum (thin film/NaCl) of compound **226**

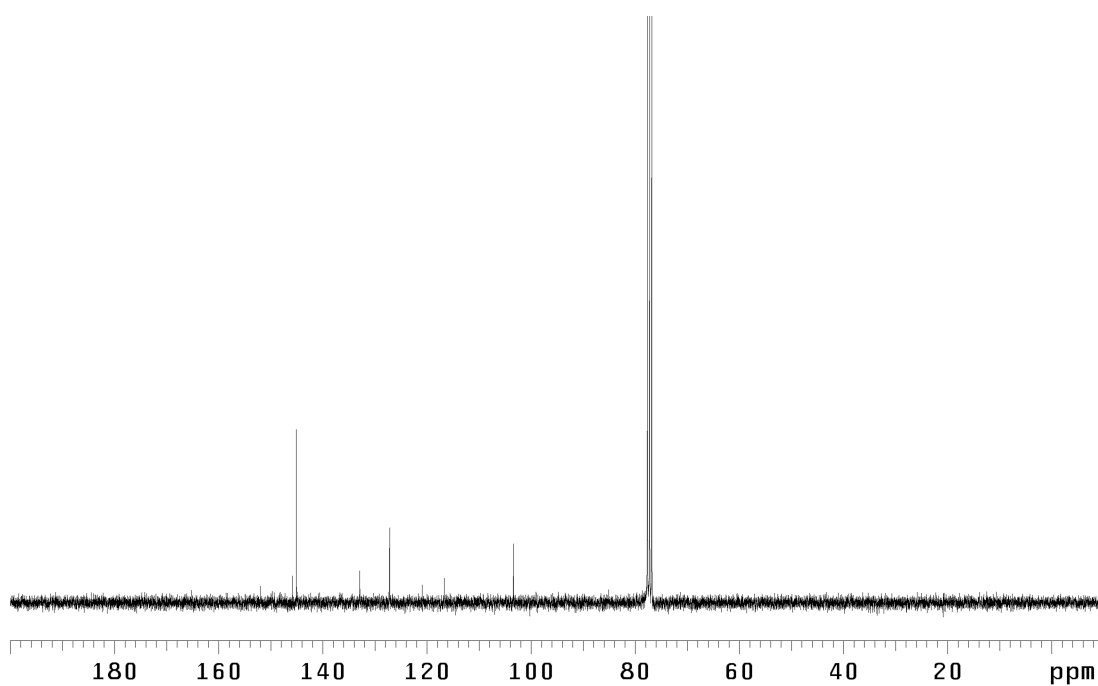
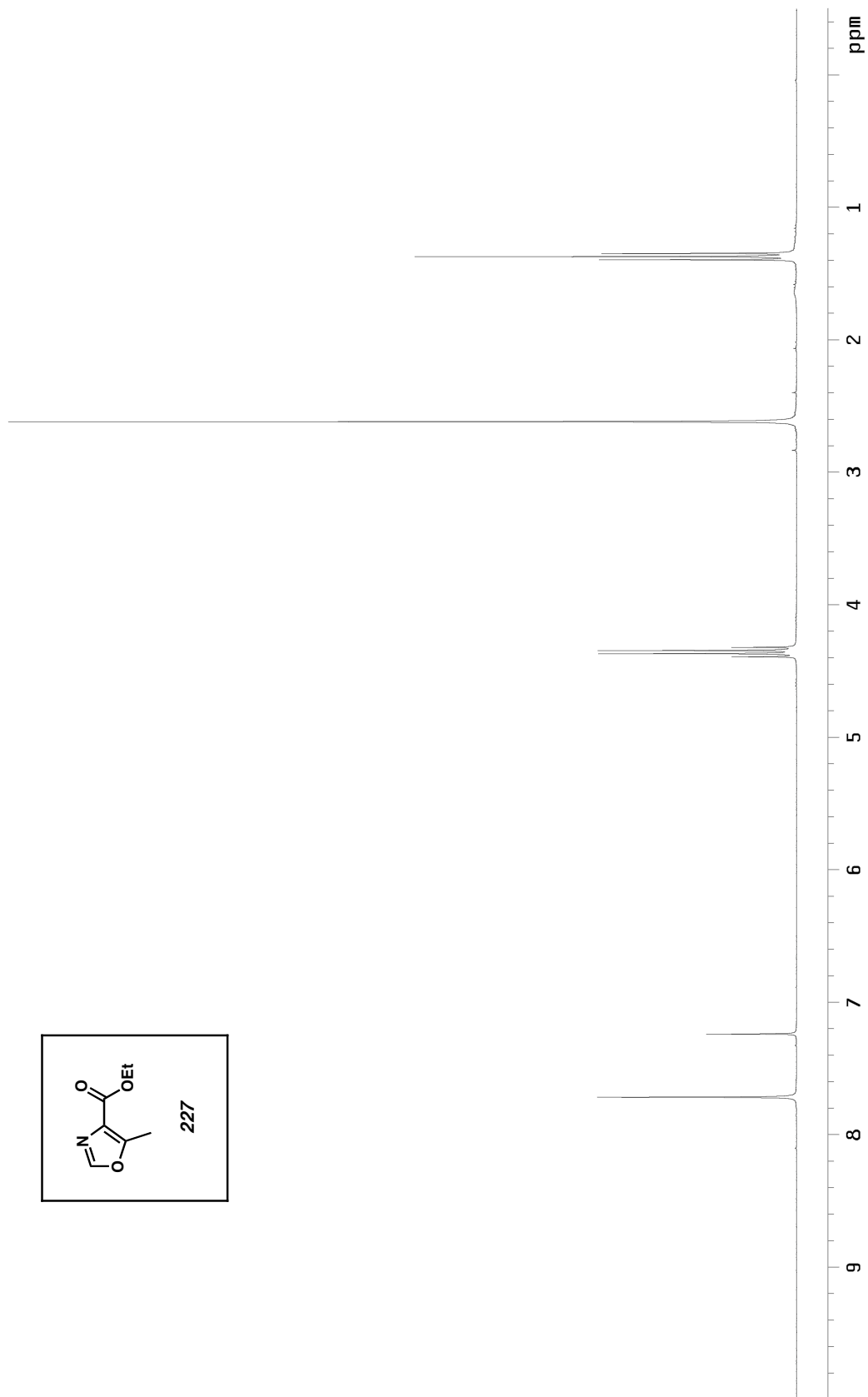
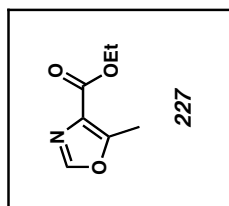


Figure A4.21 <sup>13</sup>C NMR (75 MHz, CDCl<sub>3</sub>) of compound **226**



*Figure A4.22*  $^1\text{H}$  NMR (300 MHz,  $\text{CDCl}_3$ ) of compound **227**

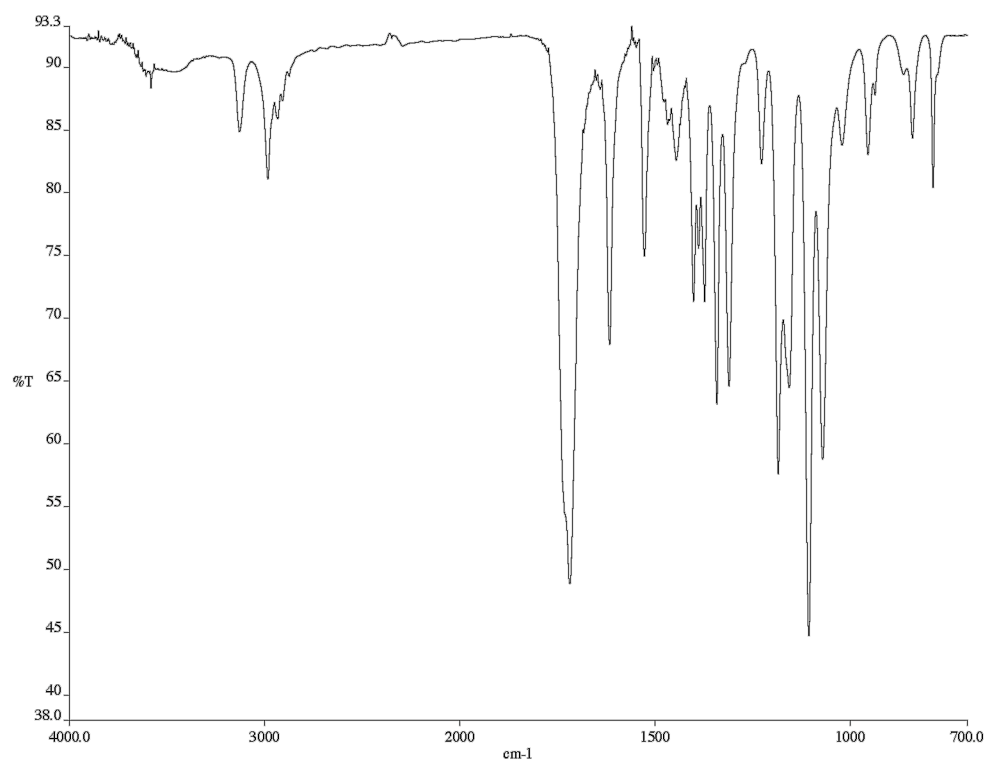


Figure A4.23 Infrared spectrum (thin film/NaCl) of compound **227**

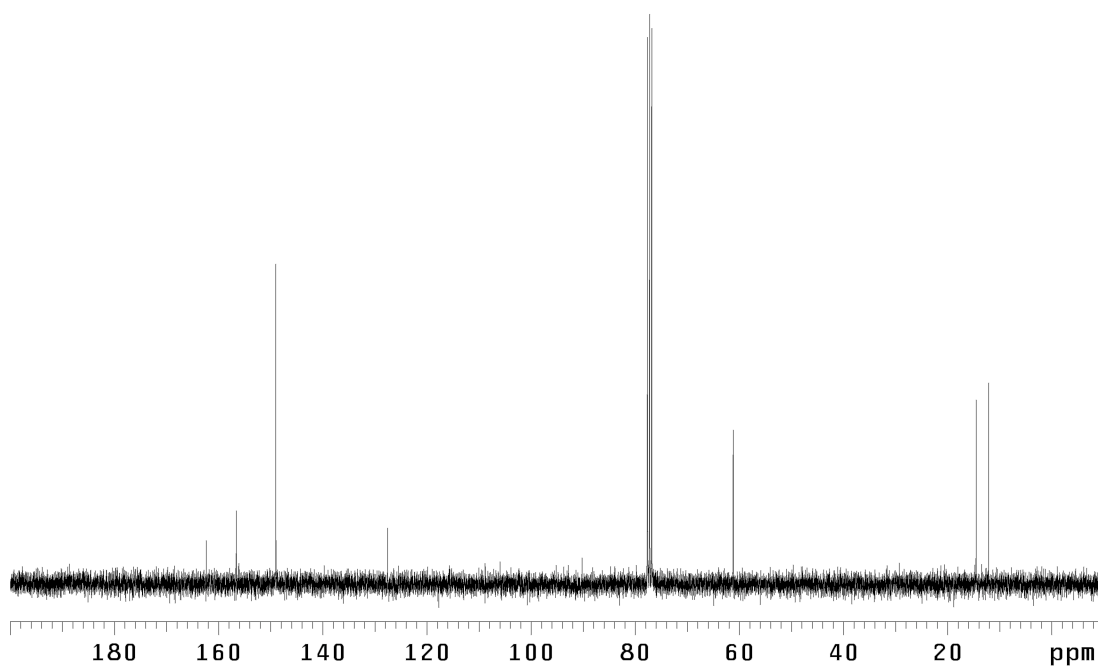
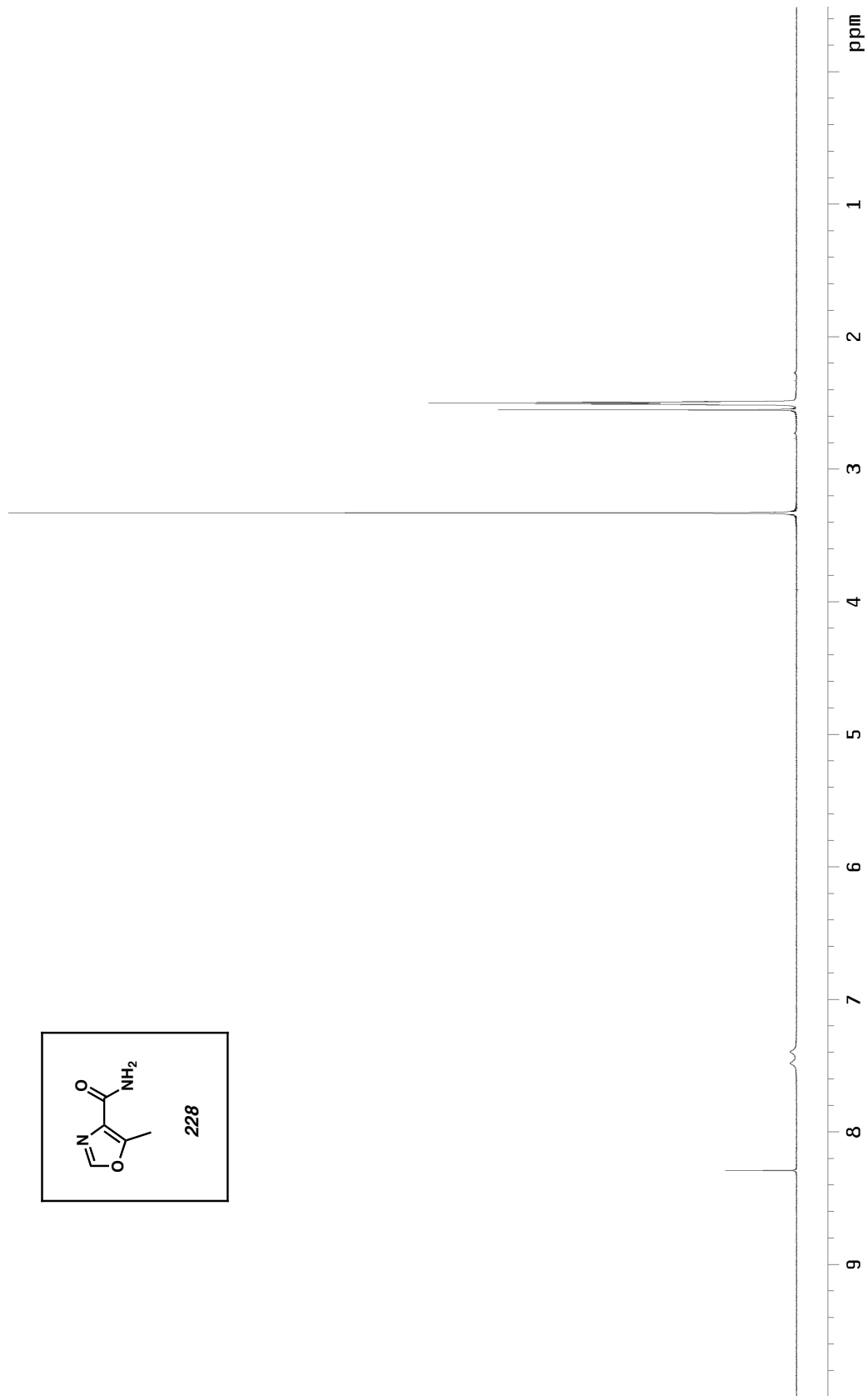
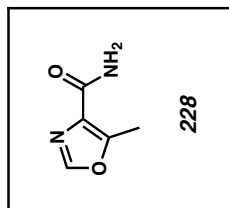


Figure A4.24 <sup>13</sup>C NMR (75 MHz, CDCl<sub>3</sub>) of compound **227**



*Figure A4.25* <sup>1</sup>H NMR (300 MHz, DMSO-*d*<sub>6</sub>) of compound **228**

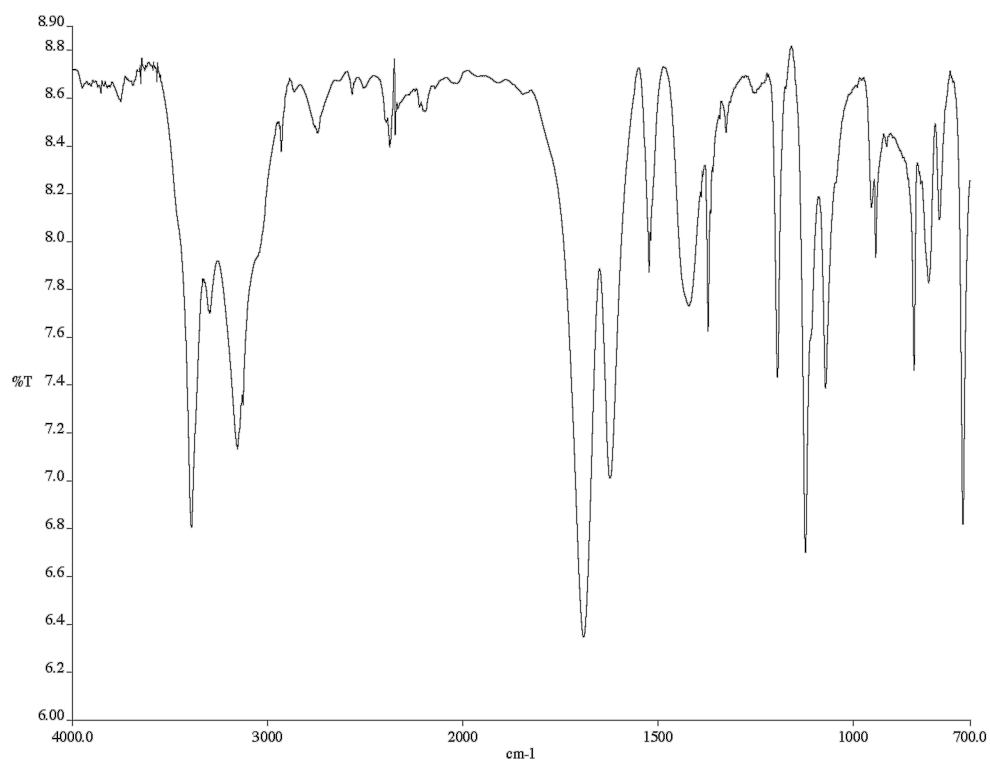


Figure A4.26 Infrared spectrum (KBr pellet) of compound **228**

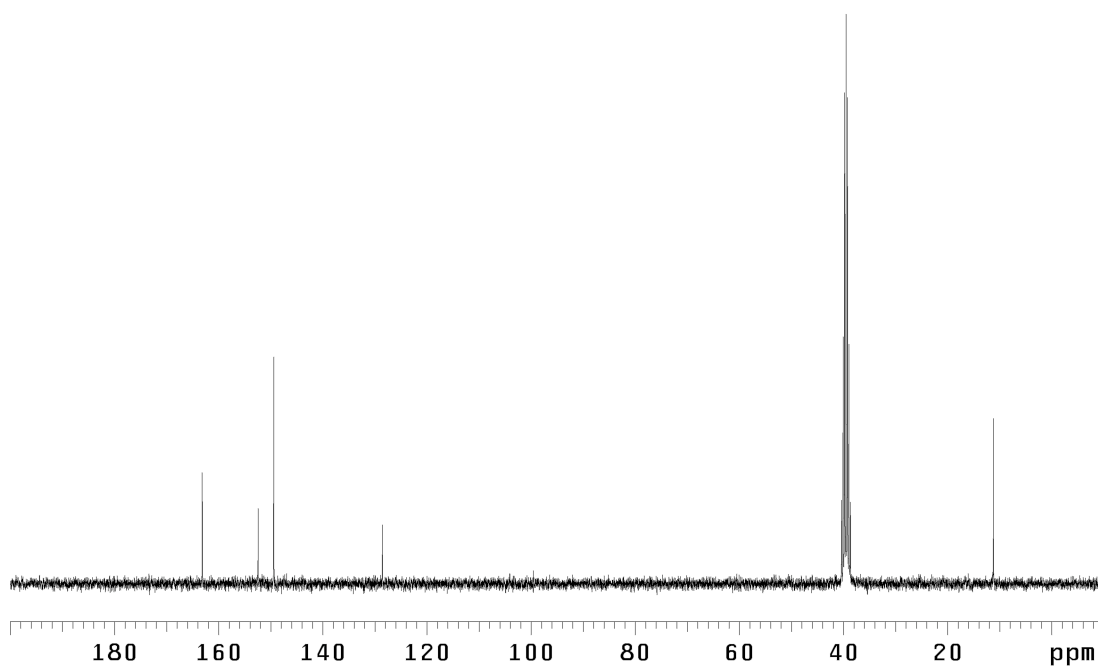


Figure A4.27  $^{13}\text{C}$  NMR (75 MHz,  $\text{DMSO-}d_6$ ) of compound **228**

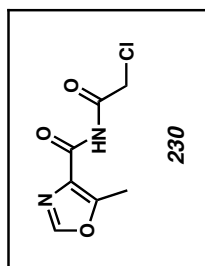
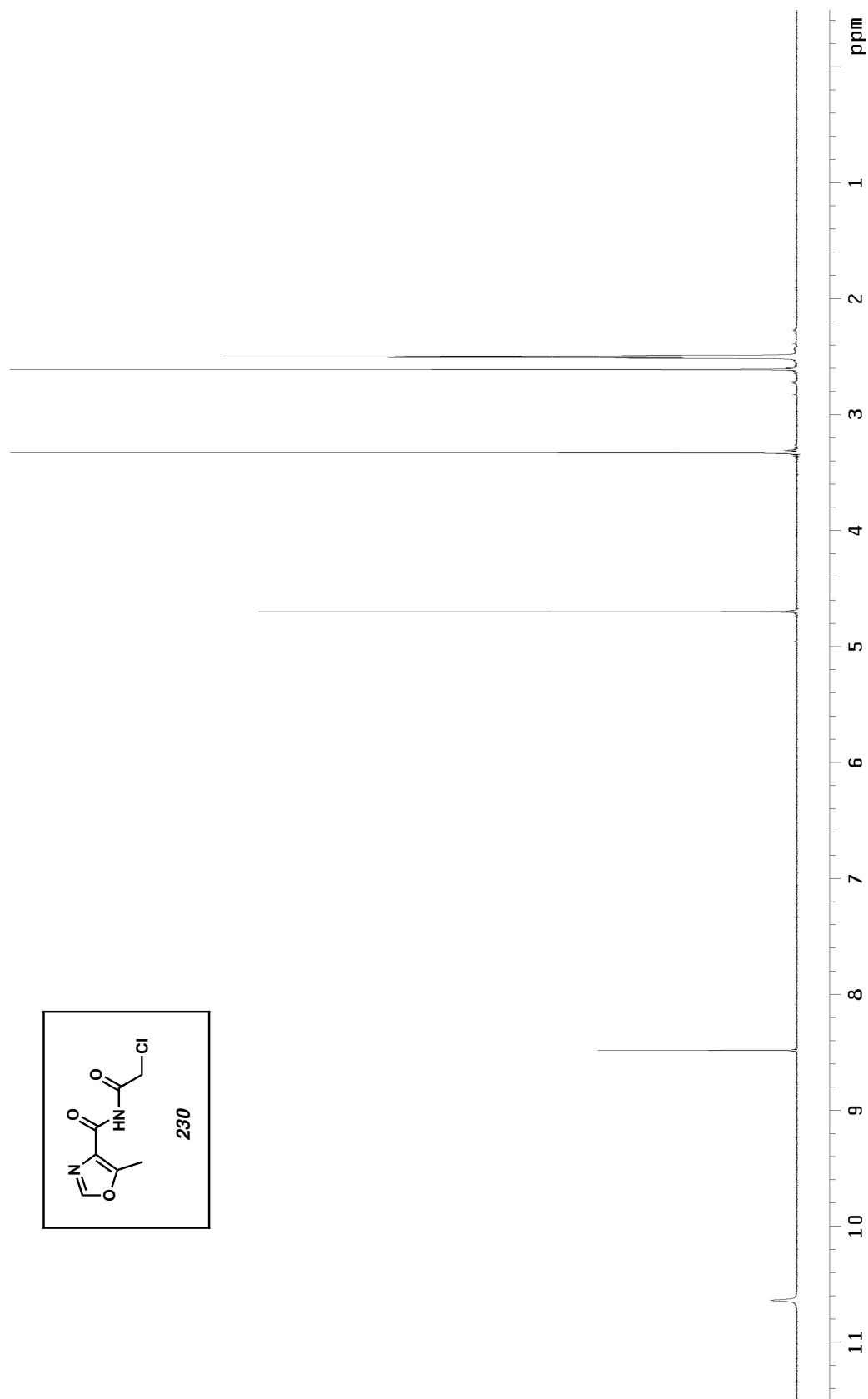


Figure A4.28  $^1\text{H}$  NMR (300 MHz,  $\text{DMSO-}d_6$ ) of compound **230**

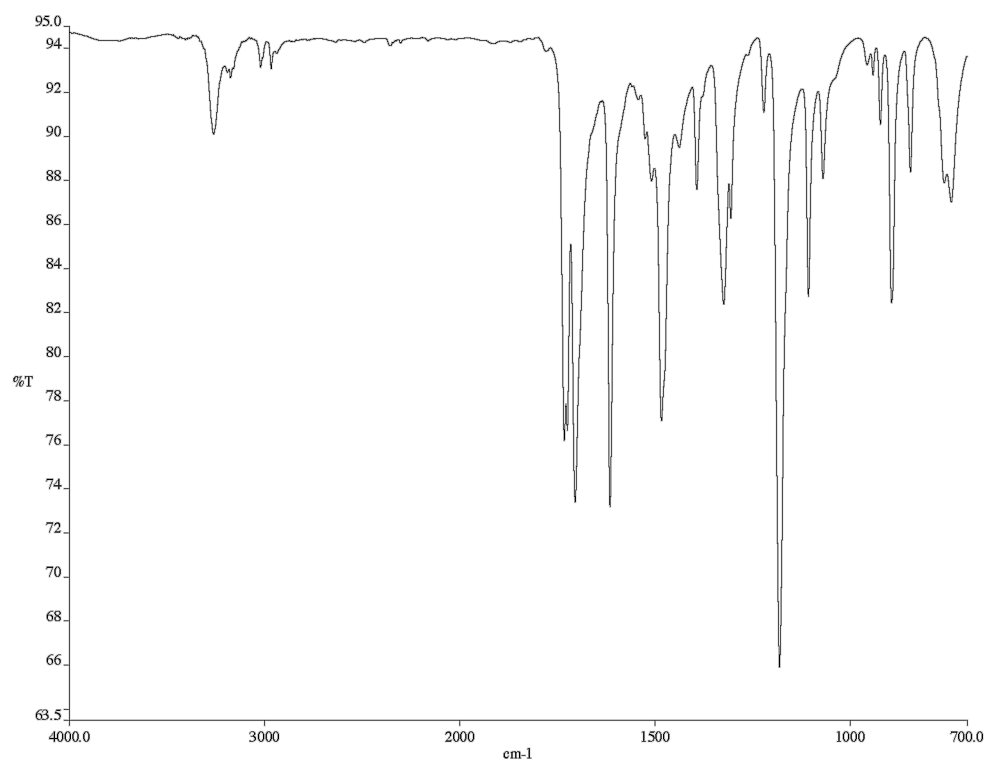


Figure A4.29 Infrared spectrum (thin film/NaCl) of compound **230**

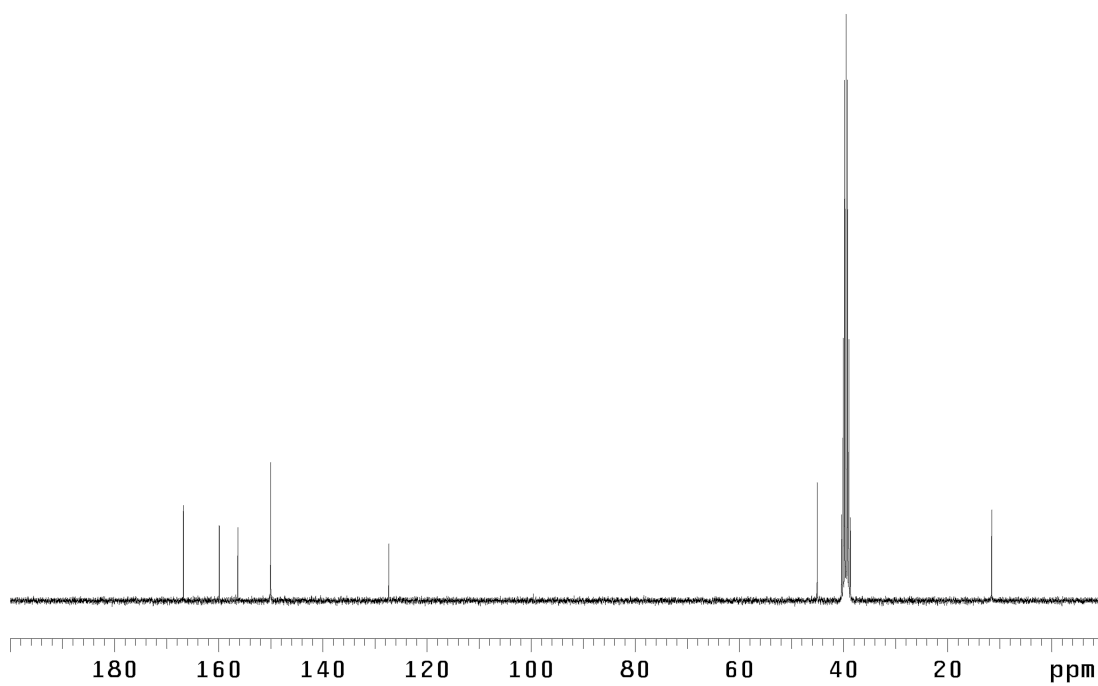


Figure A4.30 <sup>13</sup>C NMR (75 MHz, DMSO-*d*<sub>6</sub>) of compound **230**



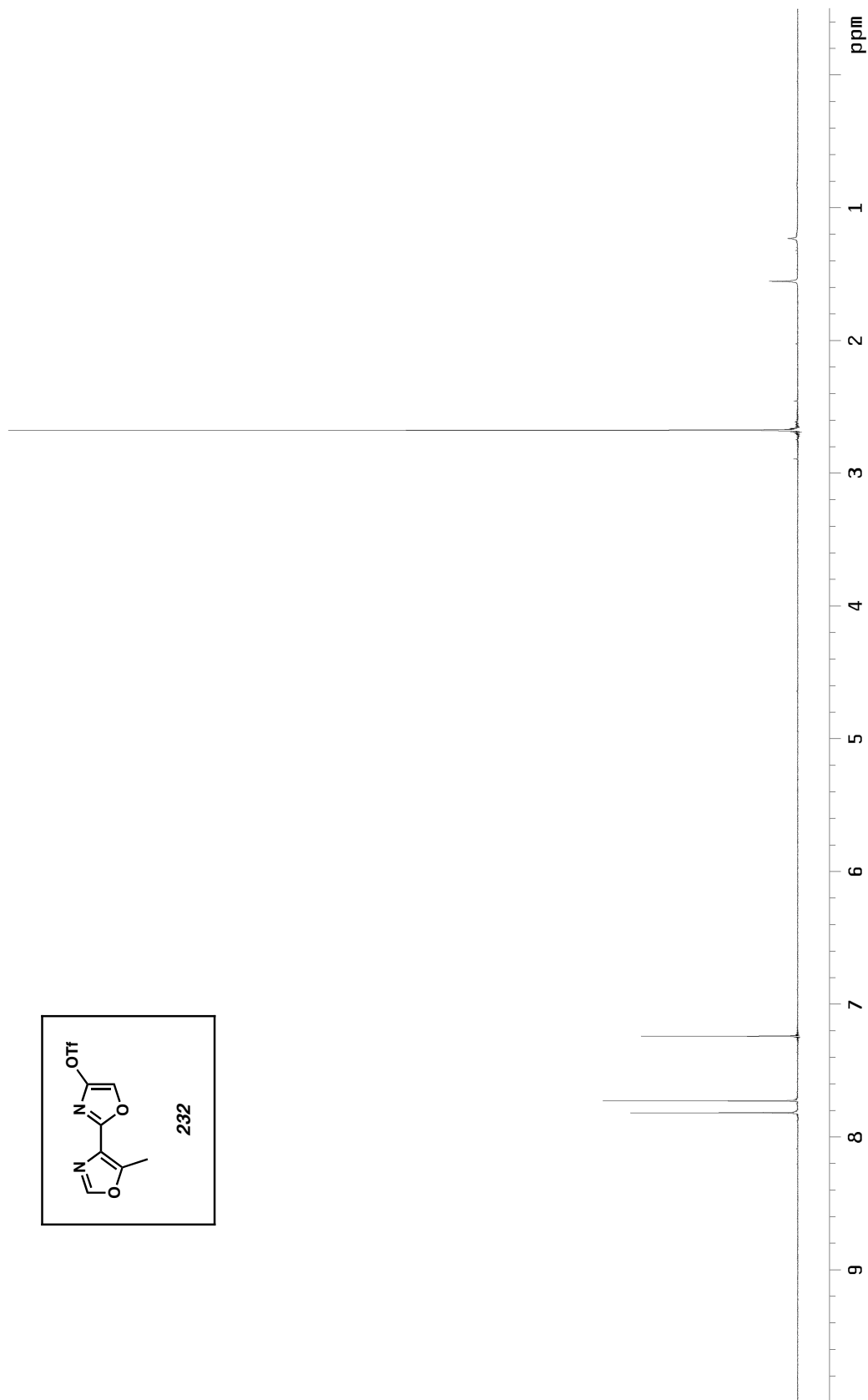


Figure A4.31  $^1\text{H}$  NMR (300 MHz,  $\text{CDCl}_3$ ) of compound **232**

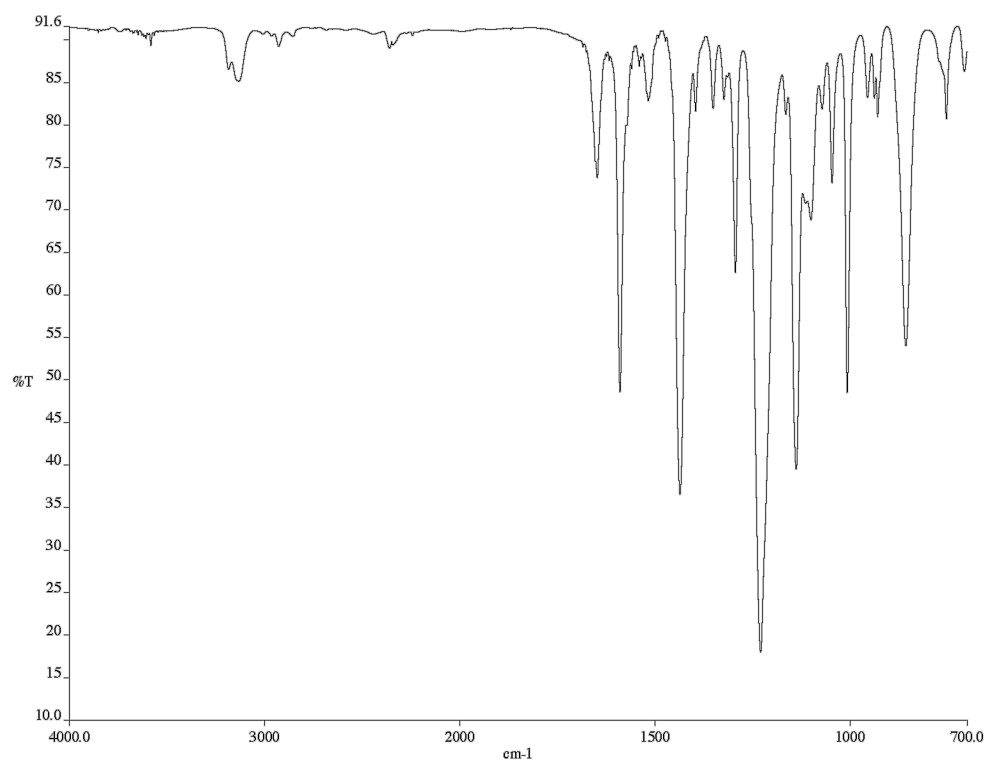


Figure A4.32 Infrared spectrum (thin film/NaCl) of compound **232**

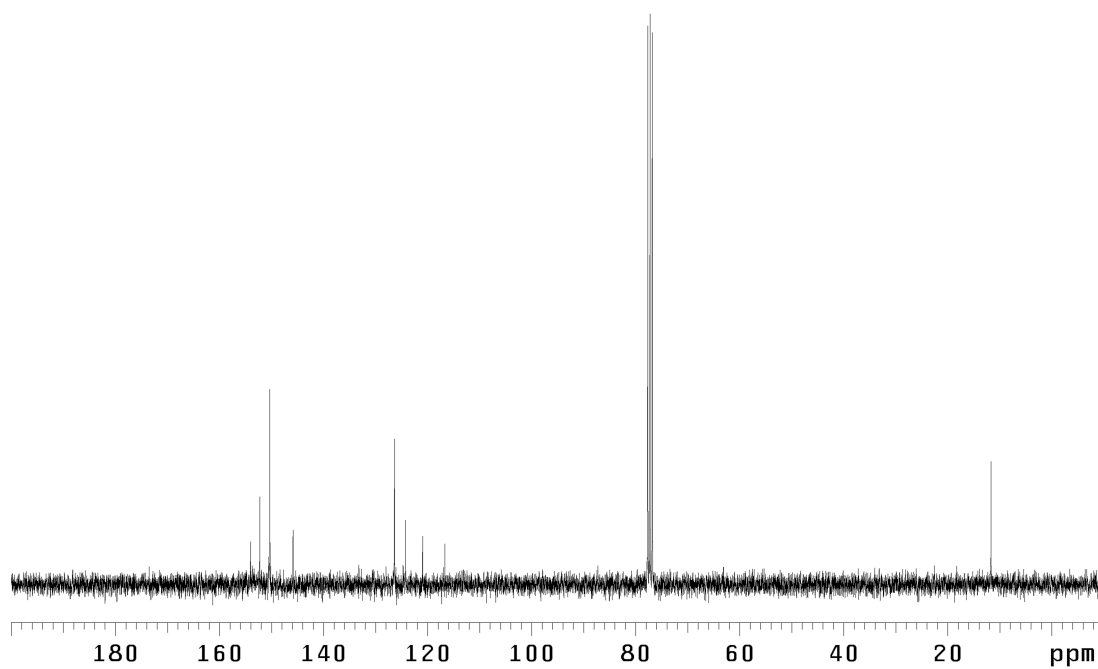
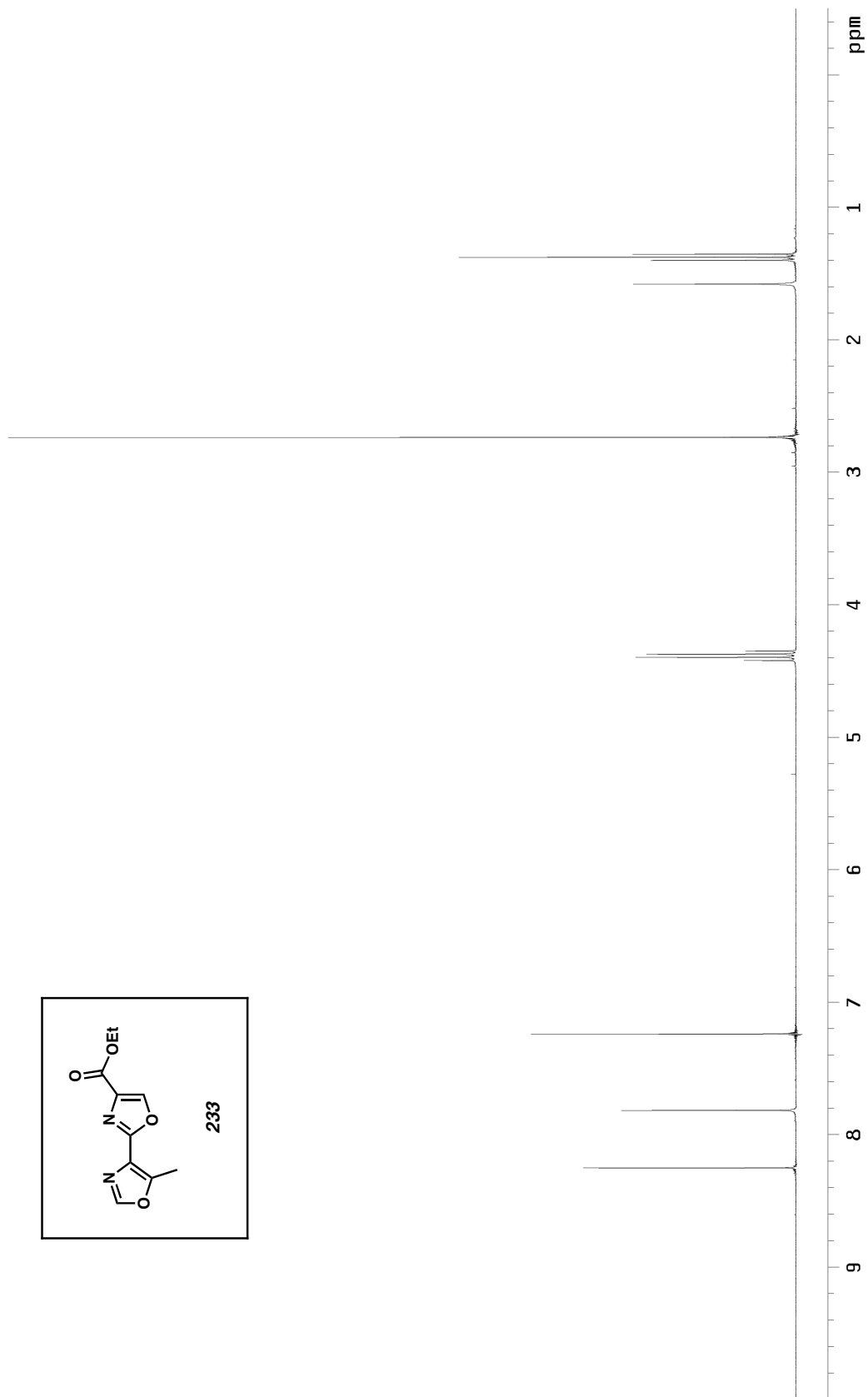
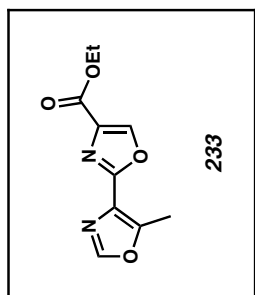


Figure A4.33 <sup>13</sup>C NMR (75 MHz, CDCl<sub>3</sub>) of compound **232**



*Figure A4.34*  $^1\text{H}$  NMR (300 MHz,  $\text{CDCl}_3$ ) of compound **233**

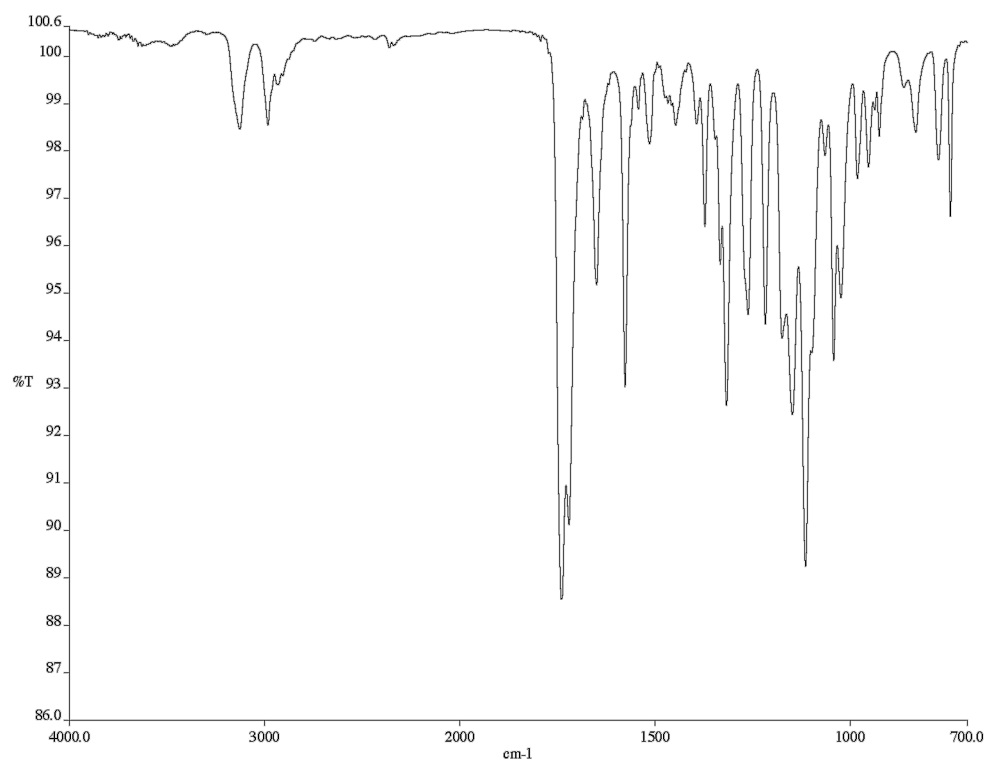


Figure A4.35 Infrared spectrum (thin film/NaCl) of compound **233**

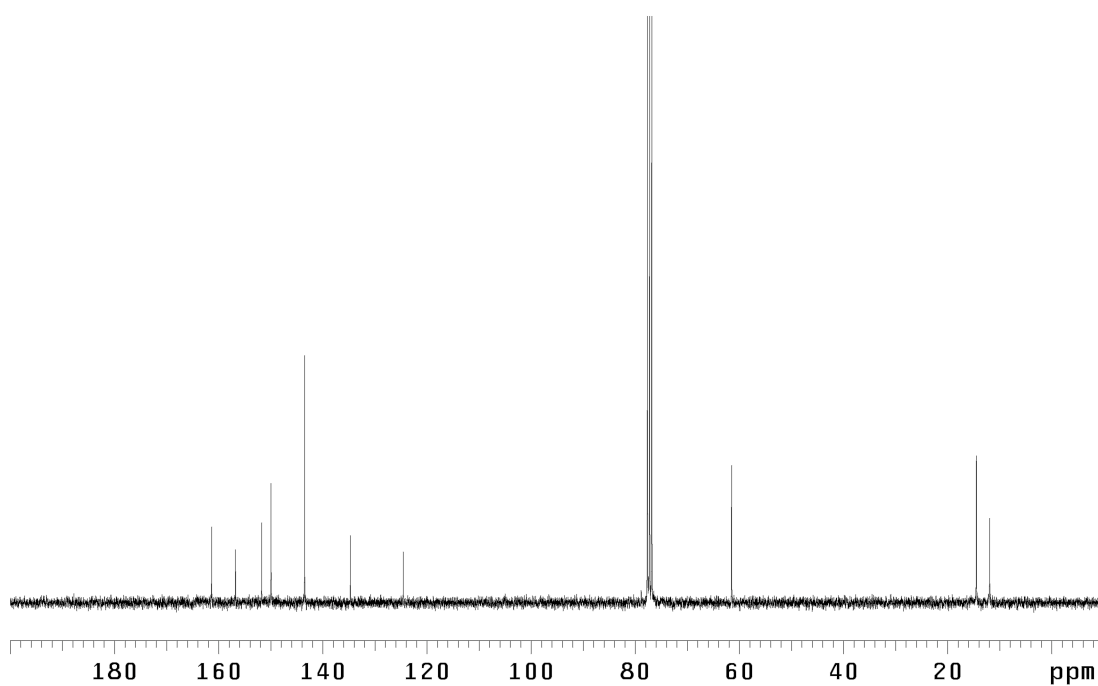


Figure A4.36 <sup>13</sup>C NMR (75 MHz, CDCl<sub>3</sub>) of compound **233**

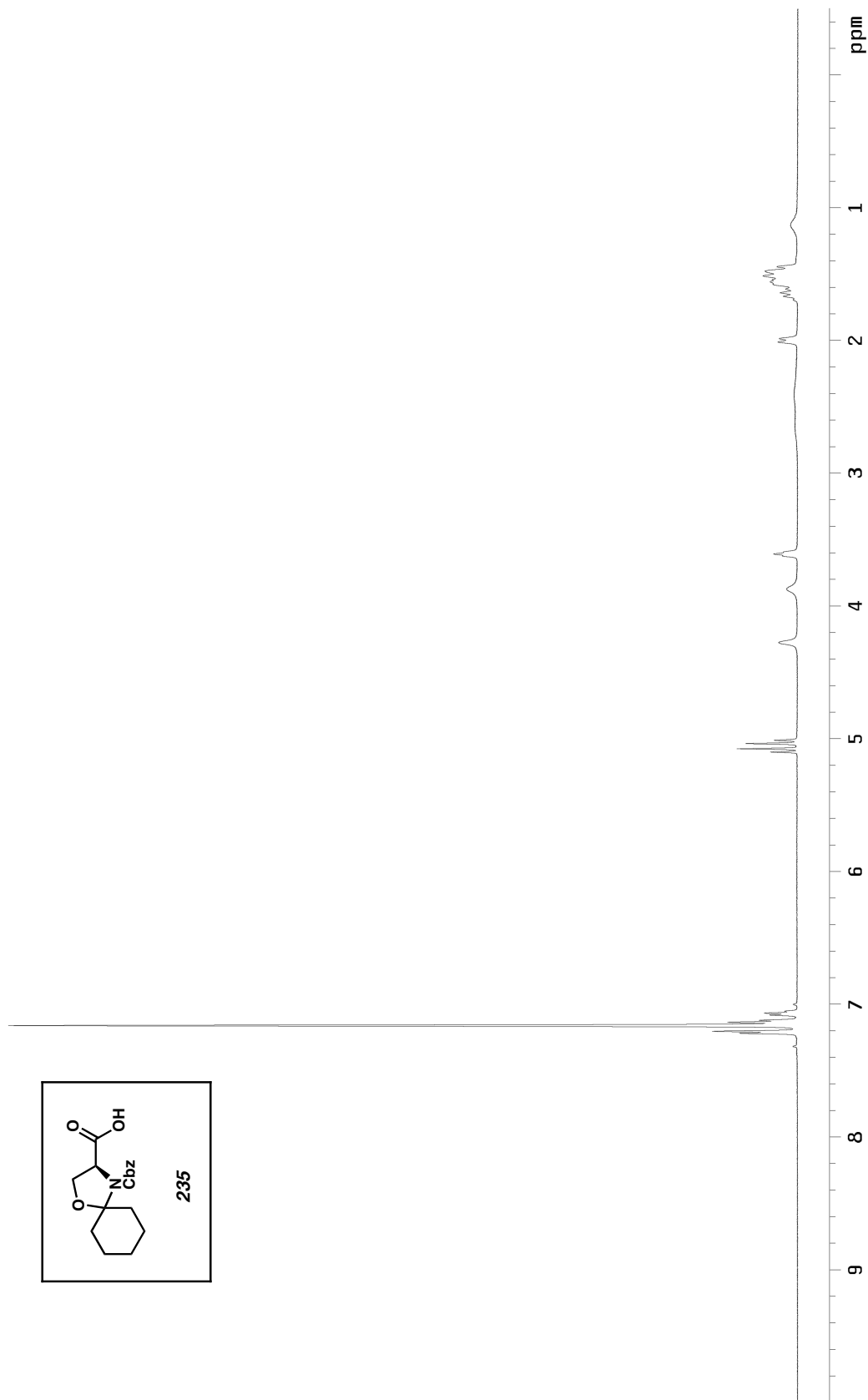


Figure A4.37  $^1\text{H}$  NMR (500 MHz,  $\text{C}_6\text{D}_6$ ,  $70^\circ\text{C}$ ) of compound **235**

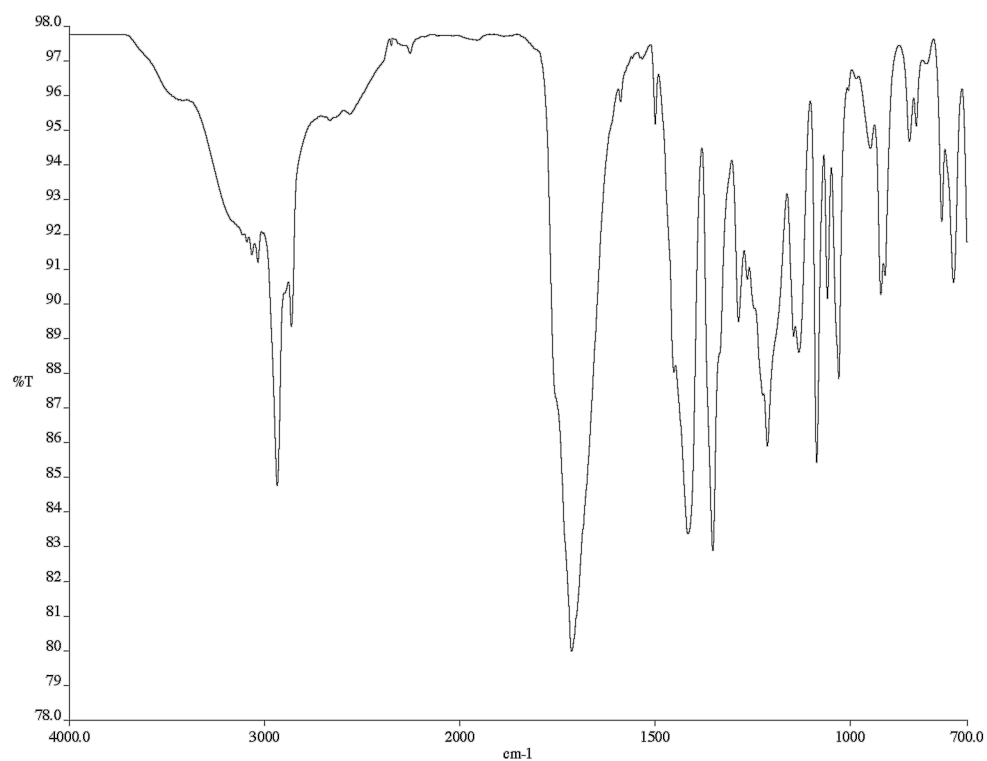


Figure A4.38 Infrared spectrum (thin film/NaCl) of compound **235**

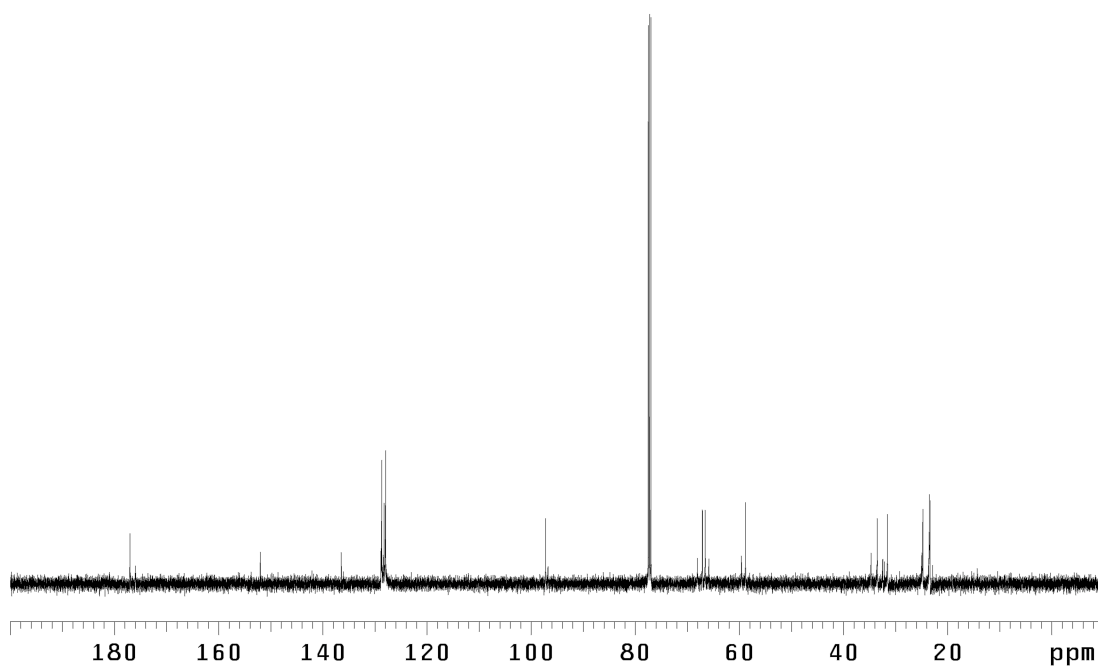


Figure A4.39 <sup>13</sup>C NMR (125 MHz, CDCl<sub>3</sub>) of compound **235**

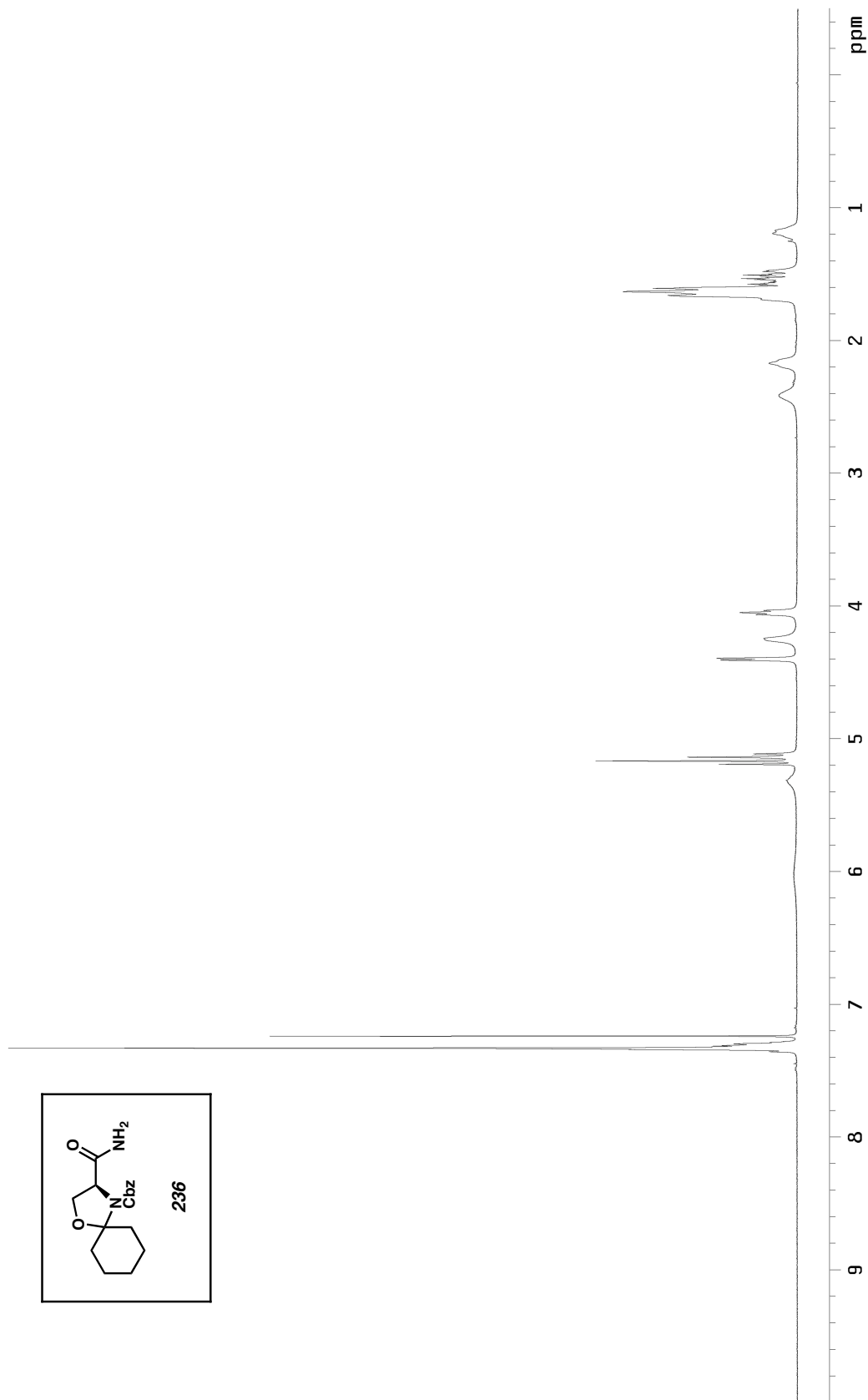


Figure A4.40  $^1\text{H}$  NMR (500 MHz,  $\text{CDCl}_3$ , 50  $^\circ\text{C}$ ) of compound **236**

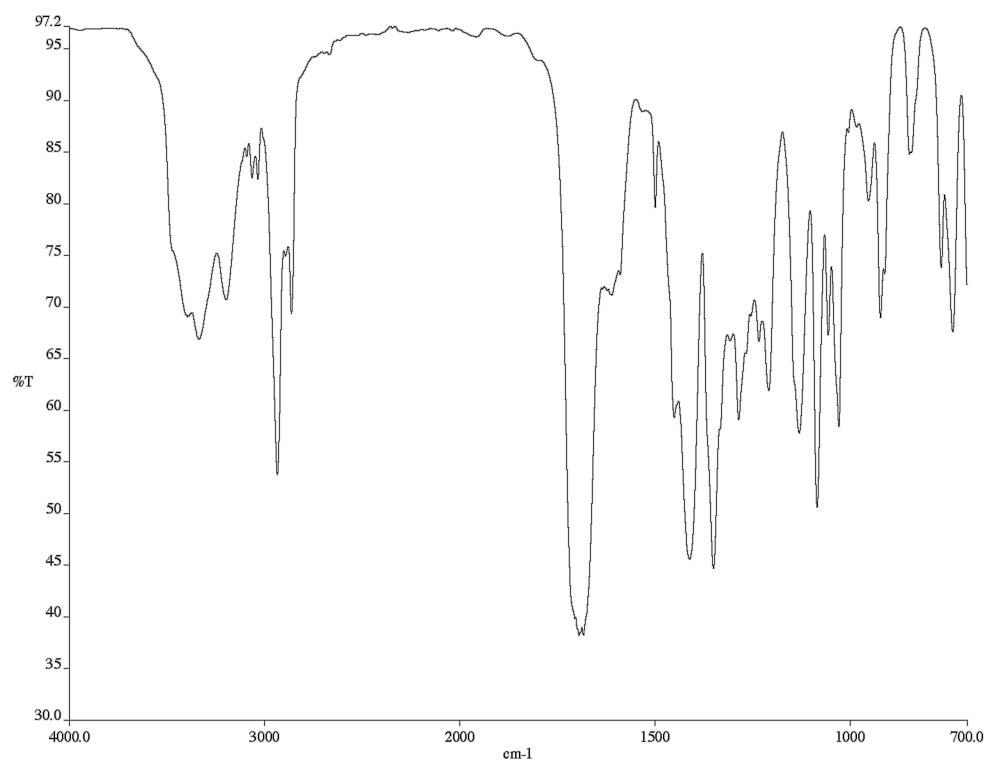


Figure A4.41 Infrared spectrum (thin film/NaCl) of compound **236**

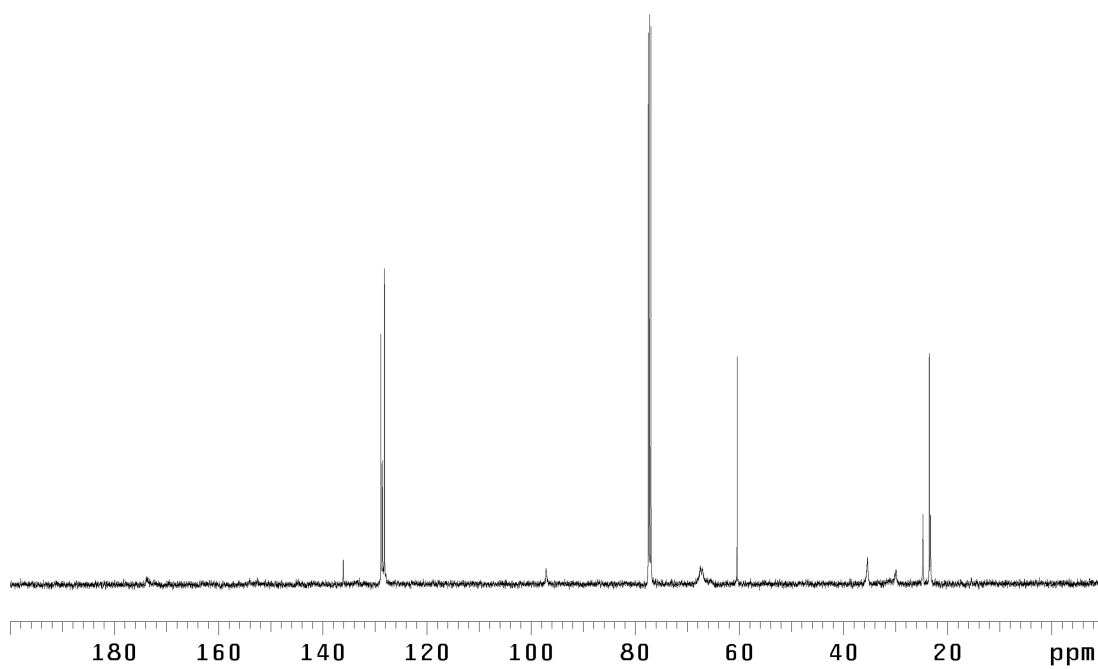


Figure A4.42 <sup>13</sup>C NMR (125 MHz, CDCl<sub>3</sub>) of compound **236**



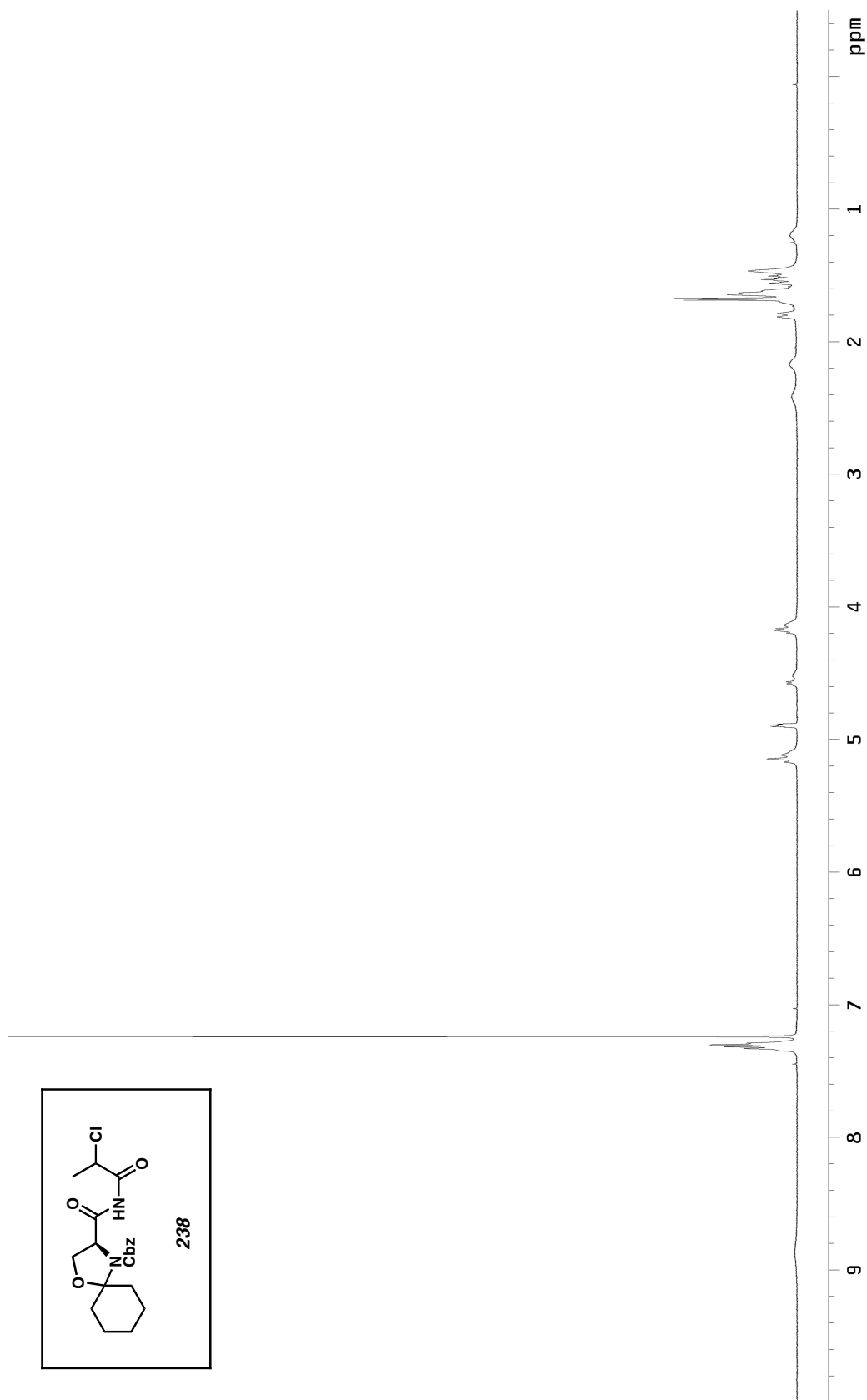


Figure A4.43  $^1\text{H}$  NMR (500 MHz,  $\text{CDCl}_3$ , 50  $^\circ\text{C}$ ) of compound **238**

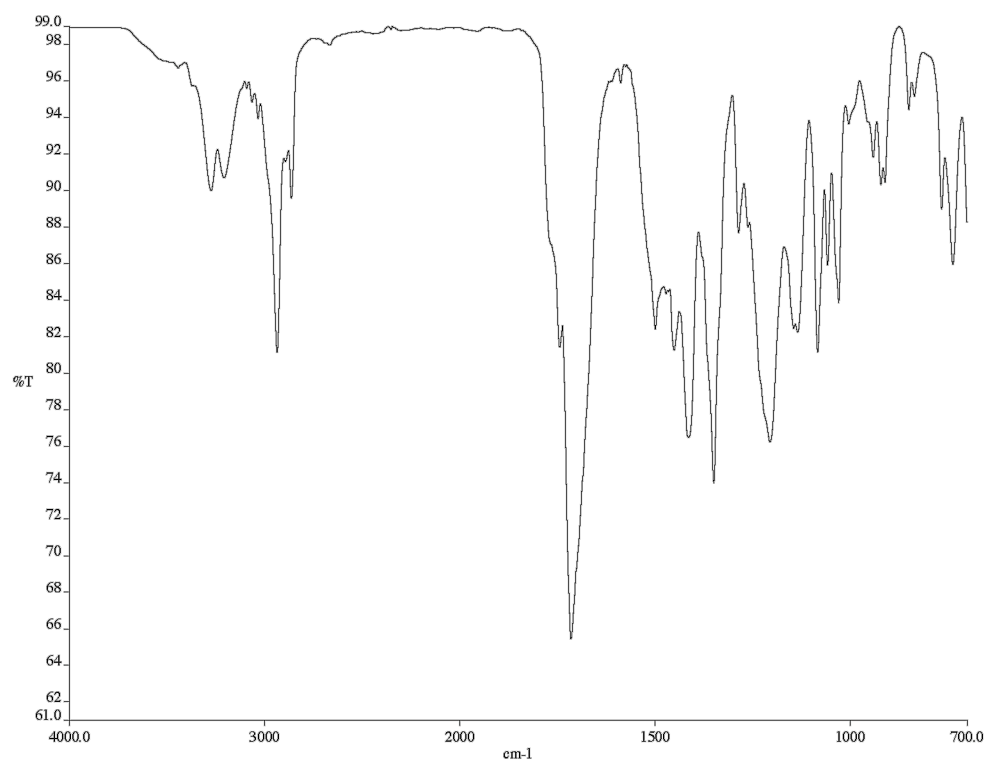


Figure A4.44 Infrared spectrum (thin film/NaCl) of compound **238**

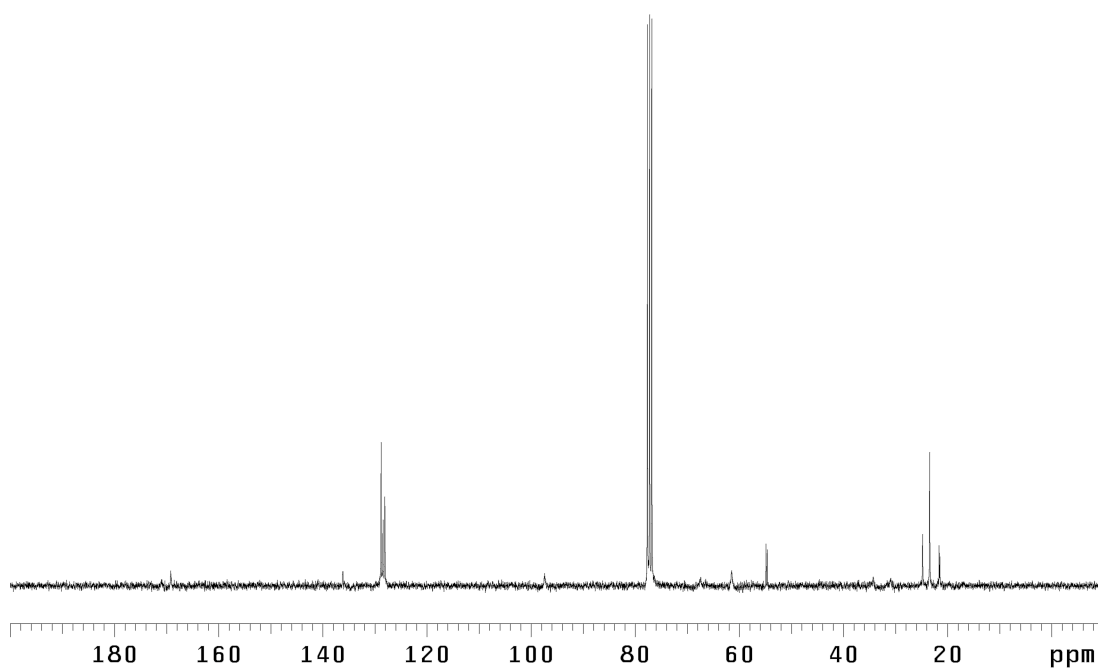


Figure A4.45 <sup>13</sup>C NMR (75 MHz, CDCl<sub>3</sub>) of compound **238**

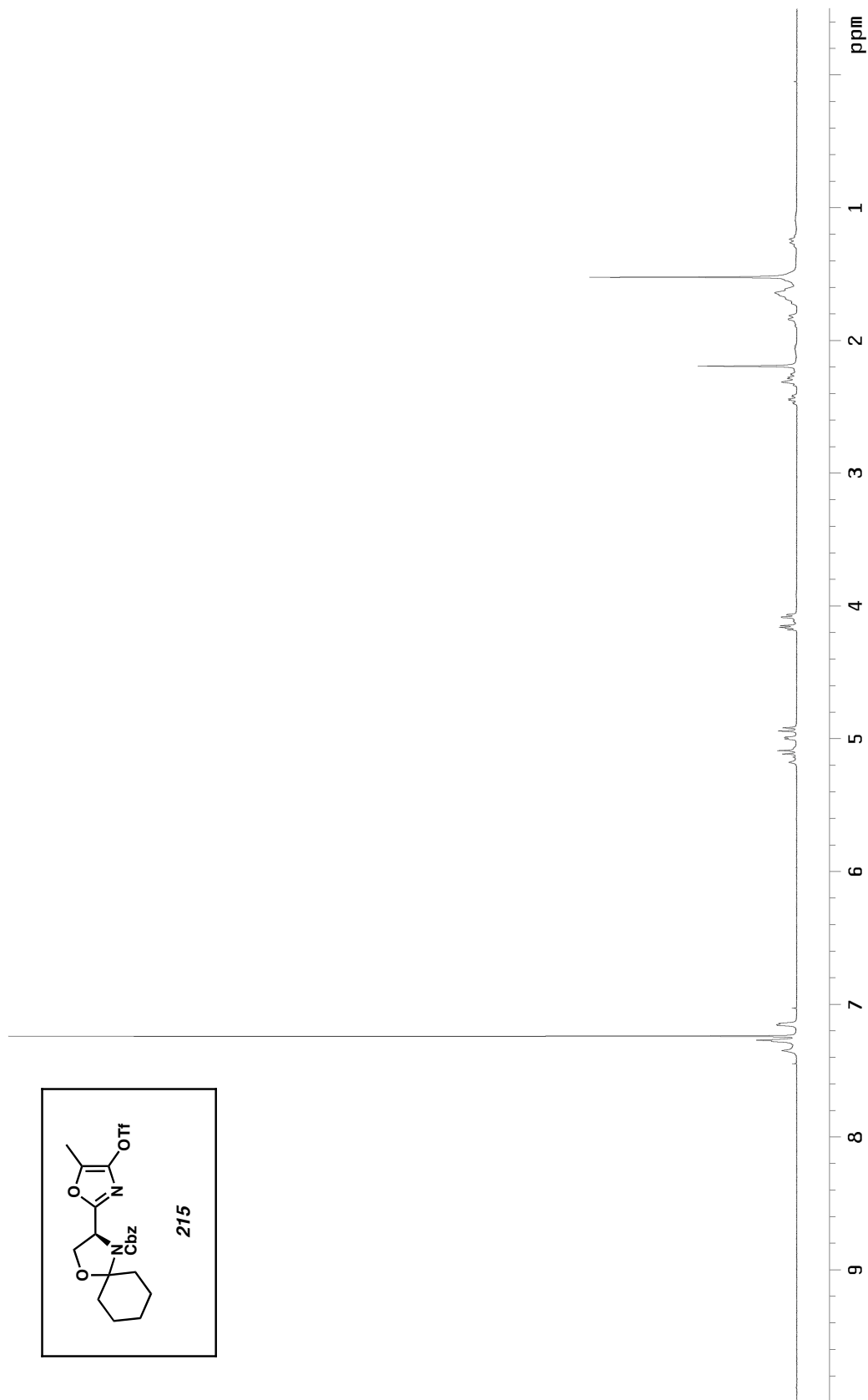


Figure A4.46  $^1\text{H}$  NMR (500 MHz,  $\text{CDCl}_3$ ) of compound **215**

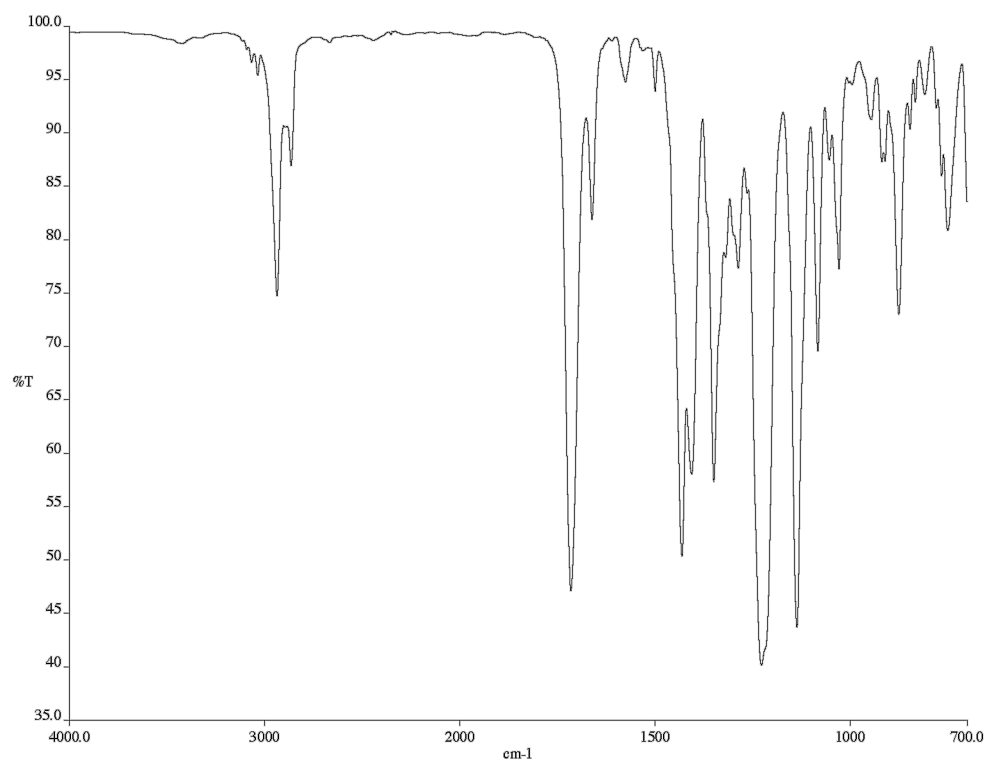


Figure A4.47 Infrared spectrum (thin film/NaCl) of compound **215**

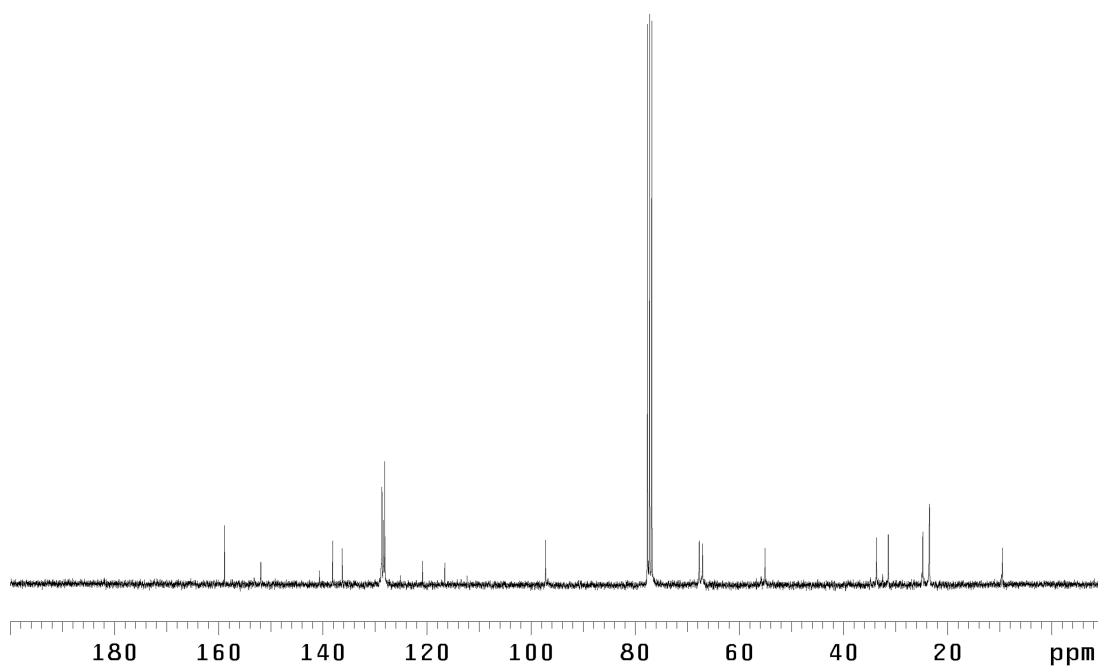


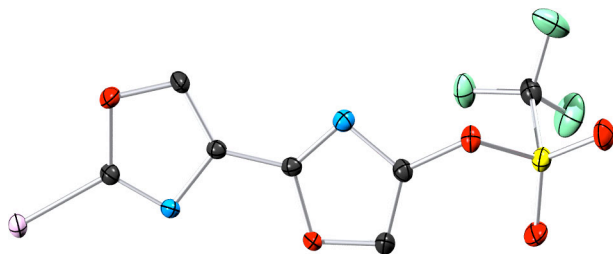
Figure A4.48 <sup>13</sup>C NMR (75 MHz, CDCl<sub>3</sub>) of compound **215**

## **APPENDIX FIVE**

### **X-Ray Crystallography Reports Relevant to Chapter Four:**

#### **Progress Toward The Total Synthesis of Telomestatin**

### A5.1 Crystal Structure Analysis of **226**



**Figure A5.1.1** Iodobisoxazole triflate **226** is shown with 50% probability ellipsoids (Note: Only Molecule A is depicted). Crystallographic data have been deposited at the CCDC, 12 Union Road, Cambridge CB2 1EZ, UK, and copies can be obtained on request, free of charge, by quoting the publication citation and the deposition number 282586.

**Table A5.1.1** Crystal data and structure refinement for **226** (CCDC 282586)

Empirical formula	C <sub>7</sub> H <sub>2</sub> F <sub>3</sub> IN <sub>2</sub> O <sub>5</sub> S		
Formula weight	410.07		
Crystallization Solvent	Diethylether		
Crystal Habit	Plate		
Crystal size	0.48 x 0.22 x 0.19 mm <sup>3</sup>		
Crystal color	Colorless		
<b>Data Collection</b>			
Type of diffractometer	Bruker SMART 1000		
Wavelength	0.71073 Å MoKα		
Data Collection Temperature	100(2) K		
θ range for 9170 reflections used in lattice determination	2.74 to 33.18°		
Unit cell dimensions	a = 5.3805(5) Å b = 14.4770(13) Å c = 14.8833(13) Å	α= 92.205(2)° β= 92.046(2)° γ = 90.356(2)°	
Volume	1157.68(18) Å <sup>3</sup>		
Z	4		
Crystal system	Triclinic		
Space group	P-1		
Density (calculated)	2.353 Mg/m <sup>3</sup>		
F(000)	776		
Data collection program	Bruker SMART v5.630		
θ range for data collection	1.93 to 33.66°		
Completeness to θ = 33.66°	82.2 %		
Index ranges	-8 ≤ h ≤ 7, -19 ≤ k ≤ 20, -22 ≤ l ≤ 22		
Data collection scan type	ω scans at 5 φ settings		
Data reduction program	Bruker SAINT v6.45A		
Reflections collected	19450		
Independent reflections	7576 [R <sub>int</sub> = 0.0597]		
Absorption coefficient	3.006 mm <sup>-1</sup>		
Absorption correction	Gaussian		
Max. and min. transmission	0.91449 and 0.56264		

## 5.1.1 (cont.)

## Structure solution and Refinement

Structure solution program	SHELXS-97 (Sheldrick, 1990)
Primary solution method	Direct methods
Secondary solution method	Difference Fourier map
Hydrogen placement	Difference Fourier map
Structure refinement program	SHELXL-97 (Sheldrick, 1997)
Refinement method	Full matrix least-squares on $F^2$
Data / restraints / parameters	7576 / 0 / 359
Treatment of hydrogen atoms	Unrestrained
Goodness-of-fit on $F^2$	1.034
Final R indices [ $I > 2\sigma(I)$ , 5482 reflections]	$R1 = 0.0311$ , $wR2 = 0.0538$
R indices (all data)	$R1 = 0.0539$ , $wR2 = 0.0583$
Type of weighting scheme used	Sigma
Weighting scheme used	$w = 1/\sigma^2(F_o^2)$
Max shift/error	0.002
Average shift/error	0.000
Largest diff. peak and hole	0.827 and -0.793 e.Å <sup>-3</sup>

## Special Refinement Details

This molecule crystallizes with two unique conformations in the asymmetric unit, differing from each other by the torsion angles around the C(6\*)-O(3\*) and the O(3\*)-S1\* bonds, as illustrated in Figures A5.1.1 thru A5.1.4 and listed in Table A5.1.6. The difference in the environment of these two molecules is illustrated in Figure A5.1.5 and A5.1.6. A short intermolecular contact between the I1 and N(1B), distance = 3.05 Å, is **NOT** present between I2 and N(1A).

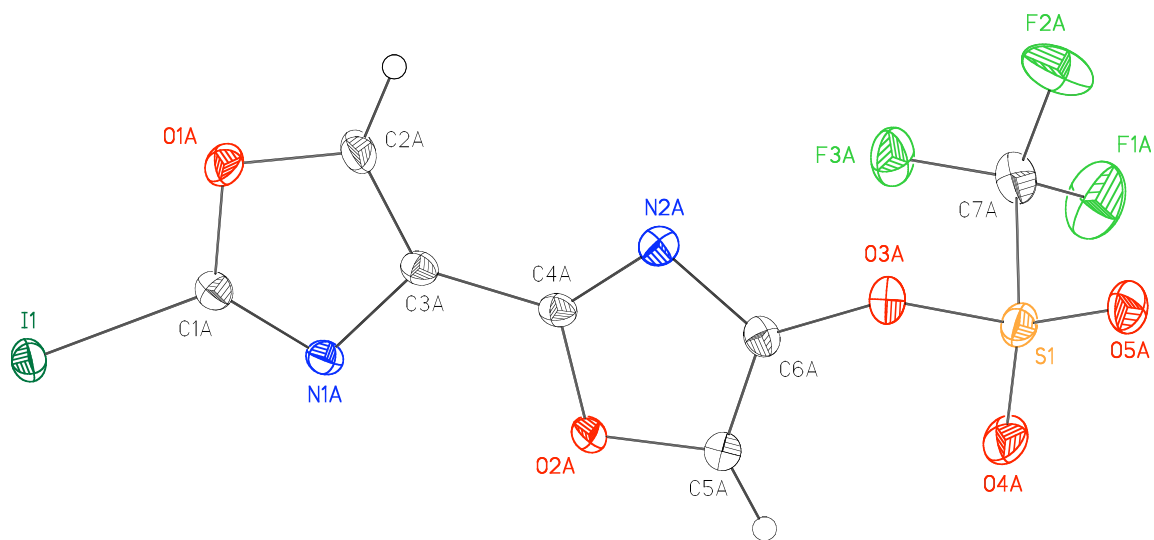
Another interesting feature observed in this structure are the CH-N and CH-O hydrogen bonds listed in Table A5.1.7. Although these are not the “classical” hydrogen bonds they are not without precedent<sup>1,2</sup> and the values observed herein are consistent with those observed elsewhere<sup>1</sup>.

Refinement of  $F^2$  against ALL reflections: The weighted R-factor ( $wR$ ) and goodness of fit ( $S$ ) are based on  $F^2$ , conventional R-factors ( $R$ ) are based on  $F$ , with  $F$  set to zero for negative  $F^2$ . The threshold expression of  $F^2 > 2\sigma(F^2)$  is used only for calculating R-factors(gt), etc., and is not relevant to the choice of reflections for refinement. R-factors based on  $F^2$  are statistically about twice as large as those based on  $F$ , and R-factors based on ALL data will be even larger.

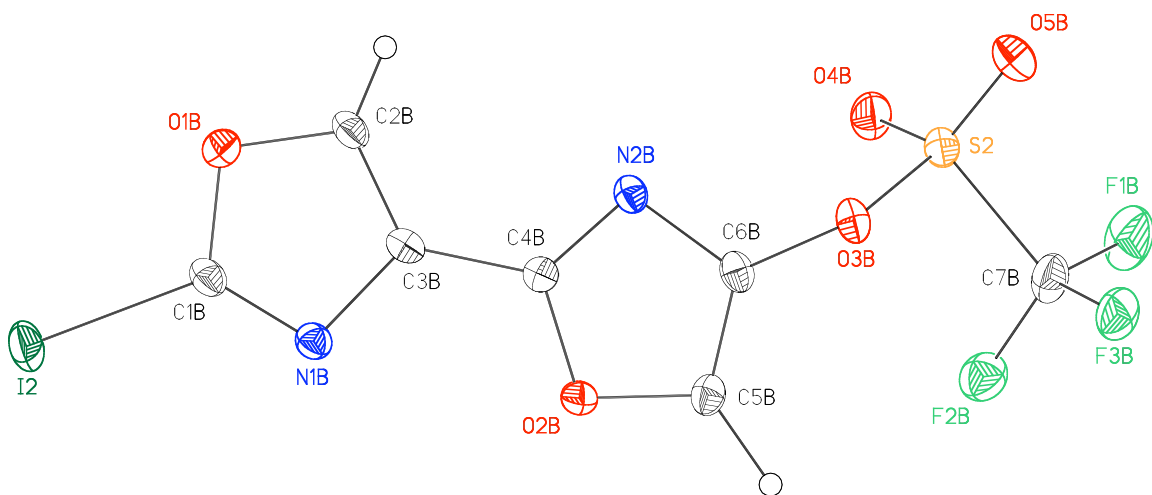
All esds (except the esd in the dihedral angle between two l.s. planes) are estimated using the full covariance matrix. The cell esds are taken into account individually in the estimation of esds in distances, angles, and torsion angles; correlations between esds in cell parameters are only used when they are defined by crystal symmetry. An approximate (isotropic) treatment of cell esds is used for estimating esds involving l.s. planes.

- 
- (1) Rahman, A. N. M. M.; Bishop, R.; Craig, D. C.; Scudder, M. L. *Eur. J. Org. Chem.* **2001**, 863–873.  
 (2) Jiang, L.; Lai, L. *J. Biol. Chem.* **2002**, 37732–37740.

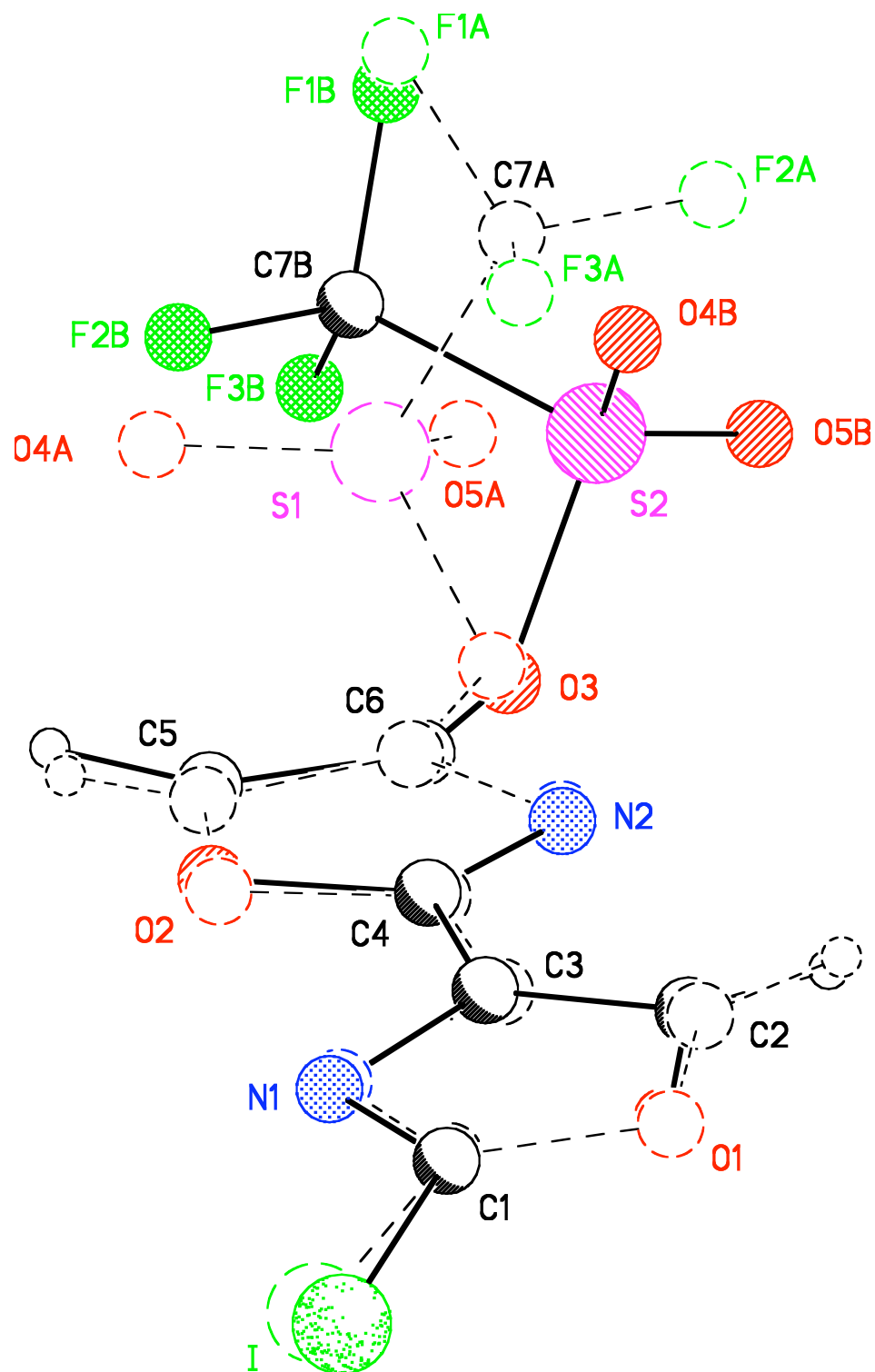




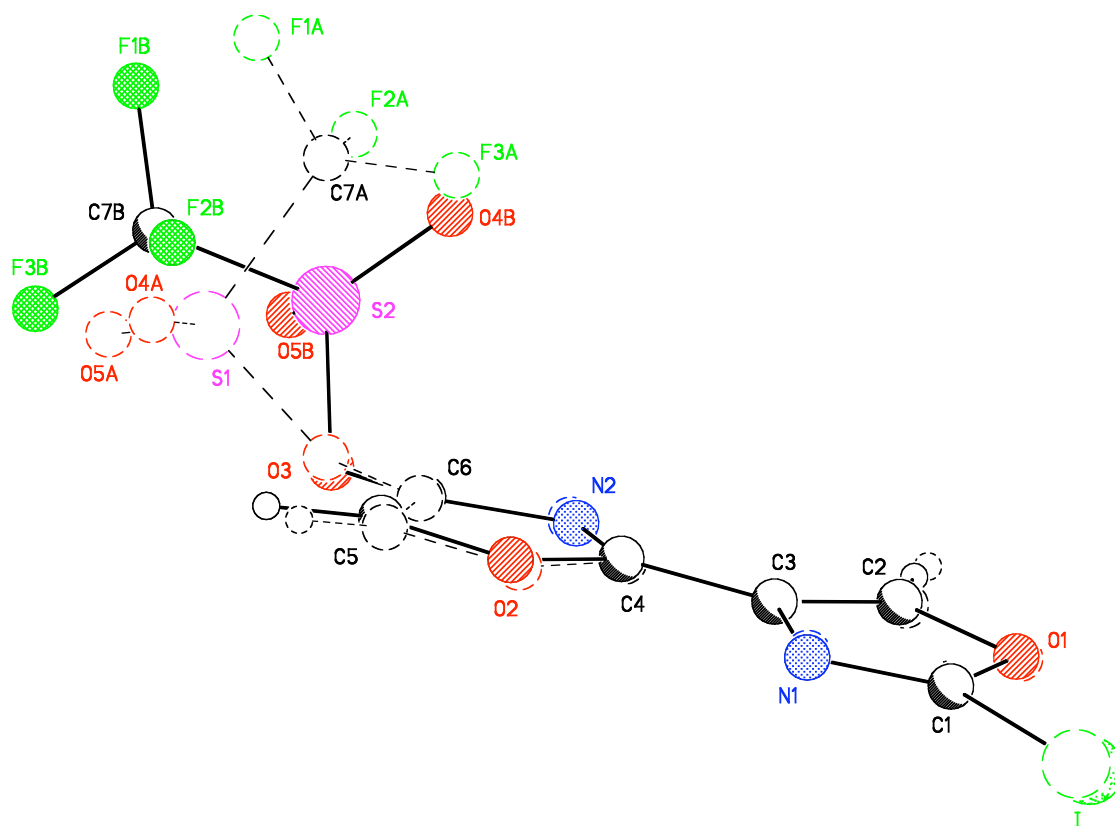
**Figure A5.1.2** Molecule A



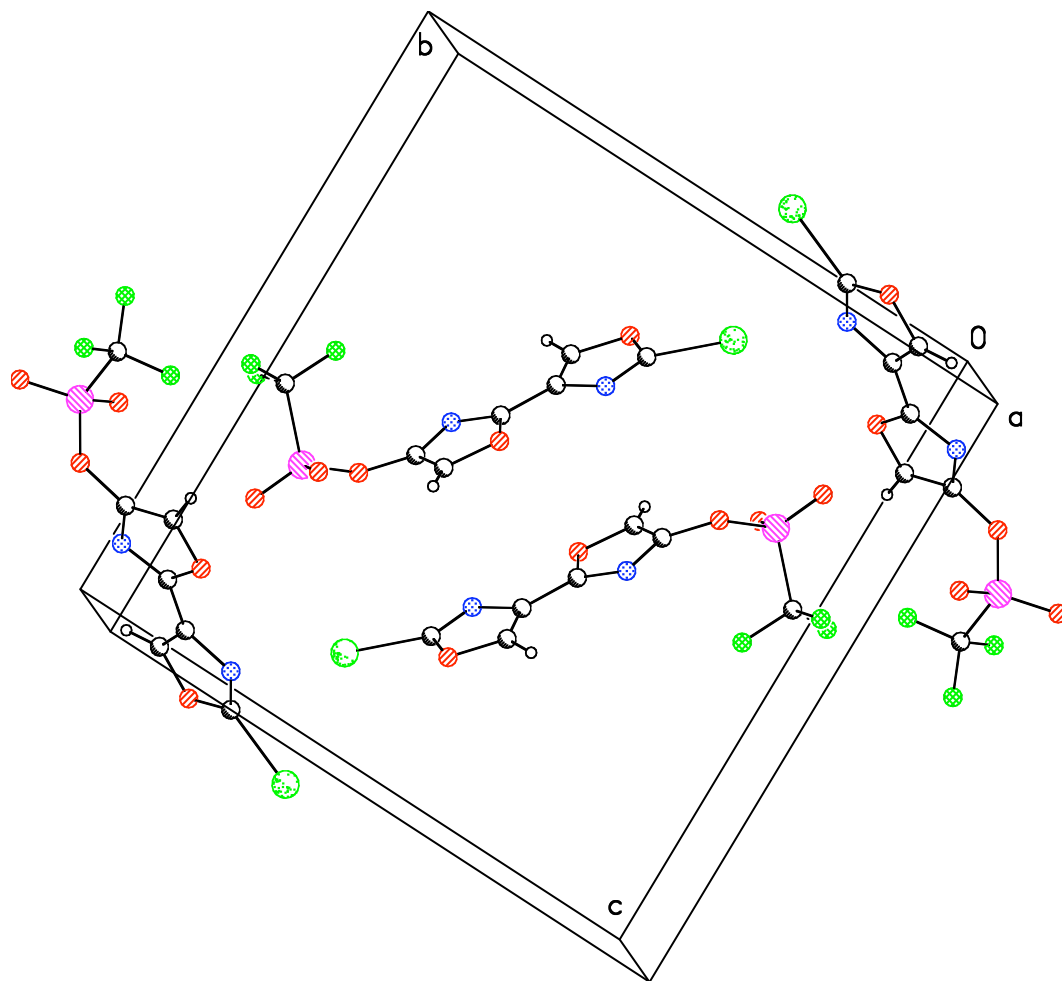
**Figure A5.1.3** Molecule B



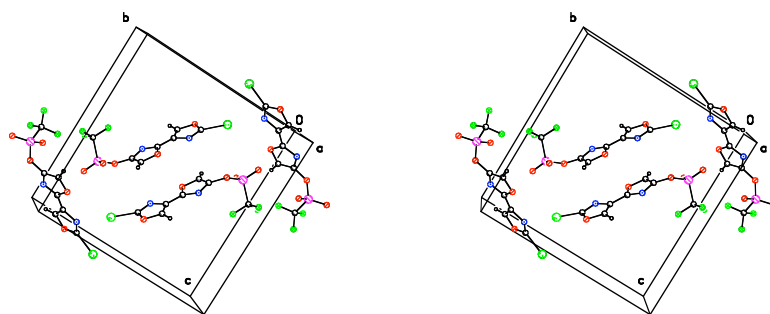
**Figure A5.1.4** *Overlap of molecule A and B emphasizing the torsion angle around the C(6)-O(3) bond*



**Figure A5.1.5** *Overlap of molecule A and B emphasizing the torsion angle around the O(3)-S bond*



**Figure A5.1.6** Packing in the unit cell with the I(1)-N(1B) interaction emphasized



**Figure A5.1.7** Stereo view of the packing in the unit cell with the I(1)-N(1B) interaction emphasized

**Table A5.1.2** Atomic coordinates ( $\times 10^4$ ) and equivalent isotropic displacement parameters ( $\text{\AA}^2 \times 10^3$ ) for **226** (CCDC 282586).  $U(\text{eq})$  is defined as the trace of the orthogonalized  $U_{ij}$  tensor.

	x	y	z	$U_{\text{eq}}$
I(1)	2611(1)	3487(1)	1553(1)	17(1)
S(1)	2125(1)	8201(1)	6603(1)	18(1)
F(1A)	2445(4)	9715(1)	5750(1)	44(1)
F(2A)	-1292(4)	9274(1)	5935(1)	39(1)
F(3A)	903(3)	8577(1)	4943(1)	29(1)
O(1A)	-1301(3)	4609(1)	2445(1)	21(1)
O(2A)	3752(3)	5878(1)	4665(1)	19(1)
O(3A)	701(3)	7278(1)	6286(1)	17(1)
O(4A)	4719(4)	8117(2)	6483(1)	28(1)
O(5A)	1112(4)	8483(1)	7431(1)	25(1)
N(1A)	2396(4)	4804(2)	3161(1)	15(1)
N(2A)	-68(4)	6392(2)	4929(1)	16(1)
C(1A)	1153(5)	4399(2)	2502(2)	15(1)
C(2A)	-1614(5)	5227(2)	3160(2)	20(1)
C(3A)	609(5)	5342(2)	3598(2)	13(1)
C(4A)	1312(5)	5888(2)	4403(2)	13(1)
C(5A)	3925(5)	6421(2)	5442(2)	20(1)
C(6A)	1616(5)	6724(2)	5578(2)	15(1)
C(7A)	954(5)	8991(2)	5757(2)	22(1)
I(2)	2895(1)	5915(1)	10688(1)	27(1)
S(2)	3024(1)	11753(1)	7553(1)	19(1)
F(1B)	3756(3)	12036(2)	5882(1)	39(1)
F(2B)	6039(3)	10962(1)	6438(1)	27(1)
F(3B)	6889(3)	12400(1)	6769(1)	29(1)
O(1B)	596(3)	7723(1)	10466(1)	19(1)
O(2B)	6105(3)	9010(1)	8594(1)	16(1)
O(3B)	4951(3)	11381(1)	8288(1)	18(1)
O(4B)	1164(4)	11076(2)	7332(1)	26(1)
O(5B)	2497(4)	12676(2)	7808(2)	32(1)
N(1B)	4077(4)	7636(2)	9688(1)	15(1)
N(2B)	3301(4)	10062(2)	9005(1)	14(1)
C(1B)	2595(5)	7220(2)	10211(2)	17(1)
C(2B)	865(5)	8548(2)	10051(2)	17(1)
C(3B)	2946(5)	8489(2)	9579(2)	14(1)
C(4B)	4040(5)	9214(2)	9059(2)	13(1)
C(5B)	6713(5)	9817(2)	8192(2)	17(1)
C(6B)	5014(5)	10439(2)	8451(2)	15(1)
C(7B)	5080(5)	11791(2)	6599(2)	23(1)

**Table A5.1.3** Bond lengths [Å] and angles [°] for **226** (CCDC 282586)

I(1)-C(1A)	2.074(3)
S(1)-O(5A)	1.4128(19)
S(1)-O(4A)	1.419(2)
S(1)-O(3A)	1.5838(19)
S(1)-C(7A)	1.833(3)
F(1A)-C(7A)	1.317(3)
F(2A)-C(7A)	1.311(3)
F(3A)-C(7A)	1.329(3)
O(1A)-C(1A)	1.357(3)
O(1A)-C(2A)	1.378(3)
O(2A)-C(4A)	1.356(3)
O(2A)-C(5A)	1.373(3)
O(3A)-C(6A)	1.404(3)
N(1A)-C(1A)	1.287(3)
N(1A)-C(3A)	1.404(3)
N(2A)-C(4A)	1.304(3)
N(2A)-C(6A)	1.372(3)
C(2A)-C(3A)	1.348(4)
C(2A)-H(2A)	0.96(3)
C(3A)-C(4A)	1.447(3)
C(5A)-C(6A)	1.340(4)
C(5A)-H(5A)	0.92(3)
I(2)-C(1B)	2.049(3)
S(2)-O(5B)	1.408(2)
S(2)-O(4B)	1.418(2)
S(2)-O(3B)	1.591(2)
S(2)-C(7B)	1.833(3)
F(1B)-C(7B)	1.323(3)
F(2B)-C(7B)	1.325(4)
F(3B)-C(7B)	1.321(3)
O(1B)-C(1B)	1.361(3)
O(1B)-C(2B)	1.374(3)
O(2B)-C(4B)	1.357(3)
O(2B)-C(5B)	1.376(3)
O(3B)-C(6B)	1.394(3)
N(1B)-C(1B)	1.295(3)
N(1B)-C(3B)	1.392(3)
N(2B)-C(4B)	1.298(3)
N(2B)-C(6B)	1.381(3)
C(2B)-C(3B)	1.345(4)
C(2B)-H(2B)	0.95(3)
C(3B)-C(4B)	1.461(4)
C(5B)-C(6B)	1.344(4)
C(5B)-H(5B)	1.14(3)
O(5A)-S(1)-O(4A)	122.97(13)
O(5A)-S(1)-O(3A)	106.06(12)
O(4A)-S(1)-O(3A)	110.99(12)
O(5A)-S(1)-C(7A)	107.22(13)
O(4A)-S(1)-C(7A)	106.61(13)
O(3A)-S(1)-C(7A)	100.73(12)

C(1A)-O(1A)-C(2A)	104.0(2)
C(4A)-O(2A)-C(5A)	105.2(2)
C(6A)-O(3A)-S(1)	119.74(17)
C(1A)-N(1A)-C(3A)	103.7(2)
C(4A)-N(2A)-C(6A)	102.6(2)
N(1A)-C(1A)-O(1A)	115.2(2)
N(1A)-C(1A)-I(1)	125.35(19)
O(1A)-C(1A)-I(1)	119.42(17)
C(3A)-C(2A)-O(1A)	107.7(2)
C(3A)-C(2A)-H(2A)	131.2(19)
O(1A)-C(2A)-H(2A)	120.6(19)
C(2A)-C(3A)-N(1A)	109.4(2)
C(2A)-C(3A)-C(4A)	130.7(2)
N(1A)-C(3A)-C(4A)	119.9(2)
N(2A)-C(4A)-O(2A)	114.1(2)
N(2A)-C(4A)-C(3A)	129.4(2)
O(2A)-C(4A)-C(3A)	116.4(2)
C(6A)-C(5A)-O(2A)	105.6(2)
C(6A)-C(5A)-H(5A)	135(2)
O(2A)-C(5A)-H(5A)	119(2)
C(5A)-C(6A)-N(2A)	112.5(2)
C(5A)-C(6A)-O(3A)	130.0(2)
N(2A)-C(6A)-O(3A)	117.5(2)
F(2A)-C(7A)-F(1A)	108.7(3)
F(2A)-C(7A)-F(3A)	108.9(2)
F(1A)-C(7A)-F(3A)	108.4(2)
F(2A)-C(7A)-S(1)	111.1(2)
F(1A)-C(7A)-S(1)	109.2(2)
F(3A)-C(7A)-S(1)	110.4(2)
O(5B)-S(2)-O(4B)	123.51(14)
O(5B)-S(2)-O(3B)	107.15(13)
O(4B)-S(2)-O(3B)	110.21(11)
O(5B)-S(2)-C(7B)	106.84(14)
O(4B)-S(2)-C(7B)	107.37(13)
O(3B)-S(2)-C(7B)	98.96(12)
C(1B)-O(1B)-C(2B)	104.3(2)
C(4B)-O(2B)-C(5B)	104.9(2)
C(6B)-O(3B)-S(2)	119.66(16)
C(1B)-N(1B)-C(3B)	103.1(2)
C(4B)-N(2B)-C(6B)	102.8(2)
N(1B)-C(1B)-O(1B)	114.9(2)
N(1B)-C(1B)-I(2)	128.2(2)
O(1B)-C(1B)-I(2)	116.89(18)
C(3B)-C(2B)-O(1B)	107.2(2)
C(3B)-C(2B)-H(2B)	131.5(18)
O(1B)-C(2B)-H(2B)	121.3(18)
C(2B)-C(3B)-N(1B)	110.5(2)
C(2B)-C(3B)-C(4B)	126.9(2)
N(1B)-C(3B)-C(4B)	122.5(2)
N(2B)-C(4B)-O(2B)	114.6(2)
N(2B)-C(4B)-C(3B)	127.2(2)
O(2B)-C(4B)-C(3B)	118.2(2)
C(6B)-C(5B)-O(2B)	105.9(2)
C(6B)-C(5B)-H(5B)	131.3(14)

O(2B)-C(5B)-H(5B)	122.7(14)
C(5B)-C(6B)-N(2B)	111.8(2)
C(5B)-C(6B)-O(3B)	128.0(2)
N(2B)-C(6B)-O(3B)	120.0(2)
F(3B)-C(7B)-F(2B)	109.7(2)
F(3B)-C(7B)-F(1B)	109.1(2)
F(2B)-C(7B)-F(1B)	109.2(2)
F(3B)-C(7B)-S(2)	110.4(2)
F(2B)-C(7B)-S(2)	109.83(19)
F(1B)-C(7B)-S(2)	108.5(2)

---



**Table A5.1.4** Anisotropic displacement parameters ( $\text{\AA}^2 \times 10^4$ ) for **226** (CCDC 282586). The anisotropic displacement factor exponent takes the form:  $-2\pi^2 [h^2 a^{*2} U^{11} + \dots + 2 h k a^* b^* U^{12}]$ .

	$U^{11}$	$U^{22}$	$U^{33}$	$U^{23}$	$U^{13}$	$U^{12}$
I(1)	213(1)	135(1)	163(1)	-16(1)	4(1)	9(1)
S(1)	183(3)	205(4)	153(3)	-35(3)	0(2)	-9(3)
F(1A)	608(14)	276(11)	434(11)	62(9)	-48(10)	-215(10)
F(2A)	367(11)	449(13)	360(10)	124(9)	119(8)	207(9)
F(3A)	441(11)	258(10)	157(8)	-11(7)	8(7)	21(8)
O(1A)	131(10)	257(11)	224(10)	-80(8)	-11(8)	-7(8)
O(2A)	136(9)	185(11)	236(10)	-76(8)	-20(8)	45(8)
O(3A)	206(10)	161(10)	152(9)	-19(7)	26(7)	-28(8)
O(4A)	150(10)	334(13)	327(11)	-115(10)	-19(8)	-27(9)
O(5A)	324(12)	273(12)	146(9)	-47(8)	16(8)	33(9)
N(1A)	124(11)	134(12)	187(11)	-6(9)	-6(8)	15(8)
N(2A)	144(11)	171(12)	151(10)	12(9)	13(8)	-11(9)
C(1A)	140(13)	128(14)	174(12)	9(10)	20(10)	-9(10)
C(2A)	145(14)	194(16)	259(14)	-88(12)	25(11)	18(11)
C(3A)	118(12)	121(13)	160(12)	17(10)	12(9)	3(9)
C(4A)	124(13)	112(13)	164(12)	28(10)	-1(10)	2(9)
C(5A)	195(15)	192(16)	195(13)	-46(11)	-42(11)	41(11)
C(6A)	157(13)	135(14)	164(12)	-2(10)	29(10)	-5(10)
C(7A)	239(15)	191(16)	226(14)	-28(12)	57(11)	-15(12)
I(2)	383(1)	149(1)	293(1)	70(1)	73(1)	31(1)
S(2)	176(3)	178(4)	232(3)	67(3)	23(3)	11(3)
F(1B)	316(11)	599(14)	258(9)	217(9)	-64(8)	-25(9)
F(2B)	304(10)	273(10)	239(8)	-8(7)	55(7)	-9(8)
F(3B)	225(9)	261(10)	377(10)	80(8)	25(8)	-79(7)
O(1B)	205(10)	185(11)	195(9)	21(8)	56(8)	14(8)
O(2B)	177(10)	152(10)	161(9)	11(7)	36(7)	36(7)
O(3B)	237(10)	140(10)	158(9)	28(7)	-17(7)	-3(8)
O(4B)	143(10)	293(12)	344(11)	134(10)	-20(8)	-26(8)
O(5B)	366(13)	186(12)	423(13)	75(10)	110(10)	88(9)
N(1B)	172(12)	139(12)	150(10)	0(9)	7(9)	14(9)
N(2B)	179(12)	122(12)	129(10)	5(8)	-3(8)	5(9)
C(1B)	210(14)	129(14)	160(12)	-2(10)	1(10)	30(10)
C(2B)	222(15)	126(14)	155(12)	4(10)	2(10)	47(11)
C(3B)	145(13)	130(14)	129(11)	-25(10)	-29(9)	18(10)
C(4B)	142(13)	144(14)	106(11)	-9(9)	-12(9)	1(10)
C(5B)	187(14)	150(14)	175(12)	18(10)	18(10)	-29(10)
C(6B)	196(14)	115(14)	145(11)	0(10)	-21(10)	-10(10)
C(7B)	189(15)	260(17)	235(14)	86(12)	-16(11)	-58(12)

**Table A5.1.5** Hydrogen coordinates ( $\times 10^4$ ) and isotropic displacement parameters ( $\text{\AA}^2 \times 10^3$ ) for **226** (CCDC 282586)

	x	y	z	$U_{\text{iso}}$
H(2A)	-3150(60)	5540(20)	3230(20)	29(9)
H(5A)	5460(60)	6530(20)	5710(20)	31(9)
H(2B)	-260(50)	9040(20)	10145(19)	16(7)
H(5B)	8370(50)	9877(18)	7738(17)	12(7)

**Table A5.1.6** Torsion angles [°] for **226** (CCDC 282586)

N(2A)-C(6A)-O(3A)-S(1)	-135.1(2)
N(2B)-C(6B)-O(3B)-S(2)	-81.0(3)
C(6A)-O(3A)-S(1)-C(7A)	81.2(2)
C(6B)-O(3B)-S(2)-C(7B)	-96.8(2)

**Table A5.1.7** CH $\cdots$ N hydrogen bonds for **226** (CCDC 282586) [ $\text{\AA}$  and  $^\circ$ ]

D-H...A	d(D-H)	d(H...A)	d(D...A)	$\angle$ (DHA)
C(2A)-H(2A)...N(1A)#1	0.96(3)	2.61(3)	3.277(4)	127(2)
C(5A)-H(5A)...N(2A)#2	0.92(3)	2.72(3)	3.348(4)	127(2)
C(2B)-H(2B)...N(2B)#3	0.95(3)	2.45(3)	3.334(4)	155(2)
C(5B)-H(5B)...O(5A)#2	1.14(3)	2.54(3)	3.269(3)	120.1(17)
C(5B)-H(5B)...O(4B)#2	1.14(3)	2.40(3)	3.323(3)	136.6(18)

Symmetry transformations used to generate equivalent atoms:

#1  $x-1, y, z$ #2  $x+1, y, z$ #3  $-x, -y+2, -z+2$

## **APPENDIX SIX**

### **Notebook Cross-Reference**

The following notebook cross-reference has been included to facilitate access to the original spectroscopic data obtained for the compounds presented in this thesis. For each compound, both hardcopy and electronic characterization folders have been created that contain copies of the original  $^1\text{H}$  NMR,  $^{13}\text{C}$  NMR, and IR spectra. All notebooks and spectral data are stored in the Stoltz archives.

**Table A6.1** Compounds appearing in Chapter 2: The Resolution of Important Pharmaceutical Building Blocks by Palladium-Catalyzed Aerobic Oxidation of Secondary Alcohols

Compound	<sup>1</sup> H NMR	<sup>13</sup> C NMR	IR
<b>67</b>	DDC-I-141	DDC-I-141	DDC-I-141
<b>68</b>	DDC-I-137	DDC-I-137	DDC-I-137
<b>69</b>	DDC-II-267-OH	DDC-II-267-OH	DDC-II-267-OH
<b>70</b>	DDC-II-269-OH	DDC-II-269-OH	DDC-II-269-OH
<b>73</b>	DDC-I-163	DDC-I-163	DDC-I-163
<b>75</b>	DDC-I-265	DDC-I-265	DDC-I-265
<b>77</b>	DDC-II-231	DDC-II-231	DDC-II-231
<b>78</b>	DDC-II-169	DDC-II-169	DDC-II-169

**Table A6.2** Compounds appearing in Chapter 3: The Total Synthesis of (+)- and (–)- Dragmacidin F

Compound	<sup>1</sup> H NMR	<sup>13</sup> C NMR	IR
<b>94</b>	DDC-IV-223	DDC-III-107	DDC-IV-223
<b>166</b>	NKG-XVI-105	NKG-XVI-105	NKG-XVI-105
<b>95</b>	DDC-III-121	DDC-III-121	DDC-III-121
<b>97</b>	DDC-VIII-65	DDC-VIII-65	DDC-VIII-65
<b>98</b>	NKG-XXIII-75	NKG-XIX-133	NKG-XXIII-75
<b>96</b>	NKG-XIX-237	NKG-XIX-131	NKG-XIX-131
<b>101</b>	NKG-XV-123	NKG-XIX-103	NKG-XIX-103
<b>170</b>	DDC-IV-221	DDC-IV-221	DDC-IV-221
<b>91</b>	NKG-XIX-107	NKG-XIX-107	NKG-XIX-107
<b>172</b>	DDC-IV-217	DDC-IV-217	DDC-IV-217
<b>92</b>	DDC-IV-61	DDC-IV-61	NKG-XVIII-63
<b>90</b>	NKG-XIV-301P3 (CDCl <sub>3</sub> ) NKG-XXI-101 (C <sub>6</sub> D <sub>6</sub> )	NKG-XXI-101	NKG-XIX-112
<b>102</b>	NKG-XVI-295P1	NKG-XVI-295P1	NKG-XVI-295P1
<b>107</b>	DDC-VI-271	DDC-VI-271	DDC-VI-251
<b>108</b>	DDC-VIII-193	DDC-VIII-193	DDC-VIII-193
<b>109</b>	DDC-VIII-167	DDC-VIII-167	DDC-VIII-167
<b>110</b>	DDC-VIII-195	DDC-VIII-195	DDC-VIII-195
<b>111</b>	DDC-VI-269	DDC-VI-269	DDC-VIII-169
<b>173</b>	DDC-VIII-171	DDC-VIII-171	DDC-VIII-171
<b>112</b>	DDC-VIII-173	DDC-VIII-173	DDC-VIII-173
<b>113</b>	DDC-VIII-175	DDC-VIII-175	DDC-VIII-175
<b>114</b>	DDC-VIII-191	DDC-VIII-191	DDC-VIII-191
<b>176</b>	NKG-XIX-118	NKG-XIX-118	NKG-XIX-118
<b>115</b>	NKG-XIX-119	NKG-XIX-119	NKG-XIX-119
<b>177</b>	NKG-XIX-121	NKG-XIX-121	NKG-XIX-121
<b>89</b>	NKG-XIX-123	NKG-XIX-123	NKG-XIX-123
<b>118</b>	NKG-XIX-135	NKG-XIX-135	NKG-XIX-135
<b>119</b>	NKG-XIX-143	NKG-XIX-143	NKG-XIX-143

Compound	<sup>1</sup> H NMR	<sup>13</sup> C NMR	IR
<b>120</b>	NKG-XIX-139	NKG-XIX-139	NKG-XIX-139
<b>124</b>	NKG-XIX-37		
<b>121</b>	NKG-XIX-151	NKG-XIX-151	NKG-XIX-151
<b>125</b>	NKG-XIX-163	NKG-XIX-163	NKG-XIX-155
<b>(+)-84</b>	NKG-XIX-227B	NKG-XIX-227	NKG-XIX-227
<b>129</b>	DDC-VIII-143	DDC-VIII-143	DDC-VIII-143
<b>180</b>	NKG-XXII-53	NKG-XXII-53	NKG-XXII-53
<b>132</b>	DDC-VII-201	DDC-VII-195	DDC-VII-195
<b>133</b>	DDC-VII-207	DDC-VII-225	DDC-VII-207
<b>131</b>	DDC-VII-217	DDC-VII-213	DDC-VII-213
<b>127</b>	DDC-VIII-99	NKG-XXII-81	NKG-XXII-81
<b>135</b>	DDC-VIII-291	DDC-VIII-291	DDC-VIII-291
<b>138</b>	DDC-IX-51	DDC-IX-51	DDC-IX-51
<b>137</b>	DDC-IX-111	DDC-IX-111	DDC-IX-111
<b>181</b>	DDC-IX-35		
<b>140</b>	DDC-IX-41	DDC-IX-41	DDC-IX-41
<b>141</b>	DDC-IX-53	DDC-IX-53	DDC-IX-53
<b>142</b>	DDC-VII-67	DDC-VII-67	DDC-VII-67
<b>143</b>	DDC-VIII-121	DDC-VIII-121	DDC-VIII-121
<b>144</b>	DDC-VIII-117	DDC-VIII-117	DDC-VIII-117
<b>145</b>	DDC-VIII-81	DDC-VIII-55	DDC-VIII-81
<b>146</b>	NKG-XXII-41	NKG-XXII-41	NKG-XXII-41
<b>147</b>	NKG-XXII-43	NKG-XXII-43	NKG-XXII-43
<b>148</b>	DDC-VIII-69	DDC-VIII-69	DDC-VIII-69
<b>149</b>	DDC-VII-299	DDC-VII-299	DDC-VII-299
<b>150</b>	DDC-VIII-213	DDC-VIII-213	DDC-VIII-213
<b>151</b>	DDC-VIII-187	DDC-VIII-187	DDC-VIII-187
<b>152</b>	DDC-VIII-225	DDC-VIII-225	DDC-VIII-215-T
<b>153</b>	DDC-VIII-273 (CDCl <sub>3</sub> ) DDC-VIII-249-Prep (C <sub>6</sub> D <sub>6</sub> )	DDC-VIII-249-Prep	DDC-VIII-273
<b>128</b>	NKG-XXII-116	NKG-XXII-116	NKG-XXII-116
<b>156</b>	NKG-XXII-131	NKG-XXII-131	NKG-XXII-131



Compound	<sup>1</sup> H NMR	<sup>13</sup> C NMR	IR
<b>157</b>	DDC-VIII-165	DDC-VIII-165	DDC-VIII-165
<b>158</b>	DDC-VIII-199	DDC-VIII-199	DDC-VIII-199
<b>159</b>	NKG-XXII-97	DDC-VIII-189	DDC-VIII-189
<b>160</b>	DDC-VIII-299	DDC-VIII-299	DDC-VIII-299
<b>161</b>	DDC-VIII-197	DDC-VIII-197	DDC-VIII-197
<b>187</b>	NKG-XXIII-57	NKG-XXIII-57	NKG-XXIII-57
<b>163</b>	NKG-XXII-213	NKG-XXII-213	NKG-XXII-213
<b>162</b>	NKG-XXIII-35	NKG-XXII-209	NKG-XXII-209
<b>(-)-84</b>	NKG-XXIII-179		

**Table A6.3** Compounds appearing in Chapter 4: Progress Toward The Total Synthesis of Telomestatin

Compound	<sup>1</sup> H NMR	<sup>13</sup> C NMR	IR
<b>219</b>	DDC-XI-191	HMZ-VII-275	HMZ-VII-275
<b>220</b>	TAD-I-137b2	HMZ-X-261	HMZ-X-261
<b>214</b>	DDC-XI-177	DDC-XI-177	DDC-XI-177
<b>247</b>	DDC-X-61	TAD-I-141	TAD-I-139
<b>224</b>	DDC-XIV-89	DDC-XIV-89	DDC-XIV-89
<b>225</b>	DDC-XIV-119	DDC-XIV-91	DDC-XIV-91
<b>226</b>	DDC-IX-291	DDC-XI-275	DDC-XI-275
<b>227</b>	DDC-XIV-87	HMZ-VII-283	HMZ-VII-283
<b>228</b>	DDC-XIII-277	HMZ-XI-235	HMZ-XI-235
<b>230</b>	DDC-XI-193	DDC-XIII-125	DDC-XIII-125
<b>232</b>	DDC-XI-205	DDC-XI-205	HMZ-IX-229
<b>233</b>	DDC-XI-269	DDC-XIII-129	DDC-XIII-129
<b>235</b>	DDC-XIV-115	DDC-XIV-115	DDC-XIV-115
<b>236</b>	DDC-XIV-111	DDC-XIV-111	DDC-XIV-111
<b>238</b>	DDC-XIV-79	DDC-XIV-79	DDC-XIV-79
<b>215</b>	JTM-XIII-247B	JTM-XIII-247B	JTM-XIII-247B

## COMPREHENSIVE BIBLIOGRAPHY

Agrofoglio, L. A.; Gillaizeau, I.; Saito, Y. *Chem. Rev.* **2003**, *103*, 1875–1916.

Alberico, D.; Scott, M. E.; Lautens, M. *Chem. Rev.* **2007**, *107*, 174–238.

Ali, I. S.; Sudalai, A. *Tetrahedron Lett.* **2002**, *43*, 5435–5436.

Altenbach, H.-J.; Himmeldirk, K. *Tetrahedron: Asymmetry* **1995**, *6*, 1077–1080.

Amatore, C.; Jutand, A. *Acc. Chem. Res.* **2000**, *33*, 314–321.

Amatore, C.; Jutand, A. *J. Organomet. Chem.* **1999**, *576*, 254–278.

Anderson, B. A.; Becke, L. M.; Booher, R. N.; Flaugh, M. E.; Harn, N. K.; Kress, T. J.;  
Varie, D. L.; Wepsiec, J. P. *J. Org. Chem.* **1997**, *62*, 8634–8639.

Anderson, B. A.; Harn, N. K. *Synthesis* **1996**, 583–585.

Anderson, S.; Anderson, H. L.; Sanders, J. K. M. *Acc. Chem. Res.* **1993**, *26*, 469–475.

Araki, H.; Katoh, T.; Inoue, M. *Synlett* **2006**, 555–558.

Araki, H.; Katoh, T.; Inoue, M. *Tetrahedron Lett.* **2007**, 48, 3713–3717.

Artandi, S. E. *N. Engl. J. Med.* **2006**, 355, 1195–1197.

Atkins, J. M.; Vedejs, E. *Org. Lett.* **2005**, 7, 3351–3354.

Audebert, P.; Bidan, G. *Synthetic Metals* **1986**, 15, 9–22.

Aygün, A.; Pindur, U. *Curr. Med. Chem.* **2003**, 10, 1113–1127.

Bagdanoff, J. T.; Ferreira, E. M.; Stoltz, B. M. *Org. Lett.* **2003**, 5, 835–837.

Bagdanoff, J. T.; Stoltz, B. M. *Angew. Chem., Int. Ed.* **2004**, 43, 353–357.

Bailey, D. M.; Johnson, R. E. *J. Med. Chem.* **1973**, 16, 1300–1302.

Baran, P. S.; Corey, E. J. *J. Am. Chem. Soc.* **2002**, 124, 7904–7905.

Barbieri, C. M.; Srinivasan, A. R.; Rzuczek, S. G.; Rice, J. E.; LaVoie, E. J.; Pilch, D. S. *Nucleic Acids Res.* **2007**, 35, 3272–3286.

Barco, A.; Benetti, S.; De Risi, C.; Marchetti, P.; Pollini, G. P.; Zanirato, V. *Tetrahedron: Asymmetry* **1997**, 8, 3515–3545.

Barros, M. T.; Maycock, C. D.; Ventura, M. R. *J. Chem. Soc., Perkin Trans. I* **2001**, 166–173.

Beccalli, E. M.; Broggini, G.; Martinelli, M.; Paladino, G. *Tetrahedron* **2005**, *61*, 1077–1082.

Beccalli, E. M.; Broggini, G.; Martinelli, M.; Sottocornola, S. *Chem. Rev.* **2007**, *107*, 5318–5365.

Beck, E. M.; Grimster, N. P.; Hatley, R.; Gaunt, M. J. *J. Am. Chem. Soc.* **2006**, *128*, 2528–2529.

Behforouz, M.; Haddad, J.; Cai, W.; Arnold, M. B.; Farahnaz, M.; Sousa, A. C.; Horn, M. A. *J. Org. Chem.* **1996**, *61*, 6552–6555.

Beletskaya, I. P.; Cheprakov, A. V. *Chem. Rev.* **2000**, *100*, 3009–3066.

Bergbreiter, D. E.; Chen, B. *J. Chem. Soc., Chem. Commun.* **1983** 1238–1239.

Bergens, S. H.; Bosnich, B. *J. Am. Chem. Soc.* **1991**, *113*, 958–967.

Bergman, J.; Venemalm, L. *J. Org. Chem.* **1992**, *57*, 2495–2497.

Bernheim, F.; Morgan, J. E. *Nature* **1939**, *144*, 290.

Bhupathy, M.; McNamara, J. M.; Sidler, D. R.; Volante, R. P.; Bergan, J. J. (Merck & Co., Inc.). WO 95/18107, 1995.

Bhupathy, M.; McNamara, J. M.; Sidler, D. R.; Volante, R. P.; Bergan, J. (Merck & Co., Inc.), U.S. Patent 5,614,632, 1997.

Billingsley, K. L.; Anderson, K. W.; Buchwald, S. L. *Angew. Chem., Int. Ed.* **2006**, *45*, 3484–3488.

Binz, N.; Shalaby, T.; Rivera, P.; Shin-Ya, K.; Grotzer, M. A. *Eur. J. Cancer* **2005**, *41*, 2873–2881.

Blackburn, E. H.; Greider, C. W.; Szostak, J. W. *Nature Med.* **2006**, *12*, 1133–1138.

Blake, A. J.; Hannam, J. S.; Jolliffe, K. A.; Pattenden, G. *Synlett* **2000**, 1515–1518.

Blankenstein, J.; Zhu, J. *Eur. J. Org. Chem.* **2005**, 1949–1964.

Blunt, J. W.; Copp, B. R.; Munro, M. H. G.; Northcote, P. T.; Prinsep, M. R. *Nat. Prod. Rep.* **2004**, *21*, 1–49.

Boehm, J. C.; Gleason, J. G.; Pendrak, I.; Sarau, H. M.; Schmidt, D. B.; Foley, J. J.; Kingsbury, W. D. *J. Med. Chem.* **1993**, *36*, 3333–3340.

Bressy, C.; Alberico, D.; Lautens, M. *J. Am. Chem. Soc.* **2005**, *127*, 13148–13149.

Brown, J. M. *Angew. Chem., Int. Ed. Engl.* **1987**, *26*, 190–203.

Buchwald, S. L.; Mauger, C.; Mignani, G.; Scholz, U. *Adv. Synth. Catal.* **2006**, *348*, 23–39.

Burgett, A. W. G.; Li, Q.; Wei, Q.; Harran, P. G. *Angew. Chem., Int. Ed.* **2003**, *42*, 4961–4966.

Cacchi, S.; Fabrizi, G. *Chem. Rev.* **2005**, *105*, 2873–2920.

Campeau, L.-C.; Parisien, M.; Jean, A.; Fagnou, K. *J. Am. Chem. Soc.* **2006**, *128*, 581–590.

Campeau, L.-C.; Parisien, M.; Leblanc, M.; Fagnou, K. *J. Am. Chem. Soc.* **2004**, *126*, 9186–9187.

Capon, R. J.; Rooney, F.; Murray, L. M.; Collins, E.; Sim, A. T. R.; Rostas, J. A. P.; Butler, M. S.; Carroll, A. R. *J. Nat. Prod.* **1998**, *61*, 660–662.

Carbonnelle, A.-C.; Zhu, J. *Org. Lett.* **2000**, 2, 3477–3480.

Caspi, D. D.; Ebner, D. C.; Bagdanoff, J. T.; Stoltz, B. M. *Adv. Synth. Catal.* **2004**, 346, 185–189.

Caspi, D. D.; Garg, N. K.; Stoltz, B. M. *Org. Lett.* **2005**, 7, 2513–2516.

Chattopadhyay, S. K.; Biswas, S. *Tetrahedron Lett.* **2006**, 47, 7897–7900.

Chattopadhyay, S. K.; Biswas, S.; Pal, B. K. *Synthesis* **2006**, 1289–1294.

Chen, M. S.; White, M. C. *J. Am. Chem. Soc.* **2004**, 126, 1346–1347.

Chen, W.; Shimada, S.; Tanaka, M. *Science* **2002**, 295, 308–310.

Chierici, L.; Gardini, G. P. *Tetrahedron* **1966**, 22, 53–56.

Chowdhury, S.; Rivalta, I.; Russo, N.; Sicilia, E. *Chem. Phys. Lett.* **2007**, 443, 183–189.

Chung, J. Y. L.; Ho, G.-J.; Chartrain, M.; Roberge, C.; Zhao, D.; Leazer, J.; Farr, R.; Robbins, M.; Emerson, K.; Mathre, D. J.; McNamara, J. M.; Hughes, D. L.; Grabowski, E. J. J.; Reider, P. J. *Tetrahedron Lett.* **1999**, 40, 6739–6743.



Ciamician, G.; Silber, P. *Chem. Ber.* **1912**, *45*, 1842–1845.

Cian, A. D.; Lacroix, L.; Douarre, C.; Temine-Smalli, N.; Trentesaux, C.; Riou, J.-F.; Mergny, J.-L. *Biochimie* **2008**, *90*, 131–155.

Clardy, J.; Walsh, C. *Nature* **2004**, *432*, 829–837.

Claridge, T. D. W. in *High-Resolution NMR Techniques in Organic Chemistry*; Pergamon: Amsterdam, 1999; pp. 320–326.

Cohen, S.; Graham, M.; Lovrecz, G.; Bache, N.; Robinson, P.; Reddel, R. *Science* **2007**, *315*, 1850–1853.

Cotton, F. A.; Koshevoy, I. O.; Lahuerta, P.; Murillo, C. A.; Sanaú, M.; Ubeda, M. A.; Zhao, Q. *J. Am. Chem. Soc.* **2006**, *128*, 13674–13675.

Crabtree, R. H. *Science* **2002**, *295*, 288–289.

Craig, B. N.; Janssen, M. U.; Wickersham, B. M.; Rabb, D. M.; Chang, P. S.; O’Leary, D. J. *J. Org. Chem.* **1996**, *61*, 9610–9613.

Cutignano, A.; Bifulco, G.; Bruno, I.; Casapullo, A.; Gomez-Paloma, L.; Riccio, R. *Tetrahedron* **2000**, *56*, 3743–3748.

Dauben, W. G.; Hance, P. D. *J. Am. Chem. Soc.* **1955**, 77, 2451–2453.

Dauben, W. G.; Hayes, W. K.; Schwarz, J. S. P.; McFarland, J. W. *J. Am. Chem. Soc.* **1960**, 82, 2232–2238.

Daugulis, O.; Zaitsev, V. G.; Shabasov, D.; Pham, O.-N.; Lazareva, A. *Synlett* **2006**, 3382–3388.

de Boer, T. J.; Backer, H. J. *Org. Synth.* **1956**, 36, 16–19.

De Carolis, M.; Protti, S.; Fagnoni, M.; Albini, A. *Angew. Chem., Int. Ed.* **2005**, 44, 1232–1236.

Deeley, J.; Pattenden, G. *Chem. Commun.* **2005**, 797–799.

Desai, L. V.; Sanford, M. S. *Angew. Chem., Int. Ed.* **2007**, 46, 5737–5740.

Desai, R. C.; Cicala, P.; Meurer, L. C.; Finke, P. E. *Tetrahedron Lett.* **2002**, 43, 4569–4570.

Doi, T.; Yoshida, M.; Shin-ya, K.; Takahashi, T. *Org. Lett.* **2006**, 8, 4165–4167.

Dounay, A. B.; Overman, L. E. *Chem. Rev.* **2003**, 103, 2945–2963.

Duddu, R.; Eckhardt, M.; Furlong, M.; Knoess, H. P.; Berger, S.; Knochel, P. *Tetrahedron* **1994**, *50*, 2415–2432.

Edwards, M. P.; Doherty, A. M.; Ley, S. V.; Organ, H. M. *Tetrahedron* **1986**, *42*, 3723–3729.

Edwards, M. P.; Ley, S. V.; Lister, S. G.; Palmer, B. D. *J. Chem. Soc., Chem. Commun.* **1983**, 630–633.

Edwards, M. P.; Ley, S. V.; Lister, S. G.; Palmer, B. D.; Williams, D. J. *J. Org. Chem.* **1984**, *49*, 3503–3516.

Eliel, E. L.; Wilen, S. H.; Mander, L. N. *Stereochemistry of Organic Compounds*; Wiley-Interscience: New York, 1994.

Endoh, N.; Tsuboi, K.; Kim, R.; Yonezawa, Y.; Shin, C. *Heterocycles* **2003**, *60*, 1567–1572.

Ercolani, G.; Mandolini, L.; Masci, B. *J. Am. Chem. Soc.* **1981**, *103*, 2780–2782.

Escobar-Nuricumbo, J. J.; Campos-Alvarado, C.; Ríos-Moreno, G.; Morales-Morales, D.; Walsh, P. J.; Parra-Hake, M. *Inorg. Chem.* **2007**, *46*, 6182–6189.

Fagnoni, M.; Albini, A. *Acc. Chem. Res.* **2005**, 38, 713–721.

Fahy, E.; Potts, B. C. M.; Faulkner, D. J.; Smith, K. *J. Nat. Prod.* **1991**, 54, 564–569.

Faulkner, D. J. *Nat. Prod. Rep.* **2002**, 19, 1–48.

Feldman, K. S.; Ngermmeesri, P. *Org. Lett.* **2005**, 7, 5449–5452.

Felpin, F.-X.; Landais, Y. *J. Org. Chem.* **2005**, 70, 6441–6446.

Ferreira, E. M.; Stoltz, B. M. *J. Am. Chem. Soc.* **2001**, 123, 7725–7726.

Ferreira, E. M.; Stoltz, B. M. *J. Am. Chem. Soc.* **2003**, 125, 9578–9579.

Ferreira, E. M.; Zhang, H.; Stoltz, B. M. *Tetrahedron* **2008**, (in press).

Fife, W. K.; Zhang, Z.-d. *J. Org. Chem.* **1986**, 51, 3744–3746.

Fincham, C. I.; Higginbottom, M.; Hill, D. R.; Horwell, D. C.; O'Toole, J. C.; Ratcliffe, G. S.; Rees, D. C.; Roberts, E. *J. Med. Chem.* **1992**, 35, 1472–1484.

Flegeau, E. F.; Popkin, M. E.; Greaney, M. F. *Org. Lett.* **2006**, 8, 2495–2498.

Freccero, M.; Fagnoni, M.; Albini, A. *J. Am. Chem. Soc.* **2003**, *125*, 13182–13190.

Garg, N. K. "The total synthesis of dragmacidins D and F." Ph.D. Thesis, California Institute of Technology, 2005. <http://resolver.caltech.edu/CaltechETD:etd-03222005-133937>

Garg, N. K.; Caspi, D. D.; Stoltz, B. M. *J. Am. Chem. Soc.* **2004**, *126*, 9552–9553.

Garg, N. K.; Caspi, D. D.; Stoltz, B. M. *J. Am. Chem. Soc.* **2005**, *127*, 5970–5978.

Garg, N. K.; Caspi, D. D.; Stoltz, B. M. *Synlett* **2006**, 3081–3087.

Garg, N. K.; Sarpong, R.; Stoltz, B. M. *J. Am. Chem. Soc.* **2002**, *124*, 13179–13184.

Garg, N. K.; Stoltz, B. M. *Chem. Commun.* **2006**, 3769–3779.

Gebhardt, K.; Schimana, J.; Krastel, P.; Dettner, K.; Rheinheimer, J.; Zeeck, A.; Fiedler, H. P. *J. Antibiot.* **2002**, *55*, 794–800.

Gilow, H. M.; Hong, Y. H.; Millirons, P. L.; Snyder, R. C.; Casteel, W. J., Jr. *J. Heterocycl. Chem.* **1986**, *23*, 1475–1480.

Gligorich, K. M.; Sigman, M. S. *Angew. Chem., Int. Ed.* **2006**, *45*, 6612–6615.

*Comprehensive Organic Synthesis*; Godleski, S. A., Trost, B. M., Fleming, I., Eds.; Pergamon Press: New York, 1991.

Gomez, D.; O'Donohue, M. F.; Wenner, T.; Douarre, C.; Macadre, J.; Koebel, P.; Giraud-Panis, M. J.; Kaplan, H.; Kolkes, A.; Shin-Ya, K.; Riou, J. F. *Cancer Res.* **2006**, *66*, 6908–6912.

Gomez, D.; Paterski, R.; Lemarteleur, T.; Shin-ya, K.; Mergny, J. L.; Riou, J. F. *J. Biol. Chem.* **2004**, *279*, 41487–41494.

Gomez, D.; Wenner, T.; Brassart, B.; Douarre, C.; O'Donohue, M. F.; Khoury, V. E.; Shin-Ya, K.; Morjani, H.; Trentesaux, C.; Riou, J. F. *J. Biol. Chem.* **2006**, *281*, 38721–38729.

Greene, T. W.; Wuts, P. G. M. *Protective Groups in Organic Synthesis*, 4<sup>th</sup> Ed.; Wiley-Interscience: New York, 2006.

Grewe, R.; Lorenzen, W.; Vining, L. *Chem. Ber.* **1954**, *87*, 793–802.

Han, X.; Stoltz, B. M.; Corey, E. J. *J. Am. Chem. Soc.* **1999**, *121*, 7600–7605.

Handy, S. T.; Zhang, Y. *Chem. Commun.* **2006**, 299–301.

Hanessian, S. In *Total Synthesis of Natural Products: The "Chiron" Approach*, Baldwin, E. J., Ed.; Pergamon Press: Oxford, 1983; pp. 206–208.

Hanessian, S.; Pan, J.; Carnell, A.; Bouchard, H.; Lesage, L. *J. Org. Chem.* **1997**, *62*, 465–473.

Harn, N. K.; Gramer, C. J.; Anderson, B. A. *Tetrahedron Lett.* **1995**, *36*, 9453–9456.

Hayashi, T. *J. Organomet. Chem.* **1999**, *576*, 195–202.

Heck, R. F. *Palladium Reagents in Organic Synthesis*; Academic Press: New York, 1985.

Helmchen, G. *J. Organomet. Chem.* **1999**, *576*, 203–214.

Hernández, D.; Riego, E.; Francesch, A.; Cuevas, C.; Albericio, F.; Álvarez, M. *Tetrahedron* **2007**, *63*, 9862–9870.

Hernández, D.; Vilar, G.; Riego, E.; Cañedo, L. M.; Cuevas, C.; Albericio, F.; Álvarez, M. *Org. Lett.* **2007**, *9*, 809–811.

Heumann, A.; Jens, K.-J.; Reglier, M. *Progress in Inorganic Chemistry*; Karlin, K. D., Ed.; Wiley and Sons: New York, 1994; Vol. 42, pp. 483–576.

Hibino, S.; Choshi, T. *Nat. Prod. Rep.* **2002**, *19*, 148–180.

Hills, I. D.; Fu, G. C. *J. Am. Chem. Soc.* **2004**, *126*, 13178–13179.

House, H. O.; Berkowitz, W. F. *J. Org. Chem.* **1963**, *28*, 307–311.

House, H. O.; Berkowitz, W. F. *J. Org. Chem.* **1963**, *28*, 2271–2276.

Huang, P.-Q. *Youji Huaxue* **1999**, *19*, 364–373.

Hughes, R. A.; Moody, C. J. *Angew. Chem., Int. Ed.* **2007**, *46*, 7930–7954.

Huntley, R. J.; Funk, R. L. *Org. Lett.* **2006**, *8*, 4775–4778.

Hutchinson, C. R.; Harmon, A. D. *J. Org. Chem.* **1975**, *40*, 3474–3480.

Hwang, D.-R.; Helquist, P.; Shekhani, M. S. *J. Org. Chem.* **1985**, *50*, 1264–1271.

Ikawa, T.; Sajiki, H.; Hirota, K. *Tetrahedron* **2004**, *60*, 6189–6195.

Incles, C. M.; Schultes, C. M.; Neidle, S. *Curr. Opin. Investig. Drugs* **2003**, *7*, 675–685.



Ishizaki, M.; Yamada, M.; Watanabe, S.-i.; Hoshino, O.; Nishitani, K.; Hayashida, M.; Tanaka, A.; Hara, H. *Tetrahedron* **2004**, *60*, 7973–7981.

Jacobs, S. A.; Podell, E. R.; Cech, T. R. *Nat. Struct. Biol.* **2006**, *13*, 218–225.

Jantos, K.; Rodriguez, R.; Ladame, S.; Shirude, P. S.; Balasubramanian, S. *J. Am. Chem. Soc.* **2006**, *128*, 13662–13663.

Jensen, D. R.; Pugsley, J. S.; Sigman, M. S. *J. Am. Chem. Soc.* **2001**, *123*, 7475–7476.

Jiang, B.; Gu, X.-H. *Bioorg. Med. Chem.* **2000**, *8*, 363–371.

Jiang, B.; Gu, X.-H. *Heterocycles* **2000**, *53*, 1559–1568.

Jiang, B.; Smallheer, J. M.; Amaral-Ly, C.; Wuonola, M. A. *J. Org. Chem.* **1994**, *59*, 6823–6827.

Jin, Z. *Nat. Prod. Rep.* **2003**, *20*, 584–605.

Kaburagi, Y.; Tokuyama, T.; Fukuyama, T. *J. Am. Chem. Soc.* **2004**, *126*, 10246–10247.

Kagan, H. B.; Fiaud, J. C. In *Topics in Stereochemistry*; Eliel, E. L., Ed.; Wiley & Sons: New York, 1988; Vol. 18, pp. 249–330.

Kanoh, K.; Matsuo, Y.; Adachi, K.; Imagawa, H.; Nishizawa, M.; Shizuri, Y. *J. Antibiot.* **2005**, *58*, 289–292.

Kawasaki, T.; Enoki, H.; Matsumura, K.; Ohyama, M.; Inagawa, M.; Sakamoto, M. *Org. Lett.* **2000**, *2*, 3027–3029.

Kawasaki, T.; Ohno, K.; Enoki, H.; Umemoto, Y.; Sakamoto, M. *Tetrahedron Lett.* **2002**, *43*, 4245–4248.

Keith, J. M.; Goddard, W. A., III; Oxgaard, J. *J. Am. Chem. Soc.* **2007**, *129*, 10361–10369.

Kelland, L. R. *Eur. J. Cancer* **2005**, *41*, 971–979.

Kelly, T. R.; Lang, F. *Tetrahedron Lett.* **1995**, *36*, 5139–5322.

Kelly, T. R.; Lang, F. *J. Org. Chem.* **1996**, *61*, 4623–4633.

Kim, M.-Y.; Vankayalapati, H.; Kazuo, S.; Wierzba, K.; Hurley, L. H. *J. Am. Chem. Soc.* **2002**, *124*, 2098–2099.

Kim, M.-Y.; Guzman-Gleason, M.; Izbicka, E.; Nishioka, D.; Hurley, L. H. *Cancer Res.* **2003**, *67*, 3247–3256.

Kim, N. W.; Piatyszek, M. A.; Prowse, K. R.; Harley, C. B.; West, M. D.; Ho, P. L. C.; Coviello, G. M.; Wright, W. E.; Weinrich, S. L.; Shay, J. W. *Science* **1994**, *266*, 2011–2015.

King, A. O.; Corley, E. G.; Anderson, R. K.; Larsen, R. D.; Verhoeven, T. R.; Reider, P. J.; Xiang, Y. B.; Belley, M.; Leblanc, Y.; Labelle, M.; Prasit, P.; Zamboni, R. J. *J. Org. Chem.* **1993**, *58*, 3731–3735.

Kiss, G. *Chem. Rev.* **2001**, *101*, 3435–3456.

Koenig, T. M.; Mitchell, D. *Tetrahedron Lett.* **1994**, *35*, 1339–1342.

Kohmoto, S.; Kashman, Y.; McConnell, O. J.; Rinehart, K. L., Jr.; Wright, A.; Koehn, F. *J. Org. Chem.* **1988**, *53*, 3116–3118.

Kopp, F.; Maraheil, M. A. *Nat. Prod. Rep.* **2007**, *24*, 735–749.

Kornfeld, E. C.; Fornefeld, E. J.; Kline, G. B.; Mann, M. J.; Morrison, D. E.; Jones, R. G.; Woodward, R. B. *J. Am. Chem. Soc.* **1956**, *78*, 3087–3114.

Kudo, N.; Perseghini, M.; Fu, G. C. *Angew. Chem., Int. Ed.* **2006**, *45*, 1282–1284.

Kuethé, J. T.; Wong, A.; Wu, J.; Davies, I. W.; Dormer, P. G.; Welch, C. J.; Hillier, M. C.; Hughes, D. L.; Reider, P. J. *J. Org. Chem.* **2002**, *67*, 5993–6000.

Kumar, A.; Ner, D. H.; Dike, S. Y. *Ind. J. Chem.* **1992**, *31B*, 803–809.

Kumar, A.; Ner, D. H.; Dike, S. Y. *Tetrahedron Lett.* **1991**, *32*, 1901–1904.

Lall, M. S.; Ramtohul, Y. K.; James, M. N. G.; Vederas, J. C. *J. Org. Chem.* **2002**, *67*, 1536–1547.

Langille, N. F.; Dakin, L. A.; Panek, J. S. *Org. Lett.* **2002**, *4*, 2485–2488.

Larock, R. C.; Hightower, T. R. *J. Org. Chem.* **1993**, *58*, 5298–5300.

Larsen, R. D.; Corley, E. G.; King, A. O.; Carroll, J. D.; Davis, P.; Verhoeven, T. R.; Reider, P. J.; Labelle, M.; Gauthier, J. Y.; Xiang, Y. B.; Zamboni, R. J. *J. Org. Chem.* **1996**, *61*, 3398–3405.

Li, J. J.; Gribble, G. W. *Palladium in Heterocyclic Chemistry*; Pergamon: New York, 2000.

Lindh, J.; Enquist, P.-A.; Pilotti, Å.; Nilsson, P.; Larhed, M. *J. Org. Chem.* **2007**, *72*, 7957–7962.

Littke, A. F.; Fu, G. C. *J. Am. Chem. Soc.* **2001**, *123*, 6989–7000.

Liu, Q.; Ferreira, E. M.; Stoltz, B. M. *J. Org. Chem.* **2007**, *72*, 7352–7358.

Liu, Y.; Gribble, G. W. *J. Nat. Prod.* **2002**, *65*, 748–749.

Magnuson, S. R. *Tetrahedron* **1995**, *51*, 2167–2213.

Mangion, I. K. "Development of Organocatalytic Direct Aldol Transformations, Total Syntheses of Brasoside and Littoralisone, and Progress Toward the Total Synthesis of Diazonamide A." Ph.D. Thesis, California Institute of Technology, 2006.  
<http://resolver.caltech.edu/CaltechETD:etd-05232006-210214>

Manthey, M. K.; González-Bello, C.; Abell, C. *J. Chem. Soc., Perkin Trans. I* **1997**, 625–628.

Marson, C. M.; Saadi, M. *Org. Biomol. Chem.* **2006**, *4*, 3892–3893.

Matsuo, Y.; Kanoh, K.; Imagawa, H.; Adachi, K.; Nishizawa, M.; Shizuri, Y. *J. Antibiot.* **2007**, *60*, 256–260.

Matsuo, Y.; Kanoh, K.; Yamori, T.; Kasai, H.; Katsuta, A.; Adachi, K.; Shin-ya, K.; Shizuri, Y. *J. Antibiot.* **2007**, *60*, 251–255.

McIntire, W. S.; Wemmer, D. E.; Chistoserdov, A.; Lidstrom, M. E. *Science* **1991**, 252, 817–824.

Meier, R.-M.; Tamm, C. *Helv. Chim. Acta*, **1991**, 74, 807–818.

Miki, Y.; Shirokoshi, H.; Asai, M.; Aoki, Y.; Matsukida, H. *Heterocycles* **2003**, 60, 2095–2101.

Minhas, G. S.; Pilch, D. S.; Kerrigan, J. E.; LaVoie, E. J.; Rice, J. E. *Bioorg. Med. Chem. Lett.* **2006**, 16, 3891–3895.

Mitchell, D.; Koenig, T. M. *Synth. Commun.* **1995**, 25, 1231–1238.

Miyake, F. Y.; Yakushijin, K.; Horne, D. A. *Org. Lett.* **2000**, 2, 3185–3187.

Miyake, F. Y.; Yakushijin, K.; Horne, D. A. *Org. Lett.* **2002**, 4, 941–943.

Miyaura, N.; Suzuki, A. *Chem. Rev.* **1995**, 95, 2457–2483.

Morris, S. A.; Andersen, R. J. *Tetrahedron* **1990**, 46, 715–720.

Muchowski, J. M.; Solas, D. R. *J. Org. Chem.* **1984**, 49, 203–205.

Muzart, J. *J. Mol. Catal. A: Chem.* **2007**, 276, 62–72.

Muzart, J. *Tetrahedron* **2005**, *61*, 5955–6008.

Muzart, J. *Tetrahedron* **2005**, *61*, 9423–9463.

Neber, P. W.; Friedolsheim, A. V. *Justus Liebigs Ann. Chem.* **1926**, *449*, 109–134.

*Handbook of Organopalladium Chemistry for Organic Synthesis*; Negishi, E., Ed.; Wiley-Interscience: New York, 2002.

Negishi, E.-i.; Anastasia, L. *Chem. Rev.* **2003**, *103*, 1979–2017.

Nicolaou, K. C.; Bulger, P. G.; Sarlah, D. *Angew. Chem., Int. Ed.* **2005**, *44*, 4442–4489.

Nielsen, R. J.; Keith, J. M.; Stoltz, B. M.; Goddard, W. A., III *J. Am. Chem. Soc.* **2004**, *126*, 7967–7974.

Nishimura, T.; Ohe, K.; Uemura, S. *J. Org. Chem.* **1999**, *64*, 6750–6755.

Nishimura, T.; Uemura, S. *Synlett* **2004**, 201–216.

Nomura, N.; Tsurugi, K. Yoshida, N.; Okada, M. *Curr. Org. Syn.* **2005**, *2*, 21–38.

O'Brien, C. *Chem. Rev.* **1964**, *64*, 81–89.

O'Brien, T.; Crocker, L.; Thompson, R.; Thompson, K.; Toma, P. H.; Conlon, D. A.; Feibush, B.; Moeder, C.; Bicker, G.; Grinberg, N. *Anal. Chem.* **1997**, *69*, 1999–2007.

Oganesian, L.; Bryan, T. M. *Bioessays* **2007**, *29*, 155–165.

Olaussen, K. A.; Dubrana, K.; Dornont, J.; Spano, J. P.; Sabatier, L.; Soria, J. C. *Crit. Rev. Oncol. Hematol.* **2006**, *57*, 191–214.

Ooi, T.; Takahashi, M.; Doda, K.; Maruoka, K. *J. Am. Chem. Soc.* **2002**, *124*, 7640–7641.

Patel, H. K.; Kilburn, J. D.; Langley, G. J.; Edwards, P. D.; Mitchell, T.; Southgate, R. *Tetrahedron Lett.* **1994**, *35*, 481–484.

Paulson, D. R.; Gilliam, L. S.; Terry, V. O.; Farr, S. M.; Parker, E. J.; Tang, F. Y. N.; Ullman, R.; Ribar, G. *J. Org. Chem.* **1978**, *43*, 1783–1787.

Pendino, F.; Tarkanyi, I.; Dudognon, C.; Hillion, J.; Lanotte, M.; Aradi, J.; Segal-Bendirdjian, E. *Curr. Cancer Drug Targets* **2006**, *6*, 147–180.

Philippe, M.; Sepulchre, A. M.; Gero, S. D.; Loibner, H.; Streicher, W.; Stutz, P. *J. Antibiot.* **1982**, *35*, 1507–1512.

Pindur, U.; Lemster, T. *Curr. Med. Chem.* **2001**, *8*, 1681–1698.



Poli, G.; Giambastiani, G.; Heumann, A. *Tetrahedron* **2000**, 56, 5959–5989.

Pontillo, J.; Chen, C. *Bioorg. Med. Chem. Lett.* **2005**, 15, 1407–1411.

Popp, B. V.; Stahl, S. S. *J. Am. Chem. Soc.* **2007**, 129, 4410–4422.

Poss, C. S.; Schreiber, S. L. *Acc. Chem. Res.* **1994**, 27, 9–17.

Punniyamurthy, T.; Velusamy, S.; Iqbal, J. *Chem. Rev.* **2005**, 105, 2329–2365.

Rao, Y. S.; Filler, R. *Chem. Commun.* **1970**, 1622.

Rapado, L. P.; Bulughapitiya, V.; Renaud, P. *Helv. Chim. Acta* **2000**, 83, 1625–1632.

Reeder, M. R.; Gleaves, H. E.; Hoover, S. A.; Imbordino, H. R.; Pangborn, J. *J. Org. Process Res. Dev.* **2003**, 7, 696–699.

Rezler, E. M.; Seenisamy, J.; Bashyam, S.; Kim, M. Y.; White, E.; Wilson, W. D.; Hurley, L. H. *J. Am. Chem. Soc.* **2005**, 127, 9439–9447.

Riego, E.; Hernández, D.; Albericio, F.; Álvarez, M. *Synthesis* **2005**, 1907–1922.

Robertson, D. W.; Krushinski, J. H.; Fuller, R. W.; Leander, J. D. *J. Med. Chem.* **1988**, *31*, 1412–1417.

Rodehorst, R. M.; Koch, T. H. *J. Am. Chem. Soc.* **1975**, *97*, 7298–7304.

Rönn, M.; Bäckvall, J.-E.; Andersson, P. G. *Tetrahedron Lett.* **1995**, *36*, 7749–7752.

Rosu, F.; Gabelica, V.; Shin-ya, K.; De Pauw, E. *Chem. Commun.* **2003**, 2702–2703.

Sajiki, H.; Ikawa, T.; Hirota, K. *Tetrahedron Lett.* **2003**, *44*, 7407–7410.

Sajiki, H.; Kume, A.; Hattori, K.; Hirota, K. *Tetrahedron Lett.* **2002**, *43*, 7247–7250.

Sasaki, S.; Ehara, T.; Sakata, I.; Fujino, Y.; Harada, N.; Kimura, J.; Nakamura, H.; Maeda, M. *Bioorg. Med. Chem. Lett.* **2001**, *11*, 583–585.

Schaus, J. V.; Panek, J. S. *Org. Lett.* **2000**, *2*, 469–471.

Scheurer, A.; Mosset, P.; Bauer, W.; Saalfrank, R. W. *Eur. J. Org. Chem.* **2001**, 3067–3074.

Schreiber, S. L. *Chem. Scr.* **1987**, *27*, 563–566.

Shafer, C. M.; Molinski, T. F. *Heterocycles* **2000**, *53*, 1167–1170.

Shay, J. W.; Wright, W. E. *Nat. Rev. Drug Discovery* **2006**, *5*, 577–584.

Sheehan, J. C.; Izzo, P. T. *J. Am. Chem. Soc.* **1949**, *71*, 4059–4062.

Shimada, S.; Li, Y.-H.; Choe, Y.-K.; Tanaka, M.; Bao, M.; Uchimaru, T. *Proc. Nat. Acad. Sci.* **2007**, *104*, 7758–7763.

Shin-ya, K.; Wierzba, K.; Matsuo, K.; Ohtani, T.; Yamada, Y.; Furihata, K.; Hayakawa, Y.; Seto, H. *J. Am. Chem. Soc.* **2001**, *123*, 1262–1263.

Sigman, M. S.; Schultz, M. J. *Org. Biomol. Chem.* **2004**, *2*, 2551–2554.

Smith, A. B., III; Minbiole, K. P.; Freeze, S. *Synlett* **2001**, 1739–1742.

Smith, A. B., III; Minbiole, K. P.; Verhoest, P. R.; Schelhaas, M. *J. Am. Chem. Soc.* **2001**, *123*, 4834–4836.

Smith, A. B., III; Minbiole, K. P.; Verhoest, P. R.; Schelhaas, M. *J. Am. Chem. Soc.* **2001**, *123*, 10942–10953.

Smith, A. B., III; Razler, T. M.; Meis, R. M.; Pettit, G. R. *Org. Lett.* **2006**, 8, 797–799.

Smith, A. B., III; Razler, T. M.; Pettit, G. R.; Chapuis, J.-C. *Org. Lett.* **2005**, 7, 4403–4406.

Sohda, K. Y.; Hiramoto, M.; Suzumura, K. I.; Takebayashi, Y.; Suzuki, K. I.; Tanaka, A. *J. Antibiot.* **2005**, 58, 32–36.

Sohda, K. Y.; Nagai, K.; Yamori, T.; Suzuki, K. I.; Tanaka, A. *J. Antibiot.* **2005**, 58, 27–31.

Stahl, S. S. *Angew. Chem., Int. Ed.* **2004**, 43, 3400–3420.

Stoltz, B. M. *Chem. Lett.* **2004**, 33, 362–367.

Stromnova, T. A.; Shishilov, O. N.; Dayneko, M. V.; Monakhov, K. Y.; Churakov, A. V.; Kuz'mina, L. G.; Howard, J. A. K. *J. Organomet. Chem.* **2006**, 691, 3730–3736.

Sumi, M.; Tauchi, T.; Sashida, G.; Nakajima, A.; Gotoh, A.; Shin-Ya, K.; Ohyashiki, J. H.; Ohyashiki, K. *Int. J. Oncol.* **2004**, 24, 1481–1487.

Tahara, H.; Shin-ya, K.; Seimiya, H.; Yamada, H.; Tsuruo, T.; Ide, T. *Oncogene* **2006**, 25, 1955–1966.

Tauchi, T.; Shin-Ya, K.; Sashida, G.; Sumi, M.; Nakajima, A.; Ohyashiki, J. H.; Ohyashiki, K. *Blood* **2004**, *104*, 925A–926A.

Tauchi, T.; Shin-ya, K.; Sashida, G.; Sumi, M.; Nakajima, A.; Shimamoto, T.; Ohyashiki, J. H.; Ohyashiki, K. *Oncogene* **2003**, *22*, 5338–5347.

Tauchi, T.; Shin-ya, K.; Sashida, G.; Sumi, M.; Okabe, S.; Ohyashiki, J. H.; Ohyashiki, K. *Oncogene* **2006**, *25*, 5719–5725.

Tauchi, T.; Sumi, M.; Nakajima, A.; Sashida, G.; Goto, A.; Ohyashiki, J. H.; Shin-ya, K.; Ohyashiki, K. *Blood* **2001**, *98*, 616A.

Temkin, O. N.; Bruk, L. G. *Russ. Chem. Rev.* **1983**, *52*, 117–137.

Tera, M.; Sohtome, Y.; Ishizuka, H.; Doi, T.; Takagi, M.; Kazuo, S. Y.; Nagasawa, K. *Heterocycles* **2006**, *69*, 505–514.

Tietze, L. F.; Ila, H.; Bell, H. P. *Chem. Rev.* **2004**, *104*, 3453–3516.

Tietze, L. F.; Sommer, K. M.; Zinngrebe, J.; Stecker, F. *Angew. Chem., Int. Ed.* **2005**, *44*, 257–259.

Tormyshev, V. M.; Mikhulina, T. V.; Rogozhnikova, O. Y.; Troitskaya, T. Y.; Trukhin, D. V. *Russ. J. Org. Chem.* **2006**, *42*, 1049–1053.

Trend, R. M.; Ramtohl, Y. K.; Ferreira, E. M.; Stoltz, B. M. *Angew. Chem., Int. Ed.* **2003**, *42*, 2892–2895.

Trend, R. M.; Stoltz, B. M. *J. Am. Chem. Soc.* **2004**, *126*, 4482–4483.

Trost, B. M. *Chem. Pharm. Bull.* **2002**, *50*, 1–14.

Trost, B. M. *J. Org. Chem.* **2004**, *69*, 5813–5837.

Trost, B. M.; Crawley, M. L. *Chem. Rev.* **2003**, *103*, 2921–2943.

Trost, B. M.; Dogra, K.; Franzini, M. *J. Am. Chem. Soc.* **2004**, *126*, 1944–1945.

Trost, B. M.; Van Vranken, D. L. *Chem. Rev.* **1996**, *96*, 395–422.

Tsuji, J. *J. Synth. Org. Chem. Japan* **1999**, *57*, 1036–1050.

*Palladium in Organic Synthesis*; Tsuji, J., Ed.; Springer: Berlin, 2005.

Tsuji, J. *Palladium Reagents and Catalysts: Innovations in Organic Synthesis*; Wiley and Sons: New York, 1995.

Tsuji, J. *Palladium Reagents and Catalysts: New Perspectives for the 21st Century*; Wiley and Sons: New York, 2003.

Tsuji, J. *Synthesis* **1990**, 739–749.

Tsuji, J.; Mandai, T. *Synthesis* **1996**, 1–24.

Tsuji, J.; Minami, I.; Shimizu, I. *Synthesis* **1986**, 623–627.

Ulibarri, G.; Audrain, H.; Nadler, W.; Lhermitte, H.; Grierson, D. S. *Pure Appl. Chem.* **1996**, 68, 601–604.

Ulibarri, G.; Nadler, W.; Skrydstrup, T.; Audrain, H.; Chiaroni, A.; Riche, C.; Grierson, D. S. *J. Org. Chem.* **1995**, 60, 2753–2761.

Van Benthem, R. A. T. M.; Hiemstra, H.; Michels, J. J.; Speckamp, W. N. *J. Chem. Soc., Chem. Commun.* **1994**, 357–359.

Vedejs, E.; Luchetta, L. M. *J. Org. Chem.* **1999**, 64, 1011–1014.

Whitlock, C. R.; Cava, M. P. *Tetrahedron Lett.* **1994**, 35, 371–374.

Williams, R. M.; Cao, J.; Tsujishima, H.; Cox, R. J. *J. Am. Chem. Soc.* **2003**, 125, 12172–12178.

Woodward, R. B.; Bader, F. E.; Bickel, H.; Frey, A. J.; Kierstead, R. W. *Tetrahedron* **1958**, 2, 1–57.

Wright, A. E.; Pomponi, S. A.; Cross, S. S.; McCarthy, P. *J. Org. Chem.* **1992**, 57, 4772–4775.

Wright, A. E.; Pomponi, S. A.; Jacobs, R. S. PCT Int. Appl. WO 9942092, August 26, 1999.

Xiao, W. *Huaxue Shiji* **1992**, 14, 363–366.

Xu, Y.; Chen, L.; Ma, Y.; Li, J.; Cao, X. *Synlett* **2007**, 1901–1904.

Yamada, S.; Shigeno, K.; Kitagawa, K.; Okajima, S.; Asao, T. (Taiho Pharmaceutical Co. Ltd., Sosei Co. Ltd.). WO2002048153; *Chem. Abstr.* **2002**, 137, 47050.

Yang, C.-G.; Huang, H.; Jiang, B. *Curr. Org. Chem.* **2004**, 8, 1691–1720.



Yang, C.-G.; Liu, G.; Jiang, B. *J. Org. Chem.* **2002**, *67*, 9392–9396.

Yang, C.-G.; Wang, J.; Jiang, B. *Tetrahedron Lett.* **2002**, *43*, 1063–1066.

Yang, C.-G.; Wang, J.; Tang, X.-X.; Jiang, B. *Tetrahedron: Asymmetry* **2002**, *13*, 383–394.

Yeh, V. S. C. *Tetrahedron* **2004**, *60*, 11995–12042.

Yu, J. Q.; Giri, R.; Chen, X. *Org. Biomol. Chem.* **2006**, *4*, 4041–4047.

Zahler, A. M.; Williamson, J. R.; Cech, T. R.; Prescott, D. M. *Nature* **1991**, *350*, 718–720.

Zeni, G.; Larock, R. C. *Chem. Rev.* **2004**, *104*, 2285–2309.

Zeni, G.; Larock, R. C. *Chem. Rev.* **2006**, *106*, 4644–4680.

Zhang, H.; Ferreira, E. M.; Stoltz, B. M. *Angew. Chem., Int. Ed.* **2004**, *43*, 6144–6148.

Zhang, L. L.; Tamura, K.; Shin-ya, K.; Takahashi, H. *Biochim. Biophys. Acta—Mol. Cell Res.* **2006**, *1763*, 39–44.

Zimmer, R.; Dinesh, C. U.; Nandanan, E.; Khan, F. A. *Chem. Rev.* **2000**, *100*, 3067–3125.

# INDEX

## A

Aerobic .....	14, 20, 22, 23
Alkaloid .....	62, 64
Aminoimidazole .....	63, 65, 66, 80, 81
Antagonist .....	19
Antidepressant .....	19, 20
Antipode .....	84, 100, 101
Antiviral .....	65
Asymmetric .....	14, 19, 23, 40
Azirine .....	82, 188

## B

$\beta$ -Hydride elimination .....	3, 5, 7, 8, 17
Bicycle .....	65, 66, 67, 71, 72, 73, 74, 75, 76, 77, 78, 79, 86, 89, 95, 96, 117, 118, 119, 128, 129, 167, 171, 172, 173, 185, 186
Biological .....	62, 65, 66, 101, 337, 342, 351, 373, 374
Biosynthesis .....	63, 84, 338, 339, 376
Bis(indole) .....	62, 63, 64
Bisoxazole .....	343, 345, 346, 347, 358, 360, 361, 363
Boronic acid .....	66
Boronic ester .....	66, 79, 80, 99, 131, 132, 175, 176
Bromination .....	79, 99, 115, 130, 175
Bromoindole .....	62, 66, 80, 126

	473
Bromopyrazine .....	132, 176
Bromopyrrole .....	66, 70, 71, 115, 116
Brown's Rh catalyst .....	99
Byproduct .....	73, 74, 93, 184
<b>C</b>	
Cancer .....	62, 336, 342, 372
Carbonylation .....	1, 347, 367
Catalysis .....	1, 4, 5, 6, 14, 342, 343, 347, 348, 350, 377
Catalyst .....	3, 5, 7, 14, 23, 43, 68, 75, 99, 183, 343
Catalytic .....	4, 7, 69, 71, 72, 74, 75, 76, 79, 338, 348
Catalytic cycle .....	3, 7, 17
Chiral .....	8, 17, 343
Chirotopic .....	189
Chloroquinoline .....	37, 38, 39
Chromosome .....	335
Cleavage .....	64, 82, 190, 349
Competitive .....	71, 88, 381
Conformation .....	88, 110, 144, 190, 192
Conversion .....	14, 21, 25, 40
Cross-coupling .....	1, 3, 5, 64, 66, 99, 100, 182, 343, 346, 348, 350, 377, 380, 381
<b>D</b>	
Dean-Stark .....	104, 348, 368
Decomposition .....	74, 98, 113, 186
Dehydrogenation .....	14, 23, 66
Deprotection .....	82, 138, 139, 140, 339

Dess-Martin periodinane .....	36, 81, 124, 134
Desymmetrization .....	14, 89
Deuterium .....	90, 185, 191
Diastereomer .....	85, 87, 97, 98, 99, 150, 151, 190, 192
Diastereoselectivity .....	69, 89, 95
Dibromopyrrole .....	113, 114, 187
DMSO .....	74, 77, 98, 119, 127, 167, 185
DNA .....	335, 336, 337
Dragmacidin .....	188
Dragmacidin D .....	62, 63, 64, 66, 80, 84, 179, 180
Dragmacidin E .....	62, 63, 84, 102, 179, 181
Dragmacidin F .....	62, 63, 65, 66, 67, 75, 79, 80, 83, 84, 85, 86, 87, 96, 98, 99, 100, 101, 140, 177, 178, 179, 180, 188
Dragmacidins .....	62, 63, 64, 84, 178, 179
<i>E</i>	
EC <sub>50</sub> .....	65
Electron .....	2, 3, 4
Electron-deficient .....	185
Electron-rich .....	6, 72
Electrophilic .....	5, 6, 7
Elimination .....	69, 87, 88, 91, 93
Enantiodivergent .....	85, 100, 189
Enantioenriched .....	27, 28, 36, 37, 39
Enantiomeric excess .....	14, 20, 21, 25, 26, 40, 92, 94, 149
Enantiopure .....	83, 189, 192

	475
Enantioselectivity .....	1, 18, 22
Enantiospecific .....	83
Ethyl nicotinate .....	72, 185
Exocyclic .....	68, 90, 191
<b><i>F</i></b>	
Friedel-Crafts .....	7, 63
<b><i>G</i></b>	
gCOSY .....	144
Glovebox .....	110, 117, 174
G-quadruplex .....	337, 351, 376
G-tetrad .....	337, 338
<b><i>H</i></b>	
Halogen-selective .....	64, 66, 79, 99, 100
Heck reaction .....	1, 8, 66, 70, 71, 74, 77, 78, 129, 180, 184, 187
Herpes simplex virus (HSV) .....	65
Heterocyclic .....	62
Heterocyclization .....	13, 14, 338
Heterogeneous .....	90, 93, 106, 183, 191, 355
Homogeneous .....	67, 93, 135, 182
Homonuclear decoupling .....	110, 144, 191, 192
Human Immunodeficiency Virus (HIV) .....	65
Hydride .....	3, 4, 5, 7, 8, 12, 17, 67
Hydrogen (H <sub>2</sub> ) .....	69, 87, 89, 91, 94, 99, 111, 126, 128, 131, 141, 147, 149, 150, 159, 161, 163, 164, 174, 175, 190, 349
Hydrogenation .....	1, 3, 69, 79, 88, 91, 95, 96, 183, 190, 192

	476
Hydrogenolysis .....	1, 92
<b><i>I</i></b>	
IC <sub>50</sub> .....	337
Imide .....	347, 348, 349, 359, 360, 366, 370
Indole .....	72, 76, 95, 97, 127, 162, 164
Inhibitor .....	92, 337, 350
Intermolecular .....	7
Intramolecular .....	7, 66, 70, 71, 72, 186, 350, 376, 382
Iodination .....	347, 362, 363
<b><i>K</i></b>	
Kinetic resolution .....	40
<b><i>L</i></b>	
Lawesson's reagent .....	349
Leaving group .....	87, 88, 93, 95
Leukotriene .....	19
Ligand .....	3, 7, 8, 14, 17, 73, 74, 78
<b><i>M</i></b>	
Macrocycle .....	337, 350
Macrocyclization .....	338, 343, 351, 377, 382, 383
Marine .....	62, 65
Mechanism .....	17, 82, 91, 92, 336
Mechanistic .....	3, 9, 12, 41
Meso .....	14, 92
Methylbisoxazole .....	347, 366, 367, 368
Methyloxazole .....	347, 364, 365, 366, 370, 371

Model ..... 9, 41, 79, 95, 338, 351

## *N*

Natural product 1, 62, 64, 65, 66, 79, 80, 81, 180, 181, 189, 337, 339, 340, 341, 342, 373

Neber rearrangement ..... 81, 82, 83, 101, 187, 188

Negishi cross-coupling ..... 343, 346, 348, 361, 380

Nisoxetine ..... 19

Nitrene ..... 188

NOE ..... 138, 144, 191, 192

Norfluoxetine ..... 19

Nucleophile ..... 7

Nucleophilic ..... 4, 5, 7, 68

## *O*

Olefin insertion ..... 5, 7, 78

Oxazole 337, 338, 339, 342, 343, 345, 348, 350, 356, 357, 358, 359, 360, 361, 373, 378, 380, 381

Oxazolone ..... 346, 347, 348, 358, 360, 366, 371

Oxidant ..... 7, 14, 16, 72, 185, 186

Oxidation .. 2, 3, 7, 8, 9, 12, 14, 17, 18, 22, 40, 41, 63, 67, 75, 81, 186, 338, 339, 340, 343

Oxidative addition ..... 3, 4, 5, 6

Oxidative carbocyclization 14, 66, 70, 71, 72, 74, 75, 76, 77, 78, 86, 97, 100, 120, 122, 169, 171, 173, 186

Oxidative kinetic resolution ..... 14, 15, 17, 18, 20, 22, 36, 42

Oxygen (O<sub>2</sub>) ..... 7, 12, 14, 17, 20, 21, 27, 28, 40, 41, 73, 74, 75, 76, 77, 120, 184

## *P*

Palladium 1, 2, 3, 4, 5, 6, 7, 8, 9, 11, 12, 13, 14, 17, 18, 20, 22, 66, 67, 68, 69, 71, 72, 73, 74, 75, 76, 77, 78, 80, 86, 87, 89, 90, 91, 92, 94, 96, 97, 98, 100, 110, 111, 117, 119,



127, 128, 132, 141, 147, 149, 150, 159, 161, 164, 167, 176, 180, 182, 183, 184, 185,  
190, 191, 342, 343, 347, 348, 349, 350, 361, 367, 377

$\pi$ -Allyl .....	4, 5, 6, 67, 68, 92, 93, 182
Palladium(0) .....	2, 3, 4, 5, 6, 7, 8, 9, 12, 66, 67, 80
Palladium(I) .....	11, 12
Palladium(II) .....	2, 3, 4, 5, 6, 7, 8, 9, 13, 17, 66, 71, 72, 76, 96, 97, 100, 185
Palladium(III) .....	12
Palladium(IV) .....	2, 9, 11
Palladium(V) .....	12
Palladium(VI) .....	12
Peptide .....	338, 339, 340
Pharmaceutical .....	1, 14, 18, 19, 20, 23, 340, 341, 376
Piperazine .....	178, 179
Protic .....	190
Prozac <sup>®</sup> (Fluoxetine) .....	19, 23
Pseudo-C <sub>2</sub> -symmetric .....	85, 89, 189
Pyrazine .....	64, 66, 176, 177
Pyrazinone .....	62, 63, 64, 65, 83, 178
Pyrrole .....	65, 66, 70, 72, 74, 79, 86, 89, 95, 96, 99, 115, 116, 117, 119, 142, 183, 184, 185, 186

## ***Q***

Quinic acid .....	66, 67, 83, 84, 85, 86, 89, 100, 104, 181, 188, 189
-------------------	---

## ***R***

Racemic .....	92, 150
Racemize .....	189
Ratio .....	71

Reduction .....	2, 4, 20, 22, 43, 68, 69, 87, 129, 182, 192
Reductive elimination .....	3, 5, 7, 8
Reductive isomerization .....	69, 87, 88, 89, 90, 92, 95, 100, 152, 154, 166, 183, 190, 191, 192
Regioisomer .....	68, 96
Regioselectivity .....	1, 6, 68, 79
Retrosynthesis .....	1, 66, 343, 378
Rhodium .....	99, 174
Rotamer .....	368, 369, 370, 371
<b>S</b>	
Selectivity factor .....	14, 20, 40
Serine .....	338, 343, 348, 350, 368
Single electron transfer .....	92
Singulair® (Montelukast sodium) .....	19, 22, 23
Sparteine .....	14, 20, 21, 27, 28
Stereocenter .....	8, 79
Stereochemistry .....	66, 84, 138, 189, 191, 192, 341
Stereoisomer .....	96
Stereoselectivity .....	1, 6, 7, 90
Steric .....	74, 97, 100, 186
Stille cross-coupling .....	1, 182, 346
Stoichiometric .....	7, 14, 16, 68, 72, 74, 75, 184
Suzuki cross-coupling .....	1, 64, 66, 79, 99, 100, 132, 133, 342, 346
Symmetry .....	189
<b>T</b>	
Tautomerization .....	99

Telomerase .....	335, 336, 337, 338, 350, 372, 373
Telomere .....	335, 336, 337, 372
Telomestatin .	335, 337, 338, 339, 340, 341, 342, 343, 345, 350, 351, 373, 374, 376, 378
Tetrakisoxazole .....	343, 347, 349, 378, 381
Thiazoline .....	337, 340, 343, 350
Tomoxetine .....	19
Total synthesis	5, 6, 62, 64, 65, 75, 77, 80, 84, 89, 180, 190, 335, 339, 340, 341, 342, 345, 350, 351, 383
Transition state .....	78, 186
Transmetallation .....	3, 5, 13
Triflate	343, 345, 346, 347, 348, 349, 350, 358, 360, 361, 363, 366, 367, 370, 371, 379, 381
Trisoxazole .....	340, 341, 343, 345, 346, 347, 348, 362, 363, 378, 381
Tryptophan .....	63
Turnover .....	75, 76
<b><i>U</i></b>	
Unnatural .....	62, 84
<b><i>W</i></b>	
Weinreb amide .....	70, 112, 114, 116, 126
Wilkinson's catalyst .....	43
Wittig olefination .....	67
<b><i>X</i></b>	
X-ray .....	346, 353, 363, 373

## ABOUT THE AUTHOR

Daniel D. Caspi was born on February 7, 1980, in Berkeley, CA. He was raised by his parents, Susan and Shlomo, and was joined shortly after his second birthday by his younger sister, Sara. Dan's childhood years were spent living in Alameda, CA, a suburb in the Bay Area and a former Naval base. He attended College Preparatory High School in Oakland, CA, where he played piano in the high school jazz band. His enthusiasm for chemistry was ignited by the AP Chemistry course, where he convinced the charismatic Mr. Coakley to add highly explosive laboratory experiments to the course repertoire.

After graduating from high school in 1998, Dan began his undergraduate studies at Revelle College at UC San Diego as a Chemistry major. After completing the organic chemistry lecture and laboratory series, and realizing that he was deeply interested in the subject, he was inspired to further his knowledge outside of the classroom. During the summer after his sophomore year, he began working at a local biotech company, Metabasis Therapeutics, Inc., where he received his first taste of medicinal chemistry research under the guidance of Dr. Jorge Gomez. Dan was also a teaching assistant for an undergraduate chemistry course for non-chemistry majors, where he tried, with limited success, to convert social science majors to the physical sciences.

In 2002, Dan's passion for organic chemistry led him to sunny Pasadena, CA, to pursue doctoral studies with Professor Brian M. Stoltz at the California Institute of Technology. In 2008, he earned his Ph.D. in chemistry for investigations involving the use of palladium in the context of pharmaceutical and natural product synthesis. Dan will join the process group at Abbott Laboratories in North Chicago, IL, in March of 2008.